INFORMATION TO USERS

This manuscript has been reproduced from the microfilm master. UMI films the text directly from the original or copy submitted. Thus, some thesis and dissertation copies are in typewriter face, while others may be from any type of computer printer.

The quality of this reproduction is dependent upon the quality of the copy submitted. Broken or indistinct print, colored or poor quality illustrations and photographs, print bleedthrough, substandard margins, and improper alignment can adversely affect reproduction.

In the unlikely event that the author did not send UMI a complete manuscript and there are missing pages, these will be noted. Also, if unauthorized copyright material had to be removed, a note will indicate the deletion.

Oversize materials (e.g., maps, drawings, charts) are reproduced by sectioning the original, beginning at the upper left-hand corner and continuing from left to right in equal sections with small overlaps. Each original is also photographed in one exposure and is included in reduced form at the back of the book.

Photographs included in the original manuscript have been reproduced xerographically in this copy. Higher quality 6" x 9" black and white photographic prints are available for any photographs or illustrations appearing in this copy for an additional charge. Contact UMI directly to order.

U·M·I

University Microfilms International
A Bell & Howell Information Company
300 North Zeeb Road, Ann Arbor, MI 48106-1346 USA
313/761-4700 800/521-0600

Order Number 9325069

Geology of parts of the Peach Lake and Brewster quadrangles, southeastern New York and adjacent Connecticut, and basement blocks of the north-central Appalachians. (Volumes I and II)

Brock, Pamela Jean Chase, Ph.D.

City University of New York, 1993

Copyright ©1993 by Brock, Pamela Jean Chase. All rights reserved.

U·M·I
300 N. Zeeb Rd.
Ann Arbor, MI 48106

GEOLOGY OF PARTS OF THE PEACH LAKE AND BREWSTER QUADRANGLES, SOUTHEASTERN NEW YORK AND ADJACENT CONNECTICUT, AND BASEMENT BLOCKS OF THE NORTH-CENTRAL APPALACHIANS

by

PAMELA JEAN CHASE BROCK

VOLUME I

A dissertation submitted to the Graduate Faculty in Earth and Environmental Sciences in partial fulfillment of the requirements for the degree of Doctor of Philosophy, The City University of New York

1993

c1993

PAMELA JEAN CHASE BROCK

All Rights Reserved

This manuscript has been read and accepted for the Graduate Faculty in Earth and Environmental Sciences in satisfaction of the dissertation requirement for the degree of Doctor of Philosophy.

4/22/93
Date

Chair of Examining Committee

4/22/93
Date

Executive Officer

Hannes K. Brueckner

Kathleen Crane

James McLelland

David E. Seidemann

Supervisory Committee

THE CITY UNIVERSITY OF NEW YORK

Abstract

GEOLOGY OF PARTS OF THE PEACH LAKE AND BREWSTER QUADRANGLES, SOUTHEASTERN NEW YORK AND ADJACENT CONNECTICUT, AND BASEMENT BLOCKS OF THE NORTH-CENTRAL APPALACHIANS

by

Pamela Jean Chase Brock

Adviser: Professor Allan Ludman

The three parts of this thesis have different focuses. Part I covers the bedrock geology of parts of the Peach Lake and Brewster quadrangles (New York - Connecticut). New interpretations of the stratigraphy, structural development, and metamorphic history of the northeastern Manhattan Prong are proposed. In Part II, a compilation of isotopic data from the north-central Appalachians is used to define five fundamental basement blocks (two juvenile, three of ancient continental crust). Part III builds upon compiled geologic data to infer the timing of the accretion of these blocks, and to model the Acadian orogeny.

Part I presents a newly recognized, rift-related Eocambrian unit, the Ned Mountain Formation (NMF). The NMF consists of bimodal metavolcanic rocks, meta-arkoses, meta-wackes, and calc-silicate rocks which crop out between the Grenvillian Fordham Gneiss and the Cambro-Ordovician Inwood Marble. The NMF is subdivided into a graphitic Basal Member, a Volcaniclastic Member (including "Pound Ridge granite"), Wacke Member, and an uppermost Calc-Silicate Member (including "Lowerre Quartzite"). NMF strata are compositionally distinct in many respects from rocks of other formations. Reconnaissance transects outside the study area confirm persistence of the NMF over a large area.

Six episodes of Paleozoic deformation are recognized in the study area. The Hartland terrane was emplaced over the Manhattan Prong during (Taconian) D_1; D_2 backfolding pro-

duced a series of large folds, which were later deformed around northeast-striking F_3 hinge surfaces. Minor recumbent D_4 folding and shearing followed. The last two events involved Carboniferous ductile faulting: first, normal-sense shearing was accompanied by a syntectonic suite of two-mica granites (previously dated as Mississippian); later, east-directed thrusting produced mylonites that yield Pennsylvanian K-Ar mica ages.

Three principal metamorphic events are recognized: granulite-facies M_1 (syn-D_1), upper-amphibolite facies M_2 (late-Taconian), and greenschist- to middle-amphibolite facies M_3 (Mississippian). M_2 and/or M_3 retrogression commonly obliterates evidence for M_1. However, inclusions in garnets indicate high pressures (>12 kb) for early-M_1, and relict spinel + quartz assemblages imply peak-M_1 temperatures approaching 1000^{o}C.

The model developed in Parts II and III places the Manhattan Prong into regional geological context.

PREFACE

The Northern Appalachians have been the inspiration and testing ground for several generations of orogenic models. Hall (1859) first noted that the sedimentary section in the Appalachian Mountains is substantially thicker than the age-equivalent section in the continental interior. Observing that many of the Appalachian rocks were of shallow-water origin, he proposed that deposition had taken place in a steadily subsiding trough. The term "geosynclinal" was introduced by Dana (1873) for the long depositional belt in which this deposition had taken place. Dana suggested that shrinkage of the earth promoted deepening of the "geosynclinal" sedimentary trough by inducing wrinkling of the earth's surface. Schuchert (1925, 1930) later subdivided the Northern Appalachians into two separate "geosynclines" and an intervening, high-standing metamorphic "geoanticline" thought to consist of Precambrian rocks. This idea encountered difficulties when the metamorphic rocks proved to contain Paleozoic fossils (Billings and Cleaves, 1934).

Kay (1944, 1947, 1951) carefully documented Lower Paleozoic facies relationships in the Appalachians, and found evidence for two contrasting lithologic belts. The western belt, dominated by carbonate rocks, he termed "miogeosynclinal"; the eastern belt, composed of clastic and volcanic rocks, he called "eugeosynclinal". Kay interpreted these facies relationships as the record of a Lower Paleozoic continental margin-volcanic island arc complex.

Plate tectonics began to influence Appalachian geologists in the 1960's. On the basis of fossil and facies distribution patterns, Wilson (1966) suggested that the Appalachian orogen marks the trace where a predecessor of the Atlantic Ocean had closed during Paleozoic time. Bird and Dewey (1970) and Rodgers (1970) offered detailed syntheses of Appalachian geology, interpreted through the prism of plate tectonics. Since then, plate-tectonic interpretations have proliferated for every orogenic event recorded in the Appalachians. Many of these interpretations differ fundamentally, calling on varying numbers of plates or opposite vergences of subduction.

It has long been recognized that mountain-building episodes occurred repeatedly in the Appalachians during Paleozoic time. Thick wedges of clastic rocks, shed by extensive highlands, were deposited during three periods: Middle Ordovician- Late Silurian time, Middle Devonian to Early Mississippian time, and Middle Mississippian to Pennsylvanian time (King, 1959; Thomas, 1977). The mountain-building events responsible for these wedges are known as the (Ordovician) Taconian orogeny, (Devonian) Acadian orogeny, and (Late Paleozoic) Alleghenian orogeny. Viewed from a plate-tectonic perspective, each of these episodes of mountain-building might be the result of a plate collision.

Today, a general consensus exists with regard to the gross tectonic framework of the Taconian orogeny in the Northern Appalachians. The accumulated weight of stratigraphic, structural, metamorphic and other data has led most geologists to believe that an arc terrane and associated accretionary prism were thrust over the North American margin, as the North American plate was shoved down an east-dipping subduction zone (for example, Hall and Robinson, 1982; Stanley and Ratcliffe, 1985; Drake and others, 1989).

The basic tectonic elements of the other major orogenic events, particularly the Acadian orogeny, remain controversial. For the Acadian orogeny, different models have invoked plate collision on a single subduction zone (e.g., Rodgers, 1981), on two subduction zones (e.g., McKerrow and Ziegler, 1971; Bradley, 1983), or no subduction at all (Hall and Robinson, 1982). Variations on these themes are almost as numerous as the geologists who have studied the region.

Almost as much dissension exists regarding the Alleghenian orogeny. At the end of the orogeny, it is agreed, the northwestern coast of Africa nestled against the Appalachian margin of North America. This supercontinent eventually split, creating the modern Atlantic Ocean. But there is no consensus on the mechanics of the pre-supercontinent collision. Each worker selects the interpretation that best suits the evidence he or she finds most telling. For instance, Sinha and Zietz (1982) proposed that Alleghenian collision occurred over a west-dipping subduction zone, because of the presence of a substantial Late Paleozoic magmatic belt on the eastern margin of

North America. On the other hand, noting the western vergence of the Central and Southern Appalachian thrust belt, Pindell and Dewey (1982) suggested that subduction occurred at a east-dipping trench. Strike-slip faulting is important in many areas (e.g., Snoke and Mosher in Hatcher and others, 1989), leading many workers to conclude that collision was oblique or that the opposing continents had irregular boundaries. Thus, Lefort (1984) invoked a rigid-indentor model to explain the structural trends in the Southern and Central Appalachians. Hatcher and Edelman (1987), among others, suggested dextral-oblique convergence between North America and Gondwana. In contrast, Sacks and Secor (1990) proposed sinistral transpression.

The extent of Alleghenian-age deformation and metamorphism in the Northern Appalachians has also been much debated. For many years, Late Paleozoic deformation was commonly believed to be limited to Rhode Island. Recently, however, more and more mineral ages from central and southern New England indicate that rocks in other areas were affected Late Paleozoic tectonism (e.g., Zartman and others, 1970; Wintsch and Sutter, 1986; Gromet, 1989; Robinson and Tucker, 1991).

More than a century after Hall and Dana, new observations can still transform our conceptions of the long-familiar Appalachians. New data continue to play a vital role in our evolving understanding of mountain belts. However, as papers and reports have proliferated, Appalachian geology has become compartmentalized. Data are more abundant than ever before, but interest wanes with distance and across barriers of specialization.

While data remain isolated, their full value cannot be realized. Data need to be integrated, played against each other, their contradictions explored, and then examined for what they reveal about geologic history and geologic process.

A multi-sided approach best serves the cause of advancing Appalachian geology. Fresh, careful observation propels us forward while keeping us on the ground; synthesis (of as many kinds of data as possible) helps us build robust models which will carry us a long way, and give the best possible mileage for our data.

Purpose. The broad purpose of this thesis is to achieve a better and more realistic understanding of the development of the Northern Appalachians. Steps are taken towards this goal through the detailed study of a small area and through synthesis aimed at the entire region. These two approaches are complementary and mutually reinforcing. Some of the observations made in the local study area shed new light on the development of the orogen. At the same time, the synthesis reveals the broad tectonic patterns experienced by the Northern Appalachians during Early to Middle Paleozoic time and explains why some orogenic events, and not others, are recorded by the rocks of the study area.

Thesis format. The thesis is divided into three parts. The first is a study of a portion of the Manhattan Prong in southeastern New York and southwestern Connecticut. The later two deal with the development of the entire Northern Appalachians. Each part has its own abstract and set of figures. A brief summary section at the end of the thesis integrates the Manhattan Prong within the broader Appalachian framework.

A variety of new observations and insights derived from field and petrographic study of the Manhattan Prong are presented in Part I. They lead to new interpretations of basic stratigraphic relationships and to recognition of previously unknown tectonic events. New evidence is presented for Eocambrian rift-basin formation, for repeated deformation and metamorphism during the Taconian orogeny, for igneous activity, metamorphism, and faulting during the post-Acadian period, and for Alleghenian-aged thrusting. In spite of this long record of deformation, no clear indications of Acadian-aged deformation were found in the study area.

Parts II and III draw on a variety of data compiled from the entire Northern Appalachians. A synthesis of these data brings a new perspective to bear on some of the fundamental questions of Northern Appalachian geology. For instance, the nature of the Acadian orogeny, the climactic tectonic event in central New England, has remained unclear. Acadian orogenesis died out to-

wards eastern and western New England, and left a strikingly varied imprint where it was recorded. A synthesis which draws on data compiled from the entire region affected by the Acadian orogeny can reveal underlying patterns missed by local workers.

Part II contains an analysis of the extensive isotopic literature on igneous rocks in the Northern Appalachians. Strontium, lead, oxygen, and neodymium isotopic data from Silurian to Carboniferous igneous rocks are compiled. The purpose of Part II is to define the fundamental basement blocks of the Appalachians: the players, so to speak, in the plate tectonic games.

In Part III, a synthesis of paleontologic, paleomagnetic, igneous, structural, and metamorphic data from the Northern Appalachians is presented. These data are used to constrain the evolving relationships between the basement blocks defined in Part II. Tectonic events of Ordovician time are outlined, but particular attention is given to building a comprehensive model for the much-debated Acadian orogeny.

Although they vary in focus, all three Parts represent steps towards a deeper and more complete understanding of the Northern Appalachians.

ACKNOWLEDGMENTS

Funding for research in the Manhattan Prong was provided by the New York State Geological Survey and by PSC-BHE grant #6-66319 (to P. W. G. Brock and D. Seidemann). A. Ludman patiently and conscientiously presided over the creation of this thesis, a process which spanned several years and generated a series of manuscripts. Over the years, helpful discussions were held with A. J. Boucot, H. K. Brueckner, C. Gariépy, J. Hopeck, A. Ludman, D. Seidemann, and J. P. Whelan. I thank Yale University for use of the K-Ar dating laboratory and D. Seidemann for instruction and assistance with K-Ar techniques. The Union Carbide Corporation provided access to its property in Fairfield County, Connecticut.

My deepest thanks, however, go to P. W. G. Brock. Not only did he give me constant encouragement and support through the years, but he accompanied me on many field trips, read all manuscripts, and drafted a number of the figures.

TABLE OF CONTENTS

PART I- GEOLOGY OF PARTS OF THE PEACH LAKE AND BREWSTER QUADRANGLES, SOUTHEASTERN NEW YORK AND ADJACENT CONNECTICUT

VOLUME I

ABSTRACT, PART I 2

INTRODUCTION
REGIONAL SETTING 4
METHODS OF STUDY 6
GEOLOGIC MAPPING 6
PETROGRAPHIC STUDY 7
Petrographic descriptions 7
STRATIGRAPHIC DESCRIPTIONS 8
Note on stratigraphic thicknesses 8

STRATIGRAPHY
PREVIOUS WORK 9
Fordham Gneiss 11
Yonkers Gneiss 11
Pound Ridge granite 12
Inwood Marble and Manhattan Schist 12
Lowerre Quartzite 13

RESOLUTION OF THE STRATIGRAPHIC CONFLICT 15
MAJOR LINES OF EVIDENCE FOR THE NED MOUNTAIN FORMATION 16

FORDHAM GNEISS 22
ORTHOPYROXENE GNEISS MEMBER 22
CLINOPYROXENE-GARNET GNEISS MEMBER 26
PLAGIOCLASE-HORNBLENDE GNEISS MEMBER 29
K-FELDSPAR-HORNBLENDE GNEISS MEMBER 30
AMPHIBOLITE MEMBER 31
GRANITIC GNEISS MEMBER 31

NED MOUNTAIN FORMATION 33
NATURE OF THE CONTACT BETWEEN THE FORDHAM GNEISS AND THE NED MOUNTAIN FORMATION 36
Apparently sharp contacts 36
Slightly diffuse contact 38
Diffuse contact 50
Interpretation of the contact between the Fordham Gneiss and the Ned Mountain Formation 52
NED MOUNTAIN FORMATION, BASAL MEMBER 53
Metabasite/mafic metasedimentary rock suite 54
Interpretation of the metabasite/mafic metasedimentary rock suite 58
Meta-arkose/K-rich metasaprolite suite 60

Coarse-textured graphitic granofels (metaconglomerate)..... 60
Interpretation of the coarse-textured granofels..... 64
Quartz-feldspar granofelses (meta-arkoses) and associated calc-silicate rocks..... 66
Interpretation of the protoliths and depositional settings of the quartz-feldspar granofelses (meta-arkoses)..... 68
K-feldspar-biotite-garnet gneiss and schistose gneiss (K-rich metasaprolite)..... 70
Lithologic associations that contain K-feldspar-biotite gneiss..... 74
Interpretation of the K-feldspar-biotite-garnet gneiss (K-rich metasaprolite)..... 75
Precambrian K-rich saprolites..... 76
Scenarios for the origins of the K-feldspar-biotite gneisses (K-rich metasaprolites)..... 78
K-feldspar-quartz gneiss (metarhyolite)..... 79
Interpretation of the K-feldspar-quartz gneiss (metarhyolite)..... 79
Facies variations within the Basal Member, Ned Mountain Formation.... 80
NED MOUNTAIN FORMATION, VOLCANICLASTIC MEMBER..... 81
Layered quartzo-feldspathic rocks..... 82
Textures of the lineated K-feldspar-rich gneisses ("felsic metatuffs")..... 85
Significance of textures in the K-feldspar-rich gneisses ("felsic metatuffs")..... 89
Interpretation of the quartzo-feldspathic rocks..... 93
Intrusive body at Ward Pound Ridge County Park..... 94
Origin of the granite..... 94
Amphibolites..... 96
Origin of the amphibolites..... 97
Facies variations in the Volcaniclastic Member..... 97
NED MOUNTAIN FORMATION, WACKE MEMBER..... 98
Quartz-feldspar-garnet-biotite-sillimanite schistose gneiss (metawacke)..... 99
Interpretation of quartz-feldspar-garnet-biotite-sillimanite schistose gneiss (metawacke)..... 100
Metabasites..... 100
Interpretation of the metabasites..... 102
Quartz-feldspar-biotite-garnet granofels..... 102
Interpretation of the quartz-feldspar-biotite-garnet granofels... 103
Garnet-K-feldspar-quartz-sillimanite-biotite-plagioclase schist (metapelite)..... 103
Transitional zone to the Calc-Silicate Member..... 103
Geographic variations within the Wacke Member..... 104
NED MOUNTAIN FORMATION, CALC-SILICATE MEMBER..... 105
Felsic metatuff..... 106
1. Felsic metatuff interbedded with marble and calc-silicate rock..... 108
Interpretation..... 110
2. Felsic metatuff interbedded with meta-arkose..... 110
Quartz-feldspar granofelses and gneisses..... 112

1) Quartz-K-feldspar granofelses..... 112
2) Quartz-feldspar-biotite-garnet granofelses..... 115
3) Miscellaneous quartz-feldspar granofelses..... 116
Interpretation of quartz-feldspar granofelses..... 116
I. Depositional history..... 116
II. Source materials..... 117
III. Summary..... 118
Calc-silicate rocks and marbles..... 119
Interpretation..... 123
Metawacke and metapelite..... 124
K-rich metasaprolite..... 125
Interpretation..... 125
Amphibolites..... 125
Interpretation..... 126
Plagioclase-magnetite rock..... 126
Interpretation..... 126
Phosphatic gneiss and Garnet-hornblende granofels..... 127
Distribution of rock types within the Calc-Silicate Member..... 127

AMPHIBOLITE DIKES IN THE FORDHAM GNEISS..... 129
Interpretation..... 129

IMPLICATIONS OF THE NED MOUNTAIN FORMATION FOR THE TECTONIC DEVELOPMENT AND GEOLOGIC HISTORY OF THE MANHATTAN PRONG..... 129
Basal Member..... 131
Volcaniclastic Member..... 131
Wacke Member..... 131
Calc-Silicate Member..... 133

NATURE OF THE CONTACT BETWEEN THE NED MOUNTAIN FORMATION AND THE INWOOD MARBLE..... 135

STRATIGRAPHIC LINKS BETWEEN THE NED MOUNTAIN FORMATION AND NEIGHBORING EOCAMBRIAN UNITS..... 135

INWOOD MARBLE..... 138
Marbles..... 139
Siliceous lithologies..... 141
Subdivision of the Inwood Marble..... 143
Interpretation..... 143

WALLOOMSAC SCHIST..... 144
Lower Walloomsac Schist (including Marble Member)..... 145
Upper Walloomsac Schist..... 152
Interpretation and geologic setting..... 154

MANHATTAN SCHIST..... 155
Interpretation..... 161

HARTLAND FORMATION..... 162
Interpretation..... 163

STRUCTURAL GEOLOGY

INTRODUCTION 168
PREVIOUS WORK 168
DESCRIPTIVE APPROACH 169

GRENVILLIAN (pre-D_1) DEFORMATION 171

PREMETAMORPHIC (Paleozoic) FAULTING 173
D_1 DEFORMATION 174
F_1 FOLDING AND FABRICS 174
D_1 THRUSTING- CAMERON'S LINE 175
INTERPRETATION OF D_1 177

D_2 DEFORMATION 177
F_2 FOLDING 177
Geometry of major F_2 folds 178
F_2 slip-line orientation 182
D_2 THRUSTING 185
F_2 FOLDING IN REGIONAL CONTEXT 185

D_3 DEFORMATION 186
F_3 FOLDING AND D_3 SHEARING 186
Orientation of F_3 folds 187
F_3 slip line 191
Correlative deformation 195
D_3 DEFORMATION: SUMMARY AND DISCUSSION 195

D_4 DEFORMATION 195
F_4 FOLDING AND D_4 SHEARING 195
INTERPRETATION OF D_4/F_4 DEFORMATION 196

D_5 DEFORMATION 199

D_6 DEFORMATION 200
Turkey Hill fault zone 200
Ridgefield and Naraneka fault zones 207
EN ECHELON D_6 SHEAR ZONES 210
D_6 SHEARING: SUMMARY AND DISCUSSION 210

D_7 DEFORMATION 213
EVIDENCE FOR LATE THRUST FAULTING 213
The Windwing thrust and other D_7 shear zones 215
Attitudes of D_7 thrust faults and conditions of deformation 217
D_7 DEFORMATION: SUMMARY AND DISCUSSION 217

HIGHLANDS BORDER FAULT 220

BRITTLE FAULTING AND FRACTURING 221

ABSOLUTE AGES OF DEFORMATIONAL EVENTS
INTRODUCTION 222

GEOLOGICAL CONTEXT FOR PUBLISHED K-AR DATA, PEACH LAKE QUADRANGLE 227

NEW K-AR AGES 229

INTRUSIVE ROCKS OF MIDDLE ORDOVICIAN AND YOUNGER AGE
INTRODUCTION 232

SMALL GRANITES OF TACONIAN AGE AND RELATED ROCKS 233
MIGMATITIC LEUCOSOMES 233
SMALL GRANITIC BODIES 235

GRANITIZED REGIONS 236

SISCOWIT GRANITE 237
DESCRIPTION 238
CONTACT AND AGE RELATIONSHIPS 239

MAFIC AND ULTRAMAFIC PODS 241
DESCRIPTION 241
CONTACT AND AGE RELATIONSHIPS 242
REGIONAL RELATIONSHIPS 243

MISSISSIPPIAN (SYN-D_6) GRANITES 244
DESCRIPTION 245
ORIGIN OF THE GRANITES 249

LAMPROPHYRE DIKE 250
DESCRIPTION 250
REGIONAL RELATIONSHIPS 251

VOLUME II

METAMORPHIC HISTORY
INTRODUCTION 252
PREVIOUS WORK 253

PROTEROZOIC METAMORPHISM (M_0) 254

EARLY PALEOZOIC METAMORPHISM- M_1-M_2 255
1. The assemblage cordierite + K-feldspar + garnet 256
2. Orthopyroxene + clinopyroxene 256
3. Corundum-bearing restites 257
4. The assemblage hercynite-rich spinel + sillimanite + K-feldspar 257
M_1 AND M_2 METAMORPHISM, ALUMINOUS LITHOLOGIES 259
1. Inclusion assemblage 1 259
2. Inclusion assemblage 2 259
3. Inclusion assemblage 3 260

4. Inclusion assemblage 4.....260
A. Reconstruction of the early M_1 metamorphic path.....264
1. Equilibria involving staurolite.....264
2. Equilibria involving kyanite.....266
3. Equilibria involving Fe-Ti minerals.....266
B. Peak-M_1, granulite-facies metamorphism.....267
Peak M_1 parageneses, aluminous rocks.....267
P-T conditions, peak-M_1.....269
C. Late-M_1 metamorphism: Granulite-facies retrogression.....272
Late M_1 parageneses in aluminous rocks.....272
Significance of textures 1 through 3.....275
Significance of textures 4 through 6.....276
S_1 fabrics: Products of late-M_1 metamorphism.....276
D. M_2 metamorphism: Upper-amphibolite-facies retrogression.....277
P-T conditions, M_2.....280
1) Pressure.....280
2) Temperature.....280
E. Garnet-biotite and garnet-cordierite "thermometry".....281
F. Behavior of Ti and Fe^{3+} during M_1 and M_2.....282
G. Petrogenetic grid for late-M_1 and M_2 reactions in aluminous rocks.286
H. Post-M_2 retrogression of surviving cordierite-bearing assemblages...289
Retrogression in KFMASH (K_2O-FeO-MgO-Al_2O_3-H_2O).....289
Retrogression in FMASH (FeO-MgO-Al_2O_3-SiO_2-H_2O).....291
Summary.....292
M_1-M_2 METAMORPHISM, NON-ALUMINOUS LITHOLOGIES.....292
M_1-M_2 assemblages, quartz-feldspar granofelses.....292
Summary.....294
M_1-M_2 assemblages, calc-silicate rocks and calcareous marbles.....294
Summary.....295
M_1-M_2 parageneses, dolomitic marbles.....295
1. M_2 metamorphic assemblages.....295
2. Relations among aluminous minerals.....296
3. Exsolution in carbonate minerals.....296
4. Pyroxene relationships.....299
5. Post-M_2 retrogression.....300
Summary.....300
M_1-M_2 parageneses, metabasites.....300

EARLY CARBONIFEROUS METAMORPHISM- M_3.....302
M_3 METAMORPHIC GRADES RECORDED IN ALUMINOUS ROCKS.....302
1) Greenschist-facies assemblages.....302
2) Lower-amphibolite-facies assemblages.....302
3) Middle-amphibolite-facies assemblages.....303
KYANITE NODULES.....304
M_3 ASSEMBLAGES IN NON-ALUMINOUS LITHOLOGIES.....308
P-T CONDITIONS, M_3 METAMORPHISM.....310
MINERAL COMPOSITIONS AND GARNET-BIOTITE THERMOMETRY FOR M_3 ASSEMBLAGES.....311

LATE CARBONIFEROUS METAMORPHISM- M_4.....313

TECTONIC DEVELOPMENT OF THE MANHATTAN PRONG
INTRODUCTION....316

TACONIAN OROGENY....316
A. REVIEW OF AGE CONSTRAINTS....316
B. GEOGRAPHIC AND TEMPORAL VARIATIONS IN TACONIAN METAMORPHISM....317
C. CORRELATION OF TACONIAN STRUCTURES....320
D. MODEL FOR THE TACONIAN OROGENY....326
1. D_1 deformation/early-M_1 metamorphism....326
2. Intrusion of mafic to intermediate igneous complexes in the eastern Prong....327
3. D_2 thrusting/F_2 folding....328
4. Post-F_2 warping....330
5. F_3 folding....330

POST-TACONIAN TECTONIC ACTIVITY....331

SUMMARY STATEMENT....333

IMPLICATIONS FOR APPALACHIAN GEOLOGY
INTRODUCTION....335

LATE PRECAMBRIAN TO EARLY CAMBRIAN TIME....335
1. Origin of the promontories and and embayments in the Appalachian margin....335
2. Age of the rift-drift transition....337

MIDDLE TO LATE ORDOVICIAN TIME....337
1. Taconian high-pressure metamorphism....337
2. Major tectonic events of the Taconian orogeny....339

MISSISSIPPIAN TECTONISM....340

PENNSYLVANIAN (ALLEGHENIAN) OROGENY....341

THE LARGER CONTEXT....342

APPENDIX 1 (to Part I) - BRIEF DESCRIPTION OF TRANSECTS, PLATE II
1. MOUNT VERNON QUADRANGLE....343
Transect A-A'....343
Transect B-B'....343
2. MOUNT VERNON AND YONKERS QUADRANGLES....344
Transect C-C'....344
3. WHITE PLAINS QUADRANGLE....345
Transect D-D'....345
Transect E-E'....346
4. OSSINING QUADRANGLE....348
Transect F-F'....348
Transect G-G'....350

5. CROTON FALLS QUADRANGLE....351
Transect H-H'....351
Transect I-I'....352
Transect J-J'....353
Transect K-K'....353
Transect L-L'....354

APPENDIX 2 (to Part I) - METHODS OF CALCULATING VALUES FOR FIGS. 19 AND 20....356

PART II - ISOTOPICALLY-DEFINED BASEMENT BLOCKS OF THE NORTH-CENTRAL APPALACHIANS

ABSTRACT, PART II....367

INTRODUCTION....368
Previous work....370

COMPILATION OF ISOTOPIC DATA....378
Sr and Pb data....378
Oxygen data....383
Neodymium data....383

COMPARISON OF ISOTOPIC AND SILICA COMPOSITIONS....386

INHERITANCE-AGE DATA....388

DISCUSSION OF ISOTOPIC AND INHERITANCE AGE CHARACTERISTICS....393
Zone A....393
Zone B....393
Zone C....394
Zone D....394
Zone E....395

RELATIONSHIPS BETWEEN THE ISOTOPIC ZONES AND OTHER ASPECTS OF NORTHERN APPALACHIAN GEOLOGY....397

COMPARISON OF ISOTOPIC AND TECTONOSTRATIGRAPHIC ZONES....397

SILURO-DEVONIAN THERMAL HISTORY AND THE ISOTOPIC ZONES....400

GEOPHYSICAL AND PALEOGEOGRAPHICAL EVIDENCE FOR CRUSTAL BREAKS....403

SUMMARY AND CONCLUSIONS, PART II....406

PART III - EARLY TO MIDDLE PALEOZOIC ACCRETION HISTORY OF THE BASEMENT BLOCKS OF THE NORTH-CENTRAL APPALACHIANS

ABSTRACT, PART III....408

INTRODUCTION....410
Basement-cover relationships....412

TIMING OF ACCRETION EVENTS....413
Penobscottian linkages....413
Taconian linkages....414
Post-Taconian paleogeography....416

TECTONICS OF THE ACADIAN OROGENY....420

PRE-ACADIAN (SILURO-DEVONIAN) IGNEOUS ROCKS....420

AN ANDEAN ANALOG....425

SEQUENCE AND TIMING OF ACADIAN ACCRETION EPISODES....433

ACADIAN DEFORMATION....436

ACADIAN METAMORPHISM....444

SUMMARY AND CONCLUSIONS, PART III....448

SUMMARY: THE MANHATTAN PRONG IN CONTEXT OF APPALACHIAN OROGENIC HISTORY....450

REFERENCES CITED....453

LIST OF TABLES

PART I - GEOLOGY OF PARTS OF THE PEACH LAKE AND BREWSTER QUADRANGLES, SOUTHEASTERN NEW YORK AND ADJACENT CONNECTICUT

page

TABLE 1- Stratigrapic Correlation Chart 10

TABLE 2- Estimated Modal Compositions of Representative Specimens, Fordham Gneiss 23

TABLE 3- Estimated Modal Compositions of Representative Specimens of Ned Mountain Formation and Related Rocks 39

TABLE 4- Chemical Analyses of Precambrian Saprolites and Aluminous Rocks of the Manhattan Prong 77

TABLE 5- Distribution of Rock Types in the Calc-Silicate Member of the Ned Mountain Formation 107

TABLE 6- Estimated Modal Compositions of Representative Specimens, Inwood Marble 140

TABLE 7- Estimated Modal Compositions of Representative Specimens, Walloomsac Schist 146

TABLE 8- Estimated Modal Compositions of Representative Specimens, Manhattan Schist 158

TABLE 9- Estimated Modal Compositions of Representative Specimens, Hartland Formation 164

TABLE 10- Tectonic Development of the Northeastern Manhattan Prong 170

TABLE 11- Principal Features of Deformational Events 172

TABLE 12- Age Constraints on Deformational Events, Northeastern Manhattan Prong. 225

TABLE 13- K-Ar Analytical Data 226

TABLE 14- Samples Used for K-Ar Age Determinations 230

TABLE 15- Microprobe Analyses From a Late-M_1 Assemblage (#966) 283

TABLE 16- Microprobe Analyses From an M_3 Assemblage (#187) 312

PART II - ISOTOPICALLY-DEFINED BASEMENT BLOCKS OF THE NORTH-CENTRAL APPALACHIANS

page

TABLE 17- Isotopic Characteristics of Silurian to Carboniferous Igneous Rocks of the North-Central Appalachians....372

TABLE 18- Isotopic Characteristics of North-Central Appalachian Igneous Rocks, Summarized by Basement Zone....385

PART III - EARLY TO MIDDLE PALEOZOIC ACCRETION HISTORY OF THE BASEMENT BLOCKS OF THE NORTH-CENTRAL APPALACHIANS

TABLE 19- Tectonic Affinities of Pre-Acadian Igneous Rocks, North-Central Appalachians....421

LIST OF PLATES

PLATE I- Geological Map of Parts of the Peach Lake and Brewster Quadrangles, New York and Connecticut....359

PLATE IA- Explanation of Lithologic Units....360

PLATE IB- Explanation of Structural Symbols....360

PLATE IIA- Map Showing Truncation of Fordham Gneiss Lithologies Beneath the Ned Mountain Formation....361

PLATE IIB- Location Map for Transects Examined Outside of the Study Area....361

PLATE IIC- Map Showing Subdivisions of the Ned Mountain Formation....361

PLATE III- Specimen Location Map....362

PLATE IV- Principal Structural Features....363

PLATE V- Geologic Cross Sections....364

PLATE VI- Model for the Taconian Orogeny in the Manhattan Prong....365

LIST OF FIGURES

PART I- GEOLOGY OF PARTS OF THE PEACH LAKE AND BREWSTER QUADRANGLES, SOUTHEASTERN NEW YORK AND ADJACENT CONNECTICUT

page

1. Geologic setting of the Manhattan Prong 5
2. Comparison of minor structures in the Fordham Gneiss (B) with those in the Ned Mountain Formation (A) and the Manhattan and Walloomsac Schists (C) ... 18
3. Attitudes of foliation from neighboring outcrops of the Fordham Gneiss and the Ned Mountain Formation 19
4. Photograph of the orthopyroxene gneiss member of the Fordham Gneiss in outcrop 25
5. Photomicrographs of orthopyroxene gneisses of the Fordham Gneiss (A) and the Hartland Formation (B) 27
6. Photomicrograph of partially retrograded orthopyroxene gneiss of the Fordham Gneiss 28
7. Schematic cross section showing the distribution of the main lithologies of the Ned Mountain Formation 35
8. (A) Photograph of the "diffuse" unconformity zone; (B) photomicrograph of silica-poor lens from the "diffuse" unconformity zone 51
9. Photograph of mafic metasedimentary rocks in outcrop 55
10. Photomicrographs of mafic metasedimentary rocks (A, B, C, D, and E) 56
11. (A, B, C) Photographs of metaconglomerates of the Ned Mountain Formation Basal Member; (D, E) photographs of meta-arkose of the Basal Member 62
12. Photographs of K-rich metasaprolite of the Ned Mountain (A) in outcrop; (B) in hand specimen; (C) photomicrograph 71
13. Composition fields of K-rich metasaprolites compared with those of quartzo-feldspathic metasedimentary and metavolcanic rocks 73
14. Photographs of layered quartzo-feldspathic rocks of the Ned Mountain Formation Volcaniclastic Member, (A) in outcrop and (B) in hand specimen 83
15. Photomicrographs of lineated K-feldspar-quartz gneisses ("felsic metatuffs") of the Ned Mountain Formation (A, B, C, D, E, F, G) 86
16. Photomicrographs of sheared granites (A, B, C) 91
17. Photomicrograph of the Volcaniclastic Member hypersolvus granite 95
18. Photograph of interbedded marble and felsic metatuff, Ned Mountain Formation Calc-Silicate Member 109
19. Feldspar and calc-silicate mineral variations in the Calc-Silicate and Wacke Members, Ned Mountain Formation 114
20. Compositional fields of marbles and calc-silicate rocks of the Calc-Silicate Member of the Ned Mountain Formation, the Walloomsac Schist, and the Inwood Marble 122
21. Photograph of amphibolite dike truncating foliation in the Fordham Gneiss 130
22. Sketch of the environment of deposition of the Ned Mountain Formation Basal Member 132
23. Sketch of the environment of deposition of the Ned Mountain Formation Calc-Silicate Member 134
24. Co-existing mineral assemblages at predominant (M_2) metamorphic conditions in marbles and calc-silicate rocks 142
25. Feldspar and calc-silicate mineral variations in the Walloomsac Schist 151
26. Photograph of the upper Walloomsac Schist in outcrop 153
27. Photographs of high-grade gneisses of the Manhattan Schist (A, B) 157

28. Feldspar and calc-silicate mineral variations in the Manhattan Schist and the Hartland Formation 160
29. Photograph of rhythmically-bedded Hartland Formation in outcrop 166
30. Photomicrograph of granulite-facies L_1 fabric in the Manhattan Schist 176
31. Schematic cross section on the east-west-striking limb of the Pound Ridge antiform 180
32. Hinge lines and slip line on northwest-striking F_2 folds 181
33. (A) Constraints on slip line orientation for east-west, northwest, and north -south striking F_2 folds. (B) Constraints on orientations for planes defined by F_2 slip lines 183
34. Simplified representation of regional F_2 folding 184
35. Photomicrograph of S_3 foliation and F_3 microfolds 188
36. Photograph of a D_3 high-strain zone 189
37. Photomicrograph of F_3 microfolds defined by S_1 sillimanite trains 190
38. F_3 hinge surfaces and hinge lines in relation to some younger structures 192
39. Structure on the north-south striking limb of the Pound Ridge antiform 193
40. Slip line determination for F_3 folds at one site 194
41. F_4 folding on the northwest-striking limb of the Pound Ridge antiform 197
42. Photographs of D_4 structures at the quarry off Mark Mead Road 198
43. Photographs of syn-D_6 granites and retrograded host schist in hand specimen 201
44. Features relating to D_6 deformation and the D_6 tourmaline granite suite, Turkey Hill fault zone 203
45. Photograph of "C-S" texture in granite from the Turkey Hill fault zone 204
46. Photograph of sheared granite dikes in outcrop, Turkey Hill fault zone 204
47. Model for deformation within the Turkey Hill fault zone 206
48. Photograph of a shear zone in the Naraneka fault zone 209
49. Major D6 shear zones in the northeastern Manhattan Prong 211
50. Photographs of a syn-D_6 granite dike in outcrop and related S_6 cleavage 212
51. (A, B) Photographs of S_7 fabrics; (C) photomicrograph of a S_7 fabric 214
52. Photograph of very-fine-grained Ned Mountain Formation Wacke Member and Fordham Gneiss, in contact, along the Windwing thrust 216
53. Attitudes of D_7 shear zones 218
54. Photograph of zoned syn-D_6 pegmatite dike offset by a D_7 thrust 219
55. Distribution of K-Ar and $^{40}Ar/^{39}Ar$ mica ages in the Manhattan Prong 223
56. K-Ar mineral ages in relation to some major structures 228
57. Photomicrograph of an S_6 fabric in a Mississippian granite 247
58. (A) Photomicrograph of inclusions of staurolite, spinel, probable kyanite and rutile in garnet. (B) Photomicrograph of kyanite, spinel, and rutile in garnet 261
59. Photomicrographs of garnet inclusion assemblage #3 (spinel-bearing, aluminosilicate-free) (A, B, C, D) 262
60. Reactions constraining the P-T trajectory of M_1-M_2 metamorphism 265
61. Photomicrographs of the peak-M_1 assemblage quartz + spinel (A, B, C) 268
62. Peak M_1 temperatures from coexisting ternary feldspars 271
63. Photomicrographs of late-M_1 textures in an aluminous lithology (A, B, C) 273
64. Photomicrographs of M_2 textures in aluminous rocks (A, B, C) 278
65. Qualitative changes in the Fe-Ti oxide compositions of late M_1 aluminous assemblages 285
66. Qualitative P-T diagram for K_2O-FeO-MgO-Al_2O_3-SiO_2-H_2O-TiO_2-O_2 (KMASHTO) 287
67. Post-M_2 retrogression of cordierite-bearing assemblages in (A) KFMASH and (B) FMASH 290
68. Photomicrographs of exsolution textures in carbonate minerals (A, B, C, D) 297

69. (A) Photograph of kyanite nodule in hand specimen. (B, C) Photomicrographs of a kyanite nodule....305
70. M_3 assemblages in marbles and calc-silicate rocks....309
71. Hall's (1979) model for the tectonic development of the Manhattan Prong....324
72. Distribution of rift-related Eocambrian felsic volcanic rocks in the Appalachians....336
73. M_1 and M_2 metamorphism in the northeastern Manhattan Prong compared with pressure-temperatures estimates for other Taconian assemblages....338

PART II - ISOTOPICALLY-DEFINED BASEMENT BLOCKS OF THE NORTH-CENTRAL APPALACHIANS

74. Locations of igneous bodies which provide isotopic data....369
75. Map distribution of strontium initial ratios....379
76. Map distribution of Pb compositions of feldspars from Devonian plutons....381
77. Pb-evolution diagram for feldspars from Devonian plutons....382
78. Map distribution of maximum $\delta^{18}O$ compositions of plutonic rocks....384
79. Plot of isotopic compositions against bulk silica content of the igneous rocks....387
80. Map distribution of zircon inheritance ages and Pb or Nd model ages from Paleozoic igneous rocks....390
81. Map of the major stratigraphic subdivisions of the north-central Appalachians....396
82. Stratigraphic criteria used to determine the Central-Avalon supracrustal block boundary....398
83. Map showing geophysical and thermochronological data in relation to the basement blocks....402

PART III - EARLY TO MIDDLE PALEOZOIC ACCRETION HISTORY OF THE BASEMENT BLOCKS OF THE NORTH-CENTRAL APPALACHIANS

84. Comparison of selected stratigraphic features with basement blocks....411
85. Paleobiological and paleomagnetic constraints on the timing of block accretion....415
86. Distribution and character of pre-Acadian igneous rocks....423
87. Distribution and character of Early Tertiary volcanic rocks of the Patagonian Volcanic Province....426
88. Geochemical gradients among North American volcanic rocks....428
89. Comparison of the "indeterminate" rocks of the Appalachians and the Patagonian Andes....430
90. Map distribution of Acadian structural features....435
91. Map-view schematic representation of the Acadian orogeny....438
92. Cross-sectional representation of the Acadian orogeny....440
93. Comparison of the present-day eastern Mediterranean with the proposed Acadian tectonic framework....442
94. Map distribution of Devonian metamorphism and thermal disturbance....445

PART I-

GEOLOGY OF PARTS OF THE PEACH LAKE AND BREWSTER QUADRANGLES, SOUTHEASTERN NEW YORK AND ADJACENT CONNECTICUT

ABSTRACT, Part I

Study of the bedrock geology (stratigraphy, structure, intrusive rocks, and metamorphic history) of the Peach Lake and Brewster quadrangles in the northeastern Manhattan Prong (southeastern New York and adjacent Connecticut) has led to recognition of 1) a new stratigraphic unit (the Ned Mountain Formation) of Eocambrian age and rift-facies origin; 2) four Ordovician (Taconian) and two Carboniferous phases of deformation; 3) a syntectonic suite of two-mica Mississippian granites and albitic pegmatites; 4) early Taconian high-pressure granulite facies metamorphism, overprinted by late-Taconian upper-amphibolite facies assemblages; and 5) Carboniferous greenschist to middle-amphibolite-facies metamorphism.

1) The Ned Mountain Formation consistently crops out between the Grenvillian Fordham Gneiss and the dolomitic, Cambro-Ordovician Inwood Marble, both in the study area and on several transects examined in other portions of the Manhattan Prong. It includes (but is not confined to) rocks previously mapped as Lowerre Quartzite, Pound Ridge granite, and Yonkers granitic gneiss. The Ned Mountain Formation comprises a graphite-rich Basal Member (metabasites, metarkose, metaconglomerate, K-rich metasaprolite, and mafic and felsic metavolcaniclastic rocks), a Volcaniclastic Member (felsic metatuffs, metabasites, and hypabyssal granite), a Wacke Member (metawacke, metarkose, and metabasites), and (at the top) a Calc-Silicate Member (metarkose, calc-silicate rock, marble, felsic metatuff, metabasite).

2) D_1 structures are west-vergent. The North American rocks of the Manhattan Prong were overthrust by the Hartland Formation on a D_1 thrust (Cameron's Line); granulite-facies assemblages compose S_1 fabrics. D_2 structures (a set of major folds), in contrast, are east-vergent. F_2 folds are deformed around the F_3 Pound Ridge antiform, the most prominent structure in the region. D_4 shearing took place on near-horizontal planes. During the first of the Carboniferous events, normal-sense motion occurred within northeast-striking shear zones. This deformation was accompanied by the intrusion of granitic dikes and pegmatites (which had previously yielded

Mississippian Rb-Sr whole-rock isochron ages; Brock, Brueckner, and Brock, 1985) and by widespread retrogression. Shallow-dipping thrusts, with east-directed displacement, cut both the normal-sense shear zones and all older fabrics. Fine-grained, recrystallized micas from fabrics in these late shear zones give K-Ar ages of 309±8 Ma (muscovite) and 294±7 Ma (biotite).

3) The Mississippian two-mica, tourmaline-bearing granites are abundant in many parts of the Manhattan Prong. Contacts of the granites are generally parallel to shortening-related cleavage in normal-sense shear zones. Many of the granites display syntectonic crystallization of muscovite and albite, but C-S textures are rare.

4) Scattered remnants of granulite-facies M_1 assemblages and inclusions in garnets in aluminous rocks record the metamorphic events which accompanied D_1 deformation. A minimum pressure of ~12 kb and minimum temperatures near 900°C are set by the early-M_1 assemblage (hercynitic) spinel + kyanite + garnet + rutile. During peak-M_1 metamorphism, spinel coexisted with quartz; this assemblage locally persists. Textures show that garnet + sillimanite replaced spinel + quartz during late-M_1. Upper-amphibolite-facies M_2 metamorphism later accompanied F_2 and F_3 deformation, and heavily overprinted M_1 assemblages.

5) Greenschist- to middle-amphibolite facies metamorphism accompanied the intrusion of the Mississippian granites. Host rocks contain coarse muscovite and young porphyroblasts of garnet, staurolite, and tourmaline. Kyanite nodules developed near granite dikes. Country rocks located further from the dikes show spotty alteration to muscovite and chlorite.

At the conclusion of Part I, a new synthetic model for the evolution of the Manhattan Prong during the Taconian orogeny is presented.

INTRODUCTION

REGIONAL SETTING

This study focuses on the region located along the New York-Connecticut border in the eastern Peach Lake and southeastern Brewster quadrangles (Fig. 1). This region is principally underlain by rocks of the Manhattan Prong.

The Manhattan Prong is the geologic province lying south of the Grenvillian Hudson Highlands, west of Cambro-Ordovician rocks of the Hartland terrane, and east of the Mesozoic Newark Basin (Fig. 1). The rocks of the Manhattan Prong consist of ancient North American basement (equivalent to the Hudson Highlands) and a sequence of highly metamorphosed cover rocks. These cover rocks have long been correlated with the fossiliferous Cambro-Ordovician sequence of North American affinity found to the north of the Hudson Highlands. The Hartland terrane is considered "exotic" with respect to Cambrian North America, and thought to have been allochthonously emplaced over the Manhattan Prong during the Late Ordovician Taconian orogeny (e.g., Hall and Robinson, 1982; Rodgers, 1985). The trace of the contact between the Manhattan Prong (and correlative units) and the Hartland terrane is known as Cameron's Line (Fig. 1).

The study area is bounded on the north by the Hudson Highlands. It is underlain principally by both the basement and cover rocks of the Manhattan Prong, though a short segment of Cameron's Line and a fragment of the Hartland terrane are present (Plate I).

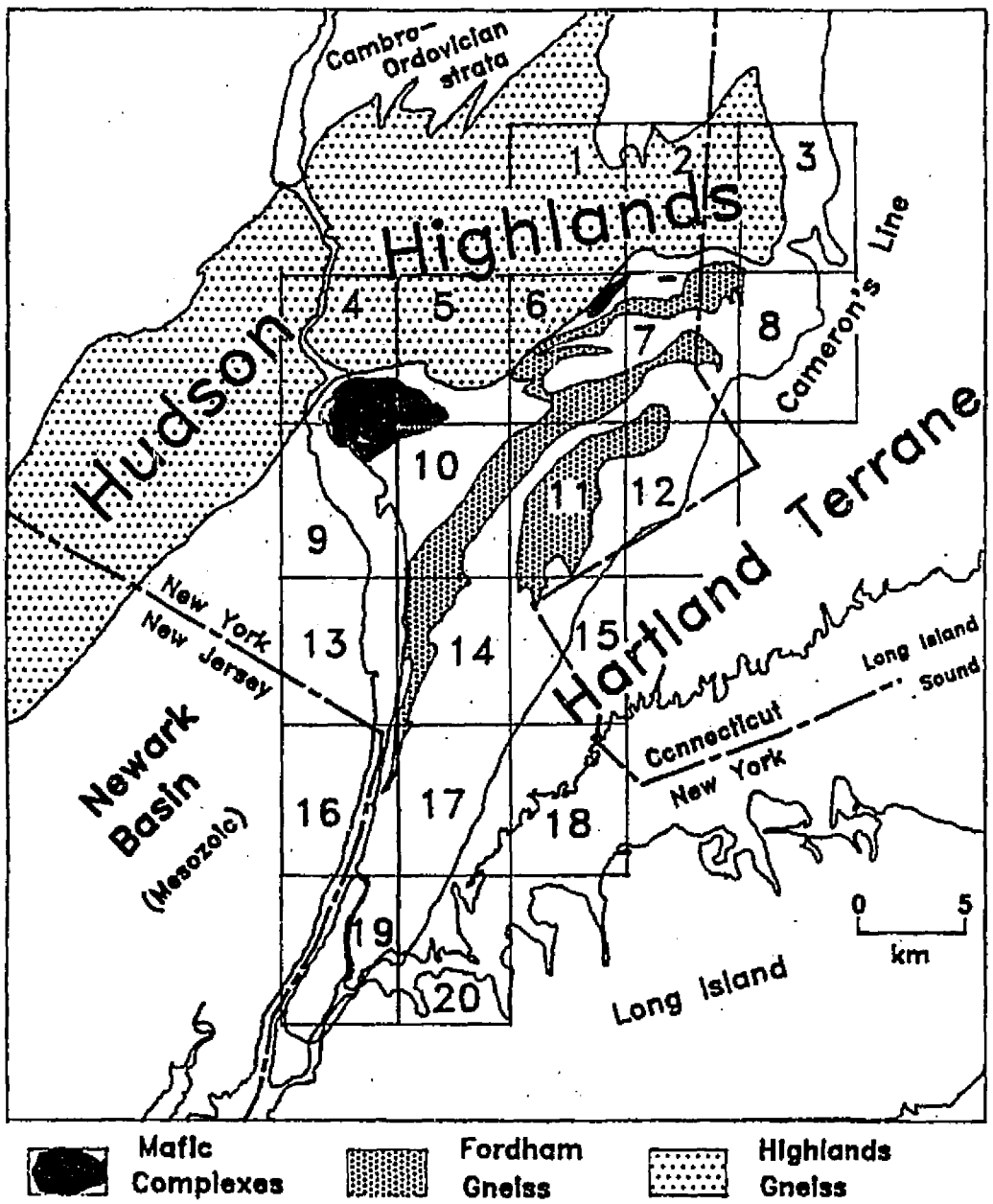

Fig. 1. Geological setting of the Manhattan Prong. Geologic contacts shown here are based on Fisher, Isachsen, and Rickard (1970) and new mapping. The 7'30" topographic quadrangles which cover the Manhattan Prong are listed below.

1 Lake Carmel
2 Brewster
3 Danbury
4 Peekskill
5 Mohegan Lake
6 Croton Falls
7 Peach Lake
8 Bethel
9 Haverstraw
10 Ossining
11 Mount Kisco
12 Pound Ridge
13 Nyack
14 White Plains
15 Glenville
16 Yonkers
17 Mount Vernon
18 Mamaroneck
19 Central Park
20 Flushing

METHODS OF STUDY

My acquaintance with the study area began during the late 1970's. In those early days, my interest focused on the youngest deformational and metamorphic events recorded in the rocks. By 1986, when I chose to study this part of the Manhattan Prong for my thesis, my interest had extended to the basic stratigraphy of the region as well as to its structure and metamorphism. During the present investigation, I have applied the tools of geologic mapping and petrographic study in order to better understand all these areas of interest. These methods were supplemented by limited K-Ar radiometric dating and by a few electron-microprobe analyses.

GEOLOGIC MAPPING. Mapping was carried out at several levels. Initially, the eastern portions of the Peach Lake and Brewster quadrangles were mapped at a 1:24,000 scale. Eventually, in order to address specific geologic problems, mapping was irregularly extended into the central and western portions of the quadrangles. Coverage was not homogeneous: certain critical areas were studied in detail (at 1:1000 or less), while some gaps occurred where access to private property was denied.

The map prepared by Prucha, Scotford, and Sneider (1968), covering the Peach Lake and southern Brewster quadrangles, illustrates the incidence of outcrop in the study area fairly well, although it is generalized, a few outcrops are misplaced, certain outcrops are not shown, and some have disappeared. Lessing (1967) and Brandon (1981) show the distribution of outcrop in parts of the study area with greater precision. No new outcrop map is provided here because the discrepancies with maps by these previous workers are not major. The locations of structure symbols on Plate I give a rough indication of the distribution of the outcrop in the eastern part of the area and delineate the irregular boundary of the study area in the west.

A new stratigraphic unit, the Ned Mountain Formation, was identified in the course of mapping in the study area. After its recognition, the regional continuity of the Ned Mountain

Formation was investigated on a reconnaissance level. Twelve transects, located in four different quadrangles (Croton Falls, Ossining, White Plains, and Mount Vernon), were intensively sampled. The locations of these transects are shown on Plate II. This reconnaissance study indicated that the Ned Mountain Formation is an important stratigraphic unit in the central and southern Manhattan Prong. The lithologic, stratigraphic, and geologic relationships encountered on each transect are briefly described in Appendix 1.

PETROGRAPHIC STUDY. Over 1400 rock specimens were collected for this thesis during the period from the spring of 1986 through the summer of 1991. These rocks were added to an older collection, jointly collected with P. W. G. Brock. In order to facilitate identification of the minerals at the hand-specimen level, many of the specimens were slabbed, etched with HF, and stained for K-feldspar. In addition, over 500 petrographic thin-sections of rocks from Peach Lake and Brewster quadrangles were examined. These were later joined by several hundred thin-sections from other parts of the Manhattan Prong.

Petrographic descriptions. The petrographic descriptions given in the Stratigraphy chapter focus on the minerals present in the predominant metamorphic assemblages. Minerals developed during late, local alteration (such as muscovite, chlorite, and epidote) are indicated in modes of individual samples, where necessary. Mineralogic variations related to metamorphic grade will be discussed in the chapter on metamorphism.

Plagioclase compositions were determined in thin section by measuring extinction angles in grains oriented perpendicular to the x-crystallographic axis. In a few cases, An content was confirmed by determining the refractive indices and extinction angles of crushed grains.

Only fourteen of the thin sections were polished. For the most part, opaque minerals were identified (using both thin sections and crushes) by properties such as color, hardness, crystal form and magnetic susceptibility. It is not possible to positively identify every minute grain by

these methods. As a result, some pyrrhotite-bearing specimens (including those listed on Tables 2, 3, 6, 7, and 8) may contain traces of undetected pyrite.

STRATIGRAPHIC DESCRIPTIONS. This thesis contains the first discussion of the Ned Mountain Formation outside of a field trip guide (Brock, 1989). As a result, special emphasis will be placed on both the description and the interpretation of the Ned Mountain Formation in the Stratigraphy chapter.

Note on stratigraphic thicknesses. The descriptions of the Paleozoic stratigraphic units include estimates of each unit's maximum thickness in the map area. These estimates are based on a combination of the unit's maximum breadth in outcrop and the average dip of layering. These estimates have only a remote relationship to original stratigraphic thicknesses because of a) repetitions of beds by folding, b) thinning of beds on fold limbs, and c) truncation of some units by faults. These estimates, inadequate as they are, grossly constrain the thickness of the newly-described Ned Mountain Formation and permit comparison of its thickness, on a relative scale, with thicknesses of better-known Paleozoic units such as the Inwood Marble.

STRATIGRAPHY

PREVIOUS WORK

Early workers in the Manhattan Prong (including Gale, 1839; Mather, 1839, 1843; and Dana, 1880) recognized that the region is underlain by a few lithologic types (such as gneiss, mica schist, and "limestone") which locally occur in traceable belts. Merrill (1890, 1896) defined and named the formations that have been in use ever since: the Fordham Gneiss, the Yonkers Gneiss, the Lowerre Quartzite, the Inwood Marble, and the Manhattan Schist.

In Merrill's original (1890) conception, the Yonkers Gneiss was described as an "arkose gneiss" and identified as the basal member of a Paleozoic sequence thought to unconformably overlie an unexposed, Precambrian basement. Stratigraphically higher portions of this sequence consisted of the Fordham Gneiss, Inwood Marble, and finally the Manhattan Schist. Merrill, like Mather and Dana before him, regarded the rocks of the "Manhattan group" as metamorphosed equivalents of the fossil-bearing Cambro-Ordovician sequence that overlies the Hudson Highlands in Dutchess County (Fig. 1; Table 1).

In 1896 Merrill reversed himself by placing the Yonkers Gneiss and Fordham Gneiss in the Precambrian, and recognizing the newly-defined Lowerre Quartzite instead as the base of the overlying Paleozoic section. The Yonkers Gneiss was now interpreted as a intrusive granite within the Fordham. Some workers, however, preferred a Precambrian age for the entire Manhattan Prong (Berkey, 1907, p. 377). Little direct evidence on stratigraphic relationships was available from the metamorphic rocks of the Prong, and their ages and affinities remained controversial for several decades. During the twentieth century, concepts of stratigraphic relationships have continued to evolve as evidence has continued to accumulate.

TABLE 1. Stratigraphic Correlation Chart

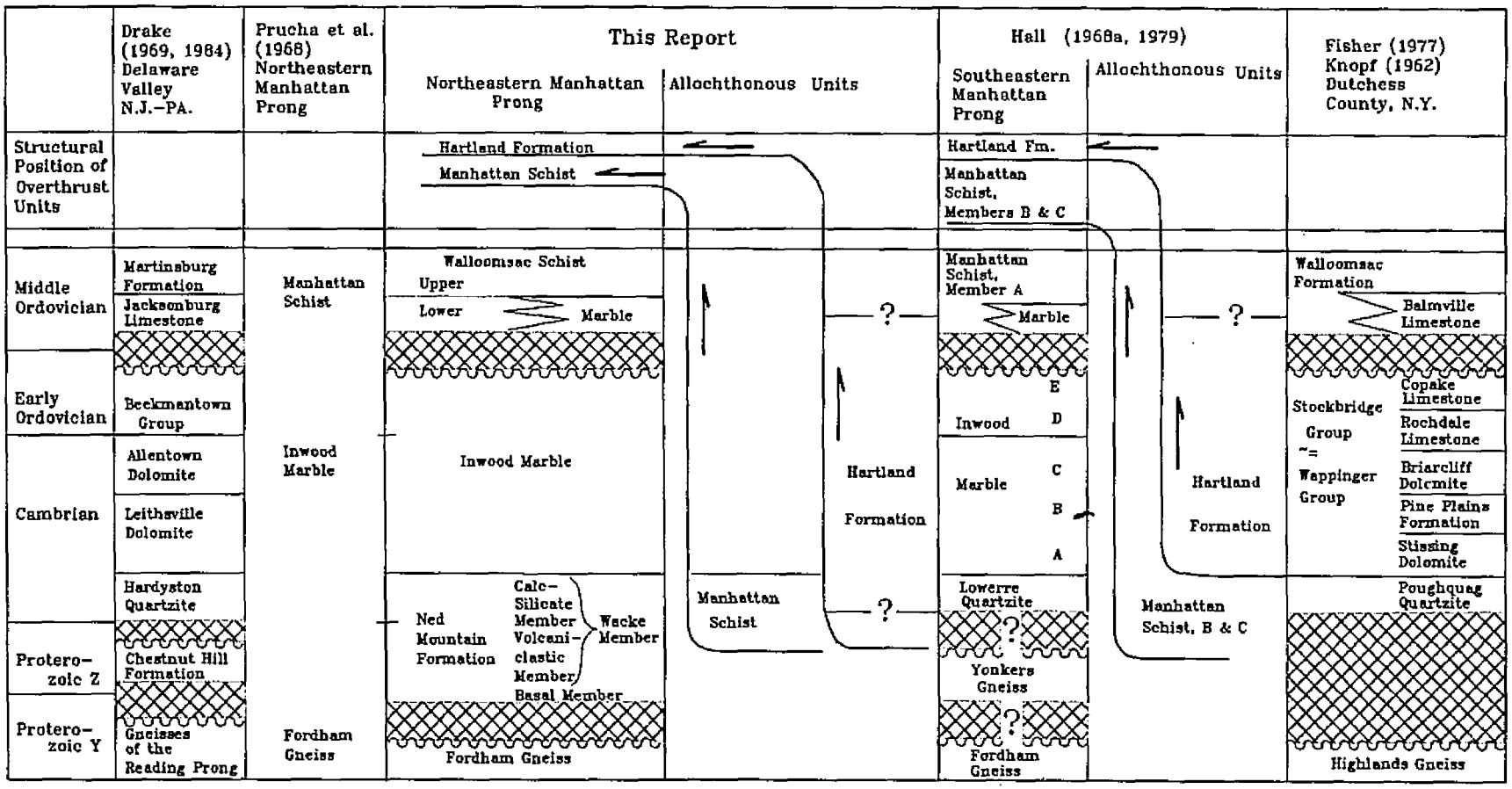

Fordham Gneiss. The Precambrian (Grenvillian) age of the Fordham Gneiss has been substantiated by both geochronological and stratigraphic studies during the past thirty years. Hall (1968a, b) subdivided the Fordham Gneiss in the White Plains quadrangle, and mapped truncation of his Fordham members beneath the Lowerre-Inwood-Manhattan sequence. Grauert and Hall (1973) documented the presence of 1.0 Ga and older zircons in the Fordham Gneiss. Subsequently, Mose (1982) obtained Grenvillian or older Rb-Sr whole-rock ages on several samples of Fordham Gneiss. Recently, a population of abraded zircons from Hall's Fordham Member C have yielded an 1170 Ma U-Pb age, indicating that the intrusion of its igneous protolith probably occurred at that time (Aleinikoff, 1985).

Yonkers Gneiss. Hall (1968a, b) originally considered the Yonkers granitic gneiss as part of the basement complex, conformable with the members of the Fordham Gneiss. Subsequent radiometric studies, however, have indicated that the Yonkers Gneiss is post-Grenvillian in age. Rb-Sr whole-rock isochron ages of 563±30 Ma* (Long, 1969) and 530±43 Ma (Mose, 1981) have been obtained on the Yonkers Gneiss. In addition, a study of zircons from the Manhattan Prong shows that the Yonkers Gneiss first crystallized during Cambrian time. For their study, Grauert and Hall (1973) separated zircons from the Fordham Gneiss, Yonkers Gneiss, Lowerre Quartzite, and Manhattan Schist. Zircons from the Fordham, Lowerre, and Manhattan gave similar ranges of Middle Proterozoic ages, but zircons from the Yonkers Gneiss yielded a nearly concordant 515 Ma age. The sampled Lowerre and Manhattan rocks were composed of recrystallized detrital sediments, and the Proterozoic zircon ages yielded support a Grenvillian sedimentary provenance. The nearly concordant Cambrian age of the Yonkers Gneiss, however, indicates that it originated as a post-Grenvillian igneous body.

* Rb-Sr ages in this thesis are based on a decay constant for ^{87}Rb of 1.42×10^{-11}/yr. K-Ar ages are calculated using decay constants of 4.962×10^{-10}/yr and 0.581×10^{-10}/yr for ^{40}K, and an $^{40}Ar/^{36}Ar$ atmospheric ratio = 295.5, as recommended by Steiger and Jäger (1977).

Hall's interpretation of field relationships evolved in concert with the geochronological evidence. In 1979, Hall described the lithologies of the Fordham Gneiss as truncated against the Yonkers Gneiss, instead of in conformable contact with it.

Pound Ridge granite. Although the Yonkers Gneiss is confined to the southern Manhattan Prong, a similar body of granitic gneiss is present in the Peach Lake and Pound Ridge quadrangles in the northeastern Manhattan Prong. Bell (1936) named this unit the Pound Ridge granite. As mapped by Scotford (1956), the Pound Ridge granite crops out in a belt at the top of the Fordham Gneiss, its contacts oriented nearly parallel to those of the nearby Inwood Marble (Plate IIB). The Yonkers Gneiss occurs in the same manner in the southern Prong (Plate IIB). In 1975, Mose and Hayes reported a 579±21 Ma Rb-Sr whole-rock isochron age for the Pound Ridge granite. This established that the Pound Ridge granite and Yonkers Gneiss have the same Rb-Sr age, within experimental error.

Inwood Marble and Manhattan Schist. The correlation of the Inwood Marble and Manhattan Schist with the Cambro-Ordovician rocks north of the Hudson Highlands (the Wappinger Group and Walloomsac Formation, Table 1) was expanded and clarified by Hall (1968a, b) and by Ratcliffe and Knowles (1969). Hall subdivided the Inwood Marble into a number of units, and then determined that these units are truncated beneath the Manhattan Schist on map scale. Hall attributed this truncation to the early Middle Ordovician unconformity that cuts across Cambro-Ordovician carbonate sequences throughout the region.

Hall (1968 a, b, c) also subdivided the Manhattan Schist. He correlated the lower Manhattan ("A") with two units of Middle Ordovician age, the Balmville Limestone and the Walloomsac Formation. These units occur above the Middle Ordovician unconformity that truncates the Cambro-Ordovician Wappinger Group carbonates in Dutchess County (Table I). Ratcliffe and Knowles (1969) discovered pelmatazoan fossils in a marble at the base of the Manhattan Schist,

thus supporting an Early Paleozoic age for Hall's Manhattan A. These pelmatazoan fragments are the only fossils that have ever been found in the Manhattan Prong; they are located on east side of the Hudson River near the Cortlandt Mafic Complex (Fig. 1).

Hall considered the upper Manhattan Schist ("B, C") to be a distinct stratigraphic unit. He noted lithologic similarities between the upper Manhattan Schist and the Waramaug Formation, a unit locally in contact with Precambrian basement in Connecticut (Rodgers, Gates, and Rosenfeld, 1959). Hall (1968a) suggested that Manhattan B and C consist of Cambrian rocks that had been emplaced over the Ordovician Manhattan A early in the Taconian orogeny; Manhattan B and C were therefore analogous to the Taconic allochthons of upstate New York. A Cambrian Rb-Sr whole-rock age on a sample of Manhattan C (Mose and Merguerian, 1985) has given some geochronological support to Hall's stratigraphic arguments.

In the present study, to avoid confusion, nomenclature will follow the usage on the Geologic Map of Connecticut (Rodgers, 1985). "Walloomsac Schist" will refer to the Early Paleozoic unit that Hall designated "Manhattan A"; "Manhattan Schist" will refer exclusively to Hall's Manhattan B and C (Plate IA).

Lowerre Quartzite. Although all workers in the Manhattan Prong have found the Fordham Gneiss, Yonkers Gneiss, Inwood Marble, and Manhattan Schist (and their subdivisions) to be useful stratigraphic units, controversy has surrounded the Lowerre Quartzite. Several workers have proposed that the Lowerre Quartzite correlates with the Poughquag Quartzite, the basal Cambrian sandstone that unconformably overlies Grenvillian basement gneisses in Dutchess County. In Dutchess County, in contrast to the Manhattan Prong, distinct discordance is commonly evident between the basement gneiss and basal quartzite (Balk, 1936). Over the years, a variety of objections have been raised to the proposed Lowerre-Poughquag correlation:

1) The stratigraphic position of the "Lowerre" did not seem constant with respect to other units. Berkey (1907, 1911) observed that the "Lowerre Quartzite" seemed to belong with the

Inwood-Manhattan sequence in some places, and with the basement gneisses in others.

2) Exposures ascribed to the "Lowerre Quartzite" were so rare that some workers doubted that they could comprise a stratigraphically valid unit. When Fluhr examined the excavations made for the Delaware aqueduct, he failed to find any trace of "Lowerre" at Fordham-Inwood contacts. He concluded that "Lowerre" did not exist (Fluhr, 1950, 1969). Some workers in the Croton Falls and Peach Lake quadrangles in the northeastern Manhattan Prong likewise recognized no "Lowerre" at the prescribed stratigraphic position (Scotford, 1956; Prucha, 1956, 1959; and Prucha, Scotford, and Sneider, 1968).

3) Several workers rejected an unconformity because they observed relationships which indicated a gradational contact between the "Lowerre" and the adjacent Fordham Gneiss. For instance, Berkey and Rice (1921) failed to see signs of unconformity. Fluhr and Bird (1939) described a "pebbly quartzite" which seemed to grade into sheared granite and then into gneiss. Prucha (1956) argued that the "Lowerre Quartzite" was merely a sheared portion of the Fordham Gneiss.

4) Some workers concluded that the Inwood Marble and the Fordham Gneiss comprise a conformable sequence. Scotford (1956), Prucha, Scotford, and Sneider, (1968), Wissig (1970), and Prucha (1956, 1959) observed interbedding of marble and gneissose rocks near the contact between the Fordham Gneiss and Inwood Marble. Prucha (1956, 1959), Scotford (1956) and Prucha, Scotford, and Sneider (1968) argued that the Fordham Gneiss and Inwood Marble could not be correlated with the Highlands Gneiss and its unconformably overlying Wappinger Group sedimentary cover.

On the other hand, Norton (1959), Norton and Giese (1957), Wissig (1970), Ratcliffe (1968), Hall (1968 a, b, c), Hall's students (e.g., Alavi, 1976; Brandon, 1981; Jackson and Hall, 1982), and Whiting-Goldberg (1977) judged the "Lowerre Quartzite" to be stratigraphically valid. They documented sparse occurrences of K-feldspar-rich quartzite below the Inwood Marble. Hall (1968b) extended recognition of "Lowerre" lithologies to a quartz-muscovite schist, which he

placed at the base of the unit. This schist was distinguished by the presence of sillimanite nodules, or bumpy-weathering clots of quartz containing fibrolitic sillimanite.

RESOLUTION OF THE STRATIGRAPHIC CONFLICT

A new perspective on this old stratigraphic controversy has emerged from the present study of the northeastern Manhattan Prong. A distinctive and hitherto unrecognized suite of rocks has been found between Grenvillian rocks of the Fordham Gneiss and the Cambro-Ordovician Inwood Marble. This suite of rocks occupies the stratigraphic position postulated for the "Lowerre Quartzite", but in the northeastern Manhattan Prong, quartzite comprises less than 1% of the unit. Instead, the suite is dominated by compositionally diverse metasedimentary and metaigneous rocks, many of which have been previously mapped as Fordham Gneiss, Pound Ridge granite, Inwood Marble, or Manhattan Schist (Scotford, 1956; Lessing, 1967; Prucha, Scotford, and Sneider, 1968; Brandon, 1981). The unit is here (informally) named the Ned Mountain Formation, after a large hill near Ridgebury, Connecticut (Plate III), where it crops out extensively. After the existence of the Ned Mountain Formation was established in the Peach Lake and Brewster quadrangles, a reconnaissance study revealed that the Ned Mountain Formation is also present in the Croton Falls, Ossining, White Plains, and Mount Vernon quadrangles. The transects studied in these quadrangles are shown on Plate II.

The question that naturally arises is, by what means was this unit distinguished now, after more than a hundred years of geological investigation of the Manhattan Prong? The answer to this question largely resides in the extensive and detailed petrographic studies carried out for this project. These studies have led to a recognition of several distinctive lithologic suites that persistently occur at the top of the "Fordham Gneiss", lithologic suites that are now separated out as Ned Mountain Formation. The suites include a number of previously unreported rock types.

The Ned Mountain Formation and the Fordham Gneiss each contain a range of metaigneous and metasedimentary rocks. The fact that two such lithologically complex units are in direct contact with each other had long militated against the realization that they are stratigraphically distinct entities. For as long as identification of lithology was based on studies in the field, the distinctive and persistent character of the Ned Mountain rock suites went unnoticed. Resemblances between certain Ned Mountain rock suites and the Paleozoic units added to the confusion.

Now, however, petrographic examination has demonstrated profound differences Ned Mountain lithologies and "look-alike" rocks of the Fordham Gneiss, Inwood Marble, and Walloomsac Schist. For example, staining of hand specimens and thin-section study has revealed that certain light-colored biotite-garnet gneisses and schists have unusual, extremely K-feldspar-rich modal compositions. Other well-bedded, graphitic, garnet-biotite schists and gneisses (some previously mapped as sillimanite schist) have instead proved to be mafic rocks rich in cummingtonite and orthoamphibole. Both these rock types are now known to be characteristic Ned Mountain lithologies.

Once the distincitive Ned Mountain lithologies and suites were distinguished in the lab, it became posssible to recognize them in outcrop and to map the Ned Mountain Formation in the field with reasonable confidence. Now, with the recognition of the Ned Mountain Formation, the geologist faces rocks in the field with a more realistic grasp of their possible compositions, though confirmation by thin-section study is still required in many cases.

MAJOR LINES OF EVIDENCE FOR THE NED MOUNTAIN FORMATION. Evidence for Ned Mountain Formation as a discrete stratigraphic entity comes from a number of sources: lithologic, structural, geochronological, and metamorphic. Map-scale relationships between the Ned Mountain Formation and other units offer some of the strongest support. Certain points will be discussed in detail later in the text; here, the evidence can be summarized as

follows:

1) The Ned Mountain Formation maintains a constant stratigraphic position between the Fordham Gneiss and Inwood Marble both in the study area and elsewhere in the Manhattan Prong (Plates I & II);

2) Mappable lithologic units in the Fordham Gneiss are truncated against the base of the Ned Mountain Formation, both in the study area and elsewhere in the Manhattan Prong (Plates I & IIA);

3) Distinctive Ned Mountain lithologies persist over long distances, stratigraphically above the truncated units of the Fordham Gneiss (Plates I & IIC);

4) Minor structures in adjacent belts of Ned Mountain Formation, Walloomsac Schist and Manhattan Schist display the same gross patterns (Fig. 2A and 2B). In contrast, attitudes of minor structures in the Fordham Gneiss can significantly diverge from those in overlying Paleozoic rocks (Fig 2C). In addition, a small but systematic discrepancy can be noted between the attitudes of foliations in the Fordham Gneiss and in the Ned Mountain Formation, at those few localities where the abundance of outcrop and simplicity of structure permit resolution of the discrepancy (Fig. 3);

5) Pronounced differences in texture, layering, and metamorphic grade exist between the Ned Mountain Formation and the Fordham Gneiss. The Grenvillian heritage of the Fordham Gneiss is manifested by its coarse-grained, commonly lineated texture and poorly developed foliation. Pyroxene and amphibole are relatively abundant in the Fordham, and biotite is generally minor. In the Peach Lake quadrangle, the Fordham Gneiss shows no recognizable bedding and may be entirely metaplutonic. In contrast, foliation is prominent in the medium-grained, well-bedded metasedimentary and metavolcanic rocks of the Ned Mountain Formation. Furthermore, relict granulite-facies mineral assemblages are observed in the Fordham Gneiss at localities scattered through most of the Manhattan Prong. In contrast, the Paleozoic Walloomsac and Manhattan Schists are restricted to middle- to upper-amphibolite grade assemblages in the western

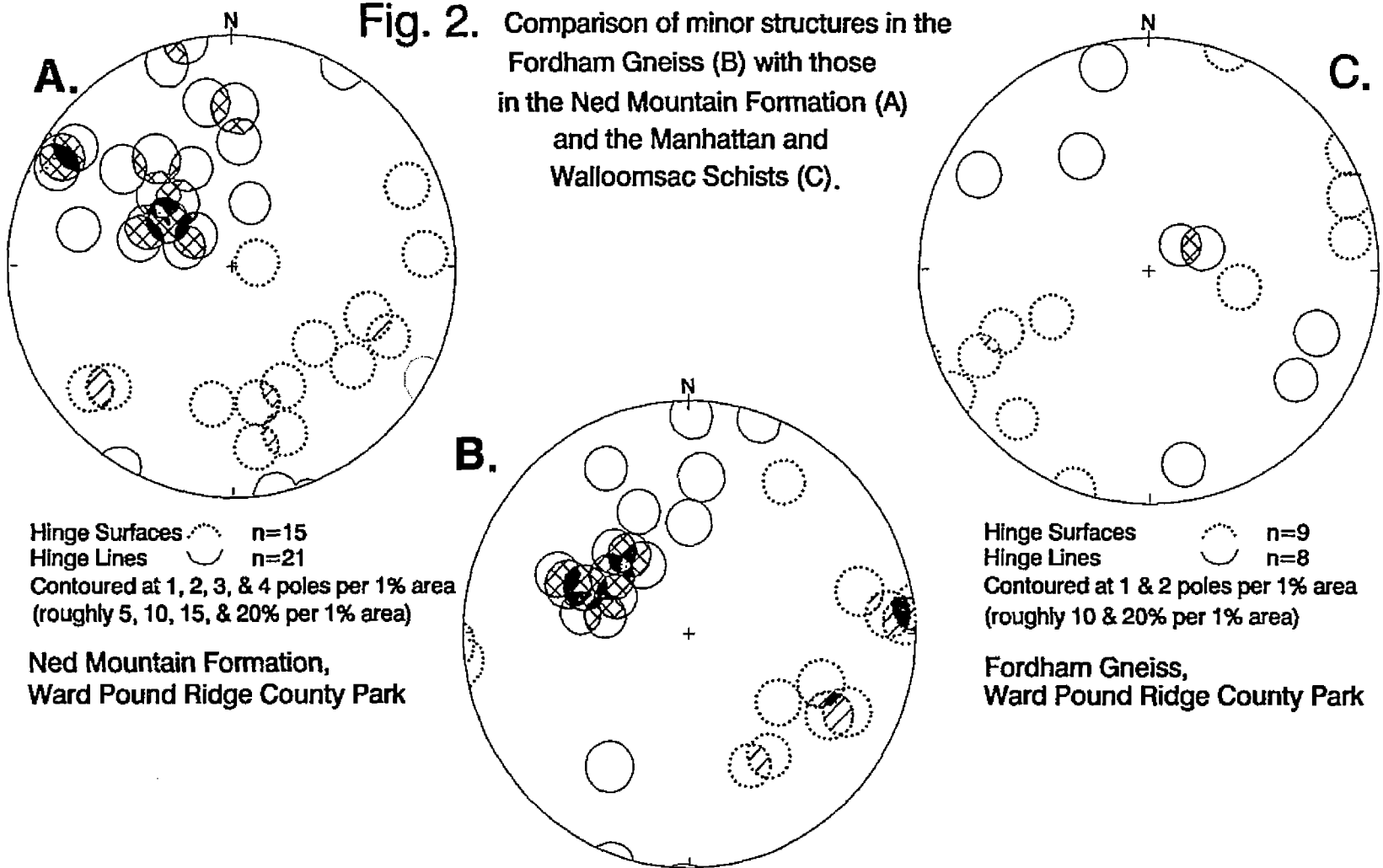

Fig. 2. Comparison of minor structures in the Fordham Gneiss (B) with those in the Ned Mountain Formation (A) and the Manhattan and Walloomsac Schists (C).

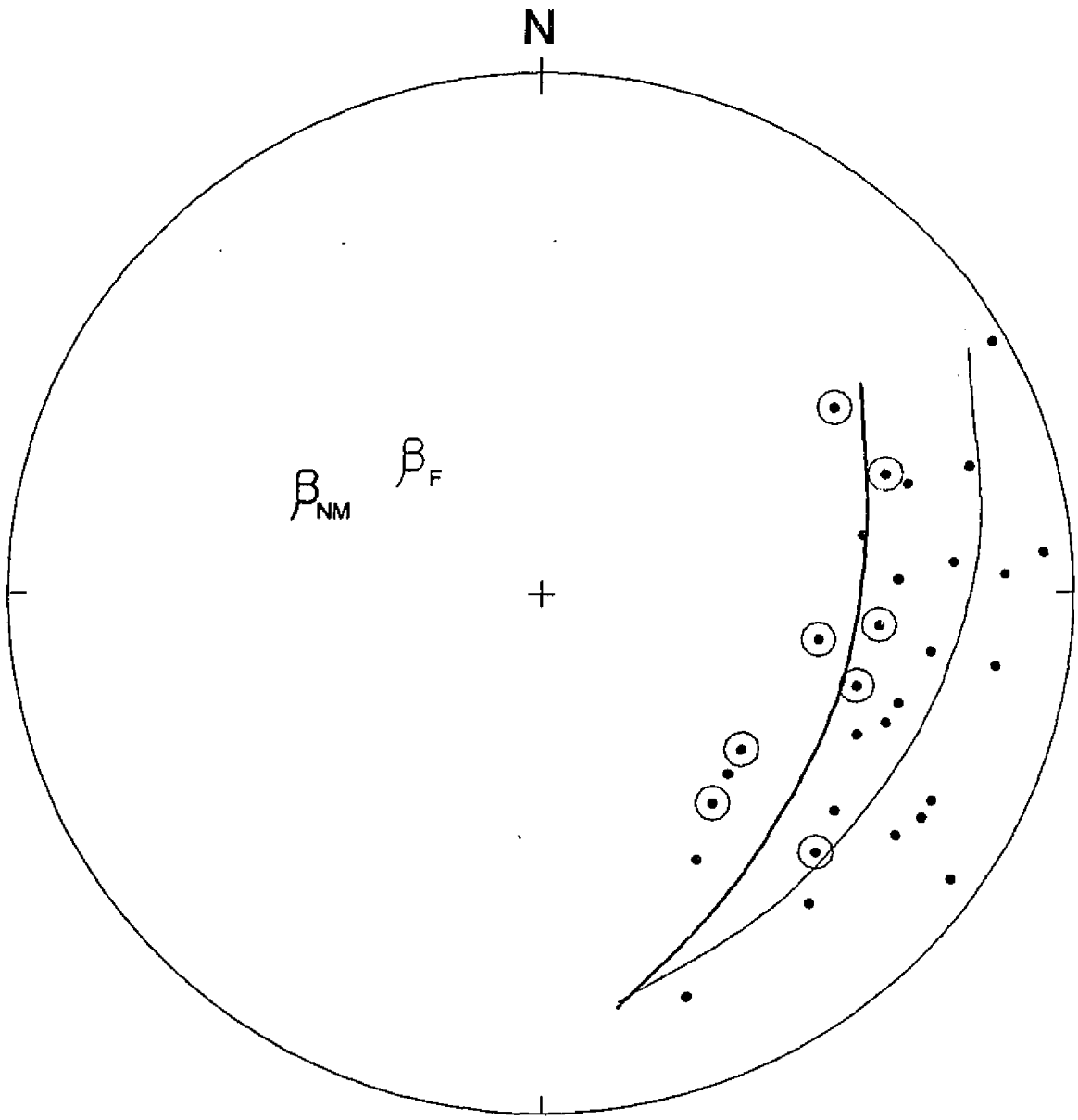

⊙ Poles to foliation, Basal Member, Ned Mountain Formation (NM)

• Poles to foliation, Fordham Gneiss (F)

β Beta Pole

Fig. 3. Attitudes of foliation from neighboring outcrops of the Fordham Gneiss and the Ned Mountain Formation between Lake Windwing and Ned Mountain Road.

portions of the Prong. The mineral assemblages in the Ned Mountain Formation everywhere reflect the same metamorphic conditions as those recorded by nearby Paleozoic units.

6) The Inwood Marble may well conformably (or paraconformably) overlie the Ned Mountain Formation in parts of the Peach Lake quadrangle. Calc-silicate rocks and calcareous marble are present near the top of the Ned Mountain Formation, which is overlain by dolomitic marble of the Inwood.

7) Geochronological evidence (discussed above) indicates that primary crystallization of the Yonkers Gneiss and Pound Ridge granite occurred during Cambrian time. These units are now interpreted to lie within the Ned Mountain Formation, and are thought to consist largely of metarhyolite flows or tuffs (with at least one hypabyssal intrusive body). The geochronological ages of the Yonkers Gneiss and Pound Ridge granite are consistent with their stratigraphic positions beneath the Cambro-Ordovician carbonate sequence.

8) The Ned Mountain Formation has several lithologic assemblages in common with equivalent Eocambrian sequences elsewhere in the Appalachians. For instance, amphibolite and feldspar-quartz gneisses (interpreted as metarhyolite) are abundant in the Ned Mountain Formation; bimodal metavolcanic rocks occur in Eocambrian sequences in Newfoundland (Williams, Gillespie, and Van Breemen, 1985), Quebec (Kumarapeli and others, 1989), Pennsylvania (Rankin, 1975), and Virginia (Rankin, 1975). Metawackes (once clay-rich sandstones) dominate part of the Ned Mountain Formation, and comparable rocks are abundant in many Eocambrian sequences. Other common Ned Mountain lithologies, such as calc-silicate rock, marble, and quartz-feldspar granofelses, are all known from Eocambrian sequences elsewhere.

The new evidence indicates that both sides in the controversy over the Lowerre Quartzite had perceived parts of a complex reality. Those who believed in the validity of the Lowerre Quartzite as a stratigraphic unit correctly interpreted the Fordham Gneiss to be Grenvillian in age, and the Inwood-Walloomsac sequence to be Cambro-Ordovician. They correctly observed that a "quartzite" is locally present just below the Inwood Marble in parts of the Manhattan

Prong. Those opposed to the concept of the Lowerre correctly observed that the "quartzite" is generally very K-feldspar rich and at some places seems to grade into rocks of granitic composition. Berkey (1911) accurately noted that quartzites are sometimes within the "Fordham Gneiss"; rare quartzites are present deep in the Ned Mountain section. Scotford (1956) and Prucha, Scotford, and Sneider (1968) reported the very real interlayering of marble and "gneiss" (amphibolite, feldspar-quartz gneiss) beneath the Inwood Marble in the Peach Lake quadrangle. They may well have been correct in inferring a conformable contact between this sequence and the overlying Inwood. (They were mistaken in considering the interbedded marbles as themselves part of the Inwood, however).

These apparently conflicting observations fit comfortably together in the light of the Ned Mountain Formation. I am not the first to propose such a solution; in 1968, at the Symposium on the New York City Group of Formations held at Queens College, John Rodgers and E-an Zen presciently suggested that a pre-Lowerre Eocambrian sequence might unconformably overlie the Fordham Gneiss. No geologist active in the Manhattan Prong at that time adopted this idea, however.

One possibly troublesome question of nomenclature still remains: is there any Fordham Gneiss in Fordham Heights? Merrill described a number of "gneiss" localities in his original 1890 paper, localities which cover occurrences of both the Grenvillian basement gneisses and the Ned Mountain Formation. However, he chose to name the formation after Fordham Heights in the Bronx. I have yet to examine the rocks in that area, and cannot predict whether any rocks of Grenvillian age will be found. I have maintained the name Fordham Gneiss for the Grenvillian basement because this usage is deeply entrenched in the geologic literature.

FORDHAM GNEISS

Six members of the Fordham Gneiss are recognized in the study area: orthopyroxene gneiss, clinopyroxene-garnet gneiss, plagioclase-hornblende gneiss, K-feldspar-hornblende gneiss, amphibolite, and granitic gneiss. Representative estimated modal compositions for each member are given on Table 2.

ORTHOPYROXENE GNEISS MEMBER. The orthopyroxene gneiss member is made up of interlayered leuco- to mesocratic coarse-grained gneisses. Compositional layers tend to be 1 to 5 centimeters thick. The appearance of this unit in the field is variable. Many leucocratic layers develop a waxy yellow or beige cast with weathering, while some portions of the gneiss are dark grey when fresh, but weather to a chalky white. Biotites generally appear deep red in hand specimen, with a bright, almost metallic luster. Cross-cutting dikes of orthopyroxene-bearing granite, usually 10 centimeters to 2 meters in thickness, are present at some localities (Fig. 4).

The mesocratic layers of the gneiss contain 25 to 55 modal % mafic minerals (generally orthopyroxene, hornblende, and biotite, ±clinopyroxene), together with plagioclase, quartz, and locally K-feldspar. Layers of leucocratic composition are abundant. They consist of ~85 modal % quartz and feldspar, with ~15% mafic minerals. A trace of garnet may also be present. Thin darker layers containing up to 65% mafic minerals (predominantly hornblende), can also occur.

Granulite-facies assemblages such as orthopyroxene + K-feldspar or orthopyroxene + clinopyroxene occur in this unit throughout the study area. The hornblende is olive-colored in thin section; biotite is dark brown or deep red-brown. The anorthite content of plagioclases ranges from An_{24} to An_{44}. Ilmenite is generally the dominant opaque mineral. A strong lineation is locally defined by orthopyroxene grains, but generally there is little preferred orientation of minerals. Some plagioclase and biotite grains have tabular or platy shapes.

The characteristic coarse-grained texture of this unit (Fig. 5A) suggests that it experienced

TABLE 2

Estimated Modal Compositions of Representative Specimens, Fordham Gneiss *

	Orthopyroxene Gneiss Member				Garnet-Clinopyroxene Gneiss Member			Plagioclase-Hornblende Gneiss Member			K-feldspar-Hornblende Gneiss Member			Amphibolite Member				Granitic Gneiss Member		
Specimen Layer	1315	1643 dark	1643 light	1725b	1678c red	1678c red/green	UC-6	1282	1284	1666	1262	1548	1704	1509 dark	1509 light	1537	1670	1555	1559	Specimen Layer
Quartz	3	5	44	34	-	tr.	-	17	25	27	25	12	20	8	20	15	4	28	25	Quartz
Plagioclase	37	28	33	29	17	10	5	33	46	38	10	30	25	28	62	34	23	28	38	Plagioclase
(% anorthite)	(32)	(44)	(33)	(24)	(70)	(80)	(bytown)	(39)	(35)	(46)	(28)	(34)	(33)	(30)	(32)	(34)	(65)	(28)	(27)	(% anorthite)
K-feldspar	28	tr.	1	-	-	19	-	-	-	-	33	10	35	-	-	-	-	25	27	K-feldspar
Hypersthene	5	10	15	20	tr.	-	-	-	-	-	-	-	-	-	-	-	4	-	-	Hypersthene
Augite	-	8	2	-	12	tr.	91	-	-	8	1	13	8	3	-	-	-	-	-	Augite
Hornblende	18	45	1	1	-	37	3	48	20	25	23	18	11	48	5	40	56	3	-	Hornblende
Cummingtonite	-	-	-	6	-	-	-	tr.	-	-	-	-	-	-	-	-	5	-	-	Cummingtonite
Biotite	6	2	2	9	-	4	tr.	tr.	8	-	6	7	tr.	12	10	10	5	12	7	Biotite
Garnet	tr.	-	-	tr.	65	29	-	-	-	-	-	-	-	-	-	tr.	-	-	-	Garnet
Apatite	tr.	-	tr.	tr.	2	tr.	tr.	tr.	tr.	tr.	tr.	4	tr.	tr.	tr.	tr.	tr.	tr.	tr.	Apatite
Zircon	tr.	-	tr.	-	-	-	-	tr.	-	-	tr.	tr.	-	-	tr.	-	-	-	tr.	Zircon
Magnetite	1	tr.	tr.	tr.	tr.	-	-	1	tr.	2	2	4	tr.	tr.	tr.	tr.	tr.	3	3	Magnetite
Ilmenite	1	1	1	1	4	1	-	1	tr.	tr.	tr.	2	tr.	1	tr.	1	3	1	tr.	Ilmenite
Pyrrhotite	tr.	-	-	tr.	-	-	-	tr.	-	-	-	tr.	1	-	-	-	tr.	-	tr.	Pyrrhotite
Sphene	-	-	-	-	-	tr.	1	tr.	-	-	tr.	tr.	-	tr.	tr.	-	-	tr.	-	Sphene
Allanite	-	-	-	-	-	-	-	-	-	-	tr.	tr.	-	tr.	tr.	-	-	tr.	tr.	Allanite
Chlorite	-	-	-	-	-	-	-	-	-	tr.	-	-	tr.	tr.	2	-	-	-	tr.	Chlorite
Calcite	-	-	-	-	-	-	tr.	-	-	-	-	-	-	-	-	-	-	-	-	Calcite

* Brief descriptions of these specimens appear on the following page.

TABLE 2, CONTINUED

Notes: 1. Specimen locations are shown on Plate III. **2. The color of the specimen's weathered surface** is specified only where it contrasts with the overall color of the rock.

Orthopyroxene Gneiss Member

1315. Medium- to coarse-grained, unfoliated, grey-green layered gneiss. (Southern Brewster quadrangle)
1643. Medium-grained, unfoliated, beige-and-black layered gneiss. (Northeastern Peach Lake quadrangle)
1725b. Medium-grained, well-foliated, grey-and-white banded gneiss, with discontinuous biotite-rich folia. (Central Peach Lake quadrangle)

Garnet-Clinopyroxene Gneiss Member

1678c. Medium- to coarse-grained, green, red, and black multicolored gneiss. Red (garnet-rich) bands are discontinuous and are cross-cut by dark coarse-grained hornblende. (Southern Brewster quadrangle)
UC-6. Coarse-grained, grey-and-white weathering, unfoliated, dark grey-green clinopyroxene gneiss. (Southern Brewster quadrangle)

Plagioclase-hornblende Gneiss Member

1282. Medium-grained, poorly foliated, dark grey hornblende gneiss. (Northern Peach Lake quadrangle)
1284. Medium-grained, black-and-white thin-layered gneiss. (Northern Peach Lake quadrangle)
1666. Medium-grained, dark grey-green and white banded gneiss. (Northern Peach Lake quadrangle)

K-feldspar-hornblende Gneiss Member

1262. Medium-grained, unfoliated, black-and-white gneiss with a coarse, heterogeneous (blotchy) texture. (Northern Peach Lake quadrangle)
1548. Medium-grained, unfoliated (though slightly lineated), black-, white-, and grey- gneiss. (Central Peach Lake quadrangle)
1704. Coarse-grained, poorly layered, white-, black- and olive- gneiss. (Southern Brewster quadrangle)

Amphibolite Member

1509. Medium-grained, dark, amphibolitic gneiss. (Southwestern Peach Lake quadrangle)
1537. Medium-grained, well-lineated, black-and-white amphibolitic gneiss. (East-central Peach Lake quadrangle)
1670. Medium-grained, dark amphibolitic gneiss, with porphyroblasts of hypersthene. (Northeastern Peach Lake quadrangle)

Granitic Gneiss Member

1555. Medium-grained, lineated, white-and-black granitic gneiss. (Central Peach Lake quadrangle)
1559. Medium-grained, slightly foliated, beige-and-black granitic gneiss. (Central Peach Lake quadrangle)

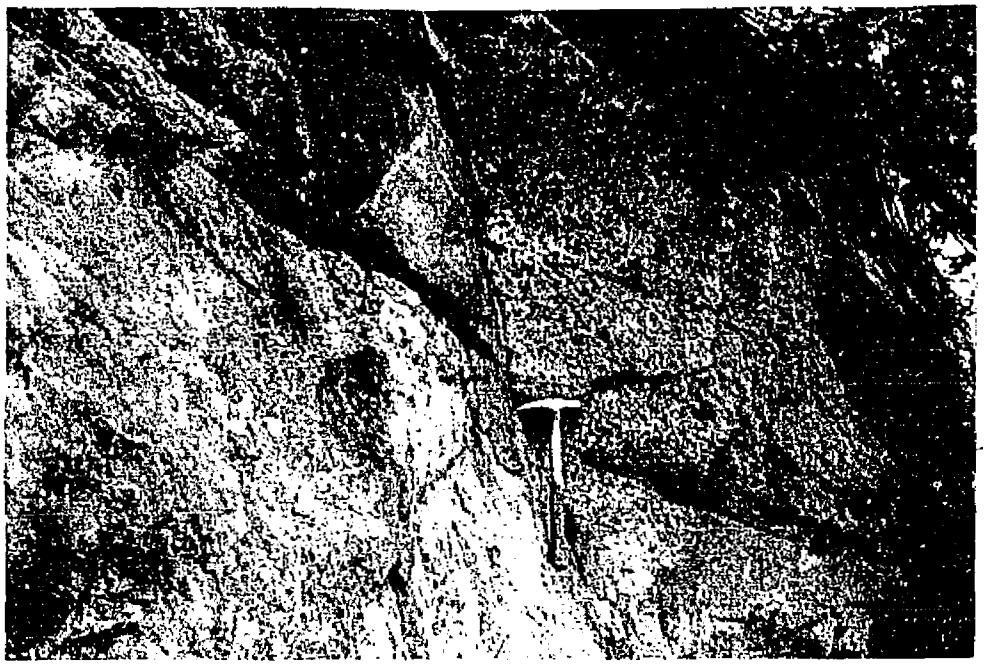

Fig. 4. The blocky weathering, grey orthopyroxene gneiss member of the Fordham Gneiss. Photo was taken south of Ned Mountain Road, near specimen #K8. The gneiss is cut by thin dikes of pinkish granite which contains rusty-weathering orthopyroxene grains. Hammer is 40 centimeters long.

static grain growth under granulite-facies conditions. Some degree of post-granulite retrogression is commonly evident in thin section. For instance, orthopyroxene megacrysts may be embayed or rimmed by cummingtonite and/or green hornblende (Fig. 6). Some grains of orthopyroxene (particularly those in contact with K-feldspar) are partially replaced by a vermicular biotite-quartz intergrowth. Some mafic layers have been transformed into amphibolite, and some leucocratic layers to a quartz-feldspar-biotite-garnet-hornblende gneiss.

The orthopyroxene gneiss member is compositionally varied, but mostly tonalitic to quartz-dioritic in bulk composition. It is interpreted as a metaigneous body that was first subjected to granulite-facies metamorphism during the Grenville orogeny.

Reconnaissance work has revealed that rocks similar to the Peach Lake quadrangle's orthopyroxene gneiss member are very abundant to the west of the study area (Plate IIB), in the Croton Falls quadrangle. However, within the Croton Falls quadrangle, orthopyroxene gneisses are commonly associated with minor amounts of Fordham calc-silicate rock. These calc-silicate rocks might represent xenoliths in a pluton, or metasedimentary beds intercalated with volcanic deposits. The tonalitic orthopyroxene gneisses of the northern Manhattan Prong may have originated as either one or as several distinct igneous bodies.

CLINOPYROXENE-GARNET GNEISS MEMBER. This member is characterized by enclaves of red-and-green rocks that display the unique mineral assemblage clinopyroxene + garnet + plagioclase. The enclaves are surrounded by amphibolites and by small (less than 10 meter-thick), well-foliated biotite granites. The red-and-green rocks grade into amphibolite.

X-ray refraction data and refractive indices indicate that the garnet is predominately almandine-pyrope. The coexisting plagioclase is a bytownite. Ilmenite is the dominant opaque mineral.

Rocks of this member range from leucocratic to melanocratic in composition. Melanocratic zones occur in two forms: as dark-green, coarse-grained rocks composed of nearly pure

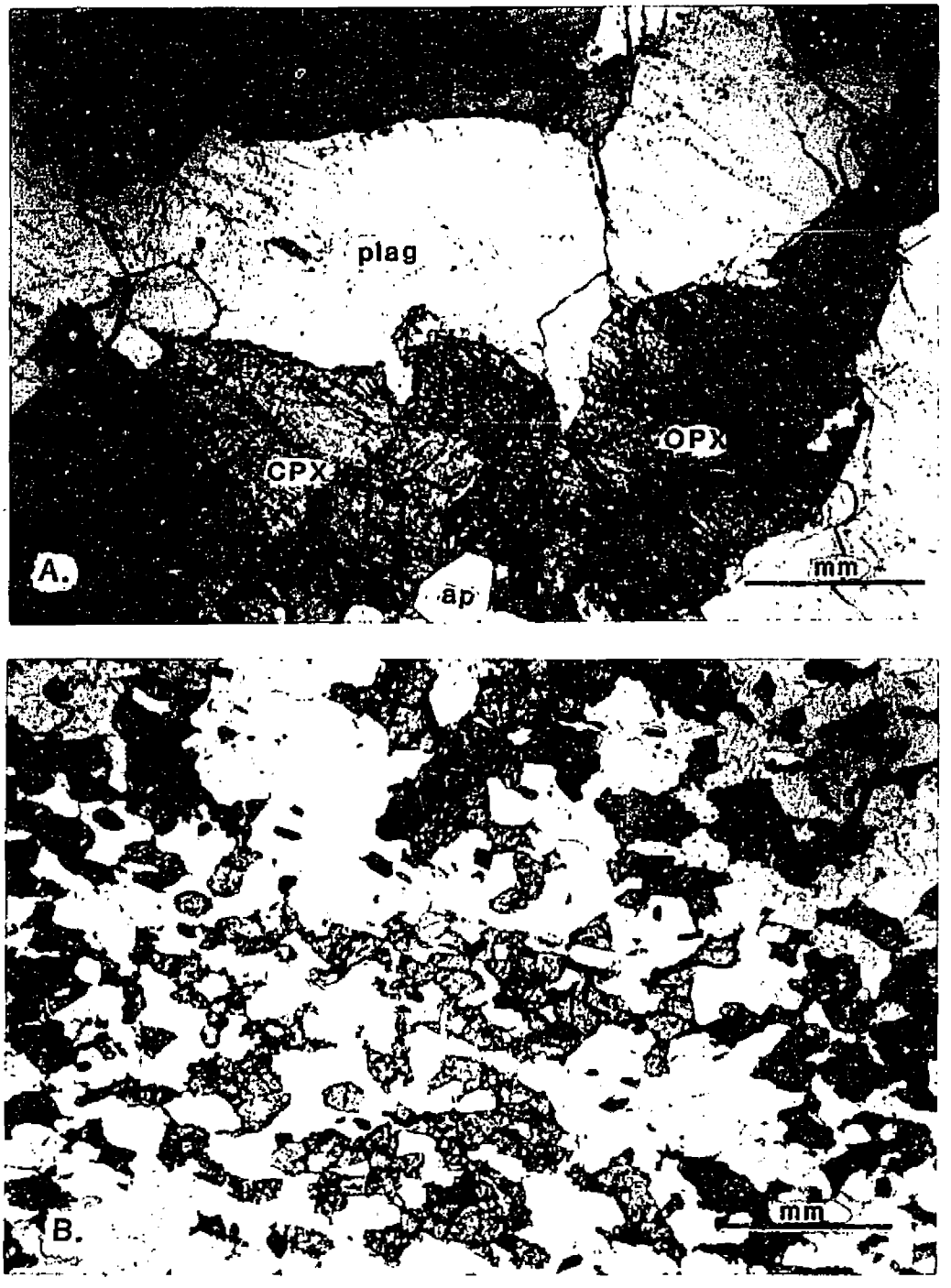

Fig. 5. (A) Typical coarse-grained texture of the Fordham Gneiss (specimen #1717 of the orthopyroxene gneiss member). OPX=orthopyroxene; CPX=clinopyroxene; plag=plagioclase; ap=apatite.

(B) Typical medium-fine grained texture of the orthopyroxene-bearing gneisses of Paleozoic age (specimen CT-7a of the Hartland Formation). High-relief grains are orthopyroxene, some with very minor alteration to hornblende; low relief grains are plagioclase and quartz.

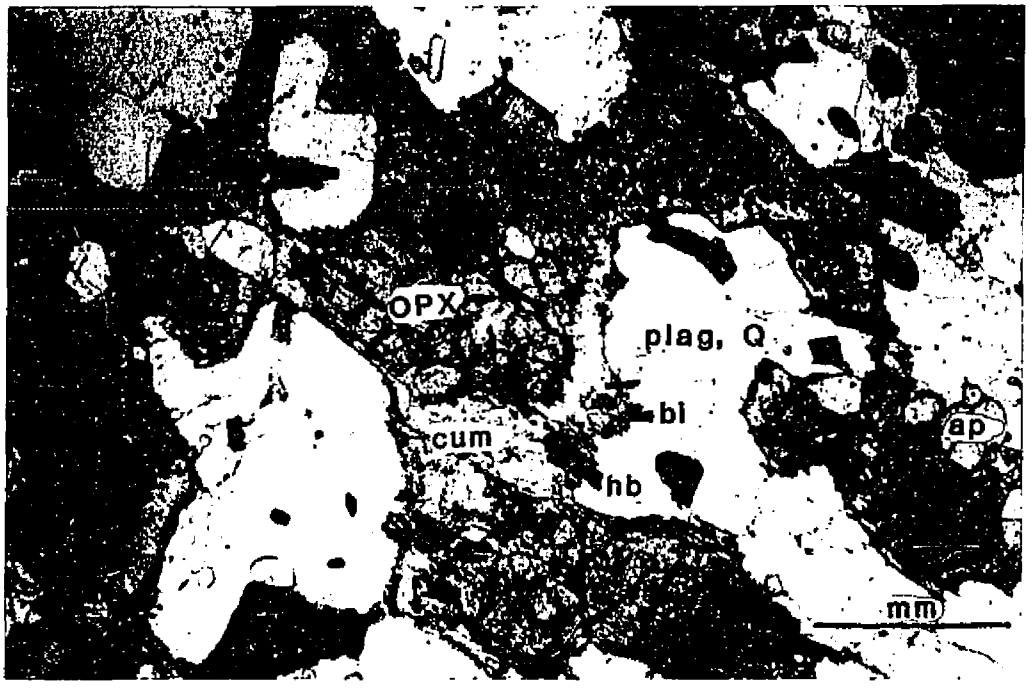

Fig. 6. Partially retrograded orthopyroxene gneiss of the Fordham Gneiss (specimen #718). Note similarity of texture to Fig. 5A. OPX=orthopyroxene; ap=apatite; bi=biotite; cum=cummingtonite; hb=hornblende; plag=plagioclase; Q=quartz.

masses of clinopyroxene, many centimeters in thickness, and as medium-grained, reddish rocks that consist of garnet-clinopyroxene intergrowths with minor plagioclase. Mesocratic zones, distinctly marked by their dark-green hornblende, surround and embay the melanocratic regions. Quartz and/or K-feldspar accompanies the hornblende; veins of K-feldspar cross-cut adjoining melanosomes. In the mesocratic zones, hornblende partially replaces the garnet + clinopyroxene assemblage.

Textural relationships indicate that the melanosomes are the oldest portions of the gneiss. The range from melanocratic- to leucocratic- compositions in this member is attributed to granitization. In spite of these granitic intrusions, the clinopyroxene-garnet gneiss member still has a more mafic average composition than does the orthopyroxene gneiss member. The clinopyroxene-garnet gneiss may have originated as a small mafic to ultramafic body positioned within a larger igneous mass of tonalitic composition.

PLAGIOCLASE-HORNBLENDE GNEISS MEMBER. The plagioclase-hornblende gneiss member consists of leucocratic to mesocratic, coarse- to medium-grained plagioclase (An_{35-47})-quartz-hornblende-biotite$\pm$clinopyroxene gneiss with amphibolitic interlayers. The unit is fairly homogeneous at the outcrop scale. Plagioclase and quartz together comprise 50 to 75% of most layers. Hornblende-rich layers are dark grey to black, plagioclase- and quartz-rich layers light grey to white. The rocks do not drastically change in color with weathering.

Many small bodies of biotite and/or hornblende granite (up to ~30 meters in thickness) are present. Granitic leucosomes also occur within the hornblende gneiss, and appear to be the result of intrusion-induced migmatization. Small amounts of K-feldspar ($\leq$8%) are present in some hornblende-bearing gneissose layers; these may reflect either K-metasomatism or a variation in primary bulk composition.

Minerals show little preferred orientation. Broadly-spaced (~0.5-2.0 meter) compositional layering and discontinuous 3 to 8 millimeter streaks are the major textural elements. The

amphibolites are commonly boundinaged because of competency differences with the leucocratic gneisses.

In thin section, the hornblende is olive green to bright blue-green. The cores of some hornblende grains contain exsolved opaque grains. Both ilmenite and magnetite are generally present in this gneiss. Coarse grains of blue-green hornblende are locally rimmed by a fine-grained hornblende-quartz symplectite. This texture suggests that clinopyroxene was formerly more abundant, and has been largely replaced by hornblende via the reaction

clinopyroxene + Na-richer plagioclase = hornblende + quartz + Ca-richer plagioclase.

The homogeneity of the plagioclase-hornblende gneiss member implies that the unit originated as an igneous body. The plagioclase-hornblende gneiss has a tonalitic bulk composition (as does the orthopyroxene gneiss member), but the greater abundance of calcic pyroxenes and amphiboles in the plagioclase-hornblende gneiss suggests that it has the higher Ca/Al bulk ratio. The contacts between the plagioclase-hornblende gneiss and the K-feldspar-hornblende gneiss are gradational; the K-feldspar-hornblende gneiss is distinguished by its substantial K-feldspar content and somewhat more leucocratic character.

K-FELDSPAR-HORNBLENDE GNEISS MEMBER. The K-feldspar-hornblende gneiss member consists of leuco- to mesocratic, medium- to coarse-grained, K-feldspar-plagioclase (An_{28-34}) -quartz-hornblende$\pm$clinopyroxene gneisses with amphibolite interlayers. This unit strongly resembles the plagioclase-hornblende gneiss in its texture and in the interplay of light-colored gneiss and dark hornblende-rich gneisses. However, leucocratic layers are more abundant in the K-feldspar-hornblende gneiss. Feldspar and quartz comprise 55 to 80 modal % of layers in this unit; modal K-feldspar ranges from 10 to 40%.

The K-feldspar-hornblende gneiss is generally poorly foliated. In thin section, biotite tends to be dark brown, and hornblende is green or pale blue-green. Although most feldspars are anhedral, some plagioclase grains display a tabular habit. Magnetite is generally the most abun-

dant opaque mineral.

The K-feldspar-hornblende gneiss is fairly homogeneous and roughly granitic in composition. The K-feldspar-hornblende gneiss is interpreted as a deformed granitoid. This granitoid and the protolith of the plagioclase-hornblende gneiss may have belonged to the same composite pluton.

AMPHIBOLITE MEMBER. The amphibolite member of the Fordham Gneiss consists of hornblende-plagioclase ($^{\sim}An_{65}$)-biotite-quartz$\pm$pyroxene amphibolite with leucocratic interlayers consisting of quartz, plagioclase (An_{30-65}), and biotite ($\pm$hornblende, pyroxene, and K-feldspar). The amphibolitic layers contain 50 to 72 modal percent mafic minerals; leucocratic layers are 60 to 80% feldspar+quartz. Small amounts ($\leq$15%) of orthopyroxene or clinopyroxene may occur in either amphibolitic or leucocratic layers, in some places in the form of megacrystic grains. Most hornblende is olive-colored in thin section. Ilmenite is the dominant opaque mineral.

The amphibolite member has gradational contacts with the orthopyroxene, clinopyroxene-garnet, plagioclase-hornblende gneiss and K-feldspar-hornblende gneiss members of the Fordham Gneiss. The age relationships between the amphibolite and these other members of the Fordham Gneiss have not been determined; their protoliths may have intruded the mafic protolith of the amphibolite member, or vice versa. The amphibolite member may also be, in part, the product of amphibolite-facies metamorphism of mafic portions of these other units. It is possible, even probable, that the rocks mapped as amphibolite member have a number of different origins.

GRANITIC GNEISS MEMBER. Many small granitic bodies of apparent Grenvillian age are found within the Fordham Gneiss. These granites are commonly hornblende-bearing, and those in the orthopyroxene gneiss member locally pyroxene-bearing. Biotite, which can be observed replacing K-feldspar, generally appears to be of secondary origin. This late biotite typically

defines any foliation that may be present.

Apatite, zircon, ilmenite, magnetite, and sphene are the most common accessory minerals in Fordham granites; a few contain allanite. One body of granite is large enough to be mapped as a separate unit at 1:24,000 scale (Plate I):

The granitic gneiss member shown on Plate I is a poorly foliated, grey-weathering granite with amphibolitic interlayers. Parts of the granite are hornblende-bearing. Plagioclase composition is ~ An_{28}. Biotite is dark brown and hornblende is green in thin section. The most remarkable feature of this particular granitic body is the modal abundance (up to 5%) of magnetite, which occurs in clots 1 to 3 millimeters in diameter. Allanite, ilmenite, pyrrhotite, and sphene are also commonly present.

NED MOUNTAIN FORMATION

The Ned Mountain Formation, proposed here, unconformably overlies the Fordham Gneiss. It contains a variety of metasedimentary and metaigneous rocks, including amphibolite, K-feldspar-quartz ("granitic") gneiss, a variety of quartz-feldspar granofelses, calc-silicate rock, and quartz-feldspar-biotite-garnet-sillimanite schistose gneiss. These lithologies occur in varying combinations and proportions through most of the Ned Mountain Formation. Individual beds, however, tend to be discontinuous, and lateral changes are commonly pronounced.

The Ned Mountain Formation has been provisionally subdivided into four members: the Basal Member, Volcaniclastic Member, Calc-Silicate Member, and Wacke Member (see Plate IA). Each member is conceived of as a package of discontinuous beds which belong to particular rock suite or suites. (A "rock suite" is defined here as a range of lithologies that commonly occurs together). Each member of the Ned Mountain Formation has its own distinctive lithologic characteristics. The members occur in a regular stratigraphic sequence between the last outcrop of Fordham Gneiss and the first beds of dolomitic Inwood Marble.

The contact between the Ned Mountain Formation and the Fordham Gneiss is exposed at scattered localities in three different 15 minute quadrangles. At most places, however, there is a gap in outcrop between the last exposure of the Fordham Gneiss and the first of the Ned Mountain Formation. These first outcrops of the Ned Mountain Formation generally belong to the Basal Member.

The Basal Member consists largely of graphitic quartz-feldspar granofelses, K-feldspar-biotite-garnet gneiss, and amphibolite. Most of the lithologies of the Basal Member contrast strikingly with rocks of the underlying Fordham Gneiss. The Basal Member is very persistent on a regional scale; it is encountered on the majority of the reconnaissance transects illustrated on Plate IIC and described in Appendix 1.

The Volcaniclastic Member overlies the Basal Member in much of the Manhattan Prong (Plate IIC) and can be seen as far north as West Mountain (Plate III) in the study area. The Wacke Member overlies the Basal Member further north. The Volcaniclastic Member contains K-feldspar-quartz ("granitic") gneiss, amphibolite, and quartz-feldspar granofelses.

The Wacke Member is in contact with Basal Member lithologies at some localities, though it locally rests directly on the Fordham Gneiss. The Wacke Member dominantly consists of quartz-feldspar-garnet-biotite-sillimanite schistose gneiss, quartz-feldspar-biotite-garnet granofels, and amphibolite. Reconnaissance study shows that the Wacke Member continues on strike to the west (Plate IIC) into the Croton Falls quadrangle. Reports by Hall (e.g., 1968b) suggest that equivalent rocks are present at other localities in the Manhattan Prong.

The Calc-Silicate Member is the most persistent and stratigraphically the highest member of the Ned Mountain Formation. As seen in the southern Peach Lake quadrangle, the Calc-Silicate Member is also the most lithologically diverse. It contains, among other things, quartz-feldspar granofelses, K-feldspar-quartz ("granitic") gneiss, amphibolite, calc-silicate rock, and marble. In contrast, in the northern Peach Lake quadrangle, the Calc-Silicate Member is largely restricted to quartz-feldspar granofels, marble, and calc-silicate rock. The southern, lithically diverse Calc-Silicate Member contains several lithologies in common with the Wacke Member, suggesting broad-scale interfingering of lithologic types (Fig. 7). A gradational contact is inferred between the laterally equivalent portions of the Calc-Silicate and Wacke Members (Plate 1A).

Outcrop of the Calc-Silicate Member occurs below all belts of the Inwood Marble in the study area except the northernmost Inwood (Plate I). Outcrop density is very low in that region, so that the apparent absence of the Calc-Silicate Member does not preclude its presence in the bedrock. Outside the study area, the Calc-Silicate Member is widespread, and both the compositionally varied and restricted types have been observed.

Rocks of post-Fordham and pre-Inwood age are not limited to the members of the Ned Mountain Formation outlined here. A few fine-grained amphibolite dikes have been observed

Fig. 7. Schematic cross section showing the distribution of the main lithologies in the Ned Mountain Formation.

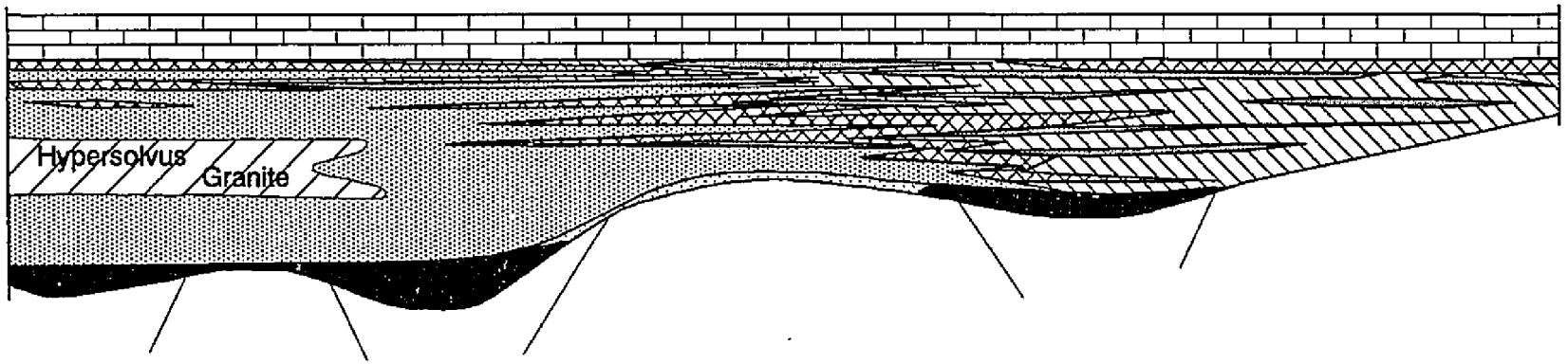

Major Lithologies of the Ned Mountain Formation

Lithologies in the Basal Member

- Graphite-bearing rocks
- Other rocks

- Metatuff and Metabasite
- Calc-Silicate Rocks and Marbles
- Quartz-Feldspar Granofelses
- Metawackes and Metabasites

Inwood Marble

Normal Fault

cutting the Fordham Gneiss. These amphibolites are interpreted as age-equivalents of Ned Mountain metabasites.

The numerous and abrupt changes in lithology that characterize the Ned Mountain Formation reflect a complex, rapidly evolving depositional setting. The major lithologies of the Ned Mountain Formation will be discussed in following sections one at a time, roughly in the sequence in which they are first encountered stratigraphically. Each rock type (or suite) will first be described; next, the protolith of the rocks will be inferred; finally, an interpretation of the depositional setting will be given. After all the lithologies and members of the Ned Mountain Formation have been discussed, the broader geologic history recorded by the Ned Mountain Formation will be considered.

Before describing the members of the Ned Mountain Formation, the nature of the contact between the Fordham Gneiss and the Ned Mountain Formation will be examined.

NATURE OF THE CONTACT BETWEEN THE FORDHAM GNEISS AND THE NED MOUNTAIN FORMATION. Outcrop is rarely continuous from the Fordham Gneiss into the Ned Mountain Formation. Where outcrop is continuous (or nearly so), the unconformity may appear to be either sharp and well-defined or diffuse and difficult to pinpoint.

Apparently sharp contacts. Apparently sharp contacts between the Fordham Gneiss and the Basal Member of the Ned Mountain Formation are exposed at two localities: on transect E-E' in the White Plains quadrangle (Plate II), and south of George Washington Highway in the northeastern Peach Lake quadrangle, (approximately 160 meters south-south-east of specimen #1669, Plate III).

Blocky, amphibolitic Fordham Gneiss is in contact with grey, quartz-rich, clinopyroxene-bearing calc-silicate rock of the Basal Member at the locality south of George Washington Highway. The bed of calc-silicate rock is less than 0.5 meter thick, and is overlain by graphitic

quartz-plagioclase-K-feldspar-biotite granofelses. The granofelses (described later) are interpreted as meta-arkoses. The graphite content of these granofelses averages about four modal percent.

On transect E-E' in the White Plains quadrangle, migmatized hornblende gneisses of the Fordham are in contact with dark-green, thin-bedded, rusty-weathering, graphitic, plagioclase-biotite-quartz-hornblende schistose gneiss of the Basal Member. The lowermost beds of the Basal Member are mesocratic gneisses, containing 30 to 50 modal percent biotite+hornblende. The quartz content of the beds varies from zero to 45 modal percent; labradorite (An_{54}) makes up the bulk of some layers. Graphite content averages about five modal percent, though some laminae contain as much as 15% modal percent.

The lithologic successions at these localities share two prominent features: 1) no systematic macroscopic changes are observed in the Fordham Gneiss as the unconformity is approached, and 2) extremely graphitic rocks of the Basal Member are present either at the unconformity or a short distance above it.

A sharp-looking contact between the orthopyroxene gneiss member of the Fordham and the Wacke Member of the Ned Mountain Formation is exposed in the northeastern Peach Lake quadrangle, just south of Ned Mountain Road (site of specimen #2565, Plate III). However, here the Fordham Gneiss closest to the unconformity is atypical in several ways. As the contact is approached, garnet appears in some layers of Fordham Gneiss; this is significant because most specimens of the orthopyroxene gneiss member contain no garnet. The typical blocky-weathering style of the Fordham Gneiss is replaced by a thin slabby-breaking habit in the uppermost several centimeters of the Fordham. A layer of mesocratic plagioclase-orthopyroxene-garnet-biotite-magnetite gneiss occurs at the very top of the Fordham Gneiss. This gneiss is remarkable because of the absence of quartz and the presence of five modal percent of garnet, the highest observed in any specimen from the orthopyroxene gneiss member.

The overlying Wacke Member consists of a medium-grained, rusty-weathering, plagioclase-garnet-quartz-biotite schistose gneiss. Similar gneisses are found at two localities where the

Wacke Member crops out within 10 meters of the Fordham Gneiss (in these cases, plagioclase-hornblende gneiss and amphibolite members). The Wacke Member schistose gneiss in direct contact with the orthopyroxene gneiss member contains about 45 modal percent plagioclase, 18 percent quartz, and 20 percent garnet. The samples from the other localities have a average modal plagioclase content of 55% (An_{30}), average quartz content of 15%, and average garnet content of 8%. One specimen (#1672, Table 3) contains 8% K-feldspar.

All the rocks collected from the lowermost Wacke Member, near outcrop of the Fordham Gneiss, are atypical compared with the bulk of the Wacke Member. Stratigraphically higher metasedimentary rocks contain more modal quartz than plagioclase, and plagioclase makes up no more than a third of modal mineralogy (Table 3). The compositional differences between rocks from the base of the Wacke Member and other metasedimentary rocks are illustrated on Fig. 13.

Slightly diffuse contact. A zone of anomalous rocks about two meters wide is present between the Ned Mountain Formation Basal Member and typical orthopyroxene gneiss of the Fordham at a locality just south of Ned Mountain Road in the northeastern Peach Lake quadrangle (site of specimen #2675, Plate III). There, the "unaltered" part of the Fordham consists of blocky-weathering dark-and-light banded plagioclase-orthopyroxene-hornblende-quartz gneisses; the stratigraphically highest exposure of blocky gneiss contains a trace of garnet. Next, a gap in outcrop about half a meter wide occurs, followed by exposure of slabby-weathering plagioclase-quartz-biotite-orthopyroxene-garnet gneisses. These gneisses contain up to 25 modal percent biotite, while the nearby "typical" orthopyroxene gneisses contain 5% biotite or less.

A bed of grey calc-silicate rock about 20 centimeters in thickness crops out stratigraphically above the anomalous gneisses. Specimen #2675 (Table 3) was collected from this bed. The calc-silicate bed is overlain by a quartz-plagioclase-K-feldspar-biotite granofels that contains about 5 modal percent graphite. This granofels grades southwards into a coarse-textured, graphitic unit (described later) interpreted as a basal metaconglomerate.

TABLE 3

Estimated Modal Compositions of Representative Specimens of Ned Mountain Formation and Related Rocks

	Contact Zone			Ned Mountain Formation, Basal Member																
	Fordham Gneiss/ Ned Mountain Fm.			Metabasite/mafic metasedimentary rock suite								Calc-Silicate rock	Meta-conglomerate	Meta-arkoses			K-rich metasaprolite				
Specimen	SG820a	SG820b		1319		SG821b	1845a	1905	SG822a	1719	1560b	2675	1742	1349	1546	1669	730	1359	1550	1593a	Specimen
Layer		host	lens	I	II						I										Layer
Quartz	8	10	-	5	12	3	8	5	44	60	70	36	31	70	60	50	1	tr.	-	2	Quartz
Plagioclase	38	51	60	53	60	28	29	63	22	15	-	15	27	25	-	15	tr.	tr.	-	-	Plagioclase
(% anorthite)	(27)	(34)	(55-75)	(50-65)	(50)	(44)	(43)	(34)	(38)	(22)	-	(70)	(47)	(50-80)	-	(47-70)	(23)	(23)	-	-	(% anorthite)
K-feldspar	-	-	-	-	-	-	-	-	-	-	-	5	15	-	30	20	57p	43p	74p	54	K-feldspar
Biotite	47	25	20	tr.	8	2	23	8	15	18	2	tr.	12	2	5	10	20	29	17	10	Biotite
Garnet	7	10	15	-	2	-	tr.	5	-	2	18	-	5	-	5	-	15	10	-	24	Garnet
Hypersthene	-	-	-	33	12	-	-	-	-	-	-	-	2	-	-	-	-	-	-	-	Hypersthene
Diopside	-	-	-	-	-	-	-	-	-	-	-	35	-	-	-	-	-	-	-	-	Diopside
Augite	-	-	-	tr.	-	tr.	-	-	-	-	-	-	4	-	-	-	-	-	-	-	Augite
Hornblende	-	-	-	4	1	67	-	-	tr.	-	-	tr.	2*	-	-	-	-	-	-	-	Hornblende
Cummingtonite	-	-	-	-	-	-	38	-	10	-	tr.	-	-	-	-	-	-	-	-	-	Cummingtonite
Orthoamphibole	-	-	-	-	-	-	-	15	-	-	-	-	-	-	-	-	-	-	-	-	Orthoamphibole
Scapolite	-	-	-	-	-	-	-	-	-	-	-	6	-	-	-	-	-	-	-	-	Scapolite
Sillimanite	-	-	-	-	-	-	-	-	-	-	-	-	-	-	-	-	6	16	8	5	Sillimanite
Apatite	-	-	-	tr.	-	-	tr.	1	-	tr.	1	tr.	tr.	tr.	tr.	-	-	-	-	-	Apatite
Zircon	-	-	-	tr.	-	-	-	tr.	-	-	tr.	tr.	-	tr.	tr.	tr.	tr.	tr.	tr.	tr.	Zircon
Allanite	-	-	-	-	-	-	-	-	-	-	-	-	tr.	-	-	-	-	-	-	-	Allanite
Corundum	-	-	tr.	-	-	-	-	-	-	-	-	-	-	-	-	-	-	-	-	-	Corundum
Green spinel	-	-	2	-	-	-	-	-	-	-	-	-	-	-	-	-	-	-	-	-	Green spinel
Tourmaline	-	-	-	-	-	-	-	-	-	-	-	-	-	-	-	tr.	-	-	-	-	Tourmaline
Anatase	-	-	-	-	-	-	-	-	-	tr.	-	-	-	-	-	-	-	-	-	tr.	Anatase
Sphene	-	-	-	-	-	-	-	-	-	-	-	1	-	-	-	-	-	-	-	-	Sphene
Graphite	tr.	4	3	-	-	-	2	3	6	2	-	-	2	-	-	4	-	tr.	-	-	Graphite
Magnetite	-	tr.	tr.	tr.	-	tr.	tr.	tr.	tr.	1	9	1	tr.	1	tr.	tr.	tr.	tr.	tr.	tr.	Magnetite
Ilmenite	tr.	tr.	tr.	3	4	tr.	tr.	tr.	-	tr.	tr.	1	tr.	2	tr.	tr.	1	2	1	1	Ilmenite
Pyrrhotite	tr.	-	-	2	tr.	tr.	tr.	tr.	2	2	tr.	tr.	tr.	tr.	-	1	-	-	tr.	-	Pyrrhotite
Pyrite	-	-	-	-	-	-	-	-	-	-	-	-	-	-	-	-	-	tr.	-	-	Pyrite
Calcite	-	-	-	-	-	-	-	-	-	-	-	tr.	-	-	-	-	-	-	-	-	Calcite
Chlorite	-	-	-	-	tr.	-	-	-	-	tr.	-	-	-	-	tr.	-	-	-	-	-	Chlorite
Muscovite	-	-	-	-	-	-	-	-	-	tr.	-	-	-	tr.	tr.	-	-	tr.	tr.	3	Muscovite

p= Perthitic K-feldspar with 20% or more exsolved plagioclase.

*= Includes both green and colorless, pargasitic hornblende.

TABLE 3, CONTINUED

Ned Mountain Formation, Volcaniclastic Member

	Layered quartzo-feldspathic rocks							Hyper-solvus granite	Amphibolites		
Specimen	1515	1524	1543	1345	1399		1415	1514	737	2496	
Layer					I	II					
Quartz	25	36	31	60	26	7	54	35	10	11	Quartz
Plagioclase	10	5	-	10	6	76	16	(60	25	23	Plagioclase
(% anorthite)	(28)	(25)	-	(75)	(23)	(32)	(30)	%	(39)	(69)	(% anorthite)
								alkali			
K-feldspar	62	41	67	19	57	-	3	feldspar)	-	-	K-feldspar
Biotite	3	15	-	5	8	tr.	26	3	-	10	Biotite
Garnet	-	-	-	-	-	-	-	-	-	16	Garnet
Diopside	-	-	-	-	-	1	-	-	-	-	Diopside
Hornblende	-	-	-	-	3	14	-	-	65	28	Hornblende
Cummingtonite	-	-	-	-	-	-	-	-	-	12	Cummingtonite
Apatite	-	tr.	-	tr.	tr.	-	-	-	tr.	tr.	Apatite
Zircon	tr.	tr.	tr.	tr.	tr.	-	tr.	tr.	-	-	Zircon
Allanite	-	tr.	-	-	tr.	tr.	-	-	-	-	Allanite
Sphene	-	-	-	-	-	-	-	-	tr.	-	Sphene
Magnetite	tr.	tr.	tr.	4	tr.	tr.	tr.	2	-	tr.	Magnetite
Ilmenite	-	2	tr.	tr.	tr.	tr.	tr.	tr.	tr.	tr.	Ilmenite
Pyrrhotite	-	-	-	tr.	tr.	2	1	-	tr.	tr.	Pyrrhotite
Pyrite	-	-	-	tr.	-	-	-	-	-	-	Pyrite
Calcite	-	tr.	-	-	-	-	-	-	-	-	Calcite
Chlorite	-	tr.	tr.	-	tr.	-	-	-	tr.	-	Chlorite
Muscovite	tr.	-	1	2	-	-	tr	-	-	-	Muscovite

TABLE 3, CONTINUED

Ned Mountain Formation, Wacke Member

	Basal Wacke Member	Metawackes					Meta-pelite	Quartz-feldspar-biotite-garnet granofels			Metabasites						K-rich metasaprolite	
Specimen	1672*	K10	193a	1249	1665	1697	1243	1641	1644	1646	552b	1252	1305	1311	1663	1679	1690a	
Layer														1	1		1	
Quartz	6	55	38	35	53	28	20	61	44	43	10	10	16	7	5	4	8	Quartz
Plagioclase	57	13	24	28	5	5	5	24	30	33	30	51	6	42	48	30	tr.	Plagioclase
(% anorthite)	(30)	(37)	(33)	(23)	(22)	(22)	(30)	(29)	(29)	(35)	(47)	(77)	(38)	(45-75)	(38)	(33)	-	(% anorthite)
K-feldspar	8	8	13	4	8	34p	21	4	2	2	-	-	-	-	-	-	74	K-feldspar
Biotite	13	7	6	17	12	8	7	6	14	12	tr.	-	3	tr.	15	5	8	Biotite
Garnet	15	10	9	11	15	12	30	4	7	7	-	-	-	20	5	-	6	Garnet
Hypersthene	-	-	-	-	-	-	-	-	-	-	7	4	-	25	-	5	-	Hypersthene
Augite	-	-	-	-	-	-	-	-	-	-	-	-	-	-	-	5	-	Augite
Hornblende	-	-	-	-	-	-	-	-	-	-	50	25	72	-	6	43	-	Hornblende
Cummingtonite	-	-	-	-	-	-	-	-	-	-	-	-	-	-	15	4	-	Cummingtonite
Kyanite	-	-	-	-	-	tr.	tr.	-	-	-	-	-	-	-	-	-	-	Kyanite
Sillimanite	tr.	5	8	4	5	12	15	-	tr.	tr.	-	-	-	-	-	-	tr.	Sillimanite
Apatite	tr.	-	tr.	-	tr.	-	-	-	tr.	-	-	tr.	-	-	3	-	tr.	Apatite
Zircon	tr.	tr.	tr.	tr.	tr.	tr.	tr.	tr.	tr.	tr	-	tr.	-	-	tr.	-	tr.	Zircon
Green spinel	-	-	tr.	tr.	tr.	tr.	tr.	-	-	-	-	-	-	-	-	-	-	Green spinel
Allanite	-	-	-	-	-	-	-	-	-	-	-	-	-	-	tr.	tr.	-	Allanite
Rutile	-	-	-	tr.	-	tr.	tr.	-	-	-	-	-	-	-	-	-	-	Rutile
Sphene	-	-	-	-	-	-	-	-	-	-	-	-	tr.	-	-	-	-	Sphene
Magnetite	tr.	1	tr.	tr.	2	tr.	1	tr.	1	1	tr.	8	tr.	1	tr.	tr.	tr.	Magnetite
Ilmenite	1	1	2	1	tr.	tr.	tr.	tr.	1	1	2	2	1	5	3	3	tr.	Ilmenite
Pyrrhotite	tr.	-	-	-	tr.	-	tr.	tr.	tr.	tr	tr.	-	1	-	-	tr.	tr.	Pyrrhotite
Calcite	-	-	-	-	-	-	-	-	-	-	tr.	-	-	-	-	-	-	Calcite
Chlorite	-	-	-	-	tr.	-	tr.	-	-	-	tr.	-	-	-	-	-	tr.	Chlorite
Muscovite	-	-	-	-	-	-	tr.	-	-	-	-	-	-	-	-	-	3	Muscovite

* From base of Wacke Member near Fordham Gneiss.

p= Perthitic K-feldspar with 20% or more exsolved plagioclase.

TABLE 3, CONTINUED

Ned Mountain Formation, Calc-Silicate Member

	Felsic metatuff				Quartz-feldspar granofelses													
					Quartz-K-feldspar			Quartz-feldspar-biotite-garnet							Miscellaneous			
Specimen	1435	1445	1470	1566b	V6-V8	311	1634	735	1421	1441	1493a		1502		1368	1520	1588b	Specimen
Layer	I						I			I	I	II	I	II	I			Layer
Quartz	29	28	22	34	70	65	78	44	41	59	33	94	75	59	64	64	61	Quartz
Plagioclase	4	12	tr.	2	-	-	-	25	35	30	42	5	-	-	1	19	10	Plagioclase
(% anorthite)	(17)	(0)	(21-27)	(18)	-	-	-	(38)	(36)	(58)	(55 - 80)		-	-	(32)	(27)	(75)	(% anorthite)
K-feldspar	65	58	63	57	25	35	18	18	-	-	-	-	10	9	32	-	20	K-feldspar
Biotite	-	tr.	12	4	4	tr.	tr.	6	15	8	19	tr.	13	4	2	15	8	Biotite
Garnet	1	-	-	-	-	-	-	4	7	1	2	-	-	27	-	tr.	-	Garnet
Calcite	-	-	-	-	-	-	-	-	-	-	tr.	-	-	-	-	-	-	Calcite
Diopside	-	tr.	-	-	-	-	3	-	-	-	-	-	-	-	-	-	-	Diopside
Hornblende	-	tr.	-	-	-	-	-	-	-	-	-	tr.	-	-	-	-	-	Hornblende
Tremolite	-	1	-	-	-	-	1	-	-	-	-	-	-	-	-	-	-	Tremolite
Clinozoisite	-	-	-	tr.	-	-	-	-	-	-	-	-	-	-	-	-	-	Clinozoisite
Cordierite	-	-	-	-	-	-	-	tr.	-	-	-	-	-	-	-	-	-	Cordierite
Kyanite	-	-	-	-	-	-	-	tr.	-	-	-	-	-	-	-	-	-	Kyanite
Sillimanite	-	-	-	-	-	-	-	tr.	-	tr.	-	-	-	-	-	-	-	Sillimanite
Apatite	tr.	tr.	tr.	tr.	tr.	tr.	-	tr.	tr.	tr.	tr.	-	1	tr.	tr.	tr.	tr.	Apatite
Zircon	-	tr.	tr.	tr.	tr.	tr.	-	tr.	tr.	tr.	-	-	tr.	tr.	tr.	tr.	tr.	Zircon
Allanite	-	-	-	tr.	-	-	-	-	tr.	-	-	-	-	-	-	-	tr.	Allanite
Tourmaline	tr.	-	-	tr.	-	-	-	-	-	-	tr.	-	-	-	-	-	-	Tourmaline
Rutile	-	-	-	-	-	tr.	-	-	-	-	-	-	-	-	-	-	-	Rutile
Sphene	-	tr.	-	tr.	-	tr.	-	-	tr.	-	-	-	-	-	tr.	-	-	Sphene
Graphite	tr.	tr.	2	tr.	-	-	-	2	-	-	2	tr.	-	-	-	-	-	Graphite
Magnetite	tr.	tr.	tr.	-	tr.	tr.	tr.	tr.	tr.	-	tr.	-	tr.	tr.	tr.	tr.	tr.	Magnetite
Ilmenite	tr.	tr.	tr.	tr.	tr.	-	-	tr.	1	tr.	tr.	-	tr.	-	tr.	tr.	tr.	Ilmenite
Pyrrhotite	tr.	tr.	-	tr.	tr.	tr.	tr.	-	1	1	2	1	1	tr.	tr.	1	-	Pyrrhotite
Pyrite	-	-	-	-	tr.	-	-	-	-	-	-	-	-	-	-	-	-	Pyrite
Chlorite	tr.	-	tr.	-	-	-	-	tr.	tr.	tr.	tr.	-	-	tr.	-	tr.	tr.	Chlorite
Muscovite	tr.	-	tr.	2	-	tr.	-	tr.	tr.	tr.	tr.	-	tr.	tr.	tr.	tr.	tr.	Muscovite

TABLE 3, CONTINUED

Ned Mountain Formation, Calc-Silicate Member

	Marbles			Calc-silicate rocks: White-and-green					Calc-silicate rocks: Dark	Metawacke		Meta-pelite	K-rich metasaprolite /		Dark phospathic gneiss		Garnet-hornblende granofels		Amphibolite			Amphibolite Dike in Fordham Gneiss	
Specimen	1383	1566a	1714	177	1308	1526a		1634	1939b	1385	1507	1565a	1379	1381	1222c	2108	1884	2468	1416	1469a	1522	2215	Specimen
Layer				I		I	II	II	I											I			Layer
Quartz	-	-	4	38	-	8	58	tr.	70	37	25	3	10	-	60	25	41	42	9	-	17	tr.	Quartz
Plagioclase	3	-	13	4	15	tr.	-	-	9	19	20	13	-	-	5	25	38	43	24	28	18	50	Plagioclase
(% anorthite)	(30)	-	-	(23)	(50)	-	-	-	(38)	(38)	(52)	(28)	-	-	(20)	(24)	(27)	(46)	(30)	(26)	(35)	(32)	(%anorthite)
K-feldspar	15	25	14	24	59	33	24	30	-	3	20	5	59	77	-	-	-	-	-	4	-	-	K-feldspar
Biotite	2	tr.	tr.	-	1	-	-	tr.	-	9	24	37	15	8	24	40	6	-	tr.	-	13	tr.	Biotite
Garnet	-	-	-	-	-	-	-	-	-	20	5	23	10	-	-	-	4	2	-	-	6	5	Garnet
Calcite	73	60	51	14	-	38	5	-	-	-	-	-	-	-	-	-	-	-	-	-	tr.	-	Calcite
Augite	-	-	-	-	-	-	-	-	-	-	-	-	-	-	-	-	-	-	3	2	-	-	Augite
Diopside	3	7	13	15	15	5	4	68	3	-	-	-	-	-	-	-	-	-	-	-	-	-	Diopside
Hornblende	-	-	2	4	-	2	1	-	8	-	-	-	-	-	-	-	8	12	60	59	42	40	Hornblende
Tremolite	3	3	-	-	2	-	-	-	-	-	-	-	-	-	-	-	-	-	-	-	-	-	Tremolite
Epidote Fam.*	-	tr.	tr.	-	3	10	6	-	4	-	-	-	-	-	-	-	-	-	-	tr.	-	-	Epidote Fam.*
Cummingtonite	-	-	-	-	-	-	-	-	-	-	-	-	-	-	-	-	-	-	-	-	tr.	-	Cummingtonite
Scapolite	tr.	-	-	-	5	-	-	-	-	-	-	-	-	-	-	-	-	-	-	-	-	-	Scapolite
Kyanite	-	-	-	-	-	-	-	-	-	-	tr.	tr.	-	-	-	-	-	-	-	-	-	-	Kyanite
Sillimanite	-	-	-	-	-	-	-	-	-	9	3	15	5	10	-	-	-	-	-	-	-	-	Sillimanite
Apatite	tr.	-	-	tr.	tr.	tr.	tr.	tr.	tr.	tr.	tr.	-	-	tr.	4	5	tr.	tr.	tr.	tr.	tr.	tr.	Apatite
Zircon	-	-	-	-	tr.	-	-	-	-	tr.	tr.	tr.	tr.	tr.	tr.	-	tr.	-	-	-	tr.	-	Zircon
Allanite	-	-	tr.	tr.	-	-	-	-	-	-	-	-	-	-	-	tr.	-	-	-	tr.	-	-	Allanite
Tourmaline	-	-	-	-	-	-	-	-	-	tr.	-	-	tr.	tr.	-	-	-	-	-	-	-	-	Tourmaline
Green spinel	-	-	-	-	-	-	-	-	-	tr.	-	-	tr.	-	-	-	-	-	-	-	-	-	Green spinel
Rutile	-	-	-	-	-	-	-	-	-	-	tr.	tr.	tr.	-	-	-	-	-	-	-	-	-	Rutile
Anatase	-	-	-	-	-	-	-	-	-	-	-	-	-	tr.	1	-	-	-	-	-	-	-	Anatase
Sphene	tr.	2	3	1	tr.	4	2	2	2	-	-	-	-	-	-	-	-	tr.	tr.	6	-	tr.	Sphene
Graphite	tr.	1	-	-	-	-	-	-	-	-	2	3	-	-	-	-	-	-	-	-	-	-	Graphite
Magnetite	tr.	tr.	-	tr.	-	tr.	tr.	tr.	2	-	tr.	tr.	tr.	tr.	-	3	tr.	tr.	tr.	tr.	tr.	2	Magnetite
Ilmenite	-	-	-	-	-	-	-	-	-	2	tr.	tr.	tr.	-	1	2	tr.	tr.	4	-	3	2	Ilmenite
Pyrrhotite	1	1	tr.	tr.	tr.	tr.	tr.	-	2	-	tr.	tr.	-	1	1	-	-	tr.	-	tr.	tr.	tr.	Pyrrhotite
Pyrite	-	-	-	-	-	-	-	-	-	-	-	-	-	tr.	-	-	-	-	-	-	-	-	Pyrite
Chlorite	-	-	-	-	-	-	-	-	-	-	-	-	tr.	-	-	-	2	-	-	tr.	-	-	Chlorite
Muscovite	-	-	-	-	-	-	-	-	-	tr.	-	-	tr.	3	4	tr.	-	-	-	-	-	-	Muscovite

* Includes clinozoisite and epidote

TABLE 3, CONTINUED

Notes: 1. Locations All the specimens collected in the Peach Lake or Brewster quadrangles are shown on Plate III. For other specimens, see Fig. 1 for the layout of topographic quadrangles and Plate II for the locations of transects. Details of location of these specimens are given verbally, with the descriptions below. **2. Nature of the descriptions** These brief descriptions touch on the color and texture of the specimen, character of the weathered surface (if any), and, (if the mode is given for a specific bed), the composition of other layers in the rock. The color of the weathered surface is specified only if it contrasts with the overall color of the rock. In a few cases, garnet color is specified; where color is unspecified, garnets are red.

Contact Zone: Fordham Gneiss/Ned Mountain Formation

SGB20. Grey-weathering, dark grey schistose gneiss with thin (<5 millmeter) white leucosomes. Collected on transect H-H' in the Croton Falls quadrangle, at a road cut on Route 22, 1.2 kilometers south of the intersection of Route 22 with Route 138. Microphotograph, Fig. 8B.

Basal Member, Ned Mountain Formation

Metabasite/Mafic metasedimentary rock suite

1319. Rusty-weathering, dark grey medium-grained gneiss; breaks in slabby fashion on biotite-rich layers. (Adjoining beds are graphitic granofelses.) (Central Peach Lake quadrangle, south of North Salem)

SGB21b. Rusty-weathering, medium-grained, dark grey gneiss. Collected on transect H-H' in the Croton Falls quadrangle, about 5 meters south of SGB20.

1845a. Rusty-weathering, medium-grained grey-green schistose gneiss. Collected on transect E-E' in the White Plains quadrangle, about 10 meters north of the Saw Mill River Parkway, and approximately 800 meters northwest of the intersection of the Saw Mill River Parkway with the Cross Westchester Expressway. Microphotograph, Fig. 10D.

1905. Rusty-weathering, medium-grained dark grey schist with greenish cast. Collected on transect B-B' in the Mount Vernon quadrangle, on the north side of Jackson Avenue, approximately 100 meters west of the south bound entrance ramp for the Sprain Brook Parkway.

SGB22a. Rusty-weathering, medium-grained, dark grey gneiss. Collected on transect H-H' in the Croton Falls quadrangle, about 32 meters south of SGB 20.

1719. Rusty-weathering, medium- to coarse-grained grey gneiss. (East-central Peach Lake quadrangle)

1560b. Rusty-weathering, medium-grained grey granofels. (Central Peach Lake quadrangle, near the north shore of Turtle Lake). Microphotographs, Figs. 10C and 12C.

Calc-silicate rock

2675. Brown-weathering, medium-grained, grey calc-silicate rock, enclosing a large disc of quartz (quartz disc was excluded from mode). (Near Ned Mountain Road in the northern Peach Lake quadrangle)

TABLE 3, CONTINUED

Metaconglomerate

1742. Brown- to rusty-weathering, grey-green, medium-grained but coarse- ("date-nut loaf") textured gneiss. (Between Lake Windwing and Ned Mountain Road in the northeastern Peach Lake quadrangle)

Meta-arkoses

1349. Grey, medium-grained, well-bedded quartz-rich granofels, pitted on the weathered surface. (Central Peach Lake quadrangle)
1546. Grey, medium-grained, well-bedded granofels with thin biotite-rich laminae. (Central Peach Lake quadrangle)
1669. Rusty-weathering, grey, fissile, medium-grained granofels with quartz- rich ovoids and green-colored discs composed of fine-grained biotite and plagioclase (mode is given for matrix material). (Northeastern Peach Lake quadrangle) Photographs, Fig. 11D and E.

K-rich metasaprolite

730. Medium-grained grey schistose gneiss. (North-central Peach Lake quadrangle)
1359. Medium- to coarse-grained grey schistose gneiss with garnet porphyroblasts. (Central Peach Lake quadrangle) Phtograph, Fig. 12.
1550. Coarse-grained, yellow-brown weathering, pinkish schistose gneiss. (Central Peach Lake quadrangle)
1593a. Medium-grained, rusty-yellowish weathering, schistose gneiss. (Central Peach Lake quadrangle)

Volcaniclastic Member

Layered quartzo-feldspathic rocks

1515. Medium-grained, buff-weathering, light-pink lineated gneiss. (Southwestern Peach Lake quadrangle) Microphotographs, Fig. 15B, C, D, and G.
1524. Medium-grained, grey, thin-layered gneiss. (Southeastern Peach Lake quadrangle)
1543. Rusty-weathering, light grey to pink banded gneiss. (East-central Peach Lake quadrangle)
1345. Medium-grained, grey and beige thin-bedded gneiss (bedding 5 to 20 millimeters in thickness). (East-central Peach Lake quadrangle) Photograph, Fig. 14B.
1399. Medium-grained, pink and grey banded gneiss with green and white bleps and streaks consisting of calc-silicate minerals. (East-central Peach Lake quadrangle) Photograph (outcrop), Fig. 14A.
1415. Medium-grained schistose gneiss with thick black biotite-rich folia. (East-central Peach Lake quadrangle)

Hypersolvus granite

1514. Unfoliated medium-grained pink granite (pink alkali feldspar plus grey quartz, black biotite, and opaque minerals). (Southwestern Peach Lake quadrangle) Microphotograph, Fig. 17.

TABLE 3, CONTINUED

Amphibolites

737. Medium-grained, dark, banded amphibolite. (Central Peach Lake quadrangle, southwest of Mamanasco Lake)
2496. Medium-grained, grey, slabby amphibolite. Collected on transect D-D' in the White Plains quadrangle, in V Everit Macy County Park, 100 meters west of the Saw Mill River Parkway, and 1.8 kilometers north of Route 138.

Wacke Member

Basal Wacke Member

1672. Medium-grained white, black, and red gneiss with quartz-rich segregations. Collected in the northeastern Peach Lake quadrangle (Plate III).

Metawackes

K10 Medium-grained, grey, schistose gneiss. (North of Lake Windwing in the northeastern Peach Lake quadrangle)
193a. Medium-grained, white, black, and red schistose gneiss. (Southern Brewster quadrangle)
1249. Medium-grained, brown- to rusty-weathering schistose gneiss. (Northern Peach Lake quadrangle)
1665. Medium-grained, brown- to rusty-weathering, white, black, and red layered gneiss. (Northeastern Peach Lake quadrangle)
1697. Medium-grained, light grey gneiss with pale pink garnets. (Southern Brewster quadrangle) Microphotograph, Fig. 58B.

Metapelite

1243. Medium-grained, medium-grey gneiss. (Near Ned Mountain Road in the northeastern Peach Lake quadrangle)

Quartz-feldspar-biotite-garnet granofels

1641. Medium-grained grey gneiss. (Northeastern Peach Lake quadrangle)
1644. Medium-grained, brown-weathering grey gneiss. (Northeastern Peach Lake quadrangle)
1646. Medium-grained, brown-weathering, light grey gneiss. (Northeastern Peach Lake quadrangle)

Metabasites

552b. Medium-grained, black amphibolite. (Southern Brewster quadrangle)
1252. Medium-grained, dark grey amphibolite, with pitted, greenish weathered surface. (Northern Peach Lake quadrangle)
1305. Brown-weathering amphibolite. (Southern Brewster quadrangle)
1311. Medium-grained, dark, brown-weathering amphibolite (Amphibolite bed is ~6.5 centimeters thick; layer II is metawacke). (Southern Brewster quadrangle)
1663. Medium to dark grey, well-bedded gneiss (layer II is quartz-feldspar-biotite-garnet granofels). (Northeastern Peach Lake quadrangle)
1679. Dark grey to black, brown-weathering amphibolite. (Southern Brewster quadrangle)

TABLE 3, CONTINUED

K-rich metasaprolite

1690a. Medium-grained, light brown weathering, beige to tan gneiss. (Southern Brewster quadrangle)

Calc-Silicate Member

Felsic metatuff

1435. Light brown-grey weathering, light grey to buff, medium- to fine-grained lineated gneiss (layer II is marble). (East-central Peach Lake quadrangle) Microphotograph, Fig. 15E; hand specimen photograph, Fig. 18.
1445. Medium-grained, yellow-tan weathering, tan granofels. (Southeastern Peach Lake quadrangle) Microphotograph, Fig. 15A.
1470. Medium-grained, grey-weathering, light grey to buff, lineated gneiss with close-spaced biotite-rich laminae. (Southeastern Peach Lake quadrangle)
1566b. Brown- to rusty-weathering, light grey lineated gneiss. (This gneiss occurs as a thin interbed within marble.) (East-central Peach Lake quadrangle)

Quartz-feldspar granofels: quartz-K-feldspar

V6-V8. Medium-grained, grey- and brown-weathering, buff-colored granofels. Collected on transect E-E' in the White Plains quadrangle, 900 meters north-north east of the intersection of the Cross Westchester Expressway with White Plains Road and 20 meters east of the Saw Mill River Parkway.
311. Medium-grained, rusty-weathering, buff-colored granofels. Collected on transect K-K' in the Croton Falls quadrangle, on a roadcut on the east side of Route I-684, 1.1 kilometers northwest of the intersection of Route 22 with Route 116.
1634. Medium-grained, buff-colored granofels, with bleps of green diopside. (Layer II is a calc-silicate rock.) (Collected by the eastern outlet of Lake Windwing in the northeastern Peach Lake quadrangle)

Quartz-feldspar-biotite-garnet granofels

735. Medium-grained, rusty-weathering, buff-colored granofels. (Southwest of Lake Mamanasco, central Peach Lake quadrangle)
1421. Medium-grained, dark brown-weathering, dark grey gneiss with well-developed quartz ribbons. (Southwestern Peach Lake quadrangle)
1441. Well-bedded, rusty-brown weathering, grey granofels. Granofelsic layer I (~1 centimeter thick) is interbedded with thin (~2 millimeter) biotite- and sillimanite-rich pelitic laminae (layer II). (Southeastern Peach Lake quadrangle)
1493a. Medium-grained, rusty-weathering grey granofels (layer I) with white quartzitic lenses (layer II) and interbedded with dark calc-silicate rock (layer III). (Southeastern Peach Lake quadrangle)
1502. Brown-grey weathering, grey granofels with very thin, close-spaced biotite folia. (Southeastern Peach Lake quadrangle)

TABLE 3, CONTINUED

Miscellaneous quartz-feldspar granofelses

1368. Brownish weathering, finely laminated tan granofels. (Layer II is a white-and-green calc-silicate rock.) (East-central Peach Lake quadrangle)
1520. Medium- to fine-grained, finely laminated medium grey granofels. (Southeastern Peach Lake quadrangle)
1588b. Medium-grained, yellow-brown to rusty weathering, light grey granofels. (Southwest of Lake Mamanasco, central Peach Lake quadrangle)

Marbles

1383. Grey-weathering, light grey marble. (Near Route 35, southeastern Peach Lake quadrangle)
1566a. Tan-weathering, buff marble. (East-central Peach Lake quadrangle)

Calc-silicate rocks: White-and-green

177. Medium-grained, thin-bedded grey granofels. (Southeastern Peach Lake quadrangle)
1308. Medium- to coarse-grained, tan- and rusty-weathering, buff and green granofels. (Southern Brewster quadrangle)
1526a. Medium-grained, thin-bedded, grey granofels. (Calcite-rich beds on this specimen are preferentially weathered out.) (Southeastern Peach Lake quadrangle)
1634. Coarse-grained, green granofels. (Layer I is a quartz-K-feldspar granofels). (Collected by the outlet on the eastern shore of Lake Windwing, northeastern Peach Lake quadrangle)

Dark calc-silicate rock

1939b. Medium-grained, rusty-weathering, thin-bedded, dark khaki-colored granofels. (Though mode is given for a K-feldspar-free layer, some beds in this dark calc-silicate rock are K-feldspar-rich). Collected on transect F-F' in the Ossining quadrangle, on the north-bound entrance ramp to the Saw Mill River Parkway at Chappaqua.

Metawacke

1385. Medium-grained, rusty-brown weathering schistose gneiss with pale-pink garnets. (By Route 35, southeastern Peach Lake quadrangle) Micrographs, Figs. 59B and 64B.
1507. Light-grey to rusty weathering grey schistose gneiss. (Southwestern Peach Lake quadrangle)

Metapelite

1565a. Dark, rusty-weathering, medium-grained schist with large garnet porphyroblasts. (East-central Peach Lake quadrangle)

TABLE 3, CONTINUED

K-rich metasaprolite

1379. Medium-grained, rusty-weathering, light grey gneiss with white (sillimanite/quartz) streaks, some of which enclose garnet porphyroblasts. (By Route 35, southeastern Peach Lake quadrangle)
1381. Medium-grained, rusty-weathering, light grey gneiss with streaks of white sillimanite. (By Route 35, southeastern Peach Lake quadrangle)

Dark phosphathic gneiss

1222c. Medium-grained, brown-weathering schist. Collected on transect K-K' in the Croton Falls quadrangle, approximately 700 meters north of the intersection of Route 22 with Route 116.
2108. Medium-grained, dark grey schistose granofels. Collected on transect G-G' in the Ossining quadrangle, 1360 meters southwest of the intersection of Spring Valley Road and Blinn Road and 200 meters due east of Spring Valley Road.

Garnet-hornblende granofels

1884. Medium-grained, grey- and brown-weathering, medium-grey granofels. Collected on transect A-A' in Mount Vernon quadrangle, on Parkview Avenue, 60 meters north of the intersection of Parkview with Pondfield Road West (just west of the Bronx River Parkway).
2468. Medium-grained, yellow-brown weathering, streaky grey granofels. Collected on transect E-E', 210 meters northeast of the Saw Mill River Parkway, 720 meters southeast of Beaver Hill, at the southern corner of a large building.

Amphibolites

1416. Medium-grained, dark-brown weathering amphibolite. (Southwestern Peach Lake quadrangle)
1469a. Brown-weathering, well-bedded amphibolite. (Layer II has 7% K-feldspar; layer III is a diopside-rich calc-silicate rock.) (Southeastern Peach Lake quadrangle)
1522. Medium- to fine-grained, grey-brown weathering amphibolite. (Southeastern Peach Lake quadrangle)

Amphibolite dike in the Fordham Gneiss

2215. Fine-grained, rusty-weathering, dark, unfoliated amphibolite. Collected on transect H-H' in the Croton Falls quadrangle, from a roadcut on Route 22, 1.7 kilometers south of the intersection with Route 138. Photograph (outcrop), Fig. 21.

Diffuse contact. The best-studied example of a diffuse, hard-to-pinpoint contact between the Fordham Gneiss and the Ned Mountain Formation is located in the Croton Falls quadrangle, on transect H-H' (Plate II). On this transect, the unconformity crops out on a road cut along Route 22, 1.2 kilometers south of the intersection with Route 138. The Fordham Gneiss here is a coarse-grained, leuco- to melanocratic orthopyroxene gneiss, similar to the orthopyroxene gneiss member of the Fordham in the study area. Mineralogically, it consists largely of plagioclase, quartz, orthopyroxene, hornblende, and biotite; minor garnet and cummingtonite are present in some samples.

A ~5.3 meter-thick lithologically heterogeneous zone occurs structurally above the continuous sequence of Fordham gneisses (Fig. 8A). Infolds of Fordham Gneiss occur within the heterogeneous interval. A dark, fine- to medium-grained, biotite- and garnet-rich gneiss repeatedly crops out in the zone. Medium-grained amphibolites and light grey quartz-plagioclase-biotite granofelses are also present. The dark biotite-garnet gneiss disappears above the heterogeneous zone, and intensely rusty-weathering, highly graphitic, schistose granofels of the Basal Member makes its first appearance.

Thin-section examination of the dark biotite-garnet gneiss shows that it consists of plagioclase, biotite, quartz, garnet, and graphite (SGB #20a and b, Table 3). Some layers have as much as 47 modal percent biotite.

The dark biotite-rich gneiss contains light-colored, discontinuous, quartz-free lenses, two centimeters or less in width. They are composed of plagioclase, garnet, biotite, graphite, green (hercynitic) spinel, and corundum (specimen #SGB 20b, Table 3; Fig. 8B). The plagioclase in these lenses is very heterogeneous in composition. Some grains are ~An_{35}, while other grains are zoned from An_{50} to An_{75}. The plagioclase-biotite gneiss, with its plagioclase-garnet-corundum-green (hercynitic) spinel lenses, forms a striking compositional contrast to the nearby tonalitic orthopyroxene gneiss of the Fordham. The plagioclase-biotite-garnet gneiss is depleted in silica and enriched in alumina and calcium in comparison with the orthopyroxene gneisses.

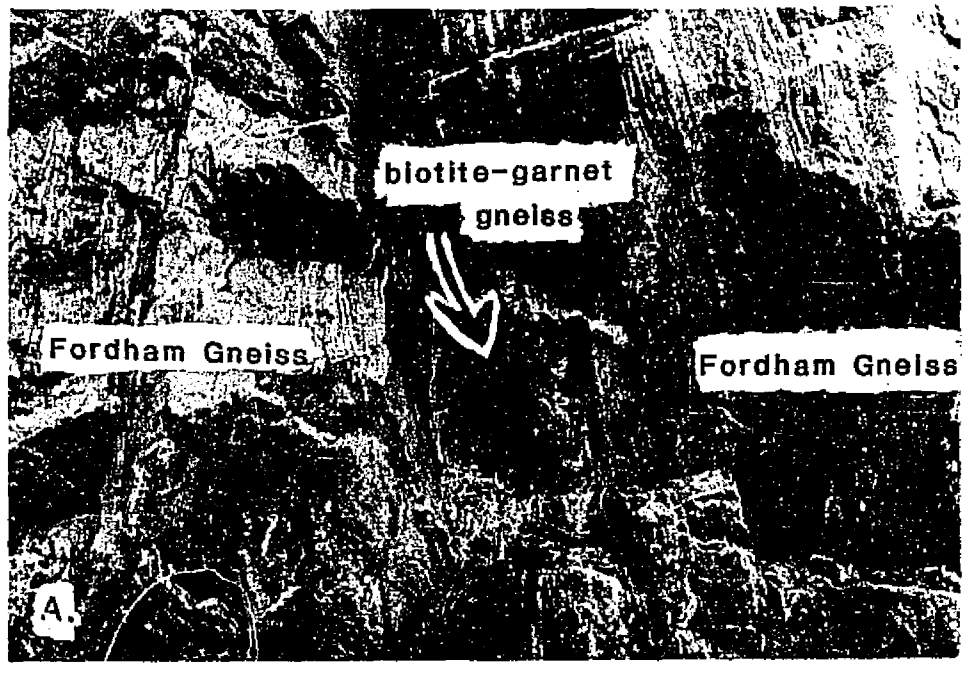

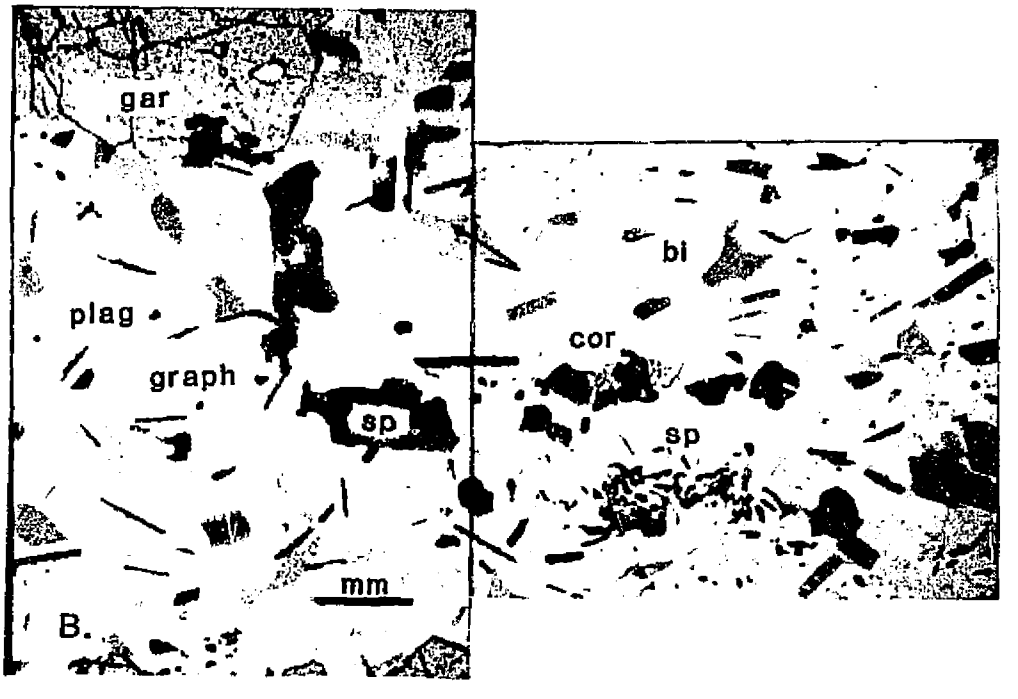

Fig. 8. (A) Blocky-weathering, layered orthopyroxene gneiss of the Fordham Gneiss with an infold of the dark biotite-garnet gneiss belonging to the "diffuse" unconformity zone, transect H-H', Croton Falls quadrangle. Hammer is 40 centimeters long.

(B) A silica-poor lens in the dark biotite-garnet gneiss from the "diffuse" unconformity zone (specimen #SGB 20b; mode on Table 4). bi=biotite; cor=corundum; gar=garnet; graph=graphite; plag=plagioclase; sp=green (hercynitic) spinel.

The dark biotite-rich gneiss and associated light-colored lenses also contrast with the stratigraphically higher Ned Mountain lithologies. None of the granofelses that outcrop above the 5.3 meter heterogeneous zone at this outcrop are deficient in silica or particularly rich in alumina. Garnet is very sparse in these rocks.

Interpretation of the contact between the Fordham Gneiss and the Ned Mountain Formation. The characteristics of the contact between the Ned Mountain Formation and the Fordham Gneiss yield clues about the conditions that accompanied the creation of the unconformity. Relationships observed at this contact, which lead to intriguing inferences, include the following:

1) Portions of the Wacke Member which immediately overlie the Fordham Gneiss contain a much higher proportion of Na-plagioclase than do other metasedimentary rocks of the Ned Mountain Formation (Fig. 13). In this respect, they resemble the Fordham Gneiss instead. Their protolith may have been a regolith of slightly weathered Fordham Gneiss, with Fordham-like proportions of quartz, plagioclase, and K-feldspar, and a minor clay component. Such a regolith may have formed in upland areas, or in regions of moderate slope.

2) The Fordham Gneiss is generally poorer in quartz and richer in biotite, garnet, and plagioclase next to the unconformity than it is elsewhere. The dark biotite-garnet gneiss from transect H-H' represents the most extreme example of this trend. These mineralogical changes indicate depletion of silica and enrichment of alumina and calcium in the Fordham immediately below the unconformity. Shifts in rock composition of this nature imply that the uppermost Fordham is locally a metamorphosed Precambrian saprolite or paleosol. Such a saprolite could have evolved from unweathered Fordham Gneiss through the destruction of primary minerals, the accumulation of such clay minerals as kaolinite, illite, and smectite, and the development of calcareous nodules. The presence of calcareous nodules would imply semi-arid climatic conditions.

3) Some specimens of the dark biotite- and garnet-rich metasaprolite contain up to three

modal percent of graphite. This graphite attests to the presence of organic matter, laid down, perhaps, in seasonal ponds. The stratigraphically higher Ned Mountain granofelses are very graphite-rich, indicating continued high organic productivity. Life-forms of some kind flourished in the inferred Late Precambrian or Early Cambrian terrestrial environment.

NED MOUNTAIN FORMATION, BASAL MEMBER. The Basal Member of the Ned Mountain Formation is the thinnest of all the stratigraphic units mapped in the study area (Plate I). Its greatest thickness in outcrop, including uncounted repetitions due to folding, is less than 300 meters. Yet the Basal Member displays many of features that characterize the Ned Mountain Formation as a whole. These features include the occurrence of certain distinctive and unusual rock types, lateral discontinuity of individual beds, and considerable lithic diversity. Most of the lithologies that are present in the remainder of the Ned Mountain Formation are represented within the Basal Member.

The Basal Member contains medium-grained, graphitic quartz-feldspar granofels (interpreted as meta-arkose), coarse-textured, dark, graphitic granofels (interpreted as metaconglomerate), quartzite, calc-silicate rock, K-feldspar-biotite-garnet gneiss (interpreted as K-rich metasaprolite), K-feldspar-quartz gneiss (interpreted as metarhyolite), amphibolite, and medium-grained, graphitic quartz-plagioclase-biotite granofelses with amphiboles or orthopyroxene (interpreted as sandy metasediments with admixtures of mafic volcanic debris). These last rocks are remarkably persistent as well as extremely distinctive, and have been encountered in the Basal Member in four different quadrangles (Plate IIC).

The Basal Member can be described in terms of two principal rock associations, the metabasite/ mafic metasedimentary rock suite and the meta-arkose/K-rich metasaprolite suite, both of which include quartz-feldspar granofelses. Descriptions of these associations (and the minor rock types) are given in the succeeding sections, and are followed by a discussion of the

regional lithologic variations in the Basal Member.

Metabasite/mafic metasedimentary rock suite. A well-bedded sequence of amphibolites, graphitic cummingtonite-, hornblende-, clinopyroxene-, or orthopyroxene-bearing quartzose granofelses, and very minor quartz-rich granofels overlies the lithologically heterogeneous zone on transect H-H' that contains the dark biotite- and garnet-rich metasaprolite. Comparable assemblages of metabasites and graphitic mafic schists and granofelses are found in the Basal Member on transects B-B', D-D', E-E', and I-I' (Plate III), as well as in the southern and central Peach Lake quadrangle.

Most beds of the metabasite/mafic metasedimentary rock suite are rusty-weathering. Sharp compositional changes occur on bedding planes; where the rocks are fresh, dark grey or black layers rich in mafic minerals contrast with light- to medium-grey quartz-feldspar granofelses. Many of the metabasite beds consist of black amphibolite, though some layers of medium-grained, dark grey-green mafic orthopyroxene gneiss occur in the Peach Lake quadrangle. Most of the metabasite layers are less than two meters in thickness; all are concordant with adjacent beds of quartz-feldspar granofels. Fig. 9 illustrates the well-defined bedding characteristic of the metabasite/mafic metasedimentary rock suite.

Abundant graphite is a hallmark of this lithic assemblage at most localities. Graphite is uncommon (though not unknown) among those rocks that contain more than 25 modal percent amphibole and/or pyroxene. All other granofelsic rock types, however, commonly contain 3 to 8 percent modal graphite.

The most abundant rock types in this suite throughout the Manhattan Prong are light- to medium-grey granofelses and schistose granofelses. The amount of biotite in each bed largely determines its color and degree of schistosity. Garnet occurs in some biotite-rich layers. Many of the granofelses contain minor amounts of pyroxene or amphibole (Fig. 10), mostly in the range of <1 to 15 modal percent. The quartz content of the granofelsic beds ranges from 25 to 70 modal

Fig. 9. Well-bedded sequence of mafic metasedimentary rocks. One bedding plane is highlighted for clarity. Ned Mountain Formation Basal Member, transect E-E', White Plains quadrangle. Lens cap is 5.5 centimeters in diameter.

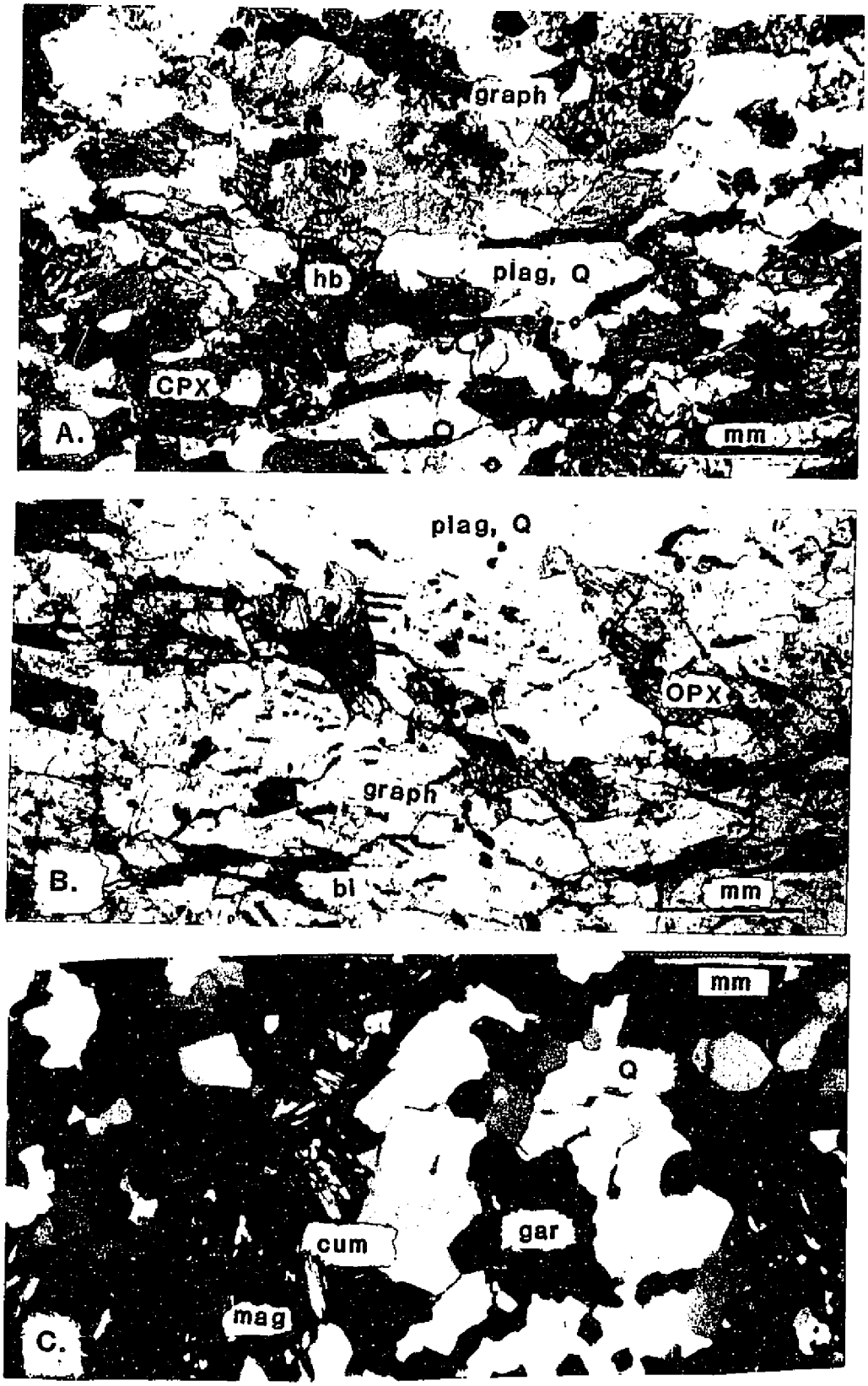

Fig. 10. Mafic metasedimentary rocks of the Ned Mountain Formation Basal Member. Caption on next page.

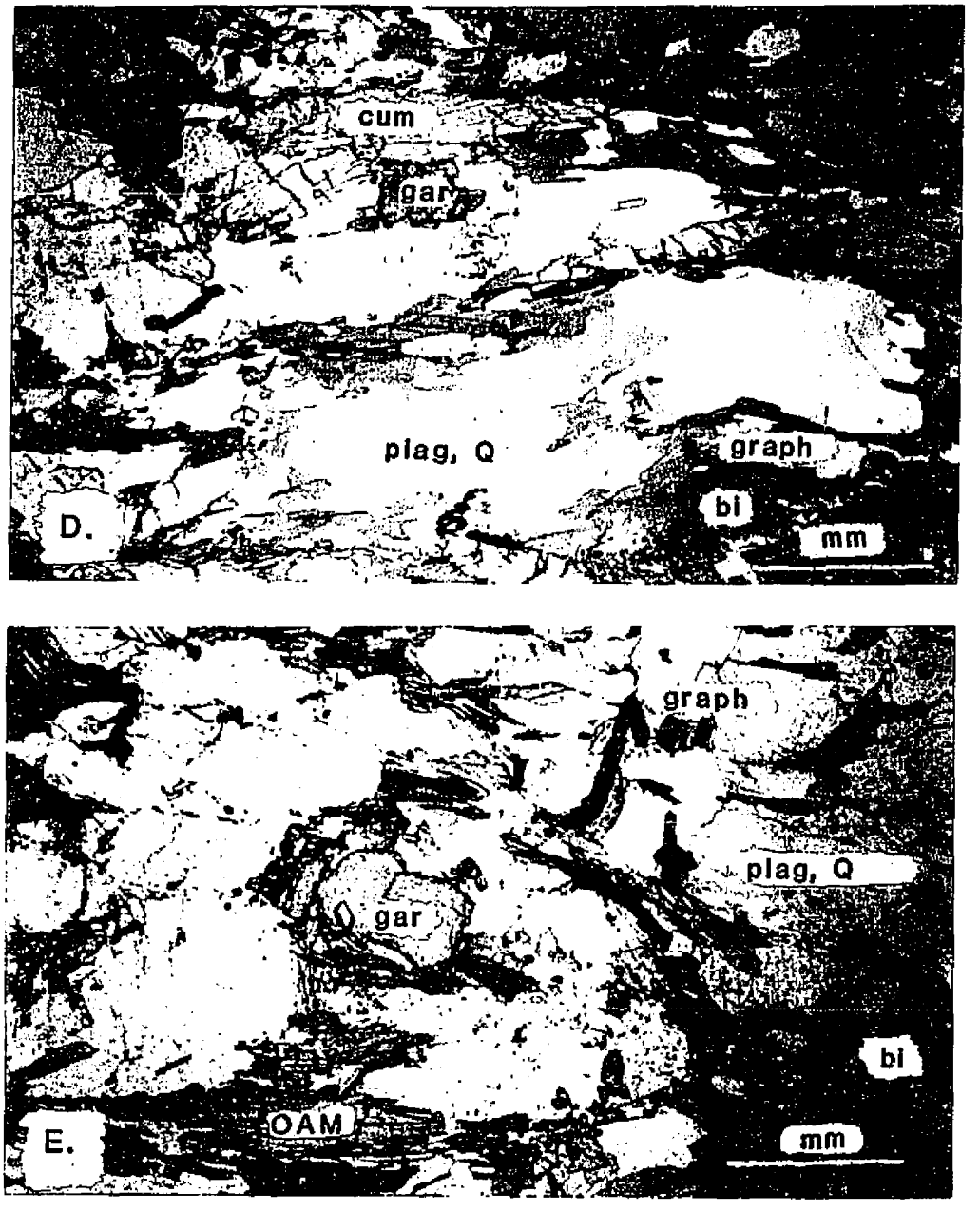

Fig. 10. Mafic metasedimentary rocks of the Ned Mountain Formation Basal Member. OAM=orthoamphibole; OPX=orthopyroxene; CPX=clinopyroxene; bi=biotite; Q=quartz; cum=cummingtonite; gar=garnet; graph=graphite; hb=hornblende; mag=magnetite; plag=plagioclase.

(A) Graphitic hornblende-augite granofels, transect H-H', Croton Falls quadrangle, specimen #SGB21a. Collected near the "diffuse" unconformity zone shown in Fig. 8.

(B) Graphitic orthopyroxene-bearing granofels, specimen #1320a.

(C) Cummingtonite-garnet quartzite (feldspar-free), with crossed nicols; specimen #1560b. (Mode is given on Table 3; contact with K-rich metasaprolite is shown on Fig. 12C.)

(D) Graphitic cummingtonite-garnet-biotite schist, specimen #1845a, transect E-E', White Plains quadrangle. (Mode is given on Table 3).

(E) Graphitic orthoamphibole-garnet-biotite schist, specimen #2280b, transect E-E', White Plains quadrangle.

percent (examples on Table 3).

The granofelses display a uniform, fine-to-medium grained texture, and dark minerals commonly occur together in biotite-rich beds or lamellae. Microscopic examination is usually necessary in order to distinguish amphibole- and orthopyroxene-bearing granofelses from those composed simply of quartz, feldspar, biotite, and garnet. Of the thirty-five thin-sections of light- to medium-grey granofels and schistose granofels from this suite that were examined, twenty-three were found to contain amphibole and/or pyroxene. These minerals had not been detected macroscopically.

Compositions of plagioclases from this rock suite correlate with modal quartz content and mafic mineralogy (see Table 3). Granofelses composed of 50 to 70 percent quartz contain plagioclase in the range of An_{22} to $_{34}$, while those that contain only 25 to 50 percent quartz, along with some amphibole or pyroxene, have a plagioclase of composition An_{34} to An_{55}. Orthopyroxene-bearing metabasites of the Basal Member, by comparison, contain plagioclase of about An_{60} composition (e.g., specimen #1319-I, Table 3), whereas hornblende amphibolites have plagioclase of An_{37} to An_{44} (e.g. SGB21b, Table 3).

One to two modal percent of opaque minerals other than graphite occur in most rocks of this suite. Of these minerals, pyrrhotite is generally dominant. One quartz-rich specimen (#1560b, Table 3) is rich in magnetite. The metabasites generally also contain substantial ilmenite. Apatite is another common accessory mineral; some granofelsic beds contain as much as one modal percent. Specimen 1395a, from a biotite-rich gneiss that crops out near mafic metasedimentary rocks, is exceptionally rich in apatite, containing 5 modal percent.

Interpretation of the metabasite/mafic metasedimentary rock suite. The amphibolites and orthopyroxene-rich gneisses are interpreted as metabasalts (or basaltic metatuffs) because of their mafic character and conformable contacts. The quartz-rich and quartz-plagioclase-biotite granofelses are considered to be subarkosic and arkosic metasandstones, respectively. The darker, rela-

tively biotite-rich garnetiferous schistose granofelses are interpreted as metamorphosed argillaceous sandstones.

The amphibole- and orthopyroxene-bearing granofelses are construed as metasedimentary rocks because they are well- bedded, commonly graphitic, and in many instances quartz-rich. The presence of amphiboles or orthopyroxene in these rocks indicates exceptionally high bulk $(Fe^{+2} + Mg^{+2})/Al^{+3}$ ratios compared to those of most metamorphosed clastic rocks. As the result of these high ratios, aluminous ferromagnesian silicate minerals such as garnet and biotite (which are commonly found in metaclastic rocks) cannot accommodate the entire $Fe^{+2} + Mg^{+2}$ content of the granofelses. These high $(Fe^{+2} + Mg^{+2})$ to Al^{+3} ratios are most readily explained by the presence of unweathered mafic material, possibly mafic tuff, in the protolith.

Those mafic metasedimentary rocks which have the lowest modal quartz contents also contain plagioclases which are compositionally similar to ones from nearby metabasites. Plagioclases from associated quartz-rich granofelses are less calcic. This correlation supports the proposal that the amphibole- and orthopyroxene-bearing granofelses represent mixtures of unweathered mafic material and siliciclastic sediments. The proportions of mafic debris and siliciclastic sediments apparently varied over time, resulting in the observed bed-by-bed compositional changes.

The principal inputs to the metabasite/mafic metasedimentary rock assemblage are inferred to have been quartz-plagioclase sands, probably derived from the underlying Fordham Gneiss; mafic flows and/or tuffs; and subordinate clay. The abundance of graphite in many beds indicates that deposition generally took place in an organic-rich, poorly oxidized environment, such as a stagnant pond. The non-graphitic granofelses probably originated as subaerial, perhaps alluvial, deposits.

Amphibole- or orthopyroxene-bearing mafic metasedimentary rocks and beds of metabasite invariably occur together in the Basal Member, but are not so linked higher in the Ned Mountain Formation. Higher in the section, metabasites remain abundant, but mafic metasedi-

mentary rocks become very rare.

The mafic minerals present in the mafic metasedimentary rocks vary geographically, and reflect local Paleozoic metamorphic grade. In the northern Peach Lake quadrangle, orthopyroxene is commonly present; in the southern Peach Lake quadrangle, cummingtonite+/-hornblende occurs; in the southern Manhattan Prong, various combinations of orthoamphibole, cummingtonite, and hornblende are encountered (Fig. 10).

Although widespread in the Manhattan Prong, the mafic metasedimentary rocks have not previously been recognized. The obvious bedding and graphite content have often led these rocks to be interpreted as some more ordinary lithology. For instance, in the Mount Vernon and White Plains quadrangles, Hall (1968b) mistook quartz-amphibole-biotite-garnet schist of the Basal Member (Fig. 10D and 10E) for a sillimanite schist of the Fordham Gneiss (transects B-B' and E-E'; see Appendix 1).

Meta-arkose/K-rich metasaprolite suite. The Basal Member contains coarse-textured, dark, graphitic granofels (interpreted as metaconglomerate), quartz-plagioclase-K-feldspar-biotite granofels (interpreted as meta-arkose), calc-silicate rock, K-feldspar-biotite-garnet±sillimanite gneiss (interpreted as K-rich metasaprolite), and K-feldspar-quartz gneiss (interpreted as metarhyolite). This suite of rocks is a major component of the Ned Mountain Basal Member in the Peach Lake quadrangle, though it is minor (compared with the metabasite/mafic metasedimentary rock suite) in the Basal Member of the southern Manhattan Prong.

Coarse-textured graphitic granofels (metaconglomerate). A distinctive dark, coarse-textured, graphitic granofels crops out at the base of the Ned Mountain Formation in a small area just south of Ned Mountain Road in the northeastern Peach Lake quadrangle. Along the unconformity, the Fordham Gneiss typically forms the crown of small hills, and the coarse-textured granofels is exposed lower on the slope. Some granofelses occur within a few meters of outcrops

of the orthopyroxene gneiss member of the Fordham Gneiss. All outcrop of the coarse-textured granofels occurs within ~15 meters of exposed Fordham Gneiss. A persistent stratigraphic succession can be traced: 1) orthopyroxene gneiss of the Fordham; 2) coarse-textured, dark, graphitic granofels, with scattered lenses of calc-silicate rock; 3) garnet-sillimanite schist (transition zone to the Wacke Member of the Ned Mountain Formation). Near Ned Mountain Road, this sequence changes to 1) Fordham Gneiss; 2) thin bed (<1 meter) of calc-silicate rock; 3) predominantly finer-grained, grey graphitic granofels; 4) feldspathic, low-quartz, garnet-sillimanite schist.

The coarse-textured granofels is grey-green in color when fresh, and generally acquires a rusty-brown color with weathering. The texture of the granofels, illustrated in Fig. 11A and B, is coarse and heterogeneous. The rocks commonly present a "date-nut loaf", blotchy appearance (Fig. 11A). The largest specimens so far recovered display dark "blotches" up to ~10 centimeters long when fresh surfaces are cut (Fig. 11B). Etched and stained cut surfaces reveal that the dark "blotches" are richer in feldspar (as well as mafic minerals) than the lighter-colored, quartz-richer matrix (Fig. 11B). No bedding, compositional layering, or ordering of the "blotches" is distinguishable either in the field or in hand specimen. The granofels is not schistose even where 15 percent modal biotite is present; what little foliation is present can be perturbed by local heterogeneities (Fig. 11A). Lenses of grey, graphitic, quartz-diopside-plagioclase-biotite-hornblende calc-silicate rock occur within the coarse-textured granofels.

A range of modal mineralogies have been derived from a suite of etched and stained hand specimens of this lithology. These granofelses contain ~3 to 38 modal percent quartz, 27 to 50 percent plagioclase, and 5 to 35 percent K-feldspar. Minor hornblende, pyroxene, and garnet are commonly present. Biotite ranges between 0 and 15 percent, and graphite from 0 to 6 percent.

A single specimen (#1742, Table 3) has been examined in thin section. Microscopically, feldspars and pyroxenes in this specimen have the coarse, granoblastic texture commonly seen in the Fordham Gneiss (e.g., Fig. 5A). Quartz is concentrated in pockets, where quartz surrounds isolated grains of feldspar. Graphite is distributed throughout the slide. Plagioclase, which has

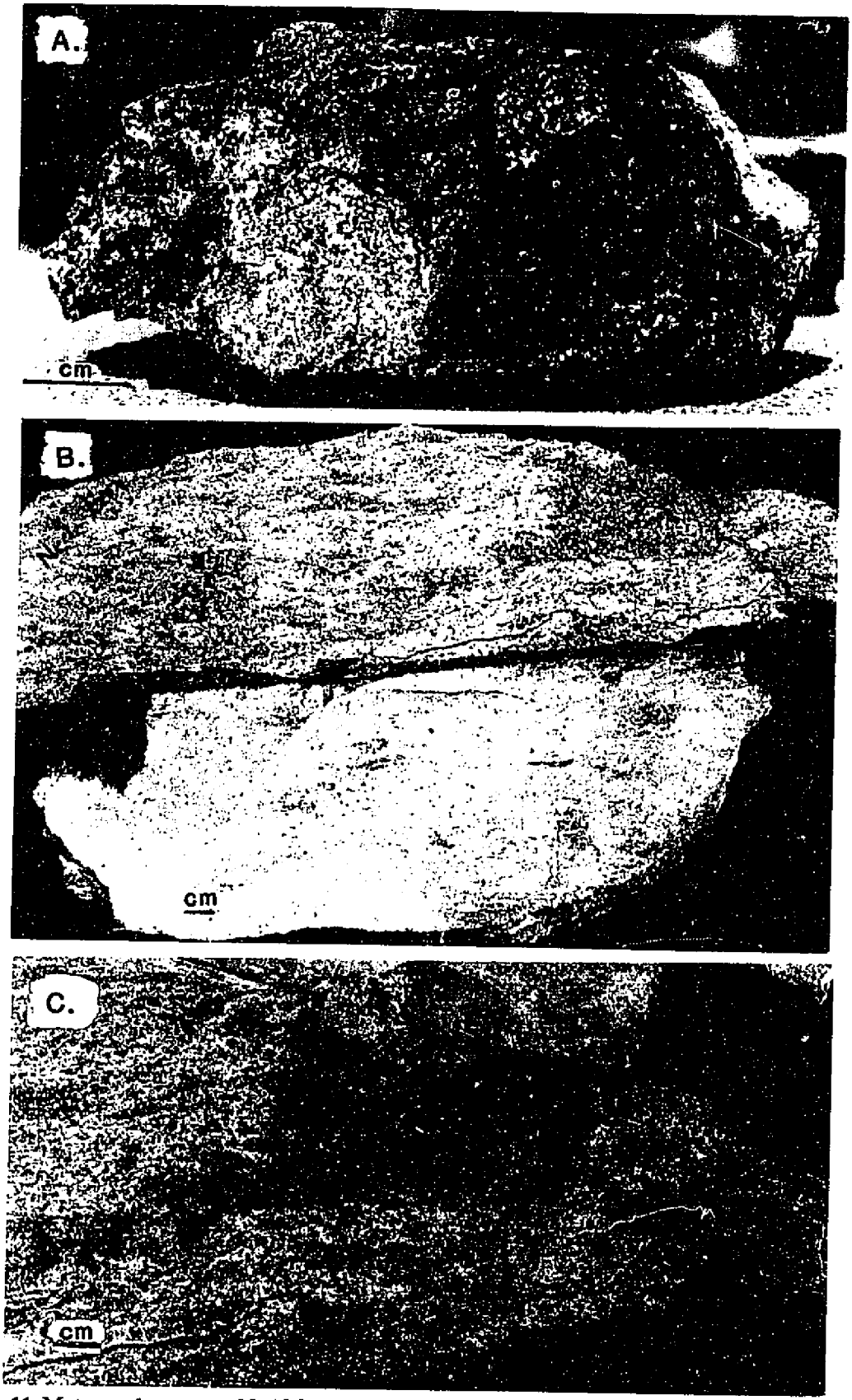

Fig. 11. Metaconglomerates, Ned Mountain Formation Basal Member. See next page for caption.

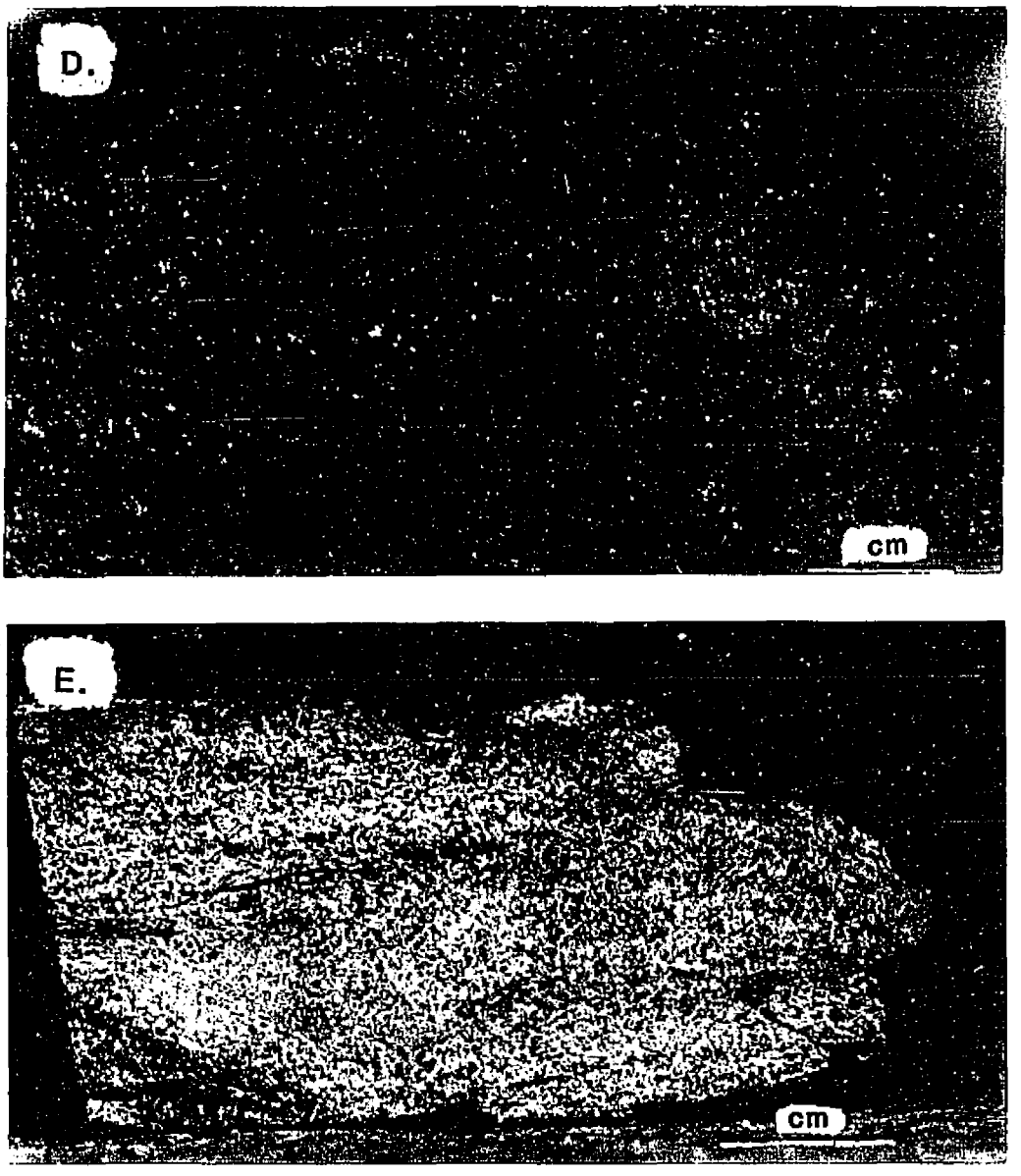

Fig. 11. Graphitic metaconglomerates and meta-arkoses of the Ned Mountain Formation Basal Member. (A) Metaconglomerate, specimen #2511a. Foliation is deflected around oval "blotches", interpreted as clasts.

(B) Metaconglomerate, specimen #1742b. Lower slab (stained for K-feldspar) fits against upper slab. Dark "blotches" on upper slab correspond to yellow, feldspathic zones on lower slab; white zones are quartz-rich.

(C) Close-up of specimen #1742b, seen above.

(D) Rusty-stained weathered surface, typical of the metaconglomerates, most meta-arkoses, and most mafic metasedimentary rocks of the Basal Member. All brightly reflecting grains are graphite. (Meta-arkose specimen #1669a)

(E) Cobble-sized quartz clast in finer-grained meta-arkosic matrix; specimen #1669a. K-feldspar is stained deep yellow; plagioclase is light yellow; quartz is grey. (Mode of matrix is given in Table 3.)

the composition ~An_{45}, is much less calcic than either the plagioclase in the adjacent lenses of calc-silicate rock (~An_{70}) or in the finer-grained graphitic granofels that crops out along strike (#1669, Table 3). It is, however, comparable to plagioclase from the nearby Fordham Gneiss (#1643, Table 2). The coarse-textured granofels contains the mineral assemblage hypersthene + K-feldspar, which also occurs in nearby outcrops of the orthopyroxene gneiss member of the Fordham Gneiss.

Interpretation of the coarse-textured granofels. The observations discussed above permit the drawing of conclusions concerning the (A) stratigraphic position and (B) the protolith of the coarse-textured granofels. The relevant points of evidence are summarized below, together with the conclusions they lead to.

A. Evidence bearing on the stratigraphic position of the coarse-textured granofels:

1) Although much of the coarse-textured granofels and adjacent exposures of the Fordham Gneiss contain comparable proportions of many minerals (quartz, feldspar, biotite, amphibole), the two units are readily distinguished in the field. The granofels sharply contrasts with the neighboring Fordham Gneiss because of its abundant graphite, its rusty stain, its susceptibility to erosion, its failure to display any gneissosity or compositional layering, and its associated lenses of calc-silicate rock.

2) The coarse-textured granofels consistently occurs in immediate proximity to exposures of Fordham Gneiss, and stratigraphically below other Ned Mountain lithologies.

3) The coarse-textured granofels interfingers with and grades northwards into a light-colored, finer-grained granofels. The granofels to the north has the same rusty-weathering, graphitic, unbedded appearance as the coarse-textured granofels, and contains similar lenses of calc-silicate rock. This finer-grained granofels is (as will be discussed in the next section) meta-arkosic in composition.

4) Orientations of foliations in the coarse-textured granofels are statistically distinguishable from those in the adjacent Fordham Gneiss. The "Ned Mountain" foliations plotted in Fig. 3 are taken from both the coarse-textured and the finer-grained graphitic granofelses of the Basal Member, north of Ned Mountain Road.

Inferences: The striking macroscopic differences between the coarse-textured granofels and the Fordham Gneiss reflect their genetically distinct characters. The discrepancy in foliation attitude between the two units points towards an unconformable contact. The map position of the coarse-textured granofels, below all other Ned Mountain lithologies, also places it at the base of the Ned Mountain Formation.

B. Evidence bearing on the protolith of the coarse-textured granofels and its depositional setting:

1) The graphite content of the coarse-textured granofels and the presence of associated calc-silcate rocks indicate a metasedimentary origin.

2) The coarse, "date-nut loaf" appearance indicates the presence of 0.5 centimeter-scale (and larger) heterogeneities in the protolith.

3) The coarse-textured granofels is compositionally similar to underlying Fordham Gneiss in several respects. These include a) feldspar-rich, relatively quartz-poor modes; b) the presence of abundant plagioclase of intermediate composition; and c) the occurrence of mafic minerals such as hypersthene and hornblende. However, graphite permeates the coarse-textured granofels, and its K-feldspar, biotite, and garnet contents are generally greater than those of the Fordham orthopyroxene gneiss. Nevertheless, the coarse-textured granofels is closer to the underlying Fordham Gneiss than to the interfingered, meta-arkosic granofels in its proportions of quartz, feldspars, and mafic minerals.

4) The coarse-textured granofels' coarse, granoblastic texture, as observed in thin section,

is reminiscent of the Fordham Gneiss. The coexisting hypersthene and K-feldspar occur in a coarse-grained, Fordham-like fabric.

5) The coarse-textured granofels has no discernable bedding, and individual specimens show erratic variations in modal compositions.

Inferences: The compositional and textural characteristics of the coarse-textured granofels are most consistent with a massive, conglomeratic protolith. The scattered pockets of granofels containing more than ~10 percent hornblende + pyroxene can be explained as relatively unweathered clasts of Fordham Gneiss. The greater K-feldspar content of the coarse-textured granofels, compared with that of the Fordham orthopyroxene gneiss, may reflect preferential survival of clasts of granite (like the orthopyroxene-bearing granite, illustrated on Fig. 4, that crops out nearby). The occurrence of coexisting hypersthene and K-feldspar in a Fordham-like microscopic texture raises the possibility that some mineral grains from the original clasts of Fordham Gneiss may have survived, at least in microscopic domains. However, any clasts of Fordham Gneiss must have been at least somewhat modified, because boundaries of clasts are not distinguishable in thin section and graphite permeates everywhere.

Quartz-feldspar granofelses (meta-arkoses) and associated calc-silicate rocks. The Basal Member contains many medium-grained, quartz-feldspar granofelses. These granofelses can be subdivided into two distinct varieties: graphite-bearing and graphite-free. Graphite-free granofelses are common in the central Peach Lake quadrangle (West Mountain region, Plate III), but most of the Basal Member granofelses that outcrop in the southern and northern parts of the Peach Lake quadrangle contain between 3 and 7 modal percent graphite. The graphite-bearing and -free granofelses differ in many respects.

The graphite-free granofelses occur in discontinuous belts or lenses several meters in

thickness. They are largely light grey, greyish- or brownish- weathering, well-bedded quartzose rocks. The light-grey beds are generally 1 to 3 centimeters in thickness, and have 5 modal percent of biotite or less. Medium-grey colored interlayers, somewhat richer in biotite and garnet, and biotite-rich laminae a fraction of a millimeter thick are commonly present. The quartz content of these rocks averages 60 to 70 modal percent, though a few beds consist of nearly pure quartz. Plagioclase is generally 0 to 20 percent; some beds contain K-feldspar in addition to or instead of plagioclase.

In contrast, the graphitic granofelses are generally rusty-weathering, poorly bedded, and fairly feldpathic rocks that outcrop in broad swaths. The typical pervasive rusty stain makes the bright flecks of graphite stand out on exposed surfaces (Fig. 11D). Feldspar content ranges from ~20 to about 55 modal percent. The graphitic granofelses are largely composed of randomly-arranged grains of quartz and feldspar, many of them 0.5 to 1 millimeter in size. Some of the graphitic granofelses contain substantial biotite; modal content ranges from <5 to ~35 modal percent, though most contain less than 15. The biotite and graphite grains tend to be evenly distributed through these poorly bedded rocks. Those rocks with substantial biotite contents generally have well-foliated, somewhat schistose textures.

The graphitic granofelses in the northeastern Peach Lake quadrangle contain ovoid quartz-rich domains 1 to 5 centimeters in diameter (Fig. 11E) and green, disc-shaped domains ~1 to 1.5 centimeters in diameter. The green domains principally consist of fine-grained biotite, plagioclase, and hornblende.

The anorthite content of plagioclases from the quartz-feldspar granofelses varies widely. Relatively sodic plagioclase (An_{34}) occurs in a graphitic quartz-K-feldspar-plagioclase-biotite granofels that crops out with rocks of the metabasite/mafic metasedimentary rock suite on transect H-H' in the Croton Falls quadrangle. Plagioclases from quartz-rich granofelses of the mafic metasediment suite at this locality have similar composition. Granofelses in the study area, however, generally contain more calcic plagioclases. Compositions of An_{50} to An_{80} are common-

ly observed, in both graphite-bearing and graphite-free rocks (e.g., #1349 and #1669, Table 3). Quartz-rich, graphite-free granofelses that contain calcic plagioclases develop a distinctive, pitted weathered surface.

Beds and lenses of calc-silicate rock locally occur with graphitic quartz-feldspar granofelses. The calc-silicate rock may be grey or white and green in color, depending on the proportions of white feldspar, grey quartz, and green diopside or hornblende. Carbonate minerals are generally very minor or absent. Graphite is present in some cases.

A bed of calc-silicate rock locally occupies the base of the Ned Mountain Formation (see the description of the "slightly diffuse" Fordham-Ned Mountain contact). This bed is overlain by graphitic quartz-feldspar granofelses. A disc of quartz some 5 centimeters in diameter was encountered in this bed; the disc appears to once have been a cobble-sized quartz clast.

The modal composition of a specimen from this bed (#2675) is given on Table 3. This specimen contains plagioclase of about composition An_{70}. Graphitic quartz-feldspar granofels that crops out nearby contains some plagioclase of similar composition (#1669, Table 3).

Zircon, tourmaline, apatite, allanite, ilmenite, magnetite, and pyrrhotite occur as accessory mineral in the quartz-feldspar granofelses. These minerals generally make up about one modal percent of the rocks.

Interpretation of the protoliths and depositional settings of the quartz-feldspar granofelses (meta-arkoses). The relatively high feldspar and moderate biotite contents of the graphitic granofelses point towards an arkosic protolith. The massive bedding style and tendency towards random distribution of biotite indicate that the sediments of the protolith could have been (at best) only poorly bedded.

The ovoid quartz-rich domains that occur in the granofelses of the northeastern Peach Lake quadrangle (Fig. 11E) probably originated as pebble- and small cobble-sized clasts. The disc-shaped green domains, with their biotite, plagioclase, and hornblende, may once have been

weathered mafic clasts of Fordham Gneiss. Thus, the graphitic granofels that grades into the coarse-textured basal metaconglomerate (discussed in the previous section) is itself somewhat conglomeratic.

Given the inferred coarseness of the protolithic sediments, their feldspathic character, and the absence of bedding, it is probable that these sediments were deposited close to their source area. The depositional setting of the graphitic granofelses (and of the related metaconglomerate) is further constrained by their protoliths' evident richness in organic matter. Modern sands generally contain very little carbonaceous material. Even though much organic material might be locally generated, most sands are deposited in oxygenated environments where organic matter is short-lived. This is true even in such relatively quiet depositional settings as deltas and deep-sea turbidites (Pettijohn, Potter, and Siever, 1973). The high graphite content of the granofelses, as well as their homogeneously distributed biotite, points towards a very quiet depositional setting, undisturbed by current action. The texture and mineralogy of the graphitic granofelses can be explained by a scenario where arkosic sands are transported, via mass-movements, into shallow, stagnant (but organically productive) ponds, situated at the bases of hillslopes.

Quite a different history is implied by texture, bedding style, and composition of the non-graphitic K-feldspar-bearing granofelses. The protolith of these rocks was arkosic but had a relatively high quartz content. The precursor sediments were probably exposed at the surface, subject to chemical weathering, for a relatively long period. The well-bedded character of these rocks implies water-lain deposition. The depositional environment was oxydizing; organic material did not accumulate. Some kind of alluvial setting is likely.

The presence of calcic plagioclase in many of the quartz-feldspar granofelses suggests that the protolithic sediments were cemented by calcite. The lenses of siliceous calc-silicate rock associated with the graphitic granofelses may also have originated as clumps of carbonate-cemented, coarse-grained siliclastic sediments.

K-feldspar-biotite-garnet gneiss and schistose gneiss (K-rich metasaprolite). Meta-arkoses of the Basal Member are commonly associated with highly distinctive K-feldspar-biotite schists or gneisses. These rocks are very rich in K-feldspar, have little or no quartz or plagioclase, and commonly contain substantial garnet and/or sillimanite. Garnet or sillimanite porphyroblasts are commonly prominent on weathered surfaces (Fig. 12A).

The K-feldspar-biotite gneisses occur in zones that range from several centimeters to a few meters in thickness. The K-feldspar-biotite gneisses are not layered compositionally, and show no evidence of internal bedding. Most of these gneisses acquire a rusty stain with weathering, though some develop a greenish-yellow cast. The yellowish-weathering gneisses are highly suspectible to weathering, and erode out preferentially compared with interbedded quartzose rocks or amphibolites. Contacts between the K-feldpsar-biotite gneisses and adjacent lithologies tend to be gradational and ill-defined, though some sharp contacts have been observed (Fig. 12C).

The most remarkable aspect of these rocks, however, is their peculiar composition. The modal K-feldspar content of these gneisses is typically 50 to 80%. Quartz is completely absent in many specimens, but can comprise up to ~12 modal percent of modal composition. Plagioclase generally occurs only as exsolved blebs in perthitic K-feldspars. One anomalous specimen, #2580d (Plate III), contains modal ~22% of a highly calcic (~An_{80}) plagioclase. Though it is fairly rich in Ca, this rock, like the other K-feldspar-biotite gneisses, is very low in Na. Aluminosilicate (sillimanite) and Fe-Mg aluminosilicate minerals (biotite and garnet) are important components of the gneisses; these mineral total, on average, about 36 modal percent. Modal biotite ranges between 5 to 30%, and 10 to 30% modal garnet and/or sillimanite is generally present.

Various combinations of opaque minerals (ilmenite, magnetite, pyrrhotite, pyrite, and graphite) together make up less than 2 modal percent of the rocks. Graphite is generally present in K-feldspar-biotite gneiss from the southern Peach Lake quadrangle, but is less common in the central Peach Lake quadrangle. Examples of modal compositions are given on Table 3.

The K-feldspar-biotite gneisses stand out compositionally from the other metasedimen-

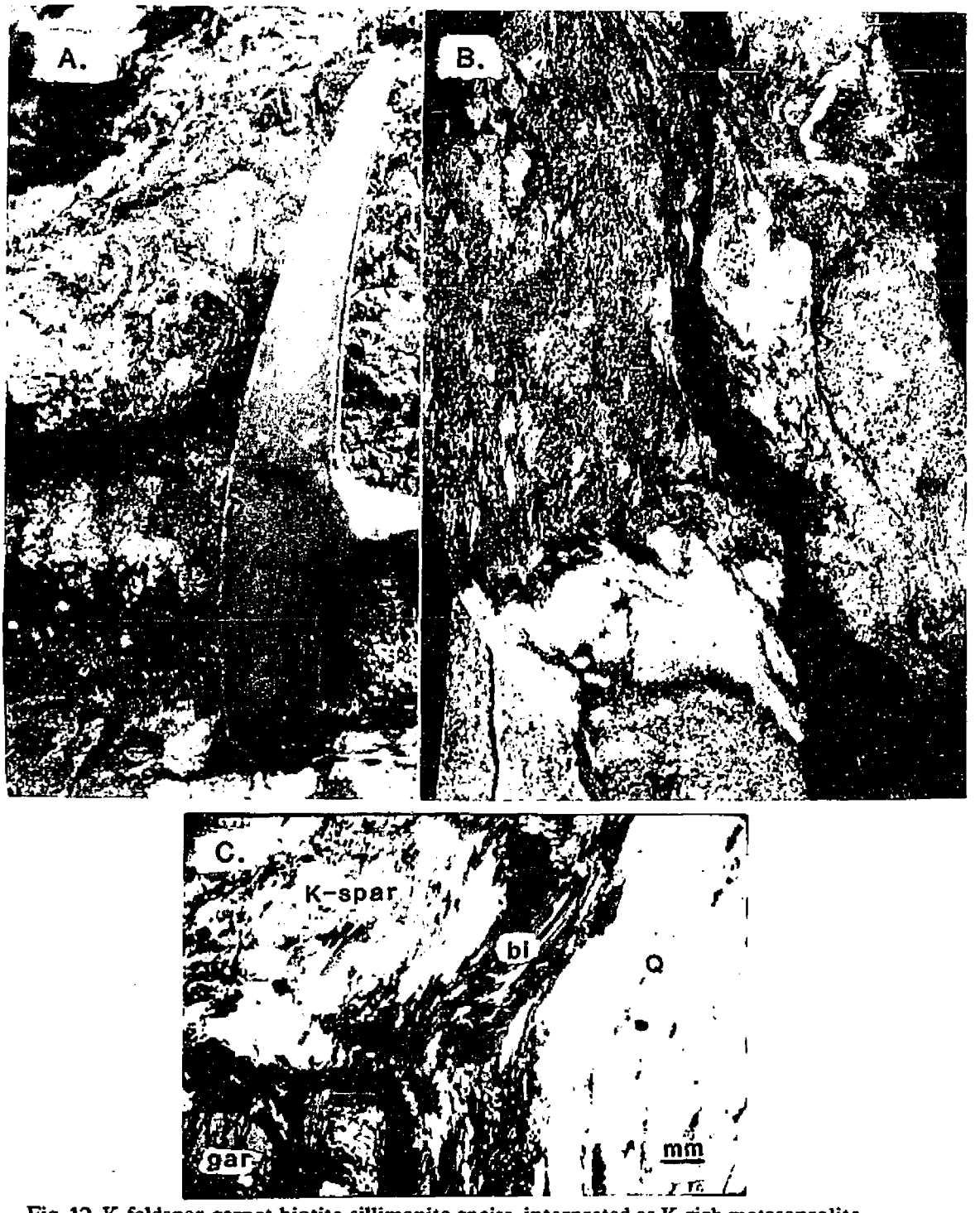

Fig. 12. K-feldspar-garnet-biotite-sillimanite gneiss, interpreted as K-rich metasaprolite.

(A) In outcrop on Old West Mountain Road, near intersection with Oreneca Road. Beige K-feldspar, white sillimanite, and garnets are prominent on the weathered surface. Hammer head is 18 centimeters long.

(B) Slabbed specimen #1359b. Photo approximately actual size. Right-hand piece shows ovoid K-feldspar-biotite "clump". (Mode of #1359 is given in Table 3.)

(C) Contact between K-rich metasaprolite and bed of cummingtonite-garnet quartzite in specimen #1560b. (The quartzite is also illustrated in Fig. 10C.) bi= biotite; gar=garnet; K-spar= K-feldspar (stained yellow); Q=quartz.

tary and metaigneous rock types that occur in the area. In order to illustrate the differences, families of lithologies (metapelite, metawacke, quartz-feldspar granofels, etc.) were first defined on the basis of modal mineralogy, and then each mode plotted on a series of ternary plots (Fig. 13). The data shown on Fig. 13 were compiled from every stratigraphic unit in the study area, except the Fordham Gneiss; rocks from all units are classified in the same fashion. Every lithologic family is shown to have its own characteristic field of modal compositions (Fig. 13).

Metapelites are defined as rocks whose modal aluminosilicate (sillimanite) and Fe-Mg aluminosilicate minerals exceed 50 percent. Rocks that contain smaller amounts of these minerals, and substantial quartz, are classified as metawackes. Fig. 13B shows that quartz predominates over feldspar in both these rock families (as do aluminosilicate minerals, by definition). The metawackes contain more quartz and fewer aluminous minerals than the metapelites, but are otherwise similar (Fig. 13C). Quartz-feldspar granofelses are still more quartzose and less aluminous than the metawackes (Fig. 13D). The K-feldspar-quartz gneisses (Fig. 13E) have roughly granitic compositions; they invariably contain moderate amounts of quartz and little, if any, Fe-Mg aluminosilicate (in these rocks, biotite). These gneisses, discussed later, will be interpreted as metarhyolites and felsic metatuffs.

In contrast with all these rock types, the K-feldspar-biotite gneisses are very high in K-feldspar, very low in quartz and Na-plagioclase, and contain moderate amounts of aluminosilicate and Fe-Mg aluminosilicate minerals. Their modal compositions are plotted in Fig. 13A. There is no overlap between these gneisses and the metapelites, the metawackes, the quartz-feldspar granofelses, or the K-feldspar-quartz gneisses; the K-feldspar-biotite gneisses evidently comprise a distinct lithologic family. In a later section, this family will be interpreted as metamorphosed K-rich saprolite.

Most K-feldspar-biotite gneisses are texturally as well as compositionally distinct from metawacke and metapelite lithologies. The metapelites and metawackes of all formations in the study area show a penetrative and ubiquitous foliation. They are generally migmatized, made

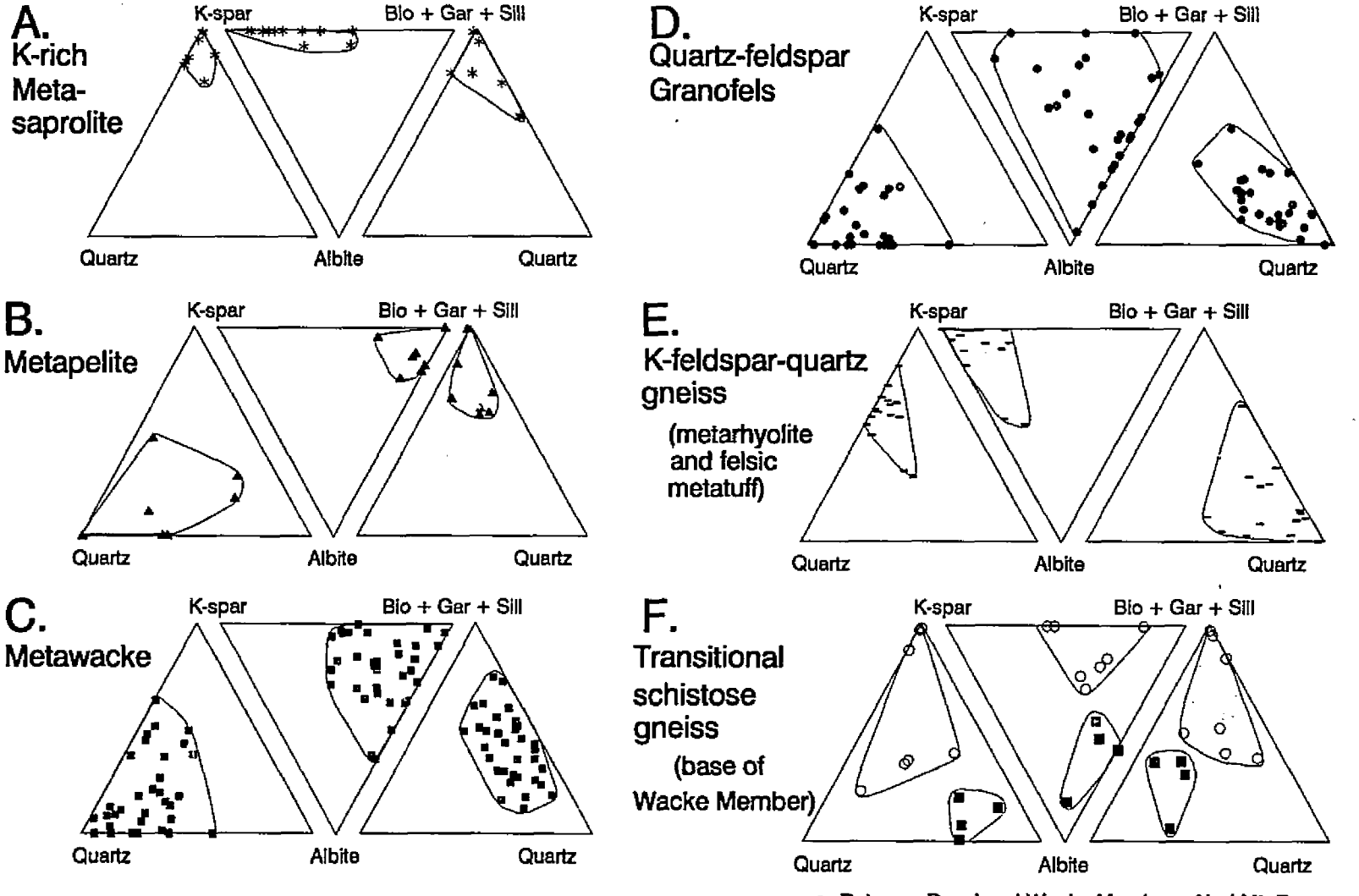

Fig. 13. Composition fields of K-rich metasaprolites compared with those of quartzo-feldspathic metasedimentary and metavolcanic rocks.

up of alternating dark biotite-rich melanosomes and light quartz-feldspar leucosomes, but a gross uniformity of texture and composition exists. The metasaprolites, in contrast, range from poorly- to well-foliated, and include rocks with striking compositional and/or textural heterogeneities as well as apparently homogeneous ones.

Lithologic associations that contain K-feldspar-biotite gneiss. The K-feldspar-biotite gneisses of the Basal Member occur in two different contexts: in the southern and central parts of the Peach Lake quadrangle, they are interbedded with meta-arkoses, the metabasite/mafic metasedimentary rock suite, and K-feldspar-quartz gneiss, while in the northern Peach Lake quadrangle, they occur within a transitional zone located between the graphitic meta-arkose and metaconglomerate of the Basal Member and the overlying Wacke Member. (K-feldspar-biotite gneisses also occur in the Ned Mountain Calc-Silicate Member.) The K-feldspar-biotite gneisses from these two contexts have different macroscopic appearances.

The K-feldspar-biotite gneisses of the southern and central Peach Lake quadrangle are readily distinguished from other Basal Member rocks (and Fordham Gneiss) in the field. They are generally beige-colored, medium to coarse-grained gneisses, with dark brown or reddish biotite concentrated into discontinuous folia. These folia contrast with domains of pink or beige K-feldspar (Fig. 12B). The biotite folia, along with trains of sillimanite, define the rock's schistosity.

Concentrations of K-feldspar, sillimanite, biotite, and garnet commonly occur in irregular clump-like masses. In some cases, the superposition of the poorly foliated "clumps" over a pre-existing fabric indicates that they are at least partially of metamorphic origin. In other cases, "clumps" have a finer grain size and different style of foliation than the surrounding host's (Fig. 12B). These "clumps" may be pre-metamorphic features.

In contrast, the K-feldspar-biotite rocks that occur in the northern Peach Lake quadrangle are fairly homogeneous in appearance. They contain medium- to fine-grained white K-feldspar, and biotite tends to be evenly distributed, instead of segregated into folia. In result, these rocks

are greyish in color and more schistose than the other K-feldspar-biotite gneisses. The K-feldspar-biotite schistose gneiss is not interbedded with other Basal Member lithologies, but instead occurs stratigraphically above Basal Member graphitic meta-arkose and metaconglomerate.

These K-feldspar-biotite schistose gneisses belong (with other lithologies) to a transitional zone between the Ned Mountain Basal and Wacke Members. Rocks of the transition zone are fairly similar to each other in macroscopic appearance, but have widely varied compositions (Fig. 13F). Those transition zone rocks which immediately overlie the Basal Member graphitic granofelses are the richest in K-feldspar and poorest in plagioclase and quartz. Some of the transitional schistose gneisses, like the Basal Member granofelses, are graphitic, though graphite is absent in the overlying Wacke Member. Rocks in upper parts of the transitional zone have compositions that grade towards metawacke, though they still have (on average) significantly more K-feldspar and less quartz and plagioclase than do the overlying schists of the Wacke Member (Fig. 13B and C; Table 3). It is instructive to remember that similar-looking schistose gneisses (but very rich in sodic plagioclase and poor in K-feldspar; Fig. 13F), occur where the Wacke Member is in direct contact with the Fordham Gneiss.

Interpretation of the K-feldspar-biotite-garnet gneiss (K-rich metasaprolite). The K-feldspar-biotite gneisses are commonly interbedded with graphitic meta-arkose and mafic metasedimentary rocks. A terrestrial depositional setting has been inferred for both these lithologies, so it is likely that the K-feldspar-biotite gneisses also originated on land. However, the modal compositions of the K-feldspar-biotite gneisses differ fundamentally from those of other aluminous or K-feldspar-bearing rocks. The compositional distinctions imply that the protolith of the K-feldspar-biotite gneiss was not one of the common varieties of sedimentary rock: it was neither a shale, a wacke, nor an arkose. Interpretation of these rocks would be difficult, except for the growing body of data in the geologic literature about a group of potassium-rich, silica- and sodium-poor, and moderately aluminous terrestrial rocks: Precambrian saprolites.

Much of the data on saprolites takes the form of chemical analyses. Fortunately, Lessing (1967) obtained an analysis of a K-feldspar-biotite gneiss from Ward Pound Ridge County Park (sample L-95, Plate III) during the course of his thesis research. This analysis can be compared with compositions of Precambrian saprolites from South Africa and the Canadian Shield, and with inferred metasaprolites of Late Precambrian age from the Appalachians (Table 4). Three analyses of metasedimentary rocks from the "Manhattan Schist", which show a comparable range in bulk silica content, are included for comparison.

The differences between modal analyses of the Precambrian saprolite and "Manhattan Schist" analyses parallel the contrasts in modal mineralogy between the K-feldspar-biotite gneiss and metawackes or metapelites (Fig. 13). The Precambrian saprolites and the "Manhattan Schist" both tend to be relatively rich in alumina and poor in silica, but their alkali contents differ strikingly. The saprolite analyses are uniformly higher in K_2O and lower in Na_2O than the "Manhattan" analyses. Lessing's L-95 analysis is comparable to the saprolites'. "Saprolite" bulk chemistry is evidently expressed by K-feldspar-rich modal compositions under the metamorphic conditions experienced in the northeastern Manhattan Prong.

Precambrian K-rich saprolites. Many workers have observed that saprolites of Precambrian age show enrichment in K_2O relative to unweathered substrate (Button, 1979; Button and Tyler, 1981; Gay and Grandstaff, 1980; Grandstaff and others, 1986; G-Farrow and Mossman, 1989; Holland, Feakes, and Zbinden, 1989; Rainbird, Nesbitt, and Donaldson, 1990; Retallack, 1986; Tyler, 1979; Zbinden and others, 1988). The abundances of Si, Ca, and Na decrease upwards in Precambrian weathering profiles (standardized against "constant" Al), but K increases upwards (e.g., Rainbird, Nesbitt, and Donaldson, 1990). The enrichment of K_2O correlates with the abundance of illite and sericite (e.g., Rainbird and others, 1990; Feakes and Retallack, 1988; Tyler, 1979). These minerals can be very abundant; sub-Huronian paleosols of Canada typically consist of "sericite, chlorite, quartz, and minor pyrite, with sericite increasing upwards in abun-

TABLE 4

CHEMCIAL ANALYSES OF PRECAMBRIAN SAPROLITES AND ALUMINOUS ROCKS OF THE MANHATTAN PRONG

	K-feldspar-rich gneiss, Basal Mem. Ned Mt. Fm.	Precambrian saprolites and metasaprolites					"Manhattan Schist"		
	1	2	3	4	5	6	7	8	9
SiO_2	52.5	64.59	46.8	47.3	44.2	42.7	68.51	45.03	54.5
TiO_2	1.75	0.29	1.02	3.6	3.4	4.6	0.57	1.28	1.51
Al_2O_3	22.0	20.76	34.35	15.7	16.6	20.2	15.68	33.76	19.4
Fe_2O_3		1.83	3.34	15.3	17.2	15.1	0.71		
FeO	11.66	0.40		2.1	2.4	0.64	2.32	8.19	7.76
MgO	5.52	0.90	.00	2.2	3.0	3.7	1.42	2.75	4.22
CaO	0.33	0.08	.00	1.5	1.5	0.16	3.83	1.85	5.23
Na_2O	0.59	.00	0.23	0.08	0.06	0.03	4.62	2.22	3.81
K_2O	6.22	8.74	9.05	7.3	6.8	7.9	2.49	4.62	3.91
MnO	0.24	0.01	0.03	0.04	0.07	0.02	n.d.	n.d.	0.20
P_2O_5		0.05	0.14	0.72	0.11	0.19	n.d.	n.d.	
H_2O+						3.1	0.13	0.91	
H_2O-				2.9	3.6	0.28	0.01	0.16	
CO_2				0.05	0.05	0.99			
LOI		2.40	4.71						
Total	100.81	100.05	99.67*	99*	99	99.61	100.29	100.77	100.54

1. Sample #L-95 of Lessing (1967). Metasaprolite of the Basal Member of the Ned Formation; location given on Plate III. (Fe is given as FeO).
2. Sub-Huronian saprolith developed over granite at Ville Marie, Quebec [sample #9 of Rainbird, Nesbitt, and Donaldson, 1990].
3. Paleosol consisting of sericite, iron oxides, and leucoxene, developed over basalt within the ?Early Proterozoic Ventersdorp Supergroup of South Africa [Sample 53c of Tyler, 1979].
4. & 5. Purple slates that cap the basaltic volcanic rocks of the Late Precambrian Catoctin Formation. These slates, and similar ones within the volcanic succession, are interpreted as metasaprolites (Reed, 1955).
6. Purple slate interpreted as metasaprolite, found with metarhyolite of the Late Precambrian Chestnut Hill Formation (Drake, 1984). Analysis given in Drake (1969).
7. "Manhattan Schist" from the Catskill Aqueduct, West 42nd Street near Fifth Ave., New York City (Fettke, 1914).
8. "Manhattan Schist" from Kensico, New York (Fettke, 1914).
9. "Manhattan Schist" from the southeastern Peach Lake quadrangle (sample L-177 of Lessing, 1967). (Fe is given as FeO).

* These totals, given in sources, do not match the sum of reported values.

dance to form an almost monomineralic cap" (Prasad and Roscoe, 1991).

K-enrichment is uncommon in modern saprolites, and the mechanism of Precambrian sericitization is controversial. Some have argued that the illite or sericite originated as a product of weathering (e.g., Allison and Ferguson, 1991), while others prefer an origin during diagenesis or low-temperature metamorphism. Nesbitt and Young (1989), for instance, suggested that the diagenesis of saprolites in a continental setting, in the presence of low Na/K meteoric waters, could promote sericitization. Either way, the K-enrichment results in rocks of very distinctive composition.

Scenarios for the origins of the K-feldspar-biotite gneisses (K-rich metasaprolites). The compositions of the K-feldspar-biotite gneisses are most consistent with a saprolitic protolith. These rocks will be referred to as "K-rich metasaprolite" from now on, to distinguish them from other feldspathic lithologies.

Many K-rich metasaprolites from the central and southern Peach Lake quadrangle are interbedded with graphitic meta-arkose and have coarse, heterogeneous textures. These characteristics point towards a non-fluvial, terrestrial depositional setting. The rare occurrence of small pockets of highly calcic plagioclase in these metasaprolites indicates the former existence of local clumps of carbonate, perhaps as calcrete.

The transitional schistose gneiss of the northern Peach Lake quadrangle is more heterogeneous in composition and more homogeneous in texture than are the other metasaprolites. In fact, only the gneisses closest to the Basal Member granofelses are predictably saprolitic in composition. Stratigraphically equivalent schistose gneiss which overlies the Fordham Gneiss is low in K and rich in Na. To explain these observations, the following scenario is suggested: 1) an illite-rich saprolite develops over valley fill (Basal Member conglomerate and arkose) while the Fordham Gneiss in the nearly-leveled uplands is converted into a plagioclase-rich regolith; 2) upper levels of the saprolite and regolith are mixed with sediments washed in from a new

source, and possibly transported short distances; 3) a continued flood of sandy sediments (the Wacke Member to-be) buries the old land surface.

K-rich metasaprolite is the only lithology to be found in the Ned Mountain Formation in the Peach Lake quadrangle but not encountered in the reconnaissance study of the southern Manhattan Prong described in Appendix 1. Its absence there may be related to metamorphic grade: where muscovite is stable, the K-rich metasaprolites are expected to be extremely muscovite-rich. A rock composed of 70% or more of muscovite would probably outcrop very poorly.

K-feldspar-quartz gneiss (metarhyolite). Scattered layers of buff-weathering, pink or white K-feldspar-quartz±plagioclase gneiss outcrop with meta-arkose, K-rich metasaprolite, metabasites, and mafic metasedimentary rocks in the Basal Member of the southern and central Peach Lake quadrangle. Similar feldspar-quartz gneisses are very abundant in the overlying Volcaniclastic Member, and are also common in the Calc-Silicate Member in the southern Peach Lake quadrangle.

The feldspar-quartz gneisses occur in concordant layers generally a meter or two in thickness. Texturally, the layers of K-feldspar-quartz gneiss are fairly homogeneous in appearance, though discontinuous, thin biotite-rich segregations are commonly present. The gneisses range from poorly- to well-foliated. At some localities, ribbons of quartz and feldspar help to define the gneissose fabric. Grain size varies from medium to coarse.

The gneisses are "granitic": K-feldspar is generally dominant, modal biotite is 15 modal percent or less, and plagioclase is minor or absent. The K-feldspar-quartz gneiss locally grades into K-rich metasaprolite, through a intermediary zone composed of feldspar-quartz-garnet-biotite gneiss.

Interpretation of the K-feldspar-quartz gneiss (metarhyolite). The granitic composition and homogeneous texture of the K-feldspar-quartz gneisses are most consistent with an igneous

protolith. The gneisses are similar to the graphite-free meta-arkoses of the Basal Member in some respects, but can be distinguished both compositionally and texturally. In contrast with the meta-arkoses, the feldspar-quartz gneisses 1) are unbedded; 2) have K-feldspar-rich compositions (Fig. 13); 3) do not contain minerals which imply a metasedimentary origin (such as graphite, garnet, or calcic plagioclase); and 4) can be coarse-grained and/or gneissose in texture.

The K-feldspar-quartz gneisses are concordant with adjoining metasedimentary rocks, suggesting a volcanic origin. Places where these gneisses grade into zones of feldspar-quartz-garnet-biotite gneiss and then into K-rich metasaprolite appear to mark pre-metamorphic compositional gradients. In addition, fabrics in the K-feldspar-quartz gneisses are qualitatively different from those observed in granitic gneisses of early intrusive origin. (The distinctive texture of the gneiss will be discussed in detail in the section on the Volcaniclastic Member.) The K-feldspar-quartz gneisses are inferred to be metamorphosed rhyolitic flows or tuffs.

Facies variations within the Basal Member, Ned Mountain Formation. The distribution of the metabasite/mafic metasedimentary and the meta-arkose/K-rich metasaprolite rock associations reflect a broad-scale, gradual facies change within the Basal Member. The mafic schists, granofelses, and amphibolites of the metabasite/mafic metasedimentary rock suite dominate the Basal Member in the southern Manhattan Prong (Plate IIC and Appendix 1), but decrease in importance northwards. In the southern and central Peach Lake quadrangle, the metabasite/mafic metasedimentary rock suite is interbedded with, but generally subordinate to, K-feldspar-bearing meta-arkoses, K-rich metasaprolites, and metarhyolites. The metabasite/mafic metasedimentary rock suite is unknown in the northern Peach Lake quadrangle. There, graphitic meta-arkose and metaconglomerate, overlain by metasaprolitic schistose gneiss, make up the Basal Member.

Volcanic activity seems to have played a key role in determining the regional variations in the Basal Member. Mafic volcanism resulted in an irregular flow of mafic detritus into the earliest clastic sediments of the Ned Mountain Formation in the southern Manhattan Prong. Evidence of

mafic volcanism is found as far north as the central Peach Lake quadrangle, where it was accompanied by felsic volcanic activity. No metavolcanic rocks of any kind are known in the Basal Member of the northern Peach Lake quadrangle.

The depositional setting of Basal Member sediments also varied from place to place. Granofelses of extraordinarily high graphite content are found in the southern Manhattan Prong and in the southern and northern parts of the Peach Lake quadrangle. The organic material was probably preserved because of deposition in stagnant, poorly oxygenated pools. Granofelses of the central Peach Lake quadrangle, in contrast, generally contain little or no graphite. Their sediments were evidently deposited in a relatively oxidizing environment. The granofelses of the central Peach Lake quadrangle are also richer in quartz, on average, than Basal Member granofelses elsewhere, indicating that precursor sediments had undergone a greater degree of weathering.

Geographic variations in 1) the nature and amount of volcanic activity, 2) characteristics of depositional environments, and 3) the degree of maturity of precursor sediments are all evident in the Basal Member. The rocks of the Basal Member also record that periods of deposition alternated with subaerial exposure and saprolite development in the region that today is encompassed by the Peach Lake quadrangle.

NED MOUNTAIN FORMATION, VOLCANICLASTIC MEMBER. The Volcaniclastic Member of the Ned Mountain Formation overlies the Basal Member in the southern and central Peach Lake quadrangle (Plate 1A). The Volcaniclastic Member contains a variety of quartzo-feldspathic gneisses and granofelses, some amphibolite, and minor amounts of calc-silicate rock. The quartzo-feldspathic gneisses include K-feldspar-quartz gneiss equivalent to the metarhyolite of the Basal Member.

The rocks previously assigned to the Pound Ridge granite (Plate IIB) fall within the

Volcaniclastic Member. The "Pound Ridge granite" contains two texturally distinct varieties of K-feldspar quartz gneiss. One of these is interpreted as a metavolcanic rock, the other as a subvolcanic intrusive body.

The apparent thickness of the Volcaniclastic Member (not adjusted for structural complexities) reaches a maximum of 1,000 meters in the southern Peach Lake quadrangle. The inferred intrusive body, which crops out in this region, makes up a substantial portion of the 1,000 meter thickness (Plate 1). The greatest apparent thickness of the Volcaniclastic Member in the central and southeastern parts of the Peach Lake quadrangle is around 250 meters.

The major lithologies of the Volcaniclastic Member will be described and discussed in the following order: first, the layered quartzo-feldspathic gneisses and granofelses, and the associated calc-silicate rocks; next, the inferred intrusive body at Ward Pound Ridge County Park; and finally, the amphibolites. After the description and interpretation of all the lithologies, facies variations within the Volcaniclastic Member will be discussed.

Layered quartzo-feldspathic rocks. Layered quartzo-feldspathic rocks in the Volcaniclastic Member range texturally from coarse-grained gneisses to fine-grained granofelses, and range compositionally from K-feldspar-rich to K-feldspar-absent. The relatively quartz-rich Volcaniclastic Member of the central Peach Lake quadrangle has conspicuous, well-defined beds several centimeters in thickness (Fig. 14A). Compositional layering is broader-spaced in the southern Peach Lake quadrangle, commonly a meter or more in thickness, but is not evident at every outcrop there.

The colors of the K-feldspar-quartz rocks loosely correlate with grain size: the finer-grained gneisses are commonly white or beige, the coarse-grained gneisses more commonly pink. All the gneisses tend to weather to a buff color. Greyish layers, relatively rich in biotite, and grey-green layers that contain hornblende or clinopyroxene are also commonly present.

The quartz, K-feldspar, plagioclase, and biotite contents of the quartzo-feldspathic rocks

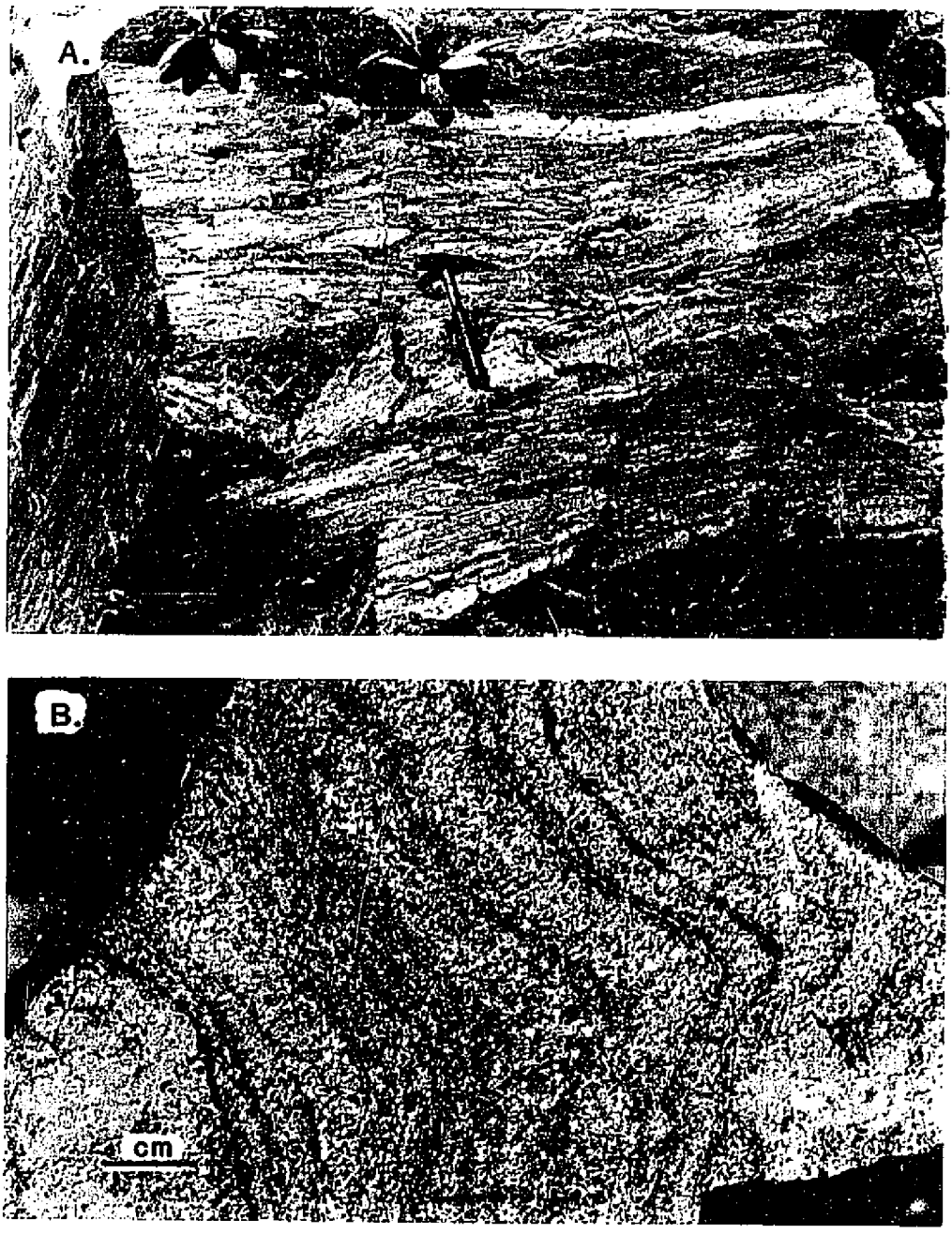

Fig. 14. Thin-bedded quartzo-feldspathic rocks, Ned Mountain Formation Volcaniclastic Member. (A) Road cut on Oscaleta Road, at site of specimen #1399. Hammer is 40 centimeters long.

(B) Bed-by-bed compositional variations in specimen #1345. K-feldspar is stained deep yellow, plagioclase is white, and quartz is grey. (The mode of a meta-arkosic bed is given in Table 3).

all vary on a bed-by-bed basis (Fig. 14B). The modal proportions of quartz and feldspar of some layers are arkosic (~65% quartz, ~30% K-feldspar+plagioclase, with ~%5 biotite), while others are rhyolitic (~60% K-feldspar, ~25% quartz, ~10% plagioclase, with ~5% biotite). The biotite content of practically all layers falls between 0 and 18 modal percent. K-feldspar, generally in the form of microcline, dominates the most feldspathic beds, but a few feldspathic layers contain subequal proportions of K-feldspar and plagioclase. The modal compositions of the more feldspathic rocks are plotted on Fig. 13E.

Sodic plagioclase (An_{22} to An_{30}) occurs in the more feldspathic beds. However, some of the meta-arkoses (e.g. specimen #1345, Table 3) contain calcic plagioclase (~An_{75}), as do many of the meta-arkoses of the Basal Member.

Interlayers of light-tan colored quartz-plagioclase (~An_{25-37})±K-feldspar-hornblende±clinopyroxene gneiss or granofels are present at some localities. Most of these layers contain 4 to 15% of a blue-green hornblende and/or diopsidic pyroxene (#1399 & 1415, Table 3). These hornblende-bearing gneisses are associated with thin beds and lenses of greenish, rusty-weathering quartz-plagioclase (~An_{30-37})-diopside-hornblende calc-silicate rock. Calc-silicate rocks are particularly abundant in the upper Volcaniclastic Member in the central Peach Lake quadrangle, near the gradational contact with the overlying Calc-Silicate Member.

Magnetite, ilmenite, apatite, zircon, and allanite are common accessory minerals among both the feldspar-rich and meta-arkosic layers. Hornblende-bearing beds may also carry minor pyrrhotite, sphene, and/or calcite.

The quartzo-feldspathic rocks show varied textures. The biotite-rich beds are generally schistose granofelses, with foliations defined by small, well-dispersed grains of biotite. The quartz-feldspar-hornblende rocks may be either poorly-foliated granofelses or streaky gneisses. The quartz-K-feldspar (meta-arkosic) rocks occur as well-layered, well-bedded, granofelses with thin biotite laminae, or (as streaking of quartz and feldspar become more prominent) as gneisses. The plagioclase-rich rocks tend to have a relatively coarse-grained gneissose texture. K-feldspar-rich

"rhyolitic" rocks can take the form of fine- to medium-grained granofelses or of lineated gneisses. The textures of these "rhyolitic" lineated gneisses show a number of remarkable features, which set them apart from deformed granites of similar modal composition. These features overlap with the range of textures observed in "rhyolitic" gneisses of the Basal and Calc-Silicate Members; the detailed description of these textures which follows will be illustrated with examples from both the Volcaniclastic and Calc-Silicate Members.

Textures of the lineated K-feldspar-rich gneisses ("felsic metatuffs"). Among those gneisses that contain the most K-feldspar (>50 modal percent) and least biotite ($\leq$5%), macroscopic fabrics largely reflect quartz-ribbon development. Macroscopic quartz ribbons are commonly accompanied by planar quartz segregations a few millimeters in thickness. Rocks which lack macroscopic quartz ribbons have a homogeneous appearance as hand specimens, but some show a linear fabric microscopically.

In rocks that lack a macroscopic linear fabric, up to 30% of feldspar and quartz grains may show a significant elongation (Fig. 15A). In these rocks, quartz and feldspar grains tend to have approximately similar sizes, with short axes of the grains generally 0.4 to 0.8 millimeter long. The elongated feldspar and quartz grains are oriented roughly parallel, and together define a rock fabric. The direction of elongation in the feldspars is random with respect to crystallographic orientation, as orientation is judged from twin lamellae. The equant grains (the majority) commonly meet in 120^{o} triple junctions, though elongate grains of quartz or feldspar subtend larger angles in triple grain junctions.

Rocks with macroscopic quartz ribbons contain prominent, elongate quartz grains in thin section. Elongate K-feldspar grains are less abundant in these rocks, but still they may comprise up to ~15% of the K-feldspar population. In addition, however, there are elongate aggregates of K-feldspar grains (Fig. 15B). These aggregates are broader as well as longer than individual elongate feldspar grains. Their component grains are large, averaging about twice the size of the

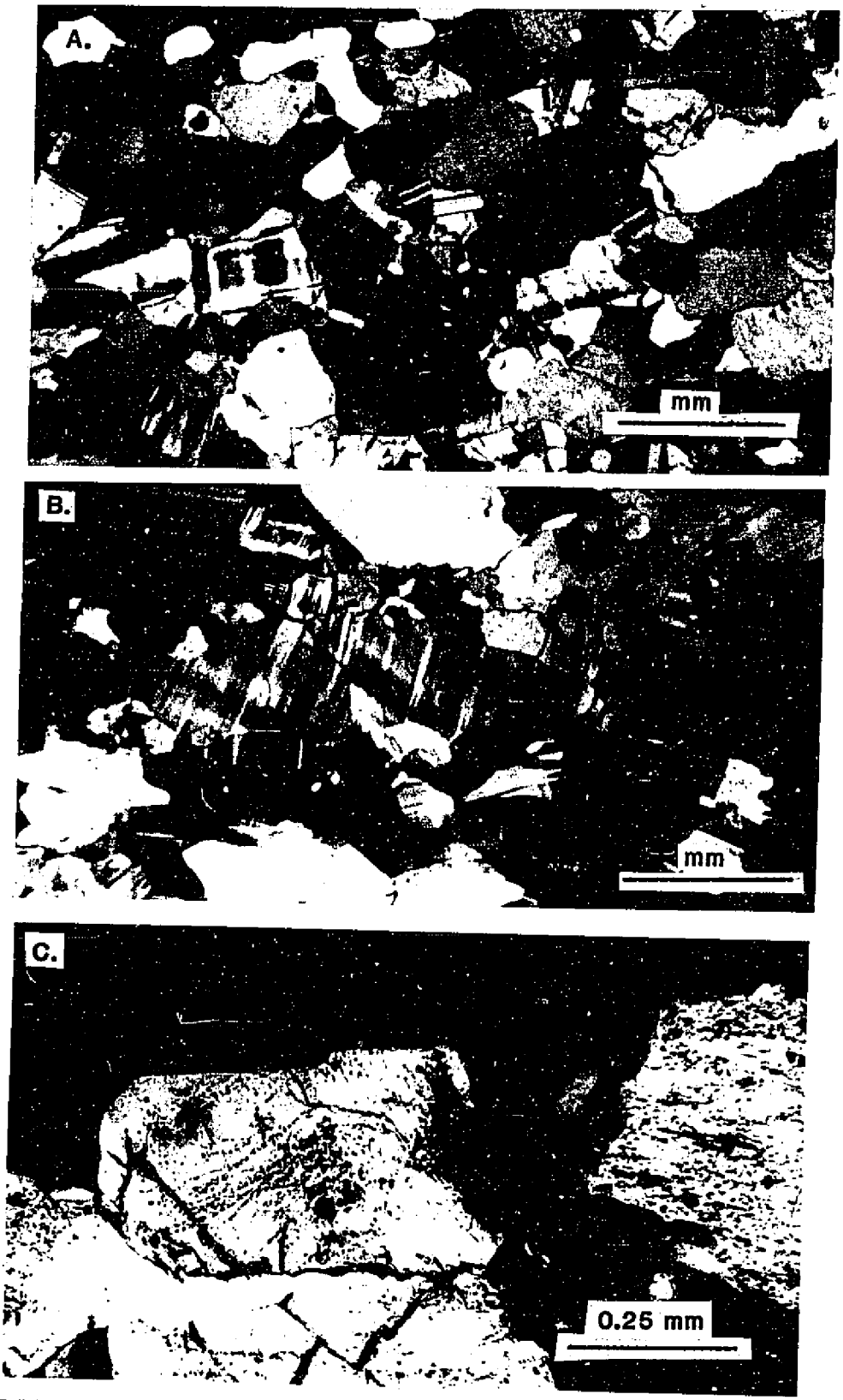

Fig. 15. Lineated K-feldspar-quartz gneisses ("felsic metatuffs"), Ned Mountain Formation. See next page for caption.

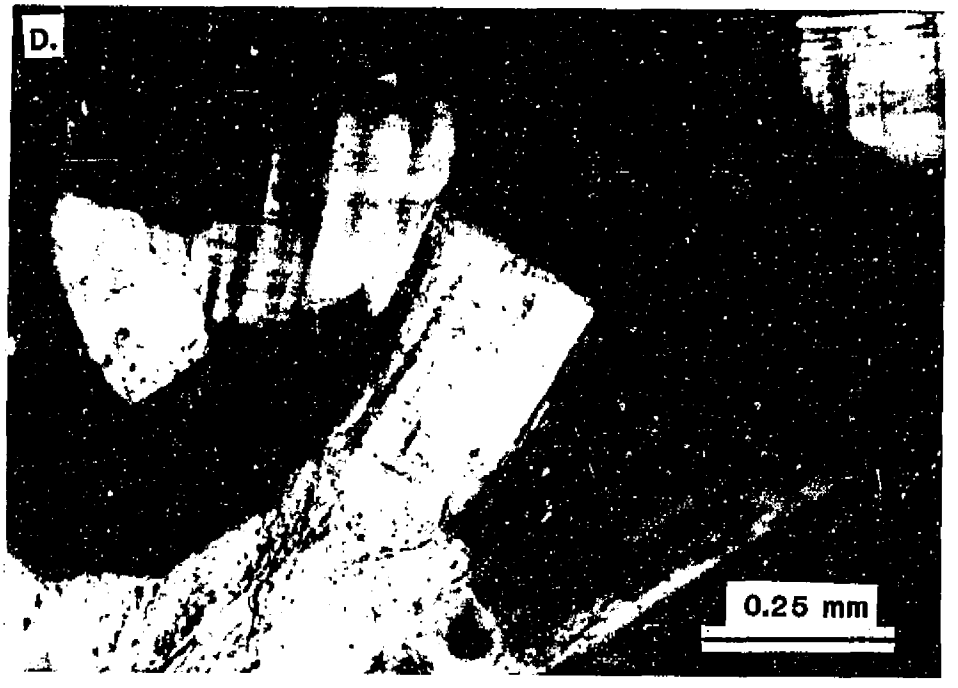

Fig. 15. Textures in lineated K-feldspar-quartz gneisses, interpreted as felsic metatuffs (page 93), from the Volcaniclastic and Calc-Silicate Members of the Ned Mountain Formation. Photographed with crossed-nicols unless otherwise indicated.

(A) A fabric is defined by the slight elongation of certain microcline, quartz, and plagioclase grains. Specimen #1445, Calc-Silicate Member. (Mode is given on Table 3).

(B) Elongate cluster of relatively coarse-grained microcline grains in somewhat finer-grained matrix. Specimen #1515, Volcaniclastic Member. (Mode is given on Table 3).

(C) Terminations on a plagioclase grain, against microcline. The (010) cleavage and the composition planes of albite twins in the plagioclase are inclined to the length of the plagioclase grain; the dominant crystal face is not (010). (Specimen #1515)

(D) Terminations on a microcline grain (center), against quartz. (Specimen #1515)

(E) Alternating ribbons of quartz (Q, low relief) and microcline (Kspar, moderate relief). Several grains of apatite (ap) and a garnet (gar) are also present. Plain light. (Specimen #1435, Calc-Silicate Member; mode is given on Table 3.)

(F) Alternating ribbons of microcline and quartz, with finer-grained inter-ribbon quartz and feldspar. Specimen #1940, Calc-Silicate Member, transect F-F', Ossining quadrangle.

(G) Broader field of view, specimen #1515. Distinct quartz ribbons and domains of K-feldspar are present.

Fig. 15. Lineated K-feldspar-quartz gneisses ("felsic metatuffs") of the Ned Mountain Formation. See previous page for caption.

matrix feldspars from the same rocks. These elongate aggregates resemble small quartz ribbons that have recrystallized into a sequence of near-equant grains.

Some feldspar grains are intergrown with quartz ribbons. These grains can have pointed projections that extend into neighboring quartz grains; these extensions are oriented parallel to the rock fabric (Fig. 15G).

Crystal faces are observed on a small proportion of matrix plagioclase and K-feldspar grains, including some elongate ones (Fig. 15C and 15D). The (010) cleavage and albite-twin composition planes of the plagioclase grains which show terminations are generally inclined to the direction of elongation (Fig. 15C.). Therefore, the dominant crystal faces are not (010), which is the best-developed direction in plagioclase crystals of igneous origin.

If quartz-ribbon development is taken as a measure of strain, changes in texture can be linked to degree of strain: 1) the least-strained rocks consist of randomly distributed, individual grains of feldspar and quartz, while the minerals are increasingly segregated with greater strain; 2) anisotropic shapes are about equally evident among the quartz and the feldspar grains of the least-strained rocks, but quartz is markedly more elongate in highly-strained rocks; 3) the development of quartz ribbons, with greater strain, is paralleled by the formation of elongate aggregates of coarse-grained K-feldspar; 4) the average size of feldspar grain decreases only slightly with increased strain.

The segregation of quartz and feldspar and the formation of elongate grains and/or aggregates of each mineral are strongly linked to strain. If strain were increased further, this progression of textures implies that, at the next stage, rocks might consist of alternating ribbons of equal-sized quartz and feldspar grains. Some stratiform K-feldspar-rich gneisses in the Ned Mountain Calc-Silicate Member (described later) display exactly these characteristics (Fig. 15E, F).

Significance of textures in the K-feldspar-rich gneisses ("felsic metatuffs"). Quartz and feldspar grains are commonly deformed via the processes of intracrystalline slip, such as disloca-

tion creep or climb. Quartz deforms readily by intracrystalline slip, forming the ribbons that are so common in sheared rocks. On the other hand, feldspar is "strong", and resists plastic deformation. As a result, where quartz and feldspar grains are deformed together, they generate contrasting textures.

Some composite textures typical of sheared granites are illustrated in Fig. 16. The granites depicted in this figure outcrop in the Peach Lake quadrangle; they underwent all or most of the same deformational and metamorphic events experienced by the K-feldspar-rich gneisses of the Volcaniclastic Member. The textures are described in the order of increasing strain:

1. (Fig. 16A) A slightly deformed hornblende-bearing granite of the Fordham Gneiss still contains some orthoclase, partly inverted to microcline. Feldspar displays a "mortar" texture, where large (commonly >0.8 millimeter) relict grains are surrounded by very small (~0.04 millimeter) new grains. Little, if any, elongation of quartz is evident. Foliation is defined, predominantly, by aligned micas.

2. (Fig. 16B) Small quartz ribbons were formed in this small anatectic granite that occurs within the Manhattan Schist. "Mortar texture" is better developed than in Fig. 16A; orthoclase grains have been largely converted into a fine-grained aggregate of microcline.

3. (Fig. 16C) This specimen comes from a penetratively deformed portion of the Ordovician Siscowit Granite. It has well- defined quartz ribbons, numerous partially-recrystallized feldspar porphyroclasts, and anastomosing zones of fine-grained (0.1 to 0.3 millimeter) recrystallized feldspar that surround feldspar porphyroclasts and separate quartz ribbons. Micas are aligned parallel to the foliation.

The textures of these granites are comparable to those of sheared granites from many localities and to products of experiments performed on granitic materials. For example, Tullis and Yund (1985) induced the creation of mortar texture and the reduction of grain-size during the experimental deformation of dry, coarse-grained plagioclase. Tullis and Yund (1985) attributed these textures to recrystallization-accommodated dislocation creep.

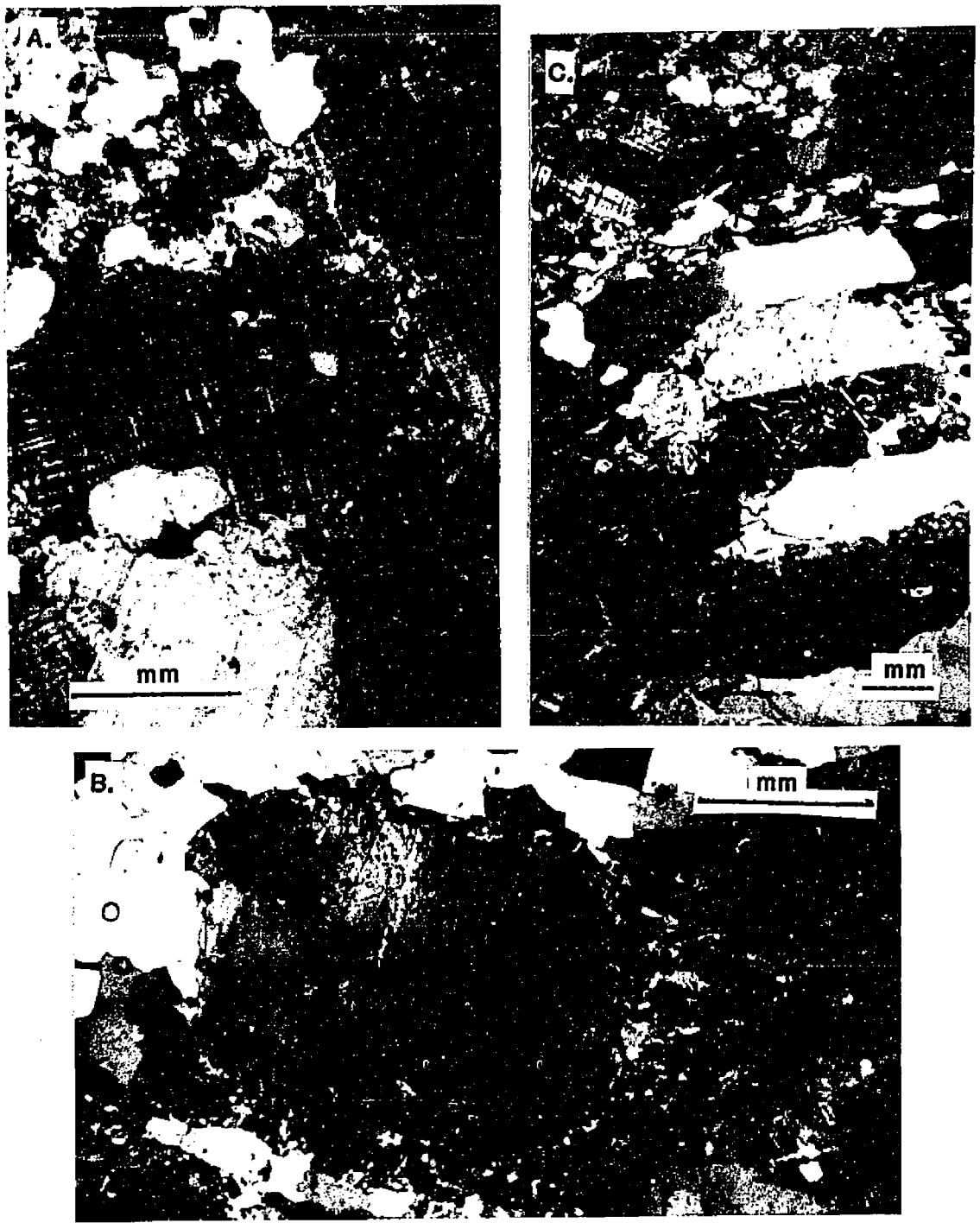

Fig. 16. Fabrics in sheared granites.

(A) Mortar texture and deformation-induced microcline twinning in a granite within the Fordham Gneiss (specimen #1288).

(B) Mortar texture around a K-feldspar porphryoclast, with a small quartz ribbon nearby. Specimen #PP30 (anatectic leucosome in the Manhattan Schist).

(C) Plagioclase porphyroclast with Carlsbad twin plane oriented parallel to rock foliation. Foliation is defined by quartz ribbons. The porphyroclast encloses numerous grains of secondary muscovite. Anastomosing domains of fine-grained feldspar occur between the quartz ribbons. Specimen #1131, Siscowit Granite.

The textures of the Volcaniclastic Member K-feldspar-rich gneisses differ from the granites' in many ways. In the gneisses, there is no sign of inversion of orthoclase to microcline; no mortar texture; no anastomosing bands of fine-grained feldspar between the quartz ribbons. The absence of these textures implies that crystal-plastic processes like recrystallization-accommodated dislocation climb were not the dominant mechanisms of feldspar deformation.

To infer what the mechanism of deformation could have been, we can reconsider the textures of the K-feldspar-rich gneisses. We saw that elongate feldspar grains were produced at low strains, and that elongation was random with respect to crystallographic orientation. Such a relationship is easiest to explain by syntectonic, selective growth of feldspar grains. The crystal faces on feldspars, though rare, strongly support the hypothesis that syntectonic grain growth took place. This grain growth indicates that some grains, or portions of grains, were lost during deformation, and new material added to existing grains in preferred sites: in other words, that deformation occurred via diffusion. The elongate aggregates and ribbons of K-feldspar, observed at higher strains, can be attributed to ongoing, syntectonic processes of segregation and grain growth.

Tullis and Yund (1991) experimentally achieved the syndeformational growth of optically unstrained, rectangular feldspar grains through the mechanism of diffusion creep. They began with fine-grained (2-10 micron) samples of plagioclase, and shortened them with varied amounts of water, and differing strain rates, temperatures, and confining pressures. They found that diffusion creep was enhanced by greater water content, by higher temperature, and by slower strain rates. Deformation by dislocation creep took place where diffusion creep did not.

Tullis and Yund established that diffusion creep can operate on feldspar grains 10 microns and less in diameter. The K-feldspar-rich gneisses are much coarser, but their textures imply that diffusion creep can be effective on a broader scale. Interestingly, Gower and Simpson (1992) have recently ascribed a texture similar to that seen in Fig. 15G (the pointed, larger feldspar grains, penetrating adjacent quartz grains) to diffusion creep.

The K-feldspar-rich gneisses of the Ned Mountain Volcaniclastic, Calc-Silicate (and

Basal) Members experienced the same temperatures and strain rates as did many of the intrusive granitic bodies in the Peach Lake quadrangle. The very different physical behaviors of the K-feldspar-rich gneisses and the granites during deformation must be attributed to characteristics of their protoliths, such as grain size and water content.

Interpretation of the quartzo-feldspathic rocks. The bedding style, the modal compositions and the textures of the quartzo-feldspathic rocks each yield clues about their origin. The feldspar-rich gneisses occur as concordant layers, interbedded with quartz-feldspar granofels and/or quartz-feldspar-hornblende gneiss, at many outcrops in the central Peach Lake quadrangle. These more feldspathic gneisses are considered to be rhyolitic metavolcanic rocks because of their concordant, bedded nature and feldspathic compositions.

The textures observed in the lineated, K-feldspar-rich gneisses are most reasonably attributed to the syntectonic recrystallization of hydrous, fine-grained material of granitic composition, such as weathered (or perhaps water-laid) tuff. Among the non-lineated gneisses, texture cannot distinguish those that originated as rhyolitic tuffs from those that once may have been rhyolitic flows. However, in order to clearly identify the bedded K-feldspar-quartz gneisses and to avoid confusing them with other K-feldspar-rich lithologies, they will be designated "felsic meta-tuffs" from here on.

The quartz-rich beds of the Volcaniclastic Member are classified as meta-arkoses, though they probably contain some felsic volcanic material. The quartz-plagioclase-clinopyroxene calc-silicate rocks and quartz-feldspar-hornblende-clinopyroxene gneisses are interpreted as mixtures of arkosic sands, carbonate, and volcanic debris. The thin-bedded sequences of quartz-richer and -poorer granofelses and gneisses that characterize the central Peach Lake quadrangle are interpreted as volcaniclastic/siliciclastic/carbonate mixtures, while the more massive, more felsic layered rocks of the southern Peach Lake quadrangle are interpreted as more purely volcanic in origin.

Intrusive body at Ward Pound Ridge County Park. A coarse-grained, homogeneous, unlayered body of salmon-pink granite lies within the Volcaniclastic Member at Ward Pound Ridge County Park in the southern Peach Lake quadrangle (Plate III). This granite crops out in a swath approximately 500 meters wide (Plate I). The granite appears to be concordant on map scale, and is cut by at least one small amphibolite dike. The color of the granite derives from the abundant, large grains of pink alkali feldspar, among which are dispersed grains of grey quartz. Foliation is poorly developed, and is generally expressed by a pronounced rock-cleavage, but biotite grains locally display parallelism. Quartz-veining is present in places.

A specimen of this granite (specimen #1514, Plate III) displays a striking texture in thin section. Almost all the feldspar occurs in large grains that have complex exsolution patterns and that contain approximately equal proportions of K-feldspar and plagioclase (Fig. 17). In some portions of the slide, a few small independent grains of orthoclase and oligoclase occur along the grain boundaries of the large alkali feldspars. These grains evidently formed by limited recrystallization of the original alkali feldspar; no primary grains of orthoclase or plagioclase appear to be present. Textures indicate that this portion of the granite has undergone relatively little strain.

Feldspar comprises about 61 modal percent of the rock; quartz, about 35%; dark-brown biotite, 2%, and opaque minerals (magnetite and a trace of pyrrhotite), 2%. A trace of zircon is also present. Magnetite occurs in octahedral crystals and in the cores of clumps of biotite. Biotite appears to be secondary in origin.

Origin of the granite. The observed textures, unique in the study area, indicate that a single phase of alkali feldspar originally existed in the granite. The presence of hypersolvus alkali feldspar indicates that primary crystallization of the granite took place at near surface-conditions, under low P_{H2O}.

Experimental work shows that Fe- biotite is not stable in granitic liquids at very low pressure (Rutherford, 1969), though observations on natural granites indicate that biotite commonly participates in solidus-liquidus equilibria at pressures greater than about 1 kilobar (Luth, 1976).

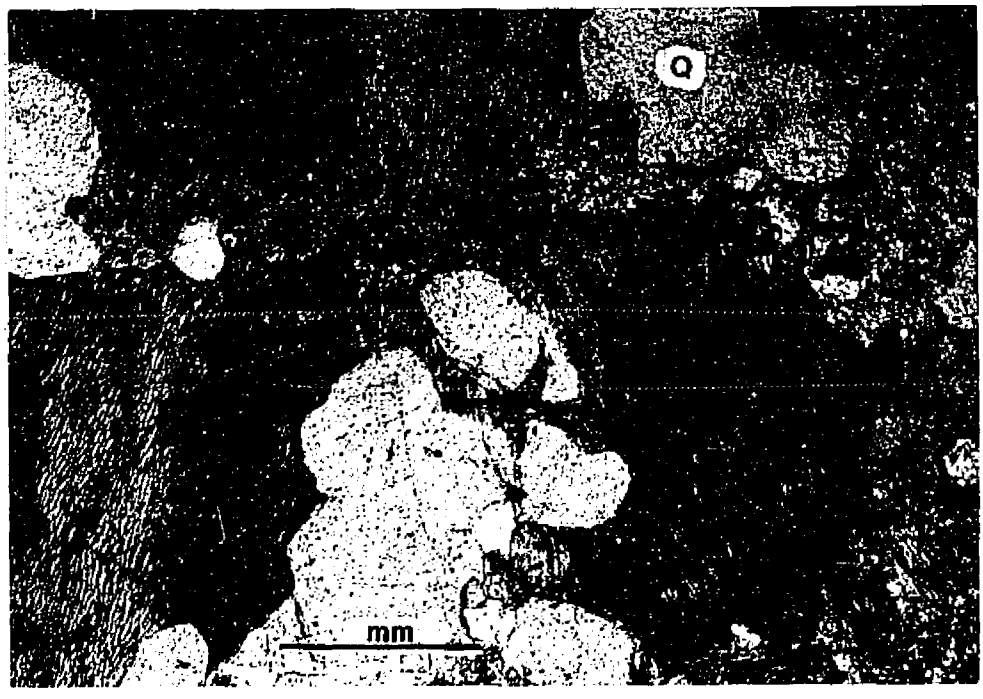

Fig. 17. Exsolution textures from hypersolvus granite within the Volcaniclastic Member, Ned Mountain Formation. Quartz (Q) was originally intergrown with a single-phase alkali feldspar. Specimen #1514 (mode is given on Table 3).

If the granite crystallized at less than 1 kilobar, the iron-rich biotite now present could not have been a liquidus phase. However, the biotites in the hypersolvus granite replace primary magnetite, and appear to be of secondary, metamorphic origin. Their presence is no barrier to an inference that granite was emplaced at a very shallow level.

The intrusion of the hypersolvus granite must have either preceded or postdated the deep burial that was associated with Paleozoic high-grade metamorphism in this region. The presence of foliation in the granite and the cross-cutting amphibolite dike place the intrusion of the granite before the regional metamorphism and deformation.

The apparently concordant nature of the granite implies it was a sill. This granite sill apparently intruded felsic metatuffs of the Volcaniclastic Member at some time between the eruption of the volcanic rocks and beginning of orogenesis. Intrusion most likely overlapped with the deposition of the Ned Mountain Formation, since younger (post-Ned Mountain) strata contain no felsic volcanic rocks.

The hypersolvus granite is most reasonably interpreted as a sub-volcanic intrusive body, and therefore as an integral part of the Volcaniclastic Member. Its bulk composition is comparable to that of those layered feldspathic gneisses which contain subequal K-feldspar and plagioclase.

The remarkable preservation of the original texture of this granite deserves comment. It was probably facilitated by the very fact that the granite did intrude a sequence of fine-grained, "wet", volcaniclastic rocks; during the initial, most intense deformation, strain would have been strongly partitioned into these "weak", fine-grained rocks, permitting textures in the coarse-grained, "hard" hypersolvus granite to survive.

Amphibolites. Amphibolites are very subordinate to layered quartzo-feldspathic rocks in the Volcaniclastic Member of the Peach Lake quadrangle. In some instances they occur in relatively thin layers (less than a meter thick), interbedded with felsic lithologies. More massive amphibolites, up to approximately 15 meters in thickness, are also known. The amphibolites are

dark rocks, generally composed of hornblende, plagioclase, and quartz, with trace amounts of ilmenite, pyrrhotite, magnetite, and sphene. Biotite occurs in zones of alteration, particularly near granitic intrusives.

Origin of the amphibolites. The more massive, homogeneous bodies of amphibolite are interpreted as metabasites. These amphibolites generally appear to be concordant and do not cut rocks stratigraphically above the Ned Mountain Formation. They are considered to largely be metamorphosed mafic flows, though some (like the amphibolite that cuts the hypabyssal granite) may have originated as diabasic dikes.

A metasedimentary origin cannot be excluded for the thin layers of amphibolite that outcrop within felsic sequences that contain calc-silicate rock and quartz-feldspar-hornblende gneiss. If they are metasedimentary, their protolith would have consisted of a mixture of carbonate, arkosic sand, and clay, with, perhaps, volcanic detritus.

Facies variations in the Volcaniclastic Member. In the southern Peach Lake quadrangle, felsic metatuff dominates the Volcaniclastic Member, and bedding is thick. Bedding is thinner and meta-arkose, amphibolite, and calc-silicate rock are more abundant in the central Peach Lake quadrangle. The Volcaniclastic Member pinches out before reaching the northern Peach Lake quadrangle (Plate IA), though some amphibolites of the Wacke Member may conceivably be correlative.

Observations by Lessing (1967) imply that the hypabyssal granite continues southwards into the Pound Ridge quadrangle. Lessing reported rocks that contain abundant mesoperthite (47 to 54 modal percent) and only minor plagioclase (5 to 15 modal%) outcrop in a belt which coincides with the hypersolvus granite in the Peach Lake quadrangle and that extends southwards, along strike. Lessing also reported sparse fluorite in some felsic rocks; this observation has not been confirmed here.

The Yonkers Gneiss occupies the same stratigraphic position in the southern Manhattan Prong as the "Pound Ridge granite" does in the northern, and has a similar radiometric age (see discussion under "Previous Work"). The Yonkers Gneiss is similar lithologically as well. It contains some lineated K-feldspar-rich gneisses, similar to felsic metatuffs of the Peach Lake quadrangle. Some other portions of the Yonkers Gneiss are homogeneous and unlayered; it is conceivable that they were once sub-volcanic intrusive bodies, like the sill at Ward Pound Ridge County Park.

The most significant difference between the Yonkers Gneiss and metafelsites of the Peach Lake quadrangle lies in mineralogy. A deep blue-green amphibole, ferrohastingsite, is common in the Yonkers Gneiss. Amphibole is unknown in hypabyssal granite and felsic metatuffs of the Peach Lake quadrangle, but hastingsite does occur in the extensive felsic metatuff section that crops out on transect K-K' (Plate II) in the Croton Falls quadrangle.

Amphibolite dominates some portions of the Volcaniclastic Member in the southern Peach Lake quadrangle. A sequence of hornblende-cummingtonite amphibolites (e.g., specimen #2496, Table 3) crops out between the Basal Member and a valley (where Inwood Marble is inferred) on transect D-D' (Plate II, and Appendix 1). These cummingtonite-bearing amphibolites are interpreted as metabasites.

NED MOUNTAIN FORMATION, WACKE MEMBER. The Wacke Member of the Ned Mountain Formation crops out in the northern Peach Lake and the southern Brewster quadrangles. The Wacke Member dies out to the south, where it is considered correlative with both the Volcaniclastic Member and with much of the Calc-Silicate Member (Plate 1A; Fig. 7)

The Wacke Member is especially well exposed in the region around Ned Mountain. The apparent thickness of this unit reaches a high of approximately 500 meters.

The base of the Wacke Member is highly feldspathic. Where the Wacke Member overlies

the Ned Mountain Basal Member, it grades downwards into K-feldspar-rich metasaprolitic schistose gneiss. Where the Wacke Member sits directly on the Fordham Gneiss, its base is rich in plagioclase (Fig. 13F). As these relationships have been considered in earlier sections, the focus here will lie on the remainder of the Wacke Member.

The Wacke Member consists (in order of abundance) of black-and-white quartz-feldspar-garnet-biotite-sillimanite schistose gneiss (metawacke), dark grey cummingtonite or orthopyroxene-bearing amphibolite or metabasite, black hornblende amphibolite, light-grey quartz-feldspar-biotite-garnet granofels, and dark garnet-feldspar-sillimanite-biotite-quartz schist (metapelite). K-rich metasaprolite and phosphathic gneiss occur at the very top of the Wacke Member, in a zone transitional to the Calc-Silicate Member.

Each of the lithologies of the Wacke Member will be described and discussed in subsequent sections. Following that, regional variations within the Wacke Member will be considered.

Quartz-feldspar-garnet-biotite-sillimanite schistose gneiss (metawacke). Extensive sequences of brown- or grey-weathering, medium-grained quartz-feldspar-garnet-biotite-sillimanite schistose gneisses make up the bulk (80-90%) of the Wacke Member. A well-developed foliation, defined by aligned biotite grains, is pervasive. The schistose gneisses are commonly segregated into white (or light grey) laminae rich in quartz and feldspar, and dark grey (or black) laminae rich in biotite and sillimanite. Coarse-grained, pink-and-white migmatitic leucosomes are abundant in some areas. Reddish garnets are commonly prominent; these, together with the dark-and-light segregations, give the gneiss a red, white, and black look.

Compositionally, the schistose gneiss is very uniform. Bedding is evident only where the schistose gneiss is in contact with another lithology, such as amphibolite or quartz-feldspar granofels. Quartz generally comprises 23 to 56 modal percent of the schistose gneiss, plagioclase (An_{22-37}) 5 to 25 percent, and K-feldspar 7 to 20 percent. The modal compositions of twelve specimens yield an average quartz-to-plagioclase ratio of approximately 2:1. Garnet, biotite, and

sillimanite combined make up 12 to 50 modal percent of these rocks. Taken individually, garnet comprises 5 to 30 percent, biotite 5 to 17 percent, and sillimanite 0 to 12 percent. The range of metawacke compositions (from all formations) is plotted on Fig. 13C; examples of Wacke Member modes are given on Table 3.

The plagioclase is commonly antiperthitic, and has semi-rectangular domains of exsolved K-feldspar. The K-feldspar is generally in the form of orthoclase, though it has been partially inverted to microcline in a few specimens. Biotite is red-brown or dark brown in thin section. Ilmenite and magnetite comprise 1 to 2 modal percent of most specimens. Green (hercynitic) spinel commonly occurs as inclusions in garnet or, less commonly, in plagioclase. Many specimens contain traces of zircon and/or apatite.

Interpretation of quartz-feldspar-garnet-biotite-sillimanite schistose gneiss (metawacke). The schistose gneiss contains substantial amounts of quartz, feldspar, and aluminous minerals. The protolith of this rock is inferred to have been a feldspathic sandstone with abundant clay-rich matrix: in other words, a wacke. For simplicity, this lithologic type will be referred to as "metawacke".

The dominance of quartz over plagioclase in the modal composition of the metawackes indicates that the precursor sediments had undergone a moderate degree of weathering. The absence of graphite and the dominance of magnetite and ilmenite over iron sulfides imply a reasonably well-oxygenated depositional environment.

Metabasites. Amphibolites and related metabasites comprise 5 to 10 percent of the Wacke Member in the Peach Lake quadrangle. They occur in layers that range in thickness from a minimum of about one centimeter, up to several meters. Their contacts are generally parallel to the foliation developed in surrounding metawackes. They are dark grey to black in color, the darkest commonly having the greatest hornblende content.

The metabasites generally display a medium-grained and uniform texture. They vary considerably in mineralogy, but the different mineralogic types generally cannot be distinguished macroscopically. The major mineralogical variations found among the metabasites include the following: 1) hornblende-plagioclase-quartz-biotite; 2) hornblende-plagioclase-orthopyroxene-quartz-biotite; 3) plagioclase-orthopyroxene-cummingtonite-quartz; 4) plagioclase-orthopyroxene-garnet-quartz; and 5) hornblende-plagioclase-orthopyroxene-clinopyroxene-quartz-cummingtonite. Those metabasites that contain substantial orthopyroxene or cummingtonite generally have plagioclase of composition An_{50} to An_{75}, while the plagioclase in simple hornblende amphibolites commonly ranges between An_{30} and An_{45}. Examples of modal compositions are given on Table 3.

Among their accessory minerals, the metabasites contain substantial amounts (1 to 5 modal percent) of ilmenite, and subordinate magnetite and/or pyrrhotite. One sample (#1252, Table 3) is exceptional in that it contains 8 percent magnetite and a highly calcic plagioclase ($\sim An_{77}$). Sphene, apatite, allanite, and zircon also occur as accessory minerals.

Evidence of metamorphic disequilibrium is found in many thin sections. Grains of calcic plagioclase tend to be strongly zoned. Pyroxenes are commonly rimmed by hornblende and/or cummingtonite. It is evident that the large array of metabasite mineralogies reflects (in part) the persistence of assemblages formed under differing metamorphic conditions.

Some of the mineralogical variation, however, cannot be explained by metamorphic disequilibrium, and must reflect variations in bulk rock composition. For example, although most of the metabasites (orthopyroxene-bearing and pyroxene-free alike) contain no garnet, a garnet-bearing zone a few centimeters in thickness is found on the boundaries of a few metabasite beds, near contacts with metawacke. The periphery of this garnetiferous zone can be very garnet-rich; the garnet content decreases toward the center of the metabasite.

One other relatively minor group of Wacke Member rocks also has mafic affinities. These rocks are well-bedded, garnet-bearing, medium-grained, grey-weathering granofelses, gneisses,

and schistose gneisses. Most beds are between 0.5 and 30 centimeters in thickness. Light-grey beds are plagioclase-rich -quartz-biotite-garnet granofelses; dark-grey beds are plagioclase (An_{38})-biotite-cummingtonite-hornblende-quartz-garnet gneiss or schistose gneiss. The total amphibole content of one dark layer studied in thin-section (specimen #1663) is 21 modal percent (Table 3). Substantial apatite (~3 modal percent) occurs in both dark and light layers.

Interpretation of the metabasites. The metabasites, in general, are interpreted as metamorphosed basaltic flows or tuffs because of their apparent concordant nature. The metabasites do not cut younger (post-Wacke Member) stratigraphic units.

Metabasite beds that have garnetiferous outer zones are interpreted as metamorphosed mafic tuffs. The garnetiferous compositions are considered mixtures of mafic tuff and argillaceous sediments.

The abundance of calcic plagioclase and magnetite found in specimen #1252 suggests local calcrete/ferrocrete development. Wacke Member mafic flows or ash falls may have (rarely) been subjected to subaerial exposure.

The well-bedded, garnetiferous, amphibole-bearing gneissose sequence resembles the mafic metasedimentary rock suite of the Basal Member in its bedded character and its layer-by-layer variation in mafic minerals. This assemblage is interpreted as a sequence of metamorphosed, moderately- to slightly-weathered mafic tuffs, mixed with varying amounts of siliciclastic sediments.

Quartz-feldspar-biotite-garnet granofels. Light- to medium-grey, grey- or brown-weathering, medium-grained quartz-feldspar-biotite-garnet granofelses make up 5 to 10 percent of the Wacke Member. The granofelses occur in beds that range from about one centimeter to about one meter in thickness. Some beds have fine biotite- and/or garnet-rich laminae; this lamination appears to be a primary bedding feature. Other granofelsic beds are massive in character and have

uniformly-distributed biotite grains.

The granofelses are composed, on average, of close to 50 percent quartz, 26 percent plagioclase (An_{29-37}), 11 percent biotite, 8 percent garnet, 3 percent K-feldspar, and 1 to 2 percent opaque minerals (ilmenite, magnetite, and pyrrhotite combined). Trace amounts of apatite, zircon, and sillimanite commonly occur. The plagioclase is generally antiperthitic; biotite is red-brown or brown in thin section. Examples of modal compositions are given on Table 3.

Interpretation of the quartz-feldspar-biotite-garnet granofels. The average quartz : plagioclase ratios of the quartz-feldspar-biotite-garnet granofels and the metawacke are both approximately 2:1. The plagioclases in these two lithologies are comparable in composition. The metawackes do contain more K-feldspar than the granofelses, but much of this excess K-feldspar can be attributed to the breakdown of the muscovite formerly present in the more aluminous metawackes. The protoliths of the granofelses and the metawackes evidently contained feldspathic sands of comparable quartz-plagioclase composition, but differing quantities of clay matrix.

Garnet-K-feldspar-quartz-sillimanite-biotite-plagioclase schist (metapelite). Rocks that have a combined total of modal garnet, biotite, and sillimanite greater than 50 modal percent (the remainder of the rock principally comprised of quartz and feldspar), are classified as "metapelites". By this standard, pelitic schist is very minor in the Wacke Member, making up less than 1 percent of the total. The range of metapelite compositions found in all formations is shown on Fig. 13B; the modal composition of one specimen (#1243) from the Wacke Member is given on Table 3.

Transitional zone to the Calc-Silicate Member. K-rich metasaprolite, locally accompanied by a phosphate-rich gneiss, occurs in a transitional zone that lies above the metawacke section but below the outcrop of any calc-silicate rock. The K-rich metasaprolite is compositionally indistin-

guishable from metasaprolite of the Basal Member, but is dissimilar in appearance. For instance, a beige-colored metasaprolite occurs at the top of the Wacke Member in Brewster quadrangle, south of Sanfords Pond (Plate III). It shows a penetrative foliation and lineation, rather than the coarse "clumpy" fabric common in the Basal Member. Garnet and quartz both occur in discontinuous, pencil-shaped lenses. Thin-section examination shows that many quartz grains contain abundant exsolved needles of rutile.

K-rich metasaprolite also crops out at the Wacke Member-Calc-Silicate Member contact in the northeastern Peach Lake quadrangle, at the eastern end of Lake Windwing (Plate III). Here, the typical K-feldspar-sillimanite assemblage of the metasaprolite has been retrogressively replaced. The metasaprolite now consists principally of muscovite (~70 modal percent), with 15 percent biotite, 5 percent relict K-feldspar, and lesser amounts of plagioclase, garnet, sillimanite, and quartz.

At Lake Windwing, a dark, phosphatic (5 percent apatite), biotite-garnet gneiss accompanies the metasaprolite. A continuous stratigraphic section is exposed from the metasaprolite/phosphatic gneiss association upwards into the calc-silicate rock and meta-arkose of the Calc-Silicate Member.

Geographic variations within the Wacke Member. A gradient in bed thickness exists within the Wacke Member in the study area. Near Ned Mountain, granofelsic or metabasic beds are most commonly 5 centimeters to 1 meter in thickness, and few beds are significantly thinner. About three kilometers northwards, many granofels beds and metabasite layers are 1.5 to 8 centimeters in thickness. About 4.5 kilometers northwards, in the southern Brewster quadrangle, it is not uncommon for beds to be 1 centimeter thick, though some large amphibolites are also present. In contrast, bedding in other units (for instance, Inwood Marble) in this area is fairly uniform; there is no evidence of a systematic tectonic attenuation of layering. The thinning of beds towards the north is interpreted to reflect a predominantly southerly provenance for the sediments of the

Wacke Member.

The Wacke Member continues westwards on strike into the Croton Falls quadrangle, where it was encountered on transect L-L' (Plate II). The Wacke Member pinches out southwards, towards the central Peach Lake quadrangle and between transects L-L' and K-K' (Plate II) in the Croton Falls quadrangle. Minor amounts of metawacke occur in the Calc-Silicate Member of the central and southern Peach Lake quadrangle, along with quartz-feldspar-biotite granofels, metabasite, and other lithologies. The Wacke and Calc-Silicate Members are considered partially correlative (Plate 1A).

Metawacke also occurs in the Ned Mountain Formation at some localities in the southern and central Manhattan Prong. Hall (1968b) noted schistose rocks in what he considered to be "basal Lowerre". I encountered a quartz-plagioclase-muscovite-sillimanite schist on traverse G-G' (Plate II) in the Ossining quadrangle, stratigraphically below a sequence consisting of meta-arkose, phosphatic gneiss and felsic metatuff that has been assigned to the Calc-Silicate Member.

NED MOUNTAIN FORMATION, CALC-SILICATE MEMBER. The Calc-Silicate Member is the uppermost member of the Ned Mountain Formation (Plates I and IA). The Calc-Silicate Member reaches its greatest apparent thickness, around 400 meters, in the central and southeastern Peach Lake quadrangle. It thins northwards, and where exposed in the northernmost Peach Lake quadrangle it appears to be less than 30 meters thick. A gradational contact is present between the Calc-Silicate and Volcaniclastic Members in the southern and central Peach Lake quadrangle. The relative abundances of felsic metatuff and amphibolite decrease stratigraphically upwards, across this boundary, while quartz-feldspar granofels and calc-silicate rock increase (Fig. 7). In addition, several lithologies unknown in the Volcaniclastic Member occur within the Calc-Silicate Member: these include K-rich metasaprolite, quartz-feldspar-biotite-garnet granofels, metawacke, quartzite, and marble. As described in the previous section, a transitional zone

containing K-rich metasaprolite occurs between the Wacke Member and the Calc-Silicate Member in the northern part of the study area. The part of the Calc-Silicate Member exposed in the southern and central Peach Lake quadrangle is the most lithically varied unit of the Ned Mountain Formation (Table 5).

Well-bedded, medium-grained, beige-colored, rusty-weathering quartz-K-feldspar granofelses (meta-arkoses) and/or K-feldspar-quartz granofelses (felsic metatuffs) occur near or at the top of the Calc-Silicate Member at a number of localities. The "Lowerre Quartzite" mapped by previous workers consists, for the most part, of these occurrences.

In the succeeding sections, the lithologies of the Calc-Silicate Member will be described and interpreted, and regional variations within the Calc-Silicate Member will be discussed.

Felsic metatuff. Felsic metatuff (stratiform K-feldspar-quartz-biotite±plagioclase gneiss, defined in the section on the Volcaniclastic Member) occurs in the Calc-Silicate Member as beds of white, medium- to fine-grained, well-foliated gneiss, or as beige to light pink, medium- to coarse-grained granofels. Felsic metatuff is found in minor amounts within sequences dominated by other lithologies; it comprises about 5 percent of the Calc-Silicate Member in the study area.

Much of the felsic metatuff of the Calc-Silicate Member occurs in one of two typical lithologic associations. 1) A few layers of light grey or beige, well-foliated felsic metatuff, 2 to 15 centimeters in thickness, are found with calc-silicate rock or marble at many outcrops. 2) Beige or pink granofelsic and gneissose felsic metatuffs, interbedded with quartz-K-feldspar granofelses (meta-arkoses), are observed at some localities. These two typical rock associations will be described separately.

Felsic metatuff also comprises parts of more complex lithologic associations. Such an association might consist of interbedded felsic metatuff, meta-arkose, and calc-silicate rock locally accompanied by additional lithologies, such as K-rich metasaprolite, quartzite, or amphibolite.

The felsic metatuffs of the Calc-Silicate Member commonly contain, in addition to micro-

TABLE 5. Distribution of rock types in the Calc-Silicate Member of the Ned Mountain Formation

Lithologies		Southern Manhattan Prong: Transects, Plate II A-A'	E-E'	F-F'	G-G'	J-J'	K-K'	L-L'	Northern Manhattan Prong: Study Area South	Central	North
Felsic Metatuff		M	m	m	m ,mG		m -U M -L	m	m -U M -L	m ,mG	m
Quartz-feldspar granofelses (and gneisses)	Quartz-K-feldspar		M		M	M	M -U	m			m
	Garnet-biotite			M ,mG				m	m G-U	m ,mG	
	Miscellaneous	M		m ,mG			m -L	M	M	M ,mG	
Marble			m	m		?				M ,mG	m
Calc-silicate rocks	White-and-green	m		m			m -L	m		M	m
	Dark, sulfidic			m					m -U	m	
Metawacke			m G		m		m -L		m ,mG	m ,mG	
Amphibolites	Cummingtonite - bearing	?		m			m -L	M	?	?	
	Cummingtonite-free	M	m	M		m	M -L	?	m	m	
K-rich metasaprolite										m	
Dark phosphatic gneiss				m	m		m -L				
Garnet-hornblende granofels		m	m	m							

KEY

M = Major amount

m = minor amount

G = Graphite present

U = upper portion of the Calc-Silicate Member

L = lower portion of the Calc-Silicate Member

cline and quartz, 0 to 12 percent plagioclase and 0 to 20 percent red or red-brown biotite. As in the Volcaniclastic Member, a few gneissose beds containing subequal K-feldspar and plagioclase occur at some localities. The plagioclase is generally An_{17} to An_{29} in composition, though one specimen (#1445, Table 3) contains albite. The felsic metatuffs contain up to ~1.5 percent Fe-Ti minerals (magnetite, ilmenite, and pyrrhotite), and trace quantities of zircon and apatite are common. Trace amounts of tourmaline, garnet, and sphene occur locally. Those metatuffs that contain the largest amounts of biotite grade texturally into schistose granofels.

Compositional gradations are common between felsic metatuff and interbedded metasedimentary rocks. Metatuffs that occur as interlayers in marble/calc-silicate sequences generally contain traces of graphite, while some felsic metatuffs have laminae containing calc-silicate minerals.

1. Felsic metatuff interbedded with marble and calc-silicate rock. Interbeds of felsic metatuff in marble sequences are readily recognized in the field: the marbles and calc-silicate rocks display little lineation (and less foliation), while the felsic metatuffs have a pronounced linear fabric and a weakly to moderately developed planar fabric (Fig. 18). The interbeds of felsic metatuff in marble sequences show more highly strained fabrics (Fig. 15E, F) than do metatuffs from any other setting. The textural contrast between the metatuff and marble is striking, and commonly provides the observer's first clue that a particular outcrop belongs to the Calc-Silicate Member. Fig. 18 illustrates the intricate interplay between marble, K-feldspar-rich calc-silicate rock, and felsic metatuff characteristic of this lithologic association.

The striking macroscopic texture of the felsic metatuffs results from its alternating "ribbons" of quartz and K-feldspar (Fig. 15E, F). The K-feldspar "ribbons" consist of microcline grains of about the same size as the quartz ribbons, or larger; most range from ~0.4 to 1.2 millimeter in diameter. Both the quartz and K-feldspar "ribbons" are a single grain in thickness (Fig. 15E). Smaller matrix K-feldspar grains, 0.1 to 0.3 millimeter in diameter, occur between some "ribbons".

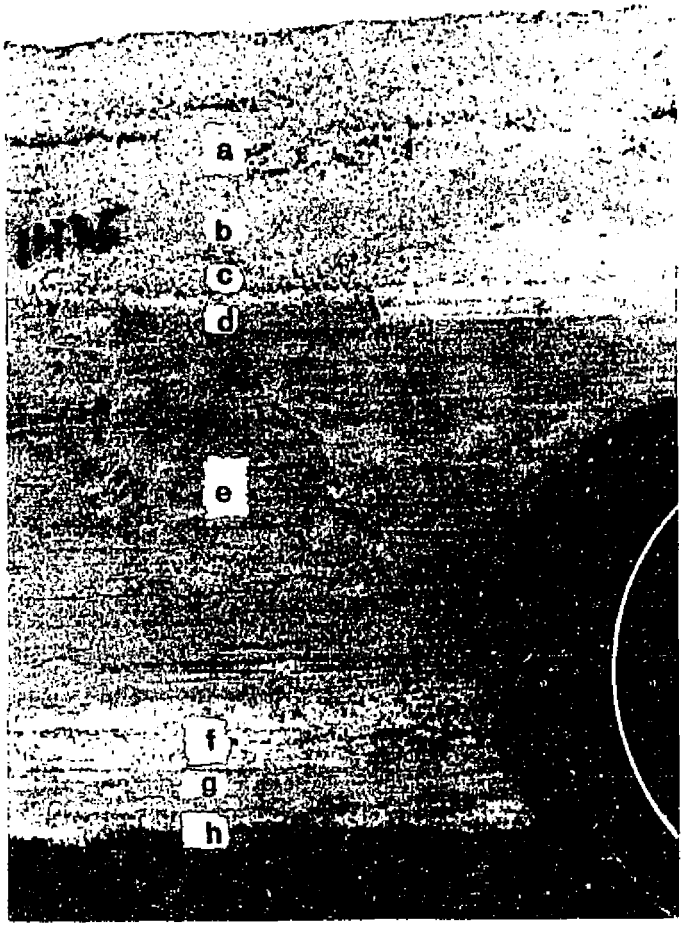

Fig. 18. Bed-by-bed variations in limey and felsic components in specimen #1435 of the Calc-Silicate Member, Ned Mountain Formation. Bright yellow grains are K-feldspar, chalky white grains are plagioclase, and grey streaks mostly quartz. Layers a, c, and h are calcitic marble; layer b is K-feldspar-bearing calc-silicate rock; layers d and f are plagioclase-quartz granofels; and layers e and g, which show the best-developed foliation, are felsic metatuff. Large grains in layer e are K-feldspar. Lens cap gives scale. A mode of layer e is given in Table 3, and Fig. 15E is a microphotograph of the same layer.

Some well-lineated felsic metatuffs contain megacrysts of feldspar, up to 7 millimeters in diameter or even larger. A few of these megacrysts show crystal terminations, though most have anhedral, ovoid shapes. Quartz and K-feldspar ribbons are commonly truncated against the largest grains and against those smaller grains that have well-developed crystal faces. Thin-section examination shows that the megacrysts can be untwinned grains of plagioclase (some antiperthitic), perthitic orthoclase, or microcline. These megacrysts commonly contain inclusions of rounded quartz or of other feldspar grains. In spite of the strong linear fabric of many of the felsic metatuffs, there is no sign of mortar texture around the megacrysts.

Interpretation. The characteristic mode of occurrence of the very-well lineated felsic metatuffs (as thin interbeds with poorly-lineated marble and calc-silicate rock) yields clues to the origin of their special texture. Marble and calcite-bearing calc-silicate rock are extremely ductile materials, which flow readily during deformation but show a high degree of textural recovery at high temperatures. High degrees of strain may leave no discernible imprint. In contrast, the thin interbeds of felsic metatuff, though initially nearly as ductile as the marbles, developed syn-tectonic fabrics that record the strain they shared with adjacent marbles: ribbons of quartz and K-feldspar.

The feldspar megacrysts that occur in the metatuffs are interpreted as poikiloblastic porphyroblasts. Once they had formed, these porphyroblasts would have behaved as porphyroclasts within the more ductile matrix of finer-grained quartz and feldspar. Both the megacrysts and the K-feldspar "ribbons" are interpreted as products of syntectonic grain growth, by a process of diffusion creep.

2. Felsic metatuff interbedded with meta-arkose. Interbedded felsic metatuff and quartz-feldspar granofels (meta-arkose) occur in sequences that can be more than 50 meters thick. Such sequences have been mapped as "Lowerre Quartzite" by Norton and Giese (1957), Hall (1968b),

Wissing (1970), Whiting-Goldberg (1977), Alavi (1976), and Brock and Brock (1985a), in the White Plains, Ossining, Mount Vernon, Pound Ridge, and Croton Falls quadrangles. These sequences display bed-by-bed variations in K-feldspar content.

The K-feldspar content of the individual beds ranges between 3 and 77 modal percent, and covers practically all intermediate values. Given the observed compositional continuum, a petrographic divide between felsic metatuff and meta-arkose must be set here. It is placed, somewhat arbitrarily, at 50 percent modal K-feldspar. In addition to the K-feldspar-rich metatuff beds, there are some feldspathic beds (also considered to be felsic metatuffs) that contain subequal amounts of K-feldspar and plagioclase, as well as 20 to 30 percent quartz. These beds tend to be coarser-grained and more gneissose than the K-feldspar-rich metatuffs.

The meta-arkoses and metatuffs are generally very similar in color and texture, and are therefore difficult to distinguish in the field. The distinction is virtually impossible to make without staining for K-feldspar or thin-section examination. Judging from collections of hand specimens, felsic metatuff comprises less than 15 percent of the interbedded felsic metatuff/meta-arkose sequences.

In many of these sequences, however, K-feldspar has been mobilized and recrystallized into numerous, very coarse-grained segregations. The segregations range from about one centimeter to a few tens of centimeters in thickness; they are composed of $\geq$85 percent, pink or beige, poikiloblastic K-feldspar. Though they resemble pegmatites in grain size, the segregations are clearly strata-bound, and their coarse grains transect only the finest scale of bedding.

These segregations contain a higher modal K-feldspar content than any felsic metatuff. K-feldspar must have migrated <u>out</u> of adjoining granofelsic beds in order to form them. The modal compositions of hand specimens must, in fact, give an under-estimate of the original proportion of felsic tuff, because of K-feldspar lost to these segregations.

Quartz-feldspar granofelses and gneisses. Quartz-feldspar granofelses and gneisses make up a significant portion (about a third) of the Calc-Silicate Member in the study area. Though the rocks are generally granofelsic, biotite-rich segregations or laminae give some a gneissose appearance.

The quartz-feldspar rocks of the Calc-Silicate Member overlap compositionally with granofelses of both the Wacke and Volcaniclastic Members, and include some additional variations. Quartz-feldspar rocks of Calc-Silicate Member are principally distinguished by 1) their stratigraphic positions, sandwiched between the Ned Mountain Volcaniclastic or Wacke Members and the Inwood Marble, and 2) by being interbedded with other Calc-Silicate Member lithologies.

The range of compositions observed among the Calc-Silicate Member quartz-feldspar rocks shows that this unit received inputs from several distinct sources. The nature of these source materials, and their depositional histories, will be examined after the description of the quartz-feldspar rocks.

For convenience, the quartz-feldspar rocks have been subdivided into three categories:

1) quartz-K-feldspar granofelses;

2) quartz-feldspar-biotite-garnet granofels and gneisses; and

3) miscellaneous quartz-feldspar granofelses.

1) Quartz-K-feldspar granofelses. Quartz-K-feldspar granofels is the predominant rock type in many of the sequences that were previously mapped as "Lowerre Quartzite". This lithology is a buff-colored, well-bedded, and generally rusty- or brown-weathering granofels. It breaks in blocky fashion and tends to outcrop well. Its K-feldspar content varies bed-by-bed. As K-feldspar increases past 50 percent, the rocks grade into felsic metatuff; as K-feldspar decreases, the rocks grade into subarkoses (quartz $\geq$75 percent), and then quartzite (quartz $\geq$ 90 percent).

Thin-bedded rocks, with cumulative thicknesses ranging from several meters up to tens of

meters, make up sequences of quartz-K-feldspar granofelses. Bedding is generally several centimeters in thickness; many beds also show fine lamination. Meta-arkose is the dominant rock type in these sequences, and is typically accompanied by minor amounts of felsic metatuff, meta-subarkose, and a few beds of quartzite. These granofelsic sequences locally contain interbeds of a dark, biotite-rich phosphathic gneiss, amphibolite, or graphitic biotite-garnet schist. Coarse-grained K-feldspar segregations (described in the previous section) are common in K-feldspar-rich portions of the sequences. In addition to occurrences within these granofelsic sequences, a few beds of quartz-K-feldspar granofels have also been observed in association with calc-silicate rock.

Rocks classified as meta-arkoses contain 50 to 75 modal percent quartz, 15 to 50 percent K-feldspar, 0 to 5 percent biotite and/or muscovite, and 1 to 5 percent accessory minerals. K-feldspar is invariably in the form of microcline. Plagioclase is absent in meta-arkosic beds, though commonly present in associated metatuffs. Accessory minerals found in quartz-K-feldspar granofelses commonly include pyrite, pyrrhotite, magnetite, zircon, tourmaline, and apatite. Sphene, ilmenite or rutile occur in a few cases. Some pyrite grains are rimmed by magnetite. In some thin sections, the grains of K-feldspar appear to be rounded.

The modal feldspar contents of Calc-Silicate Member granofelses are plotted on Fig. 19A. Alkali feldspars and calcic minerals (such as diopside and tremolite) of the granofelses are plotted on Fig. 19B. The quartz-K-feldspar granofelses are confined near the K-feldspar apices of these plots, where they coincide with most Calc-Silicate Member felsic metatuffs.

One specimen of quartz-K-feldspar granofels, collected from a bed associated with calc-silicate rocks, contains a small proportion of Ca-minerals (Fig. 19B). Modes of granofelsic and calc-silicate rock layers from this specimen, #1634, are both given on Table 3.

The foregoing description of the quartz-K-feldspar granofelsic sequences is largely based on observations from reconnaissance transects (Table 5; Plate IIB). Quartz-K-feldspar granofels is a relatively common lithology in the Calc-Silicate Member over much of the Manhattan Prong, but is a significant constituent at only one Calc-Silicate Member outcrop inside the study area. At

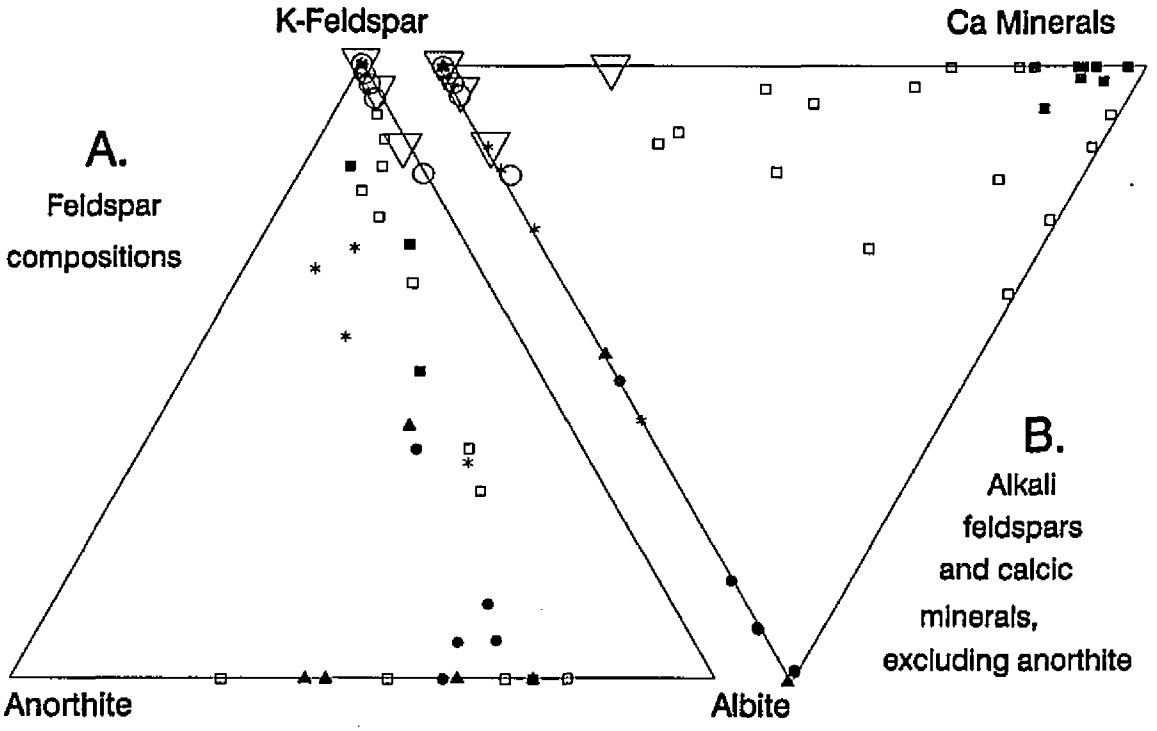

Calc-Silicate Member		Wacke Member	
Metatuff	○		
Quartz-K-feldspar granofels	▽		
Quartz-feldspar-biotite-garnet granofels	▲	Quartz-feldspar-biotite-garnet granofels	•
Miscellaneous quartz-feldspar granofelses	*		
Marble	■		
Calc-silicate rock	□		

Fig. 19. Feldspar and calc-silicate mineral variations in the Calc-Silicate and Wacke Members, Ned Mountain Formation (see text for explanation).

this site, where specimen #1634 was collected, interbedded quartz-K-feldspar granofels and calc-silicate rock occur above K-rich metasaprolite of the Wacke Member/Calc-Silicate Member transition zone. These two lithologies locally constitute the very thin Calc-Silicate Member that overlies the Wacke Member.

2) Quartz-feldspar-biotite-garnet granofelses. Brown-, rusty-, or grey-weathering, medium-grained, garnet-bearing (quartz-feldspar-biotite-garnet) granofelses occur in the Calc-Silicate Member in the central and southern Peach Lake quadrangle. These granofelses generally occur within sequences of siliceous rocks between 1 and 10 meters in thickness. Some of these granofelses have thin, sillimanite-bearing, pelitic laminae, <4 millimeter in thickness (e.g., #735 and 1441, Table 3). Other garnetiferous granofelses (#1502 and 1493, Table 3) contain thin interbeds or lenses of quartzite. A few quartz-feldspar-biotite-garnet rocks have biotite-rich segregations that give them a gneissose texture.

The modal quartz content of these granofelses ranges from 34 to 75 modal percent, the plagioclase content from 0 to 33 percent, the K-feldspar content from 0 to 18 percent, the biotite content from 0 to 15 percent, and garnet content from less than 1 to 25 percent. Plagioclase composition varies widely (An_{25} to ~An_{75}).

On Fig. 19A, the feldspar compositions of the garnet-bearing granofelses can be compared with those of other Calc-Silicate Member granofelses and with those of quartz-feldspar-biotite-garnet granofelses of the Wacke Member. The Calc-Silicate Member garnetiferous granofelses are largely confined to plagioclase-rich compositions. The fields for the garnetiferous granofelses of the Calc-Silicate and Wacke Members overlap, but calcic plagioclases occur only in the Calc-Silicate Member granofelses.

Accessory apatite, zircon, pyrrhotite, magnetite, and ilmenite are commonly present in the garnetiferous granofelses. One specimen, #735 (Table 3), contains a trace amount of cordierite. Some of the granofelses are graphitic, bearing up to ~2 modal percent of graphite.

3) Miscellaneous quartz-feldspar granofelses. The quartz-feldspar rocks of the Calc-Silicate Member include many examples which are neither rich in K-feldspar nor garnetiferous. Most of these "miscellaneous" quartz-feldspar rocks are medium-grained, grey- or brown-weathering granofelses. They generally occur in beds that range from several centimeters to a few meters in thickness, and outcrop in association with calc-silicate rock.

The proportions of quartz and feldspars in these rocks vary considerably. Modal quartz ranges from 33 to 65 percent, plagioclase from 1 to 28 percent, and K-feldspar from 0 to 33 percent. Some of these granofelses contain calcic plagioclase, others sodic plagioclase; plagioclase compositions range from An_{26} to An_{75}. Biotite content ranges from a low of 3 modal percent, to a high of 28; those rocks with the highest biotite contents are schistose granofelses. Accessory apatite and zircon are common, and sphene, tourmaline, or allanite may be present. Graphite, though uncommon, may occur in amounts up to 2 modal percent. Other opaque minerals (pyrrhotite, magnetite, and ilmenite) together comprise from 1 to 2 modal percent of the granofelses. Examples of modal compositions are given on Table 3.

The feldspar compositions of the "miscellaneous" quartz-feldspar rocks are compositionally intermediate between those of the Calc-Silicate Member quartz-K-feldspar and quartz-feldspar-biotite-garnet granofelses Fig. 19A). The "miscellaneous" granofelses are significantly richer in K-feldspar than are the granofelses of the Wacke Member.

Interpretation of quartz-feldspar granofelses. The variations in modal mineralogies of the quartz-feldspar granofelses are indicative of a wide range of source materials and depositional histories.

I. Depositional history. The range of compositions observed among the granofelses indicates their sediments must have undergone varied histories of deposition. The protolith of quartz-feldspar-biotite-garnet granofels evidently contained fairly immature, feldspathic sands. These sands had not experienced prolonged chemical weathering, but were transported, deposited, and

buried in rapid succession. However, interbeds and lenses of quartzite do occur with certain granofelses. These interbeds indicate that local accumulations of highly weathered, mature quartz sands must also have developed.

Most of the depositional environments were apparently fairly oxidizing. Graphite is uncommon, except among the garnet-bearing granofelses. Iron sulfides, on the other hand, are common. Perhaps this sulfide originated diagenetically, as pyrite in sandstones "almost entirely" does (Pettijohn, Potter, and Siever, 1973).

II. Source materials. The quartz-feldspar-biotite-garnet granofelses overlap compositionally with the granofelses of the Wacke Member. Both groups of granofelses are characterized by high (Na-rich) plagioclase to K-feldspar ratios. These ratios are comparable to the bulk proportions of plagioclase and K-feldspar in much of the Fordham Gneiss. The feldspar compositions suggest that the protolith was primarily derived from a Grenvillian (basement) source.

The quartz-K-feldspar meta-arkoses, though highly feldspathic, lack plagioclase. A second source of clastic sediments, rich in K-feldspar but poor in plagioclase, evidently also existed. This second source cannot relate to local differences in basement lithology, because a) significant amounts of plagioclase are present in every known Fordham lithology, including the granites (Table 2), b) there is no geographic correspondence between the lithologies of the Fordham Gneiss and the distribution of the quartz-K-feldspar granofels, and c) the quartz-K-feldspar granofelses overlie a lower Ned Mountain section that generally contains substantial Na-plagioclase. The characteristic bed-by-bed interplay between K-rich meta-arkose and felsic metatuff in the quartz-K-feldspar granofelsic sequences (and the compositional continuum between them) suggests a different source for the K-feldspar: viz., sanidine crystals from deposits of felsic volcanic rocks, inverted to microcline during deformation.

Even if the K-feldspar content of the granofelses can be attributed to inputs from felsic volcanic rocks, two aspects of the granofelses still must be explained: the absence of plagioclase, and presence of quartzitic interbeds. The absence of plagioclase in the granofelses implies that

any plagioclase (anorthoclase?) present in the original volcanic deposits was more vulnerable to weathering than was the K-feldspar. In addition, the absence of plagioclase indicates that basement-derived sands (of the kind that comprise the garnetiferous granofelses) made, at most, only a negligible contribution to the quartz-K-feldspar granofelses. To explain the presence of quartzitic interbeds, one may postulate either that (i) the quartzites formed as the residuum of felsic volcaniclastic deposits, weathered in place, and clays largely washed away, or that (ii) the quartzites were mature, quartz-rich sands of Grenvillian provenance that were repeatedly mixed with felsic volcanic material.

Whatever the origin of those quartzitic beds, two principal sources of clastic material can be inferred: the Grenvillian basement and ongoing felsic volcanic activity. In addition to these clastic inputs, organic matter and/or chemical precipitates also contributed to protoliths of many Calc-Silicate Member granofelses. The calcic plagioclase found in some granofelses (Table 3; Fig. 19A) testifies to former presence of calcite; the presence of graphite implies the former existence of carbonaceous matter.

III. Summary. The compositions of the granofelsic rocks indicate contributions from three principal sources: sands of Grenvillian provenance, felsic volcaniclastic material, and calcareous/organic matter. The Grenvillian basement was the primary source of detrital sodic plagioclase; most K-feldspar was derived from felsic volcaniclastic deposits; and calcite (either as a cement or as biogenic clasts) was the major source of the calcium that led to formation of calcic plagioclase. Calc-Silicate Member granofelses contain, in varying proportions, inputs from all three of these sources. The relative importance of components derived from Grenvillian basement, felsic volcaniclastic rocks and limy carbonates in each granofels is reflected by its feldspar composition (Fig. 19A).

The compositions of the granofelses record a variety of depositional histories as well as source materials. While much of the detrital material experienced little chemical weathering, at least a few small deposits reached the rank of orthoquartzite.

Calc-silicate rocks and marbles. Calc-silicate rocks and marbles make up about half of the Calc-Silicate Member in the study area. Low-lying, swampy areas tend to follow the marbles, which tend to outcrop poorly. Some of the calc-silicate rocks, on the other hand, are so siliceous that they act as topographic ridge-formers.

The calcareous rocks of the Calc-Silicate Member occur in a number of guises, and are subdivided here into three loose groupings: 1) marbles (>50 percent modal calcite); 2) white-and-green calc-silicate rocks; and 3) dark, rusty-stained calc-silicate rocks.

1) The marbles are white to beige, tan-, grey-, or rusty-weathering, and are interbedded with white-and-green calc-silicate rock. Interlayers of felsic metatuff are commonly present. The marbles are calcitic, and clinopyroxene and K-feldspar are the dominant silicate minerals. Calcite, diopside, and K-feldspar together comprise an average of ~90 modal percent of the rocks. Graphite occurs in about half of the marbles, generally in trace amounts, though locally up to 3 modal percent.

2) The white-and-green calc-silicate rocks generally occur as medium-grained granofelses, speckled white (calcite+ feldspar+quartz)-and-green (clinopyroxene+hornblende) on fresh surfaces, and tan-, brownish- or grayish-weathering. In outcrop, these rocks commonly display ribbing due to differential erosion: siliceous beds stand out in relief, while carbonate-rich calc-silicate rocks and marble beds are weathered away. Bedding is well defined, and generally ranges from 5 to 50 centimeters in thickness. White-and-green calc-silicate rock also occurs as interbeds in some quartz-feldspar granofelsic sequences.

Coarse-grained, gneissose calc-silicate rock is found at a few localities. These rocks are white to beige in color, with large, dark-green porphyroblasts of clinopyroxene and/or hornblende. Small enclaves of marble (a few centimeters in width) occur in some of these gneisses.

Graphite has <u>not</u> been found in the white-and-green calc-silicate rocks, even where it is present in associated marbles or quartz-feldspar granofelses.

3) Rusty-weathering, khaki to dark greenish calc-silicate rock occurs in relatively small

amounts. Beds range from a few centimeters to a few meters in thickness. These rocks contain several modal percent of opaque minerals, predominantly pyrrhotite, but generally including subordinate magnetite and/or pyrite. No graphite has been observed. Some beds consist of up to 75 percent clinopyroxene or hornblende, though others are quartz-rich. In contrast to the white-and-green calc-silicate rocks, K-feldspar is generally absent, though a few beds contain up to 50% K-feldspar. Plagioclase ranges from relatively sodic to calcic ($\sim An_{70}$) composition. This lithology is found in outcrop with marble, other calc-silicate varieties, or adjacent to quartz-feldspar-biotite-garnet granofels.

The calc-silicate rocks and marbles of the Calc-Silicate Member show a broad range of modal compositions. The marbles contain a substantial admixture of silicate minerals; the highest carbonate content yet observed is 77 modal percent. Beds of calc-silicate rock range from moderately to highly siliceous. The calc-silicate minerals found in these rocks include diopsidic clinopyroxene, hornblende, scapolite, tremolite, and clinozoisite. These minerals do not all coexist in textural equilibrium; some, particularly tremolite and clinozoisite, are evidently late, and replace other mineral species.

In addition to calcite and the calc-silicate minerals, K-feldspar, quartz, and plagioclase comprise significant proportions of the modal compositions of the marbles and calc-silicate rocks. Minor sphene and pyrrhotite are nearly ubiquitous, and apatite and magnetite are very common. Other accessory minerals may include biotite, graphite, tourmaline, zircon, and light-brown or yellowish allanite; the allanite is commonly overgrown by clinozoisite. Representative modes are given on Table 3.

The feldspar compositions of the calc-silicate rocks range from K-feldspar-rich to plagioclase-rich, and plagioclase composition ranges from Na-rich to Ca-rich. Plotted on Fig. 19A, these compositions cover the same field as do all the Calc-Silicate Member granofels types combined.

Fig. 19B shows the proportions of modal alkali feldspars to Ca-bearing minerals (exclusive of anorthite) in the marbles and calc-silicate rocks. To plot this figure, the mineral formulas have

been normalized to 8 oxygens (matching the alkali to oxygen ratio of the feldspars), since the minerals contain different relative amounts of Ca. Thus, a rock with equal numbers of K atoms (contained in feldspar) and Ca atoms (contained in calcite and calc-silicate minerals) plots half-way between the "Ca minerals" and K-feldspar apices. The normalized values used to plot each Ca-bearing mineral are given in Appendix 2.

On Fig. 19B, calc-silicate rocks form a belt that extends from the marbles (which plot at the "Ca-minerals" apex) nearly all the way to the K-feldspar apex. This belt nearly meets the fields of the quartz-K-feldspar granofelses and the felsic metatuffs. It implies that nearly continuous gradations in composition exist between the marbles, on one hand, and the felsic metatuffs on the other. Such a gradation is consistent with the bed-by-bed variations in limey and felsic components observed in calc-silicate sequences in the field (Fig. 18).

In contrast to the near-continuous compositional gradation observed between marbles and quartz-K-feldspar granofels, there is a compositional discontinuity between the marbles and the garnet-bearing granofelses. The calcic plagioclase that occurs in some garnetiferous granofelses (Fig. 19A) reflects a moderate enrichment in calcium, but the rocks are free of "Ca-minerals" (such as clinopyroxene) and plot on the K-feldspar-albite join in Fig. 19B. Some calc-silicate rocks, though free of K-feldspar, contain modest amounts of sodic plagioclase, and so plot on the "Ca-mineral"-albite join in Fig. 19B. However, no rocks of intermediate composition are known, and a distinct hiatus appears to exist. This hiatus is consistent with the general restriction of garnetiferous granofelses to sequences of siliciclastic rocks observed in the field.

Fig. 19 shows the range of feldspar compositions found among the calc-silicate rocks and marbles, but does not distinguish among the three most important components of most carbonate rocks: CaO, MgO, and SiO_2. This function is performed by Fig. 20, but in a special manner. Fig. 20 is intended to show an approximation of the original proportions of quartz, calcite, and dolomite, as derived by using present modal mineralogy.

In order to determine the original "quartz", "calcite" and "dolomite" content of each rock,

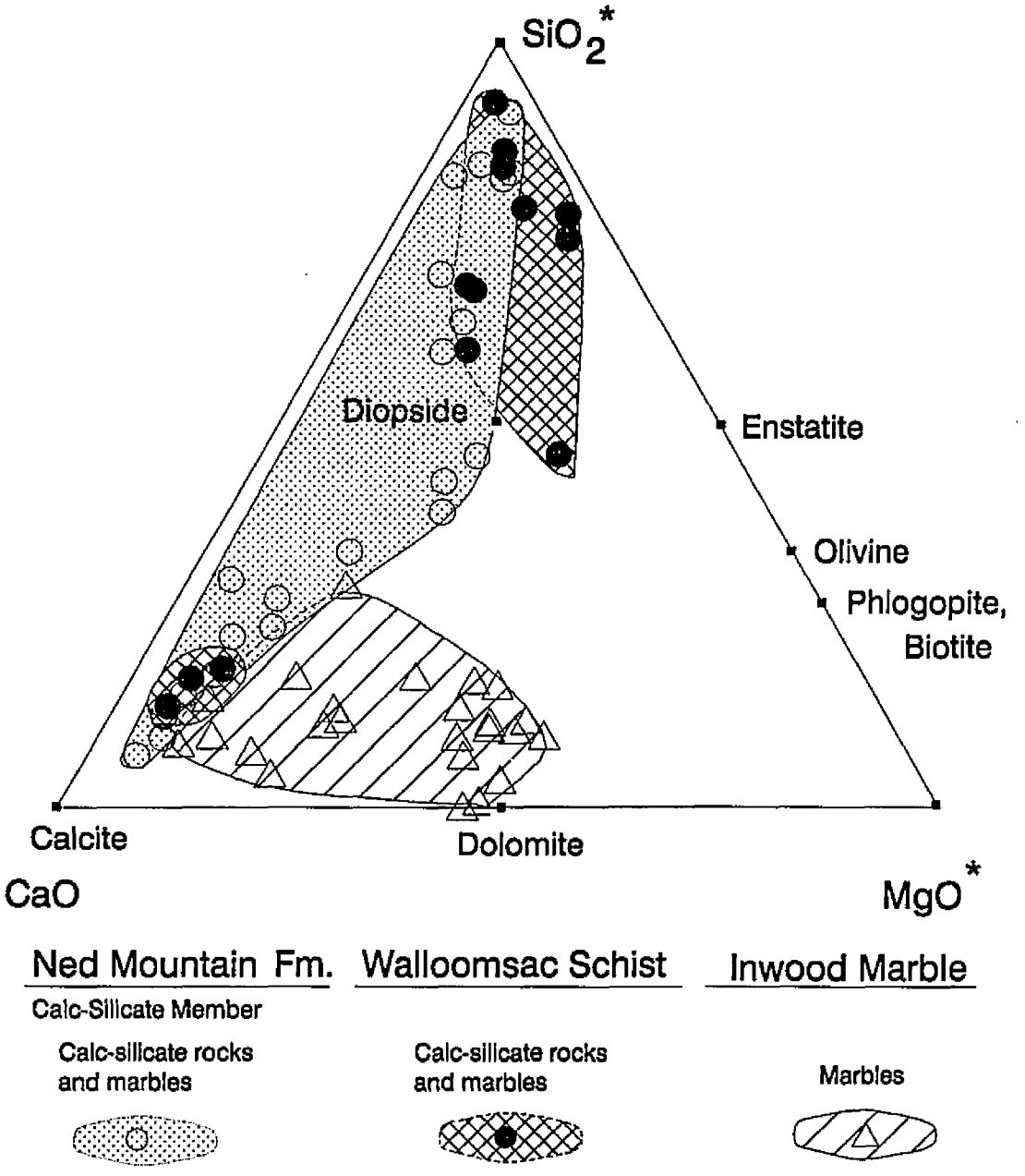

SiO_2^* = SiO_2 in excess of that in the alkali feldspars and that assigned to the original clay minerals

MgO^* = total MgO + any FeO present in the silicate minerals (see text for explanation).

Fig. 20. Compositional fields of marbles and calc-silicate rocks of the Calc-Silicate Member of the Ned Mountain Formation, the Walloomsac Schist, and the Inwood Marble.

every mineral (exclusive of Fe-Ti oxides) was normalized to 8 oxygens (this number is chosen for convenience, since 8 oxygens are used in Fig. 19B). Then, the contributions of CaO, MgO, and SiO_2 of each mineral were combined, in appropriate modal quantities.

However, the estimation of original quartz content obtained in this way must be adjusted, since some silica originally occurred in detrital minerals other than quartz. Alkalis were probably once incorporated into alkali feldspars; alumina was probably in clay minerals. In order to take these other detrital minerals in account, 1) the silica content of modal alkali feldspars is excluded from the "quartz" total; 2) Al_2O_3 (in excess of that in the alkali feldspars) is assigned to an "original clay fraction", assumed to have had an average Si:Al ratio of 1.5 : 1. The silica assigned to this "original clay fraction" is subtracted from the "quartz" total.

Another complication arises from the ferrous iron content of the calc-silicate rocks. Since no data are presently available on their mineral compositions, any Fe^{2+} that has substituted for Mg^{2+} is not readily excluded. Therefore, any FeO which occurs in micas, pyroxenes, and amphiboles is lumped with MgO on the plot (giving an MgO^* apex), although FeO contained in opaque minerals is excluded.

The various points of procedure discussed here were built into three formulas, which together define the how each rock plots on Fig. 20. These formulas are given in Appendix 2.

On Fig. 20, the calc-silicate rocks and marbles plot in a nearly continuous belt that reaches from the CaO to the SiO_2 apex. This belt records progressive degrees of mixing between calcareous and quartzose components in the rocks' protoliths. The rocks are poor in MgO, containing, at most, a modest "MgO^*" component.

Interpretation. The compositions of the calc-silicate rocks and marbles indicate that their protoliths contained mixtures of carbonate, sands derived from Grenvillian and felsic volcaniclastic sources, and clay. The compositional continuum between marble and felsic metatuff can be explained by ash-fall into carbonate-producing environments. The incomplete continuum be-

tween marble and quartz-feldspar-biotite-garnet granofels (Fig. 19B) implies that the deposition of immature, terrigenous sands and carbonates occurred in separate micro-environments. Most of the calc-silicate rocks contain only a relatively small fraction of sodic plagioclase.

The dark-green, sulfidic calc-silicate rocks generally contain little or no K-feldspar. The precursor materials of these rocks are inferred to be mixtures of sands with minor carbonate and clay, deposited in reducing, anoxic environments.

Metawacke and metapelite. Metawacke makes up 5 to 10 percent of the Calc-Silicate Member, where it is found in belts rich in meta-siliciclastic rocks. Metawacke occurs as thin, schistose interlayers in sequences of quartz-feldspar-biotite-garnet granofelses, as minor components of mixed garnetiferous granofels/ calc-silicate rock/ metawacke assemblages, and in a few metawacke-dominant sequences that attain some tens of meters in thickness.

Much of the metawacke is a medium-grained, grey, rusty-weathering, graphitic schist, though some graphite-free schist also occurs. Modal quartz ranges from 18 to 53 modal percent, K-feldspar from 0 to 36 percent, plagioclase (An_{28} to $_{52}$) from 1 to 35 percent, biotite from 9 to 28 percent, garnet from 4 to 23 percent, and aluminosilicate minerals (sillimanite and kyanite) from 0 to 9 percent. Up to 2 modal percent of graphite occurs in the metawackes.

In thin section, biotite grains are red or pale-red. Trace amounts of ilmenite, pyrrhotite, magnetite, zircon, apatite, and olive or pale-green tourmaline are common. Representative modes are given on Table 3.

Aluminous schist in one occurrence contains >50 percent modal biotite+garnet+sillimanite, and is therefore classified as a metapelite. This coarse-grained, rusty-weathering schist has 3 percent modal of graphite, and is pock-marked by large garnet porphyroblasts. Most of the biotite is bright orange-red in thin section.

K-rich metasaprolite. A number of zones or beds of rusty-weathering, K-rich metasaprolite (defined in the discussion of the Basal Member) occur within the Calc-Silicate Member. These beds, though distinctive, are volumetrically minor, and comprise <1 percent of the Calc-Silicate Member. The beds range between some tens of centimeters up to a few meters in thickness. They outcrop with quartz-feldspar granofelses, amphibolites, calc-silicate rocks, and marbles.

The K-rich metasaprolites are generally medium- to coarse-grained, light grey to beige in color (with reddish biotite), and many have porphyroblasts of garnet, sillimanite, or K-feldspar. Some show a pronounced linear and/or planar fabric. They may contain trace amounts of olive to blue-green tourmaline, zircon, apatite, ilmenite, magnetite, pyrrhotite, green (hercynitic) spinel, rutile, and/or anatase. Representative modes are given on Table 3.

Interpretation. The occurrence of K-rich metasaprolite in the Calc-Silicate Member indicates that rocks of this unit underwent episodic subaerial exposure.

Amphibolites. Amphibolites of varied compositions make up about 5 percent of the Calc-Silicate Member. They occur in homogeneous layers that range from about three centimeters to several meters in thickness. Most amphibolites outcrop with calc-silicate rock or quartz-feldspar granofelses. Beds of amphibolite (even those only a few centimeters in thickness) have sharp, planar, conformable contacts with neighboring lithologies.

Mineral assemblages found among the amphibolites include 1) hornblende-plagioclase-quartz-biotite-garnet, 2) hornblende-plagioclase-quartz-clinopyroxene, 3) hornblende-plagioclase-quartz-biotite, and 4) hornblende-plagioclase-clinopyroxene-K-feldspar. Some cummingtonite-bearing amphibolites occur in the Calc-Silicate Member outside of the study area (Table 5).

Plagioclase is fairly sodic (An_{26} to An_{35}). The amphibolites are rich in titanium, containing 3 to 6 modal percent of ilmenite and/or sphene. Trace amounts of apatite, magnetite, and pyrrhotite are common, and pale-brown allanite and epidote locally occur. Representative modes

are given on Table 3.

Interpretation. The mafic, titanium-rich character of the amphibolites implies that they are essentially metabasites. However, the presence of K-feldspar in some amphibolites is not consistent with a simple mafic protolith. It requires either a) a mixture of mafic tuff with feldspathic sediments or felsic tuffs in the protolith or b) a metasedimentary origin (from a mixture of carbonate, sand, and clay). The homogeneous nature of these beds and their sharp contacts with neighboring calc-silicate rock favor the first alternative.

Plagioclase-magnetite rock. Thin light-grey bands (<2 centimeter thick) occur with coarse-grained, hornblende-rich amphibolite at one locality. Seen in thin section, these bands consist of ~90 percent plagioclase (~An_{56}), 4 to 8 percent magnetite, a few percent of hornblende, and a number of grains of green to olive tourmaline.

Interpretation. Tourmaline has not been found in any amphibolite in the study area. The abundance of tourmaline within the bands of plagioclase-magnetite rock implies that the bands originated as sedimentary deposits, enriched in stable, heavy minerals, rather than by some process of metamorphic segregation from the amphibolite. K-rich metasaprolite collected at this locality is also tourmaline-bearing.

The bands of plagioclase-magnetite rock are reminiscent of calcic plagioclase-rich lenses and beds that occur in several other contexts, where they are also generally accompanied by abundant Fe-oxides: a) the metasaprolite that occurs at the Fordham Gneiss- Basal Ned Mountain Formation contact (SGB20b, Table 3); b) metabasite #1252 of the Wacke Member (Table 3); c) rare pockets of calcic plagioclase within K-rich metasaprolites. I suggest that the plagioclase-magnetite rock is best interpreted as a metasaprolite, which original consisted of calcrete with iron oxides, clay, and a detrital component enriched in stable heavy minerals.

Phosphatic gneiss and Garnet-hornblende granofels. Two of the lithologies assigned to the Calc-Silicate Member have been encountered exclusively outside the study area (Table 5). One of these rock types is a dark grey to black, medium-grained, biotite-rich, phosphatic gneiss. This gneiss occurs as interbeds with felsic metatuff, with quartz-K-feldspar granofels, or with calc-silicate rock. Representative modes are given on Table 3.

The second rock type is a medium-grey, garnet- and hornblende-bearing feldspathic granofels. This granofels generally shows a lineation (defined by hornblende grains), is medium- to fine-grained, and has a blocky, homogeneous appearance. It locally crops out with amphibolite. This granofels may have originated as mixture of mafic tuff and siliceous sediments, like the mafic metasediment suite of the Basal Member. Modes of representative specimens are given on Table 3.

Distribution of rock types within the Calc-Silicate Member. Lithologic variability is a hallmark of the Calc-Silicate Member at nearly every scale. On the scale of the individual outcrop, many different lithologic types (for instance, calc-silicate rock, quartz-feldspar granofels, amphibolite, and felsic metatuff) commonly occur together. The combination of rock types varies from place to place, as does the exact lithology of those rocks (graphitic versus non-graphitic, type of calc-silicate rock, etc.). Table 5 summarizes the lithologies observed in the Calc-Silicate Member at various localities in the Manhattan Prong. The relative stratigraphic position of these lithologies within the Calc-Silicate Member is indicated in some instances.

Little marble has been encountered in the Calc-Silicate Member outside of the study area. This, however, may be a function of outcrop. Only a few outcrops of Inwood Marble were found on the reconnaissance transects, and it is uncertain how much undetected Calc-Silicate Member marble is present beneath the (presumably marble-floored) valley bottoms.

Sequences of K-feldspar-rich meta-arkose and felsic metatuff up to tens of meters in thickness occur at few localities, where they have been previously mapped as "Lowerre Quartzite".

In contradiction to previous reports, however, these rocks do not invariably occur immediately below the Inwood Marble. Grey garnet-hornblende granofels and amphibolite overlie the "Lower-re" meta-arkose/felsic metatuff sequence on transect E-E'.

Some of lateral changes within the Calc-Silicate Member can be illustrated by comparing sequences separated by about 3.5 kilometers along present-day strike: transects K-K' and L-L'. On transect K-K', the Calc-Silicate Member is dominated by felsic metatuff and K-feldspar-rich meta-arkose, and contains minor amounts of other several rock types (Table 5). On transect L-L', however, quartz-feldspar schistose granofels, amphibolite, and white-and-green calc-silicate rock make up most of the Calc-Silicate Member, and K-feldspar-rich meta-arkose occurs as a single 18 centimeter-thick bed that lies just below the dolomitic Inwood Marble.

The Calc-Silicate Member and Inwood Marble outcrop within several meters of each other at two localities inside the study area. At the site in the northern Peach Lake quadrangle, by the east shore of Lake Windwing (Plate III), the Calc-Silicate Member consists of K-feldspar-rich meta-arkose and white-and-green calc-silicate rock. No other rock types are present. Multiple layers of meta-arkose and calc-silicate rock are interbedded. In the east-central Peach Lake quadrangle, the Calc-Silicate Member-Inwood Marble contact is exposed in a gully on the south side of Peaceable Road, just east of Golf Lane (Plate III). There, the Calc-Silicate Member consists of quartz-feldspar-biotite-garnet granofelses with thin, schistose, metawacke interlayers, dark, sulfidic, calc-silicate rock, K-feldspar-rich meta-arkose, and (at the very top, in contact with Inwood Marble) felsic metatuff. Specimen #1445, illustrated in Fig. 15A, was collected from this felsic metatuff. Thus, each place that the uppermost beds of the Ned Mountain Formation are observed they consist of different lithologies; a "Lowerre"-like K-feldspar-rich meta-arkose occurred at only one out of three localities.

AMPHIBOLITE DIKES IN THE FORDHAM GNEISS. Amphibolite dikes some tens of centimeters in thickness cross-cut the Fordham Gneiss in at least two localities: on transects D-D' and H-H' (Plate III). These homogeneous, dark, unfoliated dikes of hornblende-garnet amphibolite truncate folds and foliation within the Fordham Gneiss (Fig. 21). The dike on transect D-D' contains a xenolith of the host Fordham. The dikes consist of fine-grained amphibolite, though the Fordham units they cut contain much coarse-grained orthopyroxene. A mode from the transect H-H' dike is given on Table 3 (specimen #2215).

Interpretation. The amphibolites are probably metadiabase dikes genetically related to the metabasites of the Ned Mountain Formation. Hornblende-garnet amphibolite of similar modal composition occurs in the Ned Mountain Formation of the southern Manhattan Prong. These dikes are not isolated occurrences; Ratcliffe (1987) reported numerous metadiabase dikes of inferred Late Proterozoic age in the Hudson Highlands, north of the Manhattan Prong.

IMPLICATIONS OF THE NED MOUNTAIN FORMATION FOR THE TECTONIC DEVELOPMENT AND GEOLOGIC HISTORY OF THE MANHATTAN PRONG. Although there is great local variation, the Ned Mountain Formation in general shows certain persistent traits. These include: 1) presence of bimodal metavolcanic rocks; 2) abundant quartz-feldspar granofels; 3) discontinuity of individual beds; 4) abrupt and close-spaced changes in lithology; 5) repetition of many distinctive and characteristic rock types at different stratigraphic levels; 6) occurrence of metasedimentary rocks whose protoliths formed under a broad variety of environmental conditions. The layers of K-rich metasaprolite scattered through the Ned Mountain Formation record repeated subaerial exposure, and suggest terrestrial depositional settings for adjacent lithologies. It is concluded that deposition of the siliciclastic rocks occurred in a tectonically unstable terrestrial environment, accompanied by bimodal volcanic activity. A

Fig. 21. Fine-grained amphibolite dike truncates foliation in the Fordham Gneiss. Hammer is 33 centimeters long. Transect H-H', Croton Falls quadrangle. (Specimen #2215 on Table 3 was collected from this dike.)

continental rift setting is most consistent with these characteristics.

The history of the Manhattan Prong during Late Proterozoic to Early Cambrian time can be outlined by briefly considering the environmental conditions reflected by each member of the Ned Mountain Formation, in turn.

Basal Member. The typical, extremely graphitic granofelses of the Basal Member were deposited in poorly oxygenated, stagnant basins. These basins were separated by (Basal Member-free) uplands and by (subaerial?) regions where well-bedded, graphite-free granofelses were deposited. Volcanism accompanied deposition in most areas. Subsequent subaerial exposure of Basal Member rocks in the central and southern Peach Lake quadrangle is recorded by the development of K-rich saprolite. In the northern Peach Lake quadrangle, the deposition of the graphitic conglomerates and arkoses of the Basal Member was followed (at least locally) by subaerial exposure and saprolite development, before the deposition of Wacke Member sediments. Fig. 22 illustrates Basal Member depositional environments.

Volcaniclastic Member. A major volcanic episode followed the deposition of the Basal Member. Bimodal metavolcanic rocks were laid down in the central and southern Peach Lake quadrangle. Felsic tuff, the greatest single component of the Volcaniclastic Member, was erupted in quantity. Sediments of terrestrial origin were deposited in generally subordinate amounts. The presence of calcareous rocks at some localities suggests that the volcanic deposits locally settled into shallow water. Many other deposits were probably subaerial. Volcanic eruptions were evidently nearly continuous; no metasaprolite has been found in this unit.

Wacke Member. Wackes, plagioclase-rich sands, basalts and basaltic tuffs were laid down over the saprolite-capped Basal Member in the northern part of the study area. This region received little or no felsic metatuff, either on account of distance or prevailing winds. The basin of

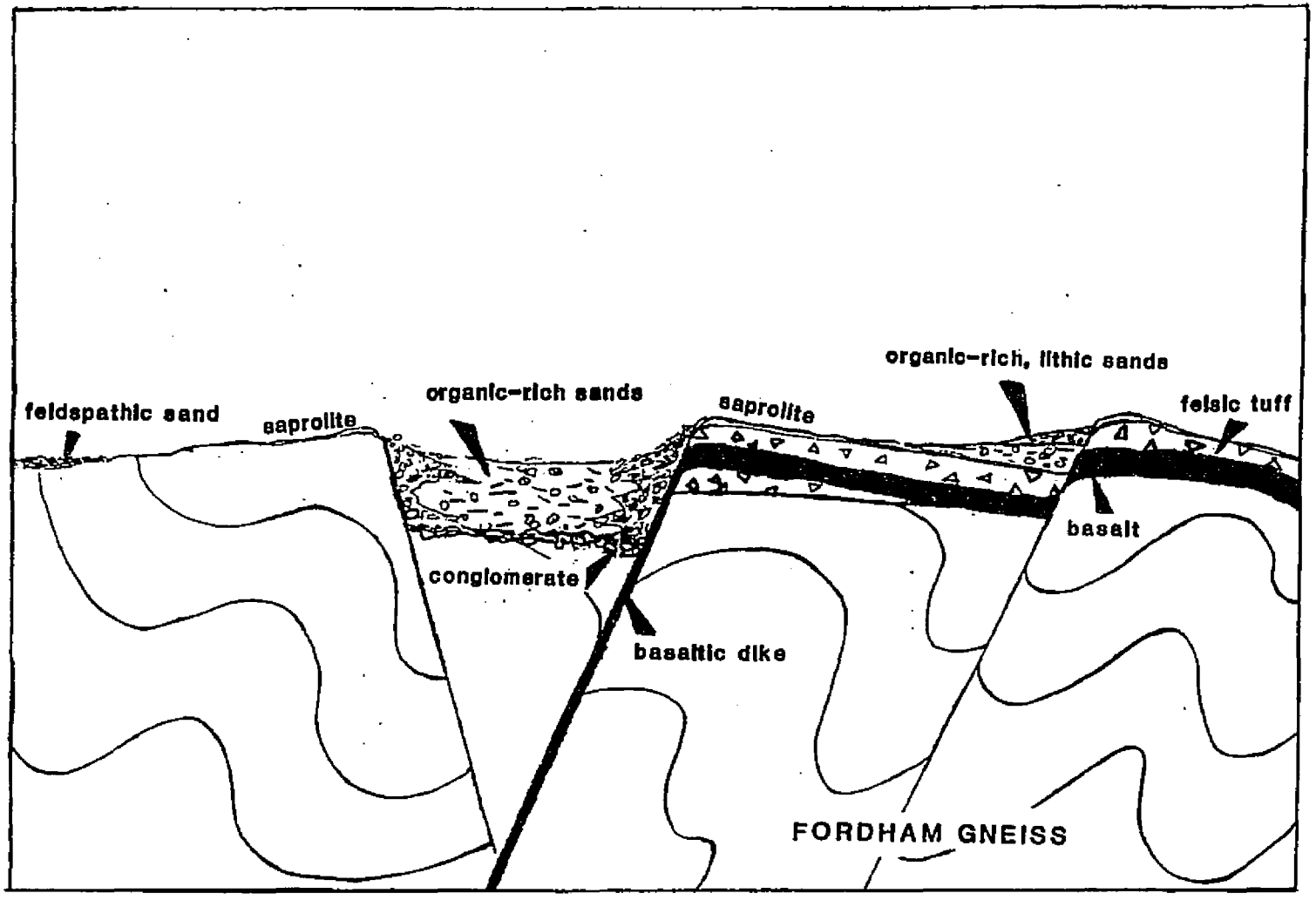

Fig. 22. Sketch of the environment of deposition of the Ned Mountain Formation Basal Member.

deposition was well-oxygenated; graphite has not been observed above the Basal Member-Wacke Member transition zone. The thinning of beds towards the north implies that sediments were derived principally from the south. Eventually, the Wacke Member basin was filled. Saprolite developed over the Wacke Member in the study area. To the west, in the Croton Falls quadrangle, a gradational transitional to the Calc-Silicate Member appears to be present (see Appendix 1, transect L-L'); there Wacke Member sediments may not have experienced subaerial exposure.

Calc-Silicate Member. The varied lithologies of the Calc-Silicate Member record a complex mosaic of environments. Limestones, apparently of shallow-water origin, were interbedded with arkosic sands and felsic and mafic volcanic material. Periodic subaerial exposure resulted in saprolite development. The Calc-Silicate Member contains relatively few argillaceous sediments; most were apparently carried away, perhaps into the basin where the Wacke Member was accumulating. The one known occurrence of graphite-rich metapelite may record an euxinic lake. The deposits of mature, quartz-rich sands which developed at some localities (lake fronts?) were periodically mixed with felsic ash falls. Although much of the Calc-Silicate Member was probably time-correlative with the Wacke Member, a thin section of arkose and siliceous carbonate rock (+/- marble) was eventually deposited over the saprolite-capped Wacke Member sediments. Fig. 23 illustrates some of the depositional environments of the Calc-Silicate Member.

Argillaceous sands (wackes) were probably deposited in a number of local basins, scattered among the upland areas and the volcanic centers of the rifted Manhattan Prong. K-feldspar-rich sediments of the Calc-Silicate Member predominate near felsic volcanic centers like the southern Peach Lake quadrangle. The shallow-water and subaerial environments of the Calc-Silicate Member ringed the built-up volcanic deposits. These shallow-water environments were generally too turbulent to permit much clay to settle out. Metawacke does occur in the upper part of the Calc-Silicate Member in the southern Peach Lake quadrangle (Table 5); this occurrence implies that topographic relief was reduced or eliminated over time.

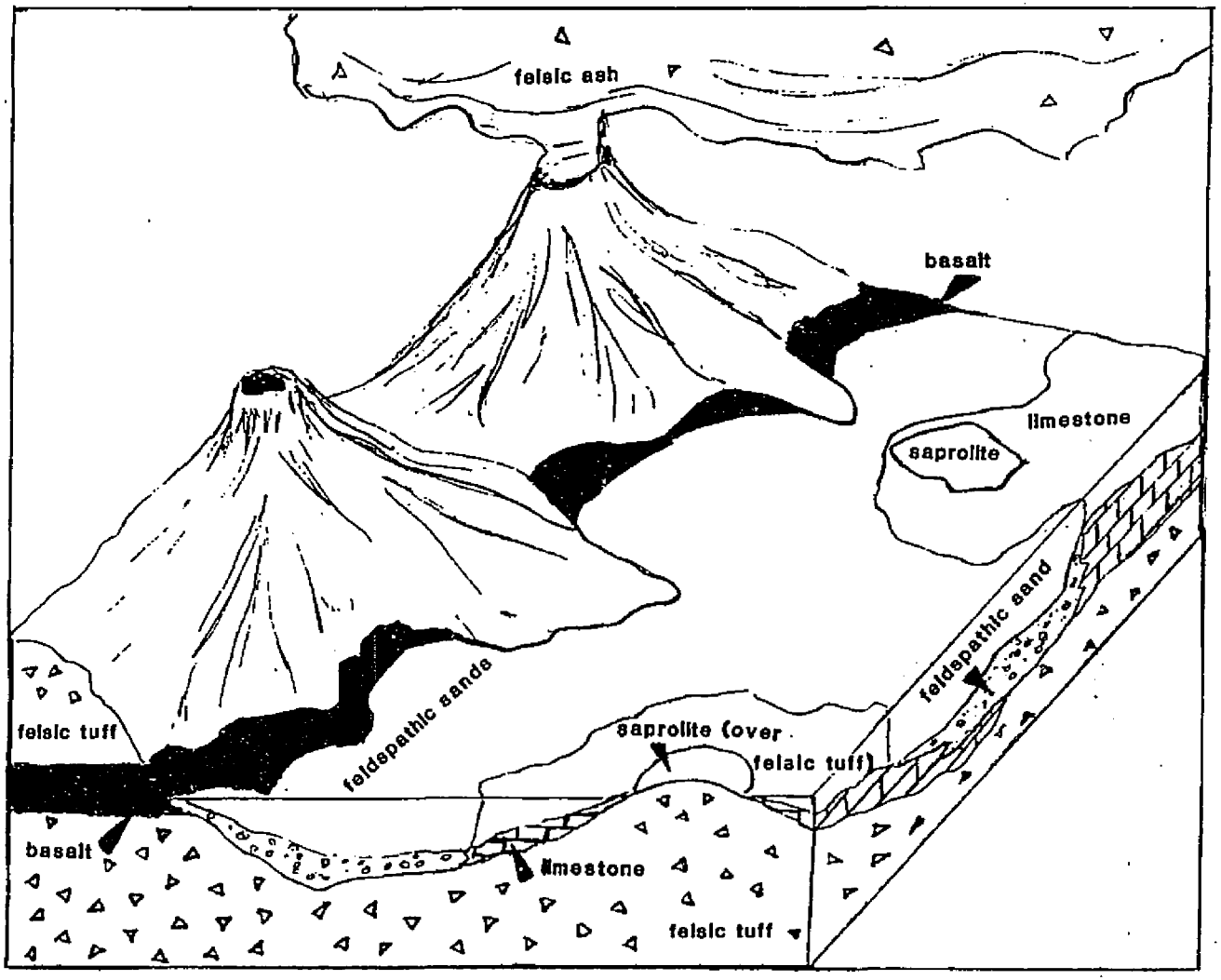

Fig. 23. Sketch of the environment of deposition of the Ned Mountain Formation Calc-Silicate Member.

The Calc-Silicate Member is probably present throughout the study area, but appears to be absent in some parts of the Manhattan Prong. On transects B-B', D-D', and H-H' (Plate III), the Basal Member (+/- the Volcaniclastic Member) is followed upsection by a pronounced valley, where Inwood Marble is presumed to lie. There is no outcrop of any Calc-Silicate Member rocks. Three interpretations are possible: 1) the Calc-Silicate Member is present, but fails to outcrop; 2) the upper Ned Mountain section has been cut out by early thrusts; and 3) these regions were uplands during the deposition of Calc-Silicate Member rocks. Explanation #3 seems the most likely to me.

NATURE OF THE CONTACT BETWEEN THE NED MOUNTAIN FORMATION AND THE INWOOD MARBLE. Although K-rich metasaprolite occurs at various horizons within the Ned Mountain Formation, none has been observed at the top. The uppermost beds observed in the Calc-Silicate Member are K-rich meta-arkose, calc-silicate rock, or felsic metatuff. The stratigraphic record implies that the mosaic of Calc-Silicate Member environments was drowned by the transgressive Inwood sea without any period of sustained erosion. In a sense, then, the Calc-Silicate Member-Inwood Marble contact is more conformable than are many of the contacts within the Ned Mountain Formation. A drastic change occurred, however, in the nature of deposition. Volcanism stopped abruptly, and transgression resulted in much greater uniformity in the character of the sediments.

STRATIGRAPHIC LINKS BETWEEN THE NED MOUNTAIN FORMATION AND NEIGHBORING EOCAMBRIAN UNITS. There are a number of lithologic similarities between the Ned Mountain Formation and the Eocambrian strata of western New England and Pennsylvania. These include the abundance of coarse clastic material, plagioclase-rich composi-

tions, and the presence of rock types such as amphibolite, quartzite, and metasaprolite.

Rift-facies Eocambrian rocks throughout western New England typically contain abundant plagioclase. The plagioclase-rich graywackes that make up the bulk of the lower Dalton, Pinnacle, and Tyson Formations are comparable to many granofelses of the Ned Mountain Formation and to metaclastic rocks of the Wacke Member in general.

The Manhattan Schist contains similar plagioclase-rich granofelses and metawackes (Table 8). According to Hall's hypothesis, the Manhattan Schist is an allochthonous Cambrian unit, correlative with the Hoosac Formation and the "lower Lowerre" (Table 1; Plate 1A). The Manhattan and Hoosac also both contain amphibolites. Manhattan Schist may indeed be a Ned Mountain correlative; if so, Eocambrian sedimentation must have been much more uniform in character at the "Manhattan" depositional site than it was within the Manhattan Prong.

Carbonaceous slate or schist, dolomite (or calc-silicate rock), and quartzite are generally present at the top of the Eocambrian rift-facies units of New England (Chang and others, 1965; Ratcliffe, 1979; Stanley and Ratcliffe, 1985; Thompson, 1972). These rocks are overlain, in turn, by the K-feldspar-bearing granofels of the Cheshire Formation. A Cambro-Ordovician dolomitic sequence correlative with the Inwood Marble overlies the Cheshire Formation.

K-feldspar-bearing granofelses or quartzites are very widespread, commonly occurring just below the Cambro-Ordovician dolomites in a region that extends from Pennsylvania to Vermont (Aaron, 1969; Jaffe and Jaffe, 1989; Tauvers, 1982). Tauvers (1982) suggested that the transition from plagioclase- to K-feldspar-rich sandstones reflected a change from a local to a "cratonal" sediment source. In the Manhattan Prong, however, the relationship between felsic volcanism and the K-feldspar-bearing granofelses is clear and consistent: felsic metatuff of the Ned Mountain Formation is the source of K-feldspar-rich sands. Felsic metatuff, possibly from the Manhattan Prong, may have been the principal source of K-feldspar for Eocambrian sandstones in neighboring areas as well.

The association of K-feldspar-rich granofels, felsic metatuff, and K-rich metasaprolite that

occurs in the Ned Mountain Formation is also found in the Chestnut Hill Formation of New Jersey-Pennsylvania (Drake, 1969, 1984) (Table 1). According to Drake (1984), the Chestnut Hill Formation consists of arkose, ferruginous quartzite, quartzitic conglomerate, metarhyolite, and aluminous metasaprolite (Table 4). The metarhyolite is made up of fine-grained chlorite, clay mineral-mica aggregate, and very fined-grained quartz (Drake, 1984). A red, fine-grained rock collected from the Chestnut Hill Formation by P. W. G. Brock contains masses of sericite, some relict K-feldspar, and hematite. These rocks appear to be remarkably similar to some Calc-Silicate Member associations.

INWOOD MARBLE

The Inwood Marble paraconformably overlies the Ned Mountain Calc-Silicate Member inside the study area. The Inwood Marble is correlative with Cambro-Ordovician carbonate sequences such as the Wappinger Group in Dutchess County, New York and the Leithsville-Allentown-Beekmantown sequence in New Jersey and eastern Pennsylvania (Table 1). The maximum thickness of the Inwood Marble in the Peach Lake quadrangle, measured perpendicular to prevailing structural trends, is around 600 meters.

The Inwood Marble is poorly exposed, and in large part underlies swampy lowlands and lakes. Topography serves as a clue to its presence; indeed, the topography of the study area loosely corresponds to its stratigraphic succession.

Rocks at the lowest stratigraphic levels, the Fordham Gneiss and much of the Ned Mountain Formation, tend to outcrop on hills or uplands. Proceeding upsection, these hills are commonly surrounded by a low-lying, swampy belt, which is underlain by parts of the Ned Mountain Calc-Silicate Member, by the Inwood Marble, and by marbles of the Walloomsac Schist. Next comes another belt of hills, which is held up by the siliceous rocks of the Walloomsac Schist and the Manhattan Schist (+/- the Hartland Formation). Stratigraphic facing direction reverses within these highlands; continuing past them, one now goes down-section, and crosses another (Inwood-) marble-bottomed valley.

In many parts of the area, however, this regular progression of hills and valleys is disrupted. Structural complexities locally interrupt the succession of formations. Still more commonly, a hilly blanket of glacial deposits buries all outcrop. Nevertheless, a rough correspondence between valleys and belts of Inwood Marble has been recognized by geologists in the Manhattan Prong for generations.

The Inwood Marble is remarkably homogeneous. Over 95% of the unit consists of marble

(that is, rocks that contain more than 50 modal percent carbonate minerals). This homogeneity contrasts markedly with the adjoining Ned Mountain Calc-Silicate Member, where marble is invariably interbedded with other lithologies.

Marbles. Marbles of the Inwood are generally pure white, cream, or buff-colored, and many have thin golden phlogopite-rich schistose interlayers. Some diopside-rich layers are somewhat greenish. Typically, bedding is pronounced, with the most obvious layers between a few centimeters and about one meter in thickness.

Inwood marbles range from dolomitic to calcitic in composition (Fig. 20). Some white, massive beds that consist of almost pure dolomite are present (e.g., #1605, Table 6). However, slightly siliceous, cream- or buff-colored marbles, containing both dolomite and calcite, are much more abundant.

Entire beds of calcitic marble occur as interlayers within dolomitic sequences in some locations. Layer-by-layer variations in dolomite content may locally be observed in laminae less than 2 centimeter thick. Thin-sectioned specimens of Inwood Marble were stained for calcite and/or dolomite to facilitate accurate mineral identification in individual layers (see specimen #178b, Table 6).

Slightly siliceous beds of Inwood Marble generally contain some nearly colorless forsterite, waxy greenish or yellowish diopside, and pale gold to tan phlogopite. In thin section, a thin rim of diopside is generally visible around grains of forsterite. Serpentine commonly pseudomorphs olivine; late tremolite or brucite are observed in some places. Enstatite and fassaite (a clinopyroxene rich in Ca, Al, and Fe^{3+}) occur in one specimen (#CT-20, Plate III).

Opaque minerals found in the Inwood Marble include pyrrhotite, pyrite, and magnetite, with pyrrhotite the most abundant. Calcitic marbles commonly contain minor amounts of graphite. Sphene and apatite occur rarely. Colorless, pale blue, grey, lavender, and deep green (almost black) spinel occurs some samples. At one time, this diversity of color led to the mistaken im-

TABLE 6

Estimated Modal Compositions of Representative Specimens, Inwood Marble

Specimen	178b		1437	1585a	1585b	1605	1625	1636	1695a	
Layer	I	II								
Dolomite	70	-	68	8	74	95	3	35	-	Dolomite
Calcite	20	62	19	80	10	4	43	50	5	Calcite
Olivine	3	-	-	-	5	-	16	10	-	Olivine
Serpentine	5	-	10	-	tr.	1	-	tr.	-	Serpentine
Phlogopite	1	-	3	3	2	tr.	10	1	tr.	Phlogopite
Brucite	-	-	tr.	-	tr.	tr.	-	-	-	Brucite
Diopside	-	30	-	3	8	-	2	-	56	Diopside
Hornblende	-	-	-	-	-	-	-	-	38	Hornblende
Tremolite	-	6	-	5	-	-	-	-	-	Tremolite
Scapolite	-	-	-	-	-	-	23	-	-	Scapolite
Mg-spinel	-	-	-	-	-	-	-	3	-	Mg-spinel
Sphene	-	-	-	-	-	-	-	-	1	Sphene
Graphite	tr.	2	-	1	-	-	tr.	-	-	Graphite
Magnetite	tr.	tr.	-	tr.	-	-	-	-	-	Magnetite
Pyrrhotite	tr.	tr.	tr.	tr.	tr.	-	1	tr.	-	Pyrrhotite
Pyrite	-	-	-	-	-	-	2	tr.	-	Pyrite

Notes: 1. Specimen locations are shown on Plate III. **2. The color of the specimen's weathered surface** is specified only where it contrasts with the overall color of the rock.

178b. Buff- and grey-weathering, white and grey banded marble. Beds are 2 to 10 millimeters thick. (Southeastern Peach Lake quadrangle)
1437. White marble. (Southeastern Peach Lake quadrangle)
1585a. Cream-colored marble with brown schistose interlayer. Schistose layer is rusty-weathering. (West-central Peach Lake quadrangle)
1585b. White- and buff-colored marble. (West-central Peach Lake quadrangle)
1605. White marble. (East-central Peach Lake quadrangle)
1625. Grey, poorly foliated marble with dark streaks, which stand up on the weathered surface. (Northeastern Peach Lake quadrangle)
1636. Buff-weathering, white to buff marble. (Eastern shore of Lake Windwing, northeastern Peach Lake quadrangle)
1695a. Medium- to fine-grained black amphibolite, with rough, pitted weathered surface. (Southern Brewster quadrangle)

pression that more than one isotropic mineral was present. Cleaved, colorless spinels were erroneously identified as periclase (Brock, 1989). X-ray-powder study has since established the identity of the colorless mineral as spinel.

The modes of the Inwood marbles were plotted on Fig. 20, where they can be compared with rocks of the Ned Mountain Calc-Silicate Member and the Walloomsac Schist. The marbles of the Inwood are distinctly more magnesian than those of these other formations. Compositional overlap between Inwood marbles and the other formations is limited to a small field near the calcite marble end-member.

Regional metamorphic conditions at one time resulted in the coexistence of forsterite and calcite in silica-poor magnesian marbles (Fig. 24A). As a result, forsterite or serpentine are found in most beds of Inwood Marble, though neither has been observed in the Ned Mountain Formation or Walloomsac Schist. The presence of olivine or serpentine serves as a key petrographic indication of a moderately magnesian bulk composition, and is an important criterion for the distinction of Inwood Marble from other stratigraphic units.

Siliceous lithologies. A few varieties of siliceous (non-marble) rock occur in the Inwood Marble. These siliceous beds are not plotted on Fig. 20. They include rare, thin grey quartzites, that occur in beds less than 20 centimeters thick. There are also a few calcareous layers that contain >30 percent modal phlogopite, and can be considered as calcite-phlogopite schist. In addition, a dark, hornblende- and diopside-rich gneiss accompanies dolomitic, forsterite-bearing Inwood at a few locations in the southern Brewster quadrangle. This gneiss resembles an amphibolite, but is free of plagioclase, and contains only diopside, hornblende, calcite, and sphene (#1695a, Table 6). One last siliceous lithology is a greyish rock, consisting primarily of calcite, scapolite, forsterite, and phlogopite (#1625, Table 6). It crops out with calcite-forsterite-phlogopite marble at one locality in the northern Peach Lake quadrangle (Plate III). Traces of scapolite have also been observed in a few other beds of the Inwood.

Fig. 24. Co-existing mineral assemblages at predominant (M_2) metamorphic conditions in marbles and calc-silicate rocks over most of the study area.

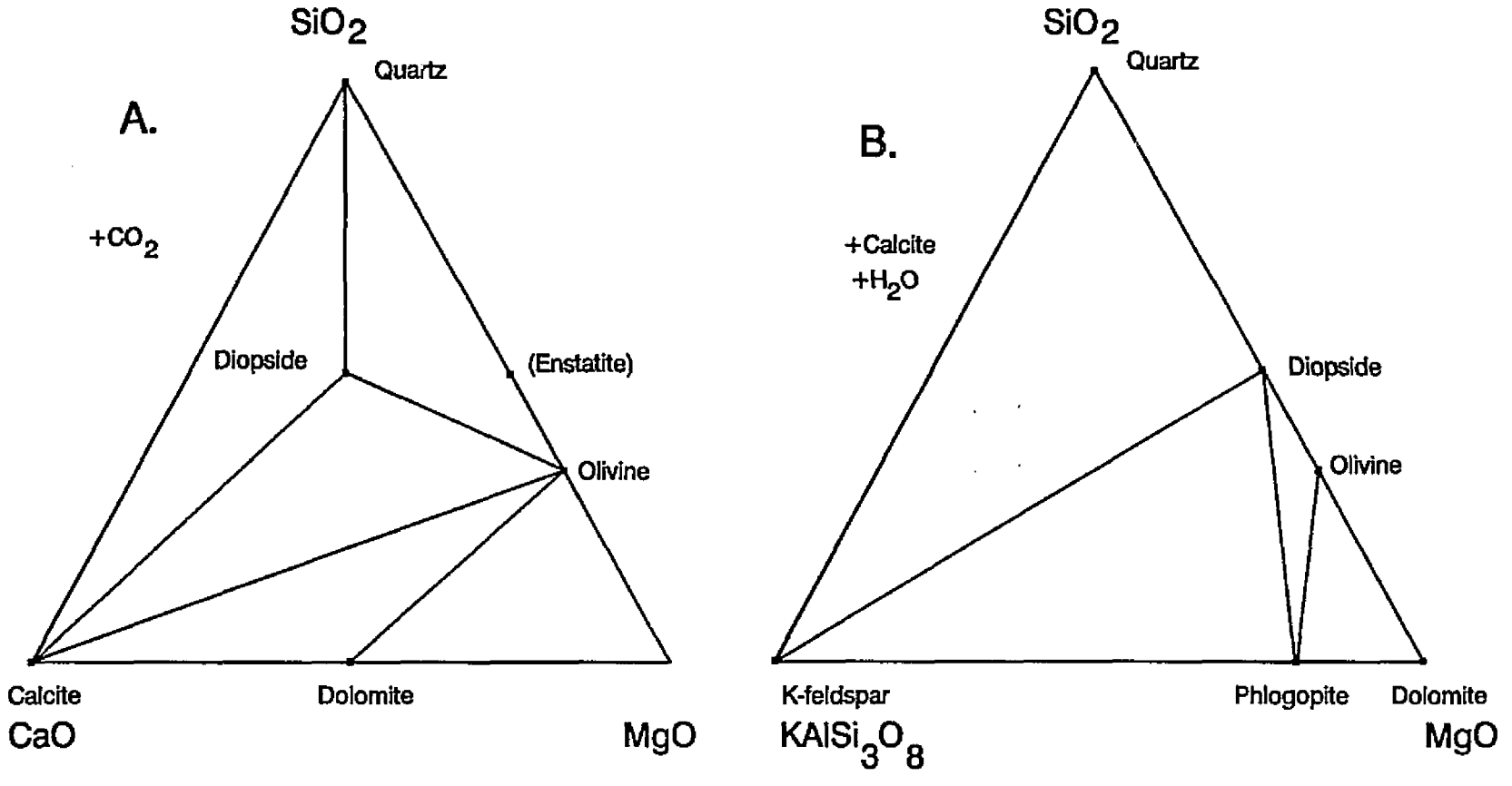

Subdivision of the Inwood Marble. Many workers, beginning with Hall, have recognized members in the Inwood Marble. This practice has not been followed here for a number of reasons. 1) Outcrop is very limited and a succession of lithologic types within the Inwood is recognizable at only a few locations. 2) Large outcrops of Inwood commonly display several lithologic variants (e.g., buff-colored calcitic and dolomitic marbles, white marble, and calcite-phlogopite schist). 3) The known distribution of the dark siliceous rocks is limited to the northern parts of the study area, but it is uncertain whether this observation has stratigraphic significance. 4) The lithologies at the base of the Inwood- where Inwood is in contact with the Ned Mountain Formation- are not identical at different locations. For example, a massive white dolomite overlies the Calc-Silicate Member at the site of sample #1445 in the southeastern Peach Lake quadrangle (Plate III). However, slightly siliceous beige and white dolomite-calcite marbles overlie the Calc-Silicate Member on the eastern shore of Lake Windwing in the northeastern Peach Lake quadrangle (Plate III). Thus, in contrast to Hall's (1968a) observations in the White Plains region, no regular stratigraphic progression within the Inwood is evident in the study area.

Interpretation. The Inwood Marble was deposited over the rift-facies rocks of the Ned Mountain Formation, possibly with local conformity in the study area. Its thick, homogeneous marbles reflect deposition in a tectonically quiescent environment. The layers of calcite-phlogopite schist suggest the presence of local clay concentrations, predating metamorphism. The dark siliceous rocks (diopside-hornblende gneiss) may be explained as metamorphosed mixtures of sand, clay, and carbonate minerals.

Many geologists have studied the Cambro-Ordovician dolomite sequences of eastern North America in recent years (e.g., Rodgers, 1968; Hall, 1968a; Drake, 1969; Friedman, 1979). Following their lead, I interpret the Inwood Marble as a shallow-shelf, marine deposit, which accumulated on the subsiding passive margin of Cambrian to Early Ordovician North America.

WALLOOMSAC SCHIST

The Lower-Middle Ordovician Walloomsac Schist overlies the Inwood Marble. The Walloomsac Schist correlates with the Balmville Limestone and Walloomsac Formation in Dutchess County, New York, and with the Jacksonburg Limestone and Martinsburg Formation of New Jersey and eastern Pennsylvania (Table 1). The maximum thickness of the Walloomsac Schist in the study area, perpendicular to structural trends, is around 500 meters.

The Walloomsac Schist is subdivided here, for purposes of description, into "upper" and "lower" parts, although the "lower" part is markedly discontinuous and commonly very thin. The "upper" and "lower" Walloomsac Schist each contain a variety of lithologic types, in distinctive combinations.

The discontinuous, lower part of the Walloomsac Schist consists largely of calcitic marbles, graphitic, rusty-weathering, quartz-feldspar granofelses and schistose granofelses, and calc-silicate rocks. Pelitic rocks are present at some localities but are generally very minor. The upper Walloomsac, in contrast, consists mostly of metawacke and metapelite, with minor amounts of granofels and amphibolite. The metawackes, metapelites, and some calc-silicate rocks of the Walloomsac tend to hold up hills, while the marbles are generally found in low-lying areas.

The succession of lithologic types within the Walloomsac Schist is most evident in the region around Ridgebury Mountain, from Lake Naraneka to Lake Windwing (Plate III). The lowland south of Ridgebury Mountain is underlain by the Inwood Marble and by marbles of the Walloomsac Schist (Plate I). Calc-silicate rocks and granofelses of the lower Walloomsac outcrop at several locations just above or below the base of the slope, and are succeeded uphill by metawacke of the upper Walloomsac. The stratigraphic sequence is reversed further north on Ridgebury Mountain, where metawacke of the upper Walloomsac is followed first by lower Walloomsac marbles, calc-silicate rocks, and granofelses, and later, at Lake Windwing, by dolomitic Inwood Marble.

Lower Walloomsac Schist (including Marble Member). The lower Walloomsac is best exposed in the northeastern Peach Lake quadrangle. Scattered, limited outcrop of the lower Walloomsac is also found in the north-central, south-central, and southwestern Peach Lake quadrangle. The rocks of the lower Walloomsac fall into two groups: 1) somewhat rusty-weathering, well-bedded marbles, and 2) slabby-bedded to finely-laminated, extremely rusty-weathering, graphitic calc-silicate rocks and quartz-feldspar granofelses. In addition to these lithologies, some graphitic metawacke occurs at a few localities.

The marbles are medium-grained, tan- to rusty-weathering rocks. They mostly consist of white calcite speckled with green diopside. Minor plagioclase (An_{28-38}), quartz, and K-feldspar are commonly present, along with trace amounts of graphite (Table 7). A Marble Member of the Walloomsac Schist is distinguished in those areas of the northeastern Peach Lake quadrangle that are primarily underlain by marbles (Plate I).

The calc-silicate rocks of the Walloomsac are generally medium- to coarse-grained, greenish or grey when fresh, and extremely rusty-weathering. They are dominantly composed of quartz, plagioclase (An_{29-85}), and (in a few cases) K-feldspar, with subordinate amounts of calc-silicate minerals (generally diopside and/or hornblende). These rocks invariably contain 1 to 3 modal percent of graphite, which helps to distinguish them from the (graphite-free) calc-silicate rocks of the Ned Mountain Formation Calc-Silicate Member.

A variety of Ca-bearing minerals, such as tremolite, clinozoisite, scapolite, and sphene, occur in some specimens of Walloomsac marble and calc-silicate rock. Tremolite and clinozoisite, where present, are texturally late. Accessory tourmaline, apatite, pyrrhotite, and magnetite are very common in both lithologies.

The marbles and calc-silicate rocks comprise two distinct and separate compositional groups, which have a large gap in silica content between them (Fig. 20). On Fig. 20, Walloomsac marbles plot in a tight cluster near the calcite end-member, while Walloomsac calc-silicate rocks define a field in the silica-rich corner of the plot. The bimodal distribution of Walloomsac

TABLE 7

Estimated Modal Compositions of Representative Specimens, Walloomsac Schist Lower Walloomsac Schist

Specimen	Marble		Calc-silicate rocks				Quartz-feldspar granofelses					Specimen
Layer	1474b 2	1623 2	CT4a	CT7	1457	1617a	1329	1370	1604	1575 I	1575 II	Layer
Quartz	2	2	36	41	44	61	17	45	35	40	5	Quartz
Plagioclase	8	8	24	32	21	20	42	20	28	33	17	Plagioclase
(% anorthite)	(38)	(28)	(69-88)	(29)	(64)	(75)	(79-85)	(45-69)	(36)	(52)	(48)	(% anorthite)
K-feldspar	7	12	-	6	2	1	1	2	20	-	58	K-feldspar
Biotite	3	-	tr.	10	20	10	26	30	8	10	15	Biotite
Garnet	-	-	-	1	1	-	4	tr.	6	4	2	Garnet
Hypersthene	-	-	-	-	-	-	-	-	-	4	-	Hypersthene
Calcite	60	69	-	-	-	-	-	-	-	-	-	Calcite
Diopside	14	3	27	5	3	6	-	-	-	-	-	Diopside
Hornblende	-	-	2	3	7	-	-	-	-	5	-	Hornblende
Tremolite	-	6	-	tr.	-	-	-	-	-	-	-	Tremolite
Clinozoisite	tr.	-	-	-	-	-	-	-	-	-	-	Clinozoisite
Cummingtonite	-	-	-	-	-	-	-	-	-	tr.	-	Cummingtonite
Scapolite	4	-	5	-	-	-	-	-	-	-	-	Scapolite
Apatite	tr.	tr.	tr.	tr.	tr.	tr.	tr.	tr.	tr.	tr.	tr.	Apatite
Zircon	-	-	tr.	tr.	tr.	-	-	tr.	tr.	tr.	tr.	Zircon
Tourmaline	tr.	tr.	tr.	tr.	tr.	tr.	tr.	-	tr.	tr.	-	Tourmaline
Allanite	-	-	-	-	tr.	tr.	tr.	-	-	tr.	-	Allanite
Sphene	1	tr.	2	-	-	tr.	-	-	-	-	-	Sphene
Anatase	-	-	-	-	-	-	tr.	-	-	-	-	Anatase
Graphite	1	tr.	2	3	1	2	2	3	2	2	3	Graphite
Magnetite	-	tr.	tr.	-	tr.	tr.	-	tr.	tr.	tr.	-	Magnetite
Ilmenite	-	-	-	-	-	-	tr.	tr.	tr.	tr.	-	Ilmenite
Pyrrhotite	tr.	tr.	1	tr.	tr.	tr.	tr.	tr.	tr.	1	-	Pyrrhotite
Pyrite	-	-	1	-	-	-	tr.	-	-	-	-	Pyrite
Chlorite	tr.	-	-	-	-	tr.	4	-	tr.	-	-	Chlorite
Muscovite	-	-	-	-	-	-	3	-	-	-	-	Muscovite

TABLE 7 (CONTINUED)

Estimated Modal Compositions of Representative Specimens, Walloomsac Schist
Upper Walloomsac Schist

	Quartz-feldspar granofelses		Metawackes					Metapelites			Amphibolites				Quartz-feldspar granofels with mafic tuff component	
Specimen	1476	1631a	1325a	1358c	1464	1618	1631	548	961	1602	181	1430	1497a	1620	1693a	Specimen
Layer		I					II					I				Layer
Quartz	50	49	30	59	37	41	22	8	22	tr.	15	10	10	4	51	Quartz
Plagioclase	35	38	4	24	25	15	21	30	18	-	24	20	10	43	23	Plagioclase
(% anorthite)	(28)	(29)	(30)	(32)	(24)	(36)	(29)	(35)	(33)	-	(67)	(40)	(64)	(65)	(62)	(% anorthite)
K-feldspar	-	-	30p	-	10	11	28p	6	-	-	-	-	-	-	-	K-feldspar
Biotite	12	5	7	10	9	2	10	23	6	37	5	3	10	-	4	Biotite
Garnet	3	5	24	5	10	20	11	18	28	33	5	-	3	-	-	Garnet
Cordierite	-	-	-	-	-	1	-	-	-	-	-	-	-	-	-	Cordierite
Sillimanite	-	tr.	4	1	5	6	5	13	20	28	-	-	-	-	-	Sillimanite
Hypersthene	-	-	-	-	-	-	-	-	-	-	-	-	-	-	-	Hypersthene
Calcite	-	-	-	-	-	-	-	-	-	-	-	-	-	-	tr.	Calcite
Augite	-	-	-	-	-	-	-	-	-	-	-	-	-	11	-	Augite
Hornblende	-	-	-	-	-	-	-	-	-	-	30	64	59	41	7	Hornblende
Tremolite	-	-	-	-	-	-	-	-	-	-	-	-	-	-	-	Tremolite
Cummingtonite	-	-	-	-	-	-	-	-	-	-	16	-	5	-	-	Cummingtenite
Apatite	tr.	tr.	-	tr.	-	-	-	-	-	-	-	tr.	-	tr.	tr.	Apatite
Zircon	tr.	tr.	tr.	tr.	tr.	tr.	tr.	tr.	tr.	tr.	-	-	-	-	tr.	Zircon
Green spinel	-	-	tr.	-	-	-	tr.	tr.	tr.	tr.	-	-	-	-	-	Green spinel
Tourmaline	-	-	-	-	-	-	-	-	-	-	-	-	-	-	-	Tourmaline
Allanite	-	-	-	-	-	-	-	-	-	-	-	-	-	-	-	Allanite
Sphene	-	-	-	-	-	-	-	-	-	-	-	-	-	tr.	-	Sphene
Rutile	-	-	tr.	-	-	-	-	-	-	-	-	-	-	-	-	Rutile
Anatase	-	tr.	tr.	tr.	tr.	tr.	tr.	-	-	tr.	-	-	-	-	-	Anatase
Graphite	-	tr.	-	-	-	tr.	tr.	-	-	-	-	-	-	-	-	Graphite
Magnetite	tr.	tr.	-	tr.	tr.	2	tr.	tr.	6	1	4	tr.	tr.	1	13	Magnetite
Ilmenite	tr.	2	tr.	tr.	1	1	1	2	tr.	tr.	1	3	2	tr.	1	Ilmenite
Pyrrhotite	-	-	tr.	tr.	-	1	tr.	-	-	-	tr.	tr.	-	-	tr.	Pyrrhotite
Pyrite	-	-	-	tr.	-	-	1	-	-	-	-	-	-	-	-	Pyrite
Chlorite	-	tr.	tr.	-	tr.	tr.	tr.	tr.	-	1	-	-	tr.	-	1	Chlorite
Muscovite	-	tr.	-	-	2	tr.	tr.	-	-	tr.	-	-	tr.	-	-	Muscovite

p= Perthitic K-feldspar with 20% or more exsolved plagioclase.

TABLE 7, CONTINUED

Notes: 1. Specimen locations are shown on Plate III. **2. The color of the specimen's weathered surface** is described only where it contrasts with the overall color of the rock. **3. Garnet color** is red unless otherwise specified.

Lower Walloomsac Schist

Marbles

1474b. Buff- to rusty-weathering, tan marble with schistose laminae. Schistose laminae are spaced approximately 15 millimeters apart. (South-central Peach Lake quadrangle)
1623. Rusty- and buff-weathering, buff-colored marble. (Northeastern Peach Lake quadrangle)

Calc-silicate rocks

CT4a. Rusty-weathering, well-bedded, greenish calc-silicate rock. One layer has been preferentially weathered out; bedding is about 2 to 9 millimeters in thickness. (Northeastern Peach Lake quadrangle)
CT7. Rusty-weathering, finely laminated grey granofels with pink garnets. (Northeastern Peach Lake quadrangle)
1457. Rusty-weathering, medium- to fine-grained, fissile grey granofels. Collected in the southeastern Peach Lake quadrangle.
1617a. Rusty-brown weathering, olive-green calc-silicate rock. (Northeastern Peach Lake quadrangle)

Quartz-feldspar granofelses

1329. Rusty-weathering, medium- to fine-grained grey granofels, with slight reddish cast. (North-central Peach Lake quadrangle)
1370. Rusty-weathering, medium- to fine-grained grey slabby granofels with pink garnets. (By Route 35, south-central Peach Lake quadrangle)
1604. Rusty-weathering, medium-grained, grey granofels with discontinuous biotite-rich folia and pink garnet. (Northeastern Peach Lake quadrangle)
1575. Rusty-brown weathering, medium- to fine-grained, slabby purplish-grey granofels. (Near Lake Naraneka, east-central Peach Lake quadrangle)

Upper Walloomsac Schist

Quartz-feldspar granofelses

1476. Medium-grained, grey granofels with dark garnet-rich interlayers. (South-central Peach Lake quadrangle)
1631a. Rusty-weathering, thin-bedded, light grey granofels (layer I) with schistose laminae (layer II). (South-central Peach Lake quadrangle).

TABLE 7, CONTINUED

Metawackes

1325a. Brown- and grey-weathering, medium- to coarse-grained schist with flattened garnet porphyroblasts. (North-central Peach Lake quadrangle)
1358c. Rusty-brown weathering, thin-bedded, grey schistose granofels. Schistose laminae are spaced ~5 millimeters apart. (South-central Peach Lake quadrangle)
1464. Rusty-brown weathering, tan to grey schistose gneiss. (East-central Peach Lake quadrangle).
1618. Rusty-weathering, medium- to coarse-grained, tan gneiss with pink garnet porphyroblasts. (Northeastern Peach Lake quadrangle)
1631a. Rusty-weathering, slightly schistose granofels. Layer II is a schistose laminae; layer I is granofelsic. (South-central Peach Lake quadrangle)

Metapelites

548. Migmatized, medium- to coarse-grained, black and white schistose gneiss. (Southern Brewster quadrangle)
961. Migmatized, medium- to coarse-grained schist with 5 to 30 millimeter-thick quartz/feldspar flasers and anastomosing sillimanite trains. (Northeastern Peach Lake quadrangle)
1602. Black and red schist with garnets 5 millimeters in diameter and wisps of white sillimanite. (Northeastern Peach Lake quadrangle)

Amphibolites

181. Thin-bedded, medium-grained, dark grey to black, amphibolitic gneiss. (South-central Peach Lake quadrangle)
1430. Brownish-weathering, medium-grained amphibolite with plagioclase porphyroblasts 3 millimeters in diameter. (East-central Peach Lake quadrangle)
1497. Brown-weathering, thin-bedded, dark-grey, medium-grained schistose amphibolite. (South-central Peach Lake quadrangle)
1620. Brown-weathering, medium-grained dark amphibolite with greyish streaks, and a pitted, spongy weathered surface. (Northeastern Peach Lake quadrangle)

Quartz-feldspar granofels with mafic tuff component

1693a. Medium- to fine-grained, thin-bedded, dark grey schistose granofels. Beds are 5 to 10 millimeters thick. (Southern Brewster quadrangle)

compositions makes a striking contrast to the near-continuum between calcareous and siliceous rocks found among the calc-silicate rocks and marbles of the Ned Mountain Formation Calc-Silicate Member (Fig. 20).

Most Walloomsac calc-silicate rocks contain substantial (5 to 20 modal percent) red biotite, and some contain minor pink or red garnet (Table 7). Many Walloomsac calc-silicate rocks plot on the right-hand side of the SiO_2-diopside join on Fig. 20 on account of their high biotite content.

Macroscopically, the calc-silicate rocks grade from greenish, relatively diopside-rich, biotite-poor granofelses, to finely laminated, grey, quartz-feldspar-biotite granofelses sprinkled with a few percent of hornblende and/or diopside. Many grey calc-silicate rocks strongly resemble nearby quartz-feldspar-biotite granofelses that are free of calc-silicate minerals. The modal compositions of the calc-silicate rocks similarly grade into "Ca-mineral"-free, quartz-feldspar-biotite-garnet granofelses. On Fig. 25B, this gradation in calcium content is expressed by the calc-silicate rocks that plot along the length of the "Ca mineral"-albite join.

The quartz-feldspar-biotite-garnet granofelses of the lower Walloomsac (# 1329, 1370, and 1604, Table 7) are greyish, medium- to fine-grained, well-bedded rocks. Beds are generally a few centimeters in thickness. Most beds have a slight reddish or purplish cast derived from distinctly reddish biotite, and contain 1 to 3 percent graphite. These granofelses, like the calc-silicate rocks, acquire a pronounced rusty stain with weathering.

Plagioclase is generally the dominant feldspar in rocks of the lower Walloomsac, though a few beds contain substantial K-feldspar. Plagioclase compositions in the granofelses vary widely, from An_{24} to $\sim An_{95}$, and correlate with the granofels' lithologic associations. Granofelses which contain calcic plagioclase tend to occur in separate sequences or near calc-silicate rocks and marble; granofelses with sodic plagioclases generally outcrop adjacent to metawacke and metapelite, and may themselves have sillimanite-bearing pelitic laminae.

Sparse orthopyroxene occurs in a few of the graphitic granofelses (e.g., #1575, Table 7).

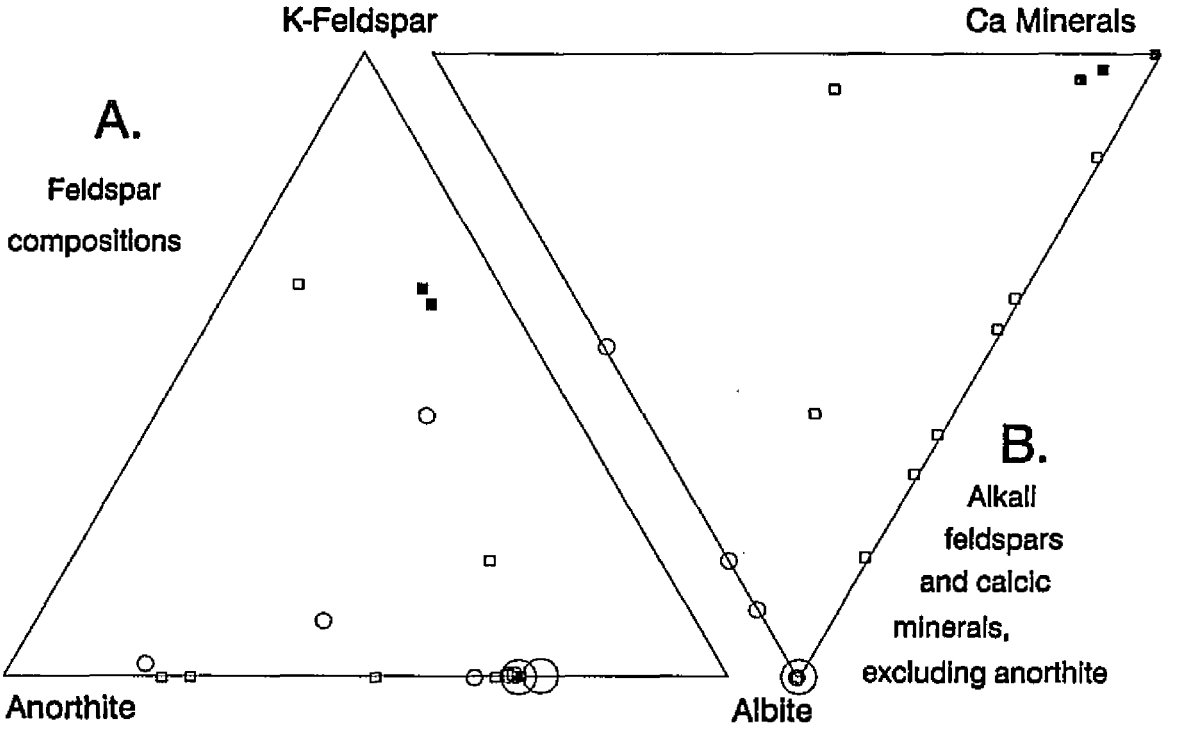

Walloomsac Schist

Lower		Upper	
Quartz-feldspar-biotite-garnet granofels	○	Quartz-feldspar-biotite-garnet granofels	◯
Calc-silicate rocks	▫		
Marbles	■		

Fig. 25. Feldspar and calc-silicate mineral variations in the Walloomsac Schist.
(Diagram is constructed in the same manner as Fig.19.)

This orthopyroxene appears to be the product of breakdown of biotite under granulite-facies conditions (discussed in the chapter on metamorphism). One anomalous specimen (#960, Plate III), has a bed that contains 7 modal percent apatite, along with quartz, plagioclase (An_{29}), biotite, and garnet. The phosphathic bed is bordered by sillimanite-bearing pelitic laminae.

Upper Walloomsac Schist. In many parts of the study area, the lower Walloomsac Schist is missing or does not outcrop, and only the upper Walloomsac is present. The upper Walloomsac consists of rusty- and rusty-brown weathering metawacke, metapelite, quartz-feldspar-biotite-garnet granofels, and minor amphibolite. Bedding is poorly defined except where granofelsic or amphibolitic beds are present.

The most easily identified Walloomsac metawackes and metapelites have a reddish cast (from red biotite), are rusty-weathering, contain graphite, and outcrop near the calcareous lower Walloomsac. Lenses of calc-silicate rock are locally present in the schists. Elsewhere, the Walloomsac metawackes are generally rusty brown-weathering rocks with red or red-brown biotite. Fig. 26 illustrates the upper Walloomsac Schist in outcrop.

The aluminous rocks are generally medium-grained schistose gneisses composed of quartz, plagioclase (An_{24-40}), K-feldspar, garnet, biotite, and sillimanite. Most are metawackes, though some contain more than 50 modal percent biotite+garnet+sillimanite, and are therefore classified as metapelites. Both these aluminous lithologies are characterized by a high degree of mineral segregation: quartz and feldspar are concentrated into white or pink leucosomes, and biotite and sillimanite into red or brown discontinuous folia. Prominent sillimanite trains are common. Some of the leucosomes (particularly those in highly aluminous rocks) are coarse-grained, discontinuous, and locally cross-cutting, giving the rocks a migmatitic appearance. Modes of representative metawackes and metapelites are given on Table 7.

Metamorphic grade has a profound effect on the appearance of the aluminous rocks. Local retrogression has resulted in transformation of some rocks into silvery (though rusty-weath-

Fig. 26. Schistose gneiss (metawacke) of the upper Walloomsac Schist, 0.7 kilometers south-southeast of Lake Naraneka. Hammer head is 18 centimeters long.

ering) muscovite schists, while parts of the Walloomsac in the northeastern Peach Lake quadrangle consist of coarse-grained, grey, rusty-weathering garnet-cordierite-sillimanite gneisses.

Beds of grey, rusty- or brown-weathering, medium- to fine-grained quartz-feldspar-biotite-garnet granofels and schistose granofels occur in the upper Walloomsac Schist (#1476 and 1631a-I, Table 7). These beds range from a few centimeters to some tens of centimeters in thickness. Plagioclase in these rocks is fairly sodic (An_{24-30}), and K-feldspar is rare; their feldspar compositions are plotted on Fig. 25A.

While most of the granofelses are essentially meta-arkoses, one well-layered, grey, quartz-rich rock, #1693a (Table 7), has an unusual modal composition. It contains 7 modal percent hornblende, 13 percent magnetite, and moderately calcic plagioclase (An_{62}). The relatively high Fe, Ca, and Mg contents of this rock suggest that it may have originated a metamorphosed sediment- mafic tuff mixture.

A few scattered metabasites are interbedded with metawacke and quartz-feldspar granofels in the upper Walloomsac Schist. The metabasites tend to be brownish-weathering, and range in thickness from a few centimeters up to a meter or so. The observed metabasite types include hornblende, hornblende-clinopyroxene, and hornblende-cummingtonite-garnet amphibolites (Table 7).

Interpretation and geologic setting. The lower Walloomsac Schist consists of metamorphosed limestone, sandstones, and minor aluminous rocks. Many of the sandstones were limey; these were later metamorphosed into calc-silicate rock. Other sandstones, which contained less Ca, became quartz-feldspar-biotite-garnet granofelses.

All the rocks of the lower Walloomsac are graphitic. The graphitic character of these rocks indicates that they were deposited in an anoxic environment. Somewhat more oxidizing conditions apparently prevailed by the time that the deposition of the sands and clays the upper Walloomsac occurred. Occasional falls of mafic tuff (and, possibly, basaltic flows) accompanied the

deposition of the sediments of the Walloomsac.

Hall (1968b) inferred that the Walloomsac Schist ("Manhattan A") lies unconformably over a truncated Inwood Marble in the southern Manhattan Prong. This unconformity is regionally extensive. The unconformity has been attributed to the growth of a "peripheral bulge" along the North American margin, created as the continental crust (with its blanket of Cambro-Ordovician carbonates) was initially jammed down an east-dipping subduction zone (Shanmugam and Lash, 1982). Thus, the development of the unconformity is thought to record the opening stage of the Taconian orogeny. The "peripheral bulge" collapsed as collision progressed, and the continental margin foundered (Rowley and Kidd, 1981; Shanmugam and Lash, 1982). After the collapse of the margin, deep-water limestone (and, later, sandstones and shales) was deposited in an anoxic basin that developed along the length of the continental margin. Thin ash beds have been observed in these sedimentary rocks (e.g., Drake and others, 1989).

Rocks of the Walloomsac Schist still preserve a recognizable record of these regional events, although the rocks were later metamorphosed to a higher metamorphic grade than were correlative rocks elsewhere. The Walloomsac Schist of the Manhattan Prong may contain more mafic rocks than occur in correlative strata, perhaps because of a greater proximity to the encroaching volcanic arc.

MANHATTAN SCHIST

The Manhattan Schist overlies the Lower-Middle Ordovician Walloomsac Schist. Hall (1968a) proposed that the Manhattan Schist ("Manhattan members B and C") is Cambrian in age, and that the unit was emplaced over the Walloomsac Schist ("Manhattan member A") on a thrust fault (Table 1 and Plate 1A) early in the Taconian orogeny. The Manhattan Schist is thus considered analogous to the Taconic allochthons of upper New York State. This hypothesis is accepted

here as the best available interpretation of regional relationships. The maximum thickness of the Manhattan Schist in the study area (perpendicular to structural trends) is around 400 meters.

The Manhattan Schist consists of metawacke, metapelite, amphibolite, and quartz-plagioclase-biotite-garnet granofels. Metawacke is the most abundant lithology, comprising perhaps 80 percent of the whole formation. Metapelite and amphibolite each make up 5 to 10 percent of the Manhattan Schist, and granofels less than 5 percent.

The metawackes are massive and poorly bedded. Most are generally brownish- or grayish-weathering, though some have a faint rusty-yellow cast. The metawackes are generally medium- to coarse-grained quartz-feldspar-biotite-garnet-sillimanite schistose gneisses. Rocks of metawacke composition grade into metapelite where combined biotite, garnet, and sillimanite exceed 50 percent.

Mineral segregation is prominent in both the metawackes and metapelites: white quartz-feldspar leucosomes commonly contrast with well-developed, dark brown- and black-colored biotite-rich folia. Garnet porphyroblasts, where present, are generally red.

The metawackes and metapelites of the Manhattan Schist contain a variety of mineral assemblages, which reflect, in turn, a range of metamorphic conditions. These aluminous rocks locally occur as coarse-grained, white-and-red garnet-cordierite-sillimanite gneisses and as silvery muscovite-biotite-garnet-staurolite schists, as well as the typical biotite-garnet-sillimanite schistose gneisses. Many of the rocks are distinctly migmatized; Fig. 27 illustrates the migmatitic appearance of some of highest-grade gneisses. Representative modal compositions of metawackes and metapelites, reflecting some of the major mineralogical variations, are given on Table 8.

The quartz-plagioclase-biotite-garnet granofelses are brown- or greyish-weathering, medium-grained rocks. The granofelses occur in beds that range between a few centimeters and ~60 centimeters in thickness. These granofelses grade texturally into gneisses as biotite content increases and mineral segregation becomes more prominent. The mode of one granofels specimen (#1817) is given on Table 8, and its feldspar content is plotted on Fig. 28.

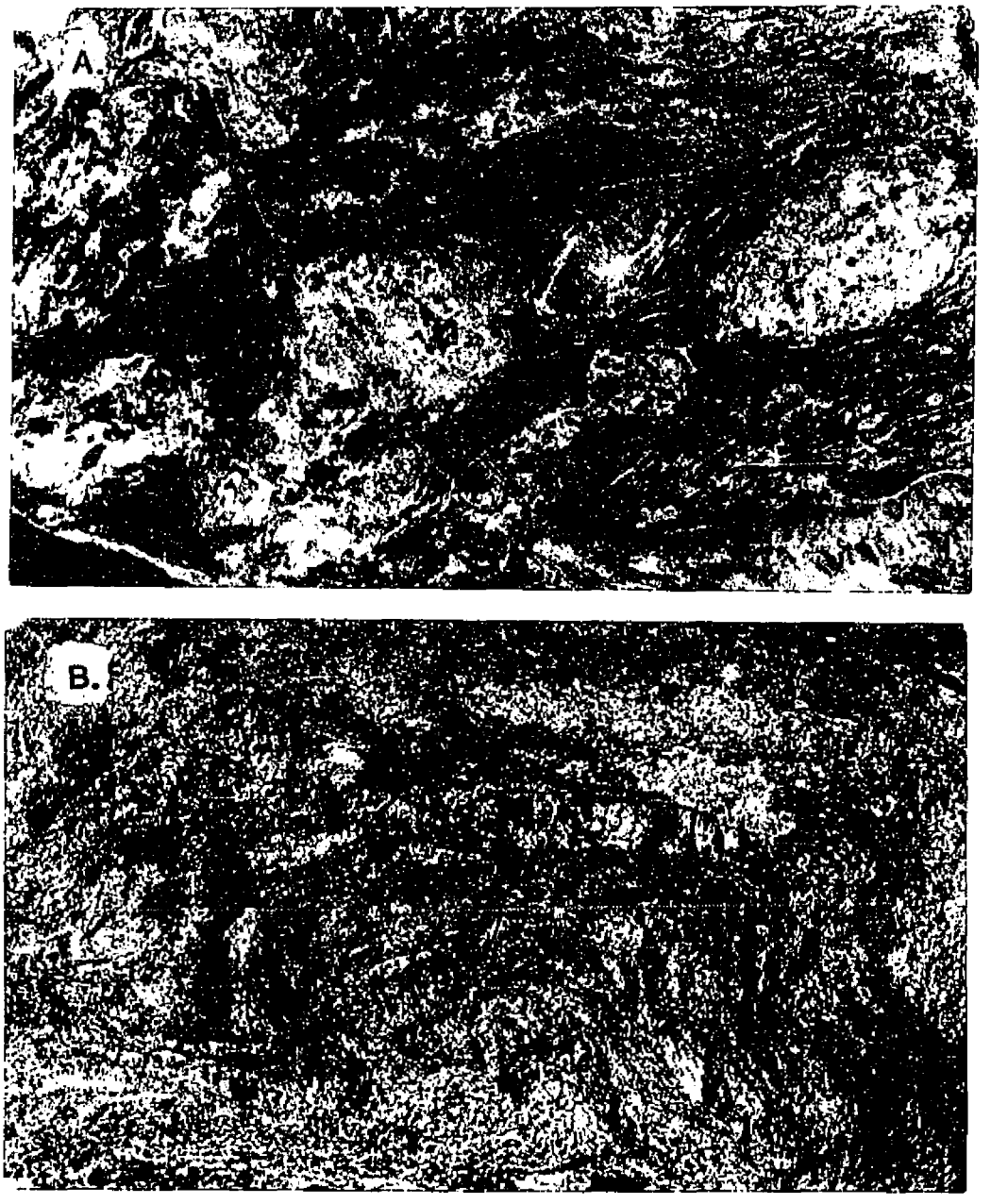

Fig. 27. High-grade gneiss (metawacke) of the Manhattan Schist, at specimen site #1001, Pierrepont State Park. Photos approximately actual size.

(A) Migmatite with oval anatectic leucosomes, which display granitic textures. Thin white streaks are (S_1) sillimanite trains. Locations of F_2 microfolds, defined by folded sillimanite trains, are controlled by the leucosomes.

(B) Doubly-plunging F_2 fold deforms both the sillimanite trains and flasered leucosomes.

TABLE 8

Estimated Modal Compositions of Representative Specimens, Manhattan Schist

Specimen	Metawackes & metapelites 180	648	966	1377	1727	Grano-fels 1817	Amphibolites 182c	1479	1499	Specimen
Quartz	21	29	20	45	40	54	4	17	22	Quartz
Plagioclase	16	25	5	7	20	25	28	17	23	Plagioclase
(% anorthite)	(25)	(30)	(43)	(23)	(23)	(28)	(38)	(38)	(59-89)	(% anorthite)
K-feldspar	5	-	-	5	20	-	-	-	-	K-feldspar
Biotite	20	7	2	31	10	16	1	12	-	Biotite
Garnet	20	15	24	5	1	4	-	-	-	Garnet
Sillimanite	15	tr.	8	6	7	tr.	-	-	-	Sillimanite
Kyanite	-	tr.	1	-	-	-	-	-	-	Kyanite
Cordierite	-	-	32	-	-	-	-	-	-	Cordierite
Staurolite	-	2	tr.	-	-	-	-	-	-	Staurolite
Gedrite	-	-	2	-	-	-	-	-	-	Gedrite
Hornblende	-	-	-	-	-	-	65	51	51	Hornblende
Apatite	tr.	tr.	-	tr.	tr.	tr.	tr.	tr.	tr.	Apatite
Zircon	tr.	tr.	tr.	tr.	tr.	tr.	-	-	-	Zircon
Tourmaline	-	tr.	-	-	-	-	-	-	-	Tourmaline
Green spinel	tr.	-	tr.	-	-	-	-	-	-	Green spinel
Rutile	-	-	tr.	-	-	-	-	-	-	Rutile
Anatase	-	tr.	-	tr.	-	-	-	-	-	Anatase
Magnetite	tr.	tr.	tr.	tr.	1	tr.	tr.	tr.	1	Magnetite
Ilmenite	3	tr.	5	tr.	tr.	tr.	2	3	3	Ilmenite
Pyrrhotite	tr.	tr.	tr.	-	1	tr.	-	-	tr.	Pyrrhotite
Pyrite	-	-	-	tr.	-	-	-	-	-	Pyrite
Chlorite	tr.	tr.	-	-	-	-	-	-	-	Chlorite
Muscovite	-	21	tr.	tr.	tr.	-	-	-	tr.	Muscovite

TABLE 8, CONTINUED

Notes: 1. Specimen locations are shown on Plate III. **2. The color of the specimen's weathered surface** is described only where it contrasts with the overall color of the rock.

Metawackes and metapelites

180. Dark grey schist with garnet porphyroblasts up to 11 millimeters in diameter. (South-central Peach Lake quadrangle)
648. Rusty-weathering, medium- to coarse-grained schist with euhedral garnets, staurolite, and tourmaline. (West-central Peach Lake quadrangle)
966. Grey and red medium-grained gneiss with anastomosing sillimanite trains. (Northeastern Peach Lake quadrangle) Microphotographs, Figs. 30, 59A, and 63.
1377. Brown-weathering, medium-grained gray schist. (Collected by Route 35, south-central Peach Lake quadrangle)
1727. Medium-grained grey schist with brown-rusty weathering biotite folia. (Alongside Route 35, south-central Peach Lake quadrangle)

Granofels

1817. Brown-weathering, medium- to fine-grained grey granofels. (Collected by Route 35, south-central Peach Lake quadrangle)

Amphibolites

182c. Dark-olive weathering, black amphibolite with white streaks. (West-central Peach Lake quadrangle)
1479. Dark-olive weathering, medium-grained black amphibolite with thin white leucosomes. (South-central Peach Lake quadrangle)
1499. Medium-grained, black amphibolite with white leucosomes (1 to 4 millimeters thick), spaced ~15 millimeters apart. (South-central Peach Lake quadrangle)

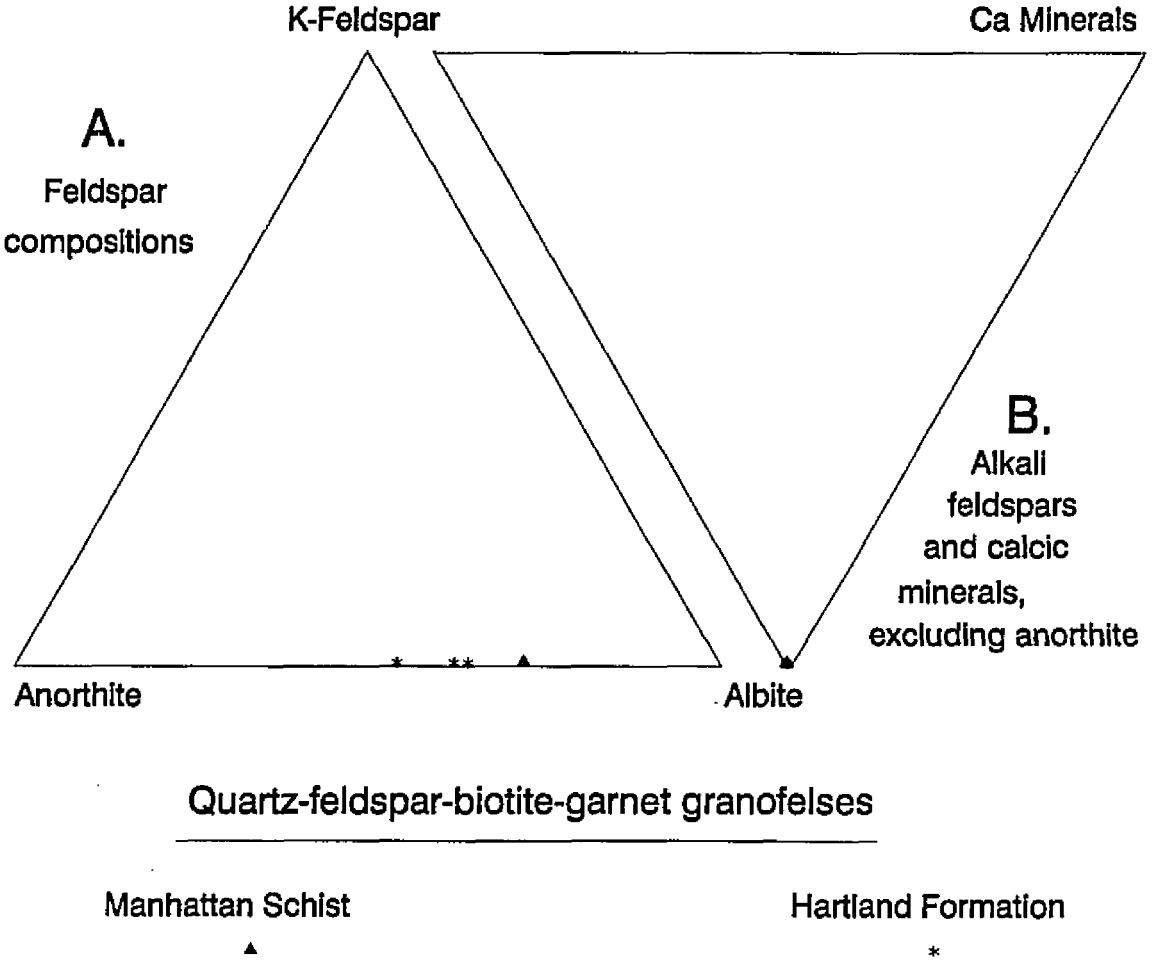

Fig. 28. Feldspar and calc-silicate mineral variations in the Manhattan Schist and Hartland Formation.
(Diagram is constructed in the same manner as Fig.19)

The amphibolites occur in homogeneous layers from 0.5 to ~5 meters in thickness. They are very dark and weather to a dark-olive or black color. All the amphibolites of the Manhattan Schist that have been examined in thin section are hornblende amphibolites. Examples of modal compositions are given on Table 8.

The Manhattan Schist resembles the upper Walloomsac Schist, with which it is in contact, in many ways. Manhattan Schist can be distinguished from the upper Walloomsac by the absence of graphite, by its darker, browner biotites, its browner weathered surfaces, and its more abundant amphibolites. Nevertheless, both formations contain rocks of varied appearances, and in some cases the distinction between Manhattan Schist and upper Walloomsac is problematic.

Interpretation. If Hall's hypothesis is correct, the Manhattan Schist was originally deposited to the east of the rocks that it presently overlies. Hall suggested that the Manhattan Schist might overlap in age with the Inwood Marble; however, the presence of amphibolites within the Manhattan suggests that it originated during the rift phase rather than under stable-margin conditions.

The Manhattan Schist resembles the Wacke Member of the Ned Mountain Formation in most aspects of appearance and composition. (The Manhattan does have better defined, more uniform layering, contains less K-feldspar, and lacks cummingtonite amphibolites.) Comparable origins for the two units are plausible.

The Wacke Member is interpreted as a deep-basin deposit, age-equivalent to the shallow-water and subaerial deposits that make up most of the rest of the Ned Mountain Formation. The Wacke Member, however, is a discrete, local body of rock, while the Manhattan Schist is continuous (and fairly homogeneous) body that extends for over a hundred kilometers. This continuity starkly contrasts with the pronounced discontinuity of practically every unit within the Ned Mountain Formation. If the Manhattan Schist were an age-equivalent of the Ned Mountain, then the mosaic of Ned Mountain environments would have been accompanied by uniform, relatively

deep-water conditions to the "east". Such a scenario may be consistent with a late-rift stage, when a water-filled trough existed along the future continental margin, but before the passive-margin carbonate bank had been established.

HARTLAND FORMATION

The stratigraphic units that have been described up to this point (the Fordham Gneiss, Ned Mountain Formation, Inwood Marble, Walloomsac Schist, and Manhattan Schist) together comprise the Manhattan Prong. The Manhattan Prong was part of Cambro-Ordovician North America. The Hartland Formation, which belongs to the Hartland terrane (Rodgers, 1985), is in thrust contact with the Walloomsac Schist and Manhattan Schist in the northeastern Peach Lake quadrangle. The Hartland Formation, of inferred Cambro-Ordovician age, was accreted to North America during the Taconian orogeny (Hall and Robinson, 1982).

The Hartland Formation occurs in the core of a tight syncline located in the northeastern Peach Lake and adjacent Bethel quadrangles (Plate I). There, the Hartland Formation consists of metabasites, thick quartz-plagioclase-biotite-garnet granofelses, and rhythmically interbedded granofels/metawacke sequences. Metabasite is the most abundant lithology (about 50 percent of the formation), and the thick granofelses and granofels/metawacke sequences each comprise about equal proportions of the remainder.

The metabasites are grey- or rusty-weathering, medium-grey, dark-grey, or black rocks. They occur in beds that vary from several centimeters to several meters in thickness. Hypersthene is the dominant mafic mineral in the medium- and dark-grey metabasites; rock color tends to darken as hornblende becomes more abundant. The grey metabasites contain hypersthene and plagioclase grains of fairly uniform size (Fig. 5B), and generally have medium- to fine-grained granofelsic textures. A few metabasites have thin, close-spaced, biotite-rich folia, and are textural-

ly fissile granofelses.

Microscopic examination of dark metabasite layers reveals small relict ortho- or clinopyroxene grains enclosed in larger hornblendes. Orthopyroxene grains in grey metabasites are commonly rimmed by hornblende. Replacement textures are so pervasive that all the hornblende may very well be secondary. Modes of representative specimens are given on Table 9.

The quartz-plagioclase-biotite-garnet granofelses are grey- or rusty-weathering, medium- to light-grey, medium-grained rocks. K-feldspar is absent, and quartz is more abundant (on average) than in granofelses of the Manhattan Schist or Walloomsac Schist. Bedding, defined by thin biotite-rich interlayers, is generally very pronounced. Quartz-rich layers are commonly 1 to 15 centimeters in thickness. The grey granofelses occur sequences generally 1 to 3 meters in thickness; such sequences weather in a massive, uniform style. Representative modes are given on Table 9.

The granofels/metawacke sequences consist of alternating beds of light grey, medium-grained, quartz- plagioclase- biotite- garnet granofels and darker, garnet- and biotite-rich metawacke. Most beds are several centimeters in thickness, though the beds of granofels are somewhat thicker on average than those of metawacke. Fig. 29 illustrates the appearance of this lithology in the field.

Mineral assemblages observed in metawacke beds include plagioclase-garnet-sillimanite-biotite-K-feldspar-quartz schist and plagioclase-garnet-biotite-(green) spinel-sillimanite gneiss (#1701, layer III, Table 9). The granofels beds generally resemble beds in the grey granofels sequences in both texture and mineralogy. Layer II in #1701 (Table 9) is exceptional, being poorer in quartz and richer in plagioclase than other Hartland granofelses.

Interpretation. The abundance of metabasite and quartz-plagioclase-biotite-garnet granofels reflects the preponderance of basaltic volcanic rocks and coarse-grained siliciclastic sediments in the Hartland's depositional environment. The rhythmic metawacke/granofels sequences sug-

TABLE 9

Estimated Modal Compositions of Representative Specimens, Hartland Formation

	Quartz-feldspar granofelses					Metabasites				
						CT-10b				
Specimen	1608	1624		1701		89		1610	1700	Specimen
Layer	I		I	II	III	I	I	II		Layer
Quartz	41	67	66	19	-	14	11	-	20	Quartz
Plagioclase	35	23	23	49	62	45	35	41	30	Plagioclase
(% anorthite)	(38)	(36)	(45)	(44)	(45)	(76)	(53)	(53)	(69)	(% anorthite)
Biotite	20	6	6	10	8	tr.	-	tr.	7	Biotite
Garnet	2	2	3	19	23	-	-	tr.	-	Garnet
Sillimanite	-	-	-	-	2	-	-	-	-	Sillimanite
Hypersthene	-	-	-	-	-	35	5	38	25	Hypersthene
Augite	-	-	-	-	-	-	-	tr.	-	Augite
Hornblende	-	-	-	-	-	tr.	45	16	12	Hornblende
Cummingtonite	-	-	-	-	-	tr.	-	tr.	-	Cummingtonite
Apatite	tr.	tr.	tr.	tr.	tr.	tr.	tr.	tr.	tr.	Apatite
Zircon	tr.	tr.	tr.	tr.	tr.	-	-	-	-	Zircon
Green spinel	-	-	-	-	3	-	-	-	-	Green spinel
Magnetite	tr.	1	1	2	-	1	1	2	2	Magnetite
Ilmenite	tr.	tr.	tr.	tr.	2	4	3	3	3	Ilmenite
Pyrrhotite	1	tr.	tr.	1	-	tr.	tr.	tr.	1	Pyrrhotite
Pyrite	tr.	-	-	-	-	-	-	-	-	Pyrite
Chlorite	-	tr.	-	tr.	tr.	-	-	-	-	Chlorite
Muscovite	tr.	tr.	tr.	-	tr.	-	-	-	-	Muscovite

TABLE 9, CONTINUED

Notes: 1. Specimen locations are shown on Plate III. **2. The color of the specimen's weathered surface** is described only where it contrasts with the overall color of the rock.

Quartz-feldspar granofelses

1608. Slightly rusty-weathering, thin-bedded, medium-grained grey granofels with biotite-rich laminae. Granofelsic beds (layer I) are 10 to 15 millimeters thick, biotite-rich laminae (layer II), ~4 millimeters. (Northeastern Peach Lake quadrangle)

1624. Well-bedded, medium-grained, grey granofels. Beds are 1 to 50 millimeters in thickness. (Westernmost central Bethel quadrangle, 130 meters east of the boundary with the Peach Lake quadrangle) Photograph (outcrop), Fig. 29.

1701. Well-bedded, medium-grained, light-grey granofels (layers I and II) with reddish, garnet-rich pelitic laminae (layer III). Granofelsic beds are 25 to 30 millimeters in thickness. (Northeastern Peach Lake quadrangle)

Metabasites

CT-10b-89. Medium-grained, dark grey gneiss, with spongy weathered surface (layer I). (Layer II is a quartz-plagioclase-garnet-biotite schistose gneiss). (Northeastern Peach Lake quadrangle)

1610. Medium grey to black banded gneiss. Black bands (layer I) are medium- to coarse-grained, and contain pale bleps of relict hypersthene. Grey bands (layer II) are finer-grained. (Northeastern Peach Lake quadrangle)

1700. Rusty-weathering, medium-grained, slabby dark-grey gneiss with numerous biotite folia. Biotite folia are spaced a few millimeters apart. (Northeastern Peach Lake quadrangle)

Fig. 29. Rhythmically-bedded quartz-feldspar granofels and metawacke of the Hartland Formation at specimen site #1624, westernmost Bethel quadrangle. Hammer is 33 centimeters long. (Mode of #1624 is given on Table 9).

gest deep-water, turbidite-style deposition. The rhythmic granofels/metawacke sequences may correspond to Hall's (1968c) Schist and Granulite Member of the Hartland Formation, recognized in the Glenville quadrangle (Fig. 1). The portion of the Hartland Formation exposed in the study area is (like the Schist and Granofels Member) probably correlative with the Moretown Formation of central New England.

Stanley and Ratcliffe (1985) noted the quartz-rich character of Moretown Formation granofelses. They suggested that the Moretown Formation originated in a forearc basin, where it received reworked sediments from uplifted portions of the accretionary prism, as well as immature sediments from the volcanic arc. Such a setting is consistent with the suite of lithologies found in the Hartland Formation in the study area.

STRUCTURAL GEOLOGY

INTRODUCTION

PREVIOUS WORK. The rocks of the Manhattan Prong have experienced several episodes of deformation and metamorphism. Scotford (1956), working in the northeastern Manhattan Prong, was the first to recognize two episodes of map-scale folding. Three or more deformational events were subsequently distinguished by workers in other parts of the Manhattan Prong (for example, Bowes and Langer, 1969; Whiting-Goldberg, 1977; Hall, 1979).

P. W. G. Brock identified a sequence of six deformational events in the Paleozoic strata of the Croton Falls quadrangle (Brock and Mose, 1979; Brock and Brueckner, 1978). A seventh event was first recognized in the Peach Lake quadrangle (Brock and Brock, 1985a and b; Brock, Brueckner and Brock, 1985). The first four of these events could be distinguished from the last three by the mineralogies of syntectonic fabrics. The fabrics that developed in pelitic rocks during the earlier events contain coexisting K-feldspar and sillimanite, but recrystallization related to the younger events produced lower-grade mineral assemblages.

Most of the deformational events that have now been recognized in the study area can be correlated with the sequence from the Croton Falls quadrangle, although the enumeration of events differs. The Croton Falls F_1 event is associated with the first foliation (S_1) and with early mineral segregations; "F_2" is defined as the event responsible for flasering of F_1 segregations. However, in the study area, the formation and the flasering of early segregations are considered parts of a single, progressive F_1 deformational event. Subsequent to flaser formation, ubiquitous tight to isoclinal folds were generated, and the flasers were deformed. In the study area, these events are assigned to F_2, though they are considered to be "F_3" in the Croton Falls quadrangle. Still later, F_3 folding in the study area and "F_4" in the Croton Falls both led to the development of

small crinkles and of reclined, fairly open folds. Though the hinge surfaces of the fold sets in the two quadrangles are oriented at about 90° to each other, the similarities in relative age, geometry, and style suggest that they may be genetically related. The study area F_4 and Croton Falls "F_5", on the other hand, are clearly distinct and unrelated episodes of deformation. Descriptions of these events are given later.

The "D_6" event of the Croton Falls quadrangle has left the clearest and most easily recognized imprint of any deformational event in the Manhattan Prong. The "D_6" was accompanied by a host of special features, including a distinctive suite of syntectonic granites and characteristic retrograde metamorphism (Brock and Brock, 1981, 1985a, and 1985b). These features make the "D_6" a regionally important structural marker event. To avoid confusion and to make the correlation explicit, this deformation is enumerated as D_6 in the study area. As a result, no D_5 event is recognized there (Table 10).

Previous structural analyses of the Manhattan Prong were developed within the traditional stratigraphic framework, which predated the recognition of the Ned Mountain Formation. Ned Mountain rocks were formerly assigned to look-alikes among the traditional units. For instance, on Brandon's (1981) map of the southeastern Peach Lake quadrangle, different portions of the Ned Mountain Formation are shown as Fordham Gneiss, Lowerre Quartzite, Inwood Marble, Walloomsac Schist (Manhattan A), and Hartland Formation. Some of the discrepancies between the major structures described in this report and those of earlier workers (including Brandon) stem from the control which the stratigraphic assignments of individual outcrops exert on map distribution patterns, and hence on map-scale structural interpretation.

DESCRIPTIVE APPROACH. An episode of deformation ("D_x"), as the term is used here, consists of all forms of deformation ascribed to the same event. Thus, the first event in post-Grenvillian rocks (D_1) includes both folding (F_1) and thrusting (D_1 ductile faulting). The relative importances of ductile faulting and folding are variable; D_6 and D_7 are essentially episodes of

TABLE 10. Tectonic Development of the Northeastern Manhattan Prong

		Principal Deformation	Igneous Activity	Metamorphism
(Meso-zoic?)		? Brittle faulting fracturing (Rifting?)	Lamprophyre dike	
Alle-ghenian	D_7	East-directed thrusting	M_4	Lower greenschist facies (in shear zones)
	D_6	Ductile normal faulting	2-mica, tourmaline granites M_3	Greenschist through amphibolite facies (primarily in shear zones)
(D_5 None recognized in study area)				(Ky-stt grade ductile shear in Croton Falls Quad.)
TACONIAN	F_4 D_4	Recumbent open folding	?	Upper amphibolite facies (Kspar- sillimanite)
	F_3 D_3	Map-scale (reclined) open folding & local tight folding & local strong shear	Q-Feldspar segregations and small granitic bodies M_2	
	F_2 D_2	Backfolding Map-scale tight to isoclinal folding Local thrusting	Q-Kspar segregations and small granite bodies mafic pods Siscowit Granite	
	F_1 D_1	Ductile thrusting Emplacement of Hartland terrane over Manhattan Prong	Migmatization small granitic bodies M_1	Granulite facies
		Emplacement of Manhattan Schist over Walloomsac Schist		
Lower Mid-Ordovician		Collapse of continental margin	Mafic (?)tuffs in Walloomsac Sch.	
		Uplift (unconformity)		
Cambrian to Early Ordovician		Subsidence of Passive margin		
Protero-zoic Z to Early Cambrian		Rifting	Bimodal volcanic suite Hypersolvus granite (in Ned Mt. Fm.)	
		Unconformity		
Gren-villian		Folding	Intrusion of hornblende and pyroxene granites	Granulite facies

ductile faulting. Brittle faulting post-dated the ductile deformational events.

The structure of the study area is complex. The post-Grenvillian strata are affected by F_1, F_2, F_3, and F_4 folding, D_1, D_2, D_4, D_6, and D_7 ductile shearing, and some brittle faulting. The Paleozoic rocks unconformably overlie the Fordham Gneiss, which was deformed during Precambrian time. In the succeeding sections, each deformational event will be described and interpreted. As aids to this discussion, the relationships between deformational and metamorphic events and episodes of igneous activity are summarized on Table 10, and many of the criteria used to distinguish structures of different ages are summarized in Table 11.

GRENVILLIAN (pre-D_1) DEFORMATION

Evidence for the Grenville orogeny in the Peach Lake quadrangle takes several forms. The truncation of Fordham units on map scale (Plate IIA) attests to discordance between the members of the Fordham Gneiss and the overlying Paleozoic strata. The divergence in attitude between foliation from the Fordham Gneiss and S_1 foliation from the Basal Member of the Ned Mountain Formation (Fig. 3) is evidence of Precambrian deformation in the Fordham Gneiss. The relict mineral assemblages and textures of the Fordham Gneiss reflect higher metamorphic grade than was attained in many parts of the Manhattan Prong during Paleozoic time.

A plot of structures from the southwestern Peach Lake quadrangle illustrates divergence between the Fordham Gneiss and younger strata (Fig. 2). Structural data from minor folds in the Ned Mountain Formation define a distinct pattern on an equal-area stereonet. Hinge surfaces, on average, form an arc, and dip towards the north, northwest, or west, while most hinge lines plunge towards the northwest (Fig 2A). Structural data from the nearby Walloomsac Schist and Manhattan Schist are very similar (Fig. 2B). Structures in the Fordham Gneiss, however, tend to be differently oriented (Fig. 2C). Hinge surfaces of minor folds in the Fordham Gneiss dip to-

Table 11. Principal Features of Major Deformational Events

EVENT	REGIONAL PATTERNS & RELATIONSHIPS	FOLIATION DEVELOPMENT	STYLE	ATTITUDE OF HINGE SURFACE	METAMORPHIC GRADE
D_1/F_1	Deforms only stratigraphic contacts (S_0); Hartland Fm. emplaced over Manhattan Prong	Penetrative S_1; Early leucosomes locally flasered	Tight to isoclinal folds	Any	Granulite facies
D_2/F_2	Deforms S_0, S_1; Folds early flasers; Responsible for major alternating bands of Fordham Gneiss and cover rocks	Biotite locally parallel to S_2	Tight to isoclinal folds, some with curved hinge lines	Strikes from north through NW to W; generally dips mod. or steep to W or N	K-feldspar-sillimanite grade
D_3/F_3	Deforms S_0, S_1, S_2; Produces Pound Ridge antiform	Locally strong crenulation cleavage	Open folds, crinkles, zones of strong shear	Generally strikes NE, dips mod. to steep NW	K-feldspar-sillimanite grade
D_4/F_4	Deforms S_0, S_1, S_2, S_3; Results in domains of shallow dip	Biotite locally parallel to S_4	Open folds, resembling flight of stairs	Nearly horizontal	?K-feldspar-sillimanite grade
D_5	(None recognized in the study area)				
D_6	Deforms S_0, S_1, S_2, S_3, and contacts of syn-D_6 granites	Discontinuous cleavages in country rocks; Slip ("C") and shortening ("S") cleavages in some syn-D_6 granites	Broad and narrow shear zones; Normal offset; West-side down	Shear zones strike ~025° dip ~75°W	Greenschist to amphibolite grade aureoles around D_6 granites
D_7	Deforms S_0, S_1, S_2, S_3, and S_6 cleavages	Mylonite and very fine-grained fabrics developed in shear zones	Narrow shear zones; Thrust offset; West-side up	Shear zones strike ~015°, dip ~10° to 40° W	Lower greenschist facies

wards the northeast or west, and hinge lines show strong scatter. The contrast in structural patterns implies the presence of Precambrian folding in the Fordham Gneiss. Given the billion-year age of Fordham Gneiss (see Stratigraphy, Previous Work), this folding is reasonably attributed to the Grenvillian orogeny.

Paleozoic folds generally cannot be distinguished from Grenvillian structures in outcrops of the Fordham Gneiss within the study area. The foliation in the Fordham Gneiss, the Paleozoic S_1 foliation, and Paleozoic bedding all presently display subparallel orientations. The discordance between attitudes of foliation in the Fordham Gneiss and S_1 in neighboring outcrops of the Basal Member of the Ned Mountain Formation is generally 15° or less (Fig. 3). Precambrian structures have evidently been strongly rotated as the result of Paleozoic deformation.

The superposition of ductile Paleozoic deformation on Precambrian structures greatly increases the difficulty of identifying map-scale Precambrian folds. The problem is exacerbated in the study area by the character of the Fordham Gneiss. The original geometry of contacts within the Fordham is uncertain, because the local Fordham evidently consists of metaigneous (and probably meta-plutonic) rocks. Given these difficulties, no attempt has been made during this study to map Precambrian folds or to distinguish episodes of Precambrian deformation.

The following discussion of Paleozoic deformation is based on evidence from post-Grenvillian stratigraphic units exclusively.

PREMETAMORPHIC (Paleozoic) FAULTING

The contact between Manhattan Schist and the Walloomsac Schist is shown as a thrust fault on Table 1 and on Plates I, IA, and IV. Hall (1968a) proposed that the Manhattan Schist ("Manhattan C") is an allochthonous Cambrian unit, emplaced over the Ordovician Walloomsac Schist ("Manhattan A") on a premetamorphic thrust. This is accepted as the best available inter-

pretation of regional relationships. There is no direct evidence for the fault within the study area.

D_1 DEFORMATION

F_1 FOLDING AND FABRICS. The first (S_1) foliation is generally oriented parallel to bedding. It is commonly defined by planar mineral segregations; granitic leucosomes commonly occur in S_1 attitudes in metawackes and metapelites. In many lithologies, platy minerals (such as graphite and biotite) tend to be aligned with S_1. The earliest (L_1) lineations are commonly defined by trains of fibrolitic sillimanite or by quartz ribbons.

Folds which display foliation exclusively in an axial planar orientation, and which do not deform any pre-existing lineation, are generally interpreted as F_1 in age. Caution must be exercised when assigning folds to F_1, however, since later fabrics locally obliterate older foliations in high-strain zones. In addition, planar fabrics are poorly developed in some granofelsic rocks, making it difficult to interpret the ages of small folds in certain localities.

F_1 folds are rarely recognizable in the aluminous lithologies, but are relatively common among the well-bedded granofelses and gneisses of the Volcaniclastic and Calc-Silicate Members of the Ned Mountain Formation. The F_1 folds observed in outcrop are tight to isoclinal, and most plunge either to the north or west and show counterclockwise rotation sense. A few F_1 folds are sheath folds that have hinge lines which curve by more than 90°.

F_1 folds of larger-than-outcrop scale are present in the area, but are difficult to identify. To do so requires tracing a specific stratigraphic horizon through gaps between outcrops and around structural features related to all younger deformations. Individual stratigraphic horizons, however, are extremely hard to correlate over distances greater than a few meters, and post-F_1 deformation is generally complex and penetrative.

Larger-than-outcrop scale F_1 folds are most readily observed in a small area located

between Ned Mountain Road and George Washington Highway, in the northeastern Peach Lake quadrangle (Plate III). There, the unconformity between the Fordham Gneiss and Ned Mountain Formation Basal Member provides a unique, readily identified stratigraphic horizon, outcrops are closely spaced, and post-F_1 deformation is relatively minor and simple. The map-trace of the unconformity defines a series of northwest-trending folds with wavelengths of a few tens of meters. The S_1 foliation in the Ned Mountain Formation is axial planar to these folds. Foliation in the Fordham Gneiss diverges from neighboring S_1 by 3 to 22 degrees, indicating that the F_1 folds are tight to isoclinal. (These folds are not shown on Plate I, which is generalized on account of scale.) F_1 folds of this size are probably abundant, though unrecognized, elsewhere in the region.

The largest F_1 folds identified in the study area are located in the south-central Peach Lake quadrangle (Plate IV), where they are outlined by the contact between the Walloomsac Schist and Manhattan Schist. These folds have a wavelength of about a half kilometer, a size which is significantly less than the largest F_2 and F_3 folds.

D_1 THRUSTING- CAMERON'S LINE. Cameron's Line separates the rocks of the Manhattan Prong from those of the Hartland Formation. In the study area, Cameron's Line truncates the contact between the Walloomsac Schist and Manhattan Schist (Plate IV), although there is no evidence of truncation of structures. Cameron's Line is subparallel to S_1 and is deformed by F_2 and F_3 folds (Plate IV). Cameron's Line is considered to be a D_1 thrust fault in this area.

The oldest mineral assemblages that occur near Cameron's Line, in rocks of both the Hartland Formation and the Manhattan Prong, are indicative of granulite-facies metamorphism. These assemblages were intensely sheared while still under granulite-facies conditions. They were cut by L_1 sillimanite trains (Fig. 30), resulting in a distinctly flasered fabric. In these same rocks, early granitic segregations first formed, then were flasered, and were subsequently deformed into F_2 folds (Fig. 27). Granulite-facies metamorphism in this area was evidently accompanied by

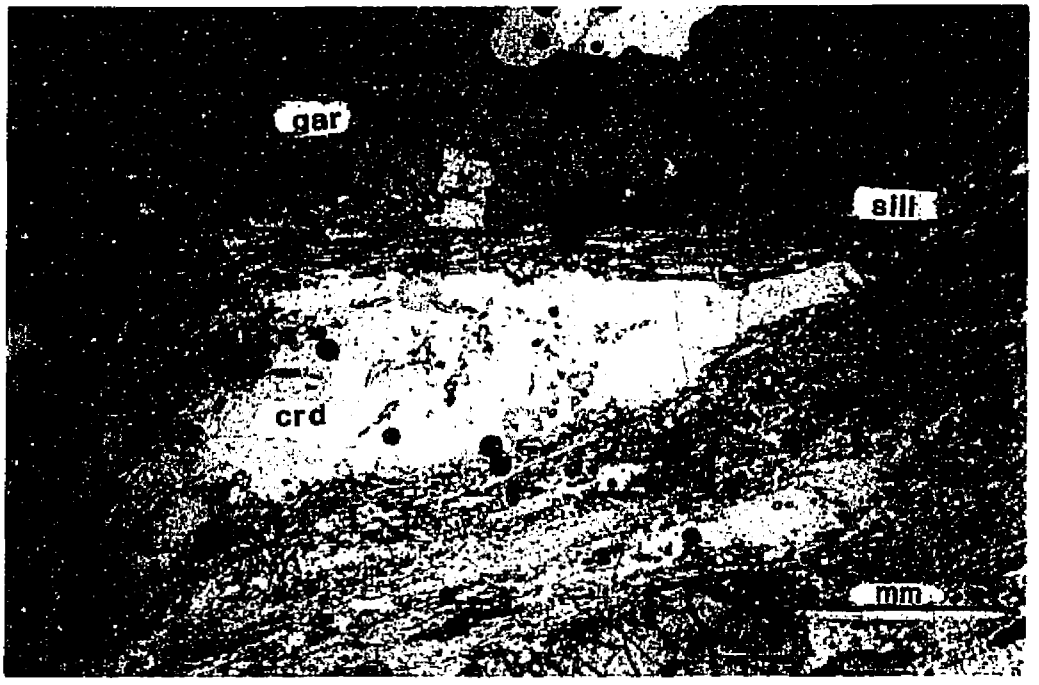

Fig. 30. L_1 fabric in a granulite-facies rock collected near Cameron's Line. Flasers of cordierite (crd), with yellow pleochroic halos around zircons, occur between anastomosing (L_1) trains of sillimanite (sill). Garnet (gar) occurs alongside. Specimen #966, Manhattan Schist. (Mode is given on Table 8).

intense D_1 strain, which may relate to motion on the Cameron's Line thrust.

INTERPRETATION OF D_1. The near-uniform counterclockwise rotation sense of the north- and west-plunging F_1 folds implies east-over-west relative motion. This sense of motion is consistent with regional-scale thrusting of the Hartland terrane westwards over North America, and with the broad tectonic framework of Taconian orogeny.

The parallelism of Cameron's Line to S_1 fabrics, and the presence of granulite-facies S_1/M_1 assemblages on both sides of the thrust, indicate that the juxtaposition of the Hartland Formation against the northeastern Manhattan Prong occurred during D_1.

D_2 DEFORMATION

F_2 FOLDING. Most of the recognizable folds of Paleozoic age are defined by deformed S_1 foliation. F_2 folds, the first to deform S_1, are the most abundant folds in the study area.

F_2 folds that have wavelengths between several centimeters and several meters are common through most of the Peach Lake and southern Brewster quadrangles. The folds are typically tight to isoclinal, and most have sharp noses. Some have curved hinge lines, and doubly-plunging F_2 folds may be observed at a couple localities (Fig. 27B).

A few F_2 folds show development of an S_2 foliation, especially in zones of strong transposition. S_2 development is generally reflected by the alignment of biotite grains, though mineral segregations were locally formed parallel to it. Pink granitic leucosomes follow S_2 in migmatized metawacke and metapelite at some localities. L_2 sillimanite or quartz lineations, where present, are commonly aligned parallel to fold hinges.

A cross-cutting sillimanite segregation defines an S_2 foliation at an outcrop located about 0.5 kilometers northwest of specimen #1625 (Plate III). The sillimanite in this segregation dis-

plays a well-developed lineation, which is oriented at high angle to nearby F_2 hinge lines. This lineation appears to record either syn-F_2 slip or the local direction of finite elongation.

The metamorphic grade of F_2 fabrics is in the upper-amphibolite-facies. Microscopic examination of metawackes and metapelites confirms that K-feldspar and sillimanite coexisted throughout the study area.

The hinge surfaces of minor F_2 folds describe a broad arc on map scale as the result of later (F_3) folding. F_2 hinge surfaces strike north-south in the South Salem region, and then swing to east-west in the West Mountain area (Plates III and IV). The contacts between the alternating belts of Fordham Gneiss and Paleozoic rocks of the study area describe parallel arcs (Plate I). Stratigraphic order is maintained along most of these contacts; the belts of Fordham Gneiss apparently define anticlines, the belts of younger rocks, synclines.

The rotation senses of minor F_2 folds are consistent with the assignment of an F_2 age to the stratigraphically-defined major folds. More direct age-control is available for the Washington Ledges syncline (Plate IV), which contains the Hartland Formation in its core. This syncline must post-date D_1, since it contains a folded D_1 thrust (Cameron's Line). The Washington Ledges syncline, and the other major lithologic belts, appear to be the products of F_2 folding.

Geometry of major F_2 folds. Two lines of evidence require that the F_2 folds be inverted. One of these is the distribution pattern of minor-fold rotation senses. The southern (or western) limbs of the major anticlines are defined as "limb A" (Figs. 31-34), the northern (or eastern) limbs as "limb B". Minor, northwesterly-plunging F_2 folds on "limb A" generally have counterclockwise rotation senses, while those on "limb B" have clockwise senses. This pattern indicates that the anticlines close downwards, and the synclines close upwards.

The second line of evidence for the inversion of the F_2 folds lies in the locations of major-fold closures. Stratigraphic units in Washington Ledges syncline pinch out towards the west, and those in the West Mountain anticline pinch out towards the south and east. Northerly- and wes-

terly- plunging F_2 minor folds predominate in both regions, implying that the Washington Ledges syncline closes upwards, and the West Mountain anticline closes downwards. On a broader scale, both the West Mountain and Shadow Lake anticlines pinch out to the south or east of the study area; the synclines open up in these directions, leading to outcrop of the Hartland Formation within short distances (Fig. 1).

Relationships among the major F_2 folds are illustrated on Fig. 31, a schematic, longitudinal cross-section of the study area. The stacking order of these folds can be inferred because of the fairly consistent northerly dips of both S_1 and S_2. The structurally highest feature within the Manhattan Prong is the Mill Plain syncline, which lies adjacent to the Hudson Highlands; the structurally lowest is "limb B" of the South Salem syncline. Plate IV provides a map-view representation of the major F_2 folds.

The orientations and rotation senses of F_2 hinge lines fall into generally consistent patterns with regard to the hinge surfaces of the major F_2 folds. On "limb A" of major F_2 folds, north- or west-plunging minor folds which show a distinct rotation sense are generally counterclockwise, while on "limb B", they are generally clockwise. Rare south- or east-plunging folds on both limbs show the reverse rotation sense (Fig. 32). The major exceptions to these generalizations occur near the major F_2 hinge surfaces, where domains (2 to ~20 meters across) showing "limb A" pattern occur on "limb B". These anomalous domains are attributed to intermediate-scale F_2 folding.

The major F_2 folds are asymmetric. The northern limbs of the South Salem and Washington Ledges synclines ("limb A") are attenuated compared with the southern limbs ("limb B"), as can be observed on cross-section A-A' (Plate V) and on Fig. 31. Plate V shows that D_2 faulting has cut out substantial portions of the "limb A" shared by the South Salem syncline and West Mountain anticline. "Limb B" appears to be the dominant limb of the F_2 folds.

The large F_2 folds are regionally important structures. The belt of Fordham Gneiss which lies in the core of the West Mountain anticline and the belt of the Walloomsac Schist in

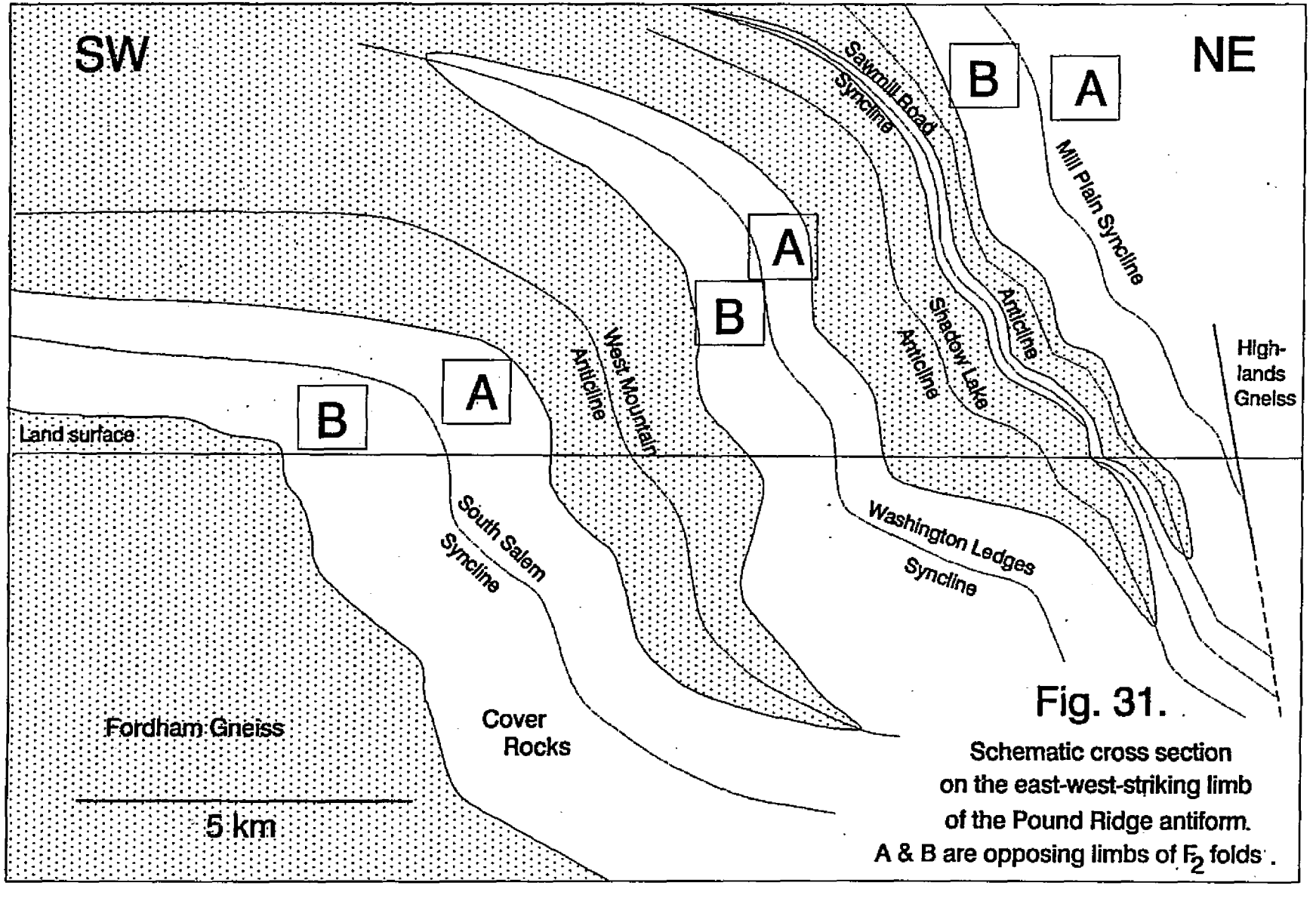

Fig. 31.

Schematic cross section on the east-west-striking limb of the Pound Ridge antiform. A & B are opposing limbs of F_2 folds.

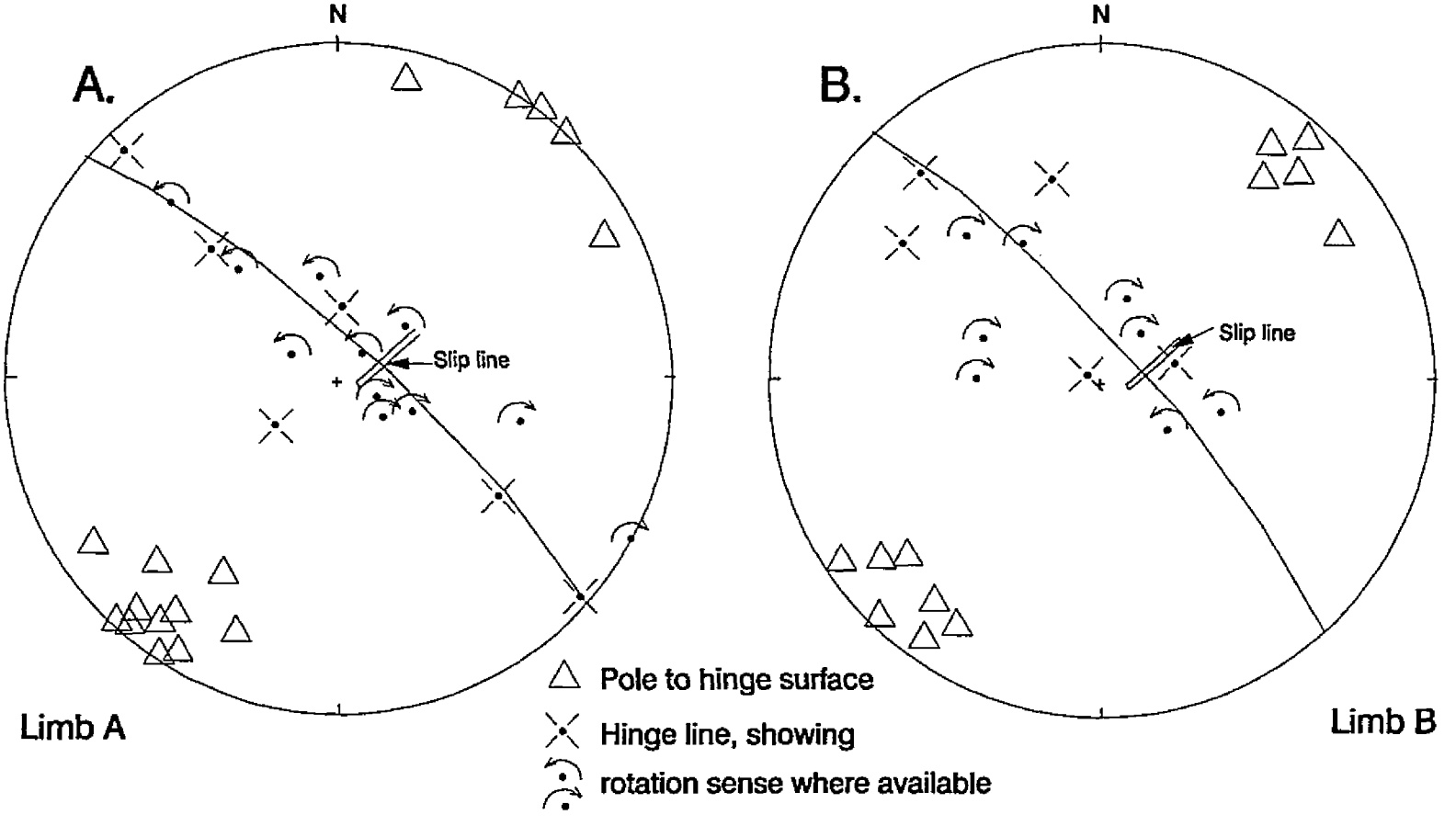

Fig. 32. Hinge lines and slip line on northwest-striking F_2 folds with steep hinge surfaces. "Limb A" and "Limb B" correspond to those on Fig. 31.

the core of the South Salem syncline can be traced over many tens of kilometers, into the southern Manhattan Prong (compare Plate V and Plate II).

F_2 slip-line orientation. The orientations and rotation senses of the hinge lines on each limb can be used to constrain F_2 slip-line orientation. According to Hansen (1971, p. 43), differential transport within the shear plane leads to varying hinge-line orientations (and rotation senses) among the resulting passive-slip folds. Hinge lines may even form at orientations approaching (but not parallel to) the direction of transport. The direction of transport coincides with the orientation at which fold rotation senses will reverse.

The hinge lines of northwest-striking F_2 folds which have steeply dipping hinge surfaces are plotted on an equal-area net in Fig. 32. For folds of this attitude, rotation sense reverses at an orientation of approximately 082° (trend), with a 78° plunge (Fig. 32). The orientation of this reversal indicates that the direction of F_2 transport plunges steeply to the east.

Data from north-south and east-west striking F_2 folds with steep hinge surfaces were plotted in the same manner. In these cases, the orientation of reversal is poorly constrained due to the paucity of east- and south-plunging minor folds (Fig. 33A). Nevertheless, the slip-line must occur within the gap between the hinges of clockwise and the hinges of counterclockwise folds, so that the data do set limits on the range of possible slip-line orientations. Fig. 33A shows where these gaps fall.

The ranges of possible slip-line orientations for F_2 folds of these varied orientations make another step in interpretation possible. If post-F_2 deformation took place by a predominantly passive-slip mechanism, then linear F_2 features (such as slip line) would collectively plot as a single great circle on equal-area net, thus defining a plane. This great circle would include the transport direction of the subsequent (F_3) folding. Fig. 33B shows how F_2 hinge-line data constrain the orientation of this great circle.

The geometry of the major F_2 folds can be modeled by combining map pattern, orienta-

Fig. 33.

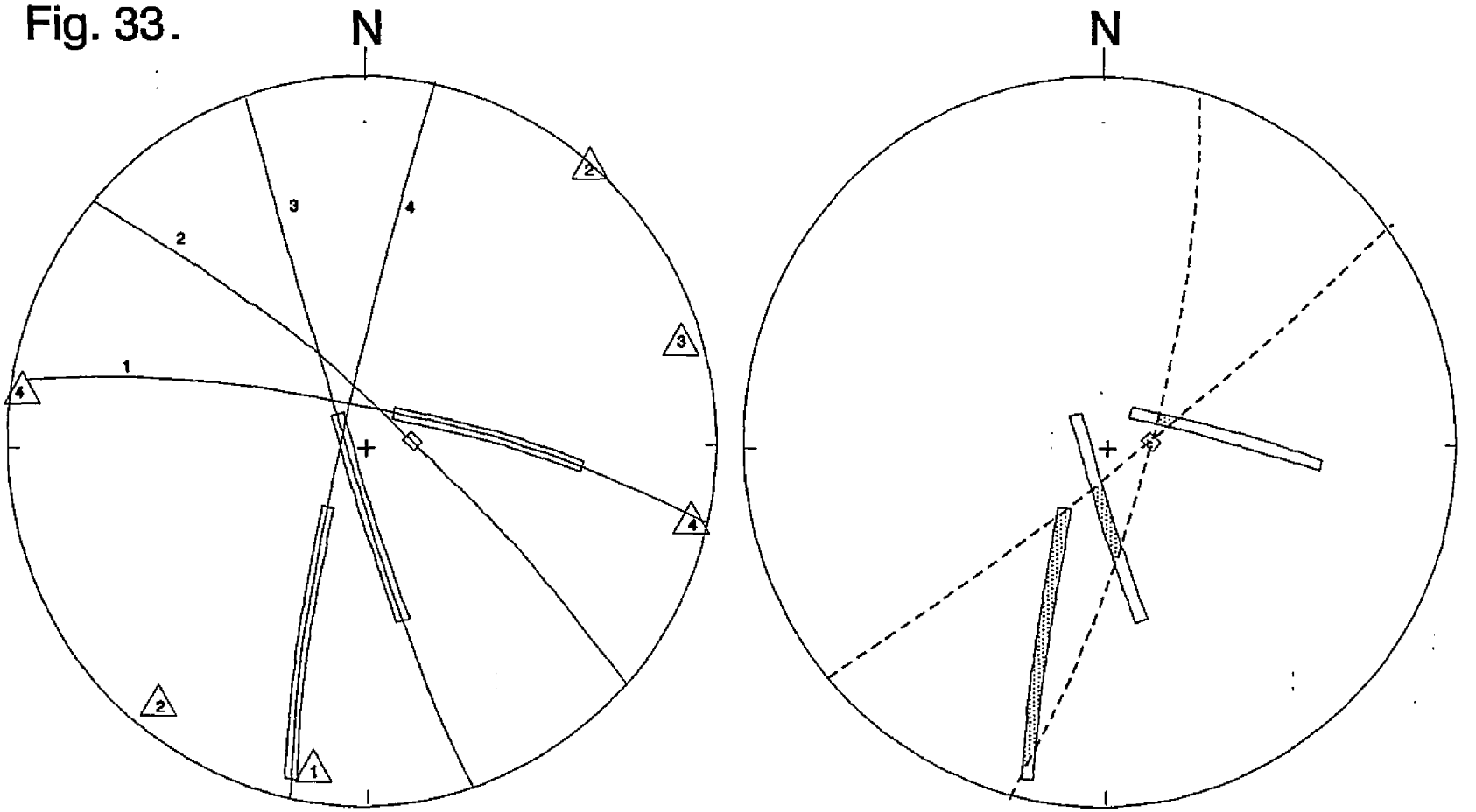

△ Pole to F_2 hinge surface

Interval within which slip line must fall (see Fig. 32)

A. Constraints on slip line orientation for east-west, northwest, and north-south striking F_2 folds

B. Constraints on orientations for planes defined by F_2 slip lines

(Construction performed on those F_2 folds having steep-dipping hinge surfaces.)

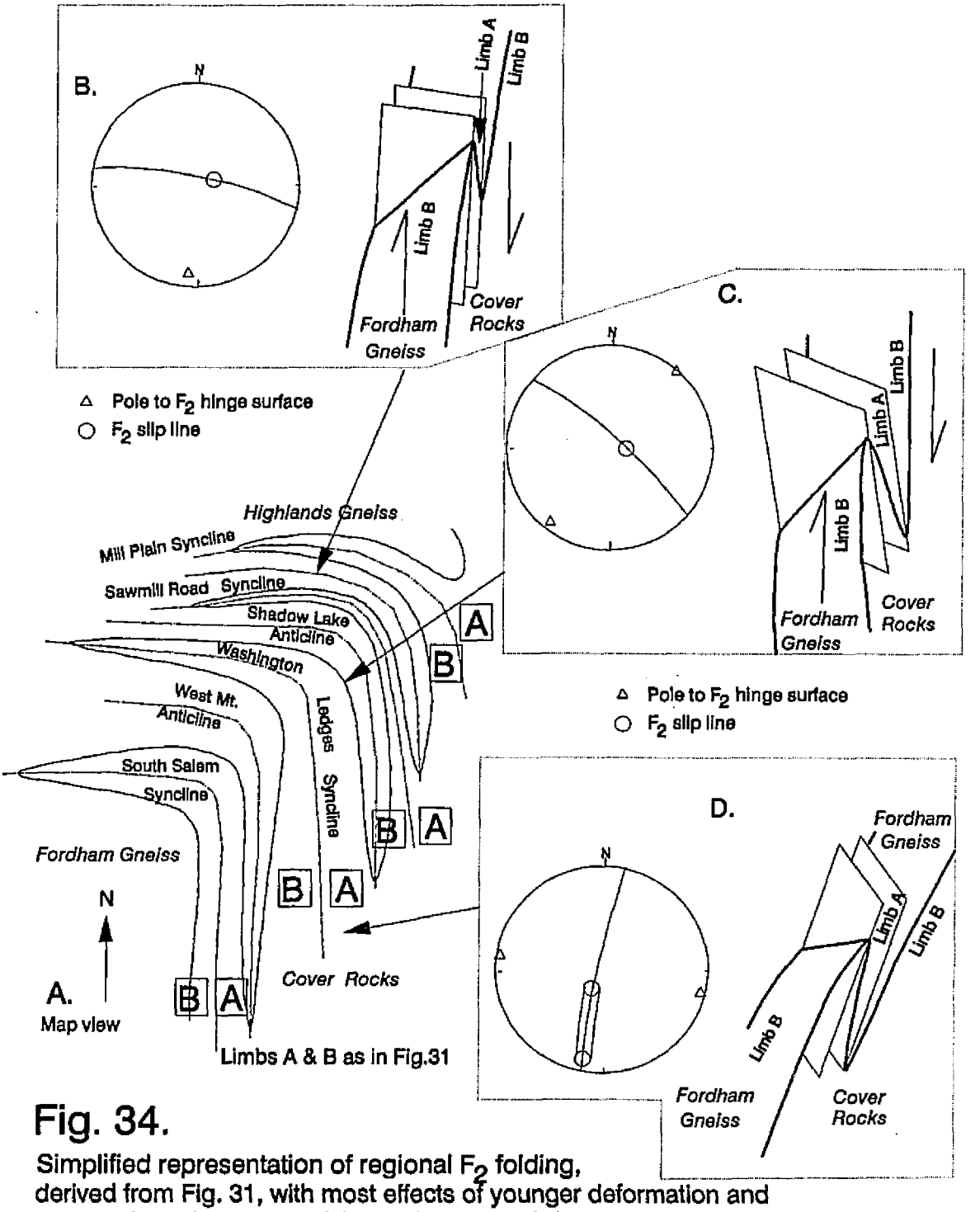

Fig. 34.

Simplified representation of regional F_2 folding, derived from Fig. 31, with most effects of younger deformation and igneous intrusion removed. The orientation of slip is shown for Figs. B and C.

tional data (e.g., the prevailing north- and west- plunges), transport directions, and asymmetry (Fig. 34B-D). Fig. 34A shows, in schematic fashion, what the "arc" of F_2 folds around the major F_3 fold might look like on a regional map scale, if plutons were removed and later deformation subtracted away.

D_2 THRUSTING. Progressively older portions of the Ned Mountain Formation have been cut out of the western limb of the West Mountain antiform, as the fold is traced southwards in the eastern Peach Lake quadrangle (Plates I, IV). A very penetrative S_2 fabric, on which intense transposition occurred, is locally developed along the zone of truncation. The truncation of units and the development of fabrics are inferred to result from D_2 thrusting, which coincided with the development of the West Mountain antiform.

On the east-west striking portion of the West Mountain antiform, northwest of Lake Rippowam (Plate III), the Fordham Gneiss is exposed almost to the base of the hillslope, leaving no room for the Ned Mountain Formation between it and the lowland (which is presumably underlain by Inwood Marble). The same D_2 thrust fault (or set of faults) which truncates the Ned Mountain Formation further east is inferred to follow the Fordham-Inwood contact here. On Plates I and IV, this D_2 fault is hypothesized to continue along the eastern boundary of the undivided Fordham Gneiss, at least as far as the southern map boundary.

F_2 FOLDING IN REGIONAL CONTEXT. With the termination of D_1 deformation, the Hartland Formation occupied the structurally highest position in the region, over the rocks of the Manhattan Prong. Subsequent F_2 folding probably affected an essentially right-side-up stratigraphic sequence (capped with allochthonous Hartland Formation), which had already been deformed into small- to medium-scale westwards-verging F_1 folds. Given these conditions, F_2 folds must originally have been upright and upwards-facing, or recumbent. However, the F_2 folds in the study area are downwards-facing (with moderately to steeply hinge lines), and have Ford-

ham Gneiss in the cores of anticlines above the Paleozoic section (Fig. 31, 34). This geometry must be the result of post-F_2 deformation.

F_2 anticlines are inverted on both limbs of the major F_3 fold. F_3 folding might, conceivably, have been responsible for the inversion of F_2 folds on one limb, but not both. Therefore, F_2 folds must have undergone rotation during a separate event, before the commencement of F_3 deformation.

The F_2 folds must be rooted in either the south or west, since structurally highest folds occur in the north or east (Fig. 31). As a result, F_2 folds appear to have originally verged towards the east or north. This vergence is opposite to the western vergence inferred for F_1 and to the generality of Taconian structures. The F_2 event is thus interpreted to be an episode of backfolding.

The "post-F_2" tilting is not given the status of a "deformational event", because its existence within the study area can only be inferred in the indirect manner described here. However, it appears to have left a substantial imprint on the geometry of the Manhattan Prong as a whole. This imprint (and related effects) will be discussed in a later section, which will treat the gross tectonic development of Manhattan Prong.

D_3 DEFORMATION

F_3 FOLDING AND D_3 SHEARING. The broad arc described by the F_2 folds outlines the largest fold in the study area, the F_3 Pound Ridge antiform (Plate IV). Outcrop-scale F_3 folds are unevenly distributed through the study area. Near the hinge surface of the Pound Ridge antiform, F_3 folding is abundant; elsewhere, it is sporadic. Few F_3 folds are seen in certain large areas.

The Pound Ridge antiform is an open fold with an interlimb angle of about 80 degrees.

Most of the minor F_3 folds are open (with interlimb angles between 65° and 100°) and have sharp noses (Fig. 35). Crinkling of F_3 age is common in metawackes. Tight F_3 folds have also been observed, though they appear to be largely confined to localized zones of strong shear.

Pronounced F_3 shear characterizes both the hinge surface of the Pound Ridge antiform and a set of subparallel high-strain zones. An S_3 crenulation cleavage is locally developed in high strain zones (Fig. 35).

The subparallel high-strain zones punctuate the "arc" defined by the F_2 folds. The zones range from about 0.2 to 10 meters in width. Some are located in the hinge regions of intermediate-scale F_3 folds. Within the high-strain zones, foliation is abruptly rotated towards the orientation of S_3 (Fig. 36). Small F_3 folds are commonly developed within and adjacent to the zones; for instance, minor F_3 folds with amplitudes around 10 centimeters are associated with the high-strain zone illustrated in Fig. 36.

F_3 folds deform upper-amphibolite facies metawackes, which have K-feldspar-sillimanite assemblages, without any evident retrogression. Laths of young sillimanite have grown across old sillimanite trains and locally define an L_3 lineation parallel to hinges of F_3 folds (Fig. 37). Metamorphic conditions which accompanied F_3 deformation were evidently in the upper-amphibolite facies.

Coarse-grained granitic leucosomes several centimeters thick occur in an axial-planar attitude to some F_3 folds, particularly in metawacke or metapelite lithologies. However, most of the anatectic granites and migmatites in the region are older, and have been deformed around F_3 folds.

Orientation of F_3 folds. The hinge surface of the Pound Ridge antiform strikes to the northeast and dips towards the northwest. Many F_3 folds in the central and southern Peach Lake quadrangle have similar attitudes, but the F_3 folds that occur northwest of the hinge surface of the Pound Ridge antiform tend to have northerly strikes (Plate IV).

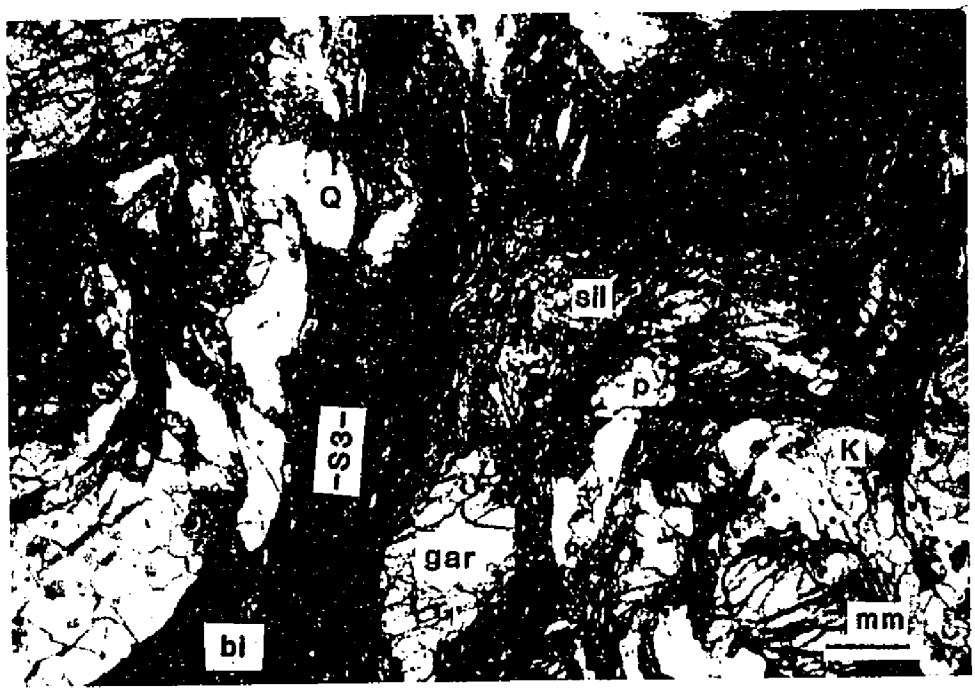

Fig. 35. S_3 foliation (-S3-) and F_3 microfolds near the hinge surface of the Pound Ridge antiform. Specimen #PP16c, Manhattan Schist, Pierrepont State Park. Some sillimanite prisms, seen in end view, are oriented parallel to the F_3 hinge line. bi=biotite; gar=garnet; K=K-feldspar; p=plagioclase; Q=quartz; sil=sillimanite (end sections).

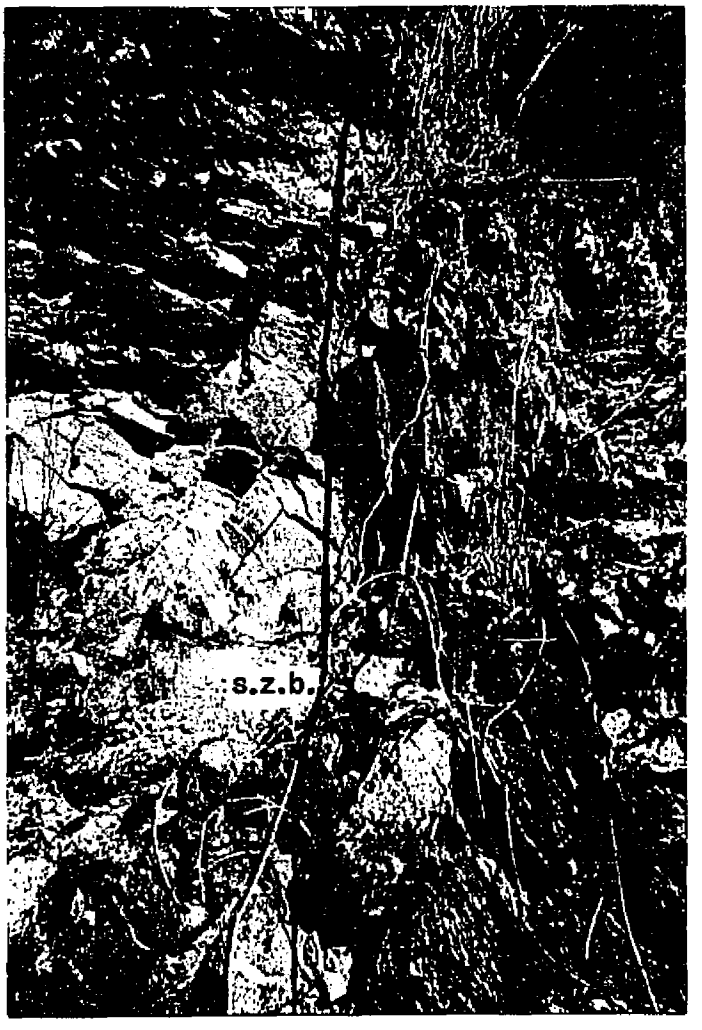

Fig. 36. D_3 high-strain zone. East-west striking, moderately north-dipping layering is rotated towards a northeasterly strike within the high-strain zone. The approximate boundary of the zone (s.z.b.) is highlighted. Hammer at the center of the photo is 33 centimeters long. Outcrop is located on Route I-84, 1.3 kilometers east of the intersection with Route I-684. (Structural data collected at this outcrop are presented on Fig. 40).

Fig. 37. S_1 sillimanite (sill) trains deformed into F_3 microfolds. End-sections of several sillimanite prisms are visible; these define an L_3 lineation parallel to the F_3 hinge line. Biotite (bi) is kinked and folded. Specimen #PP5a, Manhattan Schist, Pierrepont State Park.

The dips of the hinge surfaces of F_3 folds vary by 70°, ranging between shallow to very steep to the west (Figs. 38 and 39). The variation in dip appears to primarily relate to warping around near-horizontal F_4 hinge surfaces (Fig. 38). The scatter among the orientations of strike (which is most evident among the very steep hinge surfaces), is probably due to D_6 deformation related to the Turkey Hill fault zone (see Fig. 47, ahead).

Hinge lines of F_3 folds commonly plunge towards the north or northwest. The Pound Ridge antiform is, on average, a reclined fold, since the strike of its hinge surface is perpendicular to the trend of the average F_3 hinge line (Figs. 38, 39). On the eastern (north-south striking) limb of the Pound Ridge antiform, almost all linear elements (F_2 and F_3 hinge lines, quartz rods, sillimanite needles, foliation intersections, etc.) are subparallel, and plunge moderately to the northwest (Fig. 39).

F_3 slip line. Theoretically, if F_3 folding occurred by a passive-slip mechanism, then the intersection of the trace of S_3 on equal-area net with a plane defined by a deformed, pre-existing lineation would define the F_3 transport direction. As a practical matter, lineations known to have originally held constant orientations are rarely traceable around F_3 folds. However, the hinge line of a single F_2 fold can be measured on limbs of several minor F_3 folds at one outcrop in the Brewster quadrangle.

The outcrop is located on the north side of Route I-84, 1.5 kilometers southeast of the intersection with Route I-684 (Plate III). A zone of high F_3 strain, exposed at this outcrop, is illustrated in Fig. 36. A F_3 transport direction can be defined by data collected here (Fig. 40). This inferred transport direction trends 056° and plunges 32°.

While this direction is suggestive, only limited confidence can be placed in it, since it is based solely on data from a single locality, and especially since this locality is near the Turkey Hill fault zone. Confirmation of the slip direction at several additional localities would be desirable.

The transport direction determined on Fig. 40 does lie within the limits set for F_3 trans-

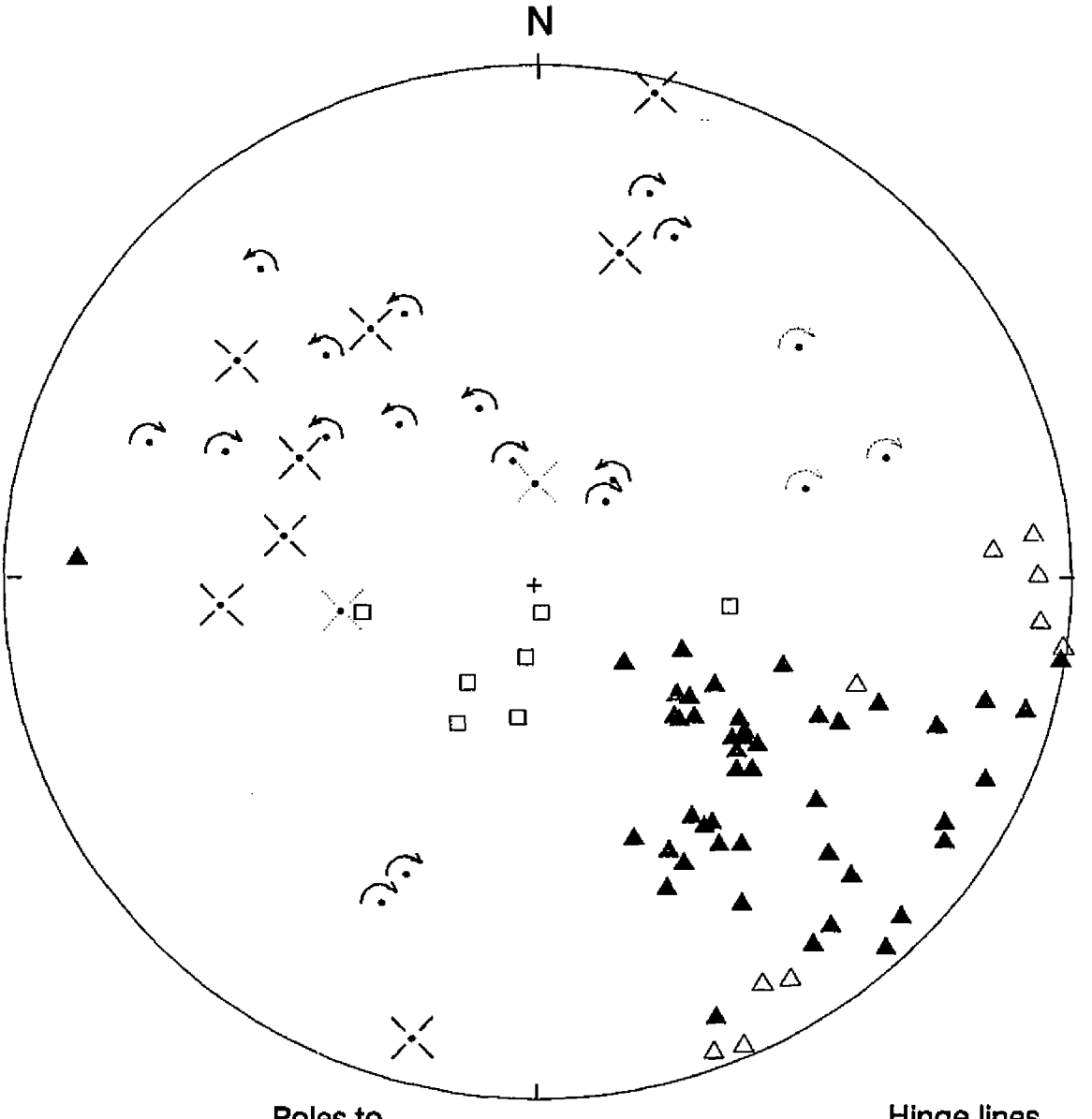

	Poles to hinge surfaces	Hinge lines showing rotation sense		Hinge lines indistinct rotation sense
F_3	▲	↶	↷	✕
F_3 adjacent to Turkey Hill Fault	△		↷	✕
F_4	□			

Fig. 38. F_3 hinge surfaces and hinge lines in relation to some younger structures.

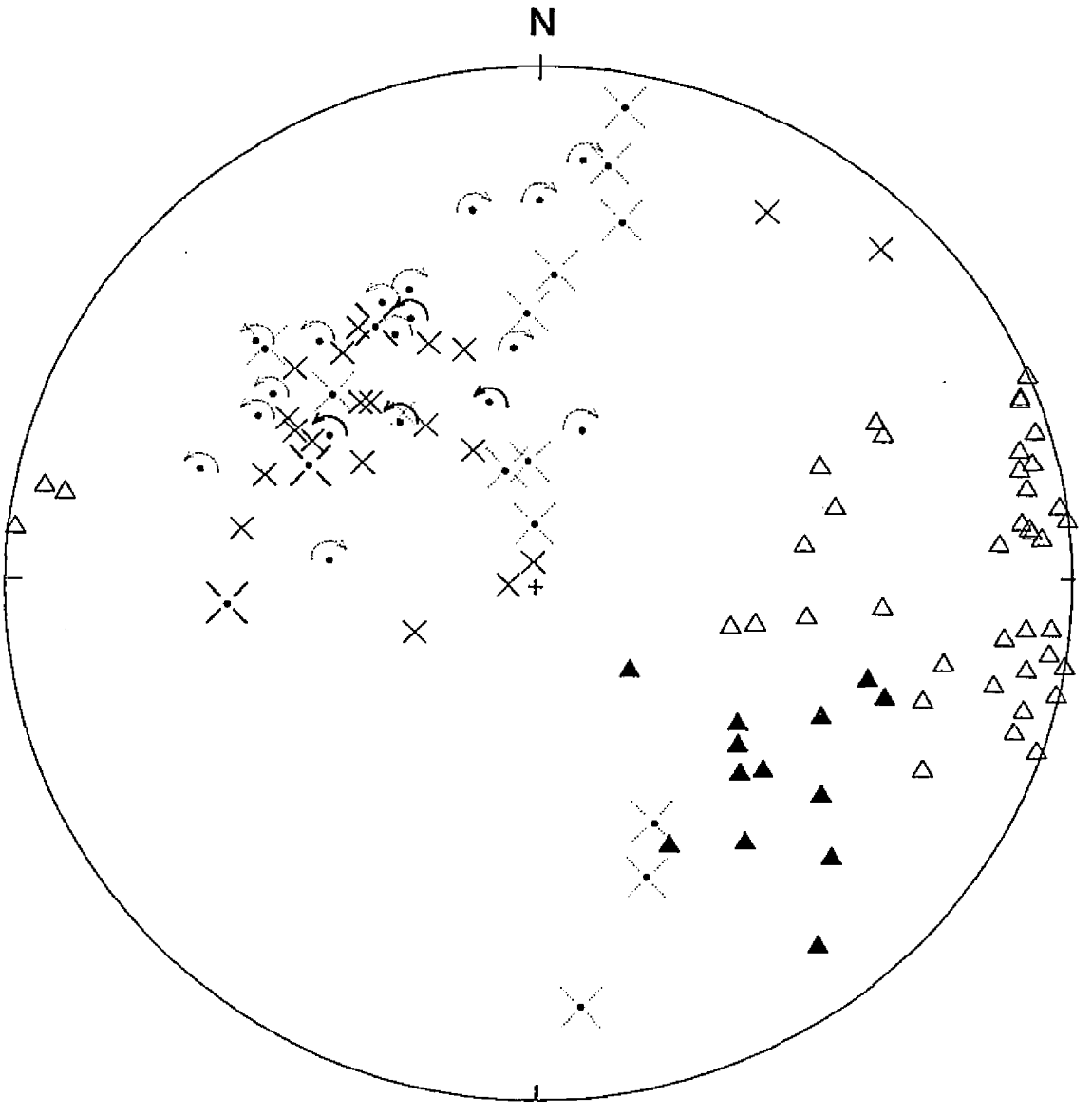

	Poles to hinge surfaces	Hinge lines showing rotation sense		Hinge lines indistinct rotation sense	Intersection of S_1 and S_2 foliations
F_2	△	↷	↷	×	×
F_3	▲	↶	↷	×	

Fig. 39. Structure on the north-south striking limb of the Pound Ridge antiform.

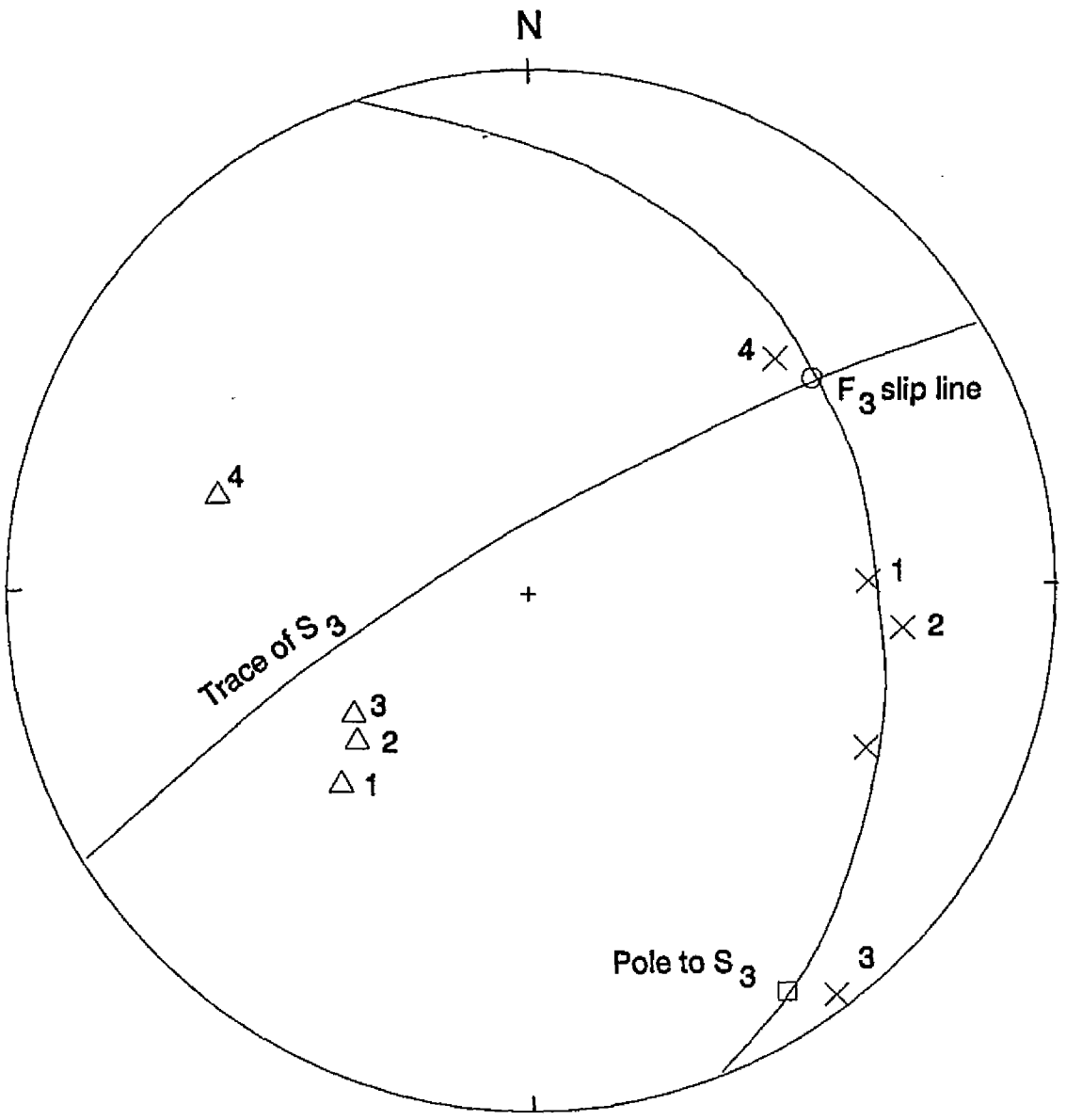

× F_2 hinge lines

△ Poles to F_2 hinge surfaces

Fig. 40. Slip line determination for F_3 folds at a site in the northwest corner of study area. See text for discussion.

port direction by the two great circles on Fig. 33B. The F_2 slip lines might, conceivably, lie in the same plane as the "F_3 transport direction" from Fig. 40, as would be expected.

Correlative deformation. "F_4" folds of the Croton Falls quadrangle are similar stylistically to Peach Lake F_3 folds, and the two fold sets deform correlative older folds. The hinge surfaces of these two fold sets also have parallel strikes. However, the dips of the hinge surfaces differ by about 80°; hinge surfaces of the Croton Falls "F_4" folds dip moderately towards the southeast. The possibility that the study area F_3 and the Croton Falls "F_4" are genetically related, conjugate fold sets should be considered in future investigations.

D_3 DEFORMATION: SUMMARY AND DISCUSSION. The F_3 Pound Ridge antiform, an open fold defined by a broad arc of F_2 hinge surfaces, is the most prominent structure in the study area. F_3 hinge surfaces, on average, strike to the northeast and dip moderately towards the northwest. An S_3 crenulation cleavage, with upper-amphibolite facies mineral assemblages, is locally developed. F_3 transport direction appears to plunge towards the northeast (Fig. 40). The "F_4" folds of the Croton Falls quadrangle are possibly correlative with study area F_3 folds.

D_4 DEFORMATION

F_4 FOLDING AND D_4 SHEARING. Through most of the study area, S_1 foliation, F_2 hinge surfaces, and F_3 hinge surfaces all display coordinated swings between steep and shallow dips, with steep to moderate dips predominating in most areas (Plates I and V; Figs. 38 and 39). This interplay of steep and shallow attitudes is attributed, in large part, to D_4 deformation.

The alternation of steep and shallow dips occurs at several scales. The largest area dominated by shallow dips is about one kilometer across; it is located west of the F_2 Shadow Lake

anticline (Plate IV). There are also several regions, each a few hundred meters across, which are characterized by shallow dips; they occur in Ward Pound Ridge County Park and on Ridgebury Mountain (Plate III). Outcrop-scale F_4 folds occur in the regions of steep dip that surround the domains of shallow foliation.

Steeply dipping fabrics are deformed around a spaced, shallow-dipping slip cleavage (S_4) in outcrop-scale F_4 folds. The hinge surfaces of the F_4 folds are spaced from several centimeters up to several meters apart. Interlimb angles on F_4 folds range between ~50° and ~120° (averaging near 90°), depending on the original attitude of the foliation and the amount of shear strain on S_4 cleavages.

Typically, steeply-dipping foliations are rotated towards moderate, and then to shallow dips as S_4 slip zones are approached. This style of deformation results in a nearly radial distribution of poles to foliations on an equal-area net. Fig. 41 illustrates this pattern for F_4 folds superimposed on northwest-striking foliations.

S_4 foliation is generally expressed as a locally-developed rock cleavage (Fig. 42A). Biotite is aligned parallel to S_4 in some folds, and small quartz-feldspar leucosomes may occur in an axial-planar orientation. There is no evident retrogression of older K-feldspar-sillimanite grade fabrics related to F_4 folding.

The upper portions of F_4 folds are generally displaced towards the southeast relative to lower portions (Fig. 42A). As a result, sets of F_4 folds resemble sets of stairs, which "mount up" towards the south or east. The opposite shear sense ("stairs" mounting to the north or west) is observed at a few localities, as are some symmetric recumbent folds (Fig. 42B and C).

INTERPRETATION OF D_4/F_4 DEFORMATION. F_4 is considered to be an episode of recumbent folding (rather than simply low-angle faulting) on account of the apparent reversals of shear sense. However, the greater abundance of the "stairs mounting to the south/ east" sense suggests differential displacement. If so, then an upper block evidently moved southeastwards

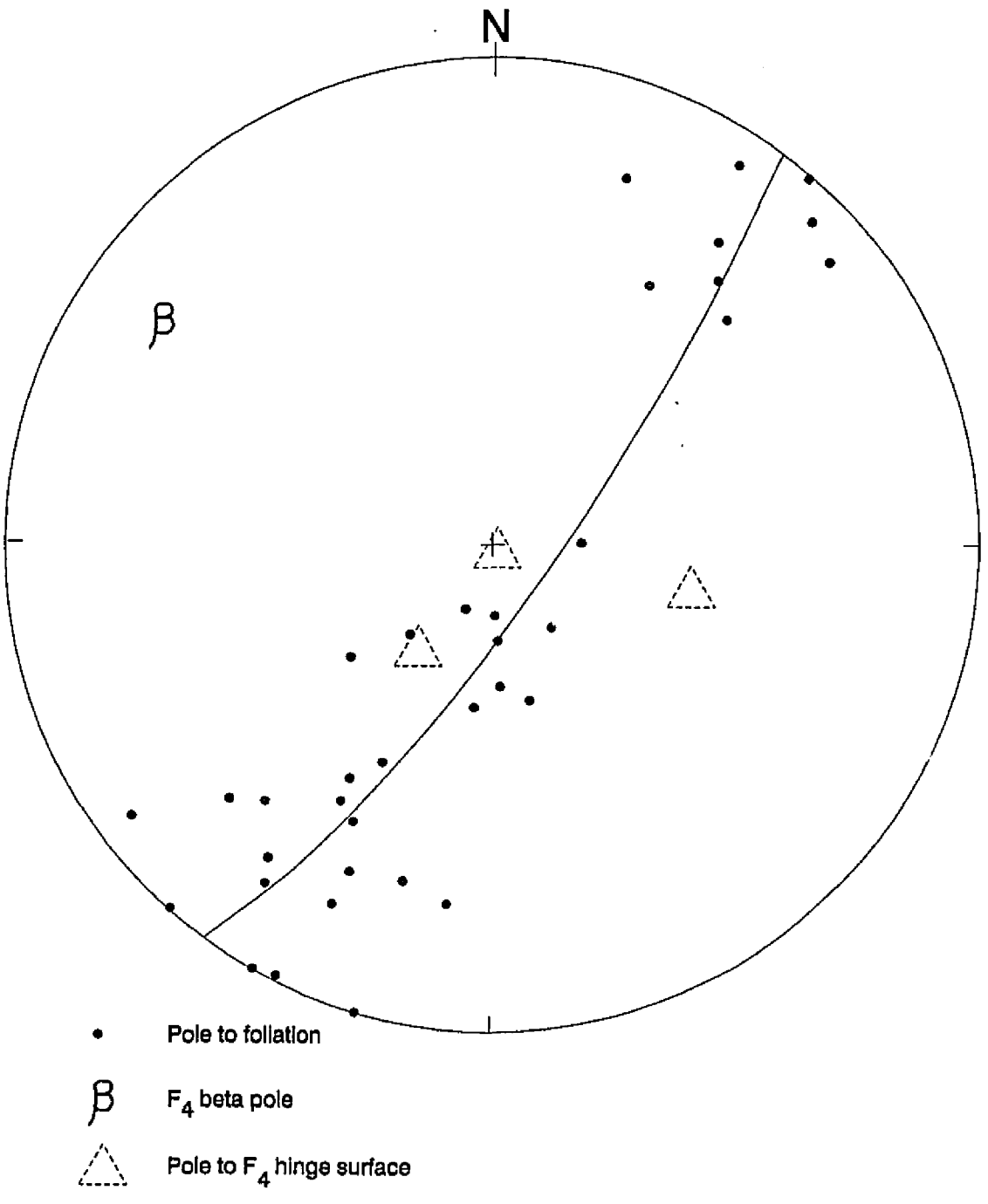

Fig. 41. F_4 folding on the northwest-striking limb of the Pound Ridge antiform.

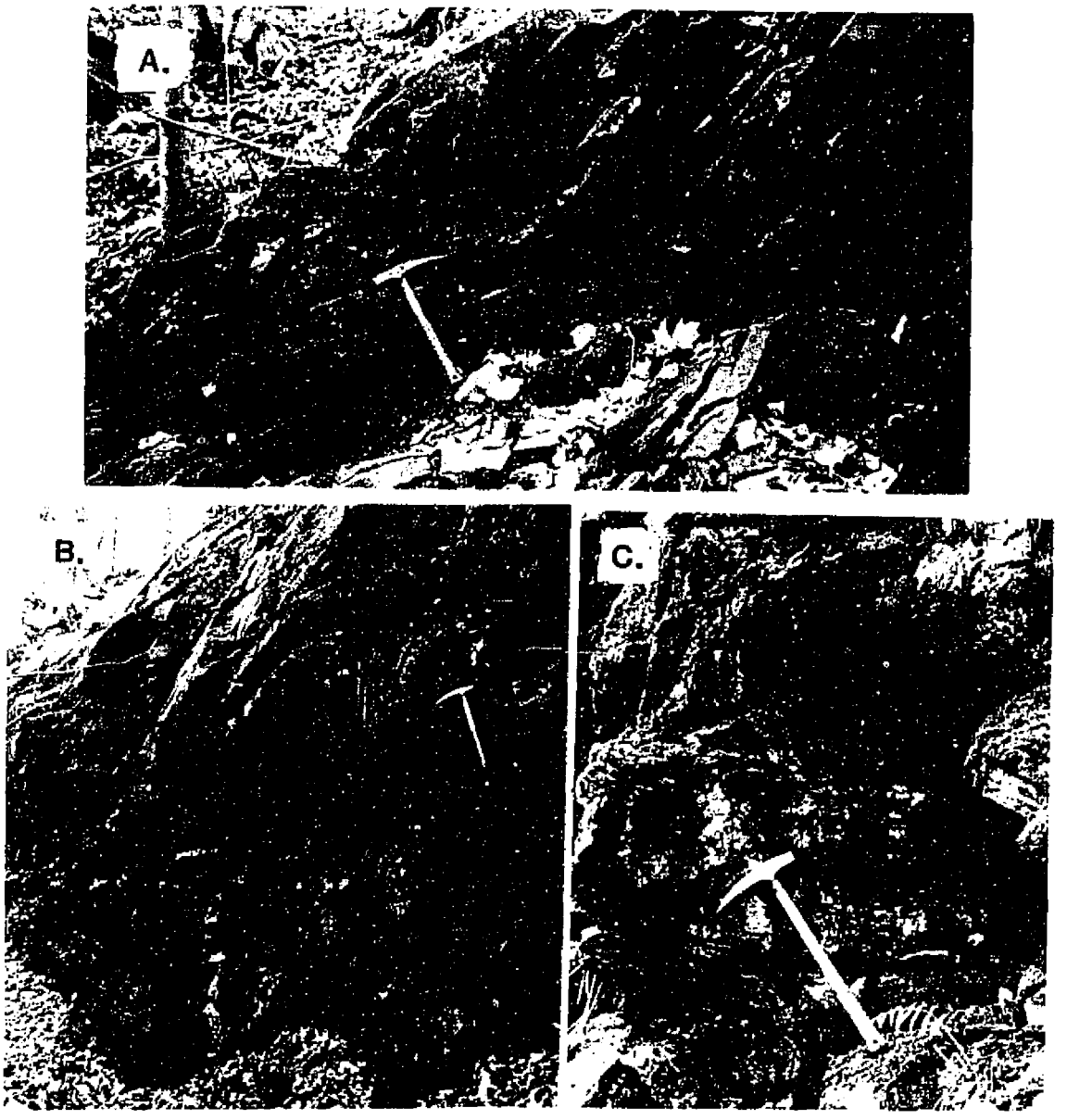

Fig. 42. D_4 structures in a small quarry off Mark Mead Road. Rocks belong to the Ned Mountain Formation Volcaniclastic Member.

(A) Shallow-dipping D_4 slip zone. Upper block is displaced towards the south. Hammer is 33 centimeters long.

(B) Open F_4 folding at two scales: warping at outcrop scale, and (at center of photo) small recumbent folds. Hammer (40 centimeters long) lies on pod of ultramafic rock (outlined).

(C) Close-up of the small recumbent folds in (B). Rocks are amphibolite and layered quartzo-feldspathic gneiss.

relative to a lower block.

Near-horizontal F_4 offset was superimposed on reclined F_3 structures, indicating a shift in deformation style. Recumbent F_4 folds might conceivably relate to either low-angle thrusting or low-angle normal faulting. Both possibilities should be considered during future studies of the Manhattan Prong. However, F_4 folding might be localized; recumbent folds comparable to the Peach Lake quadrangle's F_4 have yet to be observed in the Croton Falls quadrangle, where shallow attitudes are rare.

D_5 DEFORMATION

The "D_5" event recognized by Brock and Mose (1979) in the Croton Falls quadrangle (Fig. 1) was an episode of ductile faulting. "D_5" shear zones strike ~070° and dip steeply to the north. The zones truncate upper-amphibolite grade "F_4" folds and crinkles. Middle-amphibolite facies mineral assemblages (kyanite + staurolite) are developed in the "D_5" zones. The zones are cut, in turn, by tourmalinized fractures related to D_6.

Shear zones similar to the Croton Falls "D_5" have not been recognized in the study area. D_5 shearing may be restricted to certain localities in the Croton Falls quadrangle. Nevertheless, as explained earlier, the "D_5" slot is left vacant in this study, so that the distinctive deformation related to the next event may be assigned the same number (D_6) it bears in the Croton Falls quadrangle.

D_6 DEFORMATION

D_6 was a important deformational event throughout (at a minimum) the eastern Manhattan Prong. It resulted in substantial modification of preexisting geologic structures in parts of the study area. D_6 ductile shear was superimposed, in an extremely heterogeneous manner, on the complex geometries produced by F_1 through F_4 folding. Given the multifarious character of the resulting structures, it is not surprising that D_6 escaped recognition until recently (Brock and Brueckner, 1978; Brock and Brock, 1985a and b).

D_6 deformation in the study area is largely, though not entirely, concentrated in the shear zones delineated on Plate I. The most important D_6 shear zone in the Peach Lake quadrangle is the Turkey Hill fault (Plate IV), which makes a broad swath in the west.

Turkey Hill fault zone. The east-west striking limb of the Pound Ridge antiform is abruptly rotated counter-clockwise (towards a northeasterly strike) as it approaches the Turkey Hill fault (Plate 1). The rotated attitude is subparallel to the hinge surface of the Pound Ridge antiform; as a result, the gross map pattern gives the misleading impression of a large isoclinal fold (see, e.g., Scotford, 1956; Brandon, 1981). F_3 folds, however, are not related to this apparent western "limb", but are themselves rotated. Very steep F_3 hinge surfaces located adjacent to the Turkey Hill fault (and its extensions) tend to have anomalously easterly- or northerly-striking hinge surfaces (Plate I and Fig. 38), rather than the "limb"-parallel northeasterly strike. No definite F_3 folds have been identified within the fault zone.

The Turkey Hill fault is about three kilometers wide in the central Peach Lake quadrangle. Within this fault zone, many small dikes of tourmaline-bearing, two-mica granite and pegmatite are present. Host rocks near the granites are generally retrogressively metamorphosed (Fig. 43). Former K-feldspar-sillimanite assemblages are commonly replaced by coarse-grained muscovite, kyanite, staurolite, and garnet. Retrogression was evidently largely controlled by granite-derived

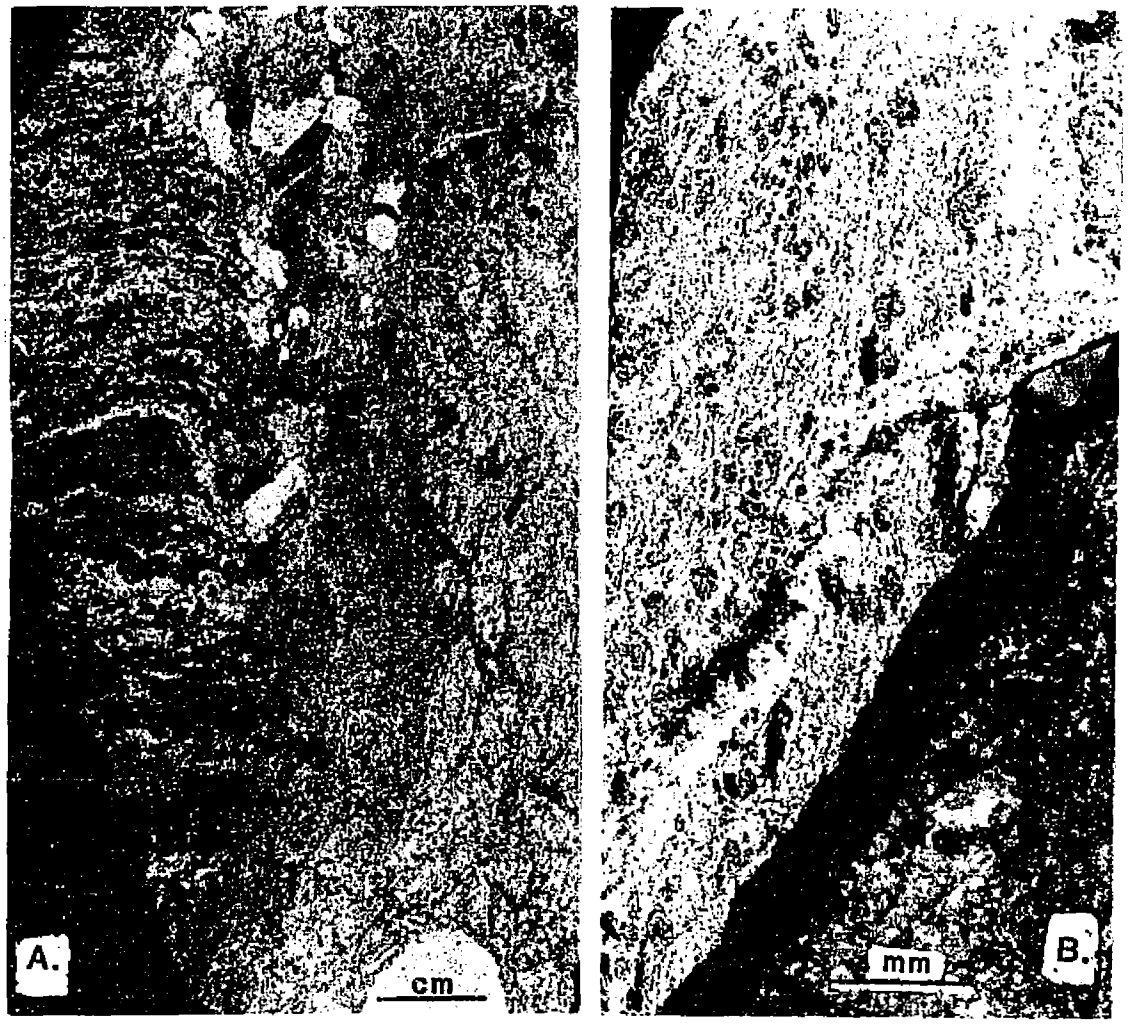

Fig. 43. Syn-D_6 granites cross-cutting foliation in retrograded Manhattan Schist, Turkey Hill fault zone.

(A) Host schist has been recrystallized to a muscovite-garnet-quartz-biotite-plagioclase assemblage. S_6 cleavage in dike (an albitic pegmatite), defined by muscovite and quartz ribbons, is aligned parallel to dike-host contact (and to length of photograph). Plagioclase appears white. Specimen #1125, easternmost Croton Falls quadrangle (Plate III).

(B) Tourmaline (black) introduced into host schist along granite-filled fracture. Host is a muscovite-garnet schist. Specimen #2673.

fluids. Where two-mica granites are closely spaced, metapelites and metawackes are nearly completely recrystallized, and sillimanite may survive only as inclusions in garnet. In apparently "drier" regions, where few granites are present, alteration (principally to muscovite and chlorite) is limited and the rocks retain more of the original minerals. The two-mica granites and the metamorphism associated with them clearly post-date the upper-amphibolite to granulite-facies conditions that accompanied D_1 to D_4 deformation.

The contacts of these granite dikes are structurally controlled. They generally dip moderately to the west (Fig. 44). Tourmalinized fractures (some with thin granite "filling", Fig. 43B) tend to follow the same orientation (Fig. 44).

The granites commonly display a well-developed, moderately dipping rock cleavage and/or a biotite/muscovite foliation parallel to their contacts (Fig. 43A, 44). A steeply-dipping slip cleavage occurs in some granites (Fig. 44). Quartz rods locally define a down-dip stretching lineation. Rarely, a C-S texture is developed (Fig. 45); when present, the slip-related ("C") cleavage dips more steeply than the shortening-related cleavage ("S"). In similar fashion, slip cleavages which cut the granites are generally steeper than foliations in the granites (Fig. 44).

The relationships between slip cleavages and foliations in the granites, together with the down-dip stretching lineation, indicate that offset on the Turkey Hill fault was dominantly normal. The west wall of the fault zone moved down relative to the east. There are few places where offset can be directly observed; however, the west-side down displacement of a granite dike can be seen on the northwest-side of the intersection of Routes 116 and 310 (Plate III), behind some small municipal buildings. A near-vertical slip cleavage and a more moderately-dipping foliation are both present at this locality (Fig. 46).

Attitudes of most dike contacts, tourmalinized fractures, and cleavages or foliations in the granites are subparallel (Fig. 44). The granites are inferred to have intruded syntectonically, preferentially following shortening-related cleavages. Deformation must have continued after solidification of the granites at least locally, in order to produce the rare C-S fabrics. Slickensides

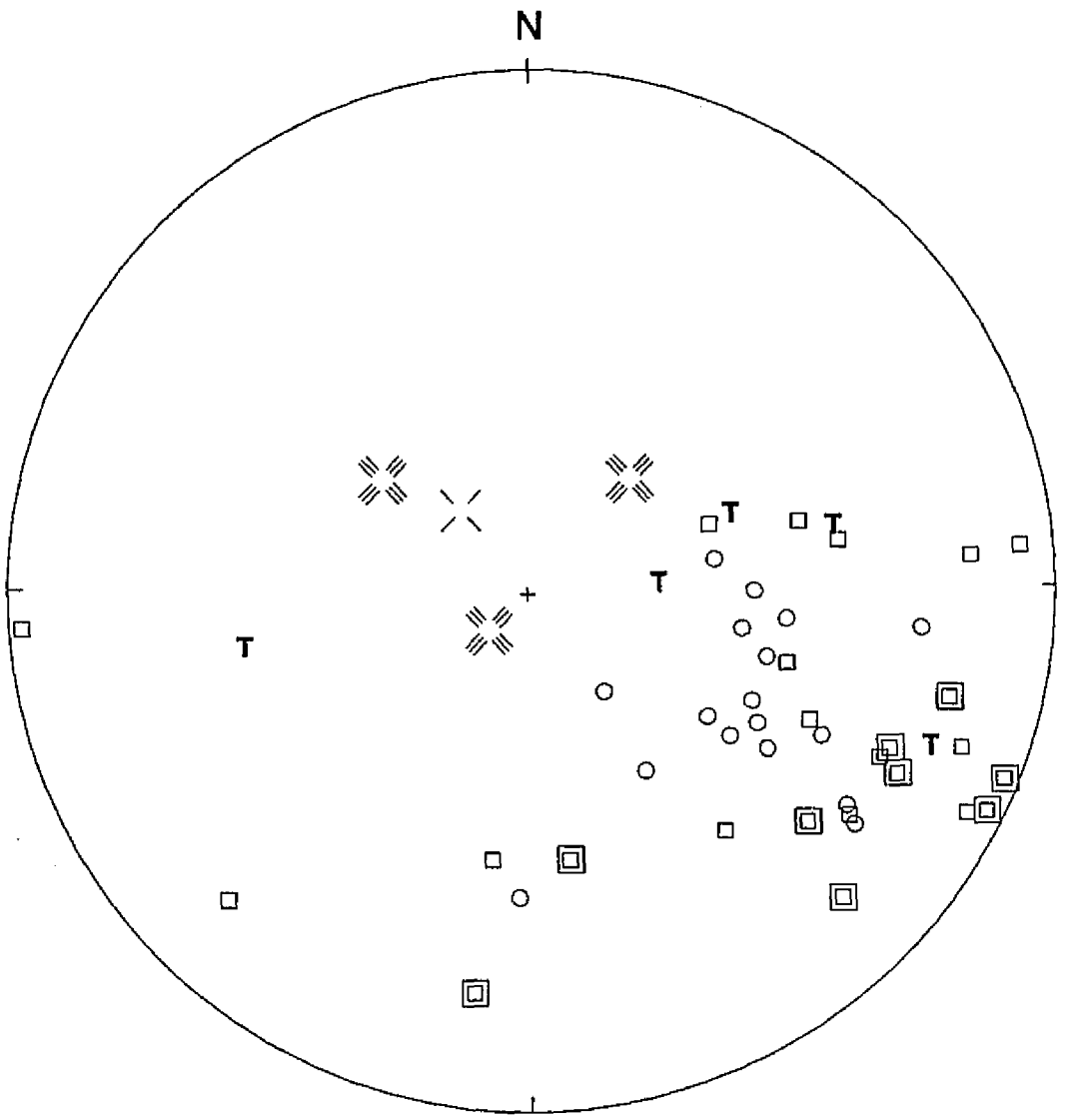

○ Granite contact

T Tourmalinized fracture

□ Fracture cleavage/ muscovite foliation in tourmaline granite

Slip cleavage

Quartz rods

Lineation in slickenside

Fig. 44. Features relating to D_6 deformation and the D_6 tourmaline granite suite, Turkey Hill fault zone.

Fig. 45. "C-S" fabric in granite from the Turkey Hill fault zone, and inferred shear sense. Black spots are tourmaline; penny provides scale. Specimen #1092. Collection site is shown in Fig. 46, below.

Fig. 46. Sheared granite dikes at the intersection of Routes 116 and 310, Turkey Hill fault zone. The steeply-dipping S_6 slip cleavage (S.C.) and more moderately-dipping foliation (F) are highlighted. Offset is down towards the northwest (right).

also occur at a few localities. They are oriented subparallel to stretching lineations (Fig. 44), and thus (like the C-S fabrics) imply continuity of deformation during cooling.

D_6 deformation and related metamorphism modified the textures as well as mineralogies of country rocks in the Turkey Hill fault. Retrograded ("wet") schists are generally coarse-grained and have large, euhedral porphyroblasts of garnet; muscovite grains mimic the S_1 fabric and, to casual inspection, appear "deformed" by old folds. Grain-size reduction is associated with strong D_6 rotation (particularly in "dry" rocks), leading in some cases to a "smeared" appearance. D_6 cleavage, where present, generally consists of sets of discontinuous, close-spaced fractures (visible in Fig. 50, ahead). Scattered grains of sulfide minerals commonly lie on this cleavage, which develops a distinct rusty stain in result. The intersection of older foliation with D_6 cleavage locally results in a strong linear fabric.

Pre-existing fabrics in the host rocks are rotated by variable amounts within the Turkey Hill fault, depending on original attitude and the degree of D_6 shear. Fig. 47 illustrates the relationship between original attitude and D_6 rotation direction. Average attitudes of D_6 slip cleavage and shortening-related cleavage are given, together with an inferred average slip direction: predicted rotation (and map offset) of planar features is shown with respect to these elements.

The east-west to northwest-striking F_2 folds intersected by the Turkey Hill fault are expected to rotate counterclockwise, resulting in apparent sinistral offset. This is the observed map pattern (Plate I). A typical, moderately northwest-dipping F_3 hinge surface should be rotated closer to the D_6 shear plane, perhaps steepening slightly but changing little in strike. Steep S_3 surfaces may be rotated either clockwise or counterclockwise, depending on their precise original orientation. Thus, small amounts of D_6 shear appears to be responsible for the anomalous attitudes of steep F_3 hinge surfaces located <u>near</u> D_6 shear zones (Fig. 38).

The minimum offset on the Turkey Hill fault can be estimated by measuring apparent sinistral displacements. A feature ideally suited for this purpose would 1) outcrop on both boundaries of the fault, 2) have a well-understood geometry within the fault zone, and 3) occur in prox-

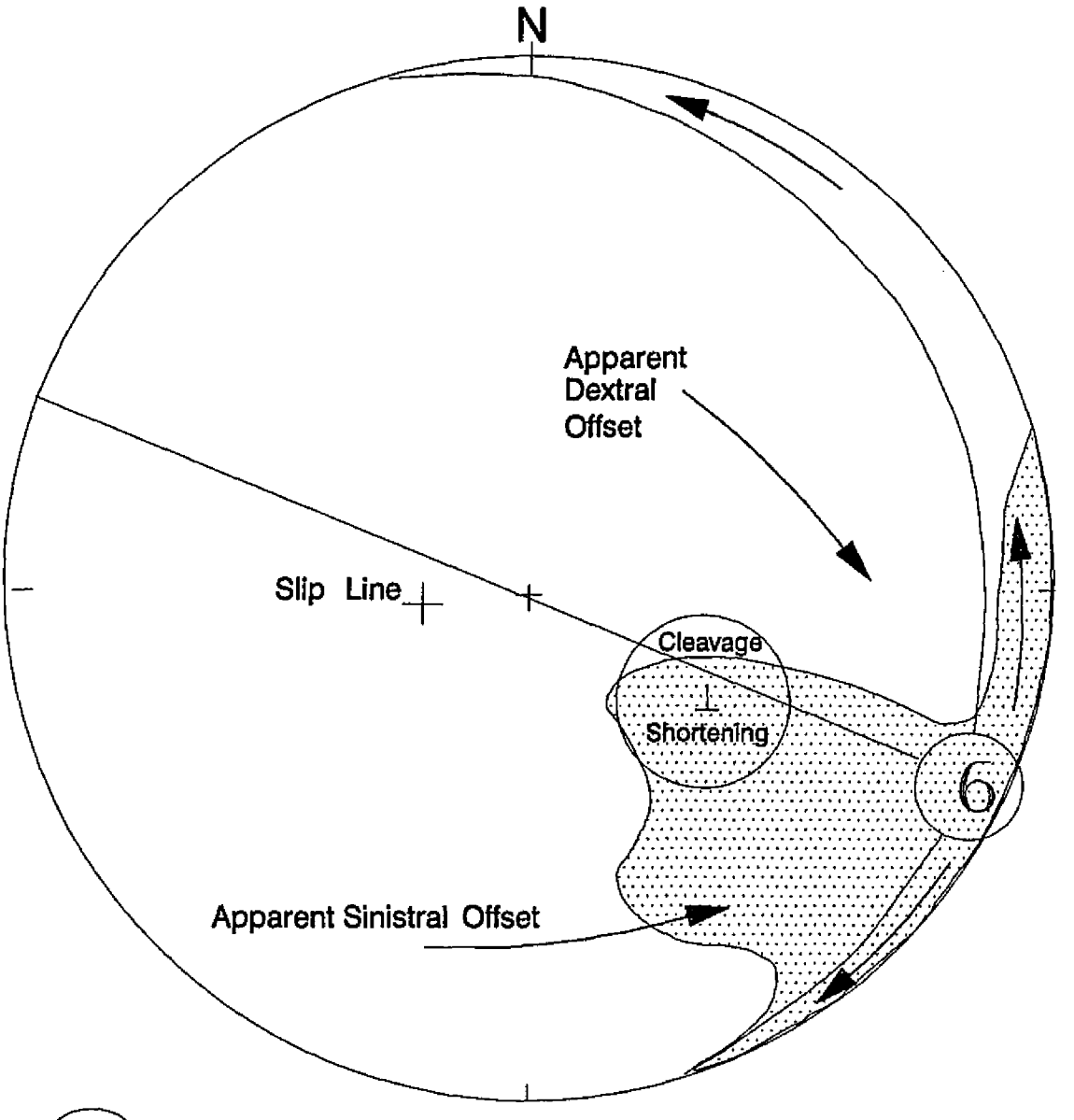

Fig. 47. Model for deformation within the Turkey Hill fault zone, showing predicted senses of rotation and map offset of planar features.

imity to the D_6 structural elements which confirm fault orientation, shear sense, and slip line. No feature fulfills all these requirements; the one which comes closest is the contact between the Inwood Marble and Walloomsac or Manhattan Schist on the southern limb of the Washington Ledges syncline (Plate IV). The apparent sinistral displacement of this contact part-way across the Turkey Hill fault is about 1.6 kilometers. With reasonable assumptions (Inwood Marble/Schist contact dipping 60° to the north on average, D_6 fault dipping 75° with movement down-dip), fault offset is estimated to be on the order of 2.9 kilometers.

Ridgefield and Naraneka fault zones. D_6 deformation occurs at a number of localities in addition to the Turkey Hill fault. The two next most prominent D_6 shear zones in the study area are the Ridgefield and Naraneka faults (Plate V). A number of small D_6 shear zones are also present. Some small D_6 shear zones overprint zones of strong F_3 shear, whose orientations predispose them to reactivation. A small D_6 shear zone located in the hinge region of an intermediate-scale F_3 fold in the east-central Peach Lake quadrangle (about one kilometer northwest of Ridgefield) illustrates this phenomenon.

The Calc-Silicate Member of the Ned Mountain Formation is juxtaposed against several other stratigraphic units along the Ridgefield fault (southeastern Peach Lake quadrangle; Plates I and V). The fault truncates F_1, F_2, and F_3 folds on map scale. South of the study area, in the Pound Ridge quadrangle, Scotford (1956), Prucha, Scotford, and Sneider (1968), and Alavi (1976) recognized shearing that appears to be related to the Ridgefield fault.

Outcrop is poor along the Ridgefield fault zone, but several D_6 characteristics can be recognized. A few small dikes of two-mica or muscovite granite are present on or near the fault. Late muscovite is moderately abundant, both in the Walloomsac Schist (to the west of the fault), and in the Siscowit Granite (to the east). Other forms of retrogressive D_6 metamorphism, discussed later, are evident in nearby calc-silicate rocks and marbles.

Cross-cutting, discontinuous D_6 cleavages are present in some places. In the Siscowit

Granite, these cleavages are defined by concentrations of aligned, fine-grained muscovite. Regional foliation within the fault generally dips moderately towards the northwest, apparently reflecting rotation towards S_6 attitudes. Fabrics in some granofelsic rocks show reduction of grain size.

The boundaries of the Ridgefield fault zone given on Plates I and IV have been primarily determined by detectable map-scale offset. Scattered evidence of D_6-related metamorphism and localized D_6 cleavages occur more than one kilometer beyond these boundaries. Diffuse edges appear to be characteristic of the larger D_6 fault zones.

The few D_6 muscovite granites exposed near the Ridgefield fault lack distinct shear fabrics, and the texture of the older Siscowit Granite is dominated by a pre-existing foliation. No direct evidence on shear sense is available for the Ridgefield fault. A normal sense is inferred by the similarities between it and other D_6 shear zones.

The Naraneka fault extends from the shore of Lake Naraneka northwards, near the northeastern boundary of the Peach Lake map sheet (Plate I). Outcrop is abundant in this area, which is largely underlain by metawackes with cordierite-K-feldspar-garnet or K-feldspar-sillimanite mineral assemblages.

The Naraneka fault contains several narrow D_6 shear zones, which are mostly less than one meter in width. They cross-cut F_2 and F_3 folds. The shear zones are steeply west-dipping, similar to the Turkey Hill fault but slightly more northerly in strike (averaging around 012°). The west sides of these shear zones moved down (Fig. 48).

Characteristic D_6 intrusive activity and remetamorphism are in evidence in the Naraneka fault. Small bodies of muscovite granite are present. Near them, host metawacke is locally transformed into a muscovite-chlorite-biotite-garnet schist. Chlorite + muscovite assemblages also occur in parts of the shear zone removed from muscovite granites.

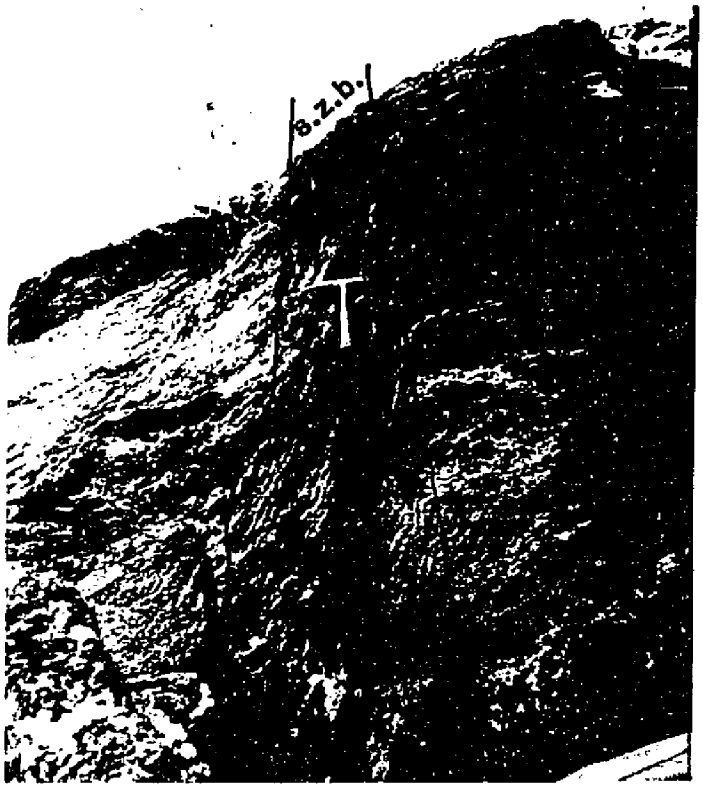

Fig. 48. Shear zone in the Naraneka fault, near the north shore of Lake Naraneka. High-grade gneisses of the Manhattan Schist have been retrograded to muscovite- and chlorite-rich schist within this shear zone. Approximate shear zone boundaries (s.z.b.) are outlined. Offset is down to the west (left).

EN ECHELON D_6 SHEAR ZONES. The Turkey Hill and Ridgefield faults seem to belong to an en echelon series (Fig. 49): in the Croton Falls quadrangle, the boundary between the Highlands Gneiss and Manhattan Prong is marked by another major shear zone which has all the characteristics of a D_6 fault.

D_6 shearing is also present on several of the transects shown on Plate II. On transect H-H', for instance, dikes of tourmaline granite intrude parallel to S_6 cleavage, cross-cutting older layering and foliation (Fig. 50A), as they do in the Turkey Hill fault. S_6 cleavage in the host rock is close-spaced and discontinuous; a prominent down-dip lineation is present (Fig. 50B). A fainter D_6 foliation occurs in the granite dike (Fig. 50B). The coarser-grained border of the granite dike shows little cleavage.

Dikes of two-mica, tourmaline granite, enveloped by retrogressive metamorphic aureoles, and associated with shearing, are found in zones scattered through most of the Manhattan Prong. This distinctive suite of common features makes it possible to recognize D_6 shear zones across the region. The special characteristics of the D_6 granites and retrograde metamorphism have only been touched on so far; they will be discussed in greater detail in later sections of this thesis.

D_6 SHEARING: SUMMARY AND DISCUSSION. D_6 is a regionally important deformational event. D_6 deformation in the study area occurred primarily in the Turkey Hill, Ridgefield, and Naraneka fault zones. D_6 displacement was normal; slip occurred on northeast-striking planes, with the west side down. The amount of displacement within the largest D_6 shear zone, the Turkey Hill fault, can be estimated from map offset of planar features. The estimate of the minimum displacement obtained this way is ~2.9 kilometers.

D_6 deformation was accompanied by the intrusion of a suite of two-mica, tourmaline-bearing granites. The contacts of these granites are oriented parallel to D_6 cleavages, and the granites are commonly cut by D_6 foliation. Retrogressive, greenschist- to middle amphibolite-facies metamorphic aureoles generally envelope the granites.

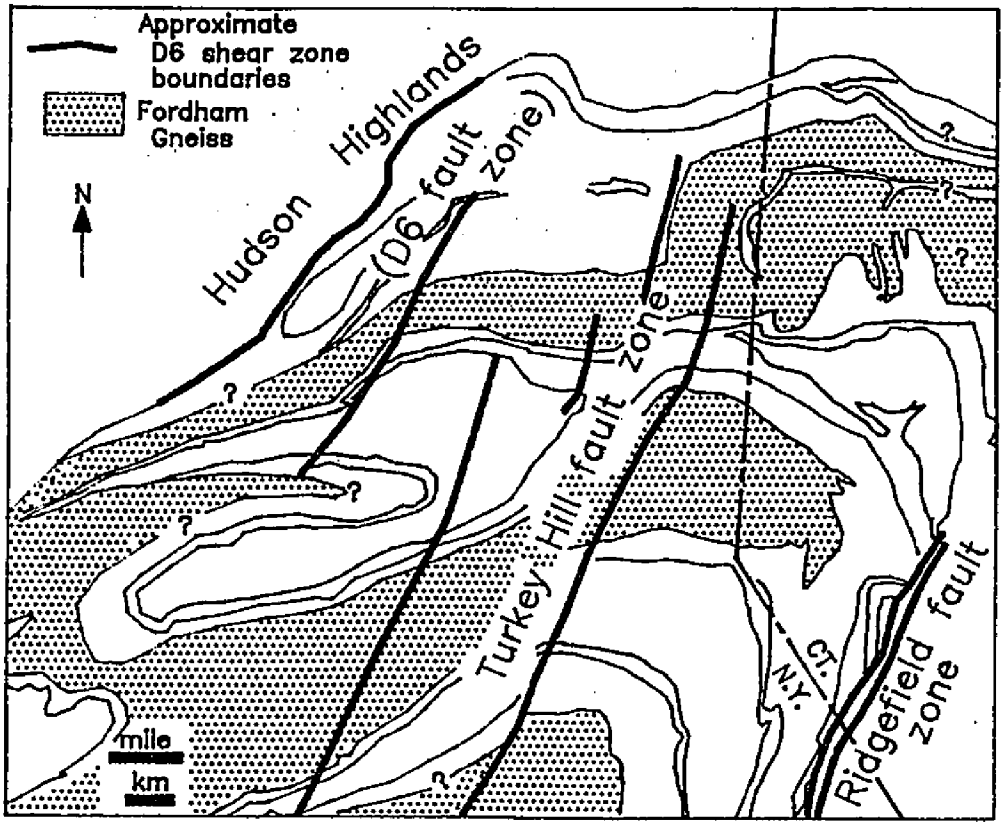

Fig. 49. Major D6 shear zones in the northeastern Manhattan Prong.

Fig. 50. (A) Dike of white syn-D_6 granite (whose contacts are parallel to outcrop surface) truncating layering in the Fordham Gneiss. Rocks of the Fordham display a S_6 cleavage roughly parallel to the dike contacts. Transect H-H', Croton Falls quadrangle.

(B) Close-up of contact between the granite shown above and the Fordham Gneiss. The Fordham Gneiss has broken on the close-spaced S_6 cleavage; the intersection of older foliation and the cleavage is marked by a pronouced mineral lineation. The dike has a planar fabric, roughly parallel to the contact, defined by micas. Tourmaline (t) occurs in the coarse-grained zone on the dike's surface.

The normal offset and the northeast-striking attitude of the D_6 shear zones imply northwest-southeast directed extension. Data from other D_6 shear zones, outside the study area, are generally comparable to those from the Turkey Hill fault, but D_6 displacement appears to have a strike-slip component in some places.

D_7 DEFORMATION

EVIDENCE FOR LATE THRUST FAULTING. The D_6 two-mica granites and their retrogressive aureoles are locally cut by thrust-related fabrics that dip moderately or shallowly to the west. For example, a slip cleavage (S_7) with a pronounced down-dip mullion lineation cuts the steeply-dipping S_6 muscovite cleavage of the Naraneka fault. Pre-existing grains of mica and kyanite are rotated into the young cleavage, with the sense of rotation indicative of thrust motion (west-side up). Apophyses of granite adjacent to the late cleavage show C-S fabrics with thrust shear sense (Fig. 51A). Small thrust displacements are visible on some cleavages. This D_7 deformation is concentrated in the Naraneka region into a few shear zones, each generally less than a meter wide; the cumulative displacement associated with these shear zones appears to be quite minor.

The textures of the rocks in D_7 shear zones relate to their pre-D_7 mineralogy. Muscovite-rich schists remain relatively coarse, though somewhat reduced in grain size; micas and quartz in these rocks behaved relatively ductilely. However, D_7 shear zones locally cut the surrounding high-grade gneisses as well as the D_6 muscovite cleavages. With D_7 shearing, K-feldspar-sillimanite-grade gneisses acquired a fine-grained, mylonitic appearance. Relict high-grade minerals show extreme reduction in grain size; for example, in one specimen, biotite grains average ~0.026 millimeters in length.

Growth of new minerals was very limited during D_7. Little, if any, water was evidently

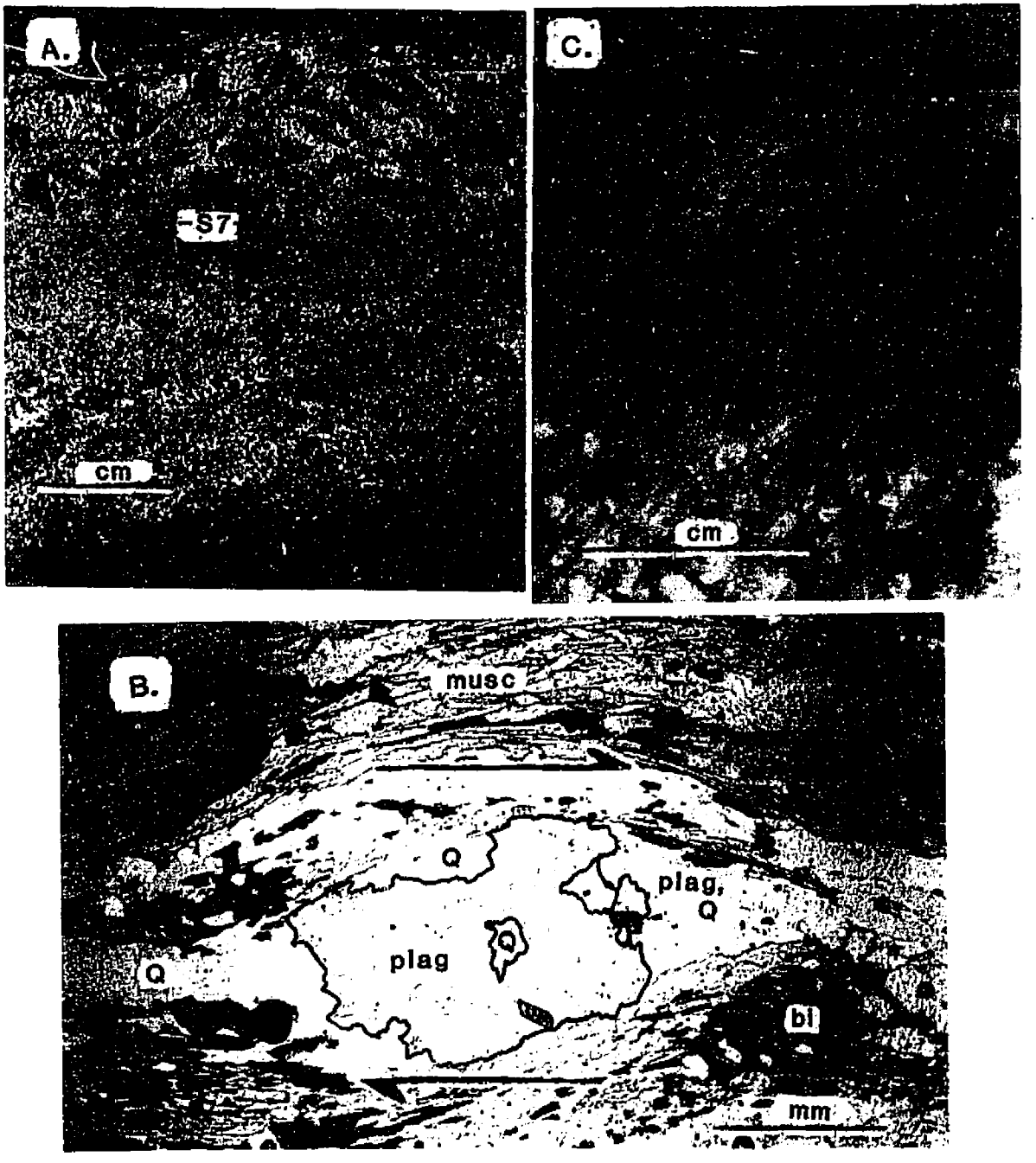

Fig. 51. D_7 fabrics. (A) Manhattan Schist cut by S_7 muscovite cleavages (one highlighted). Fabric in granite indicates that the upper block moved to the east (left). Specimen #1169.

(B) Asymmetric augen structure in muscovite schist of the Ned Mountain Formation Wacke Member. Arrows show inferred shear sense. bi=biotite; musc=muscovite; plag=plagioclase; Q=quartz. Specimen #1095.

(C) Mylonite from a narrow D_7 shear zone in the Fordham Gneiss. Fabric in granite indicates that upper block moved to the east (right). Very small, dark porphyroclasts speckle the grey host rock. Specimen #2520a.

introduced into the rocks during deformation. The low water content of the high-grade gneisses evidently limited syn-D_7 recrystallization.

The Windwing thrust and other D_7 shear zones. North and west of Lake Windwing (Plate III), narrow D_7 mylonite zones that dip from 15° to 40° to the west are fairly common. These shear zones are comparable to the D_7 shear zones found in the Naraneka region in their age relationships, attitudes, fabric development, and nature of offset.

Thrust fabrics are superimposed on D_6 mineral assemblages at a few localities (Fig. 51B), where minerals have undergone a moderate reduction in grain size. Mylonitic fabrics occur where D_7 shear is superimposed on granites (Fig. 51C). Medium- to coarse-grained, high-grade gneisses also locally show extreme reduction in grain size (Figs. 51C and 52).

The Windwing thrust (Plate IV), the most prominent D_7 fault presently known, crops out here. The Windwing thrust brings the Wacke Member of the Ned Mountain Formation in fault contact with the Fordham Gneiss. The Windwing thrust consists of a few fairly close-spaced shear zones (Plate I), each between one or two to perhaps ten meters in width.

A few small slivers of Inwood Marble and Fordham Gneiss outcrop within or adjacent to the Windwing thrust (Plate I), apparently because of displacement by the fault. Foliation in country rock is rotated from steep- or moderate- westwardly dips (which occur about 100 meters from the fault) towards nearly horizontal attitudes, as the thrust is approached. Along the trace of the fault, extremely fine-grained Fordham Gneiss (with small black hornblende porphyroclasts) can be seen in direct contact with the garnetiferous Wacke Member. The Wacke Member here is an anomalously dark, purplish rock (Fig. 52), on account of its minute, well-dispersed grains of biotite.

Significant D_7 shearing is also present near Finch Road (Plate III), in the north-central Peach Lake quadrangle. There, shear occurs in a zone about 400 meters in breadth (Plate I), but is largely concentrated within high-strain subzones, each a few meters across. Mylonitic fabrics are

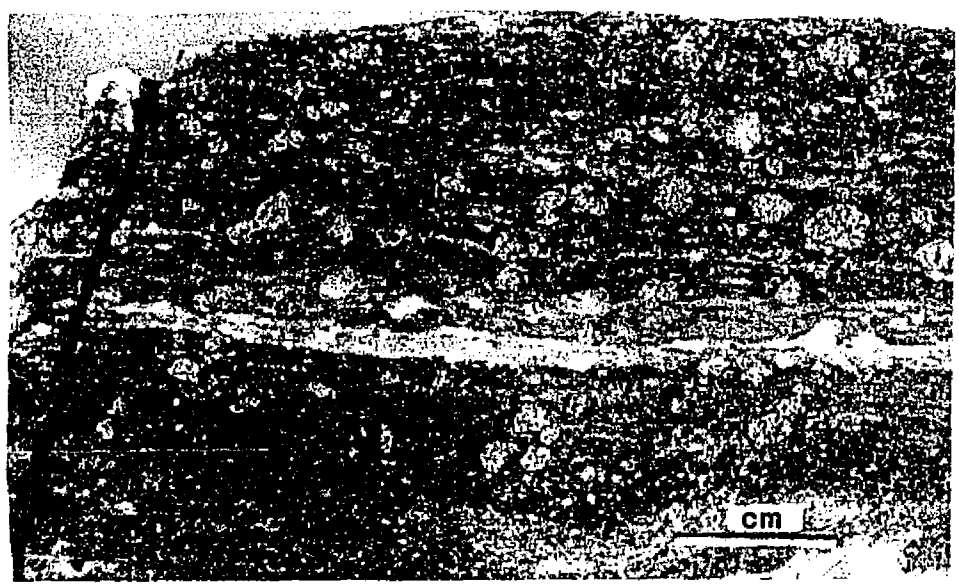

Fig. 52. Very-fine grained D_7 fabric, Windwing thrust. Ned Mountain Formation Wacke Member (reddish grey), with garnet porphyroclasts, is in thrust contact with the Fordham Gneiss (green, with black hornblende porphyroclasts). Specimen #2553.

well developed in the high-strain subzones.

D_7 features are apparently more abundant in the northern Peach Lake quadrangle than in other parts of the study area. This may be, in part, because few older structure in the northern Peach Lake quadrangle have attitudes suitable for reactivation as S_7 shear planes. Where foliations dip moderately to the west, minor D_7 shear may have been accommodated without leaving obvious clues, particularly if the rocks were "wet" and rich in muscovite. One dike of D_6 pegmatite in the Turkey Hill fault zone is cut by a small thrust fault (Fig. 54) that abruptly dies out, recording post-D_6 shortening that might otherwise have gone unnoticed.

Attitudes of D_7 thrust faults and conditions of deformation. Attitudes of D_7 slip cleavages, mullion lineations, and quartz rods from various sites in the study area are shown in Fig. 53. From these data, the average D_7 slip line is estimated to plunge 22° at 284°. Fig. 53 also illustrates the sense of rotation experienced by pre-existing foliations entering D_7 shear zones. All observations are consistent with east-directed thrusting of the overriding block.

The metamorphic conditions prevalent during D_7 deformation are difficult to determine on account of the very limited growth of new minerals. Mylonites developed in the metawackes of Manhattan Schist and Ned Mountain Formation contain syntectonically recrystallized quartz, muscovite, biotite, and chlorite. A hornblende-plagioclase-clinopyroxene assemblage of the Fordham Gneiss is replaced by very fine-grained epidote, biotite, and feldspar in the D_7 shear zone near Finch Road. It appears, therefore, that D_7 thrusting occurred under lower greenschist-facies conditions.

D_7 DEFORMATION: SUMMARY AND DISCUSSION. East-directed thrusting took place on shallow- to moderate-dipping slip surfaces during D_7 deformation. The most prominent D_7 fault is the Windwing thrust, on which the Ned Mountain Formation Wacke Member overthrust the Fordham Gneiss. West-over-east thrusting implies east-west directed shortening

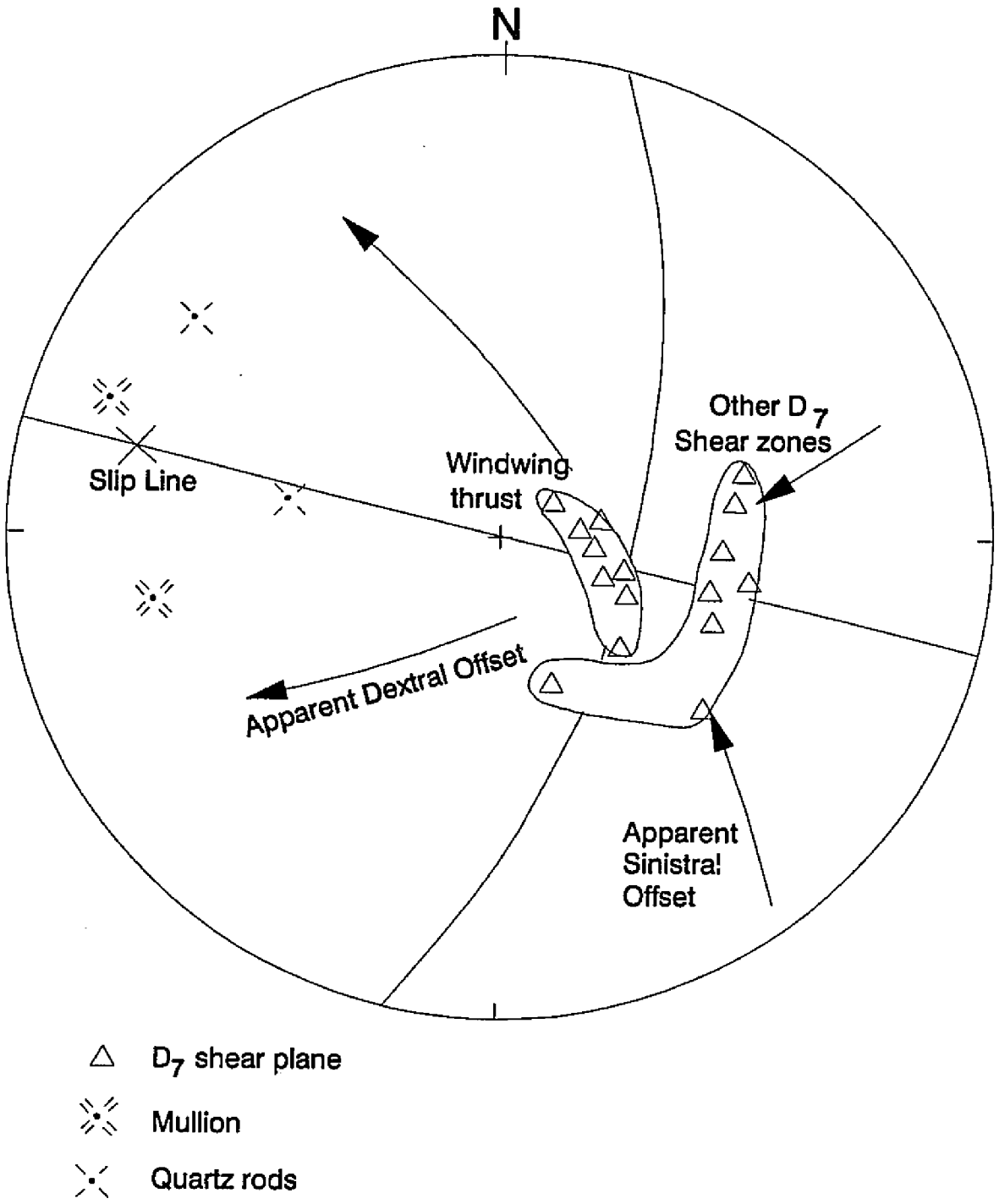

Fig. 53. Attitudes of D_7 shear zones, with sense of rotation (and map offset) of poles to planar features deformed by D_7.

Fig. 54. Zoned dike of syn-D_6 granite pegmatite, offset by small D_7 thrust (highlighted). Dike has inwards-grown grains of feldspar and muscovite, and a quartz core. Hammer head is 18 centimeters long. Specimen #1041 locality, Turkey Hill fault zone.

during D_7.

S_7 cleavages cut D_6 cleavages, granites, and metamorphic aureoles. D_7-age recrystallization was minor, but consistent with greenschist-facies conditions. D_7 shearing commonly resulted in very fine-grained fabrics, particularly where high-grade gneisses were affected. In contrast to D_6 shear zones (which were generally soaked with hydrothermal fluids) D_7 shear zones were fairly dry.

HIGHLANDS BORDER FAULT

Balk (1936), Scotford (1956), and Prucha, Scotford, and Sneider (1968) recognized faulting along the boundary between the Manhattan Prong and the Hudson Highlands. The same interpretation is adopted here: the Highlands Gneiss appears to be in contact with both the Walloomsac Schist and Inwood Marble in the Brewster quadrangle (Plate I), and is therefore in fault contact with the Manhattan Prong. The Highlands border fault, however, is difficult to study due to of the scarcity of outcrop immediately to the south of the Highlands Gneiss.

Minor slickensiding and chloritization are present along the exposed southern edge of the Highlands Gneiss, but do not appear to reflect significant motion. However, a penetrative muscovite cleavage, oriented parallel to the Highlands boundary, occurs in Manhattan Prong rocks that outcrop ~400 meters south of the Highlands Gneiss.

This cleavage is best displayed in an outcrop on the railroad tracks southeast of Sanfords Pond (Plate III). There, the cleavage is very strong and locally results in an extremely fine-grained mylonitic fabric. The cleavage cross-cuts F_3 folds (Plate I). Slickenside lineations on the cleavage plunge gently to the northeast. Asymmetrical K-feldspars in moderately-sheared, oriented specimens indicate dextral (strike-slip) motion.

Shearing of the kind seen at this outcrop probably controls the Highlands-Manhattan

Prong boundary in the central Brewster quadrangle. The exact relative age and the significance of this shearing are uncertain. Its style and metamorphic grade indicate that it postdates the amphibolite-facies, ductile F_4 event, but its relationships to D_6 and D_7 are uncertain.

BRITTLE FAULTING AND FRACTURING

The Spring Valley fault (Plate IV) is marked by a belt of intense fracturing, slickensiding, and chloritization. The nature of motion on the Spring Valley fault is unclear. The slickensides are oriented in every direction, and outcrop is not sufficient to determine how (or even whether) stratigraphic contacts have been offset.

Minor slickensides are encountered at scattered localities across the study area. These slickensides are locally accompanied by fracturing and chloritization. One set of fractures, which strikes ~065° to 085°, is commonly associated with shallow-plunging slickensides. A small dextral strike-slip fault located just south of the Spring Valley fault (Plate I) belongs to this group.

Another set of steep-dipping fractures strikes ~300° to 325°. A post-tectonic lamprophyre dike that crops out in the central Peach Lake quadrangle (Plate I) apparently intruded on a fracture belonging to this set.

ABSOLUTE AGES OF DEFORMATIONAL EVENTS

INTRODUCTION

The ages of deformational events in the Manhattan Prong can be constrained from three directions: from the stratigraphic ages of the affected rock units, from whole-rock radiometric ages of intrusions with known relationships to deformational events, and from K-Ar or $^{40}Ar/^{39}Ar$ mineral ages. The mineral ages are generally thought to record the most recent cooling through specific "closure" temperatures, and thus are expected to reflect the youngest tectonic events.

The youngest stratigraphic unit in the Manhattan Prong, the Walloomsac Schist, is Middle Ordovician in age. F_1 deformation can be no older than this. In some parts of the Manhattan Prong, K-Ar biotite ages range up to ~470 Ma* (Clark and Kulp, 1968; Long and Kulp, 1962) (Fig. 55). These ages indicate that the deformed and metamorphosed rocks had cooled below the "closure" temperature for biotite (~300°C; Harrison, Duncan, and McDougall, 1984) by Late Ordovician time. This early deformation is ascribed to the Taconian orogeny. However, most K-Ar mineral ages in the eastern Manhattan Prong are less than 400 Ma, and some are as young as ~300 Ma (Fig. 55). In recognition of these younger ages, Clark and Kulp (1968) proposed that additional metamorphic events occurred at 360 Ma and 255 Ma. [Please note that the contacts of the Fordham Gneiss shown on Fig. 55 have been based on the Geologic Map of New York (Fisher, Isachsen, and Fisher, 1970), rather than Plate II of this thesis, to facilitate comparison with Clark and Kulp's Fig. 4.]

Four phases of deformation took place under upper-amphibolite to granulite-facies conditions in the study area (F_1 to F_4). No direct measure of the absolute ages of these events is currently available in the Peach Lake quadrangle. However, a quartz-garnet-sillimanite segregation

* All K-Ar ages given by previous workers have been recalculated using the decay constants recommended by Steiger and Jäger (1977). (These constants are given on Table 13).

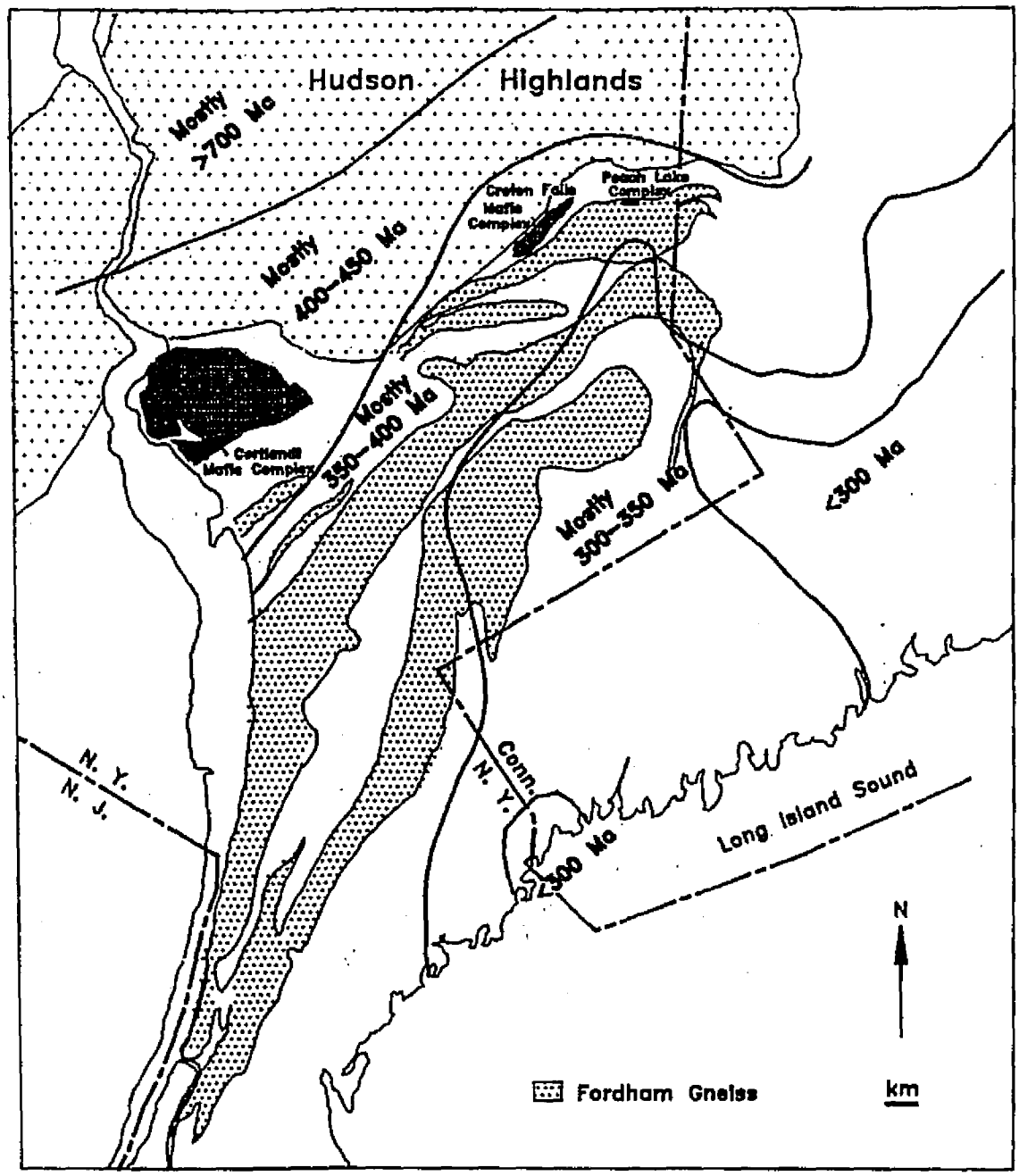

Fig. 55. Distribution of K–Ar and ^{40}Ar–^{39}Ar mica ages in the Manhattan Prong and surrounding area. Sources: Long and Kulp (1962); Clark and Kulp (1968); Dallmeyer (1975); Dallmeyer and Sutter (1976); and new data. The contacts shown here for the Fordham Gneiss are based solely on Fisher, Isachsen, and Rickard (1970), and do not agree with the contacts proposed on Plate II or Fig. 1.

associated with the Croton Falls "F_4" has given a Middle to Late Ordovician Rb-Sr whole-rock isochron age (Brock and Brueckner, pers. commun., 1985). The Croton Falls "F_4" is younger than the Peach Lake F_2 and possibly correlative with the Peach Lake F_3. The first three events in the study area (F_1, F_2, F_3) are therefore inferred to be Ordovician in age and attributed to the Taconian orogeny. The fourth event also appears to be associated with (Ordovician?) upper-amphibolite grade metamorphism, but its age is not tightly constrained.

Rb-Sr whole-rock isochron ages from the Croton Falls Granite and from the D_6 tourmaline granites loosely bracket the Croton Falls "D_5" event; "D_5" is probably Devonian, but could be older (Table 12). The absolute age of D_6 deformation can be tightly constrained because of the syntectonic nature of the two-mica tourmaline granites. Rb-Sr whole-rock isochrons obtained on three of these granites, collected from the Croton Falls and Mount Kisco quadrangles, give overlapping Mississippian ages (Brock, Brueckner, and Brock, 1985; Table 12). D_7 deformation postdates the intrusion of the D_6 granite suite, and is therefore Carboniferous in age or younger.

In view of these constraints, only two of the deformational events recognized in the study area (D_6 and D_7) are clearly post-Taconian. Some connection between the post-Taconian argon loss evident on Fig. 55 and D_6 or D_7 deformation (and related metamorphism) appears likely.

One goal of this study has been to better define the relationship between argon loss and D_6/D_7 shearing. Two approaches have been followed: 1) to evaluate the structural and metamorphic context of the sites used in Clark and Kulp's (1968) K-Ar study; and 2) to obtain new K-Ar dates from sites chosen inside D_6 and D_7 shear zones, comparing them with sites where there is not evidence of late shearing. Six new K-Ar ages were obtained, with the help of Professor D. Seidemann and the laboratory at Yale University. Four of the new samples were taken from the Peach Lake quadrangle, one each from the Mount Kisco and Croton Falls quadrangles. Analytical data for the K-Ar determinations are given in Table 13.

TABLE 12. Age Constraints on Deformational Events, Northeastern Manhattan Prong

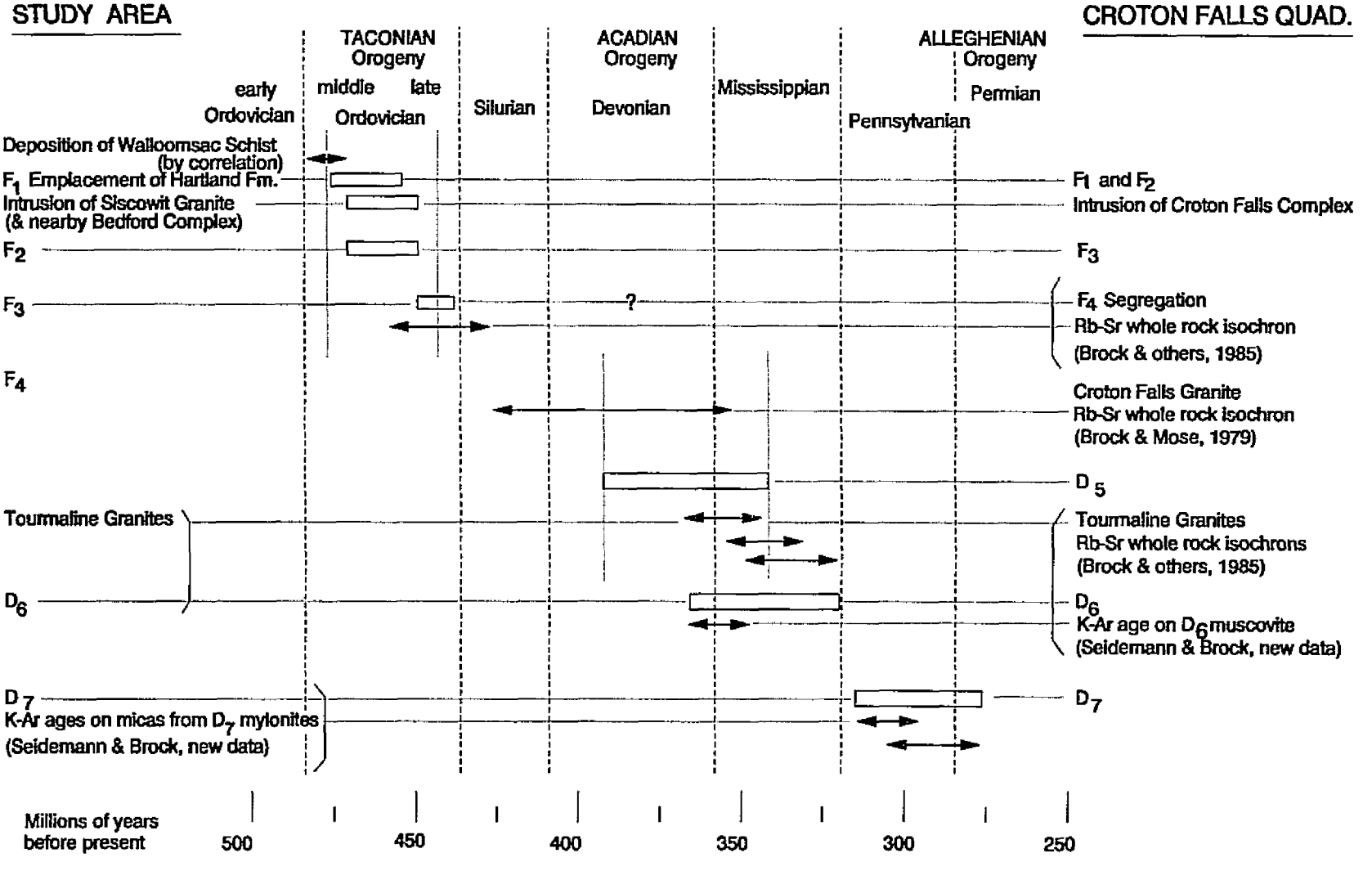

TABLE 13

K–Ar Analytical Data

Sample		Weight Percent K	Radiogenic Ar STP/gm	Percent Atmospheric Argon	Date (Ma) $\pm 1\sigma$ error
K1	(Muscovite)	6.76	99.0×10^{-6}	26	343±7
K4	(Muscovite)	7.60	116.9×10^{-6}	5	358±7
K6	(Muscovite)	8.28	108.2×10^{-6}	62	309±8
K8	(Biotite)	5.55	96.0×10^{-6}	10	398±8
K10	(Biotite)	7.57	106.3×10^{-6}	9	330±7
K11	(Biotite)	7.29	90.4×10^{-6}	55	294±7

Analytic procedures are described by Armstrong (1970)

$K\lambda_e = 0.58 \times 10^{-10}/yr$, $K\lambda_\beta = 4.962 \times 10^{-10}/yr$,

$^{40}K/K$ atom % = 0.01167

GEOLOGICAL CONTEXT FOR PUBLISHED K-AR DATA, PEACH LAKE QUADRANGLE

Seven of Clark and Kulp's (1968) sample sites were located within the Peach Lake quadrangle, and six within the study area. Of those sites, three proved to have been collected in or adjacent to major D_6 shear zones. Biotite from the Turkey Hill fault (sample L-1008, Fig. 56) yielded a K-Ar age of 329 Ma. Two samples (L-989 and 988) were collected adjacent to the Ridgefield fault (Fig. 56). Biotite from these samples gave ages of 293 and 343 Ma. These ages are consistent with the inferred Mississippian origin of the D_6 shear zones, and with possible, local, D_7 overprinting.

At sample site L-986, rocks are strongly chloritized. There is evidence nearby of young (though minor) shearing (Plate I). Biotite from this locality gave an age of 350 Ma.

In contrast, two of Clark and Kulp's sample sites were in areas where no young shearing is evident and where Taconian mineral assemblages are well preserved. Biotite from sample L-994 gave the oldest age found in the Peach Lake quadrangle, ~455 Ma. An age of approximately 383 Ma was obtained on biotite L-996, collected south of Ridgebury Mountain.

In summary, the inferred deformational history and the K-Ar mineral ages obtained by Clark and Kulp (1968) are in agreement. Samples collected in or near D_6 and D_7 shear zones give Mississippian or Pennsylvanian mineral ages. Outcrops which display undisturbed Taconian (F_1-F_4) structures and mineral assemblages give the oldest K-Ar mineral ages. Young K-Ar ages can thus be attributed to remetamorphism and deformation during D_6 and D_7.

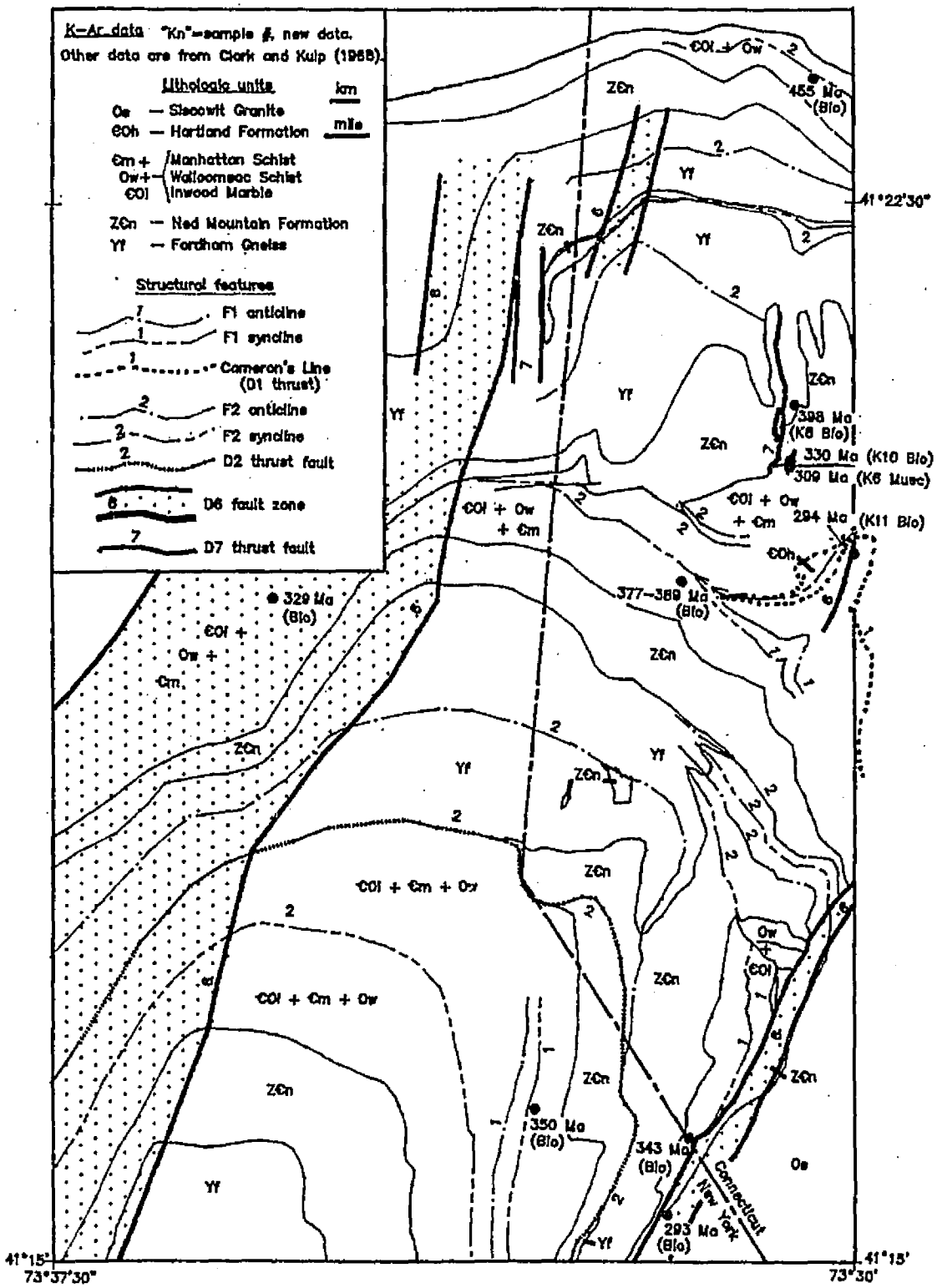

Fig. 56. K–Ar mineral ages in relation to some major structures.

NEW K-AR AGES

The new age determinations uphold the relationship between D_6 and D_7 deformation and K-Ar biotite and muscovite ages. The youngest K-Ar ages (<310 Ma) were obtained on strongly sheared samples from D_7 fault zones. An intermediate age (358±7 Ma) was obtained from a D_6 shear zone. The oldest age (398±8 Ma) came from granulites of the Fordham Gneiss located >100 meters away from any significant young shearing. A 91 million year difference in apparent ages was found among three samples collected within 600 meters of each other. A description of the samples is given in Table 14.

The two samples having the strongest D_7 shear fabrics, K6 and K11, yielded mineral ages of 294±7 Ma (biotite) and 309±8 Ma (muscovite), respectively. Micas in K6 and K11 were thoroughly recrystallized during D_7 shearing (shear textures in specimen #1095, collected at the same site as K6, are shown in Fig. 51B). Two other samples that were collected in or near D_7 shear zones, but which were not penetratively deformed, gave somewhat older mineral ages. K1 consisted of coarse-grained muscovite from a D_7 cleavage that cross-cuts a (muscovite-kyanite-staurolite grade) D_6 shear zone. This muscovite yielded an age of 343±7 Ma. No D_7 shearing is evident in outcrop where K10 was collected, but the shear zone sampled at K6 passes within several meters of the site, and minor D_6 retrogression is present within a few meters. Biotite from K10 yielded a K-Ar age of 330±7 Ma.

Argon loss during D_7 was apparently somewhat erratic. The ~300 Ma dates from K6 and K11 give the best approximation of its age, because micas from these rocks were recrystallized during D_7. Muscovite at K1 originally crystallized during D_6 deformation; the coarse grain size of K1 suggests that D_7 deformation was minor. If 300 Ma is approximately the age of D_7 deformation, K1 muscovite can only have experienced partial argon loss. The 330 Ma age of K10 implies that proximity to a major D_7 shear zone alone may result in partial argon loss from biotite. The implications of these data for the metamorphic history of the region are discussed in a later section.

TABLE 14

Samples Used For K-Ar Age Determinations

K1. (343±7 Ma). Coarse-grained muscovite from a muscovite-biotite-garnet-tourmaline schist. Sample was collected where a S_7 cleavage overprints a D_6 shear zone. Pegmatitic dikes of two-mica, tourmaline-bearing granite at this outcrop are syntectonic with D_6 deformation, and have given a Rb-Sr whole-rock isochron age of 358±9 Ma (Table 12). Location: Roadcut on the east side of Route 684, near the intersection with Beaver Dam Road, at the northern end of the Mount Kisco quadrangle. (Manhattan Schist)

K4. (358±7 Ma). Muscovite from muscovite-biotite-garnet-tourmaline schist. Sample site is within a D_6 shear zone. A small granitic pluton at the same outcrop has yielded a Rb-Sr whole-rock isochron age of 343±9 Ma. Location: behind the shopping center on the southeastern side of the intersection of Route 138 with Route 684, Croton Falls quadrangle. (Hartland Formation)

K6. (309±8 Ma). Muscovite from quartz-muscovite-garnet schist. Strong S_7 fabric development exists at the sample site; if D_7 was "dry", the abundance of muscovite indicates that D_6-related retrogression was present at this site prior to D_7 shearing. (Specimen 1095, illustrated in Fig. 51C, was also collected here). Location: northern shore of Lake Windwing (Fig. 56) (Ned Mountain Formation Wacke Member)

K8. (398±8 Ma). Biotite from a coarse-grained, two-pyroxene granulite-facies gneiss. Structures within ~ 100 meters are Taconian or older, except for a few extremely narrow (<5 cm) D_7 shear zones. Location: 600 meters north of K6 (Fig. 56). (Orthopyroxene gneiss member, Fordham Gneiss)

K10. (330±6 Ma). Coarse biotite from K-feldspar-sillimanite grade metawacke. Structures at the sample site are Taconian (F_2), but the D_7 shear zone sampled at K6 passes within several meters. Location: near northern shore of Lake Windwing (Fig. 56). (Ned Mountain Formation Wacke Member)

K11. (294±6 Ma). Fine-grained biotite from a D_7 mylonite. Mylonite contains a quartz-biotite-chlorite-muscovite-(relict?) garnet mineral assemblage. Gneisses with cordierite-K-feldspar-garnet mineral assemblages outcrop within 20 meters. Location: Pierrepont State Park, on the eastern boundary of the Peach Lake quadrangle (Fig. 56) (Manhattan Schist)

INTRUSIVE ROCKS OF MIDDLE ORDOVICIAN AND YOUNGER AGE

INTRODUCTION

Igneous rocks of a wide array of ages occur in the study area. The oldest of these comprise the Proterozoic Fordham Gneiss, which is of metaigneous origin in this part of the Manhattan Prong. A sizable proportion of the cover rock sequence consists of metavolcanic rocks of Late Precambrian through Middle Ordovician age. The metaigneous rocks of the Fordham and the metavolcanic rocks of the cover sequence have been discussed in earlier sections; this chapter will focus on the intrusive igneous rocks, of Middle Ordovician or younger age, whose emplacement coincided with, or postdated, the Taconian deformation and metamorphism of the cover rock sequence (Table 10).

The Taconian and younger intrusive bodies include granitic, mafic, and ultramafic rocks. Granitic bodies are very common, while mafic and ultramafic rocks are very rare. Most of the granites are too small to be shown on the geologic map (Plate I), but comprise ten percent or more of outcrop in many areas. A portion of one large pluton, the Siscowit Granite, crops out in the study area.

Most of the "Middle Ordovician and younger" igneous rocks are syntectonic with respect to F_1, F_2, or F_3 deformation, and are therefore Taconian in age. Some granites belong to the Mississippian D_6 tourmaline granite suite (Table 12). The youngest igneous body is a lamprophyre dike of probable Mesozoic age.

Regional stratigraphic and structural relationships are the primary concerns of this study. The brief descriptions of the igneous bodies that follow are included for the sake of completeness. The Mississippian (D_6) granite suite is treated most extensively, because these rocks are common through most of the Manhattan Prong but have not been recognized or described as distinctive entities before.

SMALL GRANITES OF TACONIAN AGE AND RELATED ROCKS

Small bodies of Taconian granite are found throughout the study area, but are especially common in sequences of migmatized metawacke and metapelite. These small granites are generally less than 10 meters wide. They range downwards in width to half a meter and less, resulting in an apparent continuum with the leucosome component of host migmatites. In general, the small granitic bodies and the leucosomes are very similar in composition and texture; the distinction between "small granitic body" and "migmatitic leucosome" is largely arbitrary, based on size.

The apparent continuities between the small granites and migmatitic leucosomes suggest that they are genetically related products of similar geological processes. In consequence, an examination of the leucosomes is requisite to a study of the granites.

MIGMATITIC LEUCOSOMES. The migmatites in the study area are generally stromatic. In stromatic migmatites, leucosomes and melanosomes form irregular layers parallel to the rock's schistosity (Mehnert, 1968). Many of the stromatic leucosomes are coarse-grained and have roughly granitic compositions, though trondhjemitic compositions are also common.

Generally speaking, migmatites have diverse origins, including anatexis, metamorphic segregation, crystallization from aqueous fluids, or injection with granitic magma. The coarse-grained character and roughly granitic compositions of most migmatitic leucosomes in the study area argue that they have anatectic origins, though a few clearly originated by other processes (i.e., magmatic injection near the Siscowit Granite).

The migmatites with the clearest anatectic features occur with granulite-facies Taconian mineral assemblages of the Manhattan Schist in the northeastern Peach Lake quadrangle. Granitic and trondhjemitic leucosomes and small granitic bodies together make up 25 to 30 percent of "Manhattan Schist" outcrop in the core of the Washington Ledges syncline (Plate IV). These migmatites are generally not stromatic; the leucosomes have rounded, pod-like shapes

(Fig. 27A). Some leucosome "pods" as small as one centimeter in diameter have granitic compositions. The leucosome "pods" have coarse-grained, uniform, igneous textures (Fig. 27A). K-feldspar in the "pods" may be white, beige, or pinkish in color.

In thin section, feldspar grains are squarish or tabular in shape, with rounded edges, while quartz is generally finer-grained and interstitial. K-feldspar is perthitic, and plagioclase is antiperthitic. In one specimen, euhedral, hexagonal quartz grains (now recrystallized into polycrystalline masses) are enclosed in a large perthite grain.

These granitic leucosome "pods" are surrounded by a restite enriched in sillimanite, opaque minerals, and garnet, and depleted in quartz and feldspar. Some leucosomes contain euhedral crystals of garnet or cordierite; the shapes of these grains suggest crystallization from melt. Nevertheless, leucosome composition and restite compositions are complementary. Compositional and textural considerations strongly argue that the "pods" are products of in-situ partial melting.

The contacts between leucosomes and restite are sharp but slightly irregular. Slivers of restite may be partially or completely enclosed by the leucosomes; where enclosed, they are schlieren-shaped. S_1 foliation clearly existed at the time of "pod" growth.

The "pods" are locally cut by S_2 foliation and are folded around those F_2 folds that have minimal wavelengths of approximately two centimeters (Fig. 27B). Smaller F_2 folds are preferentially developed in ductile restite material and so tend to conform to the shape of the pods (Fig. 27A).

The effects of later deformation events can also be recognized in many leucosomes. For instance, Fig. 16B shows quartz ribbons and mortar texture developed in an anatectic leucosome within a zone of strong F_3 shear.

Most leucosomes were affected by F_2 and F_3 folding, and formed either synchronously with D_1 or immediately following it. The relationships between leucosomes, foliation, and folding indicate that the peak of anatexis either accompanied F_1 deformation or occurred between F_1

and F_2.

SMALL GRANITIC BODIES. Most small granitic bodies display the same attributes as the granitic leucosomes, except for size. Outcrops are generally rounded, and weathered surfaces may be greyish or rusty-stained. The granites consist, for the most part, of perthitic K-feldspar, plagioclase, quartz, and biotite. Biotite-garnet schlieren are very common. Fine-grained, secondary muscovite is present in zones affected by D_6 shearing. Zircon and pyrrhotite may occur as accessory minerals. Grain size is coarse to very coarse (greater than one centimeter in diameter). Most of the granites are white, but some contain tan or pink K-feldspar.

Where small granites occur in metawacke sequences, their relationships generally parallel those observed in the granitic leucosomes. Contacts against host are sharp but irregular, and partially to completely enclosed biotite-garnet schlieren are abundant. The schlieren are oriented parallel to foliation in host rocks; contacts of the granites are commonly subparallel to this foliation.

Small granitic bodies which occur in other lithologies (such as amphibolite or calc-silicate rock) generally cross-cut compositional layering and foliation. Contacts between the granites and these lithologies are typically smooth. Field relationships indicate intrusion, rather than <u>in situ</u> anatexis.

Foliation tends to be poorly developed within small granites, and is generally expressed by aligned biotite schlieren or by rock cleavage. Where the granites occur in metawacke, strain appears to have been partitioned into more ductile host rocks. In a few instances, particularly where the host is a feldspar-rich, competent lithology, a well-developed S_2 or S_3 foliation is locally developed in the granites.

The majority of small granitic bodies appear to be deformed by F_2 folds, and are interpreted as approximately syn-F_1 in age. A substantial minority, however, are younger. Small granites may occur in the hinge zones of F_2 folds and cross-cut older foliation. Some granites cut F_2

folds or occur in zones of strong F_3 shear. A few biotite granites appear to be unaffected by F_3 deformation, and may be post-Taconian. A number of the post-F_2 granites may have clean, intrusive contacts against metawacke hosts.

Most of the granitic bodies are thought to have originated as minor accumulations of anatectic granitic liquids, since they resemble the anatectic granite "pods" in distribution, texture, composition, and contact relationships. The small syn-F_1 granites which occur within metawacke or metapelite sequences generally appear to be essentially in situ. Most granites which occur within other lithologies, and some metawacke-hosted post-F_2 granites, have apparently been mobilized and displaced from their site of origin.

GRANITIZED REGIONS

In some areas, more granite is present than could have been locally generated, though no discrete large bodies occur. The two clearest examples of this phenomenon occur 1) in the Walloomsac Schist south of Lake Windwing (northeastern Peach Lake quadrangle) and 2) in the Ned Mountain Formation Wacke Member south of Route 84 and east of Sawmill Road (southern Brewster quadrangle) (Plate III). These granitized regions are one to two kilometers long and average less than 300 meters wide on present land surface.

The two granitized areas differ in character. South of Lake Windwing, in a belt adjacent to the Walloomsac Marble Member (Plate I), granite is much more abundant than metawacke. Nevertheless, granite/host relationships resemble those seen in metawacke sequences elsewhere. The host rocks generally retain their semi-pelitic character, and resemble other Walloomsac metawackes. Fairly sharp breaks in composition occur between the granite and the remaining aluminous rocks. The granites are coarse-grained, white, and contain abundant biotite schlieren. Except for abundance, they are similar to the most common small granitic bodies. Foliation

within the granitized region is deformed by F_3 and probably by F_2 folds. This granitized area may simply represent an accumulation of anatectic liquids from a larger-than-average source region.

A different process appears to have occurred in the Wacke Member near Route 84. Rocks with distinctly granitic compositions and textures are only moderately abundant, but the Wacke Member metawackes have themselves been strongly modified. These rocks now have a granoblastic texture, with sparse grains of biotite and garnet. Plagioclase and K-feldspar grains are fairly coarse-grained and subhedral. Compared to unmodified metawacke, the feldspar content is very high, while biotite and garnet contents are low. Sillimanite remains only as inclusions in garnet. In spite of the chemical changes, the original compositional layering of these rocks is sufficiently intact to give the appearance of a well-bedded metasedimentary sequence. Granitization apparently followed beds of metawacke; interbedded amphibolites appear to be unmodified. Here, granitic components have replaced metawacke rather than having been extracted from metawacke.

Some small granites in this region contain xenoliths of foliated amphibolite. It is difficult to ascertain the exact age of granitization because of its mimetic nature.

SISCOWIT GRANITE

The Siscowit Granite is the largest body of igneous rock in the study area of Middle Ordovician or younger age. The Siscowit Granite crops out in the southeastern corner of the Peach Lake quadrangle, but continues eastwards and southwards of the borders of the study area. According to the Geologic Map of Connecticut (Rodgers, 1985), Ordovician granite contiguous with the Siscowit is the dominant lithology in a region of over 250 square kilometers.

The Siscowit Granite is one of many igneous bodies originally grouped with the Thomaston Granite of Connecticut by Agar (1934). Scotford (1956) recognized it as a distinct intrusion, and named it "Siscowit Granite" after a reservoir in the Pound Ridge quadrangle. Subsequently,

the Siscowit was described by Prucha, Scotford, and Sneider (1968), Alavi (1976), and Brandon (1981).

DESCRIPTION. The Siscowit granite occurs in small, rounded outcrops, which are fairly few and far between within the study area. Its feldspars are generally beige in color, but white, pale salmon-pink, and pale greyish-pink feldspars occur in some localities. The color of the granite varies from ecru to grey to spotted pink- white- and grey, reflecting the color of the feldspars and the abundance of quartz. On weathered surfaces, the granite may be either greyish or orange-brown (rusty-stained).

Layers or zones of medium-grained (~3 millimeter) granite alternate with layers or zones of coarser-grained granite (with grains up to ~1.5 centimeters in diameter). The coarser-grained granite locally contains feldspars showing a tabular habit. In some cases, Carlsbad twins can be seen macroscopically, with twin composition planes aligned parallel to the granite's foliation.

Tectonic fabrics are generally distinct. The least foliated granites may display a weak rock cleavage, which is oriented parallel to grains of aligned biotite. The biotite may either be dispersed through the rock or concentrated into thin, discontinuous folia. Where the tectonic fabric is more strongly developed, the biotite folia are accompanied by augened feldspars and quartz ribbons.

Younger cleavages locally cross-cut or overprint the original tectonic fabric. These younger cleavages are defined by concentrations of aligned muscovite, which typically occurs in grains smaller than 1 millimeter in diameter. The younger cleavages are generally oriented parallel to S_6 and apparently relate to the Ridgefield fault zone.

The Siscowit Granite contains, on average, about 50 percent K-feldspar, 30 percent quartz, 14 percent plagioclase, and 6 percent mica (both biotite and muscovite). Xenocrysts of garnet are common and inclusions of grey quartz-feldspar-biotite gneiss, interpreted as digested xenoliths, are known. Primary accessory minerals in the Siscowit generally include apatite, zircon, magne-

tite, pyrrhotite, and (rarely) tourmaline.

Microscopically, highly sheared specimens display anastomosing zones of fine-grained feldspar between quartz ribbons and feldspar porphyroclasts (Fig. 16C). Porphyroclasts 3 to 4 millimeters in diameter are surrounded by feldspar grains 0.1 to 0.4 millimeters long. Most of the largest plagioclase and K-feldspar grains are elongate and lie in the plane of the foliation; some of these grains show Carlsbad twinning, with the twin plane parallel to foliation (Fig. 16C). Prismatic, euhedral zircon crystals are common; where these zircons occur within quartz ribbons, the long axis of the crystal is oriented parallel to the length of the ribbon.

Most of the K-feldspar in the Siscowit is microcline, though some large grains are partially inverted from orthoclase. Many large K-feldspar grains have been replaced by myrmekite, resulting in myrmekite zones oriented parallel to the foliation. Some K-feldspar grains are partially altered to muscovite along certain crystallographic directions (Fig. 16C).

Many of the larger plagioclase grains show only Carlsbad twinning, but others have no twinning at all. Plagioclase is generally An_{22} to An_{25} in composition, but a sharply defined rim of about $\sim An_{12}$ occurs on almost every grain, even on plagioclase grains within myrmekite. Cores of plagioclase grains tend to be heavily sericitized.

Biotite is red-brown or dark brown in thin section. It is locally replaced by pale green chlorite with needles of rutile. Textural relationships between muscovite and biotite (which defines the first foliation) relate to the orientation of the first foliation. Where the old foliation is oriented at a large angle to S_6, muscovite grains may be randomly oriented, cross-cutting biotite grains and overgrowing old "mortar" feldspar. In contrast, where this foliation is subparallel to S_6 (as it commonly is within the Ridgefield fault zone), grains of muscovite and biotite may appear parallel, and it may be impossible to distinguish the two foliations.

CONTACT AND AGE RELATIONSHIPS. Walloomsac Schist and Ned Mountain Formation that outcrop near the western boundary of the Siscowit Granite have been injected

with granite. Some small dikes, interpreted as apophyses of Siscowit Granite, occur to the west of the fault. Alavi (1976) reported that the Siscowit Granite cuts the Hartland Formation in the Pound Ridge quadrangle, to the south. Intrusion of the Siscowit evidently postdated the D_1 juxtaposition of the Hartland Formation and the Manhattan Prong, because it cuts rocks on both sides of Cameron's Line.

A shear zone of probable D_3 age cuts the contact between host amphibolite and granite in one granitized outcrop of Walloomsac Schist. If the granite is part of the Siscowit, a minimum intrusive age of syn-D_2 can be inferred.

The map pattern outlined by foliation in the Siscowit Granite (Plate I) supports a late-D_1 to syn-D_2 age. The original, penetrative foliation of the Siscowit Granite, defined by quartz ribbons, commonly displays a westerly- to northwesterly- strike (with moderate to steep dip) outside of D_6 shear zones (Plate I). If the foliation were correlative with S_4, it would have a shallow dip; if it were correlative with S_3, it would strike towards the northeast. The attitudes displayed by the foliation imply that it originated during D_2 or earlier.

A comparison of the granite's magmatic and solid-state foliations provides an independent test of syntectonic intrusion. The granite's magmatic foliation is defined by the parallelism of Carlsbad twin composition planes of the large, elongate grains of feldspar (both K-feldspar and plagioclase). The twin plane of these feldspars is generally parallel to the solid-state foliation defined by quartz ribbons, whereas the twin planes of smaller plagioclase grains (including those in myrmekite textures) are randomly oriented. The coincidence of these foliations suggests syntectonic crystallization (Paterson and others, 1989), and would be consistent with either late D_1 or early D_2 intrusion.

The effects of D_6 deformation and related metamorphism are marked in the Siscowit Granite. Muscovite, which averages about 3 modal percent of the granite, postdates Taconian deformation and may be entirely D_6 in age. Sercitization and formation of sodic rims on plagioclase grains, along with minor replacement of biotite by chlorite, probably accompanied the altera-

tion to muscovite. The wide distribution of muscovite in the Siscowit Granite suggests that the region affected by D_6-related metamorphism in the southeastern Peach Lake quadrangle is much broader than the Ridgefield fault zone.

MAFIC AND ULTRAMAFIC PODS

A few small, isolated pods of ultramafic and mafic rock occur in the Ned Mountain Formation in the southwestern Peach Lake quadrangle (Plate I). One pod is ultramafic to mafic in composition; it crops out in small abandoned quarry just south of Mark Meade Road (Plate III). The other pods, mafic in composition, occur about 700 meters to the northeast of the Mark Meade quarry on Route 35.

DESCRIPTION. The Mark Meade pod is the rounded, moss-covered mass which lies beneath the hammer in Fig. 42B. This pod is less than 3 meters long and about 1 meter thick. The rocks of this pod are brown-weathering and dark grey, silvery grey, or black on fresh surfaces.

The rocks of the Mark Meade pod have a massive, unfoliated, medium-grained texture. Grains are generally 2 to 4 millimeters in diameter. Some parts of the pod show no clear evidence of metamorphic recrystallization, and appear to retain primary igneous minerals and textures. Other portions have undergone substantial metamorphic recrystallization, though without developing foliation. A faint compositional layering and a weak alignment of hornblende grains (most evident microscopically) occurs in still other portions of the pod.

The most "igneous" of the rocks consists of very pale green hornblende (~43 modal percent), olivine (~20 percent), phlogopite with blue-green (chromiferous?) rims (~32 percent), orthopyroxene (~2 percent), and opaque minerals (magnetite, pyrrhotite, and chalcopyrite, together ~3 percent), with traces of secondary minerals (serpentine and a carbonate). The mafic

minerals are strongly cleaved, but otherwise appear little modified. This rock can be classified as a olivine-phlogopite hornblendite.

Parts of the olivine-phlogopite hornblendite have been partially recrystallized under amphibolite-facies metamorphic conditions. In the recrystallized rocks, phlogopite remains abundant (but the blue-green rim disappears), olivine is gone, and the original pale green hornblende occurs as relicts in the cores of later cummingtonite grains.

The slightly layered portions of the pod contain more amphibole and much less mica than do the olivine-phlogopite hornblendite and its metamorphic equivalents. The layered portions are principally composed of green hornblende, plagioclase (An_{38}), and biotite. Some parts of the layered rock are ultramafic, consisting of >85 hornblende, while other parts contain up to 35 percent plagioclase. The macroscopic texture of this rock suggests an essentially igneous origin, though the loose alignment of the hornblende grains indicates that it may have been metamorphically recrystallized.

The pods on Route 35 are smaller than the Mark Meade pod. They range from several centimeters to tens of centimeters in thickness. They are made up of dark grey, brownish weathering, medium-grained rocks, which consist principally of olive-brown hornblende and plagioclase ($An_{38\ to\ 43}$), with minor augite, garnet, sphene, and opaque minerals (pyrrhotite, ilmenite, and magnetite). Plagioclase comprises 25 to 50 modal percent. Hornblendes tend to be aligned, and an irregular compositional layering is present. The foliated textures and garnet-bearing mineralogies of the Route 35 pods indicate that they have been metamorphosed.

CONTACT AND AGE RELATIONSHIPS. The Mark Meade pod is enclosed in a well-layered sequence of felsic metatuff, amphibolite, and quartzo-feldspathic rocks of the Ned Mountain Volcaniclastic Member. Pod contacts are roughly parallel to foliation. The foliation is parallel to S_1 and S_2; the outcrop lies on the east-west limb of the F_3 Pound Ridge antiform. The pod is not visibly affected by the F_4 folding seen in neighboring Volcaniclastic Member rocks

(Fig. 42C), and evidently behaved as a rigid mass during F_4. The boundaries of the pod show slickensides.

The pods on Route 35 are enclosed in a sequence of dark calc-silicate rock, felsic metatuff, and graphitic granofels belonging the Ned Mountain Calc-Silicate Member. The pods of mafic rock occur as boudin-like masses within more ductile lithologies, or are bounded by shear planes.

The Mark Meade and the Route 35 pods apparently represent slivers of larger ultramafic and mafic bodies. The igneous features and medium-grained texture of the Mark Meade pod indicate that its primary crystallization took place in a deep-seated pluton. The Route 35 pods have been metamorphically recrystallized, and do not preserve primary igneous features; thus, a metavolcanic origin cannot be ruled out for them. Nevertheless, their pod-like occurrence is comparable to that of the nearby Mark Meade body, and severe tectonic disruption is rare among the many amphibolite beds found in the region. The Route 35 pods are provisionally inferred to be metaplutonic rocks.

The insertion of the Mark Meade pod into its present context must have involved the dismemberment of a parental ultramafic pluton. This dismemberment probably occurred during or prior to F_2 deformation, since the Mark Meade pod is enclosed within foliation planes oriented parallel to S_2. The survival of igneous textures and mineralogies in the Mark Meade pod (including the blue-green rims on phlogopites) suggests that intrusion occurred after the peak of Taconian metamorphism during D_1. In view of these considerations, the intrusion of the parental pluton probably occurred at some time between the peaks of D_1 and F_2 deformation.

REGIONAL RELATIONSHIPS. The small pods of ultramafic and mafic rock must pertain to larger bodies. None outcrop in the immediate vicinity, however. Further afield, Taconian-aged mafic and ultramafic plutons are known to occur within the Croton Falls Complex (Plate II), the Peach Lake Complex (Plate I), and the Bedford Complex (Plate II).

Both the Croton Falls Complex and the Peach Lake Complex are located several kilome-

ters away, across structural trends, making a direct relationship with the pods unlikely. The Bedford Complex is closer than these other bodies, and some of it occurs at a roughly comparable structural level.

Alavi (1976) mapped bodies of gabbro, diorite, and biotite-augite hornblendite within the Bedford Complex. The gabbro and diorite are described as black or black-and-white mottled, medium- to very coarse-grained massive rocks with locally conspicuous foliation. These rocks may be comparable to the Route 35 pods and Mark Meade rocks of mafic composition. The Bedford biotite-augite hornblendite is a dark-green, massive, coarse- to very-coarse-grained rock that lacks olivine and phlogopite. It is evidently quite distinct from the Mark Meade olivine-phlogopite hornblendite.

According to Alavi (1976), the intrusion of the mafic and ultramafic rocks postdated crystallization of the bulk of the Bedford Complex (Bedford Augen Gneiss), which in turn followed the (F_1) juxtaposition of the Manhattan Prong and the Hartland Formation. The mafic rocks of the Bedford Complex are interpreted as post-F_1 but syn-Taconian. These constraints permit correlation with the Route 35 and Mark Meade pods. Although compelling evidence for correlation to the Bedford Complex is lacking at this time, some connection remains likely.

MISSISSIPPIAN (SYN-D_6) GRANITES

A suite of two-mica, tourmaline-bearing granites is found in association with D_6 shear zones at a number of localities in the Manhattan Prong (Brock, Brueckner, and Brock, 1985). In the Peach Lake quadrangle, two-mica granites occur near all the D_6 faults, but are particularly common in the Turkey Hill fault zone. Three granites from D_6 shear zones (two from the Croton Falls quadrangle and one from the Mount Kisco quadrangle) have been dated by the Rb-Sr whole-rock technique by H. K. Brueckner. These granites have yielded overlapping Mississippian

ages (Table 12). The intrusion of these granites was syn-tectonic with respect to D_6. (For details of these relationships, see relevant discussions in chapters on "Structural Geology" and "Absolute Ages of Deformational Events".)

DESCRIPTION. The Mississippian granite suite consists of very coarse-grained, microcline-rich pink pegmatites, medium-grained white granites, and some coarse-grained white albitic pegmatite. Most of the pink pegmatite dikes are between 5 centimeters and 2 meters in thickness. Many of the dikes have sharp, planar contacts against country rocks. Typically, the pegmatites are made up of pink microcline, white plagioclase ($^{-}An_{26}$), quartz, and muscovite. Tourmaline occurs within the pegmatites, and is commonly found in rosettes on contacts between the dikes and country rocks or in fractures within the host rocks. Some pegmatites appear to be zoned and display books of muscovite that grew inwards from pegmatite boundaries. Fig. 54 illustrates a zoned dike with a quartz core, offset by small D_7 thrust.

The granites are typically surrounded by irregular aureoles of retrograded host rocks (Fig. 43). Kyanite nodules commonly occur in host rocks near granite contacts. These nodules, and other characteristics of the aureoles, will be described in the following chapter.

The medium-grained white granites are unzoned, homogeneous bodies with equigranular texture. They occur in thin dikes (Fig. 46; Fig. 50A and B) and in very small plutons, whose length in outcrop ranges from about 5 to 200 meters. Some enclaves of pink pegmatite with books of muscovite are scattered within and around the white granites. The granites are made up of microcline, quartz, plagioclase, dark-brown biotite, and muscovite. Prisms of apatite and a trace of chlorite are generally present. Plagioclase is commonly distinctly zoned, in some places in an oscillatory manner. Small amounts of tourmaline are present within the white granites, but tourmaline is more abundant in the adjoining, altered host rocks (Fig. 43B) or in pegmatitic enclaves or borders (Fig. 50B).

The Carboniferous granites display a distinctive range of textures. Some granites display

only a faint foliation or lineation; some have distinct mica folia, but show little sign of solid-state deformation; a few granites exhibit well-developed solid-state fabrics such as C-S texture. The range of textures reflects variations in timing of granite crystallization relative to shearing, as well as variations in the intensity of D_6 deformation.

The white granite body at Goldens Bridge in the Croton Falls quadrangle shows relatively little deformation. Portions of the granite display both a foliation and lineation defined by aligned biotite grains (and, locally, muscovite). The mica grains, though aligned, are fairly evenly distributed through the rock. In the field, this granite body strongly resembles the dike in Fig. 50 (which crops out on transect H-H', about 400 meters to the southwest). The pluton at Goldens Bridge contains tabular, zoned crystals of plagioclase, predominantly of oligoclase composition ($\sim An_{25}$). Much of the fabric in this pluton is a flow foliation.

Many bodies of white granite are cut by distinct mica-rich, slightly anastomosing folia. Muscovite is concentrated in the folia, though biotite is more evenly distributed through the rock. Feldspar grains are commonly cut by aligned grains of muscovite. The muscovite folia are evidently of tectonic origin; however, in contrast with Taconian and older granites, feldspar grains in these granites show little evidence of plastic deformation. Neither small "new" feldspar grains nor "mortar texture" are present.

In these rocks, most feldspar and quartz grains have equidimensional shapes, though a few distinct quartz ribbons and elongate feldspar grains occur in certain domains. The quartz ribbons and elongate feldspar grains are oriented roughly parallel to the mica folia. The plagioclase grains generally have cores of An_{12} composition, with overgrowths of An_1 along contacts with K-feldspar.

Textural relationships around muscovite grains provide clues to the origin of this fabric. The muscovite grains typically terminate in junctions shared with quartz and/or albitic plagioclase, but do not terminate in or against K-feldspar. In one specimen, the portion of a K-feldspar grain located at the tip of a muscovite has been replaced by quartz and albite (Fig. 57). The muscovite

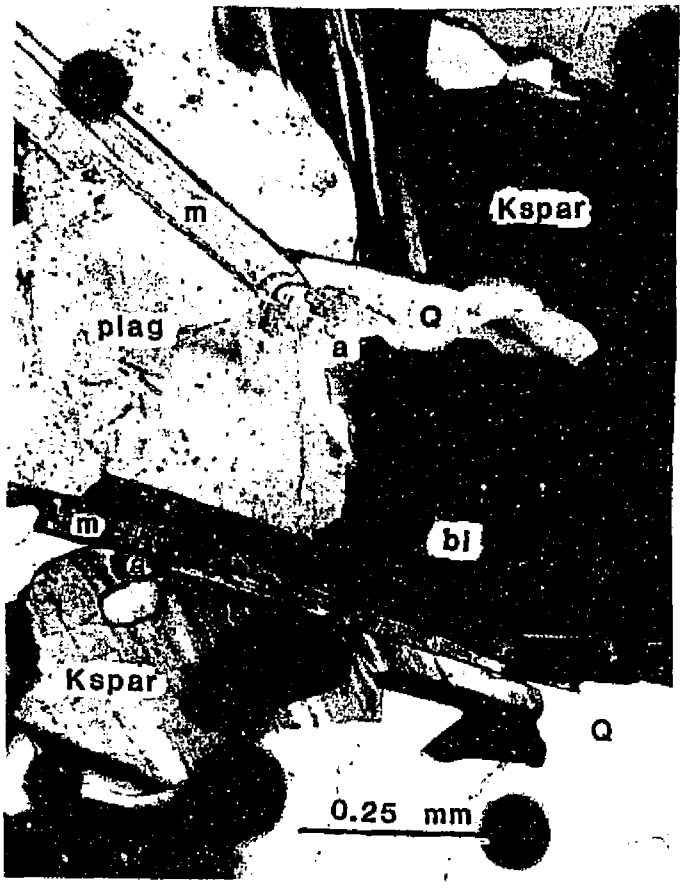

Fig. 57. S_6 fabric in syn-D_6, Mississippian granite, photographed with crossed nicols. K-feldspar (Kspar) is replaced by quartz (Q) and albite (a) at termination of muscovite (m). Plagioclase (plag) has overgrowth of albite along contacts with K-feldspar. Biotite (bi) is also present. Specimen #1220, transect K-K', Croton Falls quadrangle.

folia appear to have formed under hydrothermal, post-magmatic conditions. The creation of the tectonic fabric was accomplished by crystallization of muscovite, albite, and quartz, and accompanied by the consumption of K-feldspar.

The development of syntectonic muscovite folia and the formation of albitic overgrowths on plagioclase are analogous to effects observed in the Siscowit Granite, which was also affected by D_6. However, the muscovite grains which make up D_6 folia in the Mississippian granites average 2 to 3 millimeters in diameter, and are much coarser than the muscovite in the Siscowit. In addition, in the Siscowit Granite, oligoclase is preserved in the cores of plagioclase grains, and the rims are less albitic. The similarities in retrogressive features suggest that the alteration of the white Mississippian granites and the Siscowit Granite were promoted by similar hydrothermal fluids, which emanated out from the Mississippian granites and infiltrated D_6 shear zones.

Primary crystallization of some pegmatitic dikes appears to have been accompanied by deformation. A "granite" from the Turkey Hill fault zone (#1125, illustrated in Fig. 43A), collected in easternmost Croton Falls quadrangle (Plate III), illustrates this phenomenon. The coarse-grained "granite" has a fabric defined by folia of white mica and elongate quartz aggregates (some several centimeters long) oriented parallel to the dike contact. A second foliation is locally developed. This foliation is defined by broadly spaced, thin quartz ribbons and aligned, scattered grains of white mica. It is inclined, on average, about 30^{o} to the first, but bends into the mica-rich folia. Some large albite crystals exhibit fractures parallel to the second foliation, along which small, new grains have nucleated. Large, slightly zoned crystals of albitic plagioclase also enclose plates of white mica. The two foliations appear to be analogous to a C-S texture, but they are irregularly developed and they grade into coarse-grained, undeformed-looking pegmatite. There is no K-feldspar in this "granite", and white mica is more abundant here than in K-feldspar-bearing granites.

It appears that the growth of coarse albite, quartz, and white mica in the "granite" coincided with shearing, and the prevailing low temperatures and ongoing deformation favored the crys-

tallization of white mica over that of K-feldspar. While similar in some respects to ordinary albite pegmatites, this "granite" may be also compared with (K-feldspar-bearing) granites that have been deformed at greenschist facies in the presence of high water activity. According to Gapais (1989), feldspars in such granites break down to a quartz and a fine-grained assemblage of white mica, albite, and epidote.

Cross-cutting, hydrothermal-stage foliations defined by white mica-rich cleavages are the most common fabrics in Mississippian granites. A few also exhibit more typical C-S textures, indicative of deformation in the solid state. In the Peach Lake quadrangle, the best example is #1092, collected from another granite in the Turkey Hill fault zone. In outcrop, this tourmaline-bearing, medium-grained white granite shows a close-spaced muscovite cleavage; its etched surface reveals a fine, regularly developed C-S texture (Fig. 45).

ORIGIN OF THE GRANITES. Initial strontium ($^{87}Sr/^{86}Sr$) ratios of around .710 were obtained from the three whole-rock age determinations of D_6 granite (H. K. Brueckner and P. W. G. Brock, pers. commun.). These initial ratios, together with the abundant muscovite characteristic of these rocks, indicates that the granites are "S-type", derived from partial melting of upper-crust materials.

The granites were evidently not derived from by anatexis of the high-grade schists and gneisses of the northeastern Manhattan Prong. The host rocks of the Prong were retrograded, not melted, in the vicinity of these granites. The location of the source region of the Mississippian granites remains an outstanding question for the geology of the Manhattan Prong.

LAMPROPHYRE DIKE

A dike of biotite lamprophyre crops out 0.7 kilometer southwest of Round Pond on Old West Mountain Road in the central Peach Lake quadrangle (Plate I). The exposed portion of the dike is less than one meter in width.

DESCRIPTION. The lamprophyre is a dark-green, homogeneous-appearing, massive rock with an aphanitic-porphyritic texture. A flow foliation defined by biotite phenocrysts is parallel to the dike contacts. In thin section, several varieties of phenocrysts can be seen, all set in a matrix consisting of an altered, low-relief mineral (possibly K-feldspar), fine-grained sheet silicates, and a sprinkling of black opaques.

The largest and most abundant of the phenocrysts are biotite. These show two types of zoning: some grains have pale-red cores and deep-red rims, while others have deep-red cores and pale-red rims. Small, generally untwinned crystals of plagioclase rank next in abundance. A number of intermediate-sized crystals of augite and of a colorless clinoamphibole (probably pargasite) are sprinkled through the rock. Finally, some euhedra of apatite are present.

Patches of the lamprophyre and of the adjacent host rock are altered to green biotite, calcite, chlorite and rutile. The matrix of the lamprophyre is heavily altered (to very fine-grained material) almost everywhere. The heavy alteration is typical of this lithology (Williams and others, 1982).

The contact between the lamprophyre and host rock strikes 300^{o} and dips 72^{o} to the northeast. The dike cuts across foliation and bedding in a K-feldspar-rich granofels of the Ned Mountain Formation Basal Member. Although some minor D_6 shearing is present in the vicinity, the dike is undeformed and unmetamorphosed. The dike is inferred to be post-Mississippian in age.

REGIONAL RELATIONSHIPS. The dike on Old West Mountain Road appears to be the first lamprophyre of post-Mississippian age recognized in southwestern New England. Lamprophyre dikes of Early Cretaceous age are abundant in the Monteregian Hills of Quebec and in central to northern New England (Gold, 1967; Philpotts, 1974; McHone, 1978). The youngest of these dikes, like the Peach Lake lamprophyre, intruded on northwestwardly-striking fractures (McHone, 1978). It is possible that the Peach Lake dike is related to the same Cretaceous episode of lamprophyre intrusion that affected northern New England.

GEOLOGY OF PARTS OF THE PEACH LAKE AND BREWSTER QUADRANGLES, SOUTHEASTERN NEW YORK AND ADJACENT CONNECTICUT, AND BASEMENT BLOCKS OF THE NORTH-CENTRAL APPALACHIANS

by

PAMELA JEAN CHASE BROCK

VOLUME II

A dissertation submitted to the Graduate Faculty in Earth and Environmental Sciences in partial fulfillment of the requirements for the degree of Doctor of Philosophy, The City University of New York

1993

METAMORPHIC HISTORY

INTRODUCTION

Amphibolite-facies mineral assemblages have been reported in rocks of Paleozoic age throughout the Manhattan Prong, except for the patch at greenschist-facies-grade where the Prong's northwestern corner borders on the Hudson River. Most workers have paid limited attention to metamorphic conditions in the Prong; studies of bedrock geology have generally simply noted the predominant mineral assemblages (taken to represent the peak of metamorphism) and minor retrogressive effects such as sericitization. Metamorphic grade, it was recognized, increases eastwards, as Barth (1936) had demonstrated in his study of the Paleozoic rocks north of the Hudson Highlands (Fig. 1). Following this approach, the presence of muscovite-kyanite schists amidst upper-amphibolite-facies rocks in the Croton Falls quadrangle was initially ascribed to a folded Taconian isograd (Chase and Brock, 1976).

In contrast to this simple metamorphic picture, this study has produced evidence of 1) much higher grade (M_1) regional metamorphism than previously recorded in the Prong (or elsewhere in the Taconian orogen) and 2) extensive downgrading and obliteration of the highest grade assemblages during two later metamorphic events. Assemblages belonging to the first Paleozoic metamorphic event (M_1) reflect high-pressure granulite conditions. During the first of the later events (M_2), Paleozoic-age granulite-facies rocks were recrystallized to upper-amphibolite (K-feldspar-sillimanite) facies assemblages; during the second (M_3), parts of the Prong (particularly in D_6 shear zones) were soaked with hydrothermal fluids emanating from the Mississippian granite suite, and recrystallized at greenschist to middle-amphibolite facies grade.

Each of the metamorphic events which affected rocks of the study area will be described in sequential order. First, the conclusions of previous investigations of the northeastern Manhattan Prong will be summarized.

PREVIOUS WORK. Evidence for a metamorphic discontinuity between the Fordham Gneiss and Paleozoic strata has been presented by workers in the White Plains, Croton Falls, and Brewster quadrangles (Whiting-Goldberg, 1977; Dadourian and Brock, 1979; Brock and Brock, 1983). Granulite-facies assemblages observed in the Fordham Gneiss include orthopyroxene + K-feldspar (Dadourian and Brock, 1979; Brock and Brock, 1983) and orthopyroxene + clinopyroxene (Whiting-Goldberg, 1977). These assemblages have been interpreted as relicts of Grenvillian metamorphism which survived amphibolite-facies Paleozoic overprinting.

Most previous workers in the Peach Lake quadrangle have attributed prevalent mineral assemblages there to a single metamorphic event. Minor muscovite is commonly present in the aluminous schists; Lessing (1967) and Brandon (1981) interpreted this muscovite as a prograde mineral which survived the peak of metamorphism. However, Scotford (1956), Lessing (1967), and Brandon (1981) all placed regional metamorphism in the upper-amphibolite-facies, on account of the coexistence of K-feldspar and sillimanite. In prograde metamorphic terranes, the first appearance of K-feldspar + sillimanite indicates either 1) the breakdown of muscovite + quartz at pressures <3.5 kilobar, or 2) (at >3.5 kilobars of P_{H2O}) the disappearance of muscovite into anatectic melts generated by plagioclase-bearing rocks.

Given the K-feldspar + sillimanite assemblages, Lessing (1967) attributed the persistence of muscovite to univariant metamorphic reactions at the K-feldspar-sillimanite isograd, while Brandon (1981) invoked continuous reactions involving a phengite component of the muscovite. Retrogressive metamorphism in the region was thought to be limited to minor late uralite and sericite (Lessing, 1967) and minor chlorite (Brandon, 1981).

However, studies in the Croton Falls quadrangle (adjoining the Peach Lake quadrangle to the west) have indicated that the Paleozoic-aged rocks are polymetamorphosed. Upper-amphibolite-facies grade assemblages are followed in some localities by middle-amphibolite-facies grade assemblages (Brock and Mose, 1979; Dadourian, 1979). Emeries, formerly contact- metamorphosed by the Croton Falls Mafic Complex, have been remetamorphosed (in a complex series of

stages) at grades ranging from upper-amphibolite to greenschist facies (Brock and Brock, 1981).

Evidence for Paleozoic metamorphism of still higher grade was later recognized in the northeastern Peach Lake quadrangle. Henry Gold, then a student of P. W. G. Brock, identified cordierite in the Manhattan Schist along Washington Ledges Road in 1979. P. W. G. Brock observed granulite-facies cordierite-K-feldspar-garnet assemblages in rocks from this region in 1982.

Among the questions addressed in this study, therefore, are

1. What are the geographic limits of the Paleozoic-aged granulite metamorphism?

2. What forms does it take, in addition to the cordierite + K-feldspar + garnet assemblages?

3. How does it relate to the tectonic history of the region?

4. Can Grenvillian-aged metamorphic assemblages be distinguished from Paleozoic-aged assemblages in the study area?

5. Did the rocks of the study area undergo polymetamorphism during Paleozoic time, comparable to that observed in the Croton Falls quadrangle?

PROTEROZOIC METAMORPHISM (M_0)

The orthopyroxene gneiss and clinopyroxene-garnet gneiss members of the Fordham Gneiss contain a number of mineral assemblages indicative of the granulite facies. Clinopyroxene-bearing assemblages of the plagioclase-hornblende gneiss and K-feldspar-hornblende gneiss members are also consistent with this grade. Before attributing these assemblages to Grenvillian metamorphism, however, a method for distinguishing Precambrian from possible Paleozoic granulite-facies assemblages is necessary.

Orthopyroxene-bearing gneisses of Paleozoic age (from the Ned Mountain Formation, the

Hartland Formation, and the Walloomsac Schist) share many textural characteristics. They are well-foliated, medium- to fine-grained rocks. Orthopyroxene generally occurs as clusters of optically aligned small grains. In hand specimen, feldspars are white or grey. These orthopyroxene gneisses strongly resemble their stratigraphically equivalent, orthopyroxene-free counterparts, and the two lithologic types are difficult to distinguish without microscopic examination. In contrast, pyroxene gneisses of the Fordham are coarse-grained and poorly foliated. Most grains in these rocks are 2 to 15 millimeters in diameter. The orthopyroxene commonly grows porphyroblastically. Leucocratic orthopyroxene gneiss contains waxy-appearing, beige or slightly greenish feldspars.

The textural contrast between Fordham and post-Fordham orthopyroxene gneiss is recognizable both macroscopically and in thin section (Fig. 5). The distinctive, coarse-grained texture of the Fordham is taken as evidence that the peak mineral assemblages are the products of Precambrian metamorphism. This inference is supported by certain features unique to the Fordham Gneiss; for instance, only the orthopyroxene gneisses of the Fordham are cut by small orthopyroxene-bearing granites (shown in Fig. 4).

The precise conditions which accompanied the Grenvillian granulite-facies metamorphism are uncertain, and could be the focus of future studies. In the study area, the mineral assemblages include orthopyroxene + clinopyroxene, hypersthene + K-feldspar (both from the orthopyroxene gneiss member) and clinopyroxene + almandine/pyrope garnet + Ca-rich plagioclase (clinopyroxene-garnet member).

EARLY PALEOZOIC METAMORPHISM - M_1-M_2

Most of the Paleozoic rocks in the study area carry mineral assemblages that are compatible with middle- to upper-amphibolite facies metamorphic grade. These assemblages are now

interpreted to be the products of retrogressive, rather than of prograde metamorphism.

Relicts of granulite-facies M_1 metamorphism were first recognized in rocks collected in Pierrepont State Park and on Ridgebury Mountain in the northeastern Peach Lake quadrangle (Plate III). This region remains the best source for rocks with relict M_1 granulite-facies assemblages, though later metamorphic events are also well represented there. Traces of granulite assemblages were later found in all major F_2 synclines, and in post-Fordham strata throughout the study area. The following examples illustrate the distribution of some of the distinctive granulite-facies assemblages, and so indicate the minimum extent of M_1 granulite-facies metamorphism (for exact locations of the specimens mentioned, see Plate III):

1. The assemblage cordierite + K-feldspar + garnet replaces biotite + sillimanite in many granulite terranes. It is common in the Manhattan Schist at the core of the Washington Ledges syncline, particularly at Pierrepont State Park. It has also been observed in the Calc-Silicate Member of the Ned Mountain Formation on the northern limb of the West Mountain anticline (specimen #735). In addition, garnet- and K-feldspar-bearing rocks from three other localities contain patches of very pale or greenish, Mg-rich biotite. These patches strongly resemble the pseudomorphs of biotite after cordierite that occur in the Pierrepont area. (The rocks with patches of pale biotite are #609, from the southern limb of the Shadow Lake anticline, #1565, from the northern limb of the West Mountain anticline, and #1507, from the southern limb of the South Salem syncline). In addition, Scotford (1956) reported occurrence of the assemblage cordierite + garnet + sillimanite + biotite in a specimen collected between the "normal phase" of the Fordham Gneiss and the "Poundridge Granite" at Ward Pound Ridge County Park. This stratigraphic position corresponds with the Ned Mountain Formation Basal Member.

2. Orthopyroxene + clinopyroxene coexist in granulite-facies rocks as the result of the breakdown of hornblende. Although orthopyroxene is a common constituent of Paleozoic meta-

basites in the northern part of the study area, clinopyroxene is rarely seen in these rocks. Orthopyroxene and clinopyroxene have been observed in contact with each other in only two specimens. One is #1319, a metabasite of the Basal Member of the Ned Mountain Formation, collected from the northern side of the West Mountain antiform. The other is #CT-12A-89, a metabasite of the Hartland Formation at Pierrepont State Park. Orthopyroxene and clinopyroxene occur together (not in contact) in three other specimens: #1679 and #1603b (Hartland Formation and Walloomsac Schist, respectively, from the Washington Ledges syncline) and #1302 (northernmost belt of the Ned Mountain Formation Wacke Member, Mill Plain syncline).

3. Corundum-bearing restites are generated by anatexis of pelitic rocks under a range of granulite-facies conditions (Cartwright and Barnicoat, 1986). Corundum has been found in the Manhattan Schist at three localities: at Turkey Hill in the Turkey Hill fault zone (#876), and at two sites inside Pierrepont State Park (#1008 and PP31, Plate III). In #876, the corundum, together with green (hercynitic) spinel, occurs as inclusions inside garnet; the bulk of the rock consists of middle-amphibolite-grade mineral assemblages, and the rock is cut by a D_6 muscovite cleavage. The two other corundum-bearing specimens have upper-amphibolite to granulite-facies assemblages. All three corundum-bearing rocks occur in the core of the Washington Ledges syncline.

4. The assemblage hercynite-rich spinel + sillimanite + K-feldspar replaces muscovite + garnet in the absence of quartz under granulite-facies conditions (Selverstone and Chamberlain, 1990). Green spinel is in contact with K-feldspar (and near sillimanite) in specimen #1379. The spinel is partially rimmed by late muscovite. This specimen is from the South Salem syncline, southeastern Peach Lake quadrangle.

Thus, traces of Paleozoic granulite-facies metamorphism occur throughout the study area.

Nevertheless, the record of M_1 granulite-facies metamorphism is highly fragmentary, due to successive episodes of later metamorphic overprinting.

The aluminous lithologies retain a more complete metamorphic record than do rocks of other bulk compositions. Garnets in aluminous rocks commonly enclose relicts of older mineral assemblages. Groups of minerals that commonly occur together as inclusions inside garnet are called "inclusion assemblages" in the following sections. These inclusion assemblages indicate that a complex progression of prograde (early-M_1) and retrograde (late-M_1) metamorphic conditions occurred during the M_1 event.

After the M_1 event, granulite-facies assemblages were nearly completely replaced by upper-amphibolite-facies M_2 assemblages. The M_2 assemblages reflect a continuation of the retrogressive trend that was already evident in late-M_1. The divide between the two metamorphic events is set on tectonic grounds: M_1 accompanied the earliest Taconian deformation (D_1) and S_1 foliation development; M_2 coincided with the deformation of S_1 foliation later in the Taconian orogeny (particularly F_2 and F_3).

Most of the dominant assemblages in the non-aluminous rocks (metabasites, marbles, calc-silicate rocks, etc.) are consistent with upper-amphibolite-facies-grade and therefore appear to be M_2 in age. However, many of the assemblages in these rocks are stable over a wide range of conditions, and so do not tightly constrain metamorphic history.

To most effectively explore the sequence of metamorphic events, the following procedure has been adopted: 1) M_1 and M_2 assemblages of aluminous rocks will be described first, to establish the stages of metamorphic development and the constraints on pressure and temperature at each stage; 2) later, M_1 and M_2 assemblages found in rocks of other compositions will be summarized. After treatment of the M_1 and M_2 events, M_3 (and younger) metamorphism of rocks of all bulk compositions will be described and discussed.

M_1 AND M_2 METAMORPHISM, ALUMINOUS LITHOLOGIES. A sequence of four inclusion assemblages, representing four stages of M_1 metamorphism, can be identified by pooling observations from all the aluminous rocks. Only rarely are all four stages represented within single garnet grains. Combinations of two or three inclusion assemblages are more common, though many relatively young garnets contain only the final inclusion assemblage. Two factors contribute to the absence of older inclusions in these rocks: a) many garnets apparently formed during the late-M_1 stage, and lack older cores; and b) inclusions in a number of garnets have been replaced by biotite.

Biotite can be observed pseudomorphing inclusions of sillimanite, spinel, and rutile, or simply replacing patches of garnet. The abundance of spots of late biotite within garnets makes the identification of primary inclusions of biotite very uncertain. As a result, biotite is not counted among the minerals of the inclusion assemblages, although some might have coexisted with assemblages #1 or #2.

1. Inclusion assemblage #1. Assemblage #1 occurs as a dense cloud of very-fine-grained (~0.003 millimeter) inclusions in the "dusty" cores of certain garnets. Many of the inclusions are too small to be identified microscopically, but quartz, feldspar, and (very rarely) staurolite are apparently present. A colorless, blocky mineral is generally prominent. Fine needles of sillimanite occur as overgrowths on some "blocks"; the shape, refractive indices, and birefringence of the "blocky" grains are consistent with kyanite. Recognizable kyanite is present in one specimen (#1507). Small, rounded needles of rutile commonly occur in this assemblage. Opaque minerals can also be present.

2. Inclusion assemblage #2. The inclusions that comprise assemblage #2 are relatively large, generally 0.05 millimeters in diameter and greater. They occur in "clean" portions of certain garnet grains, surrounding the "dusty" cores with assemblage #1. Minerals species found in

assemblage #2 include spinel, kyanite, rutile, and opaque minerals. One garnet in specimen #1006 contains small inclusions of staurolite, which are intergrown with an aluminosilicate mineral (probably kyanite) and green spinel (Fig. 58A). Spinel and kyanite occur together, without staurolite, in garnets from several localities (specimens #192b, 609, 1243, and 1697). Rutile invariably accompanies the kyanite + spinel + garnet association (Fig. 58B). Assemblage #2 is the least common of the inclusion assemblages.

3. Inclusion assemblage #3. Inclusions of green spinel most commonly occur in alumino-silicate-free portions of garnet grains. Inclusion assemblage #3 consists of these spinel grains, specks of opaque that appear to be exsolved magnetite, and the mineral species that occur in adjacent inclusions. Neighboring inclusions generally consist of quartz, feldspar, and opaque minerals (Fig. 59); rutile can also be present. Inclusion assemblage #3 is most commonly found in garnet overgrowths around "dusty" cores (which contain assemblage #1), but can occur in younger garnets that lack either assemblage #1 or #2.

4. Inclusion assemblage #4. The rims of older garnets and entire grains of late-M_1 garnets commonly enclose trains of fibrolitic or acicular sillimanite. Similar sillimanite trains are generally present in the rock matrix, though in some cases (particularly in D_6 shear zones), unprotected sillimanite has disappeared. Inclusion assemblage #4 consists of this sillimanite and the minerals associated with it: quartz, feldspar, and opaque minerals (particularly ilmenite and magnetite). In contrast with assemblages #1, 2, and 3, rutile is not present. Spinel is not generally a part of assemblage #4, though it can occur as inclusions within sillimanite.

Inclusions of sillimanite are very common near the rims of older garnets. Many garnets are late-M_1 in age and contain only inclusion assemblage #4.

The significance of these inclusion assemblages must now be assessed and the assemblages

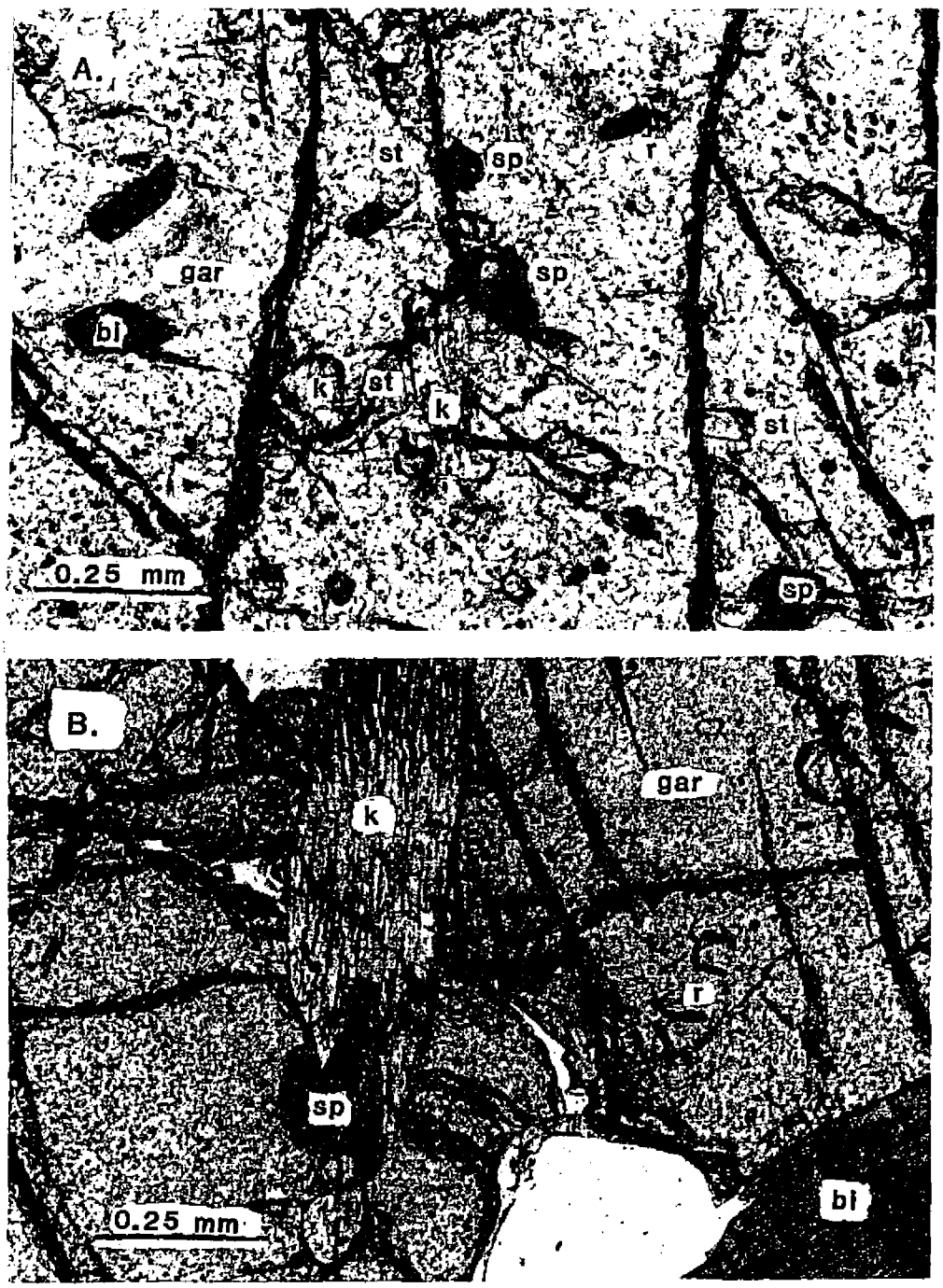

Fig. 58. (A) Inclusions of hercynitic spinel (sp), staurolite (st), probable kyanite (k), rutile (r), and biotite (bi) in garnet (gar). Specimen #1006, Manhattan Schist.

(B) Inclusions of hercynitic spinel, kyanite, and rutile in garnet (inclusion assemblage #2). Biotite occurs in matrix outside the garnet. Specimen #1697, Ned Mountain Formation Wacke Member. (Mode is given on Table 3).

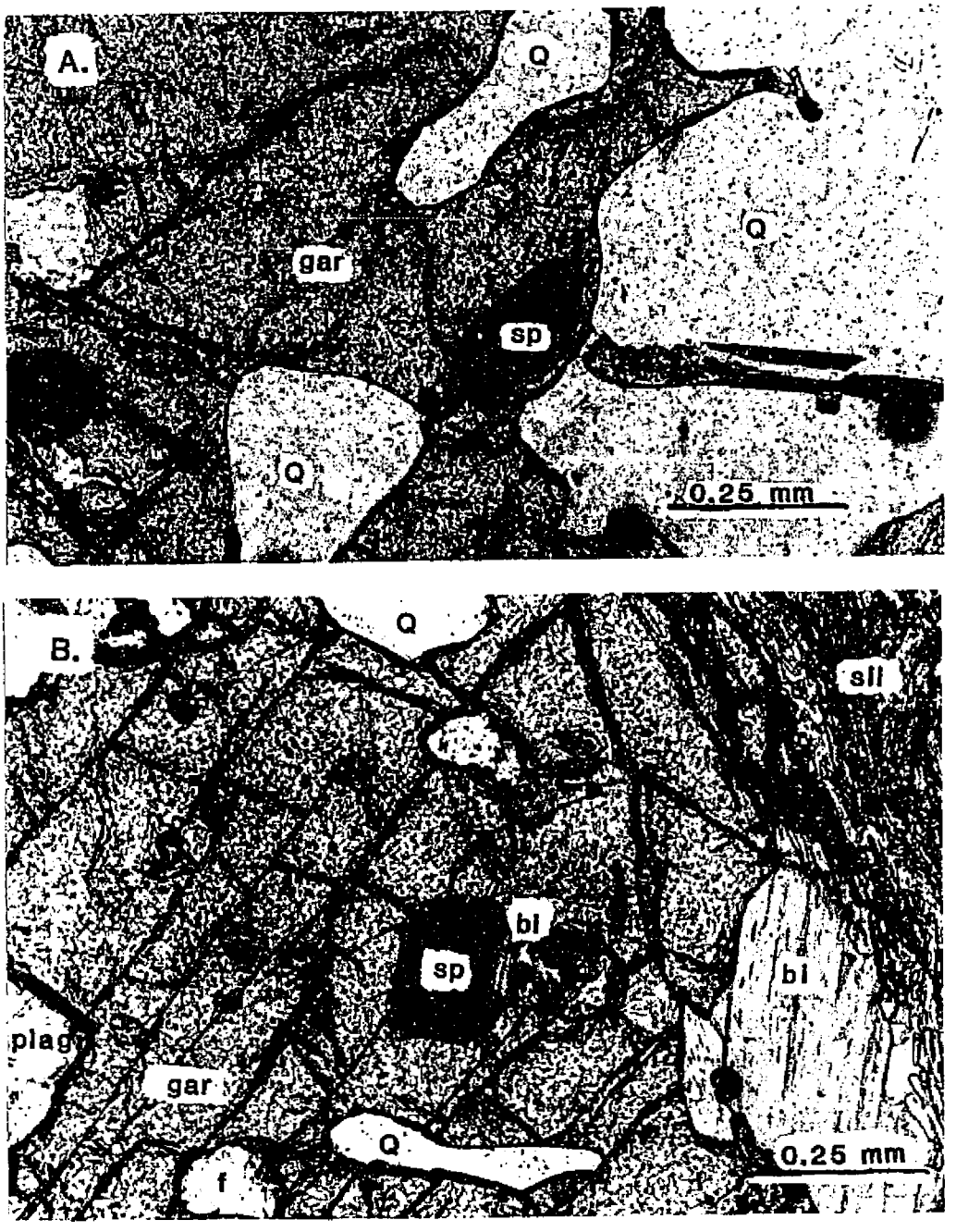

Fig. 59. Examples of garnet inclusion assemblage #3 (spinel-bearing, aluminosilicate-free). bi=biotite; f=feldspar; gar=garnet; plag= plagioclase; Q=quartz; sp=spinel.

(A) Specimen #966, Manhattan Schist.

(B) Specimen #1385, Ned Mountain Formation Calc-Silicate Member. Very fine-grained inclusions of assemblage #1 occur in the garnet core. Sillimanite occurs in the rock matrix, outside the garnet. (Mode is given in Table 3).

(C) and (D), next page

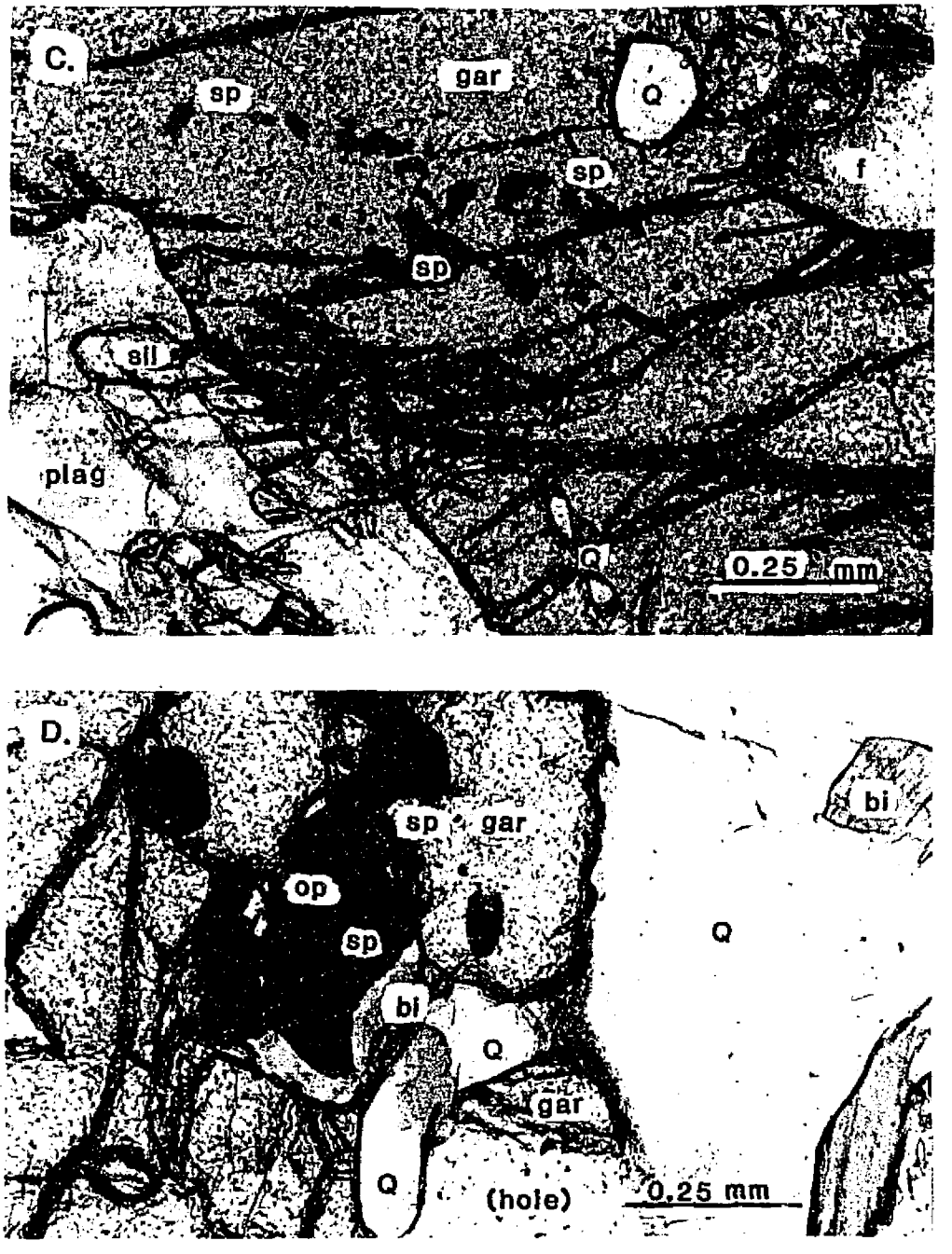

Fig. 59, continued. (C) Specimen #1243, Ned Mountain Formation Wacke Member. Spinel is associated with opaque material, probably exsolved magnetite. Sillimanite and plagioclase occur in the rock matrix.

(D) Specimen #1687, Walloomsac Schist. Spinel is intergrown with opaque material (op).

compared with surviving granulite-facies rocks. A long trail of evidence must be followed in order to distinguish the principal episodes of M_1-M_2 metamorphism and to trace the evolution of temperature and pressure conditions. Subsequent sections will each focus on a different aspect of M_1-M_2 history in the aluminous rocks. These sections will discuss: A) reconstruction of the early-M_1 metamorphic path; B) peak-M_1, granulite-facies metamorphism; C) late-M_1 metamorphism, granulite-facies retrogression; D) M_2 metamorphism, upper-amphibolite-facies retrogression; E) garnet-biotite and garnet-cordierite "thermometry"; F) behavior of Ti and Fe^{3+} during M_1 and M_2; G) petrogenetic grid for late-M_1 and M_2 reactions in aluminous rocks; and H) post-M_2 retrogression of surviving cordierite-bearing assemblages.

A. Reconstruction of the early M_1 metamorphic path. Inclusion assemblages #1 and #2 record the early stages of M_1 metamorphism. Pressure and temperature conditions during these stages are constrained by equilibria involving staurolite, Fe-Ti-minerals, and aluminosilicate polymorphs. These equilibria indicate that high pressures accompanied mounting M_1 temperatures.

1. Equilibria involving staurolite. The aluminous schists and gneisses of the study area are fairly rich in FeO, and must have contained substantial prograde staurolite at some point in their history. Staurolite would have persisted in quartz-absent domains (such as inside garnet) at temperatures above its stability in quartz-bearing assemblages (Ganguly, 1972). Staurolite-bearing assemblage #1 developed during these early stages of prograde metamorphism. With increasing temperature, however, staurolite in quartz-absent domains would break down to aluminosilicate + spinel + garnet (Fig. 60, reaction 2). The intergrowth of staurolite, spinel, and aluminosilicate in garnet found in #1006 evidently records this reaction. Staurolite almost entirely disappeared, even in quartz-free domains with further increase in temperature; the terminal breakdown of staurolite produced the assemblage kyanite + spinel + garnet (inclusion assemblage #2).

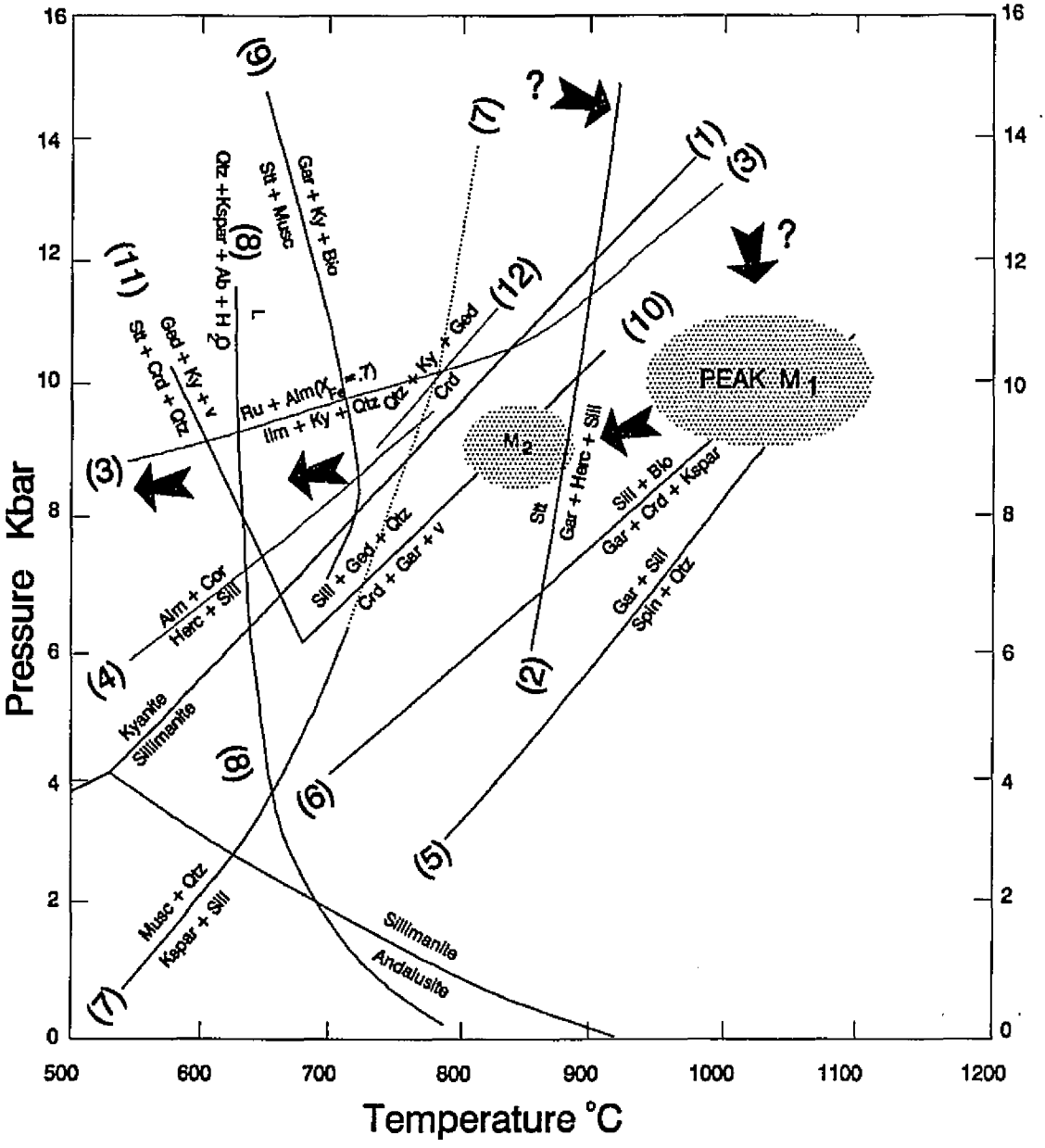

Fig. 60. Reactions constraining the P-T trajectory of M_1 - M_2 metamorphism. (4) & (5) are Fe end-member reactions. (12) is a Mg end-member reaction. See text for discussion. Sources: (1) Kerrick, 1990; (2) Ganguly, 1972; (3) Bohlen, Wall, & Boettcher, 1983; (4) & (5) Bohlen, Dollase, & Wall, 1986; (6) Thompson, 1986; (7) Chatterjee & Froese, 1975; (8) Johannes, 1985; (9) Spear & Cheney, 1989; (10), (11), & (12) Harley, 1986.

ABBREVIATIONS:-

Ab = Albite; Alm = Almandine; Bio = Biotite; Cor = Corundum; Crd = Cordierite; Gar = Garnet; Ged = Gedrite; Herc = Hercynite; Ilm = Ilmenite; Kspar = K-feldspar; Ky = Kyanite; Musc = Muscovite; Mt = Magnetite; Opx = Orthopyroxene; Qtz = Quartz; Ru = Rutile; Sill = Sillimanite; Spin = Spinel; Stt = Staurolite; v = vapor.

As a result, inclusions of prograde staurolite are extremely uncommon.

2. Equilibria involving kyanite. The regional conditions that accompanied the development of assemblage #2 are constrained by the intersection of the two reactions,

kyanite = sillimanite (1)

and

staurolite = garnet + spinel + sillimanite (2).

Taking (1) from Kerrick (1990) and (2) from the Fe-end member reaction in Ganguly (1972), minimum pressures of ~12 kilobars and minimum temperatures of ~900°C are inferred for assemblage #2 (Fig. 60). Increasing the Mg, Mn, or Zn content of the staurolite would displace (2) towards higher temperatures (Ganguly, 1972), and therefore shift the intersection towards higher pressure. A reduction in the activity of water (a_{H2O}) from unity to 0.5 would probably depress the temperature of this reaction by only 20° to 25°C (Ganguly, 1972).

Inclusion assemblages #1 and #2 both apparently contain kyanite, the high-pressure aluminosilicate polymorph, indicating that relatively high pressures prevailed through the early stages of M_1. The corundum-bearing restite parageneses already mentioned may also be the products of high-pressure prograde metamorphism during this early period.

With pressures of 10 kilobars, corundum-bearing restites would be produced by the anatexis of some bulk compositions at temperatures as low as ~670°C (Cartwright and Barnicoat, 1986). The assemblage corundum + garnet (present in specimen #876) reacts to sillimanite + hercynite with increasing temperature or decreasing pressure (reaction 4, Fig. 60). Corundum in #876 occurs in the cores of garnets, while sillimanite occurs in the rims; thus, textures suggest that the formation of corundum occurred early, predating the growth of sillimanite.

3. Equilibria involving Fe-Ti minerals. Garnet and rutile coexist in inclusion assemblages #1, #2, and #3. Rutile + garnet is a pressure-sensitive assemblage. Using Bohlen, Wall, and

Boettcher's (1983) calibration, if the garnet is assumed to be $Almandine_{70}$, this paragenesis sets a minimum pressure of 10 kilobars for a temperature circa 800° and 11 kilobars for temperatures near 900°C (reaction 4, Fig. 60). $Almandine_{70}$ is reasonable approximation of garnet composition, since the few available microprobe analyses of M_1-M_2 garnets show a range of X_{Alm} ranging from 0.65 to 0.77 (see below). The minimum pressure indicated by this assemblage would be reduced if the garnet were poorer in Fe^{2+}.

B. Peak-M_1, granulite-facies metamorphism. High-pressure, early-M_1 metamorphism was followed by the Taconian thermal peak. Evidence for conditions during this period comes from inclusion assemblage #3, and from some relict granulite-facies rocks.

Peak M_1 paragenesis, aluminous rocks. Inclusion assemblage #3 consists of spinel, quartz, feldspar, opaque minerals, and rutile. In assemblage #2, spinel, kyanite, and garnet had coexisted; but with increasing temperature, garnet + aluminosilicate are ultimately replaced by spinel + quartz (Fig. 60). The occurrence of spinel and quartz in adjacent inclusions in garnet, in the absence of aluminosilicate minerals, implies that spinel and quartz had coexisted before their enclosure by garnet.

Inclusion assemblage #3 occurs sparsely in garnets from the southern Peach Lake quadrangle, and is fairly abundant in the north. The distribution of this assemblage implies that P-T conditions permitted the coexistence of spinel and quartz throughout the study area during the peak of metamorphism.

In most of the study area, inclusion assemblage #3 is the only surviving clue to the parageneses that existed during the peak of metamorphism. However, the granulite-facies rocks in and near Pierrepont State Park locally preserve some of the peak assemblages.

The paragenesis spinel + quartz survives in specimen #PPBu4 (Fig. 61A, B). This specimen largely escaped from lower-granulite and upper-amphibolite facies retrogression, though it

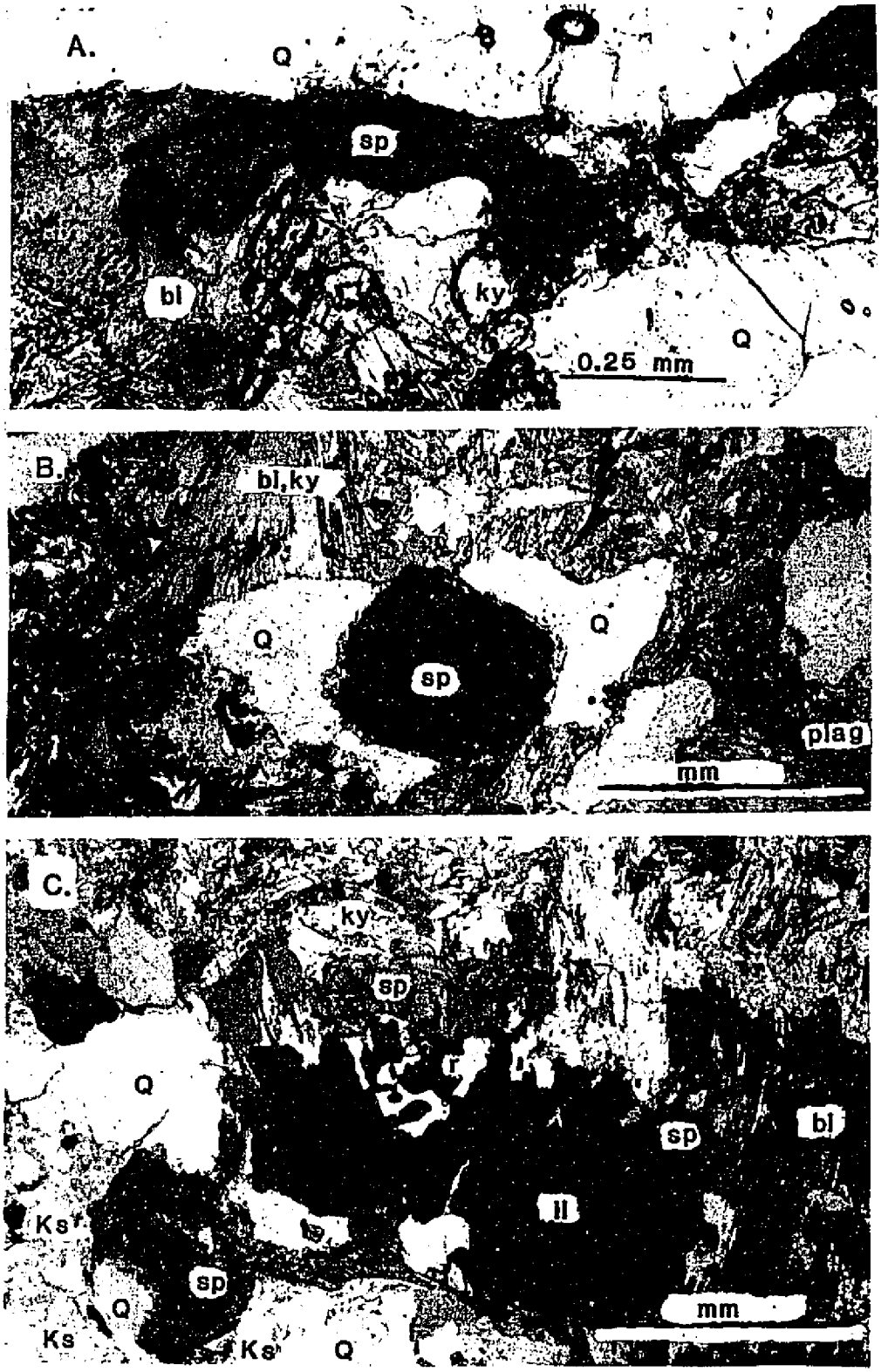

Fig. 61. (A), (B), & (C) Peak-M_1 quartz + spinel (+/- K-feldspar, plagioclase, rutile, and ilmenite) assemblages in specimen #PPBu4. Unfoliated, post-M_2 biotite and kyanite have locally replaced cordierite; garnet occurs out of field of view. bi=biotite; il=ilmenite; Ks= K-feldspar; ky=kyanite; plag=plagioclase; Q=quartz; r=rutile; sp=spinel.

displays substantial middle-amphibolite facies alteration (to muscovite, biotite, kyanite, and chlorite). The peak assemblage in this rock included cordierite, rutile, ilmenite, K-feldspar, plagioclase (An_{45}), garnet (with assemblage #1 cores), spinel, and quartz. Rutile, spinel, and quartz coexisted (Fig. 61C). An anatectic leucosome of trondhjemitic composition is present.

The "ilmenite" in this rock is actually an ilmeno-hematite which shows substantial exsolution. K-feldspar is generally perthitic, with the exsolved plagioclase component that comprises approximately 30% of the grains. Fibrolite occurs along the boundaries of some feldspar grains, and kyanite occurs with the retrogressive assemblage; these aluminosilicate minerals appear to be entirely secondary.

If cordierite were added to the list of minerals in inclusion assemblage #3, the assemblage would become comparable to the peak paragenesis in #PPBu4. No cordierite inclusions have been observed; any cordierite that might have been present in assemblage #3 may have been replaced at some later time, possibly by garnet + sillimanite + quartz (inclusion assemblage #4).

It is worth emphasizing here that the two mineral species which presently provide most of the foliation in the aluminous rocks, sillimanite and biotite, do not occur in the peak assemblage. Sillimanite and biotite are of retrograde, not prograde origin in these aluminous rocks.

P-T conditions, peak-M_1. The P-T conditions which accompanied peak-M_1 metamorphism can be loosely constrained by optically-identified mineral assemblages and compositions. Pressure, one can surmise, was relatively high, since a minimum of 12 kilobars had been experienced during the early phase of M_1. As for temperature, Fig. 60 shows the position of the multivariant reaction

$$\text{garnet} + \text{sillimanite} = \text{spinel} + \text{quartz} \quad (5)$$

determined by Bohlen, Dollase, and Wall (1986) for the system $FeO\text{-}Al_2O_3\text{-}SiO_2$. The expression

for the equilibrium constant of the reaction is

$$K_{P,T} = \frac{(a_{Alm})(a_{Sill})^2}{(a_{Herc})^3(a_{Qtz})^5}.$$

The minimum temperatures indicated by the assemblage spinel + quartz are very sensitive to the Fe^{2+} content of the spinel phase, since the value for the activity of hercynite is cubed. The X_{Mg} of spinels in quartz-bearing rocks is less than or equal to that of coexisting garnet (Grant, 1985). However, the remainder of the spinel does not necessarily consist of hercynite; spinels commonly contain magnetite (ferric iron) and gahnite (zinc) components. Reaction 5, as plotted, is at best a crude guide to peak-M_1 conditions, because the compositions of peak-M_1 phases are not presently known.

Compositions of ternary feldspars also provide a gross estimate of peak-M_1 temperatures. Stormer (1975) proposed a thermometer based on the partition of Na (albite) between coexisting alkali feldspar and plagioclase.

During this study, the compositions of feldspars were determined optically; as a result, the compositions of exsolution lamellae in alkali feldspars are only approximately known. However, the visibly exsolved albitic component defines the minimum amount of albite in the original, homogeneous alkali feldspar, if the exsolution of the two phases was constrained by the experimentally determined solvus curve. It is the minimal amount because the molecular albitic components of potassic feldspars that plot on the solvus curve surpass the potassic components of coexisting (exsolved) sodic feldspars.

In specimen PPBu4, perthite that contains between 30-40% exsolved albitic phase coexists with plagioclase of composition An_{45}. On Stormer's plots, an alkali feldspar with 30% albite, coexisting with plagioclase of An_{45}, indicates a temperature of ~950°C at a pressure of 10 kilobars (Fig. 62). A 40% albite component would indicate nearly 1200°C. At a pressure of 5 kilobars (unrealistically low for peak-M_1), these temperatures would drop to ~900°C and 1100°C, respectively. Thus, the two inaccurate measures of peak-M_1 temperatures (the spinel + quartz equili-

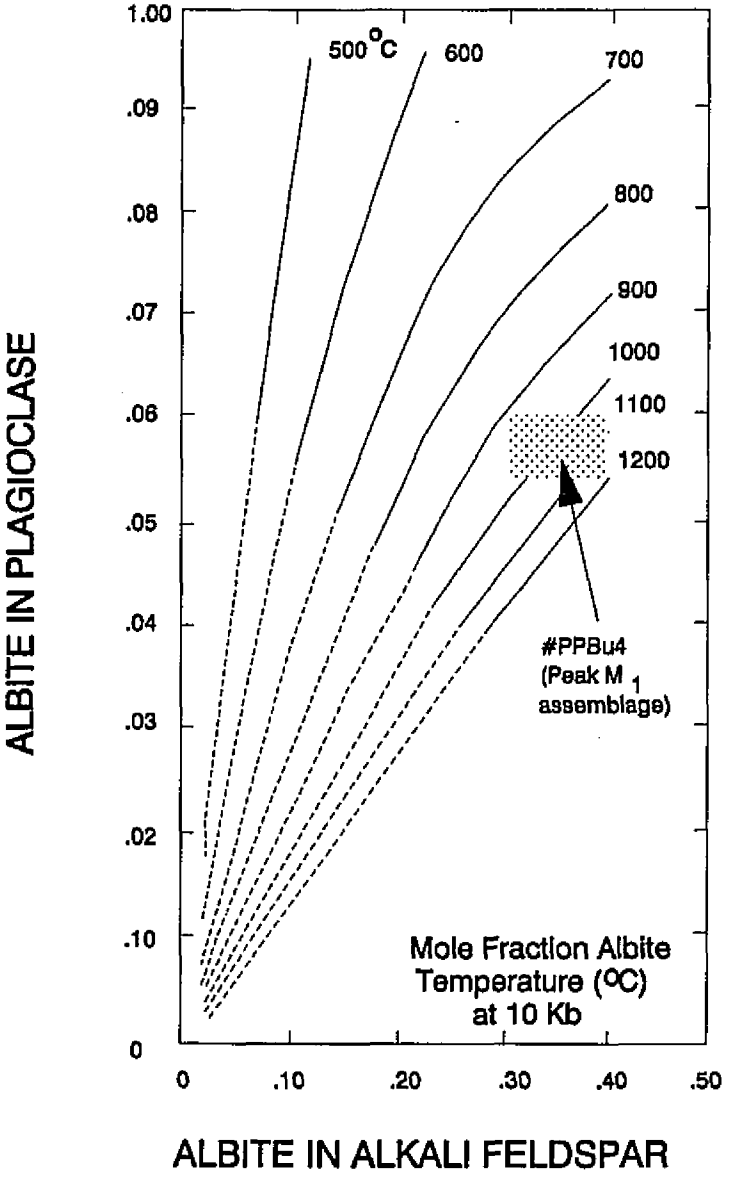

Fig. 62. Peak M_1 temperatures from coexisting ternary feldspars. Diagram after Stormer (1975).

bria on Fig. 60 and ternary feldspar compositions, Fig. 62) are in reasonable agreement with each other.

C. Late-M_1 metamorphism: Granulite-facies retrogression. The peak M_1 assemblages were overprinted by lower-grade, but still granulite-facies, assemblages in many high-grade aluminous gneisses. The mineral assemblages and textures of these gneisses record the late-M_1 metamorphic event.

Late M_1 parageneses in aluminous rocks. During the transition between the peak- and late-M_1 metamorphic stages, the spinel + quartz tie line was broken and coexisting garnet + sillimanite became stable. Prominent trains of fibrolitic sillimanite and abundant, large garnet porphyroblasts subsequently developed. Inclusion assemblage #4, which consists of the paragenesis garnet + sillimanite + quartz + feldspar + ilmenite + magnetite, first appeared during the late-M_1 metamorphic phase.

Late-M_1 assemblages, and assemblages transitional between peak- and late-M_1, are best preserved in the region around Pierrepont State Park. Late-M_1 assemblages commonly included coexisting garnet + sillimanite + quartz + plagioclase + K-feldspar + cordierite, a granulite-facies assemblage.

A number of textures, observed in the Pierrepont region, record the transition between peak- and late-M_1 parageneses:

1. In late-M_1 assemblages, spinel occurs as inclusions in garnet, sillimanite, and plagioclase. It does not coexist with quartz, though adjacent inclusions of spinel and quartz occur within garnets (Fig. 59A). Where spinel occurs in cordierite, it is rimmed by sillimanite (Fig. 63A).

2. Aligned needles of fibrolitic sillimanite project into grains of cordierite from outer grain boundaries (Fig. 63A).

3. An intergrowth of ilmenite and garnet replaces cordierite + rutile associations

Fig. 63. Late-M_1 textures in an aluminous lithology. Specimen #966, Manhattan Schist.

(A) Sillimanite (sil) separates cordierite (crd) from spinel (sp) and ilmenite (il). Sillimanite prisms (grey lines), aligned parallel to S_1, grow inwards from boundaries of cordierite grains, distinguishing them from clean quartz (Q). Rutile (r) is enclosed in ilmenite and quartz.

(B) Late-M_1 sillimanite trains define an S_1 foliation. Garnet forms a rim between an ilmenite grain (right side) and cordierite. Cordierite remains in domains between sillimanite folia (see also Fig. 30). Patches of the central cordierite grain have been replaced by post-M_2 gedrite and sillimanite.

(C) is on the next page.

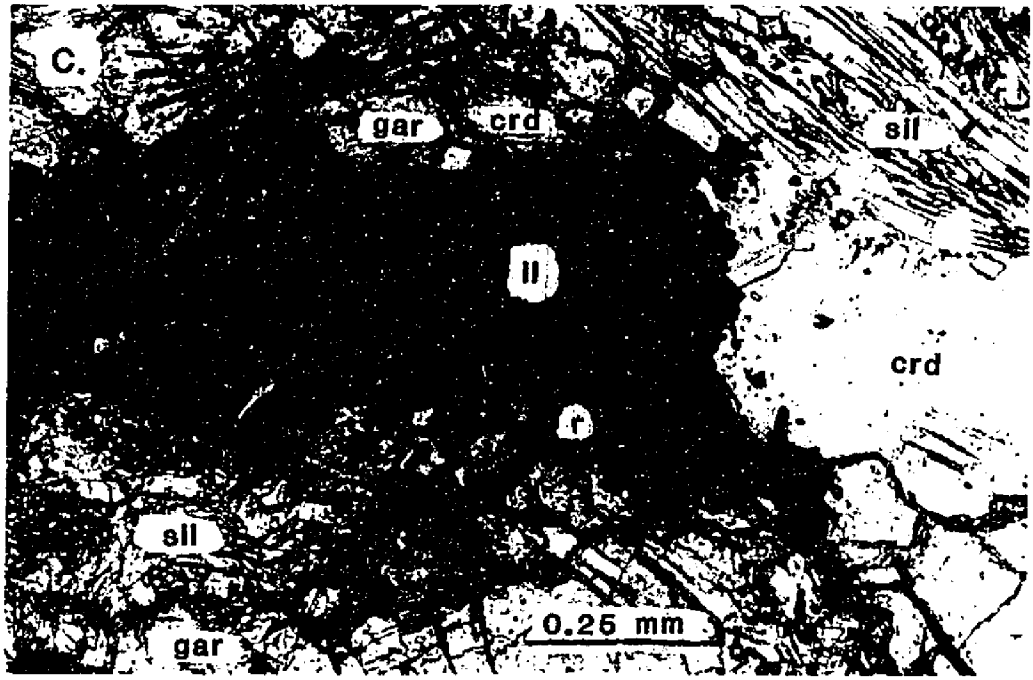

Fig. 63, continued. (C) Garnet (gar) is intergrown with ilmenite (il) and sillimanite (sil). Garnet + ilmenite + sillimanite appear to replace cordierite (crd) and rutile (r).

(Fig. 63C); ilmenite, sillimanite, or garnet shield remaining rutile from cordierite.

4. Coronas of garnet or sillimanite surround ilmenite grains that were formerly in contact with cordierite (Fig. 63A, B).

5. Overgrowths or rims of magnetite extend from some ilmenite grains into cordierite. Small, euhedral blebs of magnetite (commonly accompanied by minute grains of aluminosilicate) occur as spots in cordierite.

6. Magnetite has replaced portions of many ilmenite grains that were formerly in contact with spinel. Composite ilmenite-magnetite grains, some with relict spinel, are commonly accompanied by sillimanite. The entire ilmenite-magnetite-spinel-sillimanite assemblage is locally enclosed in late garnet.

Significance of textures 1 through 3. These textures record the replacement of the peak-M_1 paragenesis, quartz + spinel + garnet + cordierite + ilmenite + rutile, by parageneses containing garnet and sillimanite. In addition, they reveal that the modal proportions of ilmenite were increased, and those of rutile diminished.

Texture 1 indicates that the tie-lines extending from spinel to quartz and cordierite were broken in favor of garnet and/or sillimanite. Textures 1 and 2 show that the growth of garnet and sillimanite occurred at the expense of cordierite and spinel. Texture 3 demonstrates that the tie-line between cordierite and rutile was broken, and that these minerals were replaced by garnet, sillimanite, and ilmenite.

In summary, textures 1 to 3 indicate that the stability of several peak-M_1 phases (spinel, cordierite, and rutile) became restricted; these phases were replaced by garnet, sillimanite, and ilmenite. These textures may well have developed simultaneously. They can be understood in terms of a single reaction (below). The peak-M_1 assemblage is assumed to provide the reactants:

quartz + spinel + cordierite + rutile = garnet + sillimanite + ilmenite.

This reaction would not have affected quartz, spinel, and cordierite coexisting with ilme-

nite. A second reaction, involving these assemblages, would have been necessary in order to completely severe the quartz + spinel tie-line. Textures 4 through 6 provide evidence for the second reaction.

Significance of textures 4 through 6. Texture 4 shows the ilmenite + cordierite tie-line eventually became unstable, and was broken in favor of sillimanite- and/or garnet- bearing parageneses. In texture 5, cordierite is replaced by magnetite and an aluminosilicate mineral. Texture 6 reflects the rupture of the ilmenite + spinel tie-line, and the formation of magnetite- and sillimanite- bearing assemblages in its place.

In sum, these textures record the restriction of ilmenite, continued reduction of spinel and cordierite, and the growth of sillimanite, magnetite, and garnet at their expense. These changes may well have proceeded in linked fashion, as parts of a single reaction:

quartz + spinel + cordierite + ilmenite = garnet + sillimanite + (titaniferous) magnetite.

S_1 fabrics: Products of late-M_1 metamorphism. Rocks with late-M_1 assemblages occur in Pierrepont State Park and on Ridgebury Mountain. At the macroscopic level, these rocks display large garnet porphyroblasts and prominent sillimanite trains. They are speckled with black opaque minerals, and typically contain 4 to 6 modal percent ilmenite + magnetite. These rocks have little biotite. Fig. 30 is a photomicrograph of a typical, well-foliated late-M_1 assemblage, with large garnets, flasers of cordierite, prominent sillimanite trains, and opaque minerals. The assemblages present in such rocks include:

garnet + sillimanite + cordierite + magnetite,

garnet + sillimanite + ilmenite + magnetite,

garnet + sillimanite + ilmenite + rutile, and

garnet + sillimanite + magnetite + spinel;

the first three of these assemblages coexist with K-feldspar and quartz.

The mineralogies of these high-grade rocks and their garnet- and sillimanite-dominated textures are apparently of retrogressive origin. Inclusion assemblage #3 is common, and quartz + spinel assemblages locally persist. These rocks provide a useful lesson about the degree to which later metamorphic events can obscure peak metamorphic assemblages.

This was, however, just the first instance of overprinting by lower-grade assemblages. Upper-amphibolite-facies metamorphism, which followed M_1, resulted in the destruction of cordierite and reappearance of biotite. However, the late-M_1 sillimanite trains survived, and form a prominent part of many upper-amphibolite-facies rocks (Fig. 37).

D. M_2 metamorphism: Upper-amphibolite-facies retrogression. Almost all the biotite contained in aluminous rocks in the Pierrepont State Park area is texturally late. Biotite replaces spinel, cordierite (Fig. 64A), and garnet, and overprints trains of late-M_1 fibrolitic sillimanite. Some biotite "inclusions" in garnet (Fig. 59A) conceivably have crystallized during prograde M_1, but even these biotite "inclusions" may be largely or entirely the product of retrogression of other minerals.

The reappearance of biotite in the aluminous rocks commenced before the F_2 deformational event. Biotite is concentrated in areas around late-M_1 anatectic leucosomes in some granulite-facies rocks. Though this biotite overprints S_1 fabrics, some is clearly deformed by F_2 folds.

The relationship between the anatectic leucosomes and host-rock biotite implies that pockets of melt (and partially crystallized, slushy leucosomes) acted as H_2O "reservoirs" during the M_1 event. When this water was released into host with the crystallization of the melt, it promoted the rehydration of the surrounding rock. It is uncertain whether there were any other sources of H_2O during M_2. In any event, sufficient water became available to allow widespread development of hydrous phases during upper-amphibolite grade M_2 metamorphism.

The textures of rocks throughout the study area commonly reflect the retrogressive nature of M_2. Patches of unaligned biotite overprint trains of M_1 fibrolitic sillimanite, and replace por-

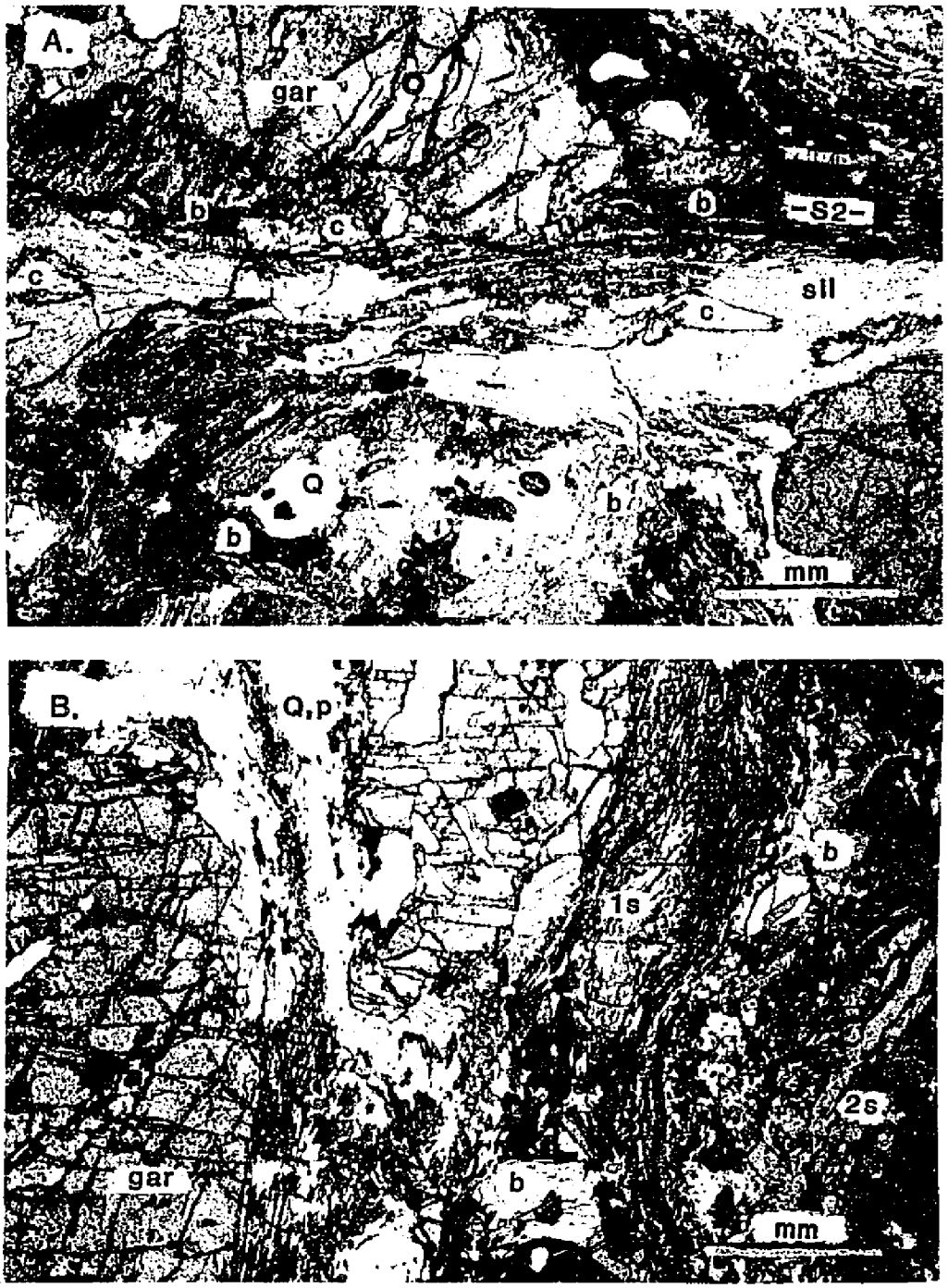

Fig. 64. M_2 textures in aluminous rocks. (A) S_2 foliation (-S2-), defined by aligned biotite (b), is oriented parallel to S_1 folia (late-M_1 sillimanite train). Optically continuous, relict cordierite grains (c) occur within S_1 folia. Cordierite grain adjacent to sillimanite train has been partially replaced by biotite. Biotite grains outside S_2 folia show varied orientations. Garnet (gar) in upper left consists of early-M_1 core (with very-fine-grained inclusions) and a partial overgrowth of late-M_1 garnet-opaque symplectite. Q=quartz. Specimen #1002, Manhattan Schist.

(B) Late-M_1/S_1 sillimanite train (1s) and neighboring garnet have been partially replaced by biotite. Coarse prisms of younger sillimanite (end sections, 2s) coexist with biotite. A close-up of the central garnet is given in Fig. 59B. p=plagioclase. Specimen #1385, Ned Mountain Formation Calc-Silicate Member. (C) is on the next page.

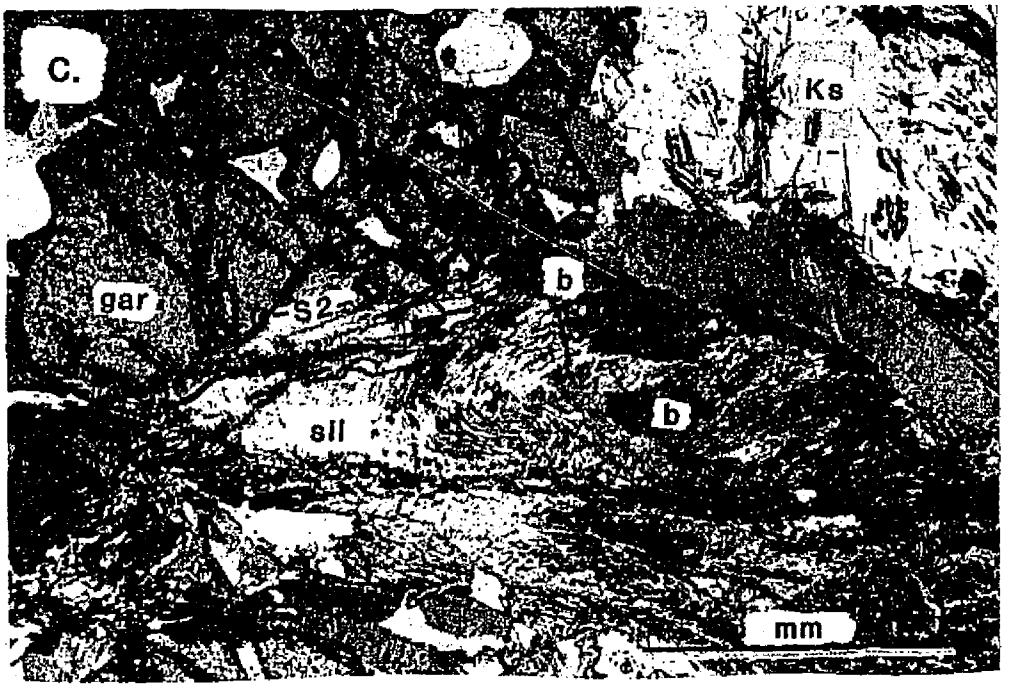

Fig. 64, continued. (C) Folded M_1/S_1 sillimanite (sil) trains, garnet (gar), and K-feldspar (Ks) are partially replaced by biotite (b). M_2 sillimanite prisms define an S_2 foliation (-S2-), axial-planar to folded M_1 sillimanite. Specimen #2197, Walloomsac Schist, transect H-H', Croton Falls quadrangle.

tions of garnet; a second generation of sillimanite, in the form of coarse prisms, grows within and across both biotite and fibrolite trains (Fig. 64B). Similar textures can be observed in rocks collected in the Croton Falls quadrangle (transect H-H') (Fig. 64C).

The Fe-Ti oxide minerals participated in M_2 retrogressive reactions to some degree. M_2 assemblages generally contain significantly lower amounts of opaque minerals (<1 to 2 modal percent) than the late-M_1 assemblages (which generally had 4 to 6 modal percent). M_2 biotite commonly nucleated over (and partially replaced) magnetite. Rutile is not present in M_2 assemblages, except for the thin needles exsolved in quartz grains.

Cordierite- and spinel-bearing late-M_1 assemblages were replaced by biotite-bearing parageneses (garnet + sillimanite + biotite + magnetite + ilmenite) at most localities during M_2. During M_2, cordierite nearly disappeared; spinel co-existed only with sillimanite; and biotite partially or completely replaced many spinel inclusions in garnets (Fig. 59B, D).

P-T conditions, M_2. 1) Pressure. Though few good quantitative measures are available, M_2 metamorphic conditions can be qualitatively placed in P-T space. Sillimanite, not kyanite, was the stable Al_2SiO_5 polymorph, and rutile + garnet did not coexist in M_2 assemblages. M_2 pressures were evidently significantly lower than those experienced during prograde-M_1 (Fig. 60). However, the presence of the assemblage garnet + sillimanite + quartz indicates that pressure remained moderate to high, since this assemblage is replaced by cordierite at low pressures (Holdaway and Lee, 1977; Martignole and Sisi, 1981).

2) Temperature. M_2 mineral assemblages correspond to substantially lower temperatures than do assemblages of the late-M_1 stage. M_2 assemblages are bounded in P-T space, on the high-temperature side, by the rehydration reaction,

garnet + cordierite + K-feldspar = biotite + sillimanite (6).

The approximate position of this reaction is shown on Fig. 60.

A distinctive assemblage developed in the quartz-free, remetamorphosed emeries of the Croton Falls Complex (Croton Falls quadrangle) sets an upper thermal limit for M_2 metamorphism there. The emery assemblage, corundum + garnet + spinel, is replaced by masses of staurolite. The crystallization of this staurolite must have been accompanied by the addition of silica, but the reaction is still analogous to the formation of staurolite from garnet, spinel, and sillimanite (reaction 2 on Fig. 60). Reaction (2) defines the limits of staurolite stability at high temperatures. It is uncertain whether the constraint this reaction sets is also valid for M_2 conditions in the Peach Lake quadrangle.

The presence of syn-F_2 and syn-F_3 granitic leucosomes indicates that temperatures remained high enough to allow the presence of melt, though melt was probably much reduced in volume compared with the M_1 stage. A minimum temperature is set by the stability of the K-feldspar + sillimanite tie-line. Muscovite did not appear in quartz-bearing assemblages. However, the absence of muscovite may have been due to the presence of melt, rather than to the thermal limits of muscovite stability. Therefore, a low-temperature boundary for M_2 assemblages can be set somewhere between the reaction

K-feldspar + sillimanite = muscovite + quartz (7)

and the minimum-melting curve (reaction 8, Fig. 60).

E. Garnet-biotite and garnet-cordierite "thermometry". Only very limited microprobe study of M_1 and M_2 assemblages has thus far been done. When the few existing data are fed into thermometric equations, they give unrealistically low temperatures.

Late-M_1 cordierites and garnets from specimen #966 were analyzed on the 9-channel Camica Camibax (S3117C) automated microprobe at Lamont-Doherty Geological Observatory. The analyses showed that the garnets are approximately binary solutions of almandine and pyrope, with spessartine and grossular components together comprising less than 6 molar percent. Pyrope content ranges up to 30 molar percent.

These are reasonable granulite-facies garnets. However, the cordierite in the rocks is very magnesian (Table 15). Application of the data to Fe-Mg exchange thermometry gives maximum temperatures of 560°C and 549°C, using the calibrations of Thompson (1976) and Perchuk and Lavent'eva (1983), respectively.

At an earlier stage, P. W. G. Brock had analyzed coexisting garnets and biotites from an M_2 assemblage in the Croton Falls quadrangle (on transect K-K', Plate II). (These analyses were performed on the 9-channel automated ARL-SEMQ electron microprobe at the American Museum of Natural History). His data yield a maximum temperature of 577°C when combined with an estimated pressure of 8 kilobars and Perchuk and Lavent'eva's (1983) calibration, or up to ~ 565°C with Thompson's calibration.

These limited data sets suggest that many M_1-M_2 Fe-Mg silicates underwent extensive re-equilibration as they cooled or during subsequent metamorphic events. Geothermometers applied to granulite-facies minerals commonly yield temperatures attained after the granulite metamorphism, because of rapid diffusion through the initial stages of cooling (Selverstone and Chamberlain, 1990). Still, the temperatures recorded by these assemblages are surprisingly low, and may relate to an M_3 overprint. This study strongly supports Selverstone and Chamberlain's contention that "petrographic relationships can place better constraints on P-T histories of granulites than can thermobarometric calculations on minerals whose compositions have been modified...".

F. Behavior of Ti and Fe^{3+} during M_1 and M_2. The textural relationships observed in late-M_1 and M_2 assemblages clearly demonstrate the participation of oxide phases in retrogressive reactions. The modal content of opaque minerals reached a peak during late-M_1 and declined thereafter, confirming this participation.

It is instructive to follow the "flow" of Ti, Fe^{3+}, and Fe^{2+} through different phases, from the peak-M_1 stage through M_2. The changing assemblage of Fe-Ti oxides (from rutile + ilmeno-

TABLE 15

MICROPROBE ANALYSES FROM A LATE-M_1 ASSEMBLAGE (#966)

	garnet 6	garnet 7	garnet 8	cordierite 11	cordierite 12
SiO_2	38.81	38.42	38.17	46.11	48.22
TiO_2	0.02	0.02	0.0	0.01	0.0
Al_2O_3	20.76	20.76	21.11	33.93	33.62
FeO	29.89	30.74	31.80	3.90	3.90
MnO	0.98	0.91	1.00	0.04	0.01
MgO	7.67	7.44	6.38	10.98	10.39
CaO	1.22	1.24	1.29	0.01	0.03
Na_2O	0.0	0.0	0.0	0.15	0.08
K_2O	0.0	0.0	0.0	0.03	0.08
Total	99.36	99.53	99.76	95.15	96.32
		------ Formula based on 24 oxygens ------			
Si	6.09	6.05	6.03	6.43	6.62
Ti	0.0	0.0	0.0	0.0	0.0
Al	3.84	3.85	3.93	5.58	5.44
Fe	3.92	4.05	4.20	0.45	0.45
Mn	0.13	0.12	0.13	0.0	0.0
Mg	1.79	1.75	1.50	2.28	2.13
Ca	0.21	0.21	0.22	0.0	0.0
Na	0.0	0.0	0.0	0.04	0.02
K	0.0	0.0	0.0	0.01	0.01
Total	15.98	16.03	16.01	14.79	14.67
X_{Fe}	0.65	0.66	0.69	0.16	0.17
X_{Mg}	0.30	0.29	0.25	0.84	0.83

hematite to ilmeno-hematite + titaniferous magnetite) can be illustrated on an FeO-TiO_2-1/2 Fe_2O_3 plot (Fig. 65). The amount of Fe^{3+} present in the entire bulk composition is assumed to remain constant throughout.

In the peak M_1 assemblage, Fe^{2+} resided primarily in spinel, garnet, and cordierite, Fe^{3+} in ilmeno-hematite and spinel, and Ti in rutile and ilmeno-hematite. On Fig. 65, a point in the field of coexisting rutile + ilmeno-hematite is selected to represent this initial assemblage.

During the first late-M_1 retrograde reaction, garnet and ilmenite formed at the expense of spinel, rutile, and cordierite. As Ti was transferred from rutile to ilmenite, it must have been accompanied by an equivalent amount of Fe^{2+} (which would have been derived from spinel, garnet, or cordierite). In addition, as spinel broke down, any Fe^{3+} formerly held in solid solution would have gone into ilmeno-hematite. As a result, this late-M_1 reaction involved a net <u>increase</u> in the modal content of Fe-Ti oxide minerals.

The addition of Fe^{2+} and Fe^{3+} to the Fe-Ti oxides would also lead in a shift of the "bulk" composition plotted on Fig. 65. This composition would migrate downwards, until meeting the ilmenite-hematite join as the last rutile was consumed. The exact direction of the downward shift would depend on the relative inputs of Fe^{2+} and Fe^{3+}.

During the next stage of late-M_1, garnet and magnetite formed at the expense of spinel, ilmenite, and cordierite. Ti moved from ilmeno-hematite to titaniferous magnetite (magnetite-ulvospinel$_{ss}$). Fe^{3+} was transferred from ilmeno-hematite and spinel to magnetite. Fe^{2+} moved from ilmenite, spinel, and cordierite to magnetite and garnet.

The Ti/Fe^{2+} ratio of the reactant ilmeno-hematite was probably much greater than that of the product titaniferous magnetite. If so, the silicate minerals must have again contributed Fe^{2+} to the oxide phases, leading to still greater modal amounts of Fe-Ti oxides.

The trend towards increasing amounts of Fe-Ti oxides was reversed during M_2. Textures show that biotite formed at the expense of cordierite, magnetite, spinel, and (to some extent) garnet. At the end of M_2, Ti and Fe^{3+} resided in ilmeno-hematite, in magnetite, and in biotite.

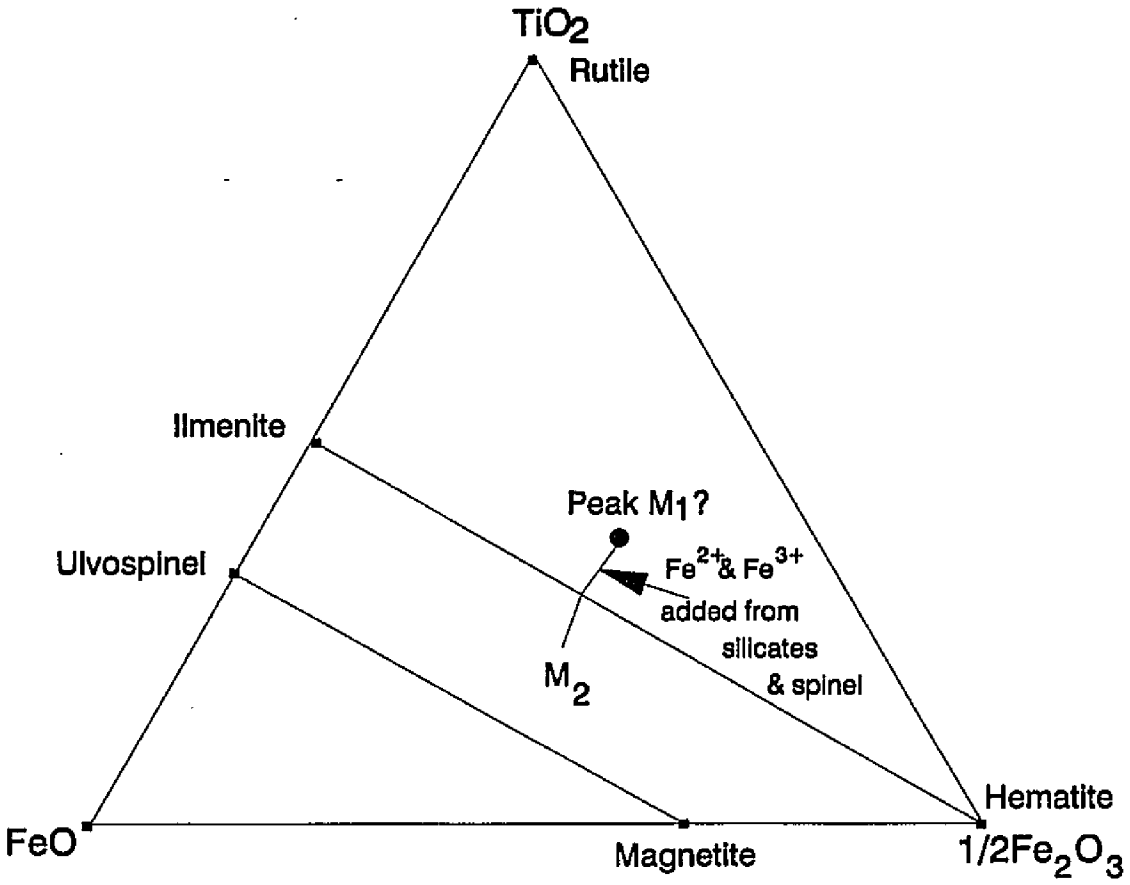

Fig. 65. Qualitative changes in the Fe-Ti oxide compositions of late M_1 aluminous assemblages. See text for discussion.

As Ti and Fe^{3+} were transferred from oxide to silicate phases, some proportion of oxide Fe^{2+} must also have moved. With M_2 reactions, modal Fe-Ti oxides generally dropped from 4 to 6 modal percent to 2 percent or less.

The varied colors of M_2 biotites reflect inputs from the oxide phases. Deep-reddish brown or dark greenish-brown biotites are common in rocks containing ilmenite + magnetite; more reduced, graphite-bearing rocks contain deep-red biotite. However, patches of very pale or light-green biotite can occur alongside the predominant red or brown grains. These pale biotites pseudomorph cordierite in micro-domains where opaque minerals are absent. Contributions of Ti and Fe^{3+} from the oxide phases evidently controlled the colors of M_2 biotites.

Hayama (1959) observed that biotites with high-Ti contents have deep red-brown colors, while low-Ti biotites which have high Fe^{3+} contents are green. The dark greenish-brown biotites probably contain both substantial Ti and Fe^{3+}, while the deep red colors seen in graphite-bearing rocks indicate high Ti and but very low Fe^{3+}.

G. Petrogenetic grid for late-M_1 and M_2 reactions in aluminous rocks. Textures indicate that quartz, garnet, sillimanite, cordierite, spinel, biotite, ilmenite, rutile, magnetite, and melt were major participants in retrograde reactions during late-M_1 and M_2. These phases can be represented by the components K_2O, FeO, MgO, Al_2O_3, SiO_2, H_2O, TiO_2, and O_2 (KFMASHTO).

Clarke, Powell and Guirand (1989) and Clarke and Powell (1991a and b) proposed a petrogenetic grid for the system KFMASHTO in portions of the granulite facies. Fig. 66, a qualitative P-T diagram in projection from quartz, K-feldspar, and melt, is an adaptation of Fig. 5 from Clarke and Powell (1991b). This projection is appropriate for use here since quartz, K-feldspar, and anatectic leucosomes coexist with most late-M_1 and M_2 assemblages.

The assemblage spinel + cordierite + rutile + ilmenite existed at the thermal peak. As cooling began, the rocks passed through the inferred late-M_1 reactions

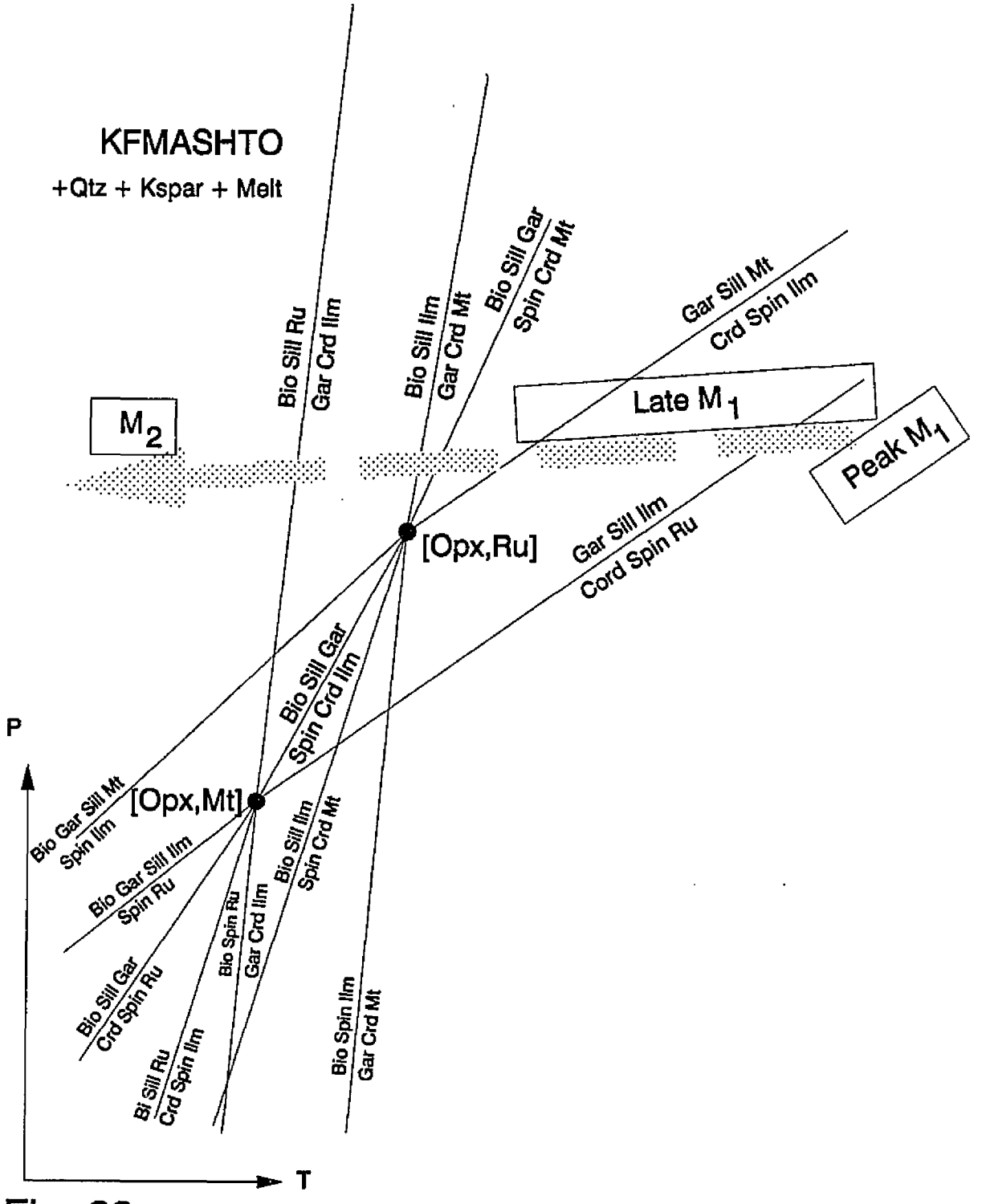

Fig. 66. Qualitative P-T diagram for K_2O-FeO-MgO-Al_2O_3-SiO_2-H_2O-TiO_2-O_2 (KMASHTO) in the projection from quartz, K-feldspar, and melt, showing the inferred P-T path from peak M_1 through M_2. Diagram after Clarke & Powell (1991b, Fig.5). For abbreviations, see Fig. 60.

spinel + cordierite + rutile = garnet + sillimanite + ilmenite

and

spinel + cordierite + ilmenite = garnet + sillimanite + magnetite.

There is good textural evidence (discussed earlier) for both of these reactions.

The replacement of spinel and cordierite by biotite, and the nucleation of biotite on magnetite during the M_2 stage is consistent with two reactions on Fig. 66:

spinel + cordierite + magnetite = biotite + sillimanite + garnet, or

garnet + cordierite + magnetite = biotite + sillimanite + ilmenite.

As the observed M_2 assemblage consists of biotite + sillimanite + garnet + ilmenite + magnetite, either or both of these reactions may have taken place.

The four proposed reactions from Clark and Powell's petrogenetic grid considered so far are supported by textural relationships and mineral assemblages from rocks of the study area. The geometry of their grid implies that this sequence of retrogressive reactions may have taken place during near-isobaric cooling (Fig. 66).

The next "down-temperature" reaction on the petrogenetic grid,

garnet + cordierite + ilmenite = biotite + sillimanite + rutile

is not observed in the study area, since rutile does not occur in M_2 assemblages. This reaction may have been prohibited by previous retrograde reactions; virtually all cordierite may have been consumed by this stage. In addition, judging from textures in late-M_1 assemblages, what little cordierite remained did not coexist with ilmenite, since coronas of late-M_1 sillimanite or garnet covered all mutual contacts.

Where Fe-Ti oxide minerals were not available, M_2 retrogression could have continued as the KFMASH reaction

garnet + cordierite + K-feldspar = biotite + sillimanite

or, where garnet was not available,

cordierite + K-feldspar = biotite + sillimanite.

These reactions could have generated the pale biotite observed as pseudomorphs after cordierite.

H. Post-M_2 retrogression of surviving cordierite-bearing assemblages. Taconian F_2 and F_3 deformation and fabric development were associated with M_2 assemblages. Most late-M_1 assemblages were replaced or heavily overprinted during these episodes of deformation. A small amount of cordierite did survive M_2 metamorphism; however, much of this cordierite underwent partial or complete retrogression after deformation ceased.

The post-M_2 alteration of cordierite followed two parallel sequences of retrograde reactions. Where K-feldspar was available, reactions in the KFMASH system took place, resulting in the formation of biotite. In K_2O-deficient domains, retrogression proceeded in the FMASH system.

Retrogression in KFMASH (K_2O-FeO-MgO-Al_2O_3-H_2O). Fig. 67A illustrates the retrogressive sequence in the KFMASH system. During M_2, cordierite had broken down to biotite + aluminosilicate (+ garnet, where hercynite or another Fe-rich phase was involved). These reactions had produced the biotite and sillimanite grains that defined late Taconian fabrics (e.g., Fig. 35). However, unfoliated masses of biotite and kyanite (Fig. 61B) later formed as pseudomorphs after cordierite. This post-M_2 stage of retrogression evidently occurred after the region had cooled past the sillimanite = kyanite equilibrium (1, Fig. 60). The unfoliated character of the assemblage implies that it is post-kinematic.

Post-M_2 retrogression passed from an early stage where biotite + garnet + kyanite assemblages were stable, down-temperature to a later stage where staurolite-bearing parageneses were formed (Fig. 67A). During the earlier stage, kyanite grew into grains of cordierite, biotite, or garnet. However, some rocks which show this early assemblage also contain late staurolite. This staurolite coexists with kyanite, biotite, and/or garnet. Muscovite is also present. Staurolite appears to have formed by the reaction

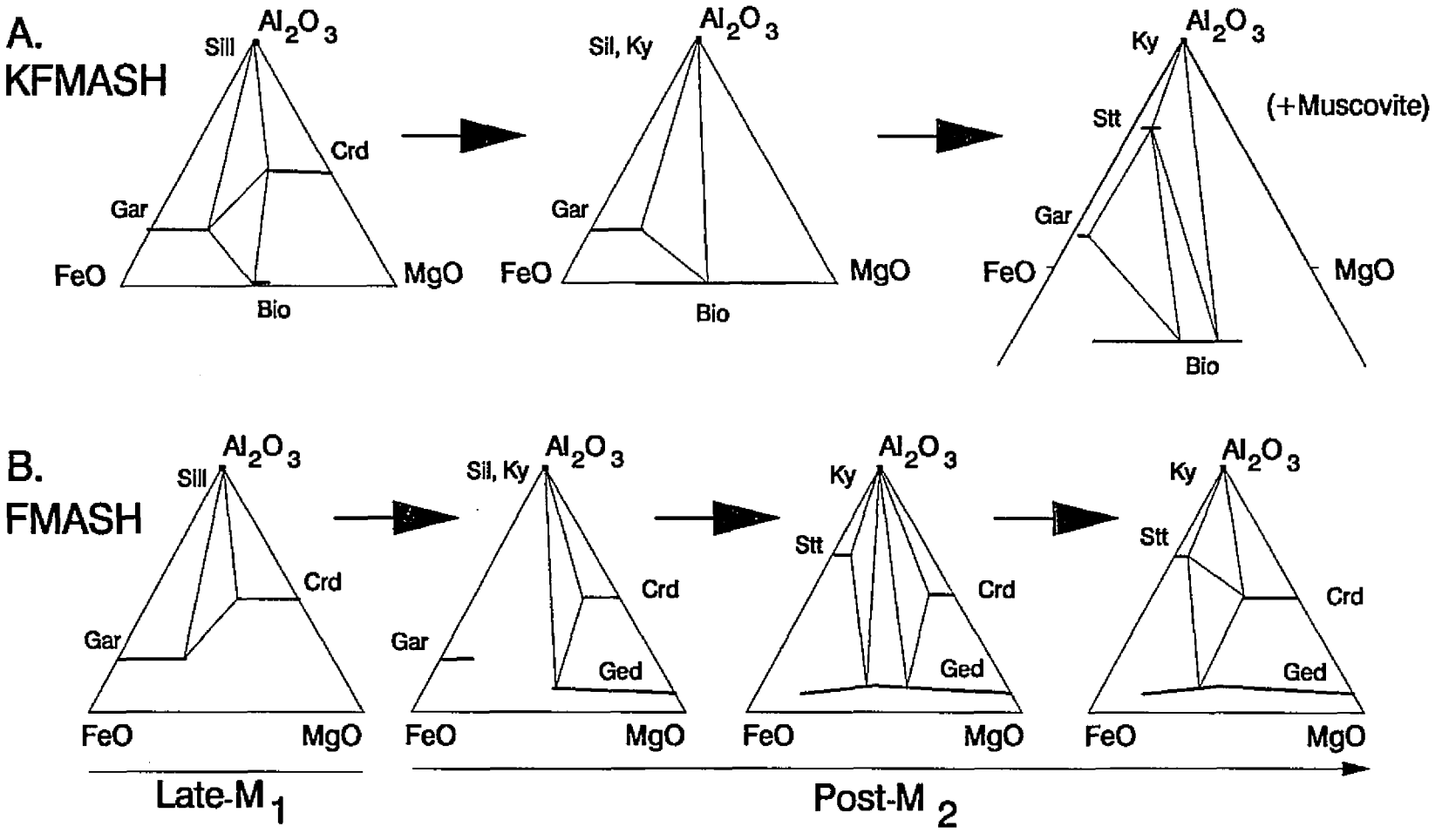

Fig. 67. Post-M_2 retrogression of cordierite-bearing assemblages that survived M_2 metamorphism. Assemblages are shown on AFM diagrams and on Thompson's (1957) AFM muscovite projection Slopes of FMASH tie lines are based on Harley (1986). Abbreviations as on Fig.60.

garnet + biotite + kyanite = staurolite + muscovite.

The P/T conditions associated with this later stage of retrogression can be estimated from the intersection of the reaction

garnet + biotite + aluminosilicate = staurolite + muscovite

(reaction 9, Fig. 60), with

kyanite = sillimanite (1, Fig. 60).

These two equilibria, combined, indicate a minimum pressure of 8 kilobars and minimum temperature of 700°C for cases where $P_{Total} = P_{H2O}$, assuming garnets are almandine-pyrope$_{ss}$ (Spear and Cheney, 1989). If $P_{Total} > P_{H2O}$ during post-M_2 retrogression, the staurolite-forming reaction would be displaced down-temperature.

Retrogression in FMASH (FeO-MgO-Al_2O_3-SiO_2-H_2O). Where K-feldspar was not available, retrogressive reactions belonging to the FMASH system occurred. In these instances, orthoamphibole (gedrite) plus aluminosilicate minerals locally replaced cordierite (Fig. 63B). Gedrite is intergrown with sillimanite in some places, intergrown with kyanite in others. These textures imply that the replacement of cordierite by gedrite + aluminosilicate, (like its replacement by biotite + aluminosilicate) proceeded as the region cooled through the sillimanite = kyanite equilibrium. The coexistence of gedrite with kyanite, and the absence of gedrite in tectonic fabrics, indicate that the formation of gedrite post-dates Taconian-aged M_2 assemblages.

Staurolite-bearing parageneses (cordierite + staurolite, gedrite + staurolite) appeared in the FMASH sequence with continued cooling. Fig. 67B illustrates the sequence of tie-lines for the FMASH retrogressive assemblages.

Harley (1985) studied assemblages involving gedrite in the FMASH system. He developed a "semi-quantitative" petrogenetic grid for conditions where $P_T = P_{H2O}$. Three equilibria from his grid are plotted onto Fig. 60 (reactions 10, 11, and 12). Reactions (10) and (11) define the limits of the stability field for gedrite + aluminosilicate.

Fig. 60 shows that the assemblage gedrite + aluminosilicate is restricted to pressures greater than 6 kilobars for $P_{Total} = P_{H2O}$. Retrogressive replacement of cordierite by gedrite + aluminosilicate requires minimum temperatures of ~670°C. Staurolite-bearing assemblages would develop temperatures continued to drop.

Summary. Retrogressive post-M_2 replacement of cordierite by KFMASH and FMASH assemblages occurred post-kinematically, as the region cooled past the sillimanite = kyanite equilibrium. Post-M_2 retrogression did not necessarily take place at temperatures and pressures as high as those implied by reactions (9) to (12) (Fig. 60); the values of P_{H2O} which accompanied post-M_2 retrogression probably varied a good deal, but were almost certainly less than P_{Total}. Still, the KFMASH and FMASH retrogressive assemblages (along with other assemblages discussed earlier) help constrain the regional P-T trajectory and place M_2 at relatively high pressures (6 to 11 kilobars) and temperatures (700° to 850°C) (Fig. 60).

This concludes discussion of M_1-M_2 assemblages in the aluminous rocks. A brief summary of M_1-M_2 parageneses in rocks of other bulk compositions follows:

M_1-M_2 METAMORPHISM, NON-ALUMINOUS LITHOLOGIES. The "non-aluminous" lithologies have been divided into the following compositional categories: quartz-feldspar granofelses; calc-silicate rocks and calcareous marbles; dolomitic marbles; and metabasites. The nature of M_1-M_2 mineral assemblages in each compositional category will be discussed separately.

<u>M_1-M_2 assemblages, quartz-feldspar granofelses.</u> Granofelsic rocks generally contain some combination of quartz, K-feldspar, plagioclase, biotite, and garnet, depending on their bulk compositions. The plagioclase can be rich in anorthite (see Figs. 19, 25, and 28). In granofelses of more calcic compositions, hornblende or clinopyroxene may occur. These lithologies grade into

calc-silicate rock.

The biotite-bearing mineral assemblages are consistent with M_2 upper-amphibolite-facies metamorphic grade. However, two specimens of quartz-feldspar granofels, both from Walloomsac Schist, contain relict orthopyroxene-bearing assemblages that are not compatible with the amphibolite facies.

One of these specimens, #1603b, is a calcareous granofels with an extremely calcic ($\sim An_{80}$) plagioclase. This rock has a well-developed S_1 foliation, defined by alternating quartz ribbons and trains of plagioclase, which give the rock a fine-laminated appearance.

Grains of ortho- and clinopyroxene occur in neighboring "laminae". Most grains of clinopyroxene are surrounded and embayed by pale green hornblende. A rust-stained grain, lying in contact with clinopyroxene, appears to be an altered orthopyroxene. Orthopyroxene and clinopyroxene apparently coexisted in this specimen during M_1.

The other minerals in specimen #1603b include garnet, ilmenite, and pyrrhotite. The garnet is poikiloblastic, and encloses plagioclase and quartz. K-feldspar occurs in hand specimen, but is not present in the thin section. Red biotite grows in irregular patches around quartz and feldspar; it appears to post-date the "laminated" S_1 fabric.

Taken together, the textural and mineralogical relationships indicate that the hornblende and biotite formed during M_2. The biotite probably formed during a reaction involving orthopyroxene, such as

orthopyroxene + ilmenite + K-feldspar = biotite + quartz.

The other orthopyroxene-bearing granofels, #1575, presently has layers of two contrasting compositions: (I) quartz + plagioclase + biotite + orthopyroxene + hornblende + cummingtonite + garnet and (II) K-feldspar + plagioclase + biotite + garnet. Modes for both layers are given on Table 7. The plagioclase is intermediate in composition ($\sim An_{50}$); accessory graphite, pyrrhotite, ilmenite, and magnetite are also present.

Textural relationships demonstrate that a minimum of two mineral assemblages are

present. The hornblende and cummingtonite grains cloak orthopyroxene; much of the biotite occurs in small patches around quartz, feldspar, and garnet; the garnet forms overgrowths over pyrrhotite and has crystal faces against biotite and plagioclase. Grains of hornblende, cummingtonite, biotite, and garnet evidently grew late, presumably during M_2.

In contrast, the orthopyroxene, quartz, plagioclase, K-feldspar, and pyrrhotite in this rock predated M_2 alteration. These minerals evidently once belonged to an older, M_1 assemblage. Although grains of orthopyroxene and K-feldspar are not currently in contact, they do occur in close proximity, in adjacent layers. Coexistence of these minerals during M_1 is inferred.

Summary. M_1 mineral assemblages in quartz-feldspar granofelses included orthopyroxene + K-feldspar, and, in calcareous compositions, orthopyroxene + clinopyroxene. The biotite, hornblende, and at least some of the garnet observed in these rocks either partially or entirely post-date the M_1 metamorphic peak. These later minerals were stable during M_2.

M_1-M_2 assemblages, calc-silicate rocks and calcareous marbles. The calc-silicate rocks and marbles generally contain some combination of the following minerals: calcite, diopside, quartz, K-feldspar, plagioclase, and sphene. Many calc-silicate rocks also contain hornblende, which replaces diopside in a number of cases. Marbles of the Walloomsac Schist generally carry red biotite as well. Fig. 24 gives tie-lines for the predominant assemblages on SiO_2-MgO-CaO and quartz-K-feldspar-dolomite plots. These mineral assemblages are consistent with the upper-amphibolite-facies grade of M_2, but may also have existed during the later stages of M_1.

In addition to these phases, scapolite occurs in intergrowths with diopside and/or plagioclase in several specimens. This scapolite is moderately to highly calcic. Compositions, determined from refractive indices, range from 70 +/-5% to 85 +/-10% meionite (calcic) component. Scotford (1956) reported scapolite of similar composition from this area.

Experimental work has shown that highly calcic, meionite-rich scapolites are restricted to

high-temperature metamorphic rocks. The meionite-end member replaces the assemblage anorthite + calcite at temperatures above 870°C (Goldsmith and Newton, 1977). This reaction is insensitive to both pressure and fluid-phase composition. Typical granulite-facies scapolites, which contain X_{mei} of 75 to 85%, form at lower temperatures.

Almost all the plagioclase that coexists with calcite in the marbles and calc-silicate rocks of the study area is sodic in composition. This plagioclase is generally An_{23} to An_{33}, and almost invariably $<An_{40}$, even though many quartz-feldspar granofelses, metawackes, and calcite-free calc-silicate rocks contain highly calcic plagioclases. The one known exception is a calcic ($\sim An_{78}$) plagioclase that occurs with both calcite and a highly calcic (85+/-10% meionite) scapolite. Evidently, most of the calcic plagioclase that once may been have present in calcitic rocks has reacted with calcite to produce scapolite. This reaction would have occurred during M_1 prograde metamorphism.

Summary. Scapolite replaced anorthite-rich plagioclase + calcite during M_1. Many other minerals in the calc-silicate rocks, such as diopside, quartz, and K-feldspar, were probably stable during both M_1 and M_2. Hornblende is most likely of M_2 origin.

M_1-M_2 parageneses, dolomitic marbles. Most metamorphic assemblages of the dolomitic marbles appear to be M_2 in age, but a few clues regarding earlier metamorphic stages persist. Observations bearing on the marbles' metamorphic history will be discussed in the following order: 1) the predominant mineral assemblages; 2) relations among aluminous minerals; 3) exsolution in carbonate minerals; 4) pyroxene relationships; and 5) post-M_2 retrogression.

1. M_2 metamorphic assemblages. The main assemblages of the Inwood Marble include

a) dolomite + forsterite +/- phlogopite,

b) dolomite + forsterite + calcite +/- phlogopite, and

c) calcite + forsterite + diopside +/- phlogopite.

Tie-lines for these assemblages are shown on Fig. 24. These assemblages are consistent with M_2 upper-amphibolite-facies metamorphism.

2. Relations among aluminous minerals. Phlogopite is the dominant Al-bearing phase observed in the dolomitic marbles. Other Al-bearing phases, except for spinel, occur in trivial amounts. Fassaite, a clinopyroxene rich in Fe^{3+} and Al, has been identified in one specimen (#CT-20). Traces of scapolite occur in a couple rocks. One specimen (#1625), which shows textural evidence of metasomatism, has a substantial amount of scapolite (Table 6).

In a number of marbles, small amounts of pale, Mg-rich spinel coexist with calcite, dolomite, and forsterite. In one case, a deep-green, hercynitic spinel (partially replaced by phlogopite), is intergrown with magnetite and accompanied by calcite, scapolite, and forsterite (#1695b).

The question raised here is: from what mineral(s) did the spinel form? Given the alumina-poor character of the dolomitic marbles, there seem to be few alternatives: spinel most likely formed during M_1, as a product of the breakdown of phlogopite. The alteration to phlogopite shown by some grains of spinel seems to imply a reversal of the original, prograde reaction.

3. Exsolution in carbonate minerals. The dominant Ca-rich carbonate in spinel-bearing marble #CT-20 contains remarkably well-preserved exsolution textures. The exsolved phase has distinctively higher refractive indices than the host, and evidently is dolomitic. Coarse-grained, primary dolomite also occurs in the rock; it is distinguished from the Ca-rich carbonate by the absence of exsolution textures as well as by refractive indices.

The exsolved dolomite occurs in clusters of rods, which fan through the grains, apparently without regard to crystallographic orientation (Fig. 68). "Rods" tend to disappear near the periphery of the host grains (Fig. 68A and C). Instead, smaller, irregular grains of single-phase carbonate have grown along the grain boundaries (Fig. 68D).

A minority of Ca-rich carbonate grains are visibly zoned (Fig. 68B; C and D). Cores and

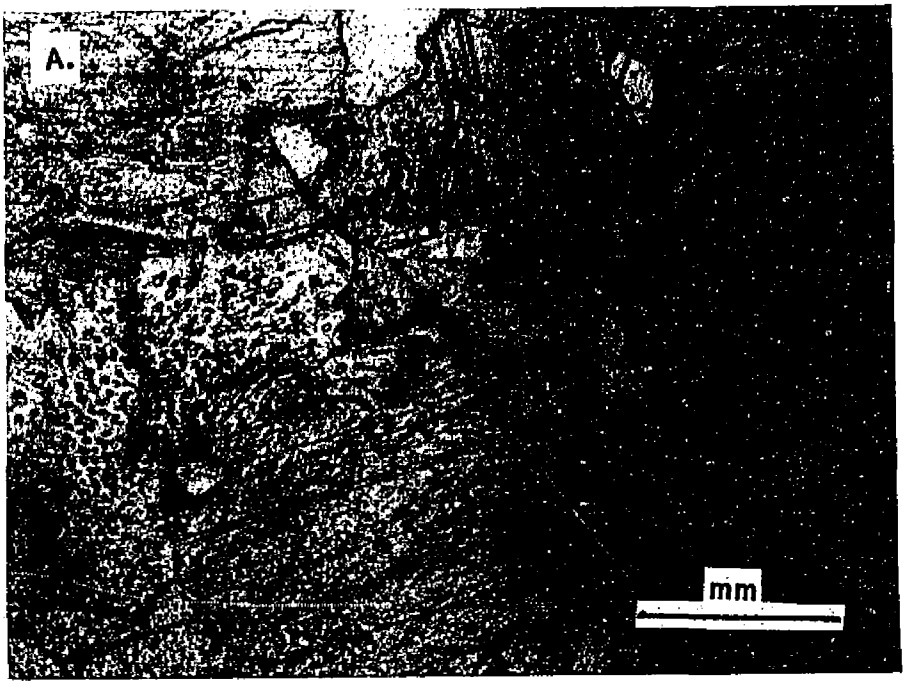

Fig. 68. Exsolution textures in carbonate minerals, specimen #CT-20.
(A) Exsolved rods of dolomite fan through calcite grains but are concentrated in cores.
(B) Optically discontinuous, zoned calcite grain, with dolomite rods nucleated along the core/rim boundary.
(C) and (D) are on the next page.

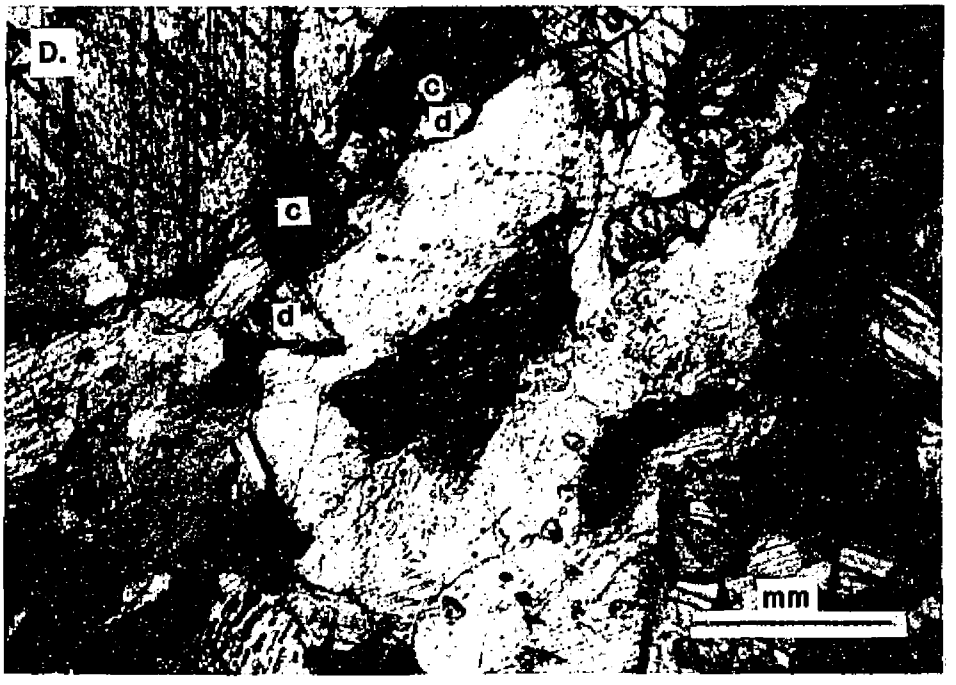

Fig. 68, continued. (C) and (D) Zoned calcite grain in two orientations, showing exsolved dolomite rods in both rim (C) and core (D). Rods disappear towards grain periphery. Small, single-phase calcite (c) and dolomite (d) grains occur alongside the zoned grain (D).

rims are optically discontinuous (Fig. 68B; C and D). Both the cores and the rims contain rods of dolomite, though dolomite seems to be more abundant in the cores. Exsolved grains preferentially occur along boundaries between the cores and rims (Fig. 68B). The exsolution of the rods clearly occurred after the creation of the zoned pattern.

According to Essene (1983), exsolved dolomite is hardly ever preserved inside calcite grains at high temperatures, with the result that thermometry based on the calcite-dolomite solvus is most useful for rocks metamorphosed in the 400-650° C temperature range. #CT-20, with its abundant exsolution, is evidently a rare exception.

The relative proportions of host and rod were examined in grains where a cross-sectional view of the rods is visible. The grains with the highest proportion of dolomitic rods were estimated to contain ~30% exsolved dolomitic carbonate. The exact compositions of the two carbonate phases are unknown. However, since Mg is much more soluble in calcite than Ca is in dolomite, the minimum Mg content of the original carbonate grain can be obtained by assuming the host to be pure calcite. Calcite with 15% $MgCO_3$ (30% dolomite) gives a minimum temperature of ~760°C (for a pressure of 9 kilobars) on Goldsmith and Newton's (1969) $CaCO_3$-$MgCO_3$ solvus curve.

4. Pyroxene relationships. In addition to extraordinarily well-preserved carbonate exsolution textures, CT-20 also contains a disequilibrium assemblage of silicate minerals. This assemblage includes components of probable M_1, M_2, and M_3 ages. Optical and X-ray study of this rock demonstrate that pyroxenes of at least three compositions are present: diopside, fassaite, and enstatite.

Enstatite has also been observed in a marble from the Croton Falls quadrangle. It might be a relict of M_1 metamorphism. Both the Croton Falls rock and CT-20 also contain spinel.

The pyroxenes are very difficult to distinguish petrographically, and their age-relationships are still unclear. More work will be needed to clarify the role played by pyroxenes in the

early phases of metamorphism.

5. Post-M_2 retrogression. Nearly all forsterite grains in the dolomitic marbles are encased in narrow rims of diopside. In many cases, grains of calcite near forsterite have been altered, apparently to dolomite. The textures suggest that the forsterite + calcite tie-line was broken in favor of dolomite + diopside. This reaction implies middle-amphibolite-facies grade, and may have occurred during post-M_2 cooling.

Summary. The most likely M_1 assemblages in dolomitic marbles consisted of dolomite, magnesian "calcite", +/- forsterite, pyroxene(s), and spinel. Spinel probably formed by decomposition of phlogopite during prograde metamorphism; it is unclear whether phlogopite was present at the peak of metamorphism. Phlogopite was certainly present during M_2.

Tie-lines on Fig. 24 reflect M_2 mineral assemblages, though these lines disregard the substantial dolomite-calcite solid solution that must have then existed. After M_2, rims of diopside formed over forsterite grains, probably as the forsterite + calcite tie-line was broken.

M_1-M_2 parageneses, metabasites. Orthopyroxene is abundant in much of the northern part of the study area, including Pierrepont State Park, where late-M_1 aluminous granulite assemblages are found in outcrop. Orthopyroxene is inferred to have been the dominant mafic mineral in many late-M_1 assemblages. Parageneses observed in the high-grade metabasites include

1) plagioclase + orthopyroxene + quartz (Fig. 5B)

and

2) plagioclase + orthopyroxene + clinopyroxene + quartz.

The stability of hornblende in late-M_1 assemblages is open to question. Textures in #CT-12A-89 (which contains the assemblage orthopyroxene + clinopyroxene) suggest that all hornblende in this specimen is secondary. In this and in many other metabasites, hornblende is observed rim-

ming or engulfing grains of pyroxene. However, in other cases, textural evidence for replacement is lacking. It is uncertain whether hornblende persisted in metabasites of certain bulk compositions throughout M_1, or whether rocks with texturally equilibrated hornblende were simply more completely recrystallized during M_2. Studies of whole-rock chemistry may help resolve this question.

M_2 assemblages in metabasites include the following:

1) hornblende + plagioclase + quartz +/- biotite

2) hornblende + garnet + plagioclase + quartz

3) cummingtonite + hornblende + plagioclase + quartz +/- biotite

Orthopyroxene commonly occurs in hornblende and/or cummingtonite amphibolites in the northern portion of the study area, though it has not been found in the south. Orthopyroxene is partially replaced by amphiboles in many specimens, but appears to coexist with the amphiboles in others. Possible explanations include a) orthopyroxene + amphibole is a relict late-M_1 assemblage; b) orthopyroxene locally survived metastably, along with M_2 amphibole; and c) orthopyroxene + amphibole is a stable M_2 assemblage in at least some bulk compositions.

The cummingtonite amphibolites come in two varieties, with and without garnet, but only the garnet-free assemblage is interpreted as M_2. In portions of some cummingtonite amphibolites, euhedral garnets grow over grains of magnetite and/or ilmenite, replacing cummingtonite, hornblende, plagioclase, and quartz. This replacement is local and partial; the paragenesis cummingtonite + hornblende + garnet thus appears to post-date cummingtonite + hornblende, and is therefore excluded from M_2.

EARLY CARBONIFEROUS METAMORPHISM - M_3

M_3 metamorphism left a complex and varied imprint on older, higher-grade assemblages. This imprint is most evident in D_6 shear zones, particularly near Mississippian granites.

In the following sections, the range of metamorphic grades recorded by aluminous rocks will be described first. This will be followed by discussions of the distinctive M_3 kyanite nodules, the nature of M_3 assemblages in non-aluminous lithologies, and finally, constraints on P-T conditions during the M_3 event.

M_3 METAMORPHIC GRADES RECORDED IN ALUMINOUS ROCKS.

1) Greenschist-facies assemblages. M_2 assemblages show some signs of greenschist-to-middle-amphibolite-facies retrogression at many localities, but the degree of recrystallization and the grade of the new mineral assemblages are variable. Minor amounts of alteration are most common. Patches of muscovite overprint old foliations, and parts of garnets are replaced by chlorite. Plagioclase is locally sericitized. Specimens showing minor retrogression to muscovite and chlorite commonly carry anatase, a polymorph of TiO_2 which is associated with low-temperature, hydrothermal environments (Lindsley, 1976, p. L-67).

Aluminous rocks in or near D_6 shear zones show the greatest degrees of M_3 recrystallization. In a few cases, the rock is recrystallized into a muscovite-chlorite-biotite schist. Old garnets are largely replaced by chlorite + muscovite, and old titaniferous biotites by chlorite grains which are criss-crossed with needles of rutile. These assemblages indicate greenschist-facies conditions; where dikes of Carboniferous granite are present, however, mineral assemblages are generally lower- to middle-amphibolite facies grade.

2) Lower-amphibolite-facies assemblages. Porphyroblasts of staurolite are prominent in the lower-amphibolite-facies aluminous schists. Large tourmaline crystals also occur. Chlorite

remains an important constituent of these rocks; their textures indicate that garnet + chlorite and staurolite + chlorite tie-lines are stable. However, the staurolite + biotite tie-line is not stable. Where porphyroblasts of staurolite overgrown relict M_2 biotite, they are surrounded by coronas of chlorite. Muscovite is moderate in abundance; it replaces both biotite and sillimanite of M_2 age.

3) Middle-amphibolite-facies assemblages. The two most striking characteristics of the middle-amphibolite-facies aluminous schists are a) the great abundance of muscovite (commonly 20 modal percent or more) and b) the numerous euhedral porphyroblasts of staurolite and garnet, each several millimeters in diameter. The euhedral garnets of these rocks contrast with the anhedral garnets characteristic of older assemblages. The schists are striking in appearance, with the euhedral porphyroblasts standing out against the silvery, coarse-grained, muscovite-rich matrix. Prisms of black tourmaline are also common, particularly along contacts with Carboniferous granites (Fig. 43B). Occurrences of chlorite are limited to small inclusions in garnets. Biotite occurs in small patches, mostly surrounded by muscovite. Sillimanite mainly occurs as inclusions in old garnets, though a trace may be present in the matrix, with micas.

Kyanite and/or sillimanite occur as sparse, euhedral crystals in certain M_3 assemblages. Kyanite is more abundant. Both aluminosilicate minerals are observed in contact with muscovite and with biotite. However, it is difficult to determine which mica/aluminosilicate pairs record equilibrium relationships. In some cases, biotite may be relict; in others, the aluminosilicate mineral might be. Some textures imply that late sillimanite formed after M_3 kyanite, implying increasing metamorphic grade, but further work is needed to completely resolve this question.

Chlorite inclusions occur inside garnets even where the staurolite + biotite tie-line appears to be stable and chlorite is absent in the rock matrix. Inclusions in M_3 garnet may consist of chlorite, of chlorite + biotite, or of chlorite + muscovite. Some garnets have internal crystal faces against these inclusions. Rocks with amphibolite-facies M_3 assemblages evidently first passed through a greenschist-facies phase, during which garnets were replaced by chlorite or chlorite +

muscovite.

Large crystals of tourmaline are abundant in M_3 assemblages. This abundance contrasts with the extreme scarcity of tourmaline in older, higher-grade aluminous parageneses. Most of the tourmaline originally present in the pelitic rocks was evidently lost during M_1-M_2 anatexis.

Fettke (1914) astutely observed many of the connections between the pegmatite dikes of the Manhattan Prong and the aluminous host rocks. He noted that kyanite was "apparently of contact origin", occurring where the schist was "saturated with pegmatitic material"; he identified "emanations" from the tourmaline-bearing granites as the source of similar-looking tourmaline found in adjacent host rock. It is unfortunate that his insightful comments have been forgotten or ignored through the intervening years.

KYANITE NODULES. Fettke (1914) was the first worker to note that "bands very rich in cyanite" occur with muscovite and quartz in some aluminous schists of the Manhattan Prong. These "bands", or nodules, of kyanite generally occur in aluminous schists that are immediately adjacent to dikes of Carboniferous granite. The nodules have irregular, bulbous shapes (Fig. 69A), and are up to ~10 centimeters in length. They consist of >80% euhedral kyanite, plus (in descending order) minor staurolite, fibrolitic sillimanite, muscovite, biotite, quartz, apatite, and tourmaline.

A kyanite-free mineralogic "front" commonly occurs in borders around the nodules. The "front" is composed of quartz and muscovite grains that contain needles of acicular sillimanite (Fig. 69B). Intergrowths of muscovite + fibrolitic sillimanite and quartz + fibrolitic sillimanite comprise the matrix of the nodules (Fig. 69C). The proportion of fibrolite in many of these intergrowths is very high; in some places, no sign of quartz or muscovite is visible, and fibrolite alone apparently forms dense, solid mats. Coarse-grained, euhedral kyanite and staurolite overgrow the matted sillimanite, the muscovite-fibrolite intergrowths, and quartz-fibrolite intergrowths (Fig. 69C). In one nodule, a few prisms of young sillimanite cut the kyanite crystals.

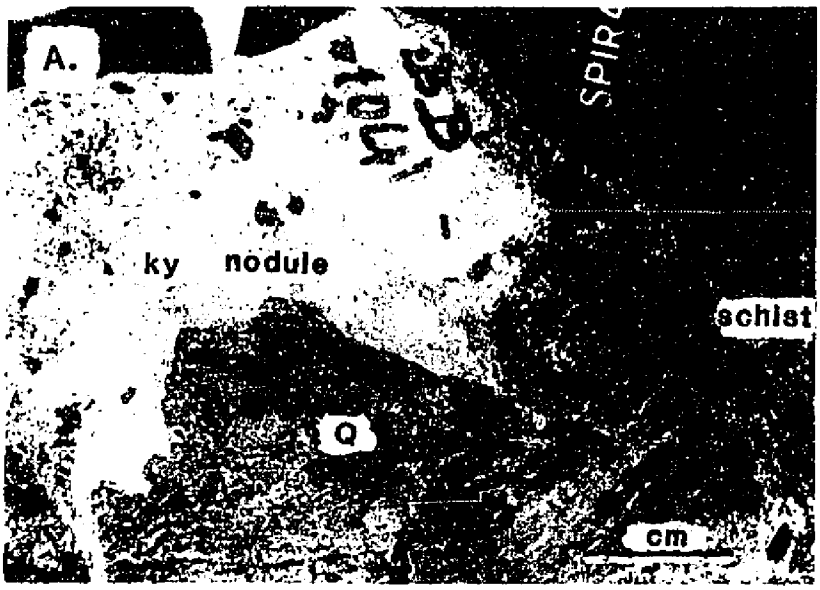

Fig. 69. M_3 kyanite nodule, specimen #1041, Manhattan Schist, Turkey Hill fault zone.
(A) Irregular contact between kyanite nodule (white, with brown staurolite porphyroblasts) with aluminous schist and vein quartz. Manhattan Schist, specimen #1041.
(B) and (C) are on the next page.

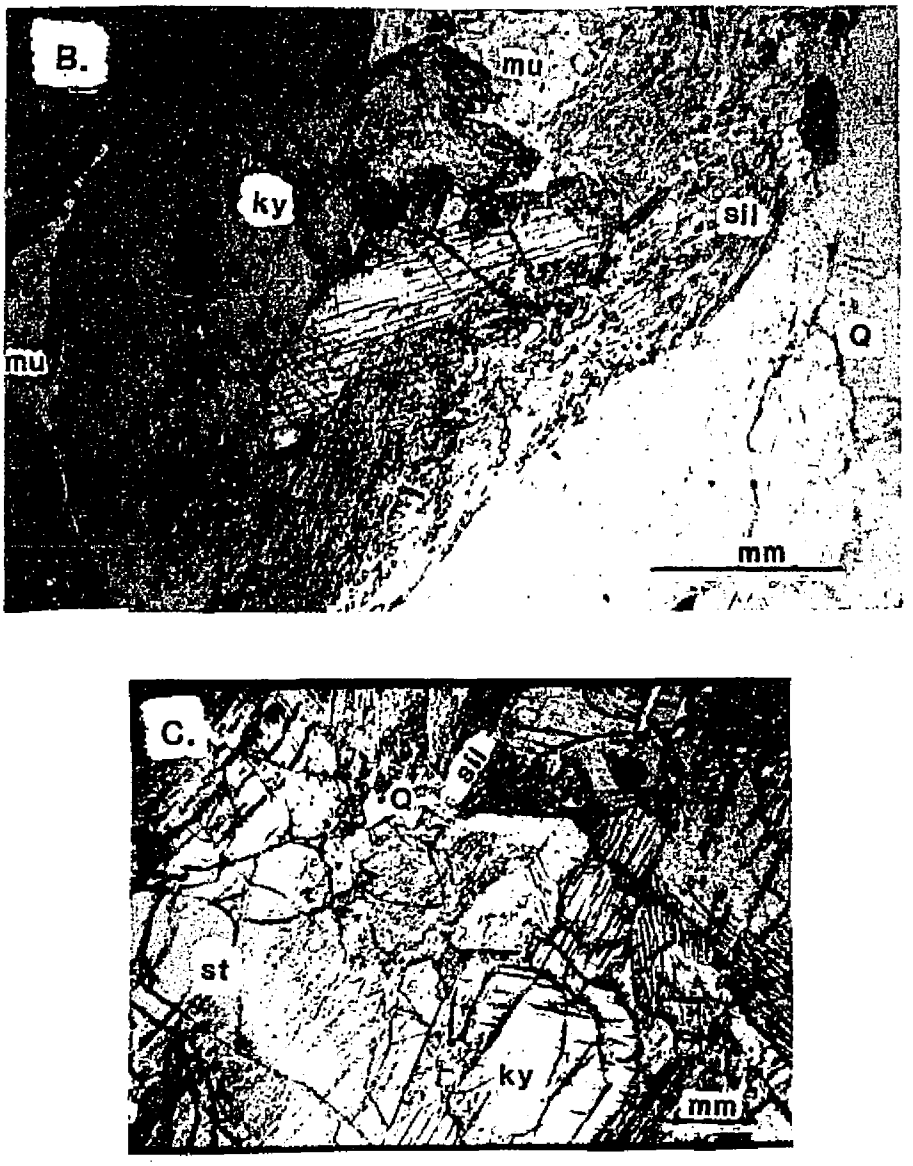

Fig. 69, continued. Specimen #1041b.

(B) Sillimanite "front" on kyanite nodule. Sillimanite (sil) occurs in quartz (Q) and muscovite (mu).

(C) Core of nodule. Porphyroblasts of staurolite (st) and kyanite (ky) overgrow and enclose a matrix of quartz densely packed with aligned sillimanite (-sil-) needles.

The textures suggest two independent processes: 1) a progressive enrichment in alumina, as fibrolite replaced quartz and muscovite, ending in the development of solid mats of sillimanite; and 2) the transformation of fibrolite to kyanite within the nodules. Both these processes require careful consideration.

Alumina is generally thought as one of the least mobile chemical components during metamorphism. Yet, alumina must have undergone substantial transport in order to form the several-centimeter-in-diameter nodules of 80% kyanite.

Nodules of aluminosilicate minerals are uncommon, but they are not unique to the Manhattan Prong. Kerrick (1990) reviewed many occurrences of aluminosilicate nodules and discussed possible mechanisms of formation. Of the occurrences he describes, the nodules of the Manhattan Prong are most similar to nodules found in the aureoles of the Donegal Granites in Ireland. In this occurrence, swarms of fibrolite needles transect muscovite grains; the fibrolite is overgrown by coarse sillimanite prisms. The nodules are closely associated with tourmaline. These nodules were interpreted to be the products of metasomatism, attributed to the flow of boron-bearing magmatic fluids (Pitcher and Read, 1963; Kerrick, 1987).

A comparable origin can be inferred for the M_3 aluminosilicate nodules, associated as they are with dikes of tourmaline granite. The presence of tourmaline may be vital for this aluminosilicate nodule-forming process; experimental work by Morgan and London (1989) suggests that the solubilities of Al and Si are enhanced by the presence of boron in aqueous fluids.

Fibrolite of the M_3 nodules is directly overgrown by kyanite, not by sillimanite. A question then follows: what is the relationship between these aluminosilicate minerals? The alternatives include:

1) fibrolite in the nodules formed early, at higher temperatures, near the still-crystallizing granite dikes; later, with cooling, fibrolite was transformed into kyanite; or

2) fibrolite in muscovite and quartz grew metastably (while P-T conditions were in the kyanite field), to be later replaced by the stable kyanite phase.

A definitive choice cannot presently be made between these two alternatives. However, the fact that kyanite is the dominant mineral in all M_3 nodules appears to favor the second. Kerrick (1990) noted that considerable evidence for the metastable growth of fibrolite is available; fibrolite growth in micas and quartz may be favored for kinetic reasons.

M_3 ASSEMBLAGES IN NON-ALUMINOUS LITHOLOGIES. Many varieties of greenschist-through-middle amphibolite-facies retrogressive assemblages occur in D_6 shear zones and in surrounding areas. Calc-silicate rocks and marbles offer some of the best examples.

In calc-silicate rocks, calcite + plagioclase is commonly replaced by poikiloblastic clinozoisite. This reaction indicates, unsurprisingly, that a water-rich (CO_2-poor) fluid phase accompanied M_3 retrogression (Storre, 1970). This reaction evidently proceeded very readily; clinozoisite occurs in calc-silicate rocks even where other forms of M_3 recrystallization are modest.

Two other forms of M_3 retrogression have been observed in some calc-silicate rocks:

1) Poikiloblastic tremolite crystals locally cross-cut and replace diopside. Tremolite replaces the M_2 assemblage, quartz + diopside + calcite (Fig. 24A). Instead, quartz + tremolite + calcite locally coexist (Fig. 70A).

2) Diopside is replaced by phlogopite in quartz-bearing assemblages. The M_2 tie-line K-feldspar + diopside (Fig. 24B) has been broken in favor of phlogopite + quartz (Fig. 70B).

These retrograde assemblages are consistent with lower- to middle-amphibolite facies grade of M_3 recrystallization.

The serpentinization of olivine is the most common form of M_3 retrogression observed in the dolomitic marbles. Olivine grains are fringed by serpentine, criss-crossed by veins of serpentine, or are completely pseudomorphed. Only a small proportion of marbles completely escaped serpentinization.

Brucite occurs with serpentine in marbles at some localities. In addition, brucite and a carbonate (dolomite?) locally replace spinel. Tremolite euhedra cut across diopside grains in the

Fig. 70. M_3 assemblages in marbles and calc-silicate rocks.

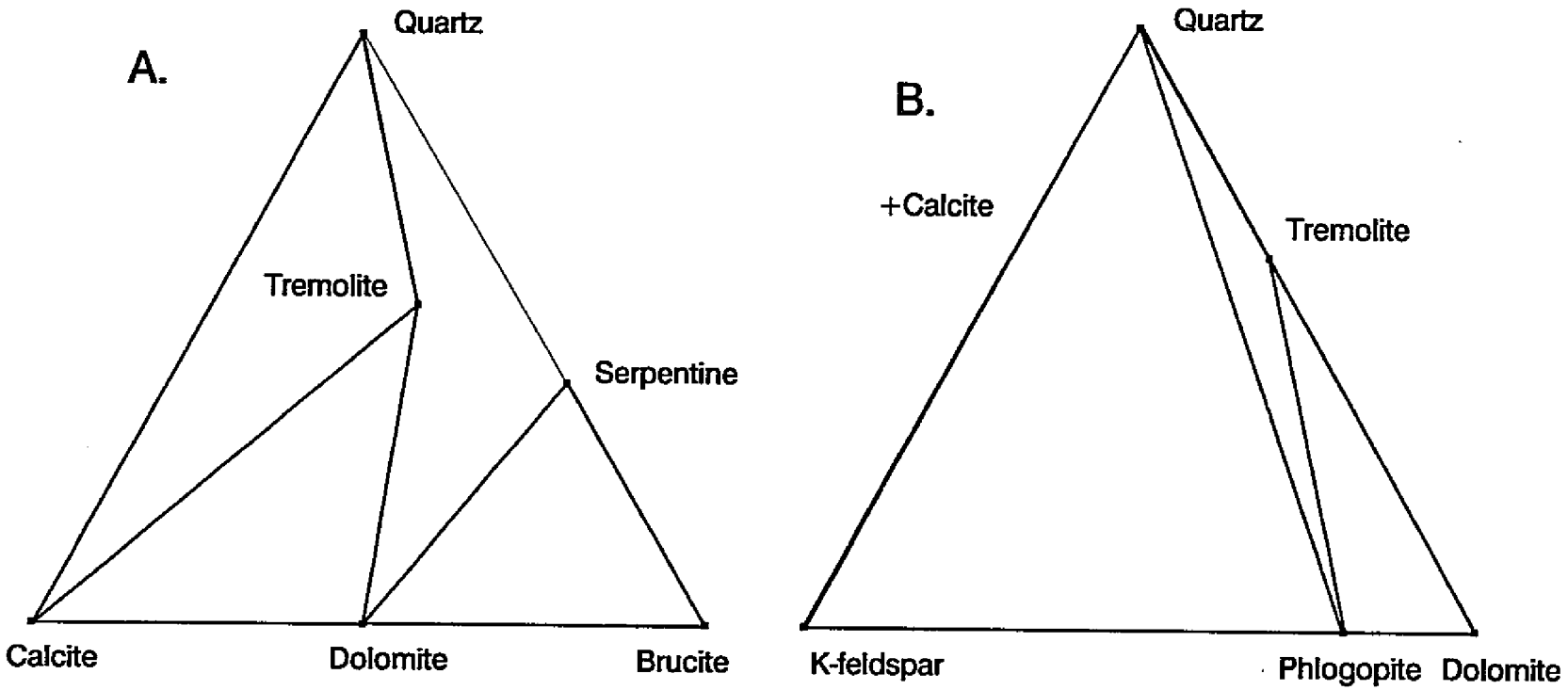

more siliceous M_3 assemblages. Fig. 70 shows the M_3 tie-lines inferred for the dolomitic marbles.

The effects of M_3 metamorphism leave fewer obvious marks on the metabasite lithologies. Amphibolites they were (during M_2), amphibolites they remained. However, a number of retrogressive features can be identified.

Several amphibolites contain M_3 epidote, generally in trace amounts. M_3 amphiboles appear to differ compositionally from M_2 amphiboles; amphibolites from D_6 shear zones tend to have pale blue-green or green hornblende, rather than the usual olive-colored amphibole. The most visually striking change in many metabasites, however, is the rimming (or replacement) of ilmenite grains by sphene. In the sphene-rich amphibolites, plagioclase grains are zoned, with rims more albitic (e.g., An_{40}) than the cores (e.g., An_{50}, #1303). Calcium from the plagioclase appears to have combined with ilmenite in order to form sphene.

P-T CONDITIONS, M_3 METAMORPHISM. The highest-grade, amphibolite-facies M_3 mineral assemblages occur in D_6 shear zones and, in particular, near Carboniferous granites. Greenschist-facies assemblages occur in areas with few (if any) granite dikes. The M_3 event was evidently a form of hydrothermal-cum- contact metamorphism.

Before the commencement of M_3, and beyond the reach of M_3 hydrothermal fluids, prevailing temperatures must have been below those recorded by the lowest-grade M_3 assemblages. The assemblage serpentine + brucite sets an upper limit on the temperatures experienced during lowest-grade M_3 recrystallization. At 7 kilobars (or lower) pressure ($P_{Total} = P_{H2O}$), this assemblage is restricted to temperatures below ~470° C (Johannes, 1968). The greenschist-facies alteration to chlorite + muscovite observed in the aluminous rocks, and the formation of clinozoisite in the calc-silicate rocks, are also consistent with temperatures below 470°C.

The absence of andalusite in M_3 assemblages sets minimum pressure at around 4 kilobars (Fig. 60). Peak- M_3 is represented in the aluminous rocks by the assemblage staurolite + muscovite + biotite; aluminosilicate (sillimanite and/or kyanite) may have coexisted with biotite.

The minimum temperatures for peak aluminous assemblages can be estimated from Spear and Cheney's (1989) quantitative petrogenetic grid for the system KFMASH. Given a pressure of 4 kilobars, they indicate that the staurolite + biotite tie-line becomes stable at ~550°C, replacing garnet + chlorite (assuming the garnet to be an almandine-pyrope$_{ss}$). Spessartine and grossular components in garnets displace this temperature upwards. Where garnets contain MnO + CaO/MnO + Ca + MgO + FeO = ~0.2, minimum temperature needed to stabilize the staurolite + biotite tie-line would be ~570°C (Spear and Cheney, 1989, Fig. 4). The minimum temperature required for coexistence of sillimanite with biotite at 4 kilobars would be about 585°C. If pressure were greater than 4 kilobars, somewhat greater minimum temperatures would be required to stabilize both the staurolite + biotite and aluminosilicate + biotite tie-lines.

MINERAL COMPOSITIONS AND GARNET-BIOTITE THERMOMETRY FOR M_3 ASSEMBLAGES. Limited compositional data on M_3 assemblages are presently available. In 1979, P. W. G. Brock and I obtained analyses of a few garnets, biotites, staurolites, and a muscovite from specimen #187, an aluminous schist from the (D_6) Turkey Hill fault zone in the southwestern Peach Lake quadrangle (Plate III). The compositions are given on Table 16. The rock contains a muscovite + staurolite + garnet + biotite assemblage. Garnets and staurolites are euhedral; some garnets contain chlorite inclusions.

Mineral compositions in #187 are consistent with other constraints on M_3 metamorphism. The muscovite has substantial paragonite and phengite components, suggestive of moderate- to low-grade conditions. The garnet "core" composition (gar 2) is Mn-rich (X_{Mn}=.18) relative to rim (gar 1, X_{Mn}=.10) and relative to older, M_1-M_2 garnets (Table 15). This kind of compositional zoning is common in lower-amphibolite-facies rocks, and suggests that M_3 garnet growth began during cool conditions and continued as temperature increased. Mg-rich biotite (bio 1) occurs as an inclusion in garnet.

Compositions of garnet rim (gar 1) can be paired with those of matrix biotite (bio 2) for

TABLE 16

MICROPROBE ANALYSES FROM AN M_3 ASSEMBLAGE (#187)

	stt 1	stt 2	gar 1	gar 2 (core)	bio 1 (in stt)	bio 2	musc
SiO_2	27.87	27.51	37.91	37.98	36.36	36.81	45.64
TiO_2	0.52	0.55	0.07	0.30	1.20	1.46	0.45
Al_2O_3	55.12	55.02	21.94	22.10	19.40	20.10	34.38
FeO	14.46	14.45	31.59	29.46	16.13	17.44	2.89
MnO	0.27	0.24	4.44	8.15	0.07	0.08	0.0
MgO	1.70	1.88	3.49	3.77	11.82	11.44	0.73
CaO	0.03	0.01	2.93	1.40	0.03	0.02	0.01
Na_2O	0.09	0.11	0.10	0.12	0.34	0.40	1.27
K_2O	0.0	0.0	0.0	0.0	7.28	7.27	8.57
Total	100.06	99.77	102.47	103.28	92.63	95.02	93.94
------- Formula based on 24 oxygens ------					¦¦¦--- on 22 oxygens -------		
Si	3.96	3.92	5.93	5.93	5.52	5.46	6.16
Ti	0.06	0.06	0.01	0.0	0.14	0.16	0.05
Al	9.23	9.25	4.05	4.06	3.47	3.52	5.47
Fe	1.71	1.72	4.14	3.84	2.05	2.17	0.33
Mn	0.03	0.03	0.59	1.08	0.01	0.01	0.0
Mg	0.36	0.40	0.81	0.88	2.67	2.53	0.15
Ca	0.0	0.0	0.49	0.24	0.0	0.0	0.0
Na	0.02	0.03	0.03	0.04	0.10	0.11	0.33
K	0.0	0.0	0.0	0.0	1.41	1.38	1.48
Total	15.37	15.68	16.05	16.07	15.37	15.34	13.94
Fe/Fe+Mg	0.82	0.81	0.84	0.81	0.43	0.46	
X_{Fe} (almandine)			0.68	0.63			
X_{Mg} (pyrope)			0.14	0.15			
X_{Mn} (spessartine)			0.10	0.18			
X_{Ca} (grossular)			0.08	0.04			

Abbreviations: stt = staurolite; gar = garnet; bio = biotite; musc = muscovite.

thermometry. If pressure is set at 4 kilobars, Perchuk and Lavent'eva's (1983) calibration gives temperatures of 581° to 588°C; Thompson's (1976) calibration gives about 550°C. Temperatures derived from Perchuk and Lavent'eva's calibration are more consistent with petrographic observations, and seem to give an approximation of peak M_3 conditions.

Temperatures over 550°C evidently occurred in localized hot spots, near dikes of Carboniferous granite, and surrounded by regions where lower-amphibolite- and greenschist-grade conditions prevailed. The brucite + serpentine assemblage of some of the dolomitic marbles reflects recrystallization at temperatures below 470°C. In areas free of D_6 shearing and M_3 hydrothermal fluids, ambient temperatures could have been significantly less than 400°C.

The distribution of K-Ar ages in the study area (and elsewhere in the Manhattan Prong) confirms this pattern. Outside of D_6 shear zones and regions of hydrothermal alteration, biotite mineral ages range up to ~375 Ma or older (Fig. 56). During Mississippian time, these regions apparently experienced temperatures less than ~260°-300°C, the "closure" temperature for biotite (Harrison and McDougall, 1980; Purdy and Jager, 1976). Rapid diffusive argon loss is expected to occur at the "closure" temperature, "resetting" the K-Ar clock. In the study area, Carboniferous mica ages are characteristic of D_6 and D_7 shear zones, their environs, and zones of alteration.

LATE CARBONIFEROUS METAMORPHISM - M_4

Very limited amounts of recrystallization occurred during D_7 deformation. In contrast with M_3, there is no sign of related igneous activity or any influx of water-rich fluids. Comminuted grains of relict minerals tend to persist in S_7 fabrics (Fig. 52). In D_7 shear zones, recrystallization was prompted by tectonic strain, but limited by scarcity of water. As a result, S_7 fabrics tend to be localized and very-fine-grained.

One of the dated D_7 shear zones (K11) cuts the Manhattan Schist at Pierrepont State

Park. This shear zone is superimposed on an M_2 (upper-amphibolite-facies) mylonite fabric. Rocks in and around the D_7 shear zone show alteration to white mica and chlorite, particularly along the many rust-stained fractures.

Another D_7 shear zone cuts the plagioclase-hornblende gneiss member of the Fordham Gneiss. A mylonitic S_7 fabric developed, consisting of fine-grained epidote, recrystallized quartz, feldspar, biotite, chlorite, and porphyroclasts of relict hornblende (specimen #1240). Some larger hornblende grains are partially rimmed by epidote, but replacement reactions apparently did not keep pace with mechanical breakage during D_7 deformation. Temperatures were sufficiently high to permit the development of quartz rods.

Where D_7 shear zones are superimposed on M_3 assemblages, most minerals are rotated, sheared, and reduced in size, but do not show obvious metamorphic changes. The lowest-grade M_3 assemblages remained stable. At some localities, where both D_6 and D_7 deformation are present, some greenschist-facies assemblages (such as serpentine + brucite in #1266), may be either M_3 or M_4 in origin.

M_4 metamorphism clearly belonged to the greenschist-facies. Shear-related heating would have boosted temperatures inside D_7 shear zones, yet even there, the instability of hornblende (in #1240) indicates that temperatures remained fairly low.

K-Ar mineral ages help constrain the absolute values and the distribution of temperatures experienced during M_4. Fine-grained muscovite and biotite from D_7 shear zones (K6 and K11) have yielded two of three youngest K-Ar ages found in the region (309 Ma and 294 Ma, respectively). In contrast, most K-Ar age determinations have fallen between ~330 and 455 Ma (Fig. 56). The distribution of K-Ar mineral ages implies that peak temperatures were attained within shear zones, where they reached a minimum of ~350°C ("closure temperature" for muscovite, Purdy and Jager, 1976). However, surrounding regions generally remained below ~300°C ("closure temperature" for biotite).

Southeast of the Manhattan Prong, ~300 Ma K-Ar mica ages become much more abun-

dant (Fig. 55). In this region, M_4 regional temperatures apparently surpassed 350°C.

TECTONIC DEVELOPMENT OF THE MANHATTAN PRONG

INTRODUCTION

The stratigraphic, structural, metamorphic, and geochronologic findings in this thesis provide new constraints on the tectonic development of the northern Appalachians in general, and, in particular, for the Manhattan Prong. For the sake of simplicity, the implications of these findings for geologic history at the local and the broader scales will be treated in separate chapters. Each of these chapters will be brief; detailed treatments of all aspects of regional tectonic development are beyond the scope of this thesis.

This chapter will focus on the tectonic development of the Manhattan Prong and the surrounding area. The tectonic development of the Prong during Late Precambrian through early Middle Ordovician time, as recorded by the stratigraphic sequence consisting of the Ned Mountain Formation, Inwood Marble, and Walloomsac Schist, has already been discussed. Here, events that occurred at deep levels in the crust during the Taconian orogeny will be emphasized. First, I will outline some of the major constraints on Taconian-aged structures and metamorphism; later, I will present a step-by-step model for the Prong's tectonic development. A brief description of post-Taconian tectonism will follow.

TACONIAN OROGENY

A REVIEW OF AGE CONSTRAINTS. K-Ar mineral ages from the Ordovician rocks in the western Manhattan Prong commonly range up to 450 Ma (Fig. 55). The Middle to Late Ordovician Taconian orogeny was clearly responsible for regional metamorphism and penetrative deformation of this region. In contrast, many K-Ar mineral ages in the northeastern Prong are

Carboniferous. However, relationships between structures and radiometric ages indicate that regional high-grade metamorphism and penetrative deformation in these areas are also Taconian.

F_2 and F_3 folding in the study area were accompanied by regional M_2 upper-amphibolite-facies metamorphism, with temperatures probably surpassing 700°C. Biotite K-Ar ages are "reset" at temperatures of a mere ~300°C. The scattered K-Ar mica ages of ~400 Ma or older (Fig. 56) are consistent with post-Taconian cooling ages, and attest that F_3 deformation took place long before the Devonian Acadian orogeny. More direct constraints on deformational ages are available in the Croton Falls quadrangle, where an upper-amphibolite facies, syn-F_4 segregation has yielded a Late Ordovician Rb-Sr whole-rock isochron age (Table 12). (As discussed earlier, the Croton Falls F_4 is tentatively correlated with the Peach Lake F_3.) The D_1, D_2, and D_3 deformational events in the study area, and the related M_1 and M_2 episodes of metamorphism, can be regarded as Taconian in age.

B. GEOGRAPHIC AND TEMPORAL VARIATIONS IN TACONIAN METAMORPHISM. To gain a proper appreciation of Taconian metamorphism, the sequence of metamorphic assemblages in each part of the Manhattan Prong would, ideally, be described, and effects due to post-Taconian remetamorphism recognized and discounted. Existing data permit an approach to this ideal at few, if any, localities.

In the study area, the early (M_1) metamorphic history was heavily obscured by M_2 and M_3 recrystallization. The most telling evidence for M_1 derives from a small proportion of the several hundred thin-sections that have been examined. Preservation of M_1 assemblages appears to be even more fragmentary in the the Croton Falls quadrangle. There, upper-amphibolite-facies M_2 assemblages are most common, though M_3 overprinting is strong in many areas. However, rocks collected in the southern portions of the quadrangle (beginning in the Washington Ledges syncline) locally contain Paleozoic orthopyroxene. In addition, many aluminous rocks from the south have textures which imply a retrograde origin for biotite (e.g., Fig. 64C), and spinel has been

observed in the Inwood Marble. From this limited evidence, it is inferred that at least the southern portions of the Croton Falls quadrangle experienced a granulite-facies M_1, and have a metamorphic history similar to the study area's.

Significant transitions in M_1 and M_2 metamorphic grade occur southwest of Croton Falls, in the Ossining quadrangle (Fig. 1). In the eastern part of the Ossining quadrangle (transect F-F', Plate II), co-existing garnet, sillimanite, and biotite occur in M_2 assemblages, indicating upper-amphibolite-facies-grade. However, no sign of a relict granulite-facies M_1 has yet been encountered. Middle-amphibolite facies assemblages occur to the west, on transect G-G'. These assemblages appear to belong to Taconian M_1 or M_2, rather than Carboniferous M_3, for the following reasons: 1) sillimanite grows in muscovite and quartz, in a typical prograde manner, but neither I nor Wissig (who mapped the quadrangle, Wissig, 1970), have observed the characteristic M_3 polymorph, kyanite; 2) relicts of higher-grade metamorphism (such as sillimanite inclusions in garnet), which are commonly observed in retrograde M_3 assemblages, appear to be absent; 3) according to Ratcliffe, Bender, and Tracy (1983, Fig. 9), regional metamorphic grade declines to the west, reaching garnet grade at the Hudson River by the Cortlandt Complex (Fig. 1, Plate II).

The aureole of the Cortlandt Complex is superimposed on closely-spaced Taconian isograds. Several geochronological studies (summarized in Ratcliffe, Bender, and Tracy, 1983, p. 23-27) indicate that the Complex is Ordovician in age. The isograds trend northeast from the Cortlandt Complex, and can be traced across the Hudson Highlands into the Paleozoic rocks of Dutchess County (Ratcliffe, Buden, and Burton, 1985, Fig. 9). The biotite and sillimanite + muscovite isograds are separated by only 5 to 13 kilometers of the earth's surface over this distance.

Studies of the metamorphism in and around the Cortlandt Complex constrain the P-T conditions associated with the isograds. Waldron and Tracy (1986) estimated that the garnet- and staurolite + kyanite-grade country rocks near the western end of the Cortlandt Complex were metamorphosed at 500-600°C and 3 to 4 kilobars. They deduced temperatures of 600° to 650°C and pressures of 6 to 7 kilobars for regional metamorphism in country rocks near the eastern end

of the Complex (above the sillimanite + muscovite isograd). In contrast to these country rocks, barometric calculations on contact metamorphosed rocks in the aureole of the Cortlandt Complex and on emery inclusions, yielded pressures of 6 to 7 kilobars at both sides of the Complex. These thermometric and barometric results imply that early Taconian (M_1?) isobars had been rotated into very steep (or even vertical) orientations before the intrusion of the Cortlandt Complex, and that a second episode of loading followed intrusion.

Early Taconian metamorphism is poorly constrained in the most of the Manhattan Prong on account of M_2 and M_3 overprinting. Mineral assemblages in the central and eastern portions of the Prong are generally middle- to upper-amphibolite-facies grade. The location of the isograd separating upper- and middle-amphibolite-facies assemblages of M_2 age is uncertain, but the middle-amphibolite-facies assemblages observed in the northeastern Prong have invariably been the products of M_3 retrogression.

Large areas of the southern Prong were remetamorphosed during M_3. On recent field trips to northern and central Manhattan Island, P. W. G. Brock observed swarms of syn-D_6 granite dikes, associated with typical M_3 retrograded schists. The aluminous schists have coarse-grained muscovite, abundant tourmaline, and euhedral porphyroblasts of garnet (and, more rarely, staurolite). Kyanite nodules are present (Taterka, 1987).

As Taterka (1987) observed in Central Park, the garnets in these muscovite schists commonly contain grains of relict sillimanite. This garnet-sillimanite assemblage records a time when upper-amphibolite-facies conditions prevailed; during that period, much less mica would have been present, and the rocks probably had gneissose textures. The Manhattan "Schist" probably owes its very name to coarse-grained M_3 muscovite.

A few clues imply that the southern Prong experienced a prograde metamorphic history comparable to the study area's, though precise pressure-temperature conditions are unclear. In the study area, high pressure and climbing temperatures were experienced during early-M_1; rutile coexisted with garnet, and kyanite was stable. Corundum-bearing restites locally formed as the

result of anatexis. Metamorphism peaked high in the granulite facies. M_2 metamorphism produced somewhat lower pressure, upper-amphibolite-facies assemblages; sillimanite was stable, and rutile did not coexist with garnet.

In the southern Prong (and adjoining Hartland Formation), the following parallels to study-area metamorphic history have been observed:

1) Relict kyanite occurs in upper-amphibolite-facies sillimanite schist of the Hartland Formation, in the eastern Bronx and nearby southwestern Westchester County (Mount Vernon quadrangle) (i.e., kyanite predated sillimanite)

2) Rutile inclusions occur in garnets of the Hartland Formation in southwestern Westchester County (Mount Vernon quadrangle).

3) A specimen of Walloomsac Schist recently collected by P. W. G. Brock in the central Bronx (Flushing quadrangle) contains relict corundum (evidently of restite origin) in a retrograded M_3 assemblage. Pod-like anatectic leucosomes (like those in Pierrepont State Park) occur in the same area.

4) Upper-amphibolite-facies aluminous assemblages commonly contain sillimanite and ilmenite (but not kyanite or rutile) as matrix phases (Mount Vernon quadrangle).

The southern Prong, like the northern, probably experienced a high-pressure early-M_1 (when kyanite grew and garnet + rutile coexisted), granulite-facies peak-M_1 (when anatexis resulted in corundum-bearing restites), and upper-amphibolite-facies M_2 (when sillimanite, garnet, biotite, and ilmenite coexisted).

C. CORRELATION OF TACONIAN STRUCTURES. Cameron's Line, the thrust-contact between Hartland Formation and the Manhattan Prong, is the most prominent D_1 structure in the study area. This D_1 thrust is folded by the Washington Ledges syncline, which belongs to a set of F_2 folds which trend to the northwest in the central Peach Lake quadrangle. North of the study area, to the east of the Hudson Highlands, Cameron's Line is again deformed around a

northwest-trending fold (Rodgers, 1985) (north of HH, Plate VI-4, 5). Like the F_2 synclines in the study area, this fold opens to the southeast, and its hinge surface appears to be deformed by the F_3 Pound Ridge antiform. The fold is therefore tentatively correlated with the study area's F_2. If this is correct, then the intervening, easternmost Highlands apparently define an eastwards-closing F_2 anticline (analogous to the Shadow Lake and West Mountain anticlines), situated structurally above the F_2 Mill Plain syncline. This fold is termed the "Hudson Highlands anticline" on Plate VI.

F_2 folds in the study area and easternmost Highlands evidently verged to the east. However, Taconian shear zones in the Hudson Highlands northwest of the study area show southwest-directed thrust or oblique-thrust motion (Ratcliffe, Buden, and Burton, 1985). Late motion on these faults has been related to F_2 folding in Paleozoic rocks on the northern side of the Highlands (Ratcliffe, Buden, and Burton, 1985). Structures in this entire region, north and west of the study area, apparently verged westwards throughout the Taconian orogeny. The southern extension of this west-verging belt passes through the Cortlandt Complex (Plate VI-5,6).

Two structural domains apparently existed in the region during late Taconian time. In the western domain (which included the bulk of the Hudson Highlands, Paleozoic rocks north of the Highlands, and the corner of the Manhattan Prong near the Cortlandt Complex), west-vergent D_2 structures developed; in the eastern domain (which included the study area), east-vergent D_2 structures developed.

The boundary between these two domains within the Manhattan Prong must lie somewhere between the study area and the Cortlandt Complex. Its position can be constrained by tracing the east-vergent F_2 folds west and south from the study area. Regional map patterns imply that two of the folds, the South Salem syncline and the West Mountain antiform, can be followed for much of the length of the Manhattan Prong (Plate II; Plate VI-4,5). The structurally higher folds (Washington Ledges, Shadow Lake, Mill Plain, etc.) appear to be confined to the northern part of the Prong. An extensive belt of Walloomsac Schist occurs in the northeastern Ossining

quadrangle, at the structural level equivalent to the Washington Ledges syncline, but there is no readily recognized correlative fold.

Workers in the southern Prong have generally observed two (Paleozoic) episodes of tight to isoclinal folding, followed by more open, northeast-trending, upright folds (Hall, 1968b; Whiting-Goldberg, 1977; Taterka, 1987). The younger folds control much of the map pattern. These fold events appear to correspond to the F_1, F_2, and F_3 episodes recognized in the study area. To confirm this correspondence, however, the predicted locations of the major F_2 hinge surfaces, and the basic geometry predicted by F_1-F_2-F_3 relationships in the north, should be compared against the structural relationships that have actually been observed in the southern Prong.

The correlation can be tested in either southern Westchester County or the northern Bronx, but the F_2 West Mountain anticline and South Salem syncline apparently pinch out further south. Hall's major relevant published work is his (1968b) field trip guide to the White Plains vicinity. The guidebook, unfortunately, gives few details of structure, and is not useful for testing the correlation. Luckily, Whiting-Goldberg's observations of structures in the Mount Vernon quadrangle are carefully recorded and interpreted in her thesis.

Whiting-Goldberg observed only a few F_1 minor folds in the Mount Vernon quadrangle (Fig. 1), though a number of F_2 folds were recognized. The majority of her F_2 folds show a clockwise rotation sense when viewed from the south. However, the map pattern defines a number of narrow antiforms and synforms (visible on Plate II, at the latitude of transect A-A'.) Whiting-Goldberg reasoned that the folds so prominent on the map belong to F_3, since clockwise F_2 folds occur on both their limbs. Most of the F_3 folds, she inferred, must deform a single limb of a large F_2 fold. This F_2 fold-limb must be upwards-facing, since the stratigraphically highest rocks are exposed in the cores of north-plunging, southwards-closing F_3 synforms.

If F_2 folds were traced south from the Peach Lake quadrangle, the hinge surface of the West Mountain antiform would pass west of Mount Vernon, outside Whiting-Goldberg's area.

The hinge surface of the South Salem syncline would lie in the Mount Vernon quadrangle's westernmost synform, and then pass southwards out of the area, unless it were folded back around a F_3 fold.

Whiting-Goldberg's data does in fact permit correlation of her westernmost synform with the South Salem syncline. On a compilation of F_2 minor folds, she shows only two within the Paleozoic rocks west of the hinge surface of this fold, and one of the two has a counterclockwise sense. The F_2 minor folds with clockwise rotation senses that occur in the remainder of the area, and the right-side-up character of the rocks, accord with the proposed correlation.

The geometry proposed here contrasts with the model of the Manhattan Prong advanced by Hall (1979). In Hall's model, (equivalents of the) West Mountain anticline, Washington Ledges syncline, Shadow Lake anticline, and Mill Plain syncline are conceived as west-vergent F_1 folds, with the West Mountain structurally above the Shadow Lake anticline (Fig. 71). These "F_1" folds are subsequently backfolded around a very large, westwards-closing, F_2 fold equivalent to the South Salem syncline. The "F_1" anticlines, as a result, then close towards the east, as they are observed to do in the northern Prong. The (equivalents of the) West Mountain anticline, Washington Ledges syncline, and Shadow Lake anticline are inferred to continue structurally below the (equivalent of the) South Salem syncline. Upright "Acadian" F_3 folds are later superimposed on this complex structure.

Hall was strongly influenced by a site at Silver Lake (in the White Plains quadrangle; Hall, 1968b) in the construction of this model. There, granofelsic rocks assigned to the Lowerre Quartzite appear to plunge beneath more layered, gneissose rocks assigned to the Fordham Gneiss. Hall inferred that the "Lowerre Quartzite", Inwood Marble, and Manhattan Schist in the easternmost syncline in the Prong (where Silver Lake lies) represent an otherwise hidden lower structural level (marked "x" on Fig. 71), and that the surrounding "Fordham Gneiss" belongs to inverted nappe-like structure.

There are a number of disparities between Hall's model and structural and stratigraphic

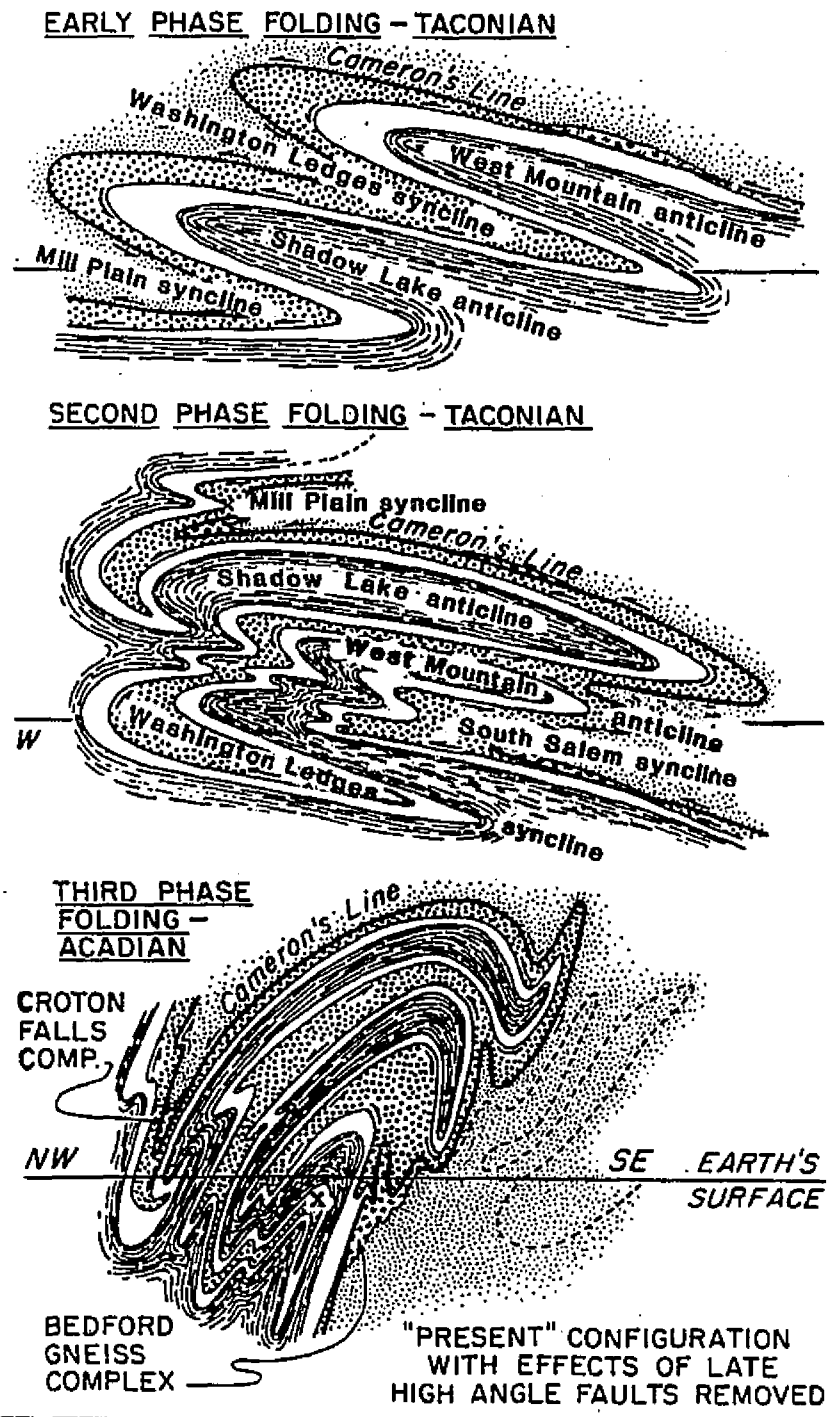

Fig. 71. Sketches modified from Hall (1979, Fig. 4), showing his model for the tectonic development of the Manhattan Prong. Folds equivalent to structures in the study area are identified by name. "X" in bottom sketch indicates rocks which Hall viewed as the exposed portion of an otherwise hidden lower structural level.

relationships in the northeastern Prong, but the clearest contradictions are in the Mount Vernon and White Plains quadrangles. These contradictions largely stem from Hall's identifying the rocks of the Ned Mountain Formation as Fordham Gneiss.

Hall's model requires that the "Fordham Gneiss" cut by transect A-A' (Plate II) be a section through the entire thickness of the West Mountain "nappe", close to its root. As a result, the Inwood Marble at either end of the transect would occupy different structural levels. However, none of the rocks examined on transect A-A' appear to be true Fordham; all are typical Ned Mountain lithologies. The Fordham core of the West Mountain "nappe" is simply not exposed. Therefore, the belts of Inwood Marble that outcrop at either end of the transect must belong to the same structural level.

In addition to rocks from transect A-A', I also examined Whiting-Goldberg's petrographic thin sections, which include rocks collected at several different latitudes along this same belt of "Fordham Gneiss". Only one of these rocks, collected at the center of the antiform, is true Fordham. The oldest rocks exposed in most parts of this belt belong to the Ned Mountain Formation.

Similar stratigraphic relationships occur at the northern termination of transect A-A"s marble belt (Plate II). Hall's Silver Lake site is situated at this termination. The granofelsic "Lowerre", biotite-quartz-feldspar "Fordham Gneiss", and K-feldspar-quartz "Yonkers Gneiss" that occur north and west of the Inwood Marble all belong to the Ned Mountain Formation. The "Fordham" belt is narrow, and is largely or entirely composed of Ned Mountain Formation. Little if any true Fordham can be exposed between the two belts of Inwood that are supposed to occupy different structural levels.

Another point of conflict involves the plunge of the easternmost syncline, particularly around the termination of Inwood Marble at Silver Lake. Minor structures in the region display many reversals of plunge, so that the syncline's net plunge (as it closes on map scale) is difficult to determine. The Inwood disappears beneath Silver Lake; north of the lake, "Lowerre" granofelses outcrop, followed further north by "Fordham".

Hall believed the northwards plunge of this "Lowerre" beneath the "Fordham" to provide a firm facing direction for the entire fold. The north-dipping beds were evidently upside-down; therefore, the Inwood Marble that crops out further south must lie beneath the "Lowerre", and the entire stratigraphic sequence in this syncline must be inverted.

This logic of this argument falters when it is recognized that both the "Lowerre" and "Fordham" belong to the same formation, and that relationships between the two lithologies do not mandate a particular facing direction. Although "Lowerre" quartz-feldspar granofelses commonly lie at the top of the Ned Mountain section, they do not necessarily comprise the uppermost lithology (see description, transect E-E'). Broad stratigraphic relationships, described earlier, require that the syncline be right-side-up; such an interpretation is permitted by both minor structures along the syncline and by the observed stratigraphic succession.

D. MODEL FOR THE TACONIAN OROGENY. The most telling structural and metamorphic data presently available in the study area, the remainder of the Manhattan Prong, and the surrounding region have been selected and synthesized into a model for the Taconian orogeny. The model applies specifically to southeastern New York and adjacent Connecticut, though comparable events may have occurred in other parts of the orogen. Some aspects of this model, and its consequences, are speculative. Much careful work (mapping, petrography, metamorphic petrology) will be needed in order to fully test the predictions of this model against reality.

1. D_1 deformation/early-M_1 metamorphism. During D_1, the Hartland terrane was emplaced over the North American margin along west-directed thrusts. The garnet-grade rocks near the west end of the future Cortlandt Complex were buried to ~15 kilometers (4 kilobars), and the sillimanite + muscovite grade rocks at the east end were buried to ~20 kilometers (~7 kilobars). If one moves eastwards to the study area, however, the rocks of the Mill Plain syncline already

record evidence of burial to a minimum of ~ 40 kilometers (~ 12 kilobars). Within the study area, available data are consistent with either a constant depth of burial, or a gradual thickening southeastwards.

A cross-sectional view of "D_1 deformation" in the northern Manhattan Prong was constructed on the basis of these metamorphic data (Plate VI, cross-section 1A-A'). Early-M_1 7 and 12 kilobar isobars are shown; these isobars are used as markers and repeated in representations of later deformational phases. To construct cross-section A-A', the isobars were assumed to record equivalent amounts of M_1 loading along their traces, beginning from the vicinity of the Cortlandt Complex and north through the Hudson Highlands.

On cross-section 1A-A', the linear distance between the intersection of the Fordham/Ned Mountain contact with the 7 and the 12 kilobar isobars is ~35 kilometers. This 35 kilometers represents a very rough approximation of the pre-D_2 separation between the sillimanite-muscovite isograd (in the Hudson Highlands) and the Mill Plain syncline's south limb.

The geometry that results from this construction shows a wedge of Hartland that abruptly thickens, and then (nearly?) planes off. This geometry is reminiscent of the ramps and flats of low-angle thrust faults. It indicates that, by early stages of the Taconian orogeny, a slightly thickened (40 kilometers thick?) continental block (Hartland terrane) had already overthrust this part of the North America margin.

At this time, there is no compelling evidence in the central Manhattan Prong for very high pressures during M_1. For this reason, a more moderate amount of burial is postulated in cross-section 1B-B'. As a result, the overthrust Hartland there is shown as a gently tapering wedge.

2. Intrusion of mafic to intermediate igneous complexes in the eastern Prong. The extreme early-M_1 loading experienced in the northern Prong was followed by a moderate reduction in pressure and temperature, during which deformation continued (late-M_1; Fig. 60). After cessation of D_1 deformation, a series of mafic to intermediate igneous bodies were intruded. These

bodies included the Croton Falls Complex, the Peach Lake Complex, the Bedford Complex, and the small mafic to ultramafic pods found in the Peach Lake quadrangle. The moderate post-D_1 uplift of the eastern Prong and the intrusion of the Croton Falls and Peach Lake Complexes are indicated schematically on Plate VI, cross-section 2A-A'.

The intrusion of these mafic bodies may well be linked to the release of the basement from the severe loading associated with D_1. Rapid decompression of the mantle can lead to mafic magmatism. Mafic magmas may intrude during the decompression of granulite terranes developed deep in an overthickened crust. These mafic magmas may mix with anatectic granitic liquids (Harley, 1989, p. 240), resulting in rocks of intermediate composition.

Additional syn-Taconian plutons of mafic to intermediate composition which intruded after D_1 are known from other portions of western Connecticut (for instance, the Hodges Complex; Merguerian, Mose, and Nagel, 1984). If the post-D_1 mafic-to-intermediate plutons of the northeastern Prong were the products of decompression, then occurrence of similar bodies elsewhere in western Connecticut would suggest that severe M_1 loading was of regional scope. If so, then high-pressure metamorphic assemblages, and subsequent granulite-facies metamorphism, may once have been extensive.

Fragmentary metamorphic evidence does in fact support such a scenario. Retrograded Taconian eclogites have been recognized in rocks of the Berkshire massif in northwestern Connecticut (Maggs, Cheney, and Spear, 1986). These eclogites were subsequently remetamorphosed, first in the granulite facies, and later in the amphibolite facies. Thus, their history parallels the record of the northeastern Manhattan Prong.

3. D_2 thrusting/F_2 folding. During D_2, west-directed thrusting in the western Hudson Highlands resulted in steepening of isobaric surfaces (Plate VI, 3A-A', 3B-B'). East-vergent F_2 folds (West Mountain, Shadow Lake, and Hudson Highlands anticlines) developed further east.

F_2 folding involved substantial shortening of the northern Manhattan Prong. If F_2 folds

had formed concentrically, conserving lengths of contacts and stratigraphic thicknesses, then point "a" on the post-Grenville unconformity (cross-section 1A-A') would have been translated westwards by approximately 80 kilometers. However, the roughly similar style of most F_2 folds implies a passive-slip fold mechanism. Passive-slip folding would have led to thinning on the fold limbs and stretching of the apparent length of the unconformity.

Even if a significant fraction of the length of the unconformity is attributed to stretching by passive-slip, it still must have been some tens of kilometers long before deformation. Therefore, a section of basement some tens of kilometers long once lay below the cover rocks that are now within the F_2 folds. However, only a thin sliver of basement was actually incorporated into the F_2 folds. What happened to the expanse of crust that formerly underlay these tens of kilometers?

The amount of crustal shortening required by the F_2 folds is most readily accommodated by underthrusting along a basement detachment (Plate VI 3A-A'). This detachment would have continued westwards, at depth, within the Grenvillian basement (cross-sections 3A-A' and 3B-B').

The two structurally highest F_2 anticlines (Hudson Highlands and Shadow Lake) die out in the northern Prong. Only the West Mountain anticline is traced southwards into the central Prong (Plate VI, 3B-B'). In the southernmost Prong, even the West Mountain anticline may pinch out. The disappearance of major F_2 folds suggests that F_2-related basement shortening decreases towards the south (Plate VI, cross-section 3B-B').

Plate VI-3C shows a "map" view (at the level of plane "d") for the period following F_2 deformation. Basement rocks "outcrop" in the central region, cover rocks towards the northeast and southwest. Rocks affected by the highest grade of metamorphism, east of the early-M_1 12 kilobar isobar, occur in the northern Prong.

F_2 folding in the northern Prong was accompanied by M_2 metamorphism, which reflects pressures in the range of 7 to 10 kilobars. It is uncertain whether these pressures give a measure of the total unroofing between D_1 and D_2, or whether a larger amount of post-D_1 unroofing was

followed by some degree of D_2 re-burial.

4. Post-F_2 warping. After D_2, F_2 folds in the northern Prong were rotated into reclined attitudes, with hinge lines plunging (on average) moderately to the north. Their hinge surfaces were swung towards northwesterly strikes (Plate VI-4A). In the central Prong, F_2 hinge lines today average approximately horizontal, and hinge surfaces are northeast-striking. In the southernmost Prong, F_2 folds plunge towards the south (Merguerian and Baskerville, 1987; Taterka, 1987). Yet, in spite of these differences among F_2 folds, F_3 hinge surfaces are remarkably constant in orientation. The north-south change in F_2 attitudes are attributed, therefore, to the development of a post-D_2 dome-like structure.

Uplift related to the dome would have centered in the northern Manhattan Prong, near the Bedford Complex (Plate VI-4A). A cross-sectional view is given in Plate VI-4B (note similarity between the northern end of this cross-section and Fig. 31). Uplift must have fallen off towards the northwest, since warping has not been noted in the Hudson Highlands.

The Cortlandt Complex and the northwest-trending Cortlandt-Beemerville lamprophyre dike swarm may have been emplaced during this post-D_2 period. The Cortlandt Complex postdated two or three episodes of folding (Ratcliffe, Bender, and Tracy, 1983) and intruded across the steepened (post-D_2) isogradic surfaces. The position of the Cortlandt Complex corresponds to the culmination of the proposed domal structure. This intrusive event and uplift of the "dome" may conceivably stem from a similar source: upwelling of buoyant mantle, coupled with a temporary reduction in compressive stresses.

5. F_3 folding. F_3 folds deformed the "domed" F_2 hinge surfaces and hinge lines (Plate VI-5), recording an apparent renewal of compressive stress. In the northern Prong, F_3 folding of reclined F_2 anticlines resulted in the inverted, downwards-closing orientation they display on the north-south limb of the F_3 Pound Ridge antiform (Fig. 34).

S_3 maintains a fairly constant orientation throughout the Prong; attitudes of F_3 hinge surfaces from the Peach Lake and Mount Vernon quadrangle overlap. In contrast, F_3 hinge lines are regionally variable. This variation results from the dependence of hinge lines on pre-existing attitudes of planar (S_2) surfaces. F_3 folds in the Peach Lake quadrangle generally have north-plunging hinge lines, because they deformed north-dipping surfaces. In contrast, F_3 hinge lines in the central Prong have plunges that average nearly zero. The surfaces deformed by these folds must have been (on average) nearly horizontal. The orientations of F_3 hinge lines thus support the hypothesis of a post-D_2 "dome".

Syn-F_3 and syn-F_2 metamorphism in the northeastern Prong both belong to the M_2 metamorphic event, and do not have petrographically distinguishable metamorphic grades. This appears, at first, to contradict the structural model, since uplift is implied by the post-D_2 "doming". However, Waldron and Tracy (1986) inferred that the region around the Cortlandt Complex experienced an episode of loading after the emplacement of the Complex. This episode of loading may well reflect the same compressional episode recorded by F_3 folding further east. Perhaps loading during F_3 compensated for uplift during post-D_2 "doming".

POST-TACONIAN TECTONIC ACTIVITY

The oldest K-Ar biotite mineral ages in the Manhattan Prong probably record the time when temperatures first dropped beneath ~300°C ("closure" point for argon diffusion) following the Taconian orogeny. Temperatures of ~300°C would occur at a depth of ~18 kilometers (~5 kilobars) under a "normal" geothermal gradient. Therefore, if the Taconian orogeny waned at ~450 Ma, the presence of scattered mineral ages as old as 440 Ma in the eastern Prong implies uplift from depths of ~28 kilometers (8 kilobars, post-M_2 metamorphism) to 18 kilometers occurred within a period of about 10 million years. A rapid post-Taconian rate of uplift (~1.0

millimeter/year) is implied.

After the post-orogenic period, the crust may have reached equilibrium, and uplift stalled. Mississippian-aged M_3 metamorphic assemblages record minimum pressures of 4 kilobars. It is conceivable that substantial uplift did continue, and that renewed burial occurred during the Acadian orogeny (Early to Middle Devonian time). Either way, by Mississippian time, ~340-360 Ma, during D_6 deformation, the eastern Prong was at a minimum depth of ~15 kilometers.

D_6 deformation, together with the intrusion of the syntectonic Mississippian granite suite and its associated M_3 metamorphism, had by far the greatest impact of any post-Taconian tectonic event in the Manhattan Prong. It has, however, gone almost completely undetected. Where M_3 muscovites followed pre-existing layering (as they often did), Taconian folds appear to "deform" post-Taconian muscovite. (I speak from hard experience, for I originally tried to distinguish "pre-" from "post-muscovite" folding in the Turkey Hill fault zone. I eventually realized that most rocks showing "post-muscovite" folding were merely more completely retrograded.) Attitudes of D_6 slip planes and F_3 hinge surfaces are generally parallel, thus adding to the confusion. In addition, D_6 shear zones are commonly quite broad, with irregular, diffuse boundaries, and with heterogeneously distributed shear. It is not surprising that previous workers generally did not recognize D_6-related shearing, or that they failed to distinguish D_6 deformation and M_3 metamorphism from older features.

A rough correspondence does exist between some of the D_6 shear zones (Turkey Hill fault zone, Ridgefield fault zone, and the Highlands border fault in the Croton Falls quadrangle) and the aeromagnetic lineaments plotted by Tillman (1981, Fig. 5). However, many areas strongly affected by D_6 do not show up as lineaments, and some lineaments appear to follow D_6 shear zones for a certain distance, and then switch to features of other ages.

Most of the map-scale effects of D_6 remain unclear. In the northern Prong, where S_6 is oriented at high angles to F_2 hinge surfaces, D_6-related rotation and map-scale offset are easiest to recognize. In the central and southern Prong, where all planar structural elements tend to be

subparallel, this is very difficult. For the time being, the presence of M_3 retrogression, Mississippian granites, and S_6 fabrics are the main evidence for the existence of D_6 shearing at many localities in the central and southern Prong.

Map-scale deformation of other ages is even more difficult to recognize and correlate. Open folding of post-F_3 age has been reported by workers in many parts of the Manhattan Prong (e.g., Alavi, 1976; Whiting-Goldberg, 1977; Ratcliffe, Bender, and Tracy, 1983; Taterka, 1987), and Brock and Mose (1979) reported post-Taconian shearing. However, the significance and traceability of these deformational events are unclear. For instance, the F_4 deformation observed in the study area (with its near-horizontal hinge surface) has no recognizable counterpart in descriptions from other areas. Similarily, Brock and Mose's (1979) D_5 shearing in the Croton Falls quadrangle appears to be localized. Post-F_3 folds recognized in various parts of the Prong probably do no correlate with each other, but instead span the entire period from late in the Taconian orogeny through the Carboniferous D_6 or D_7 (and perhaps even later). The impact of these open folds on overall map pattern is uncertain but appears to be minor.

Small brittle faults are also abundant in the Manhattan Prong. Map-scale offsets of stratigraphic contacts occur in a few places, but again, these structures appear to be of minor importance.

SUMMARY STATEMENT

Most of the geometry of the Manhattan Prong is the product of Taconian deformation. The tectonics of the Taconian orogeny were complex, and involved temporal and spatial changes in the style and the vergence of deformation. The eastern Prong experienced severe loading early in the orogeny, followed by granulite-facies metamorphism. Subsequent decompression of the mantle may have led to intrusion of mafic to intermediate igneous complexes. This

compression/relaxation cycle may have been repeated twice more during the Taconian orogeny (F_2 folding, post-D_2 "domal" uplift; F_3 folding, post-Taconian uplift).

The early (M_1) metamorphic history of the Prong was obscured by pervasive retrogression late in the Taconian orogeny (M_2) and again, during the Mississippian (M_3) metamorphic event which accompanied D_6 deformation. The diffuse character of many D_6 shear zones and the parallelism of D_6 shear planes with Taconian structures make the impact of D_6 deformation on the map pattern difficult to evaluate in many areas.

IMPLICATIONS FOR APPALACHIAN GEOLOGY

INTRODUCTION. In this chapter, the broader implications of the evidence presented in this thesis for Appalachian geology will be briefly considered. An historical framework is adopted here. Implications of this study for the North America of Late Precambrian time will be discussed first, and then its significance for subsequent periods, ending with the Pennsylvanian.

LATE PRECAMBRIAN TO EARLY CAMBRIAN TIME. 1. Origin of the promontories and embayments in the Appalachian margin. The Ned Mountain Formation is the first major Eocambrian felsic volcanic sequence recognized on a promontory (i.e., a segment curved concave to the craton: Fig. 72) in the Appalachian orogen. The well-known felsic volcanic sequences (which are located at Mount Rogers, Virginia; South Mountain, Pennsylvania; and the Sutton Mountains, Quebec) are all located on embayments in the Appalachian orogen (Fig. 72).

The locations of felsic volcanic centers relative to orogen promontories have implications for the evolution of the North American margin during Late Precambrian to Cambrian time. Rankin (1976) proposed that the shape of the Appalachian orogen had been inherited from the configuration of the Late Precambrian rifts which linked RRR (continental rift) triple junctions. According to his model, the triple junctions developed over hot spots, and felsic volcanism centers developed in the aulocogens (or failed arms) of the triple junctions. A competing interpretation, offered by Thomas (1977, 1991), holds that the shape of the Appalachian orogen reflects a sequence of rift segments and transform faults inherited from an ancient oceanic rift system.

The Ned Mountain Formation occurs on a promontory of the Appalachian orogen. Its felsic metavolcanic sequences formed in a rift segment parallel to the continental margin, not an aulocogen, and are therefore consistent with Thomas's model, but not with Rankin's.

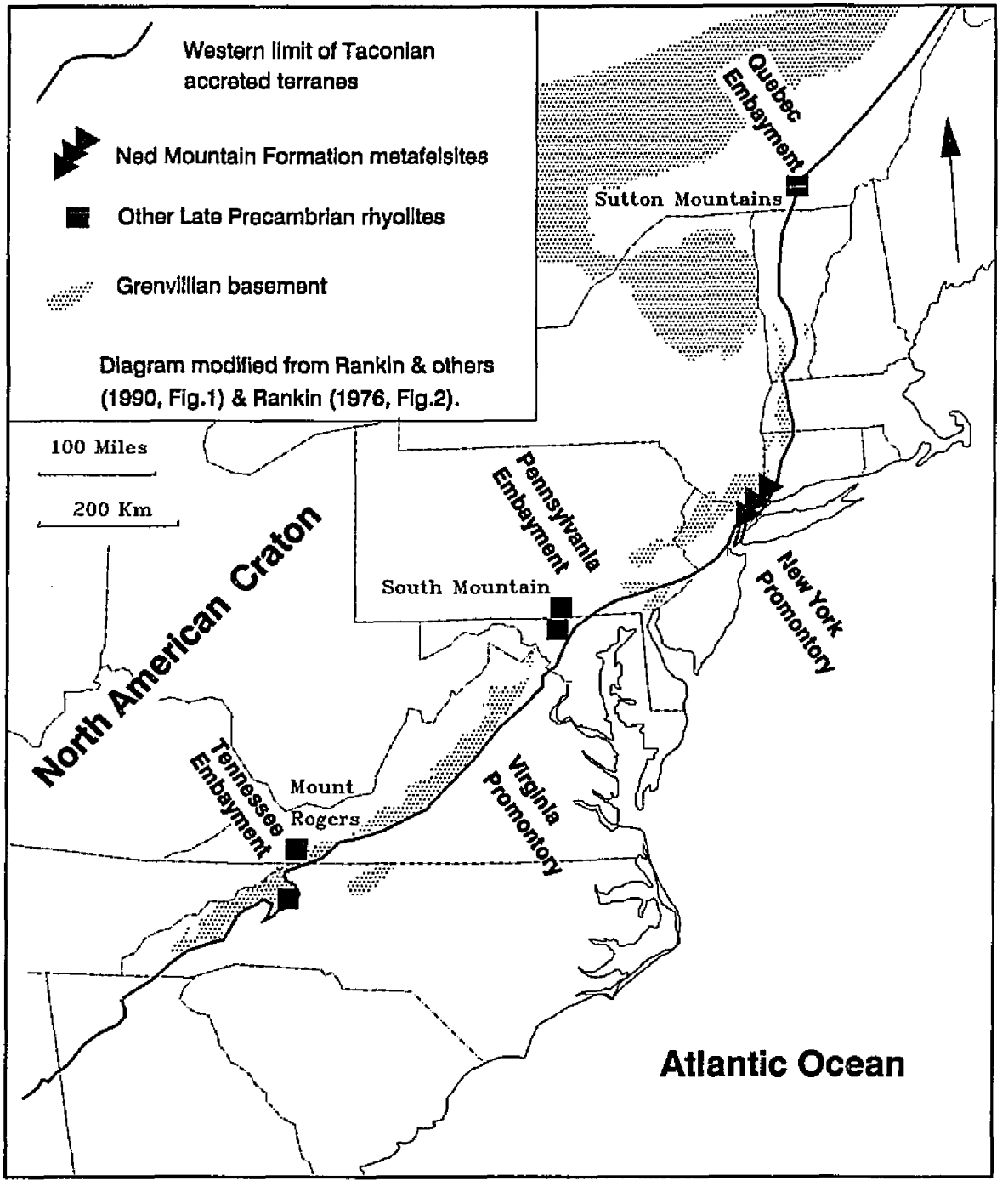

Fig. 72. Rift-related Eocambrian felsic volcanic rocks in the Appalachians.

2. Age of the rift-drift transition. Some debate has centered on the age of the (pre-Iapetan) rift-drift transition in the Appalachians. Some workers (e.g., Hatcher, 1987) have inferred an Early Cambrian Proto-Atlantic (Iapetan) ocean of substantial width. However, Early Cambrian (~550-570 Ma) radiometric ages have been obtained on rift-related volcanic rocks in Vermont (Kumarapeli and others, 1989), and Virginia (Badger and others, 1988). The Cambrian (~530-580 Ma) radiometric ages of the Ned Mountain Volcaniclastic Member (Yonkers and Pound Ridge granitic gneisses) suggest crystallization at around the same time as these other rift-related volcanic rocks. Taken together, the ages suggest that drifting did not commence before late Early Cambrian time.

MIDDLE TO LATE ORDOVICIAN TIME. 1. Taconian high-pressure metamorphism. Taconian amphibolite-facies-grade mineral assemblages are commonly taken to record approximate peak metamorphic conditions. In the northern Appalachians, this approach has led to a contradiction between the apparent P-T conditions of metamorphism and other measures of depth of exposure.

Laird observed (in Drake and others, 1989) that metamorphic grade along the Grenville basement increases southwards; this, along with north-plunging lithologic contacts, indicates that deeper structural levels are exposed in southern New York than in northern Vermont. However, the Taconian mineral assemblages suggest to Laird a southwards decrease (!) in metamorphic loading. The structures and mineral assemblages of the northeastern Manhattan Prong provide insight into how this contradiction came about, and demonstrate how later metamorphic events can effectively obscure early ones.

Although the Taconian orogeny is thought to be the result of a continent-arc collision, evidence for high-pressure metamorphism is sparse. Most Taconian metamorphic assemblages in the Appalachians belong to medium-pressure facies (Fig. 73). In the northern (U. S.) Appalachians, pressures of 7 kilobars or more (or presence of eclogite) have been inferred at only four local-

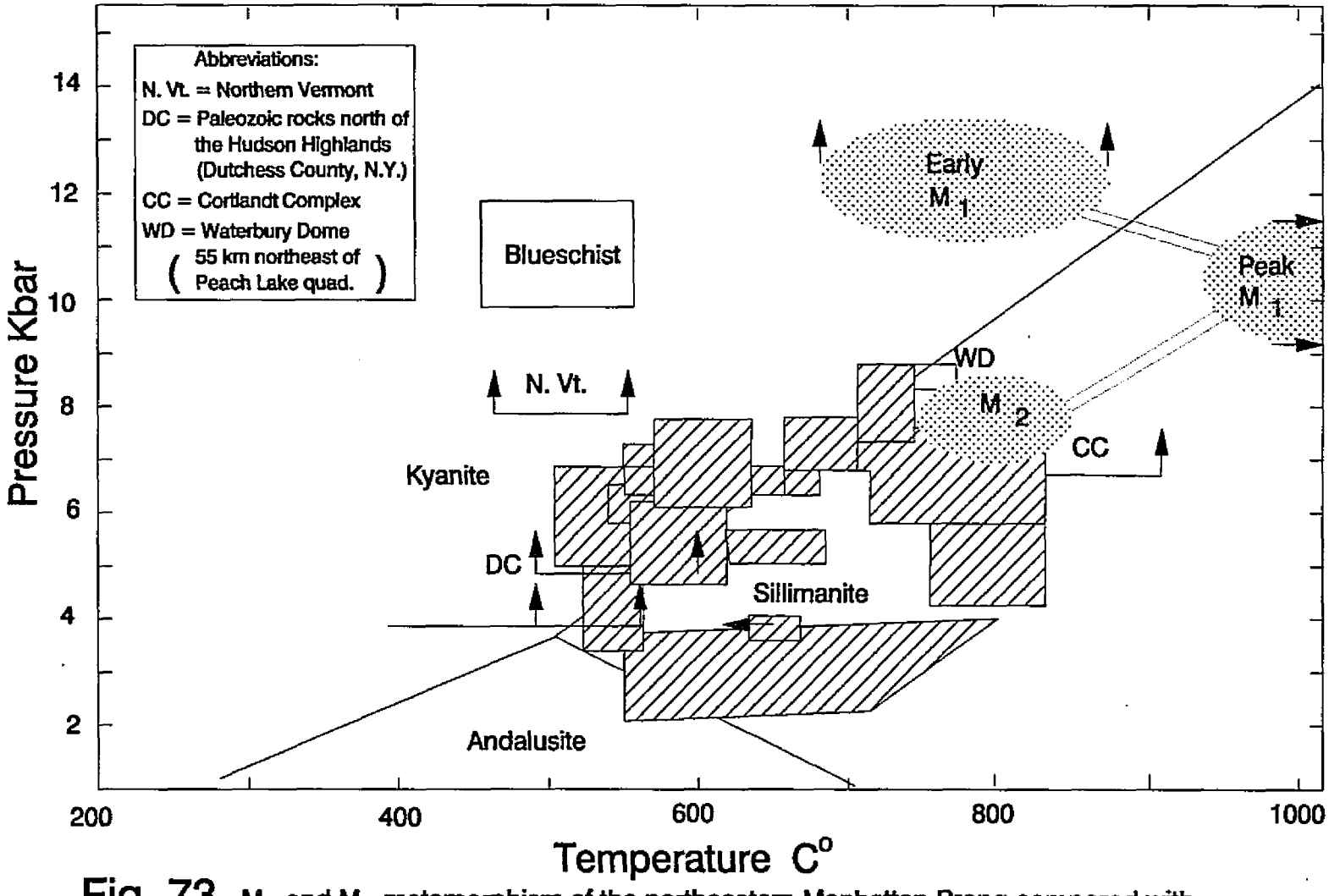

Fig. 73. M_1 and M_2 metamorphism of the northeastern Manhattan Prong compared with pressure-temperature estimates for other Taconian assemblages in the Appalachians. Based on Fig. 19 in Drake & others, 1989. (Data compiled by Laird.)

ities: northern Vermont (Laird and others, 1984), northwestern Connecticut (Berkshire massif) (Harwood, 1976; Maggs, Cheney, and Spear, 1986), the western Manhattan Prong (Cortlandt Complex) (Ratcliffe, Bender, and Tracy, 1983; Waldron and Tracy, 1986), and west-central Connecticut (Waterbury Dome) (Dietsch, 1985). The minimum pressures inferred in the northeastern Manhattan Prong (12 kilobars) are greater than those deduced from any other Taconian terrane in the U. S. Appalachians (Fig. 73). These rocks fill a glaring gap in the metamorphic record of the Taconian orogeny.

2. Major tectonic events of the Taconian orogeny. A single deformation event (D_1) accompanied the deep burial, subsequent granulite-facies metamorphism, and the first stages of cooling and decompression of the Manhattan Prong. Peak temperatures were very high, probably in the vicinity of 950 to 1000°C. The rapid rise in temperatures after burial implies a "hot" overriding slab, and fairly high thermal conductivity. The pressures correspond to burial of $\geq \sim 40$ kilometers, consistent with slab's identity as an active continental margin.

The thinning of the overriding slab after D_1, and consequent decompression of the mantle, may have led to the generation of the mafic to intermediate magmas which intruded both the Manhattan Prong and the Hartland terrane in western Connecticut. During the following (D_2) stage of the Taconian orogeny, compression (and shortening) continued, but loading was distinctly reduced.

After a pause (and possible release of compression stress), another (D_3) pulse of shortening (and loading?) occurred. Pervasive amphibolite-facies M_2 metamorphism associated with these last two tectonic pulses overprinted early higher-grade assemblages. They left a Barrovian, middle-pressure metamorphic imprint similar to that of "high-grade" Taconian assemblages elsewhere in the Appalachians (Fig. 73).

MISSISSIPPIAN TECTONISM. During Mississippian time, the Manhattan Prong was cut by normal-sense (D_6) shear zones, a suite of syntectonic two-mica granites was intruded, and host rocks were extensively retrograded. Orientations of the shear zones and dikes imply northwest-southeast directed extension. The timing of this extensional event falls between the Acadian and Alleghenian orogenies.

Deformation of Mississippian age has not been previously recognized in this part of the Appalachians, although evidence for the Devonian Acadian orogeny exists elsewhere in southwestern New England. One may speculate that D_6 deformation was the product of local transtension on the post-Acadian continental boundary. Some workers have proposed that dextral-transcurrent motion between the colliding plates resulted in propagation of the Acadian orogeny towards the south (Ettensohn, 1985, 1987; Ferrill and Thomas, 1988). Though the orogeny is of Early to Middle Devonian age in southern New England, it is recorded by clastic wedges as young as early Mississippian in age in the southern Appalachians. Independent evidence for transcurrent motion comes from Atlantic Canada, where dextral strike-slip faulting of Late Devonian through Carboniferous age is associated with basin formation (Belt, 1968; Webb, 1969; Bradley, 1982). Devonian through Carboniferous dextral strike-slip faulting may have affected the entire margin of eastern North America.

The Mississippian D_6 normal shear zones, two-mica granite suite, and associated M_3 retrogressive metamorphism that are so prominent in the Manhattan Prong have not been distinguished elsewhere. Still, this event had long gone unrecognized in the Manhattan Prong, and careful investigation may reveal its presence in other areas. At least some granites of appropriate age are known outside the Manhattan Prong. For instance, in central Connecticut, Brookins (1980) reported Rb-Sr whole-rock ages of 348±15 Ma for a folded pegmatite and 354±10 Ma for a dike in the Glastonbury Gneiss. Alleghenian deformation is much more pronounced in southern Connecticut than it is in the Manhattan Prong, which must substantially increase the difficulty of recognizing the Mississippian event.

PENNSYLVANIAN (ALLEGHENIAN) OROGENY. The Windwing thrust and other D_7 shear zones are the first structures of demonstrably Alleghenian age to be recognized between the Valley and Ridge province in New Jersey-Pennsylvania (Geiser in Hatcher and others, 1989) and south-central Connecticut (Wintsch and Sutter, 1986). Geiser and Engelder (1983) and Marshak and Tabor (1989), among others, have proposed that some of the deformation in the Hudson Valley fold-thrust belt of New York State is Alleghenian. The presence of Alleghenian thrusting in the Manhattan Prong implies continuity of Alleghenian deformation across the gap between New Jersey and central Connecticut.

The K-Ar radiometric ages obtained on D_7 micas (294 Ma biotite, 309 Ma muscovite) are similar to many other Alleghenian mineral ages in New England. In central Massachusetts, at the Pelham Dome, Gromet and Robinson (1990) obtained a 292±2 Ma Rb-Sr mineral isochron, a 304±20 Ma Sm-Nd mineral isochron, and 292±5 Ma U-Pb sphene ages. In the same area, Robinson and Tucker (1991) obtained a U-Pb monazite age of 297±2 Ma. In eastern Connecticut, at the Willimantic Dome, mineral isochrons and a concordant (U-Pb) sphene fraction give Pennsylvanian (294±3 and 304±2 Ma) ages. These ages predate the Permian amphibolite-facies metamorphism of Rhode Island and southern Connecticut. In Rhode Island, Dallmeyer, Hermes, and Gil-Ibarguchi (1990) found 276-266 Ma $^{40}Ar/^{39}Ar$ plateau ages for hornblende of the Scituate Granite; in southern Connecticut, Wintsch and Sutter (1986) obtained a 258±3 Ma $^{40}Ar/^{39}Ar$ hornblende plateau age. The Pennsylvanian and Permian mineral ages probably represent different stages of the Alleghenian orogeny.

The early, Pennsylvanian phase may record regional-scale east-west compression. In the Manhattan Prong, east-directed low-angle thrusting occurred during Pennsylvanian time. In central Massachusetts, Pennsylvanian deformation was associated with north-south longitudinal shearing (Robinson and Tucker, 1991). Geiser and Engelder (1983) proposed that a cleavage that trends 010° in the Hudson Valley relates to early Alleghenian (Lackawanna phase) deformation, although other geologists believe this cleavage to be Acadian (e.g., Marshak and Tabor, 1989).

THE LARGER CONTEXT

Here, in Part I of this thesis, the results of my study of the bedrock geology of the northeastern Manhattan Prong have been presented. Although these rocks are fascinating for their own sakes, they gain in significance when set in the broader contexts of the Manhattan Prong and of Appalachian geology as a whole. The framework into which the northeastern Prong can be placed has been built up through the efforts of the entire geologic community.

It is difficult, however, to clearly discern some of the essential aspects of that larger Appalachian context, when one is confronted with ever-growing mountains of conflicting interpretations. In Parts II and III, an attempt is made to meet the need for a coherent framework for Northern Appalachian geology. First, in Part II, the sub-Appalachian basement is divided into blocks, primarily on the basis of isotopic data. In Part III, these blocks are used to constrain the accretion history and nature of the orogenic events in the Appalachians. A wealth of published data on paleogeography, igneous activity, structure, and metamorphism are synthesized, leading to the development of a model for the Early to Middle Paleozoic accretion of the blocks, with an emphasis on the Acadian orogeny.

APPENDIX 1 (to Part I) - BRIEF DESCRIPTION OF TRANSECTS, PLATE II

Place names given in these descriptions can be found on the appropriate topographic quadrangles.

1. MOUNT VERNON QUADRANGLE

Transect A-A'. A continuous section of Ned Mountain Formation underlies the Inwood Marble on this transect. The relatively thick and homogeneous "Yonkers granite" was the lowest unit encountered; then came an interbedded series of amphibolites, felsic metatuffs, and a variety of quartz-feldspar-biotite granofelses. These granofelses include the leucocratic hornblende-garnet granofels whose mode is given in Table 3 (specimen #1884). At the top of this section, a thin-bedded lithologic sequence containing calc-silicate rocks was encountered.

The metamorphic grades of rocks collected on this transect range from the middle-amphibolite to greenschist facies. Intense chloritization is evident at some localities. These low- to middle-grade mineral assemblages are probably correlative with the Mississippian M_3 of the Peach Lake quadrangle.

Transect B-B'. A sequence of characteristic Ned Mountain lithologies lie to the west of a belt of Manhattan Schist and Walloomsac Schist, and alongside an intervening valley where Inwood Marble is presumed to run through. Most of these Ned Mountain lithologies are graphitic; the entire section is assigned to the Basal Member. The lithologies include quartz-plagioclase-biotite-cummingtonite-garnet-graphite granofels, quartz-biotite-graphite schist, orthoamphibole-plagioclase-garnet-biotite-graphite schist (specimen #1905, Table 3), fine-grained, grey, plagioclase-hornblende-clinozoisite-quartz granofels, rusty, clinopyroxene-bearing calc-silicate rock, and felsic metatuffs. Textures confirm the secondary nature of much of the clinozoisite. This mineral most likely formed during the Mississippian M_3 event, as did clinozoi-

site occurrences in the northern Manhattan Prong.

Hall (1968b) reported occurrence of sillimanite schist here. This was an understandable mistake. The almost colorless, prismatic orthoamphibole and cummingtonite, in association with biotite, garnet, quartz, and graphite, may be readily confused with sillimanite. However, the mafic metasedimentary rocks have a slight greenish cast that helps to distinguish them from true pelitic schist.

The top of the Ned Mountain Formation is missing here, since the Basal Member is exposed adjacent to the "Inwood" valley. A sequence of layered, non-rusty, coarse-grained, hornblende-quartz-plagioclase-K-feldspar-clinopyroxene gneisses are exposed to the west of the Basal Member. Minor calcite is present, and the rocks appear to have calc-silicate affinities. The coarse-grained texture and massive, grossly homogeneous character of these rocks indicate that they belong to the Fordham Gneiss.

2. MOUNT VERNON AND YONKERS QUADRANGLES

Transect C-C'. Layered, coarse-grained, dark to light colored, quartz-plagioclase-hornblende gneisses outcrop to the west of the Walloomsac Schist and a valley where Inwood Marble is presumed to lie. The gneisses resemble the Fordham unit that crops out on the western end of transect B-B', but these rocks appear to lack clinopyroxene and calcite. The Ned Mountain Formation seems to be missing at this locality.

To the west of the gneisses, in the Yonkers quadrangle, a sequence of quartz-plagioclase-biotite±muscovite±garnet±K-feldspar schists and granofelses occurs. Highly sheared granitic gneisses, which are possible (though not definite) former felsic ash beds, are associated with these rocks. The textures and compositions of these rocks suggest Ned Mountain Formation, although no absolutely diagnostic lithologies are present.

Continuing west, a pronounced valley marks the belt where the N.Y.S. geological map

(Fisher, Isachsen, and Rickard, 1970) shows Inwood Marble. However, the marble that crops out near the Hudson River (in the town of Hastings-on-Hudson), is not Inwood. It is a calcareous marble containing skeletal clinopyroxene, phlogopite, and quartz, and interbedded with fine-grained granofelses consisting of quartz, plagioclase, K-feldspar, red biotite, and garnet. This lithologic association might conceivably be found in either the Ned Mountain Formation or the Walloomsac Schist, but is more typical of the Walloomsac. The outcrop is provisionally assigned to the Walloomsac Schist, pending future confirmation of Inwood Marble between it and the inferred Ned Mountain Formation.

3. WHITE PLAINS QUADRANGLE

Transect D-D'. The Fordham Gneiss at the western end of this transect was assigned to Fordham Member B by Hall (1968b). A rather variable suite of metasedimentary and metaigneous rocks proved to be present in this part of "Member B". They include coarse-grained quartz-plagioclase±K-feldspar-biotite-garnet gneisses, mesocratic hornblende-garnet-plagioclase-quartz±cummingtonite gneiss, and some quartz-plagioclase-clinozoisite-hornblende rocks of possible calc-silicate affinity. Some layers of mafic composition are also present. These layers contain relict orthopyroxene+clinopyroxene, now largely replaced by hornblende. This suite of "Member B" rocks is cut by a dike of fine-grained hornblende-garnet amphibolite of probable Eocambrian age, and is overlain by the Basal Member of the Ned Mountain Formation.

The Basal Member here consists of a well-bedded sequence of quartz-feldspar granofelses (many of which are graphitic), mafic metasedimentary rocks, amphibolites, and sparse possible felsic metatuff. Lithologies include fine-grained quartz-plagioclase-biotite-graphite±muscovite granofels with biotite-rich, schistose laminae, quartz-plagioclase-biotite-garnet-hornblende-cummingtonite-graphite granofels, and quartz-rich granofelses. The Basal Member is overlain by a sequence of hornblende-cummingtonite-garnet amphibolites, which are interpreted as meta-

morphosed mafic flows and assigned to the Volcaniclastic Member. The mode of one of these amphibolites, #2496, is given on Table 3. To the east of the amphibolites is a valley in which the Inwood Marble is assumed to lie.

The dominant mineral assemblages here are consistent with middle- to upper-amphibolite facies grade. Their age is uncertain. The clinozoisite observed in the Fordham is probably of Mississippian M_3 age.

Transect E-E'. This transect, one of exceptional interest, was investigated in particular detail. Hall's (1968b) Fordham Member C makes up the bulk of the basement in this region. Member C is, as Hall described it, a remarkably homogeneous unit, mostly consisting of coarse-grained, quartz-plagioclase-K-feldspar-hornblende rock. It commonly has a strong linear fabric, and minor biotite locally defines a foliation. The leucocratic composition, absence of compositional layering, and the homogeneous nature of Member C over a large area suggest that it originated as a hornblende-bearing granitoid. Aleinikoff (1985) reported relict plagioclase phenocrysts and other textures indicative of a coarse-grained, intrusive protolith. Member C is in contact with a variety of other Fordham lithologies, so that (in contradiction with Hall's mapping) it appears to truncate the metasedimentary units of the Fordham (such as Members B and D).

Cross-cutting relationships indicate that at least three ages of rock are present in the Fordham Gneiss. The oldest rocks are the boudins of amphibolite, mafic orthopyroxene-clinopyroxene gneisses, and calc-silicate rocks seen in scattered (and isolated) outcrops. These rocks are similar lithologically to parts of Member B. The younger Member C granitoid surrounds and embays the older ("Member B-type") lithologies. Intrusion of the Member C pluton was estimated at 1170 Ma by Aleinikoff (1985) on the basis of U-Pb zircon systematics. After intrusion of Member C, these gneisses were cross-cut by younger biotite granites.

The graphitic Basal Member of the Ned Mountain Formation overlies the Fordham Member C and a variety of "Member B" xenoliths on this transect. Beautiful exposures of massive,

dark, rusty-greenish-weathering, sulfidic, quartz-plagioclase-biotite-graphite-hornblende±garnet±cummingtonite±orthoamphibole schists are found in the parking lot of the Fuji film company (west side of Taxter Road, just south of White Plains Road). (A photomicrograph of a graphitic orthoamphibole schist from this locality, #2280b, appears in Fig. 10E). The contact between the grey and black Fordham Gneiss and the rusty-weathering graphitic rocks of the Ned Mountain Formation is exposed in a cut behind one building. A sequence of well-bedded quartz-plagioclase-biotite-garnet granofelses with interlayers of amphibolite and biotite-garnet schist occurs above the dark, massive rocks, slightly higher in the Basal Member. The well-bedded sequence is illustrated in Fig. 9. A thick volcaniclastic section, dominated by felsic metatuffs, overlies the Basal Member to the northeast.

About 1 kilometer to the northwest (and across a valley that may follow a fault zone) the Basal Member crops out, discontinuously, for several hundred meters on either side of the Saw Mill Parkway. Various lithologic changes can be observed in this portion of the Basal Member. At the northwestern end of the outcrop zone, the Basal Member is a well-bedded, fine-grained quartz-plagioclase-biotite-garnet granofels, interbedded with quartz-plagioclase-biotite-cummingtonite-garnet-graphite schist. Greenish, graphitic hornblende-biotite schist and cummingtonite-garnet-biotite schist are found to the east, but these lithologies either pinch out or fail to outcrop in the west. Amphibolite is also present. Some quartz-plagioclase-biotite-garnet granofelses, interbedded with biotite-garnet schist, occur on the north side of the Saw Mill Parkway. These rocks, which resemble the well-bedded sequences at the Fuji outcrop, also appear to pinch out further west.

A photomicrograph of graphitic cummingtonite schist collected near the parkway appears in Fig. 10D; a mode for this specimen (#1845a) is given in Table 3. Hall (1968b) mapped the Basal Member rocks by the parkway (like those further south at the Fuji parking lot) as a sillimanite schist within the Fordham Gneiss.

A thick sequence of quartz-K-feldspar granofelses overlies the Basal Member at the

western end of the outcrop belt. These rocks constitute the "Lowerre Quartzite" mapped by Hall (1968b). The K-feldspar content varies layer by layer, and some are sufficiently K-feldspar-rich to be considered felsic metatuffs. Numerous coarse-grained K-feldspar-rich segregations are also present. The "Lowerre" here appears to be a lateral equivalent of the gneissose, felsic metatuffs which overlie the Basal Ned Mountain ~1 kilometer to the southeast. The mode of one granofels specimen, #V6-V8, is given in Table 3.

The quartz-K-feldspar granofelses are overlain in turn by minor quartz-plagioclase-hornblende- garnet- K-feldspar granofels (specimen #2468, Table 3) and amphibolite. Norton (1959) reported finding marble at this locality, before the rock cut (located behind large factories) was covered with talus. A hiatus in outcrop follows; Hall (1968b) shows a broad belt of Inwood Marble reaching to the "Lowerre".

4. OSSINING QUADRANGLE

Transect F-F'. This transect begins in the Manhattan Schist in the east. It passes through the Inwood Marble, the Ned Mountain Formation, and several units of Fordham Gneiss, before finally finishing in the west within the Walloomsac Schist.

The Walloomsac Schist is in fault contact with the Fordham Gneiss near the western end of the transect. Rocks along the fault commonly show strongly sheared fabrics. A sliver of the Fordham Gneiss is present in the fault zone, apparently surrounded by Walloomsac Schist. There is little room for the Inwood Marble, which may be locally missing. The Ned Mountain Formation appears to have been entirely cut out. Walloomsac metawackes, which contain stable sillimanite-biotite-garnet assemblages nearby, are locally retrograded to muscovite-staurolite-garnet schist. Pseudomorphs of muscovite after sillimanite are observed in some specimens. Tourmaline is abundant. Calc-silicate rocks of the Walloomsac located near the fault contain a great deal of texturally late clinozoisite, and a small amount of relict diopside.

The textures and mineralogies of the strongly retrograded rocks strikingly resemble those of M_3 assemblages in the Peach Lake quadrangle. These observations imply that M_3 metamorphism is responsible for the observed retrogression of formerly upper-amphibolite facies assemblages. The close association between the M_3 assemblages and this fault zone implies that the fault is a D_6 shear zone.

The Fordham Gneiss in the center of this transect consists of several lithologic units (Plate IIA). West to east, they are: I) coarse-grained, layered, leuco- to melanocratic, hornblende-clinopyroxene-plagioclase-quartz-K-feldspar gneisses; II) coarse-grained, rusty-weathering, quartz- plagioclase-K-feldspar-biotite± garnet± graphite gneiss; III) [within (II)] yellow-weathering, sulfidic, quartz-plagioclase- sillimanite-biotite-garnet schist; IV) quartz-clinopyroxene-hornblende-plagioclase gneiss interlayered with mafic, hornblende-garnet-plagioclase-orthopyroxene gneiss.

Lithologies similar to Unit I are fairly common in the Fordham Gneiss and are seen at number of places in the Manhattan Prong (Plate IIA). Unit II appears to be equivalent to Hall's Member B, which lies along strike to the south. Unit III strongly resembles the sillimanite schist of Hall's Member D in the White Plains quadrangle. Unit IV is similar to some xenoliths in Hall's Member C, and to mafic layers in Member B.

The Fordham Gneiss is overlain by a complex and varied sequence of Ned Mountain lithologies. Although a distinct Basal Member is absent, some highly graphitic granofels is present near the base of the Ned Mountain. Ned Mountain lithologies here include felsic metatuff, amphibolite, sulfidic, rusty-weathering calc-silicate rock, graphitic quartz-plagioclase-biotite granofels, plagioclase-rich granofels (±quartz, clinopyroxene, hornblende, epidote), and a quartz-plagioclase-hornblende-garnet-biotite gneiss containing a distinctive pink allanite. Some layers of the hornblende-garnet gneiss contain up to 10% modal apatite, and the gneiss appears to grade into calc-silicate rock. Cummingtonite-bearing metabasites and quartz-plagioclase-biotite-garnet-graphite granofels become abundant higher in the section.

The uppermost Ned Mountain Formation is well exposed on the entrance ramp of the Saw Mill Parkway at Chappaqua. At this locality, described by Wissig (1970) as an example of interlayered Fordham Gneiss and Inwood Marble, the Calc-Silicate Member crops out. Lithologies here include calcareous marble, clinopyroxene-K-feldspar-bearing calc-silicate rocks, quartz-(red) biotite-plagioclase-garnet-graphite granofelses, garnet-hornblende-cummingtonite amphibolite, quartzite, and felsic metatuff with graphitic interlayers. A felsic metatuff from this outcrop is shown in Fig. 15F; the mode of a dark calc-silicate rock (#1939b) is given in Table 3. Dolomitic Inwood Marble, followed by Manhattan Schist, overlies the Ned Mountain Formation to the east.

Transect G-G'. This transect focuses on the uppermost Ned Mountain Formation, which is exposed in two neighboring belts formerly mapped as Fordham Gneiss and Lowerre Quartzite (Wissig, 1970). Walloomsac Schist crops out between the two belts.

A sequence of well-bedded felsic metatuffs and quartz-feldspar granofels was encountered in the eastern belt. The metatuff contains minor amounts of ferrohastingsite amphibole, which Hall (pers. commun.) considered diagnostic of "Yonkers Gneiss".

An outcrop of "Lowerre Quartzite", mapped by Wissig (1970), occurs in the western belt, alongside a valley which Inwood Marble might underlie. This "Lowerre" strongly resembles the "Lowerre" that crops out on transect E-E'; it contains interbedded quartzite, quartz-K-feldspar granofels, felsic metatuff, and coarse-grained, K-feldspar-rich segregations. It also includes dark, biotite-rich interlayers. These dark layers proved to be apatite-rich, quartz-plagioclase-biotite-magnetite-ilmenite granofelses. The mode of one of these dark granofelses, #2108, is given on Table 3. A thin, reddish layer, composed largely of rutile and apatite, is present between a coarse-grained K-feldspar segregation and bed of phosphatic granofels; the origin of this curious layer is uncertain.

Quartz-muscovite-biotite-staurolite-garnet-plagioclase-graphite-sillimanite schist (metawacke) crops out slightly north of the "Lowerre". This metawacke appears to lie stratigraphically

below the granofels/metatuff section, and belongs to the Ned Mountain Formation.

These schists are quite different from the familiar upper amphibolite-facies grade metawackes. Sillimanite occurs here only within quartz and muscovite grains, resulting in the bumpy-weathering quartz-sillimanite "sillimanite nodules" considered characteristic of the "basal Lowerre" by Hall (1968a, p. 22). The development of these "sillimanite nodules" appears to be dependent on metamorphic grade. In the Peach Lake quadrangle, sillimanite may be enclosed in K-feldspar, plagioclase, and garnet, intergrown with biotite, or (most commonly) concentrated into sillimanite-rich laminae. A relatively small proportion of sillimanite occurs inside quartz, except in M_3 kyanite nodules.

The thickness of the metawacke section on this transect is uncertain. Rocks of the Ned Mountain Formation on this transect are assigned to the Calc-Silicate Member.

5. CROTON FALLS QUADRANGLE

Transect H-H'. The Fordham Gneiss on this traverse largely consists of coarse-grained, well-layered, dark-to-light (though largely leucocratic) quartz-plagioclase-biotite-orthopyroxene-hornblende± garnet gneiss. Minor amounts of sulfidic, clinopyroxene-hornblende calc-silicate rock are present. Except for the calc-silicate rock, the Fordham here is similar to the tonalitic orthopyroxene gneiss member in the Peach Lake quadrangle. It does not resemble any Fordham unit observed in the southern Manhattan Prong.

The Fordham Gneiss is cut by a fine-grained hornblende-garnet amphibolite dike of probably Eocambrian age near the southern end of the transect. This dike is mineralogically and texturally identical to the dike that cross-cuts Fordham "Member B" in White Plains quadrangle (transect D-D'). The dike is illustrated in Fig. 21, and a mode is given in Table 3 (specimen #2215).

The unconformity is folded here, so that rocks of the Ned Mountain Formation Basal

Member and Fordham Gneiss alternate several times along the transect. The contact between the Fordham Gneiss and the Ned Mountain Formation is diffuse; a mixed zone of metasaprolite, mafic metasedimentary rocks of the Ned Mountain Formation, and infolds of Fordham Gneiss occupies several meters. The beginning of this diffuse unconformity zone is illustrated in Fig. 8A. (This contact zone is described in detail in the Stratigraphy chapter, near the beginning of the section on the Ned Mountain Formation.)

Minor D_6 shearing is observed on the transect. The Fordham Gneiss is cut by S_6 cleavages and by dikes of syn-D_6 granites. These features are illustrated in Fig. 50.

Almost all of the Ned Mountain Formation on this transect belongs to the metabasite/mafic metasedimentary rock suite. The rocks consist of rusty-weathering quartz-plagioclase-biotite±garnet granofelses, fine-grained, hornblende +/- cummingtonite amphibolites (some with minor augite), graphitic quartz-plagioclase-biotite-cummingtonite (+/- hornblende) granofelses, graphitic quartz-plagioclase-biotite granofelses and a few beds of quartz-feldspar-biotite granofels (free of pyroxene, amphibole, and garnet). One mafic metasedimentary rock from this locality, #SGB21a, is illustrated in Fig. 10A; the modes of two (#SGB21b and SGB22a) are given in Table 3. These graphitic rocks outcrop in zone that extends from ~ 15 centimeters to a minimum of 4 meters above the base of the Ned Mountain Formation.

A sequence of amphibolites, dark quartz-plagioclase-biotite-cummingtonite granofelses interbedded with quartz-plagioclase-biotite-garnet schists, and granitic gneisses (metatuffs?) are the uppermost rocks of the Ned Mountain Formation here. These rocks are exposed on a north-facing hillslope; (Inwood?) marble crops out on the north side of the valley. Still further north, a substantial section of graphitic Walloomsac marbles, metawackes, and granofelses is present. A photomicrograph of one metawacke, #2197, appears in Fig. 64C.

Transect I-I'. The Fordham Gneiss lithology that crops out at the northwest end of this traverse is a plagioclase-hornblende-orthopyroxene-garnet gneiss. This gneiss resembles both the

orthopyroxene gneiss member of the Peach Lake quadrangle and the Fordham Gneiss lithology on transect H-H'. Further south, the Fordham consists of hornblende gneiss and clinopyroxene-bearing calc-silicate rock. Continuing south, the Fordham is overlain by the Basal Member of the Ned Mountain Formation. The Ned Mountain contains graphitic orthopyroxene- or clinopyroxene-bearing granofelses (like those on transect H-H'), quartz-plagioclase-biotite-graphite granofels, and amphibolite. The Inwood Marble does not outcrop; the Manhattan Schist occurs to the south.

Transect J-J'. This locality, at the dam below Titicus Reservoir, was used by Prucha, Scotford, and Sneider (1968) to illustrate "interlayering" of Fordham Gneiss and Inwood Marble. The Fordham Gneiss here is a coarse-grained plagioclase-hornblende-biotite-orthopyroxene gneiss. There is no distinct Basal Member of the Ned Mountain Formation; instead, Calc-Silicate Member quartz-K-feldspar granofels, amphibolite, and possibly marble overlie the Fordham Gneiss. Forsterite-bearing Inwood Marble and graphitic Walloomsac Schist outcrop above the Ned Mountain Formation. Both the Ned Mountain and Inwood are extremely thin. Tectonically induced attenuation of these formations is probable.

Transect K-K'. The Fordham Gneiss on this transect has been rotated and retrograded as the result of Mississippian D_6 shearing. No orthopyroxene has been found in it. The Fordham consists of dark- and light-colored quartz-plagioclase-biotite-hornblende gneisses and minor sulfidic, clinozoisite-rich calc-silicate rock. Two small plutons of foliated, two-mica, albitic granite are present on this traverse. One has yielded a 335±13 Ma Rb-Sr whole-rock isochron age (P. W. G. Brock and H. K. Brueckner, pers. commun.). A photomicrograph of one these granites, showing the S_6 fabric, appears in Fig. 57.

Going north, after a gap in outcrop, a sequence of homogeneous, leucocratic, quartz-K-feldspar-plagioclase-biotite±amphibole gneisses and granofelses overlie the Fordham Gneiss.

These rocks were termed the "?late Precambrian slabby-weathering unit" in Brock and Brock (1985a). This section is interpreted to consist primarily of layered, metamorphosed felsic volcaniclastic rocks. Minor calc-silicate rock is interbedded with the felsic rocks, along with some amphibolites, very minor biotite-quartz-plagioclase-garnet-chlorite schist, dark phosphathic schist (specimen #1222c, Table 3), and cummingtonite-hornblende-garnet-quartz-plagioclase schist. A compositional transition to occurs as one continues upsection, towards the north, culminating in a thick sequence of quartz-K-feldspar granofelses ("Lowerre Quartzite"). These granofelses, like other "Lowerre" occurrences, show bed-by-bed variation in proportions of quartz, K-feldspar, and micas. The mode of one specimen, #311, is given in Table 3. Some interbeds of amphibolite are found with the "Lowerre"-type granofelses. The Inwood Marble appears to be missing; Walloomsac metawackes and probable Walloomsac marble overlie the "Lowerre" granofelsic sequence.

Transect L-L'. The Fordham Gneiss lithology at the southern end of this transect is a well-layered, leuco-to mesocratic quartz-plagioclase-hypersthene-hornblende-garnet-antiperthite gneiss. It is essentially identical to the Fordham orthopyroxene gneiss member of the Peach Lake quadrangle. To the north of the Fordham, there is a gap in outcrop. After the gap, quartz-plagioclase-garnet-biotite-sillimanite metawackes, quartz-plagioclase-biotite-garnet granofelses and amphibolites of the Ned Mountain Formation Wacke Member outcrop. Hornblende and hornblende-garnet-cummingtonite amphibolites are both present. These rocks lie on strike with the Wacke Member of the Peach Lake quadrangle. The Wacke Member is overlain by a lithologically diverse suite of rocks, which consists of quartz-feldspar-garnet-biotite granofelses, amphibolites, granitic gneisses (metatuffs?), quartz-plagioclase-hornblende-garnet-biotite±cummingtonite granofelses, and minor calc-silicate rock. This heterogeneous section is assigned to the Calc-Silicate Member. Diopside and K-feldspar-bearing calc-silicate rock appears at the top of this section, interbedded with quartz-plagioclase-biotite schistose granofels and amphibolite.

A continuous section from the uppermost Calc-Silicate Member, into the Inwood Marble,

is exposed at one locality. There, an 18 centimeter-thick bed of white quartz-K-feldspar granofels of the "Lowerre" type appears precisely at the Calc-Silicate Member-Inwood contact.

The Ned Mountain Formation is overlain by olivine-bearing, dolomitic Inwood Marble. Calc-silicate rock and metawackes of the Walloomsac Schist outcrop above the Inwood.

APPENDIX 2 (to Part I) -

METHODS OF CALCULATING VALUES FOR FIGS. 19 AND 20

Fig. 19. Fig. 19A shows the modal feldspar proportions [K-feldspar:albite:anorthite] of the quartz-feldspar granofelses, calc-silicate rocks, and marbles, while Fig. 19B shows the modal proportions of alkali feldspars to Ca-bearing minerals other than anorthite. To construct Fig. 19B, the Ca content of the calcic minerals was normalized to 8 oxygens, matching the alkali : oxygen ratio of the feldspars, because their mineral formulas contain different relative amounts of Ca. The normalizing factors are given below:

Diopside $CaMgSi_2O_6$	= 1.33 Ca per 8 oxygens
Sphene $CaTiSiO_5$	= 1.60 Ca per 8 oxygens
Tremolite $Ca_2Mg_5Si_8O_{22}(OH)_2$	= 0.67 Ca per 8 (O+OH)
Epidote $Ca_2Fe^{+3}Al_2Si_3O_{12}(OH)$	= 1.23 Ca per 8 (O+OH)
Scapolite $(Ca_3Na)Al_5Si_7O_{24}(OH)$	= 0.96 Ca per 8 (O+OH)
Calcite $CaCO_3$	= 2.67 Ca per 8 oxygens
Dolomite $CaMg(CO_3)_2$	= 1.33 Ca per 8 oxygens

Figs. 25 and 28 were constructed in the same manner as Fig. 19.

Fig. 20. was designed to illustrate the relative proportions of quartz : calcite : dolomite in the protoliths of the calc-silicate rocks and marbles, as determined from their present mineralogies.

The "calcite" and "dolomite" content are derived from the modal sum total of Ca- and Mg-bearing minerals. The Ca, Mg, and Si contents of the minerals are first normalized to 8 oxygens, in the same manner as for Fig. 19 (above). Some Fe^{+2} substitution for Mg is expected in certain minerals, particularly the micas. In the absence of chemical analyses, this Fe cannot be excluded; therefore, modal "Mg*" (which includes this Fe) is determined instead.

The "Ca" and "Mg*" contents thus arrived at are ascribed to sedimentary carbonate minerals. However, the normalized "Si" value must undergo further adjustments before realistically representing the quartz content of the protolith. 1) The Na and K were probably originally contained within detrital alkali feldspars; therefore, the silica content of the present alkali feldspars is excluded from the "Si" total. 2) It is also assumed that the Al (in excess of that in the alkali feldspars) was originally combined with Si in "clay minerals" with the approximate Si : Al ratio of 1.5 : 1. The silica content of these "clay minerals" is likewise excluded.

Anorthite is assumed to have formed by combination of Ca from carbonates with Al and Si from the "clay minerals". Since anorthite has a Si : Al ratio of 2 : 2 (for 8 oxygens), 1.0 free Si is produced from the anorthite-forming reaction. This Si must be substracted from the total "Si" to give the original quartz content of the protolith. Thus, while the Ca of anorthite contributes to total "Ca", an amount equal to 50% of anorthite Si is subtracted from the "Si" total derived from other sources.

The normalizing procedure, and adjustment for "Si", are outlined below.

	Mineral Formulas										Normalized values			
				A						B	C	D		
Mineral	K	Na	Ca	Mg*	Fe	Al	Si	O	OH	8/Ox	Al	Si	Ca	Mg
Quartz							1	2		4	0	4.00	0.00	0.00
Anorthite			1			2	2	8		1	2	-1.00	1.00	0.00
Scapolite		1	3			5	7	24	1	0.3	1.6	0.16	0.96	0.00
Epidote			2		1	2	3	12	1	0.6	1.2	0.00	1.23	0.00
Biotite	2			5.5		2.5	5.5	20	4	0.3	0.8	0.58	0.00	1.83
Clinoamphibole			2	5			8	22	2	0.3	0	2.67	0.67	1.67
Clinopyroxene			1	1			2	6		1.3	0	2.67	1.33	1.33
Orthopyroxene				1			1	3		2.7	0	2.67	0.00	2.67
Olivine				2			1	4		2	0	2.00	0.00	4.00
Serpentine				3			2	5	4	0.9	0	1.78	0.00	2.67
Brucite				1					2	4	0	0.00	0.00	4.00
Calcite			1					3		2.7	0	0.00	2.67	0.00
Dolomite			1	1				6		1.3	0	0.00	1.33	1.33
Sphene			1				1	4	1	1.6	0	1.60	1.60	0.00
Spinel				1		2		4		2	4	-6.00	0.00	2.00

Explanation

Column A. Mineral formulas. Mg^* and MgO^* include both Mg and Fe^{2+}

Column B. The normalizing factors needed to obtain 8-oxygen-equivalents for each mineral. "8/Ox" = 8 divided by the number of oxygens in the mineral formula. The cations in the formula are then multiplied by this number in order to normalize them to 8 oxygens.

Column C. Al content of each mineral, normalized to 8 oxygens. This number, times 1.5, will later be subtracted from total Si. (This Al and Si are assigned to an "original clay fraction").

Column D. First, the Si, Ca, and Mg of each mineral are normalized to 8 oxygens by multiplying by the number in column B. Next, silica equal to 1.5 times the amount Al in column C is subtracted, giving negative numbers in some cases. Finally, to calculate the proportions of "SiO_2", "CaO", and "MgO^*" in the protolith of each rock, the numbers given in this column are multiplied by the modal mineral percentages. The results are plotted on Fig. 20.

The procedure can also be summarized by these equations:

Protolith "SiO_2" = 4 x modal quartz + 0.58 x modal biotite + 2.67 x modal orthopyroxene + 2 x modal olivine + 1.78 x modal serpentine + 2.67 x modal hornblende + 2.67 x modal clinopyroxene + 0.16 x modal scapolite + 1.6 x modal sphene - modal anorthite - 6 x modal spinel;

Protolith "CaO" = modal anorthite + 0.67 x modal hornblende + 1.33 x modal clinopyroxene + 1.33 x modal dolomite + 2.67 x modal calcite + 0.96 x modal scapolite + 1.23 x modal epidote + 1.6 x modal sphene; and

Protolith "MgO^*" = 1.83 x modal biotite + 2.67 x modal orthopyroxene + 4 x modal olivine + 2.67 x modal serpentine + 4 x modal brucite + 2 x modal spinel + 1.67 x modal hornblende + 1.33 x modal clinopyroxene + 1.33 x modal dolomite.

PLEASE NOTE:

Oversize maps and charts are filmed in sections in the following manner:

LEFT TO RIGHT, TOP TO BOTTOM, WITH SMALL OVERLAPS

The following map or chart has been refilmed in its entirety at the end of this dissertation (not available on microfiche). A xerographic reproduction has been provided for paper copies and is inserted into the inside of the back cover.

Black and white photographic prints (17" x 23") are available for an additional charge.

University Microfilms International

PLATE I—

GEOLOGICAL MAP OF PARTS OF THE PEACH LAKE AND BREWSTER QUADRANGLES, NEW YORK AND CONNECTICUT

Intrusive Rocks

- Oum — Ultramafic and mafic pods
- Os — Siscowit Granite

Allochthonous Rocks

- €Oh — Hartland Formation
- 1
- €m — Manhattan Schist
- 0

Autochthonous Rocks

- Ow — Walloomsac Schist
  - Owm — Marble Member

UNCONFORMITY

- €Oi — Inwood Marble
- Z€n — Ned Mountain Formation, undivided
  - Z€nc — Calc-Silicate Member
  - Z€nw — Wacke Member
  - Z€nv — Volcaniclastic Member
    - Z€nvg — Hypersolvus granite
  - Z€nb — Basal Member

UNCONFORMITY

- Yf — Fordham Gneiss, undivided

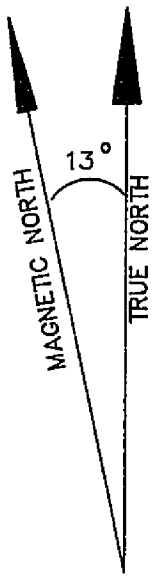

TER

RK

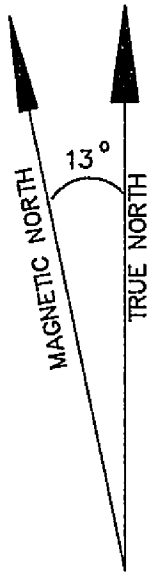
13°
MAGNETIC NORTH
TRUE NORTH

vided

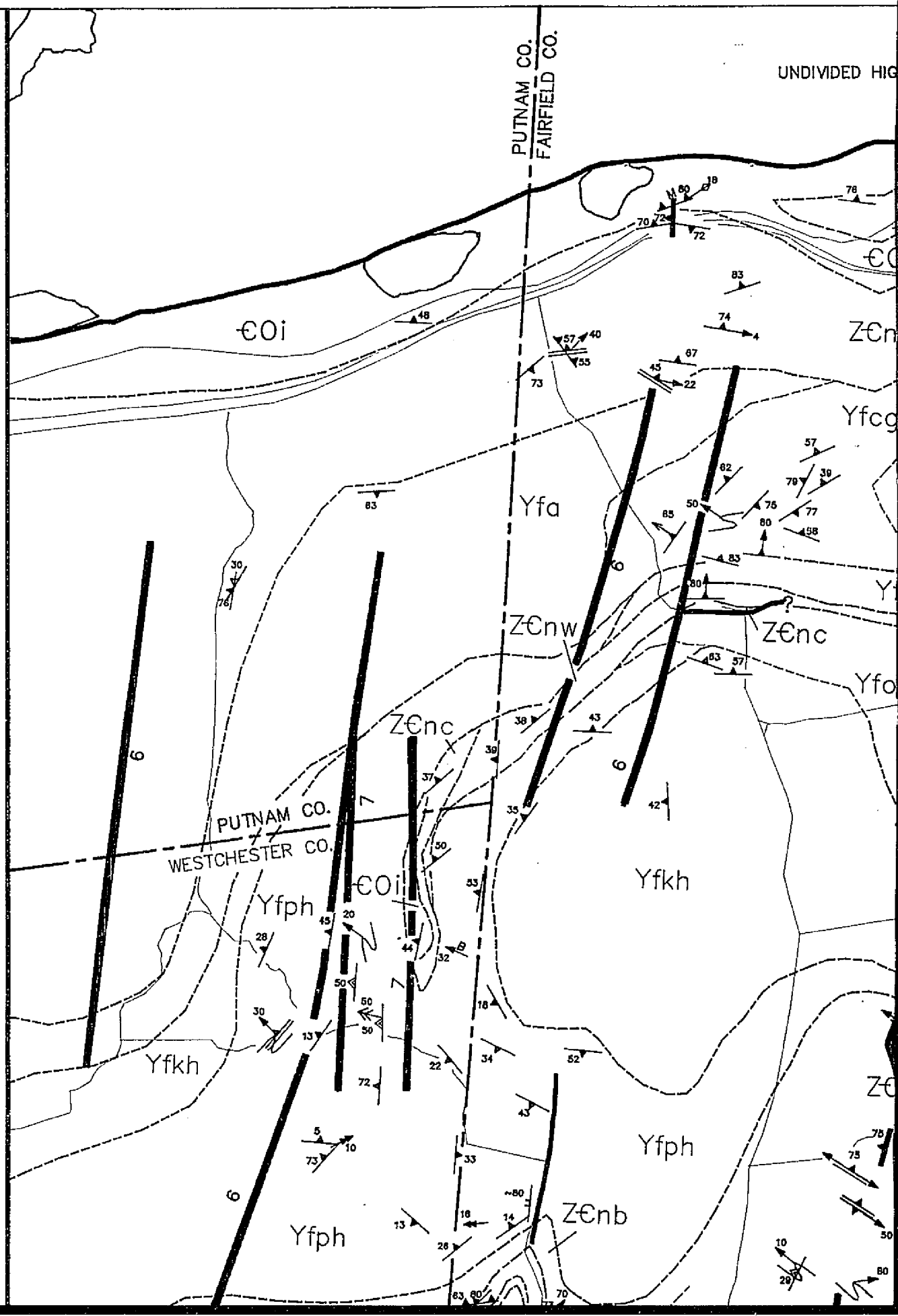
UNDIVIDED HIG
PUTNAM CO.
FAIRFIELD CO.
PUTNAM CO.
WESTCHESTER CO.
€Oi
Yfa
Yfcg
Z€nw
Z€nc
Yfkh
Yfph
Z€nb
6
7

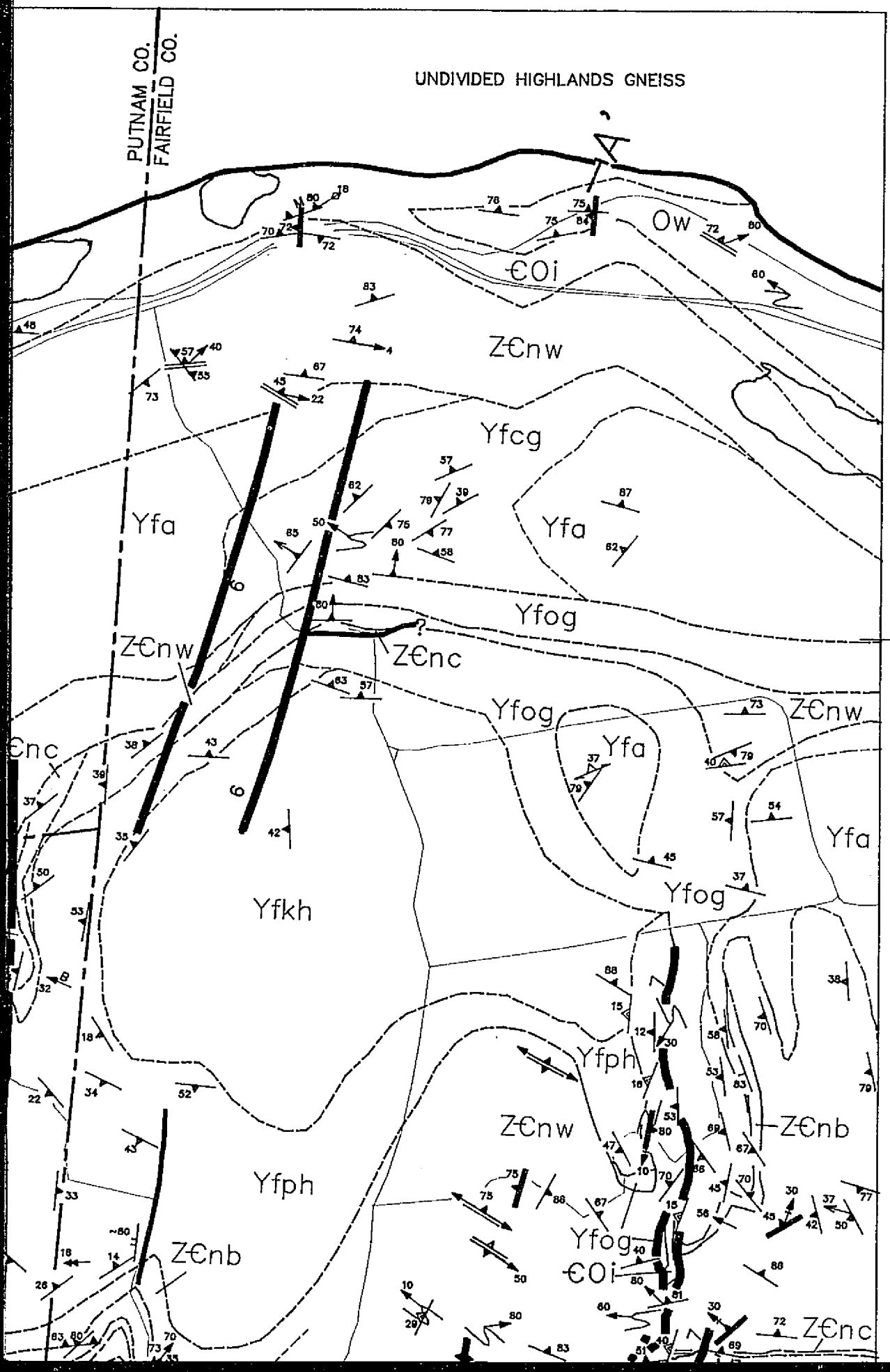
PUTNAM CO.
FAIRFIELD CO.
UNDIVIDED HIGHLANDS GNEISS
A
A'
Ow
€Oi
Z€nw
Yfcg
Yfa
Yfog
Z€nc
Yfkh
Yfph
Z€nb
41° 22' 30"

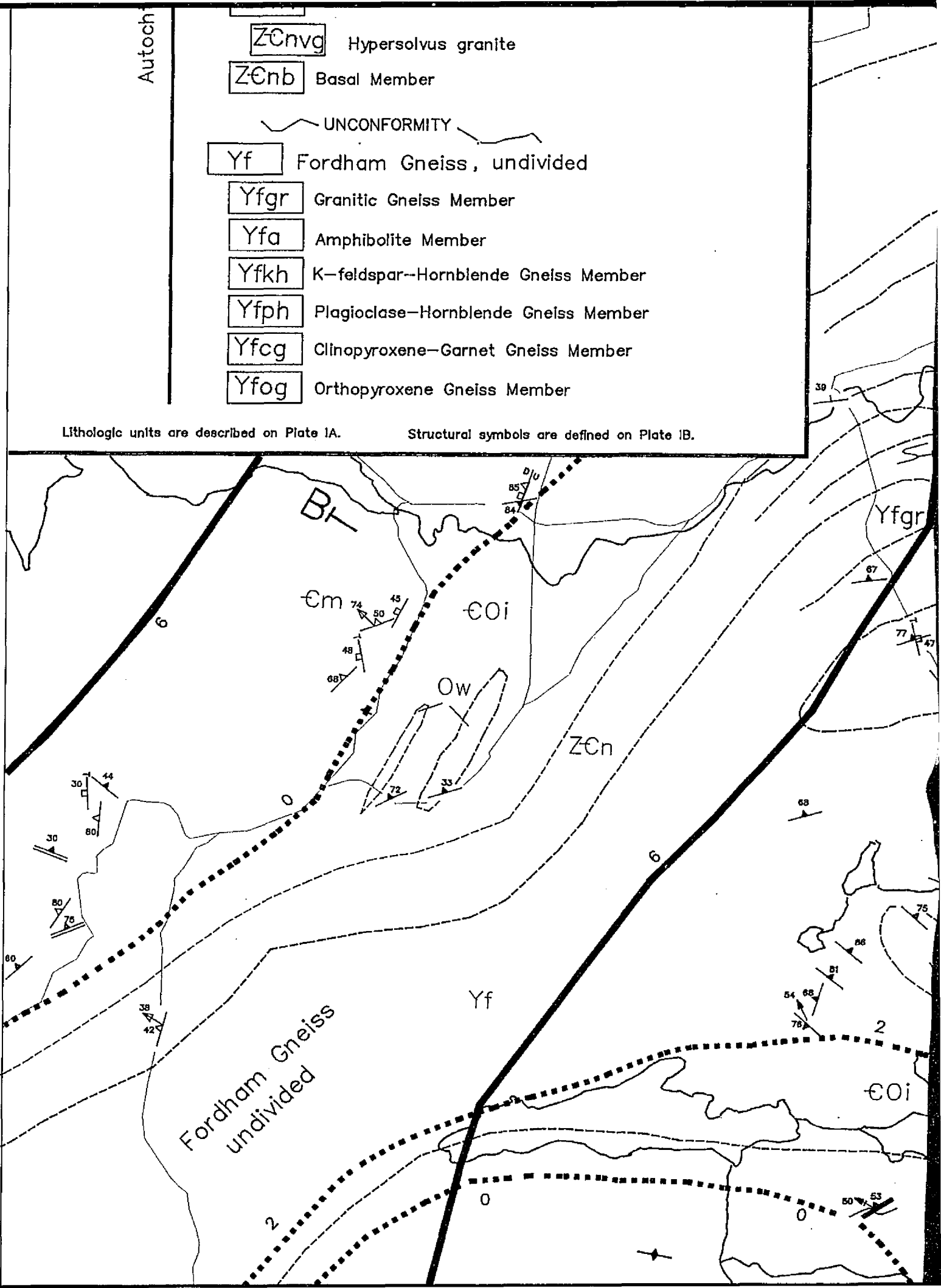
Autoch
Z€nvg Hypersolvus granite
Z€nb Basal Member
UNCONFORMITY
Yf Fordham Gneiss, undivided
Yfgr Granitic Gneiss Member
Yfa Amphibolite Member
Yfkh K–feldspar–Hornblende Gneiss Member
Yfph Plagioclase–Hornblende Gneiss Member
Yfcg Clinopyroxene–Garnet Gneiss Member
Yfog Orthopyroxene Gneiss Member
Lithologic units are described on Plate 1A.
Structural symbols are defined on Plate 1B.
Bt
€m
€Oi
Ow
Z€n
Yf
Yfgr
Fordham Gneiss undivided
6
0
2

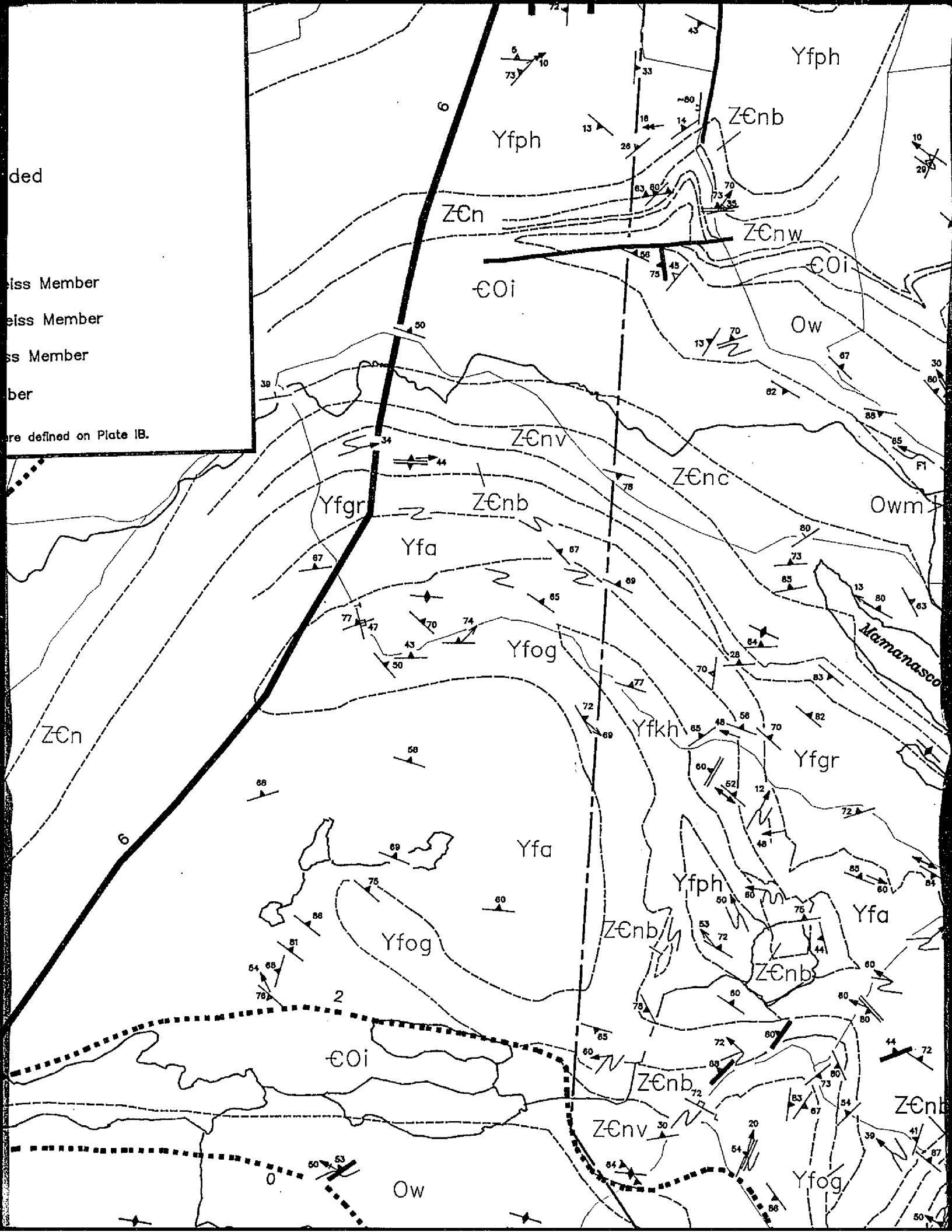
ded
iss Member
eiss Member
ss Member
ber
re defined on Plate IB.
Yfph
Z€nb
Yfph
Z€n
Z€nw
€Oi
€Oi
Ow
Z€nv
Z€nc
Owm
Yfgr
Z€nb
Yfa
Yfog
Mamanasco
Z€n
Yfkh
Yfgr
Yfa
Yfph
Yfa
Yfog
Z€nb
Z€nb
€Oi
Z€nb
Z€nv
Yfog
Ow

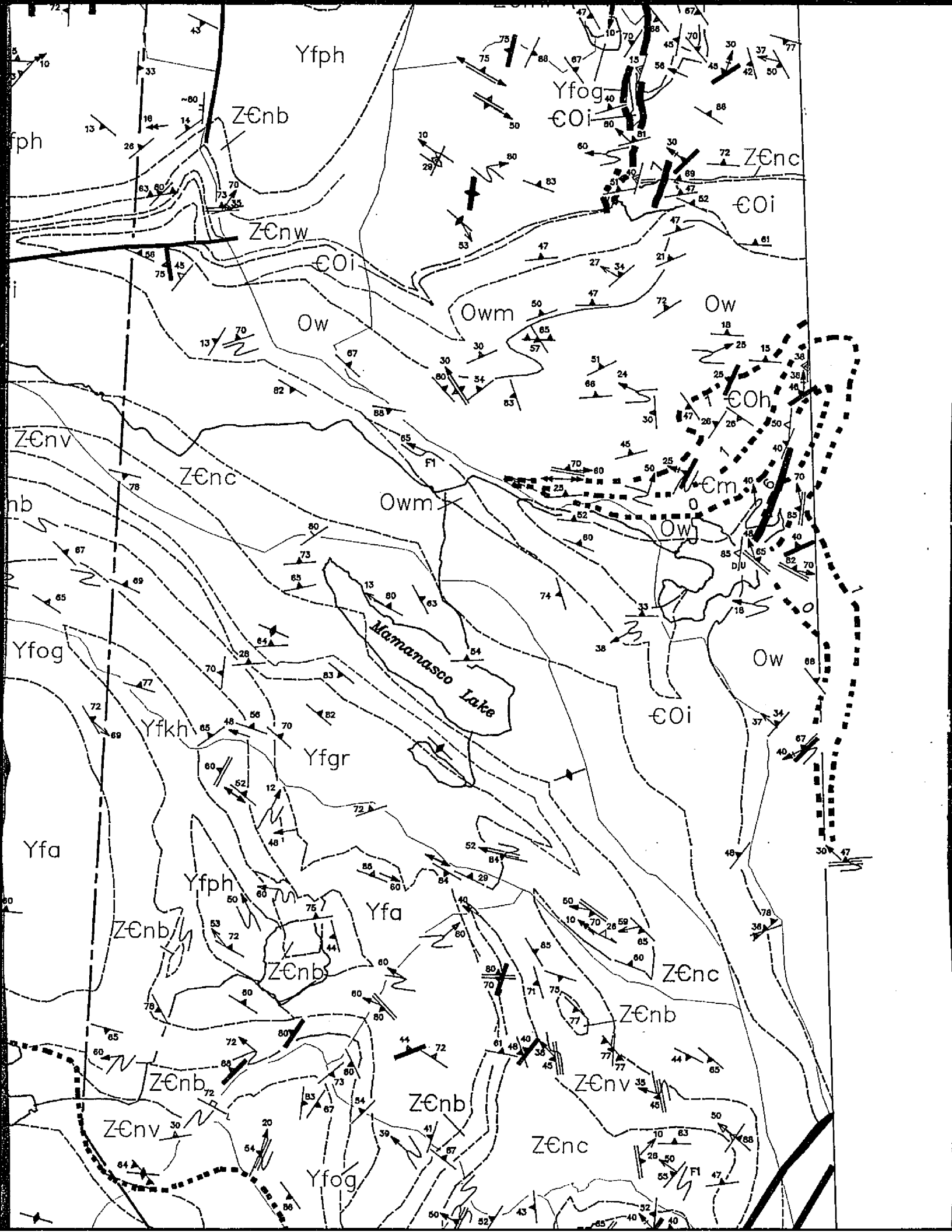
Yfph
Yfog
Z€nb
€Oi
Z€nc
Z€nw
Ow
Owm
€Oh
Z€nv
€m
Yfkh
Yfgr
Yfa
Mamanasco Lake

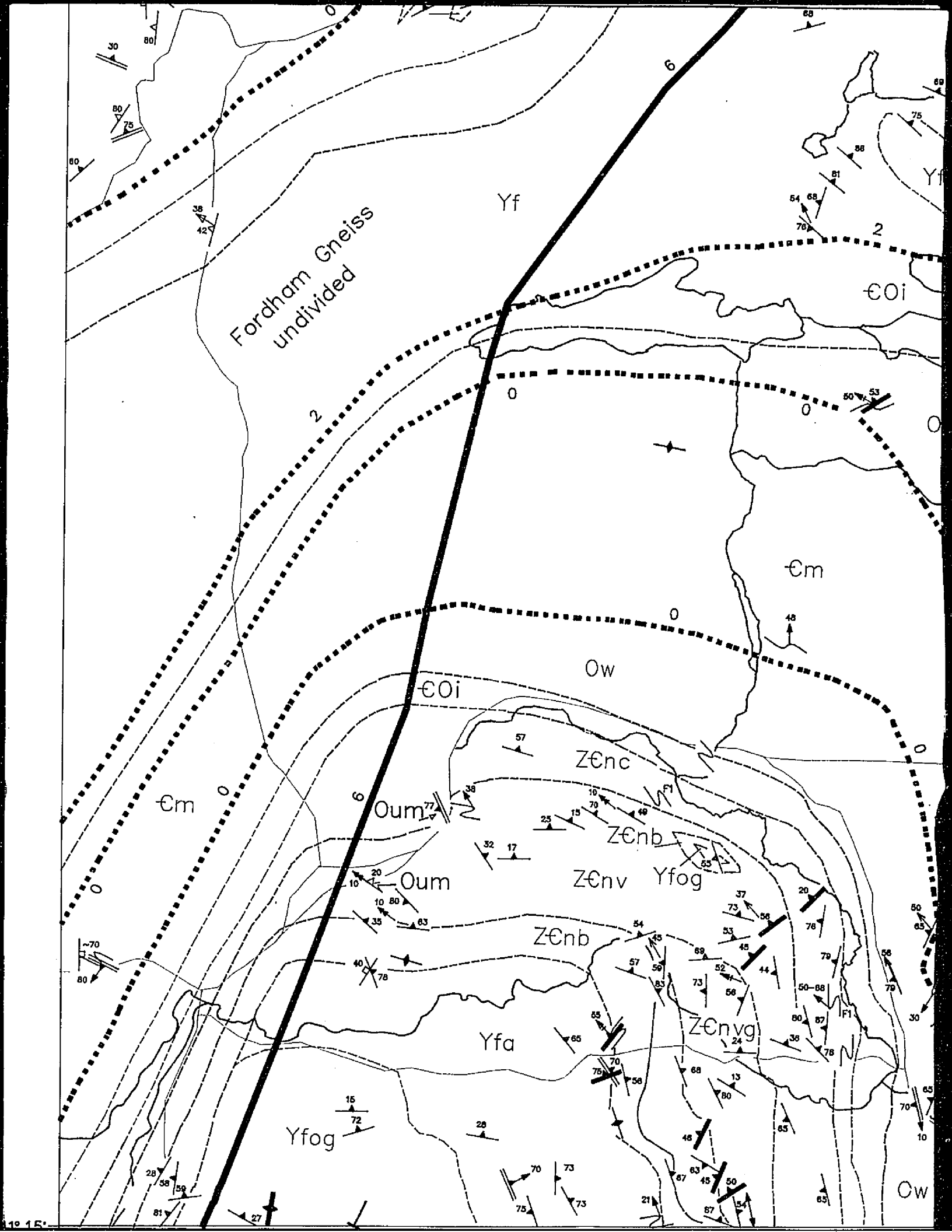
Yf
Fordham Gneiss
undivided
€Oi
€m
Ow
Z€nc
Oum
Z€nb
Z€nv
Yfog
Z€nvg
Yfa
0
2
6
F1

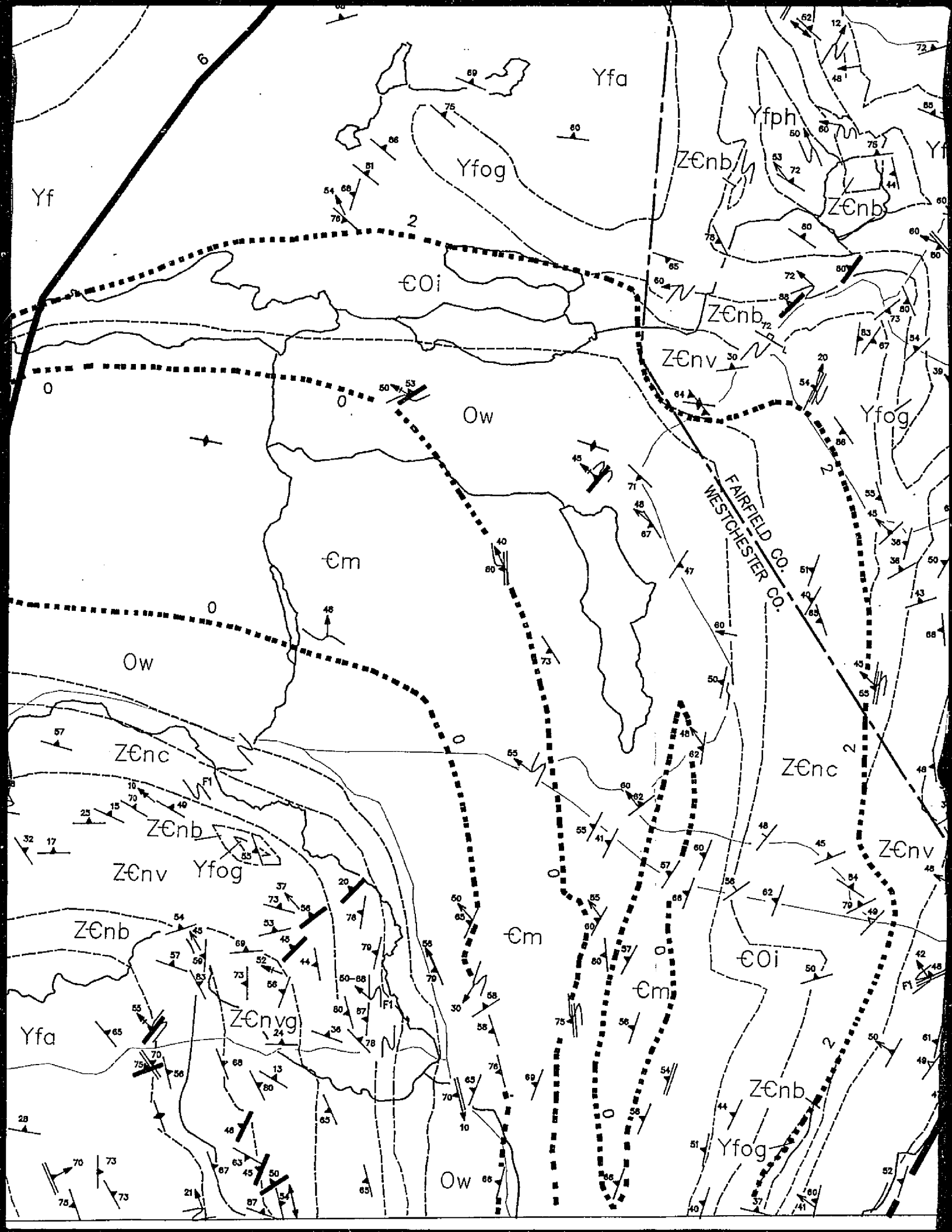
Yf
Yfa
Yfog
Yfph
Z€nb
Z€nv
€Oi
Ow
€m
Z€nc
Z€nvg
FAIRFIELD CO.
WESTCHESTER CO.
F1

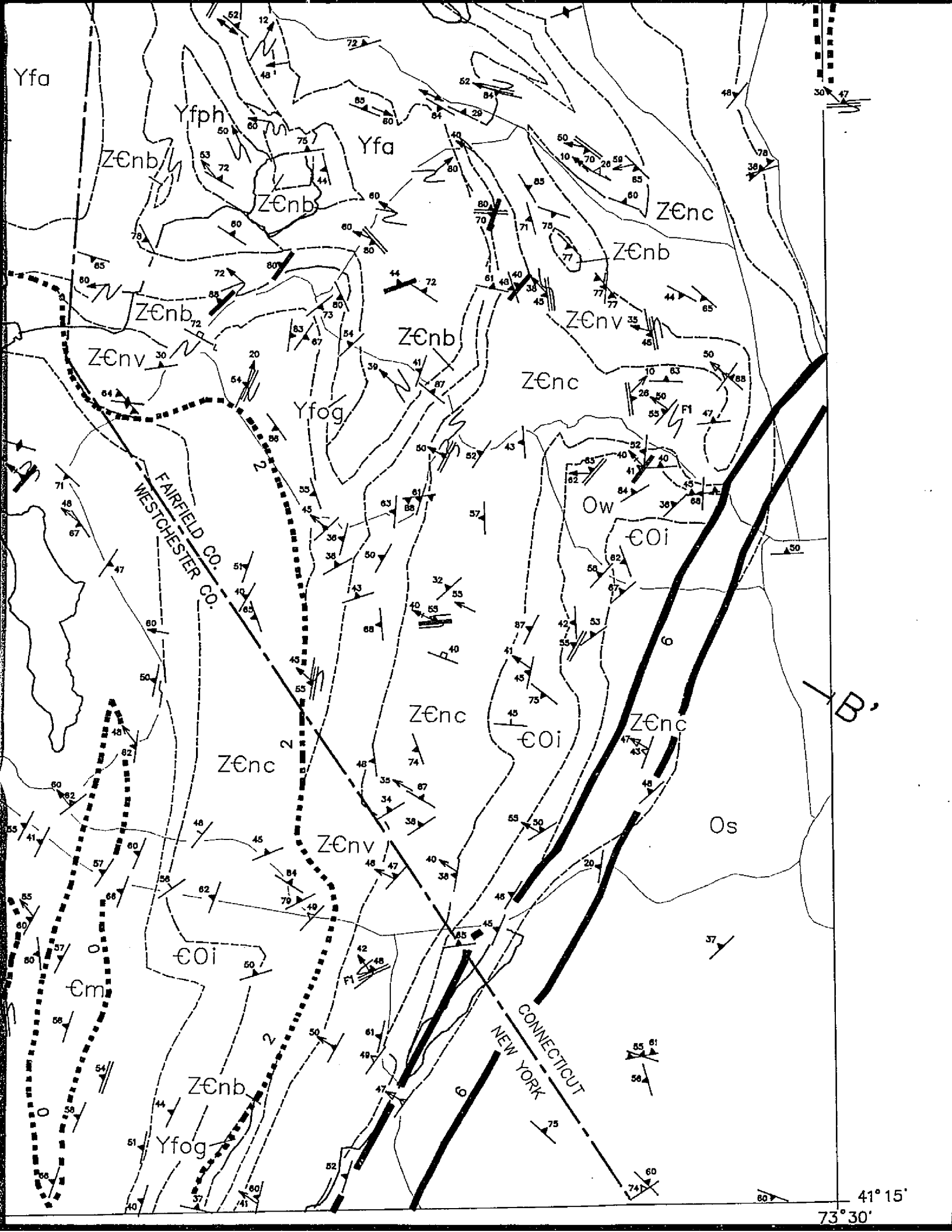
Yfa
Yfph
Z€nb
Yfa
Z€nb
Z€nc
Z€nb
Z€nb
Z€nv
Z€nb
Z€nv
Z€nc
Yfog
F1
Ow
€Oi
FAIRFIELD CO.
WESTCHESTER CO.
Z€nc
Z€nc
€Oi
Z€nc
Os
Z€nv
€Oi
€m
Z€nb
Yfog
CONNECTICUT
NEW YORK
B'
41° 15'
73° 30'

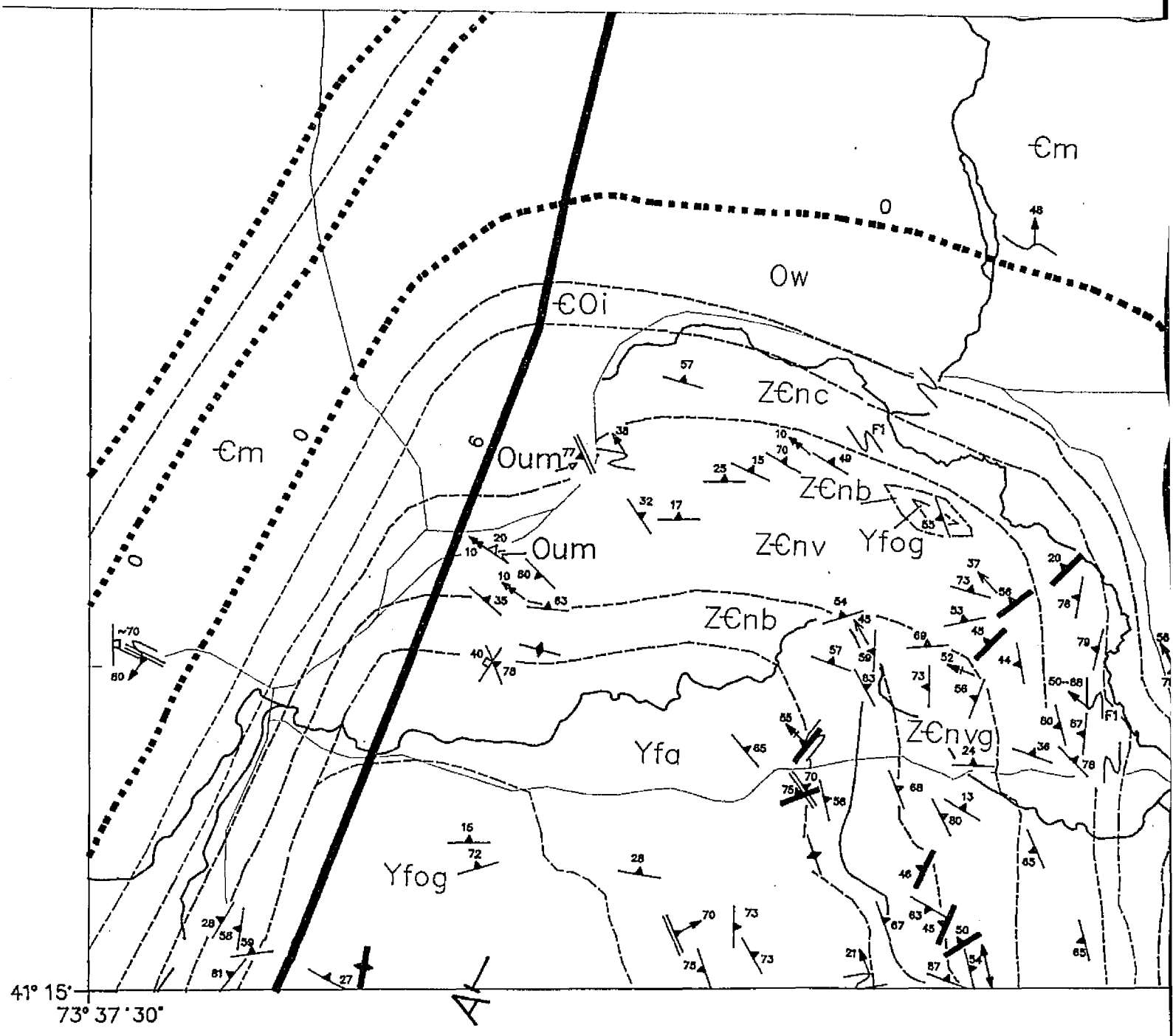

Selected roads

For identification of roads and landmarks, see Plate III.

1 0.5

1 0.5

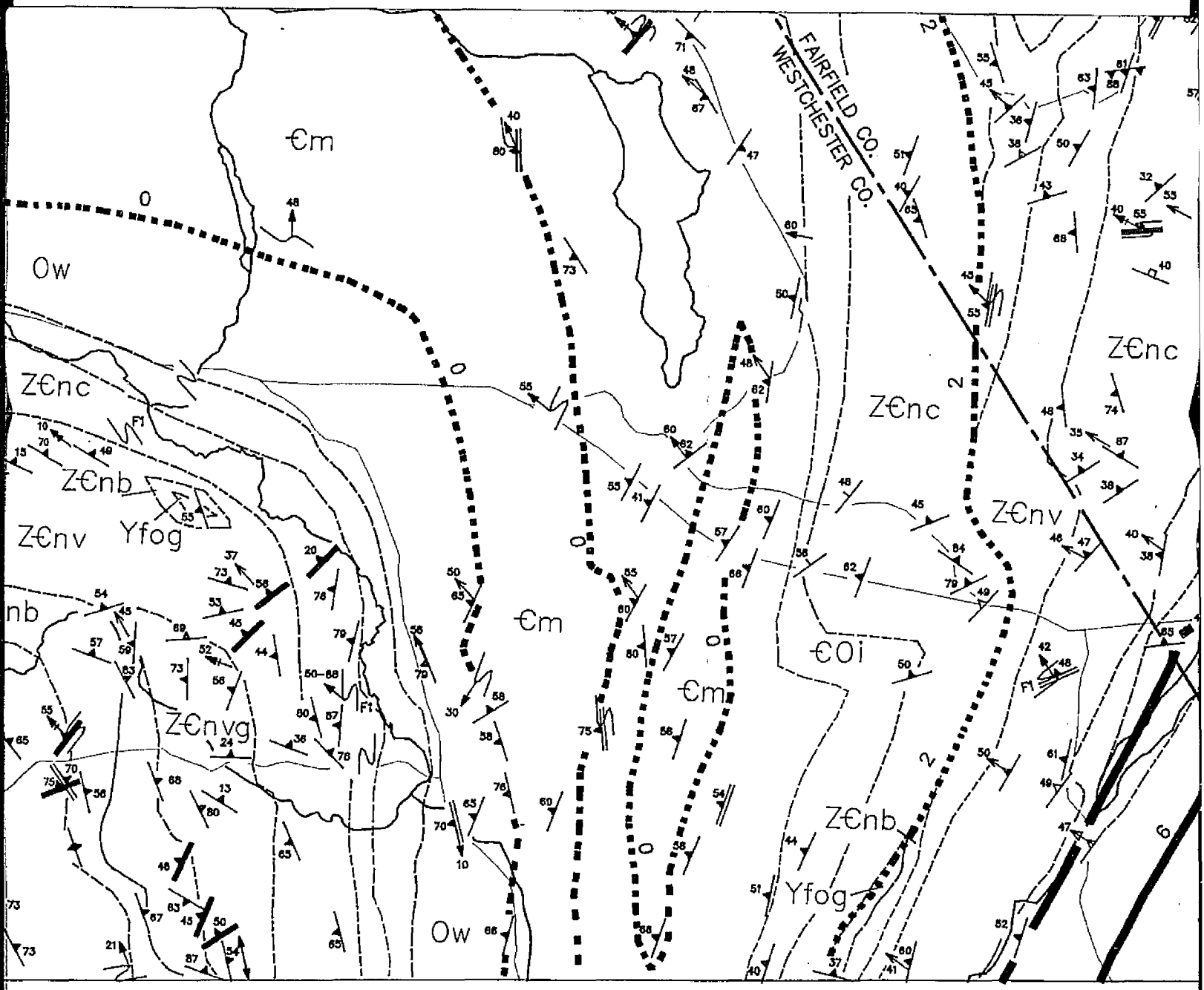

SCALE 1:24000

1 0.5 0 0.5 1 MILE

1 0.5 0 0.5 1 KILOMETER

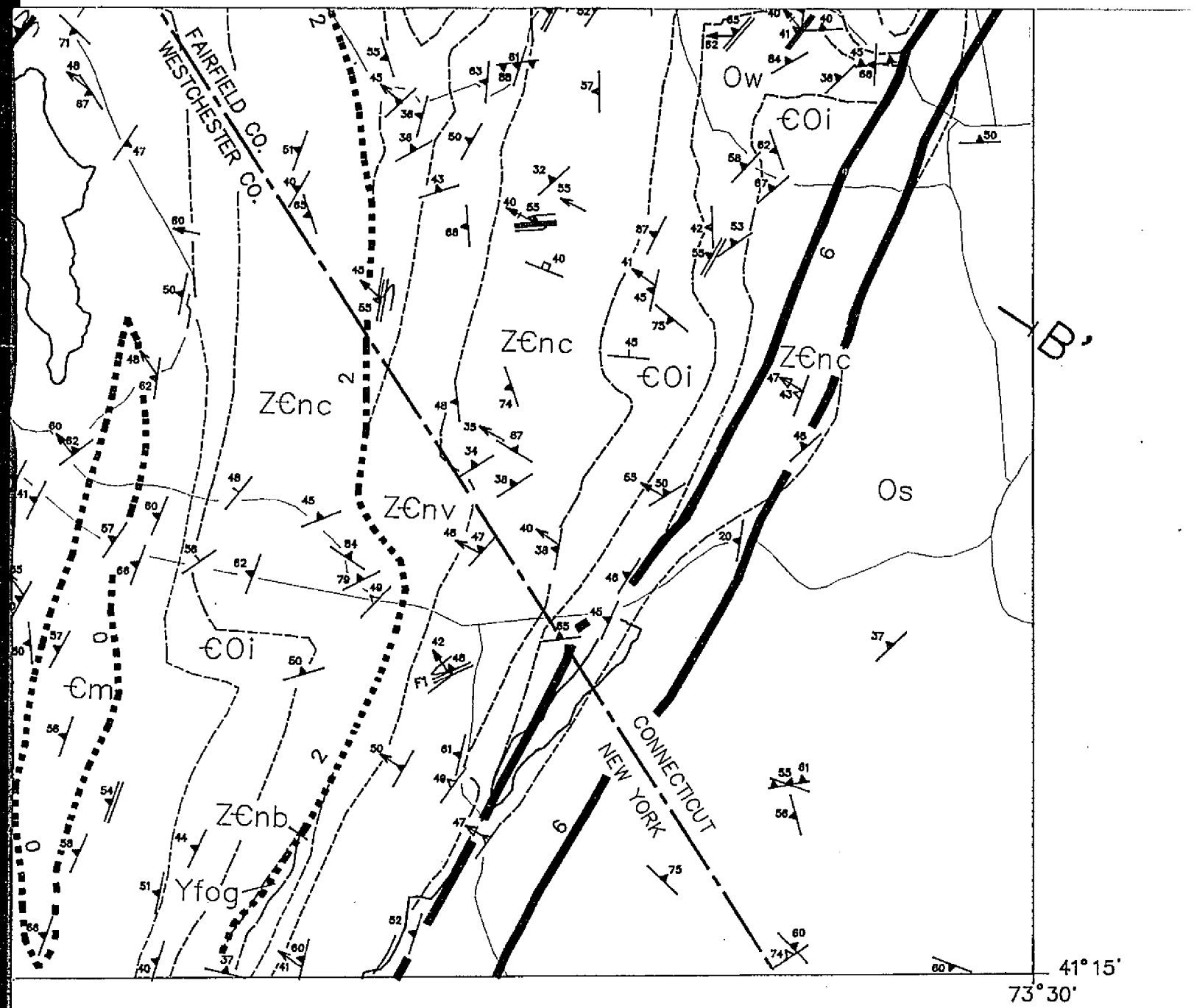

Geology by Pamela Chase Brock, 1992.

0.5 1 MILE

1 KILOMETER

PLEASE NOTE:

Oversize maps and charts are filmed in sections in the following manner:

LEFT TO RIGHT, TOP TO BOTTOM, WITH SMALL OVERLAPS

The following map or chart has been refilmed in its entirety at the end of this dissertation (not available on microfiche). A xerographic reproduction has been provided for paper copies and is inserted into the inside of the back cover.

Black and white photographic prints (17" x 23") are available for an additional charge.

University Microfilms International

PLATE IA– EX

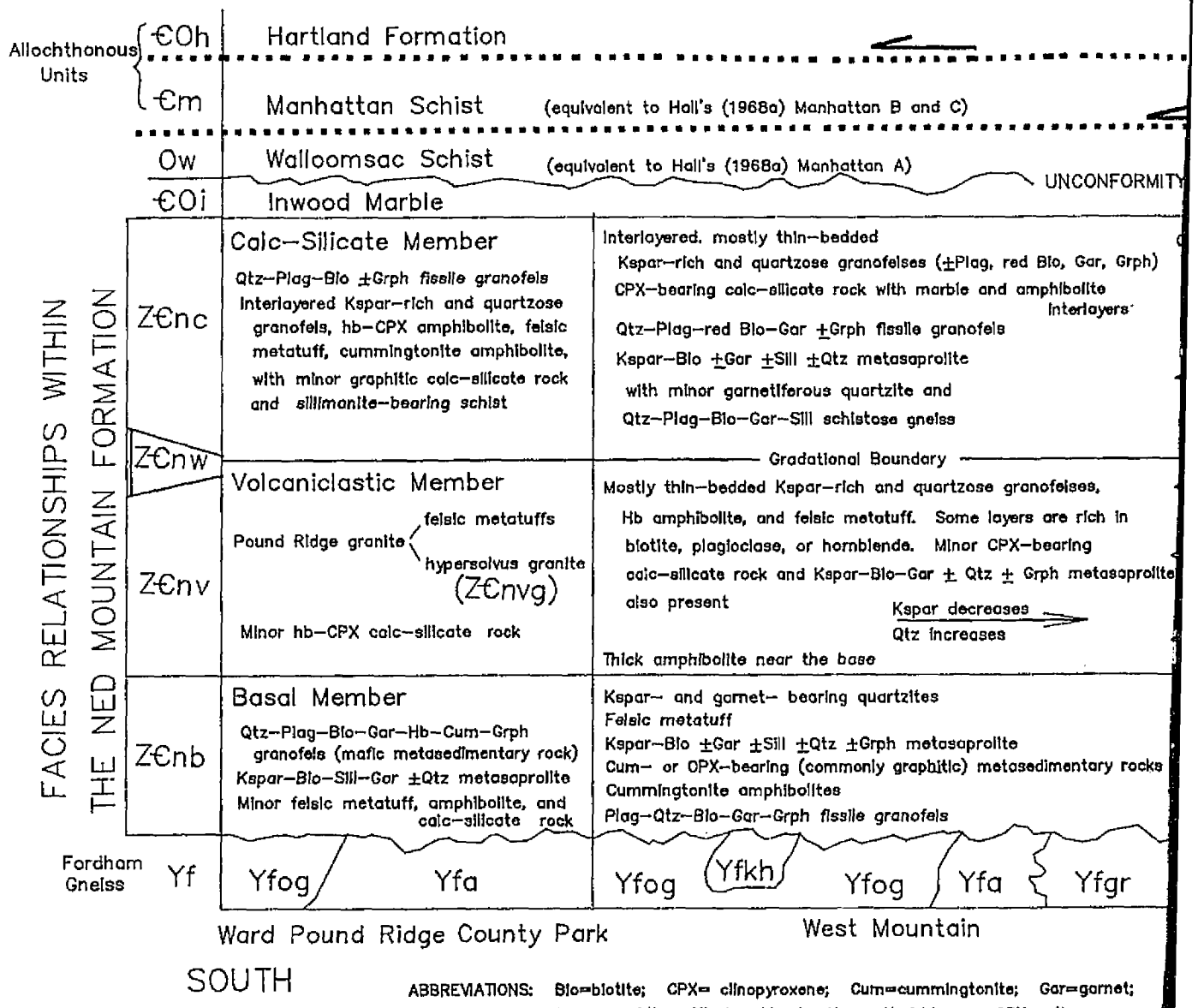

ABBREVIATIONS: Bio=biotite; CPX= clinopyroxene; Cum=cummingtonite; Gar=garnet; Grph=graphite; Hb=hornblende; Kspar=K–feldspar; OPX=orthopyroxene; Qtz=quartz; Sill=sillimanite.

INTRUSIVE ROCKS

MESOZOIC

Lamprophyre

Dark green, fine–grained, porphyritic lamprophyre dike less than 0.5 meter in thickness. Biotite phenocrysts are abundant and display a flow foliation parallel to dike contacts.

CIAN

Ow Walloomsac Sc

Rusty–weathering, poorly bedded, migmatitic quartz–pl
garnet–sillimanite schistose gneiss and biotite–garnet–s
schist. Well–bedded, graphitic, quartz–plagioclase–biot
marble, and calc–silicate rock are present near the b
gives many rocks a distinctive red cast. Bedding vari
greater than one meter in thickness. The Walloomsac
(+/–) clinopyroxene amphibolite and a few very thin b

LATE IA– EXPLANATION OF LITHOLOGIC UNITS

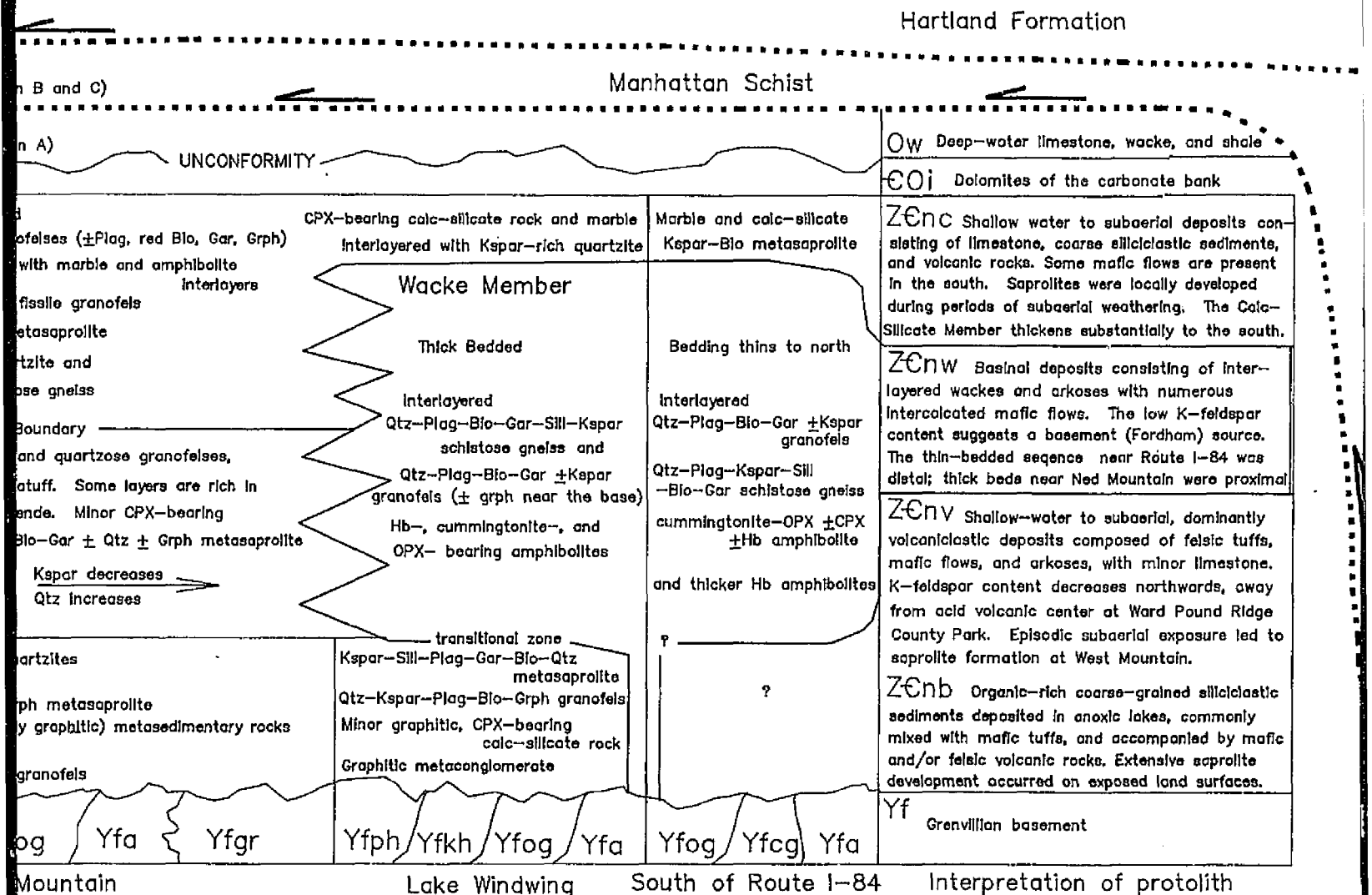

n=cummingtonite; Gar=garnet;
=K–feldspar; OPX=orthopyroxene;

AUTOCHTHONOUS UNITS

Ow Walloomsac Schist

orly bedded, migmatitic quartz–plagioclase K–feldspar–biotite
histose gneiss and biotite–garnet–sillimanite–quartz–feldspar
graphitic, quartz–plagioclase–biotite granofels, calcareous
ate rock are present near the base. The typical reddish biotite
distinctive red coat. Bedding varies from several centimeters to
er in thickness. The Walloomsac Schist contains minor hornblende
mphibolite and a few very thin beds of cummingtonite amphibolite.

Owm Marble Member

–silicates of the Walloomsac Schist are distinguished as the
their thickness in outcrop permits.

€Oi Inwood Marble

n, and greenish magnesian marble with calcareous interlayers.

Yf Fordham Gneiss

Yfgr Granitic Gneiss Member

Coarse–grained, poorly layered, light grey, hornblende–bearing granitic gneiss with abundant clots of magnetite, one– to three–millimeters in diameter. Amphibolitic interlayers are also present.

Yfa Amphibolite Member

Massive hornblende–rich amphibolite with minor leucocratic quartz–feldspar–biotite +/– hornblende gneiss. Small amounts of pyroxene are commonly present in both the mafic and leucocratic layers. Contacts with with Yfog, Yfcg, and Yfph are gradational.

Yfkh K–feldspar–Hornblende Gneiss Member

AMBRO–ORDOVICIAN

HOLOGIC UNITS

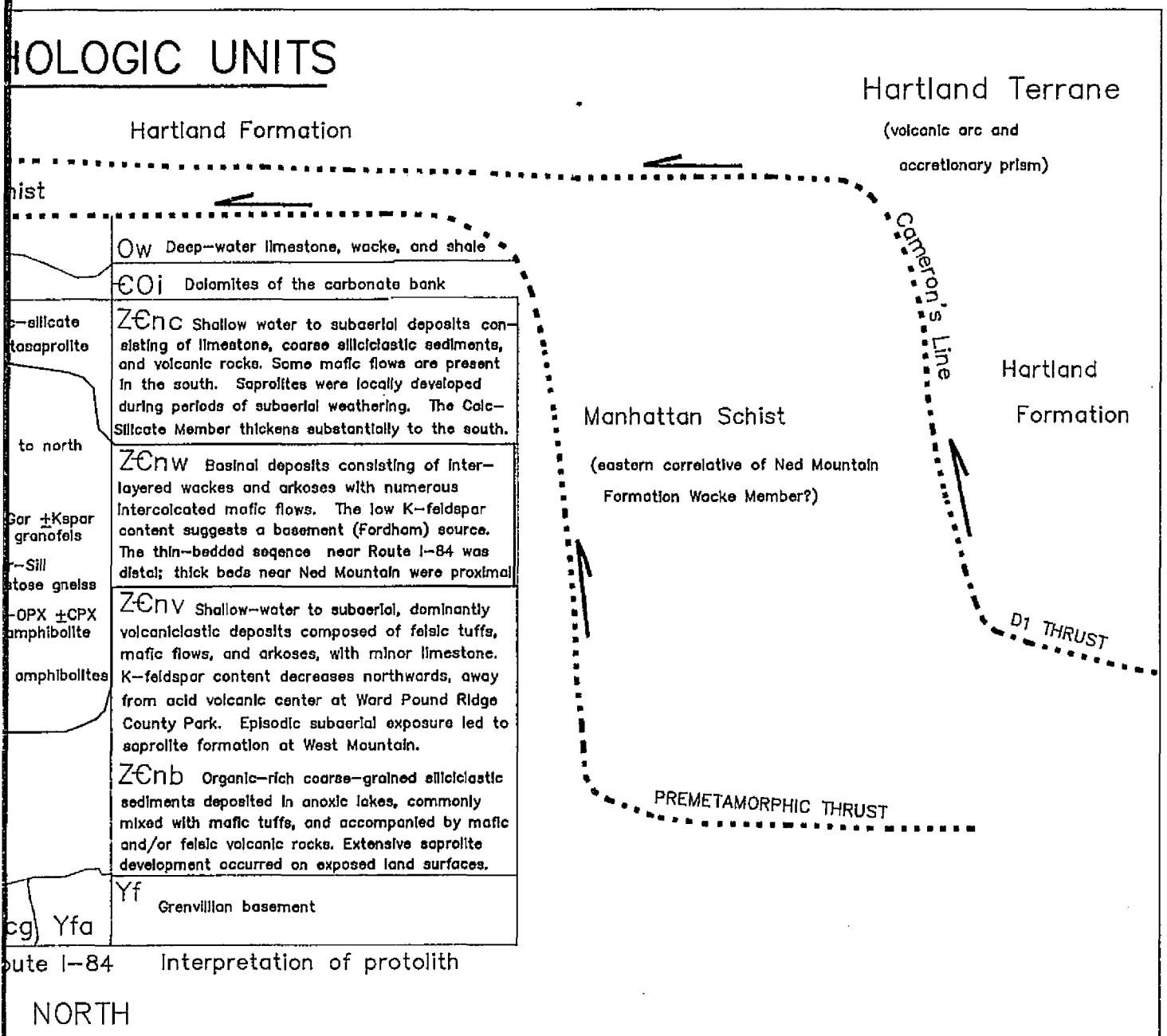

ALLOCHTHONOUS UNITS

Yf Fordham Gneiss

Yfgr Granitic Gneiss Member

poorly layered, light grey, hornblende-bearing granitic gniess
clots of magnetite, one- to three-millimeters in diameter.
erlayers are also present.

Yfa Amphibolite Member

nde-rich amphibolite with minor leucocratic quartz-feldspar-
rnblende gneiss. *Small amounts of pyroxene are commonly*
the mafic and leucocratic layers. Contacts with
and Yfph are gradational.

MBRO-ORDOVICIAN

€Oh Hartland Formation

Well-bedded sequence of thick, dark grey to black, hornblende-, cummingtonite-, or orthopyroxene-bearing amphibolites, thick white quartz-plagioclase-biotite-garnet granofelses, and thin (~10 centimeter) layers of white granofels rhythmically interbedded with grey quartz-feldspar-biotite-garnet-sillimanite schistose gneiss.

€m Manhattan Schist

ABBREVIATIONS: Bio=biotite; CPX=clinopyroxene; Cumm=cummingtonite; Gar=garnet; Grph=graphite; Hb=hornblende; Kspar=K-feldspar; OPX=orthopyroxene; Qtz=quartz; Sill=sillimanite.

INTRUSIVE ROCKS

MESOZOIC

L Lamprophyre

Dark green, fine-grained, porphyritic lamprophyre dike less than 0.5 meter in thickness. Biotite phenocrysts are abundant and display a flow foliation parallel to dike contacts.

MISSISSIPPIAN

Mississippian Granite Suite

Very small bodies of tourmaline-bearing, two-mica white granite, pink microcline-rich pegmatite, and white albitic pegmatite. Cleavages defined by muscovite +/- biotite are commonly present. Aluminous host rocks are typically retrograded to muscovite-rich schists.

ORDOVICIAN

Os Siscowit Granite

Medium to coarse-grained, pinkish-weathering, pale beige granite and granitic gneiss. Foliation is variably developed; micas are generally aligned, and quartz ribbons locally prominent. Biotite is ubiquitous, and secondary muscovite is generally present. Contains metasedimentary xenoliths and garnet-biotite schlieren.

Oum Ultramafic and mafic pods

Isolated pods of grey to black mafic and ultramafic rock, each less than two meters in diameter. Pods consist of olivine-phlogopite hornblendite (partially converted to unfoliated amphibolite) or garnet-hornblende amphibolite.

AUTOC

CAMBRO-ORDOVICIAN

Ow Walloomsac Schist

Rusty-weathering, poorly bedded, migmatitic quartz-plagioclase K-feldspar-garnet-sillimanite schistose gneiss and biotite-garnet-sillimanite-quartz-fe schist. Well-bedded, graphitic, quartz-plagioclase-biotite granofels, calcar marble, and calc-silicate rock are present near the base. The typical red gives many rocks a distinctive red cast. Bedding varies from several cent greater than one meter in thickness. The Walloomsac Schist contains min (+/-) clinopyroxene amphibolite and a few very thin beds of cummingtoni

Owm Marble Member

The marbles and calc-silicates of the Walloomsac Schist are distinguish Marble Member where their thickness in outcrop permits.

€Oi Inwood Marble

Well-bedded white, tan, and greenish magnesian marble with calcareous in Silica-poor magnesian beds consist of dolomite, +/- phlogopite, calcite, spinel. The more siliceous of the magnesian beds contain calcite-olivine-phlogopite. Scattered interbeds of brown phlogopite-calcite schist, white and dark diopside-rich amphibolite are locally present.

PROTEROZOIC Z- CAMBRIAN

Z€n Ned Mountain Formation

See diagram above for description of geographical and facies-related v

Z€nc Calc-Silicate Member

Z€nw Wacke Member

Z€nv Volcaniclastic Member

Z€nb Basal Member

PLATE IB- EXPLANATION

PLANAR FEATURES

Strike and dip

	Vertical	Inclined
Bedding		35 / 48

LINEAR FEATURES

Trend and plunge

Horizontal	Inclined

AUTOCHTHONOUS UNITS

Walloomsac Schist

ded, migmatitic quartz–plagioclase K–feldspar–biotite
neiss and biotite–garnet–sillimanite–quartz–feldspar
, quartz–plagioclase–biotite granofels, calcareous
are present near the base. The typical reddish biotite
red cast. Bedding varies from several centimeters to
ckness. The Walloomsac Schist contains minor hornblende
te and a few very thin beds of cummingtonite amphibolite.

Marble Member

es of the Walloomsac Schist are distinguished as the
hickness in outcrop permits.

Inwood Marble

greenish magnesian marble with calcareous interlayers.
onsist of dolomite, +/– phlogopite, calcite, olivine, and
the magnesian beds contain calcite–olivine–diopside–
eds of brown phlogopite–calcite schist, white quartzite,
bolite are locally present.

Mountain Formation

cription of geographical and facies–related variations

Calc–Silicate Member

Wacke Member

Volcaniclastic Member

Basal Member

PROTEROZOIC Y

Yf Fordham Gneiss

Yfgr Granitic Gneiss Member

Coarse–grained, poorly layered, light grey, hornblende–bearing granitic gniess with abundant clots of magnetite, one– to three–millimeters in diameter. Amphibolitic interlayers are also present.

Yfa Amphibolite Member

Massive hornblende–rich amphibolite with minor leucocratic quartz–feldspar–biotite +/– hornblende gneiss. Small amounts of pyroxene are commonly present in both the mafic and leucocratic layers. Contacts with with Yfog, Yfcg, and Yfph are gradational.

Yfkh K–feldspar–Hornblende Gneiss Member

Leuco– to mesocratic, coarse–grained, well–layered, K–feldspar–plagioclase–quartz–hornblende +/– clinopyroxene gneiss with amphibolitic interlayers.

Yfph Plagioclase–Hornblende Gneiss Member

Coarse–grained, well–layered, leuco– to mesocratic plagioclase–quartz–hornblende +/– clinopyroxene gneisses with amphibolitic interlayers.

Yfcg Clinopyroxene–Garnet Gneiss Member

Massive, poorly layered, generally melanocratic, green– or red–and–green clinopyroxene–garnet–plagioclase–quartz gneiss. Irregular black patches occur where hornblende has replaced clinopyroxene and garnet.

Yfog Orthopyroxene Gneiss Member

Coarse–grained, well–layered, leuco–to mesocratic orthopyroxene–bearing gneisses with dark hornblende–rich interlayers, cross–cut in places by orthopyroxene–bearing granite. Dark grey or greenish when fresh; beige or pinkish when weathered.

CAMBRO–ORDOVICIAN

Well–b
cumm
white
(~10
with g
gneiss

Poor
K–fe
quart
hornb

EXPLANATION OF STRUCTURAL SYMBOLS

EAR FEATURES

Trend and plunge

Horizontal Inclined

FOLD STYLE AND CROSS–CUTTING RELATIONSHIPS

CONT

	F1	F2 and unspecified age	F3	F4
Tight clockwise fold				
	F1			

ALLOCHTHONOUS UNITS

CAMBRO–ORDOVICIAN

€Oh Hartland Formation

Well–bedded sequence of thick, dark grey to black, hornblende–, cummingtonite–, or orthopyroxene–bearing amphibolites, thick white quartz–plagioclase–biotite–garnet granofelses, and thin (~10 centimeter) layers of white granofels rhythmically interbedded with grey quartz–feldspar–biotite–garnet–sillimanite schistose gneiss.

€m Manhattan Schist

Poorly bedded, migmatized, dark grey quartz–plagioclase–K–feldspar–biotite–garnet–sillimanite schistose gneiss and white quartz–plagioclase–biotite–garnet granofels, with interlayers of hornblende amphibolite.

Yf Fordham Gneiss

Yfgr Granitic Gneiss Member

ed, poorly layered, light grey, hornblende–bearing granitic gniess t clots of magnetite, one– to three–millimeters in diameter. interlayers are also present.

Yfa Amphibolite Member

blende–rich amphibolite with minor leucocratic quartz–feldspar– hornblende gneiss. Small amounts of pyroxene are commonly oth the mafic and leucocratic layers. Contacts with cg, and Yfph are gradational.

K–feldspar–Hornblende Gneiss Member

esocratic, coarse–grained, well–layered, K–feldspar–plagioclase– lende +/– clinopyroxene gneiss with amphibolitic interlayers.

Plagioclase–Hornblende Gneiss Member

ned, well–layered, leuco– to mesocratic plagioclase–quartz– +/– clinopyroxene gneisses with amphibolitic interlayers.

Clinopyroxene–Garnet Gneiss Member

rly layered, generally melanocratic, green– or red–and–green –garnet–plagioclase–quartz gneiss. Irregular black patches hornblende has replaced clinopyroxene and garnet.

fog Orthopyroxene Gneiss Member

ned, well–layered, leuco–to mesocratic orthopyroxene–bearing gneisses ornblende–rich interlayers, cross–cut in places by orthopyroxene– ite. Dark grey or greenish when fresh; beige or pinkish when

RAL SYMBOLS

AND CROSS–CUTTING RELATIONSHIPS

F1 F2 and unspecified age F3 F4

old

CONTACTS AND FAULTS

Tightly constrained contacts

Interpolated contacts

ORDOVIC

biotite schlieren.

Oum Ultramafic and mafic pods

Isolated pods of grey to black mafic and ultramafic rock, each less than two meters in diameter. Pods consist of olivine–phlogopite hornblendite (partially converted to unfoliated amphibolite) or garnet–hornblende amphibolite.

PROTEROZOIC Z– CAMBRIA

Z€n Ned Mountain Formation

See diagram above for description of geographical and facies–related

Z€nc Calc–Silicate Member

Z€nw Wacke Member

Z€nv Volcaniclastic Member

Z€nb Basal Member

PLATE IB– EXPLANATION

PLANAR FEATURES

Strike and dip

	Vertical	Inclined
Bedding		35
Foliation		46
Cross–cutting foliation		55

Hinge surfaces and refoliation zones

F1		47 F1
F2 and unspecified age		63
F3		37
F4		12

Fabrics in late faults and shear zones

S6 cleavage and sense of displacement, where available.	55 D U
Cleavage in D7 shear zone	25
Late (post–F3) mylonite zone (exact age uncertain)	M 81
Brittle fault cleavage	87
Tourmalinized fractures	42 T

LINEAR FEATURES

Trend and plunge

	Horizontal	Inclined
Quartz rod (age unspecified)		44
Boudin line		51

Hinge lines

F1		F1 54
F2 and unspecified age		43
F3		42
F4		11

Intersection of D6 with older foliation	33
L7 mullion and quartz rods	36
Slickensides	7

Cn Ned Mountain Formation

ove for description of geographical and facies-related variations

Z€nc Calc-Silicate Member

Z€nw Wacke Member

Z€nv Volcaniclastic Member

Z€nb Basal Member

Yfcg Clinopyroxene-Garnet Gneiss Member

Massive, poorly layered, generally melanocratic, green- or red-and-green clinopyroxene-garnet-plagioclase-quartz gneiss. Irregular black patches occur where hornblende has replaced clinopyroxene and garnet.

Yfog Orthopyroxene Gneiss Member

Coarse-grained, well-layered, leuco-to mesocratic orthopyroxene-bearing gneisses with dark hornblende-rich interlayers, cross-cut in places by orthopyroxene-bearing granite. Dark grey or greenish when fresh; beige or pinkish when weathered.

IB- EXPLANATION OF STRUCTURAL SYMBOLS

LINEAR FEATURES

Trend and plunge

Horizontal Inclined

rtz rod (age unspecified) 44

din line 51

nge lines

1 F1 54

2 and unspecified age 43

3 42

4 11

tersection of D6 with older foliation 33

7 mullion and quartz rods 36

lickensides 7

FOLD STYLE AND CROSS-CUTTING RELATIONSHIPS

	F1	F2 and unspecified age	F3	F4
Tight clockwise fold				
Tight counterclockwise fold	F1			
Open counterclockwise fold				
Open clockwise fold				
Symmetric fold				

Examples of folds showing hinge surface and hinge line 42 55 37 48

Examples of folds showing hinge surface and limbs 75 83 87 72 51 56

Fold showing hinge line and limbs 85 21 23

Examples of cross-cutting foliations 87 55 37 42

(Intersections of structural symbols are plotted at the outcrop location. The centers of fold symbols are plotted at the outcrop location.)

pyroxene–Garnet Gneiss Member

generally melanocratic, green– or red–and–green
lagioclase–quartz gneiss. Irregular black patches
has replaced clinopyroxene and garnet.

thopyroxene Gneiss Member

yered, leuco–to mesocratic orthopyroxene–bearing gneisses
ich interlayers, cross–cut in places by orthopyroxene–
grey or greenish when fresh; beige or pinkish when

SYMBOLS

ROSS–CUTTING RELATIONSHIPS

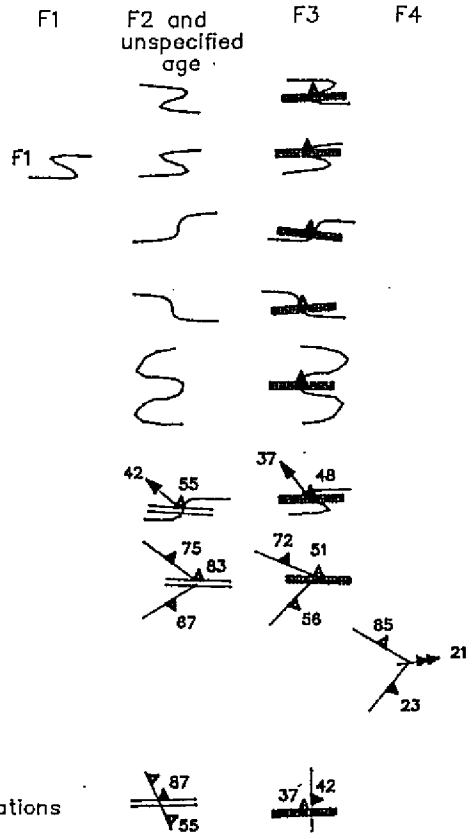

line

d

foliations

symbols are plotted at the outcrop location.
mbols are plotted at the outcrop location.)

CONTACTS AND FAULTS

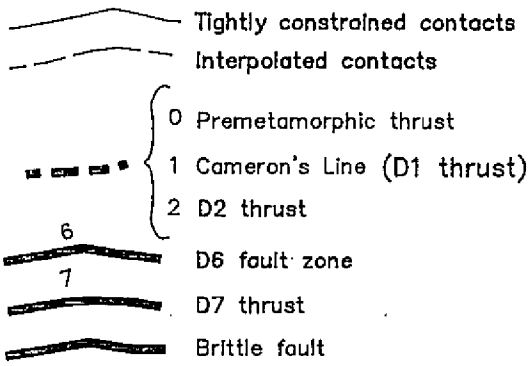

PLEASE NOTE:

Oversize maps and charts are filmed in sections in the following manner:

LEFT TO RIGHT, TOP TO BOTTOM, WITH SMALL OVERLAPS

The following map or chart has been refilmed in its entirety at the end of this dissertation (not available on microfiche). A xerographic reproduction has been provided for paper copies and is inserted into the inside of the back cover.

Black and white photographic prints (17" x 23") are available for an additional charge.

University Microfilms International

Plate II—A. Map showing truncation of Fordham Gneiss lithologies beneath the Ned Mountain Formation.

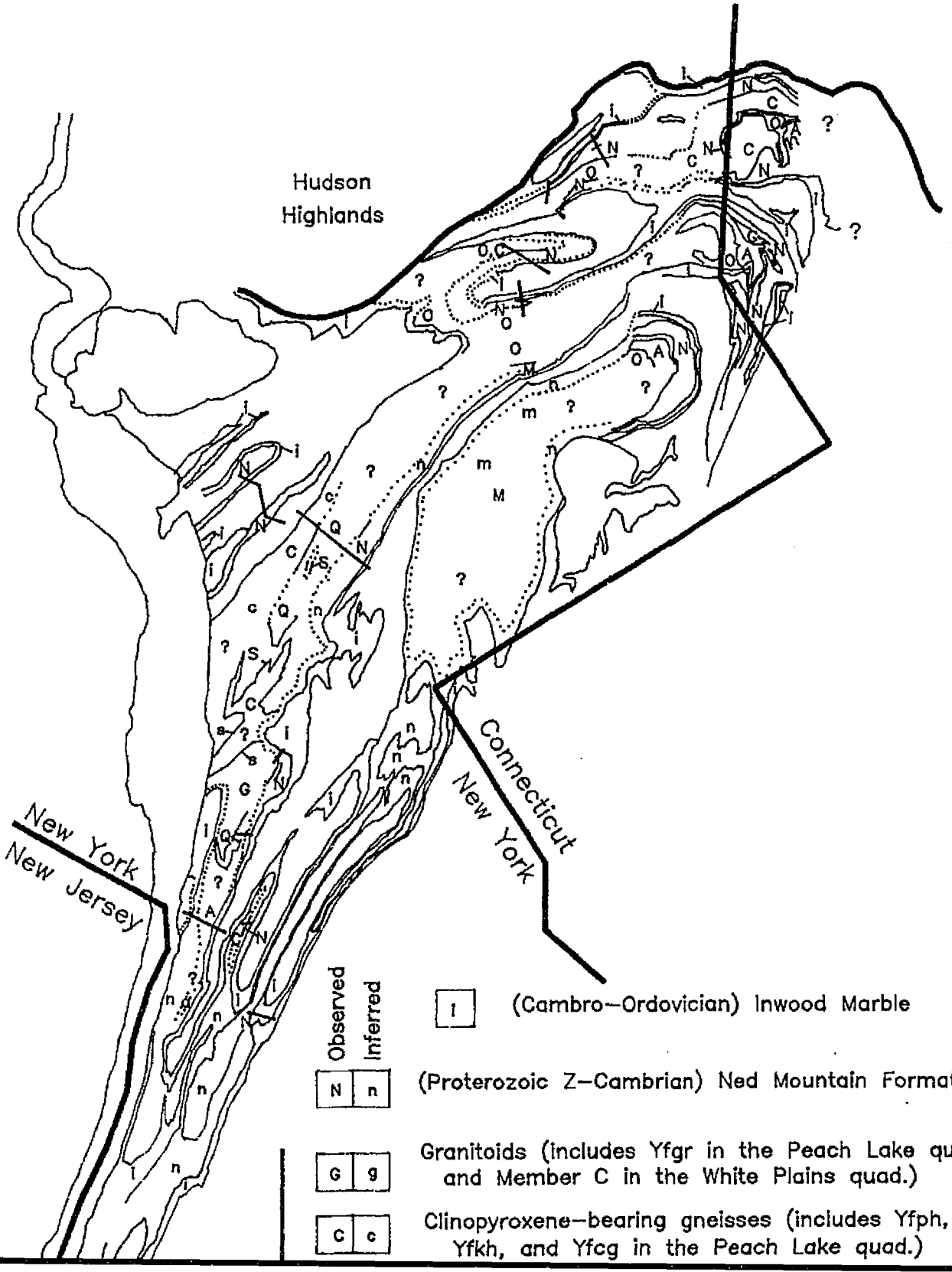

Plate II–B. Location map for transects examined outside of the study area.

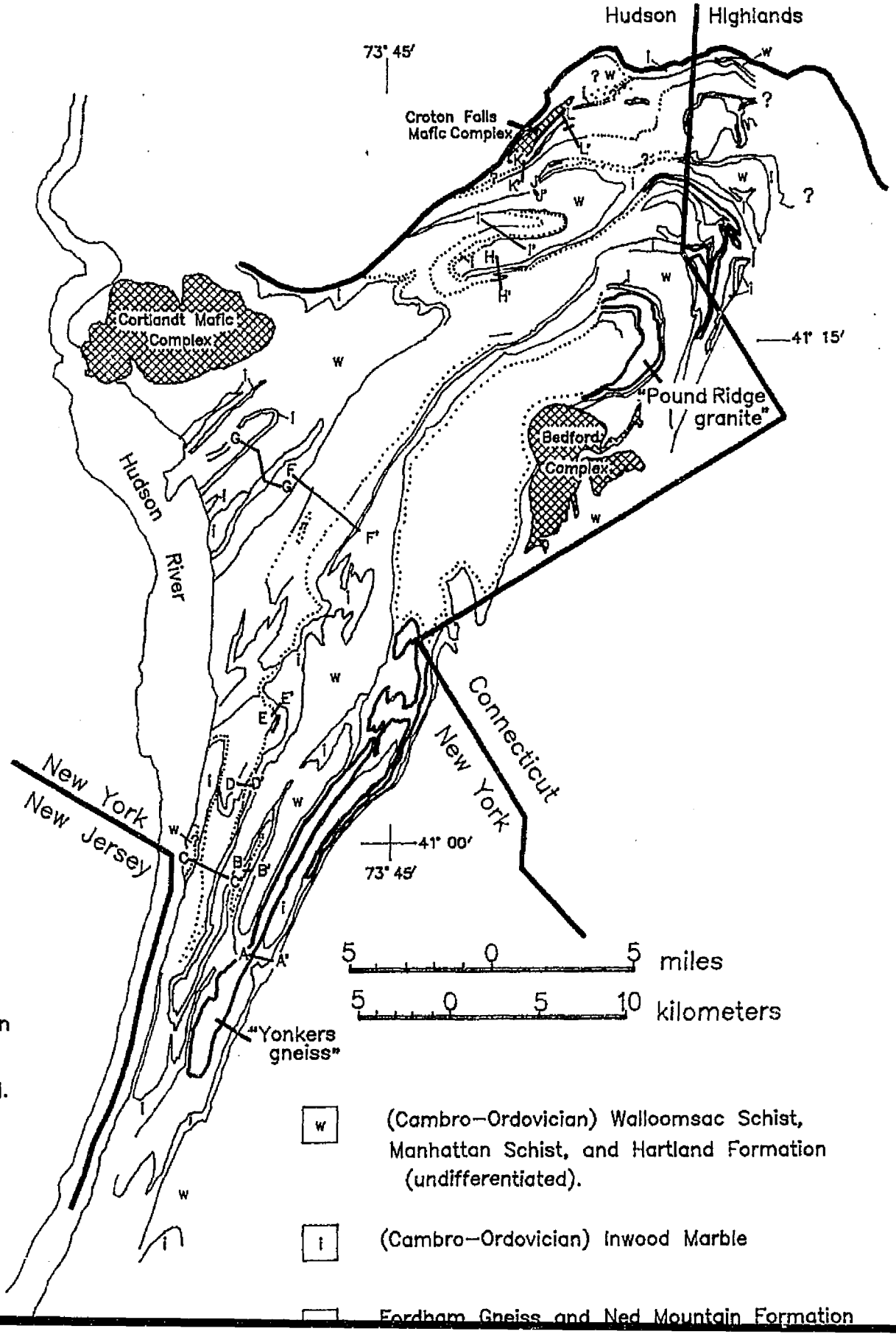

. Location map for transects examined outside of the study area.

Plate II–C. Map showing subdivisions o

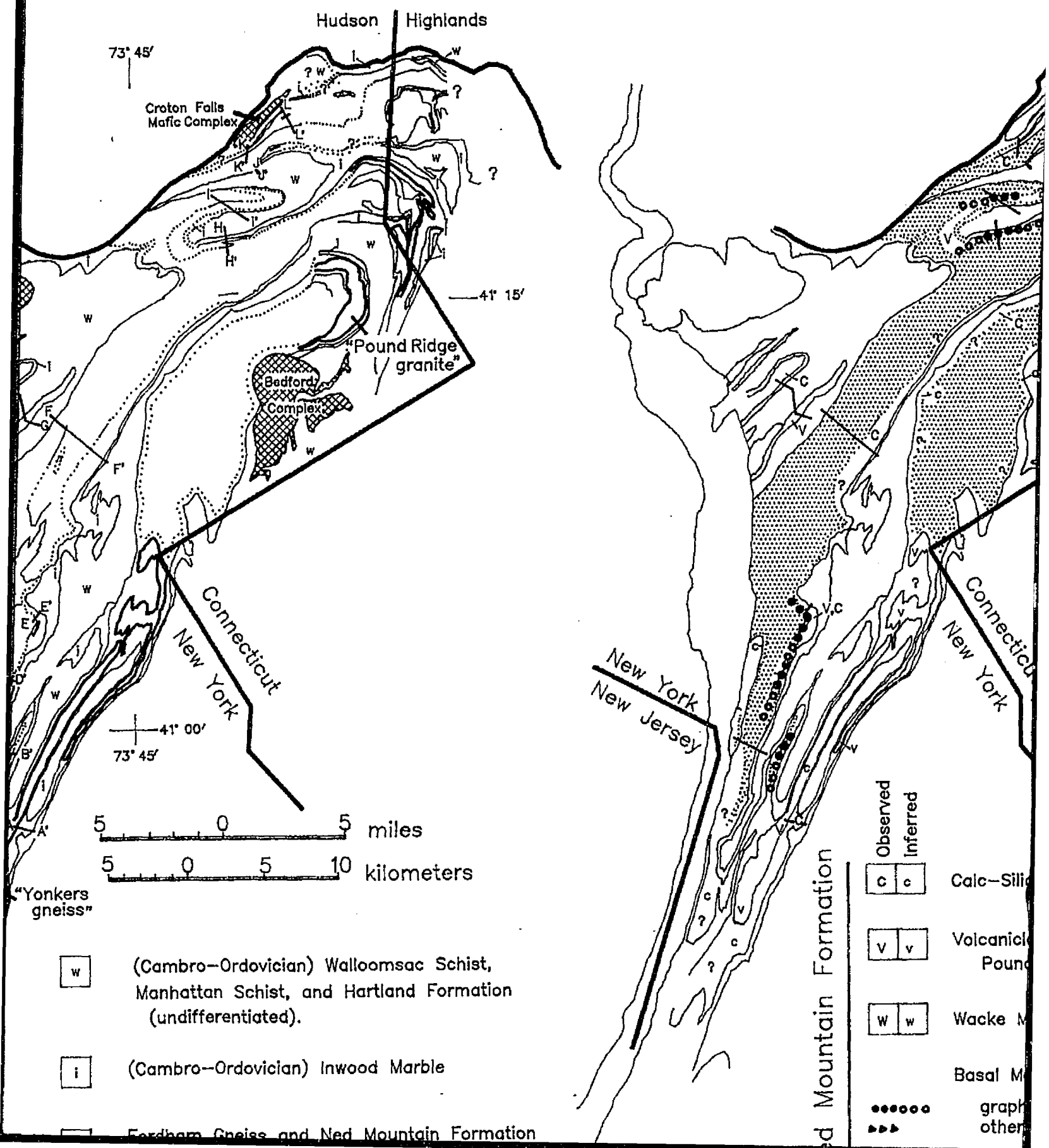

(Cambro–Ordovician) Walloomsac Schist, Manhattan Schist, and Hartland Formation (undifferentiated).

(Cambro–Ordovician) Inwood Marble

Fordham Gneiss and Ned Mountain Formation

Plate II–C. Map showing subdivisions of the Ned Mountain Formation.

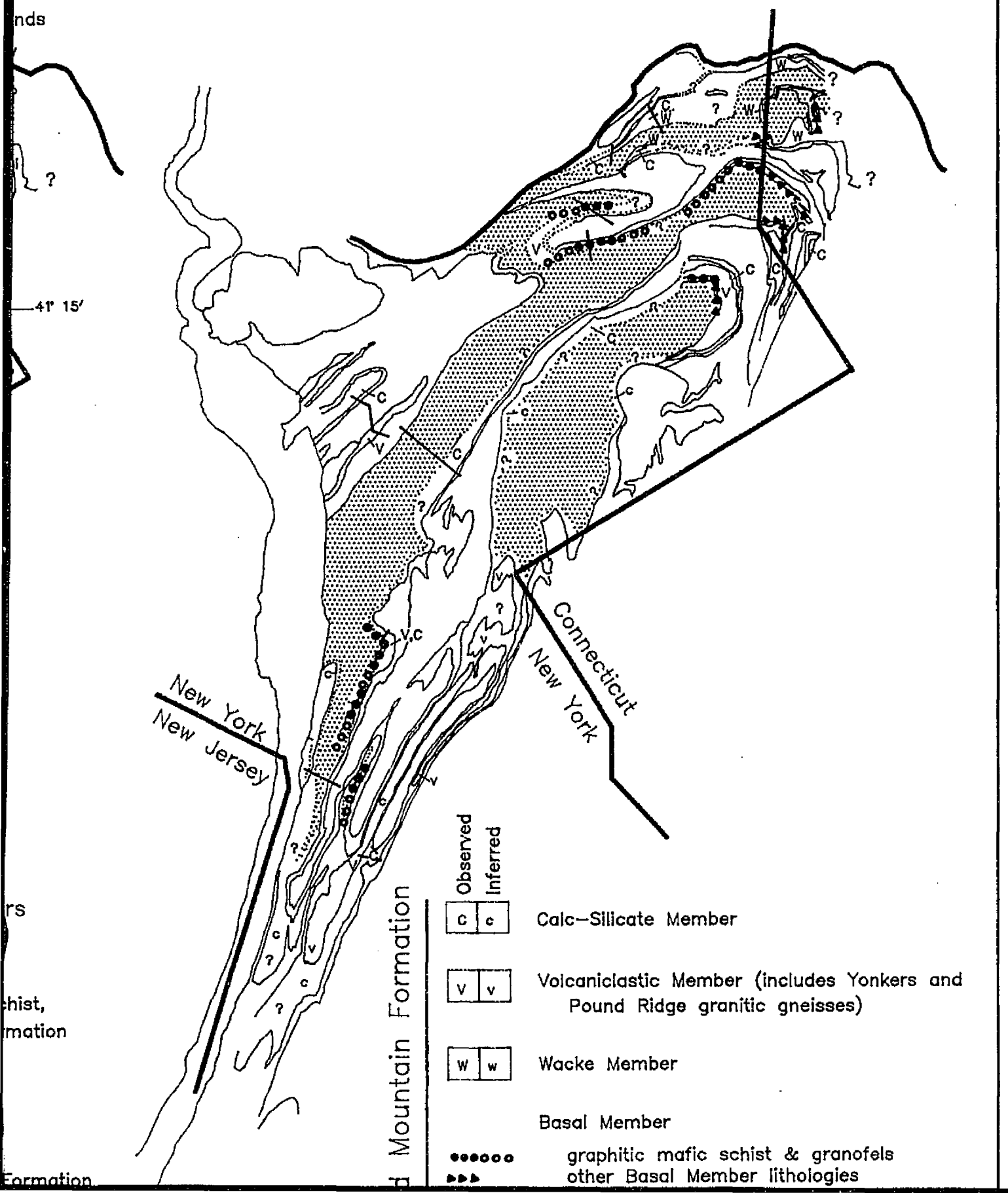

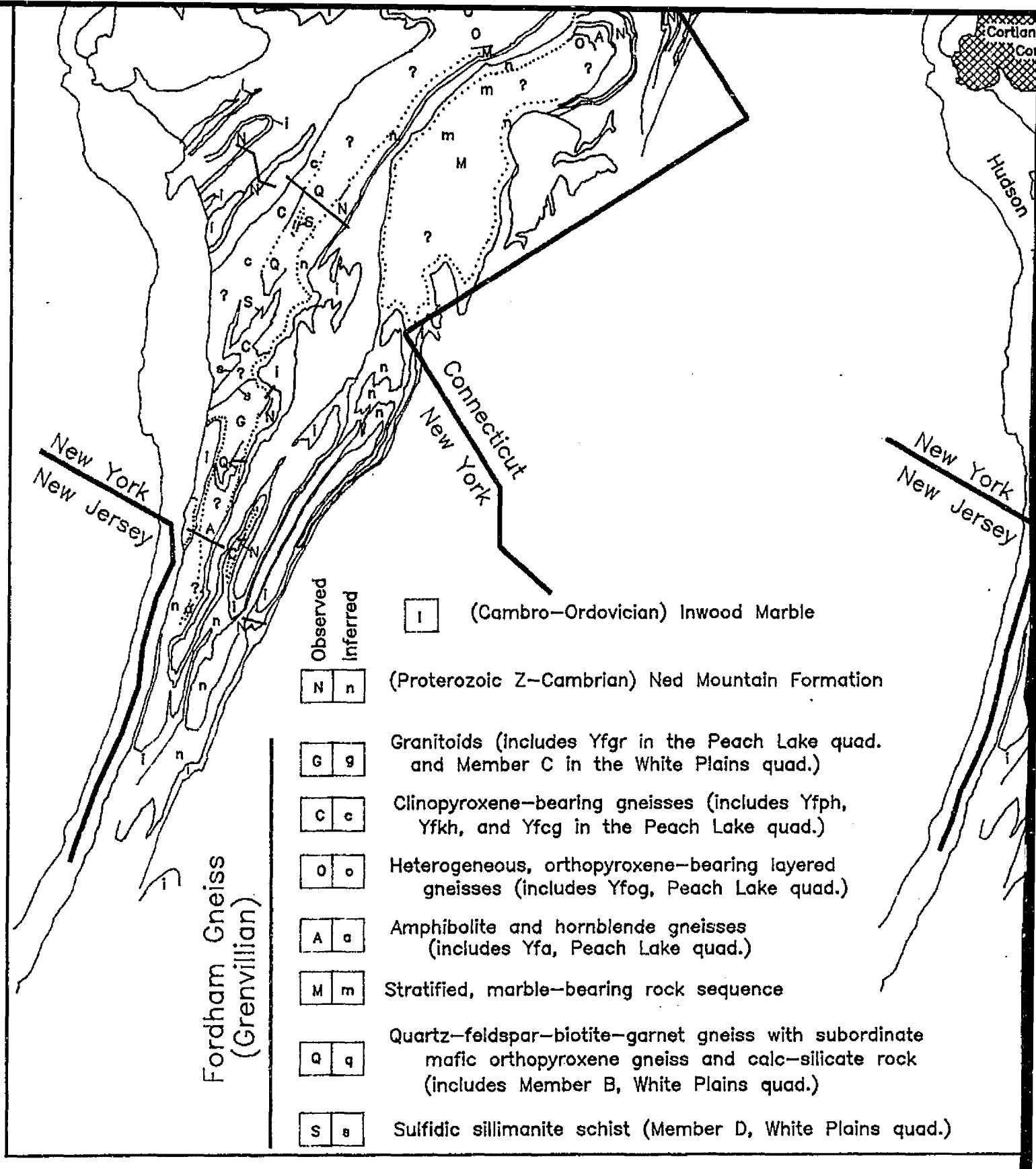
Cortlan
Co
Hudson
New York
New Jersey
Connecticut
New York
New York
New Jersey
Observed
Inferred
Fordham Gneiss
(Grenvillian)
I (Cambro–Ordovician) Inwood Marble
N n (Proterozoic Z–Cambrian) Ned Mountain Formation
G g Granitoids (includes Yfgr in the Peach Lake quad. and Member C in the White Plains quad.)
C c Clinopyroxene–bearing gneisses (includes Yfph, Yfkh, and Yfcg in the Peach Lake quad.)
O o Heterogeneous, orthopyroxene–bearing layered gneisses (includes Yfog, Peach Lake quad.)
A a Amphibolite and hornblende gneisses (includes Yfa, Peach Lake quad.)
M m Stratified, marble–bearing rock sequence
Q q Quartz–feldspar–biotite–garnet gneiss with subordinate mafic orthopyroxene gneiss and calc–silicate rock (includes Member B, White Plains quad.)
S s Sulfidic sillimanite schist (Member D, White Plains quad.)

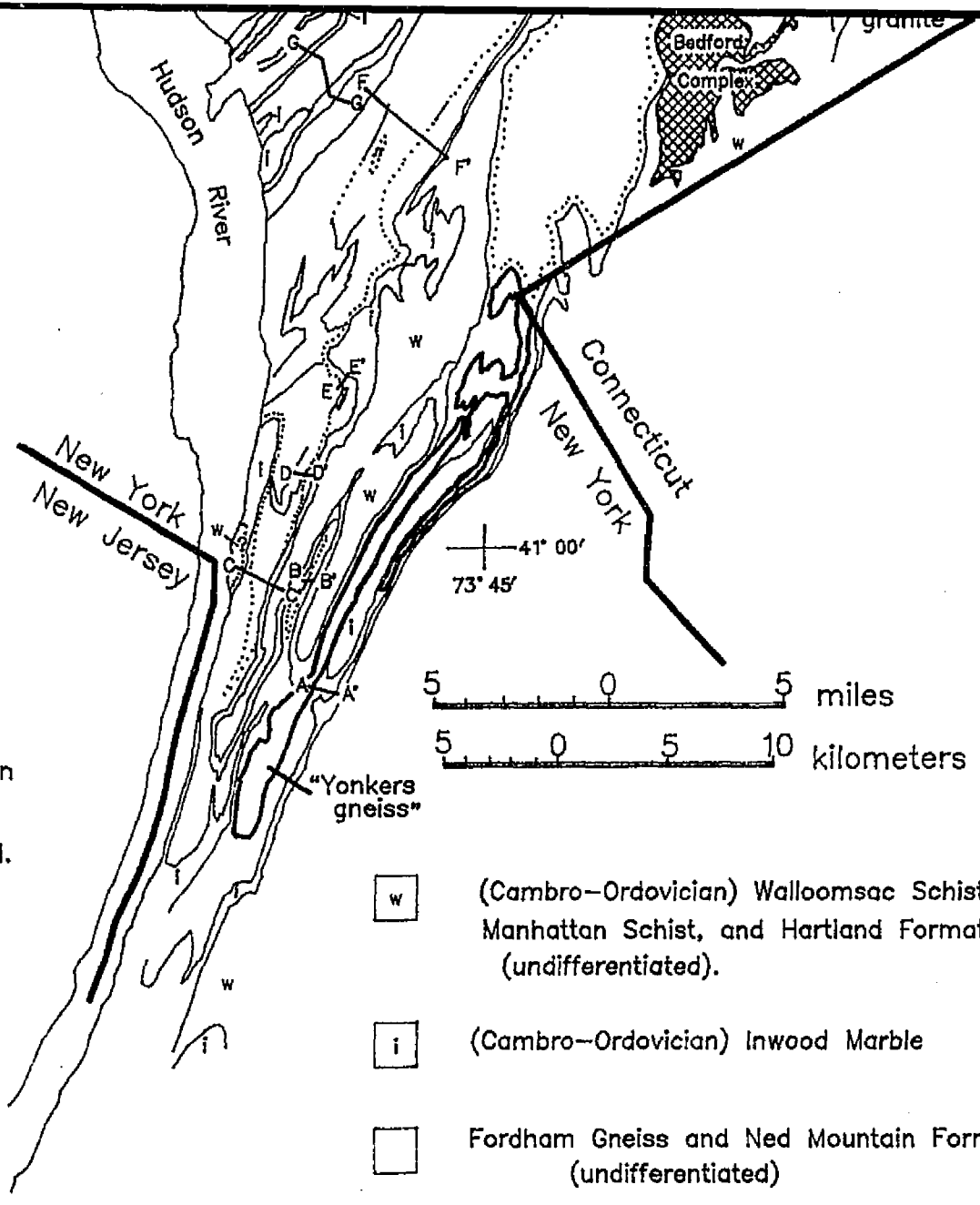

cian) Inwood Marble

) Ned Mountain Formation

in the Peach Lake quad.
White Plains quad.)

neisses (includes Yfph,
e Peach Lake quad.)

oxene–bearing layered
fog, Peach Lake quad.)

nde gneisses
Lake quad.)

g rock sequence

garnet gneiss with subordinate
gneiss and calc–silicate rock
White Plains quad.)

t (Member D, White Plains quad.)

w (Cambro–Ordovician) Walloomsac Schist, Manhattan Schist, and Hartland Formation (undifferentiated).

i (Cambro–Ordovician) Inwood Marble

Fordham Gneiss and Ned Mountain Formation (undifferentiated)

Contacts within Ned Mountain Formation

Contacts within Fordham Gneiss

Contacts are based on Fisher, Isachsen and Rickard (1970), Alavi (1976), and new mapping.

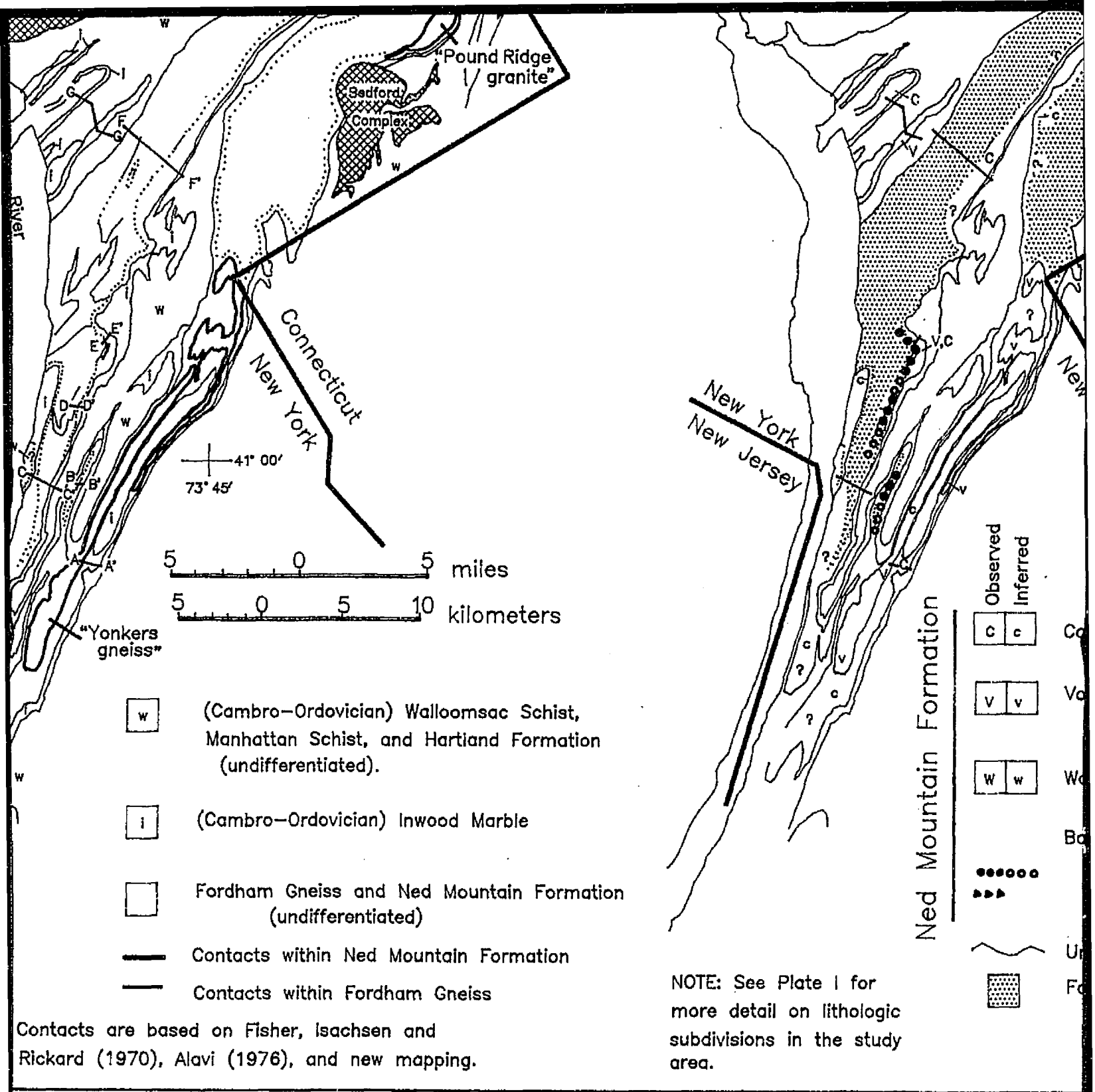
"Pound Ridge" granite
Bedford Complex
Connecticut
New York
New York
New Jersey
41° 00′
73° 45′
5 0 5 miles
5 0 5 10 kilometers
"Yonkers gneiss"
River
Ned Mountain Formation
Observed
Inferred
(Cambro–Ordovician) Walloomsac Schist, Manhattan Schist, and Hartland Formation (undifferentiated).
(Cambro–Ordovician) Inwood Marble
Fordham Gneiss and Ned Mountain Formation (undifferentiated)
Contacts within Ned Mountain Formation
Contacts within Fordham Gneiss
Contacts are based on Fisher, Isachsen and Rickard (1970), Alavi (1976), and new mapping.
NOTE: See Plate I for more detail on lithologic subdivisions in the study area.

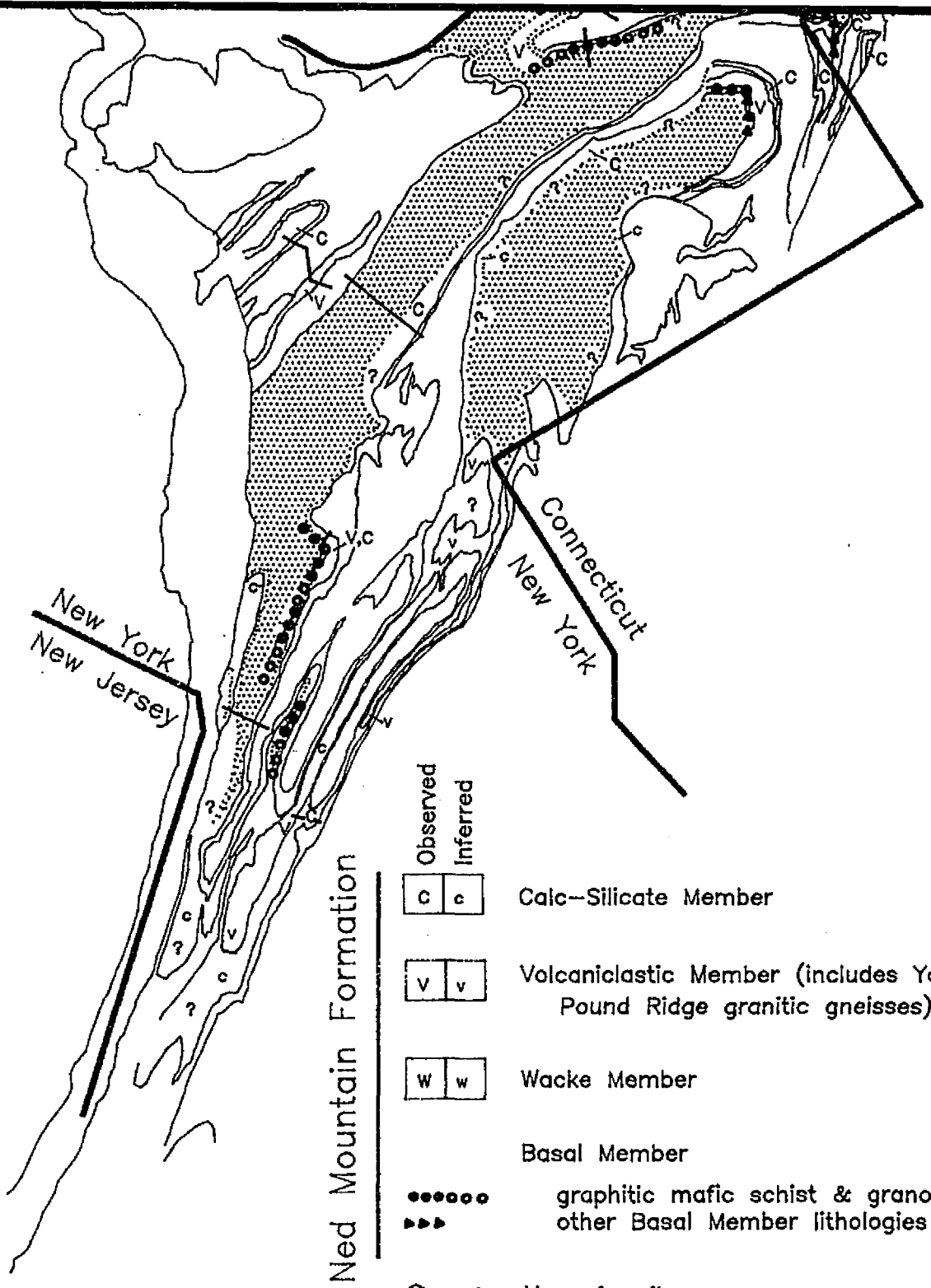

NOTE: See Plate I for more detail on lithologic subdivisions in the study area.

PLEASE NOTE:

Oversize maps and charts are filmed in sections in the following manner:

LEFT TO RIGHT, TOP TO BOTTOM, WITH SMALL OVERLAPS

The following map or chart has been refilmed in its entirety at the end of this dissertation (not available on microfiche). A xerographic reproduction has been provided for paper copies and is inserted into the inside of the back cover.

Black and white photographic prints (17" x 23") are available for an additional charge.

University Microfilms International

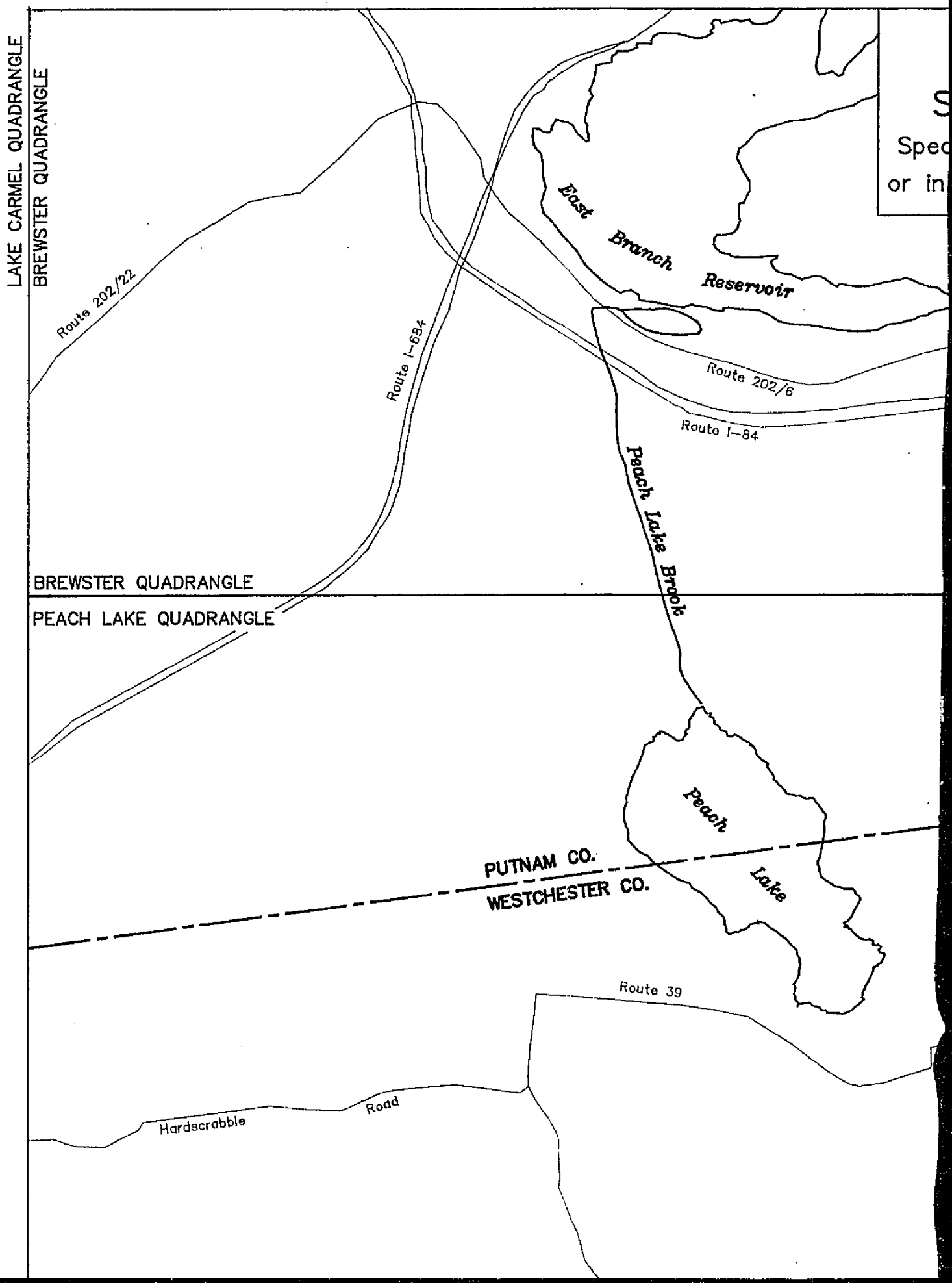
LAKE CARMEL QUADRANGLE
BREWSTER QUADRANGLE
Route 202/22
Route I-684
East Branch Reservoir
Route 202/6
Route I-84
Peach Lake Brook
BREWSTER QUADRANGLE
PEACH LAKE QUADRANGLE
Peach Lake
PUTNAM CO.
WESTCHESTER CO.
Route 39
Hardscrabble Road

PLATE III –

Specimen Location Map

Specimens cited in the text, on tables, or in illustrations are indicated by number.

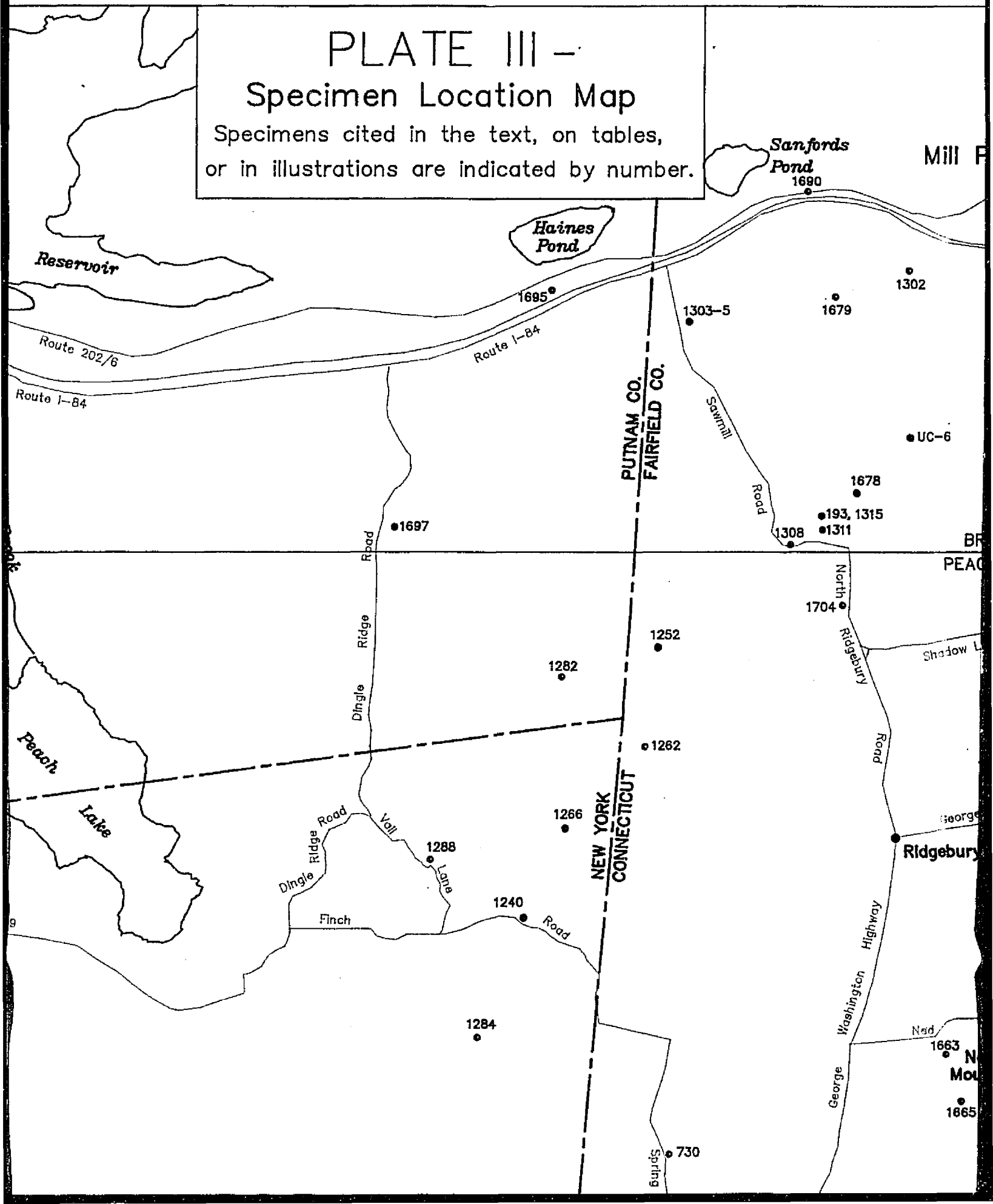

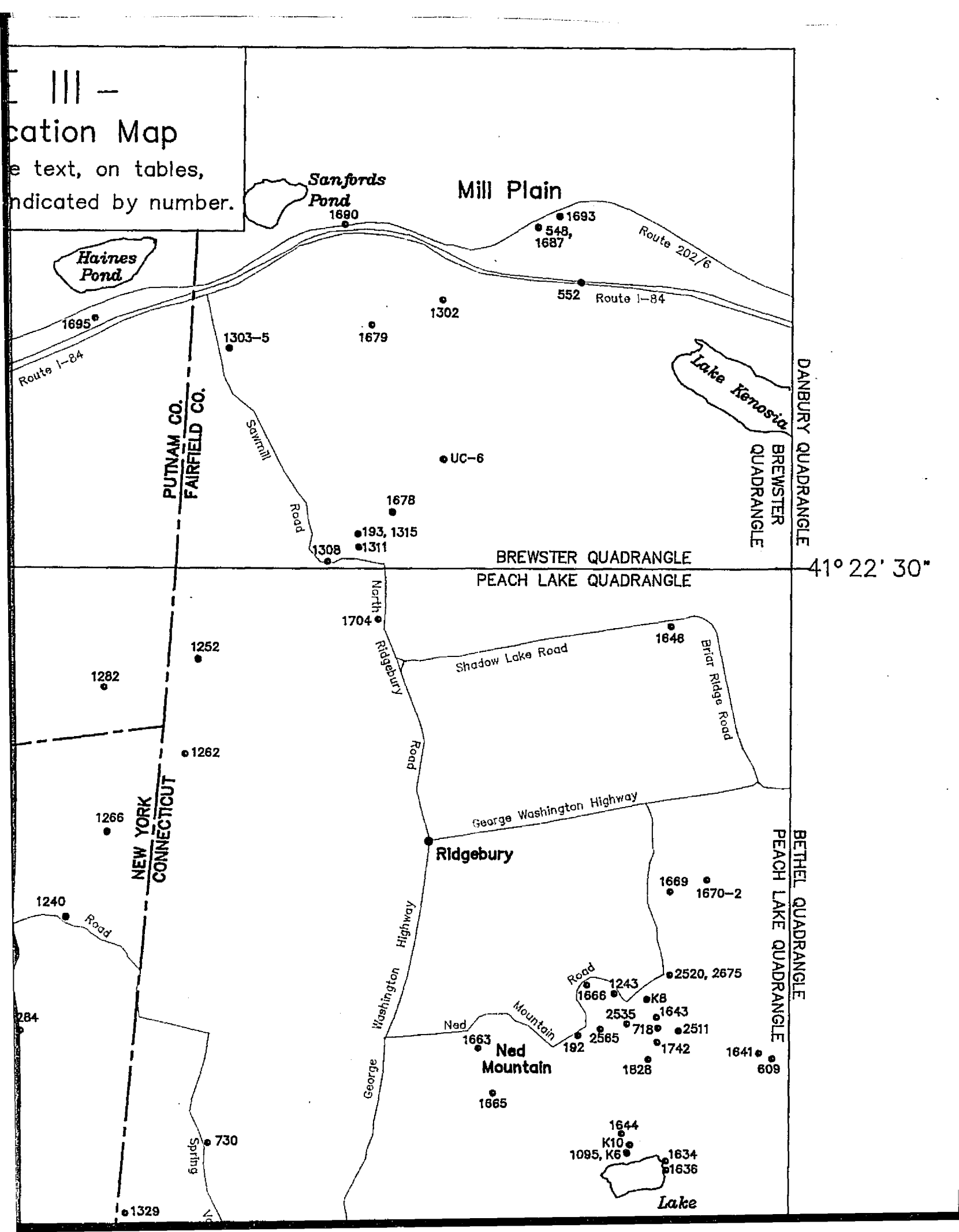
III –
cation Map
e text, on tables,
ndicated by number.
Sanfords Pond
1690
Mill Plain
1693
548, 1687
Route 202/6
Haines Pond
552
Route I–84
1695
1302
1303–5
1679
Route I–84
Lake Kenosia
DANBURY QUADRANGLE
BREWSTER QUADRANGLE
PUTNAM CO.
FAIRFIELD CO.
Sawmill Road
UC–6
1678
193, 1315
1308
1311
BREWSTER QUADRANGLE
PEACH LAKE QUADRANGLE
41° 22' 30"
North Ridgebury Road
1704
1252
1282
1262
1648
Shadow Lake Road
Briar Ridge Road
NEW YORK
CONNECTICUT
1266
George Washington Highway
Ridgebury
1669
1670–2
1240
Road
BETHEL QUADRANGLE
PEACH LAKE QUADRANGLE
Washington Highway
Road
1243
2520, 2675
1666
K8
2535
1643
718
2511
Ned Mountain
1663
Ned Mountain
192
2565
1742
1641
609
1828
George
1665
284
730
Spring
1644
K10
1095, K6
1634
1636
Lake
1329

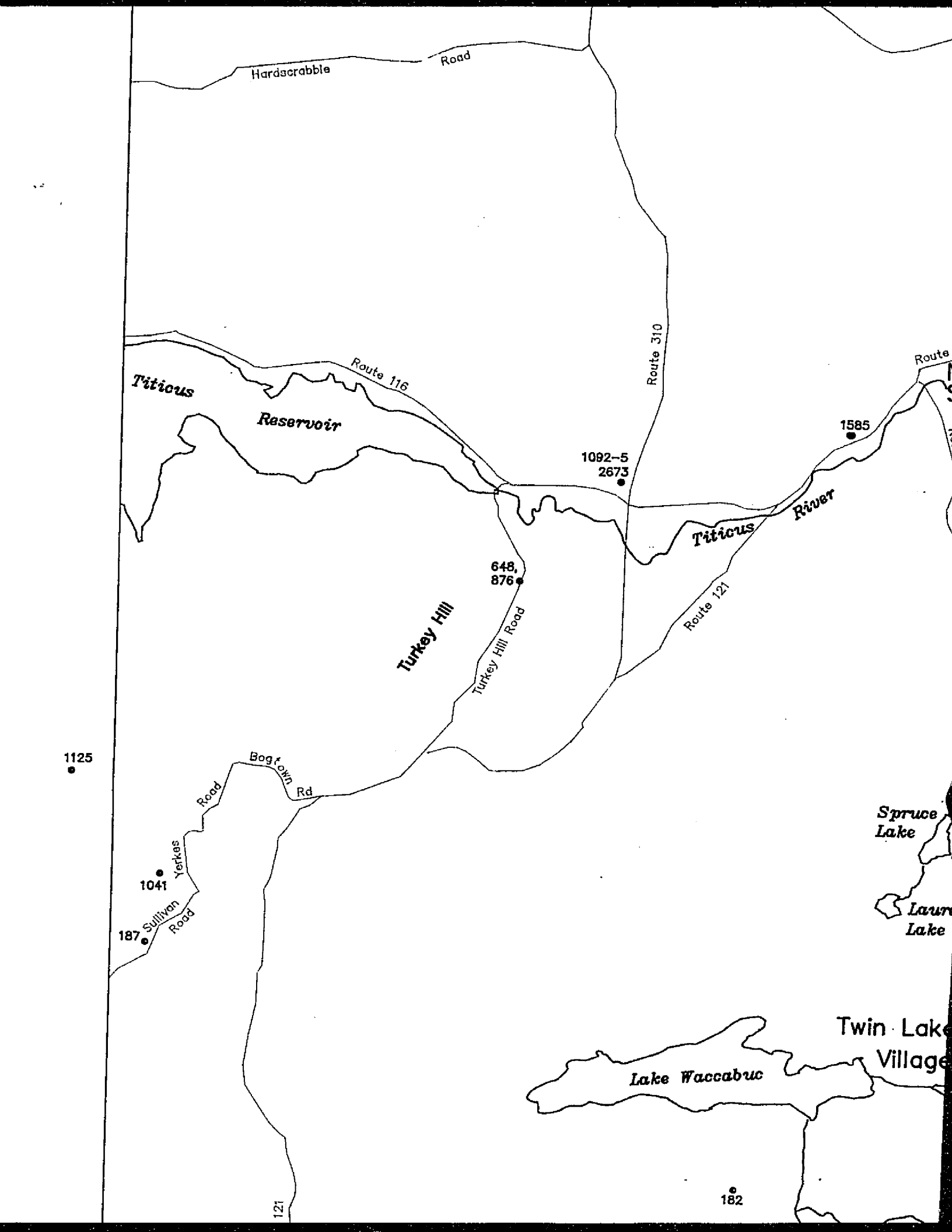
Hardscrabble Road
Route 116
Titicus Reservoir
Route 310
Route
1585
1092–5
2673
Titicus River
Route 121
648,
876
Turkey Hill
Turkey Hill Road
1125
Bogtown Rd
Road
Yerkes
1041
Sullivan
Road
187
Spruce Lake
Laur
Lake
Twin Lake
Village
Lake Waccabuc
182
121

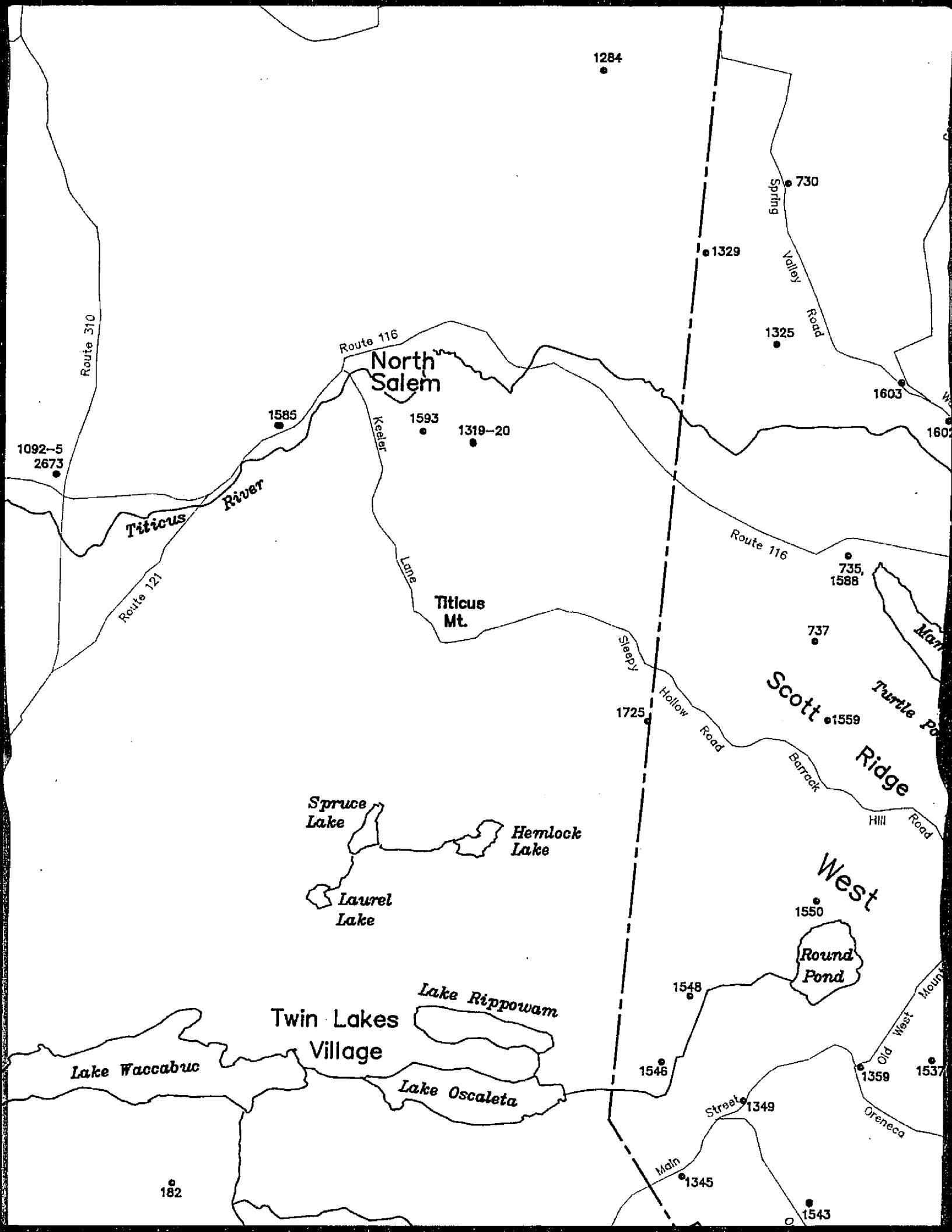
1284
730
Spring Valley Road
1329
1325
1603
Route 310
Route 116
North Salem
1585
1593
1319–20
Keeler Lane
1092–5
2673
Titicus River
Route 121
Route 116
735, 1588
Titicus Mt.
737
Sleepy Hollow Road
Scott
1559
1725
Ridge
Barrack Hill Road
Spruce Lake
Hemlock Lake
Laurel Lake
West
1550
Round Pond
1548
Lake Rippowam
Twin Lakes Village
Lake Waccabuc
Lake Oscaleta
1546
1359
1537
Old West Mount
Street
1349
Oreneca
Main
1345
182
1543

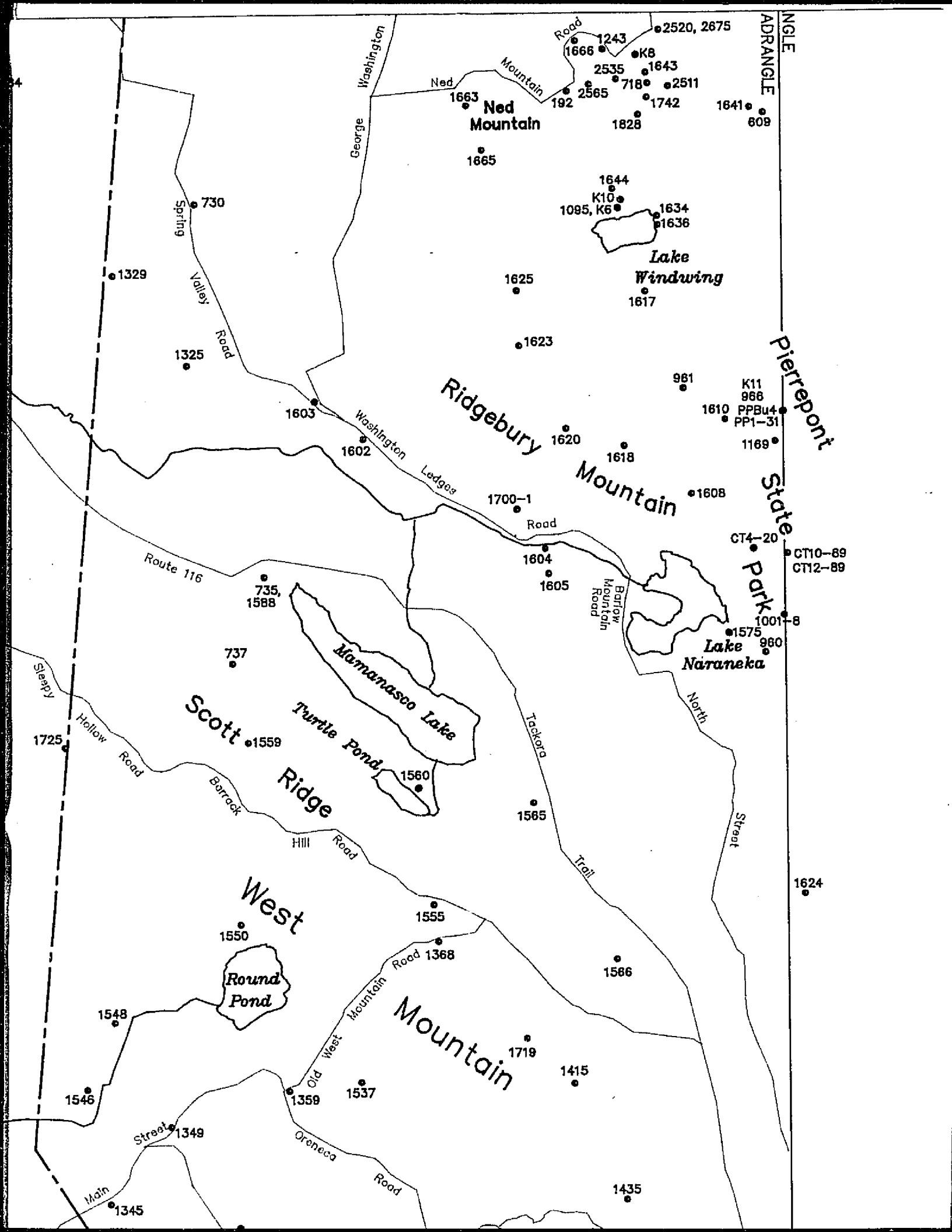
NGLE
ADRANGLE
Washington
George
Ned
Mountain
Road
2520, 2675
1666
1243
K8
2535
1643
718
2511
2565
192
1742
1641
609
1828
1663
Ned Mountain
1665
1644
K10
1095, K6
1634
1636
Lake Windwing
1617
1625
730
Spring
Valley
Road
1329
1325
1623
961
K11
966
1610
PPBu4
PP1–31
1169
Pierrepont State Park
Ridgebury Mountain
1603
1602
Washington Ledges Road
1620
1618
1608
1700–1
Road
1604
1605
CT4–20
CT10–89
CT12–89
Route 116
735, 1588
Barlow Mountain Road
1001–8
1575
960
Lake Naraneka
737
Mamanasco Lake
Turtle Pond
Scott Ridge
1559
1560
Sleepy Hollow Road
1725
Barrack Hill Road
Tackora Trail
North Street
1565
1624
West Mountain
1555
1550
1368
Round Pond
1586
1548
Old West Mountain Road
1719
1415
1546
1359
1537
Street
1349
Oreneca Road
Main
1345
1435

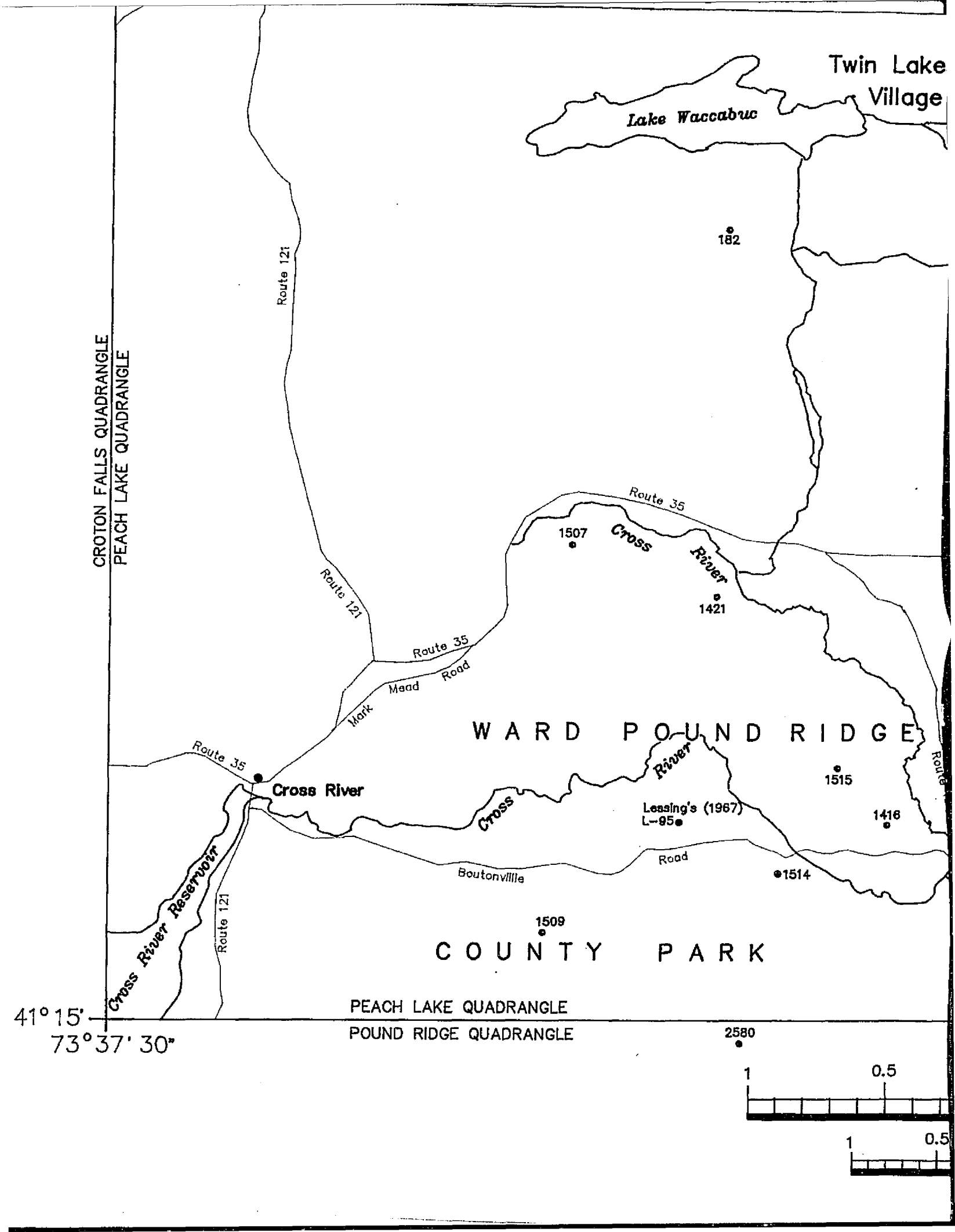
Twin Lake Village
Lake Waccabuc
182
Route 121
CROTON FALLS QUADRANGLE
PEACH LAKE QUADRANGLE
Route 35
1507
Cross River
1421
Route 121
Route 35
Mead
Road
Mark
WARD POUND RIDGE
Route 35
Cross River
Cross River
1515
Lessing's (1967)
L-95
1416
Boutonville
Road
1514
Cross River Reservoir
Route 121
1509
COUNTY PARK
41°15'
73°37'30"
PEACH LAKE QUADRANGLE
POUND RIDGE QUADRANGLE
2580
1
0.5
1
0.5

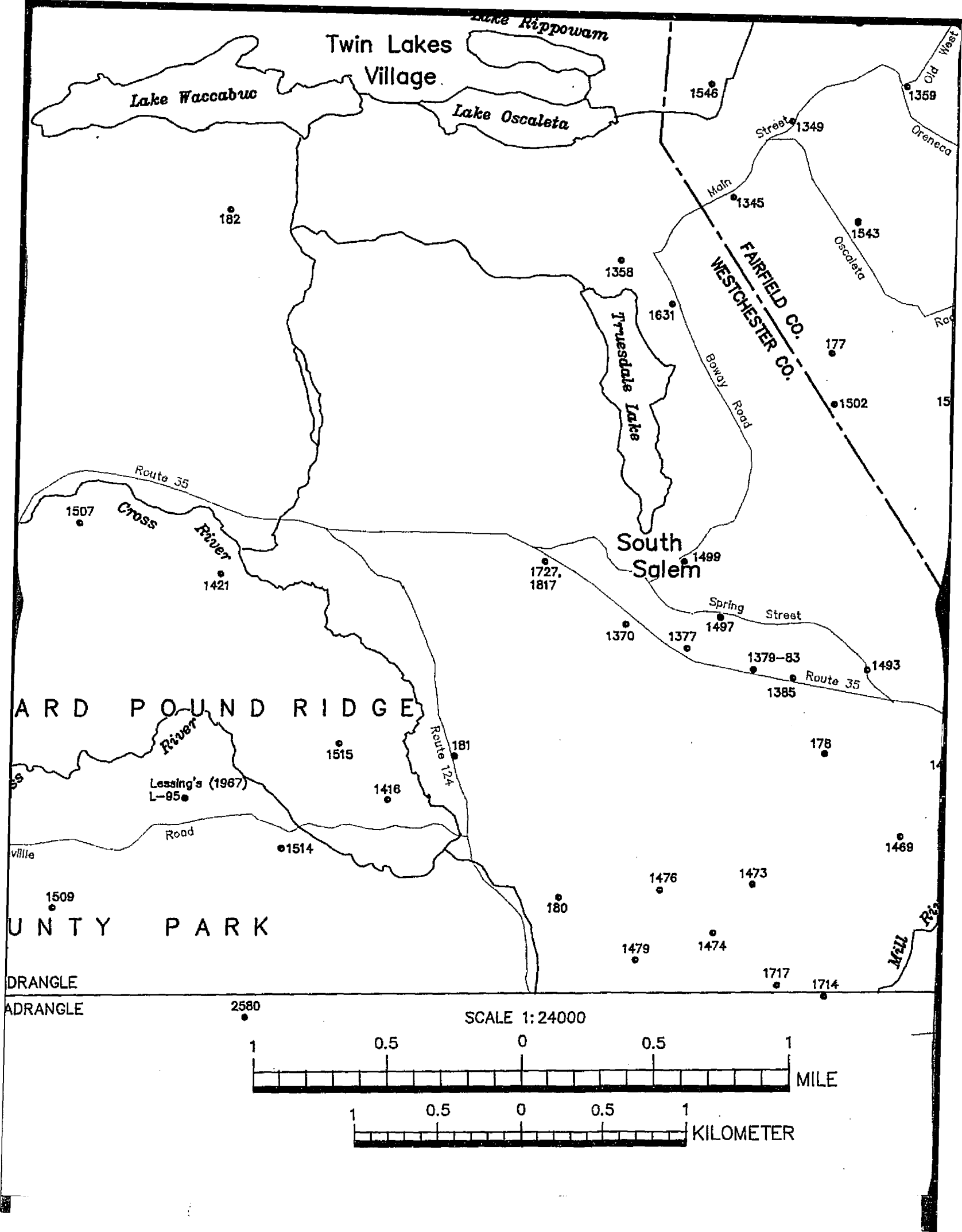
Lake Rippowam
Twin Lakes Village
Lake Waccabuc
Lake Oscaleta
1546
Old West
1359
Street
1349
Oreneca
Main
1345
182
1543
Oscaleta
1358
1631
Truesdale Lake
FAIRFIELD CO.
WESTCHESTER CO.
Boway Road
177
1502
Route 35
1507
Cross River
1421
South Salem
1499
1727, 1817
Spring Street
1497
1370
1377
1379–83
1493
Route 35
1385
A R D P O U N D R I D G E
River
1515
Route 124
181
178
Lessing's (1967) L–95
1416
Road
1514
1469
1509
1476
1473
180
U N T Y P A R K
1479
1474
Mill Ri
1717
1714
DRANGLE
ADRANGLE
2580
SCALE 1: 24000
1 0.5 0 0.5 1
MILE
1 0.5 0 0.5 1
KILOMETER

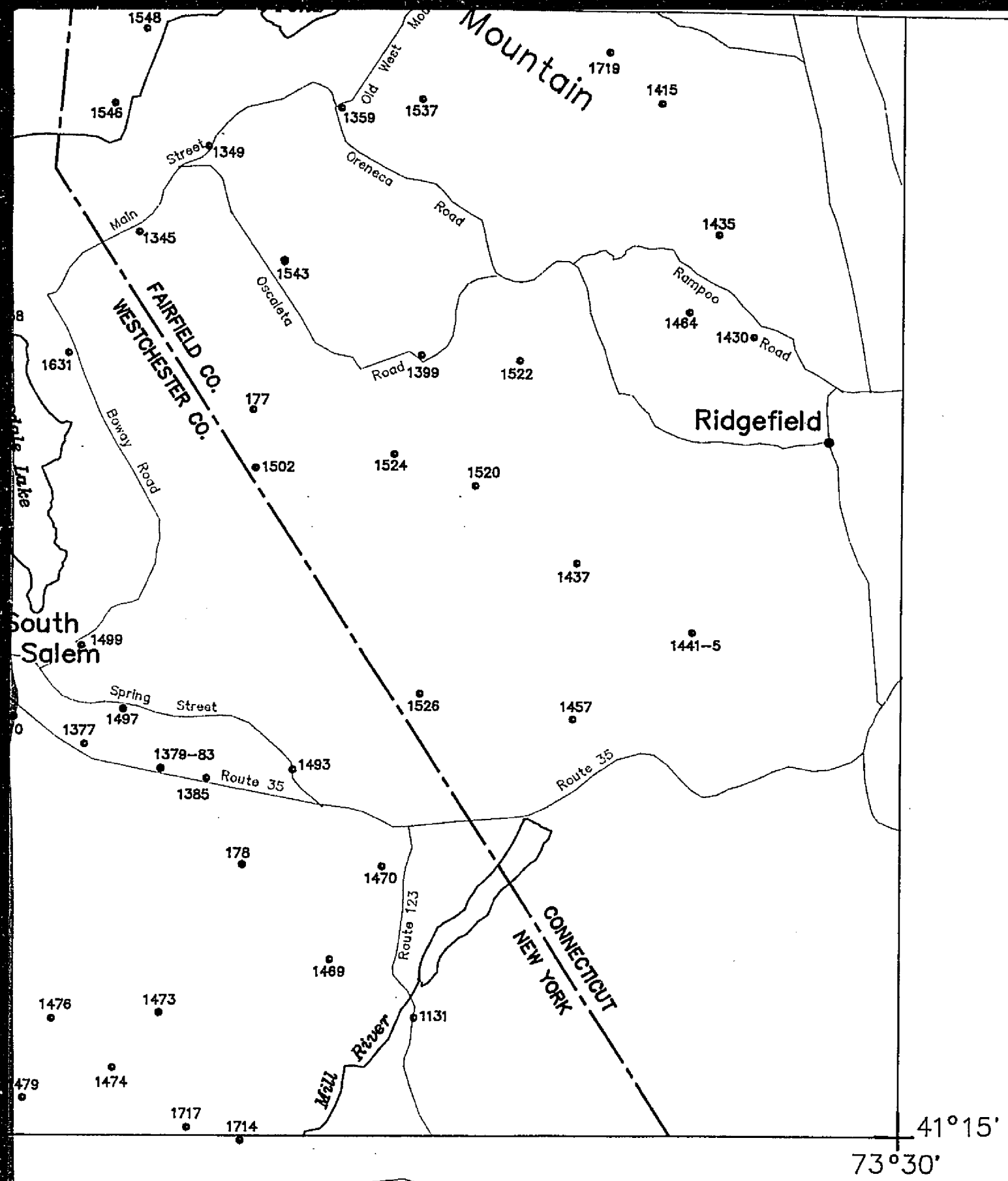
Mountain
Old West
Street
Oreneca
Road
Main
Oscaleta
Road
Rampoo
Road
Ridgefield
FAIRFIELD CO.
WESTCHESTER CO.
Boway Road
South
Salem
Spring
Street
Route 35
Route 35
Route 123
CONNECTICUT
NEW YORK
Mill
River
1548
1546
1359
1537
1719
1415
1349
1345
1543
1435
1464
1430
1631
1399
1522
177
1502
1524
1520
1437
1499
1441–5
1526
1457
1497
1377
1379–83
1493
1385
178
1470
1469
1476
1473
1131
1479
1474
1717
1714
41°15'
73°30'
0.5
1
MILE
1
KILOMETER
Selected Roads

PLEASE NOTE:

Oversize maps and charts are filmed in sections in the following manner:

LEFT TO RIGHT, TOP TO BOTTOM, WITH SMALL OVERLAPS

The following map or chart has been refilmed in its entirety at the end of this dissertation (not available on microfiche). A xerographic reproduction has been provided for paper copies and is inserted into the inside of the back cover.

Black and white photographic prints (17" x 23") are available for an additional charge.

University Microfilms International

PLATE IV - PRINCIPAL STRUCTURAL FEATURES

See Plate I for explanation of lithologic symbols.

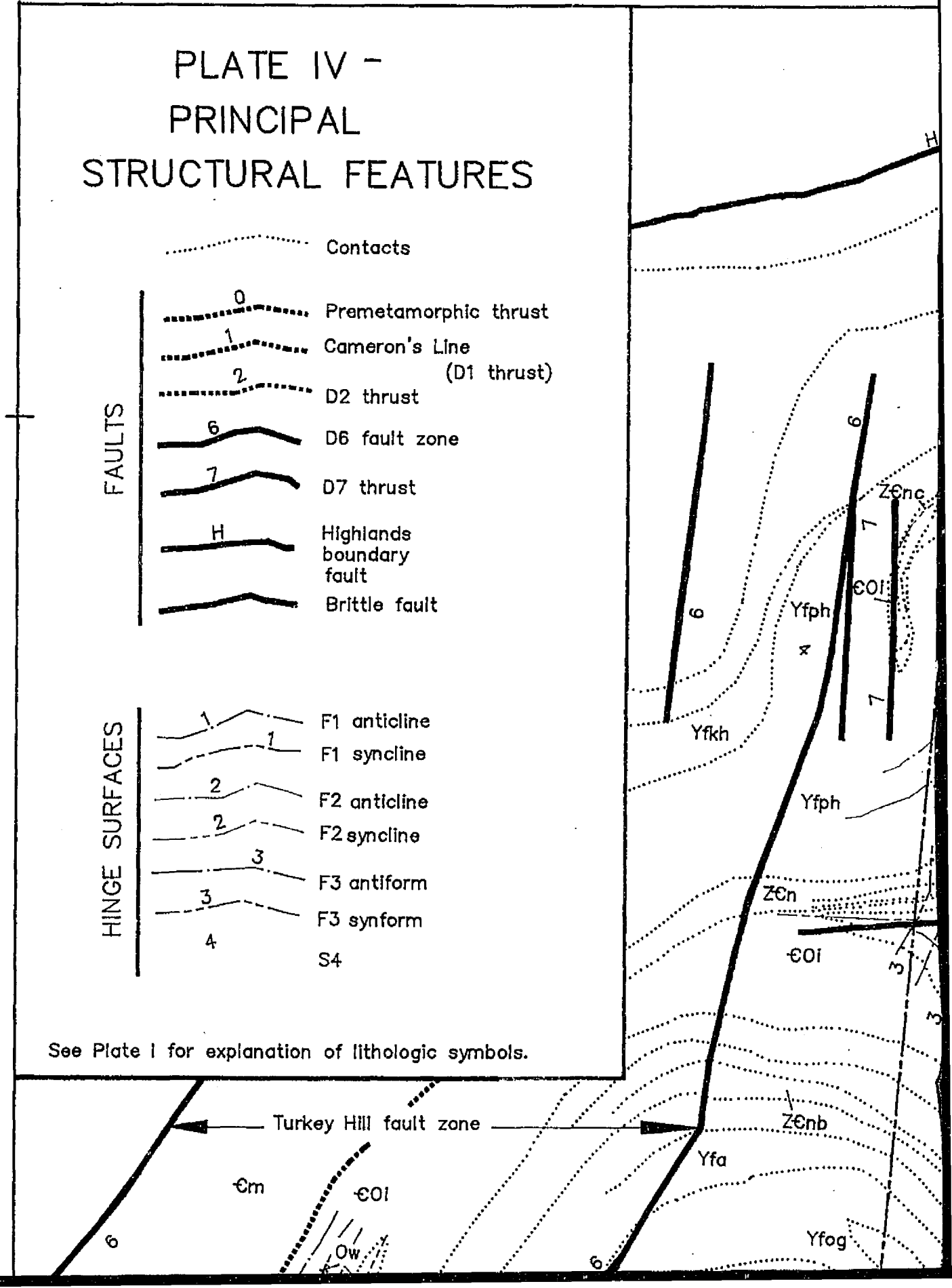

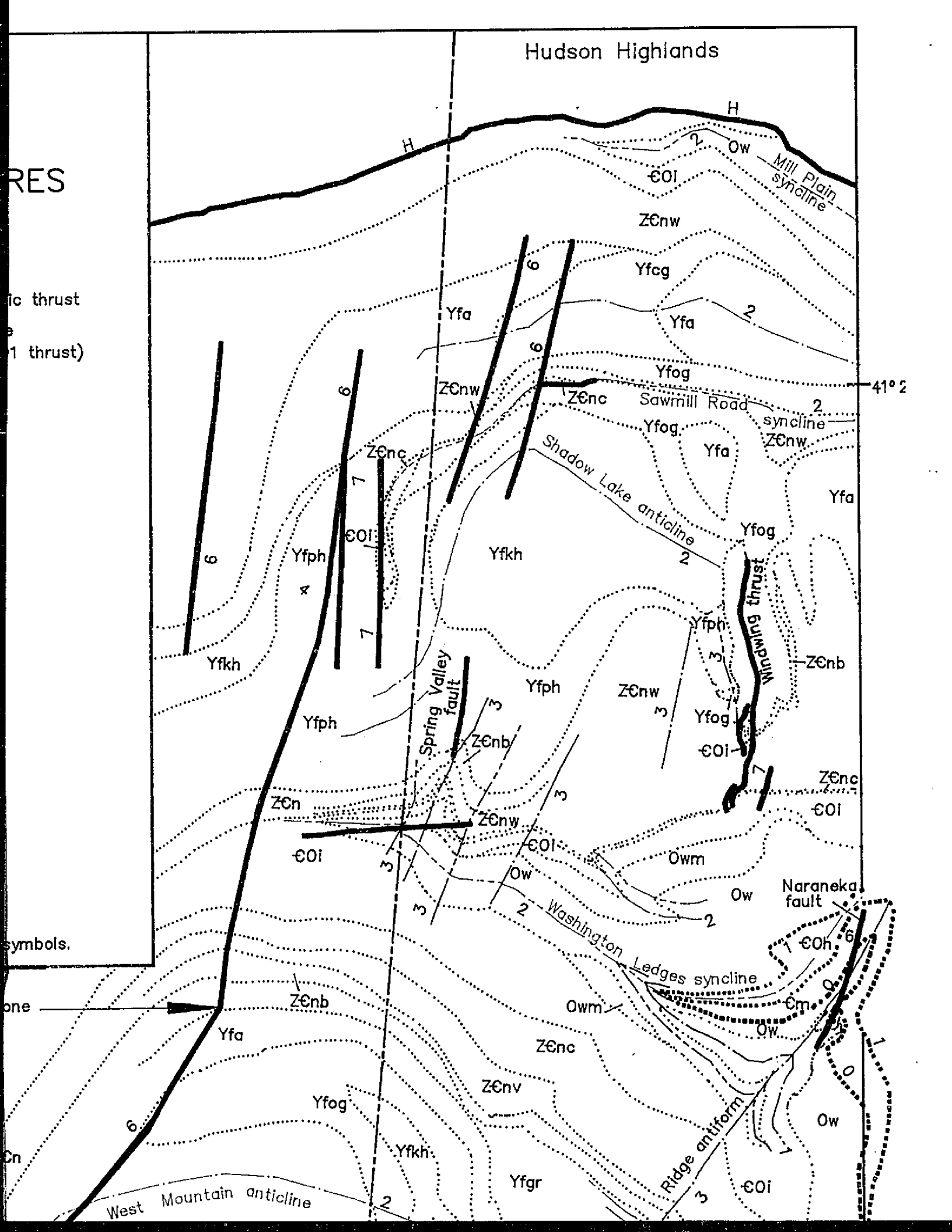
Hudson Highlands
RES
ic thrust
1 thrust)
symbols.
one
H
Ow
Mill Plain syncline
€Oi
Z€nw
Yfcg
Yfa
Yfog
Z€nc
Sawmill Road syncline
41° 2
Shadow Lake anticline
Yfkh
Yfph
Windawing thrust
Z€nb
Spring Valley fault
Z€n
Owm
Naraneka fault
Washington Ledges syncline
€Oh
€m
West Mountain anticline
Z€nv
Yfgr
Ridge antiform

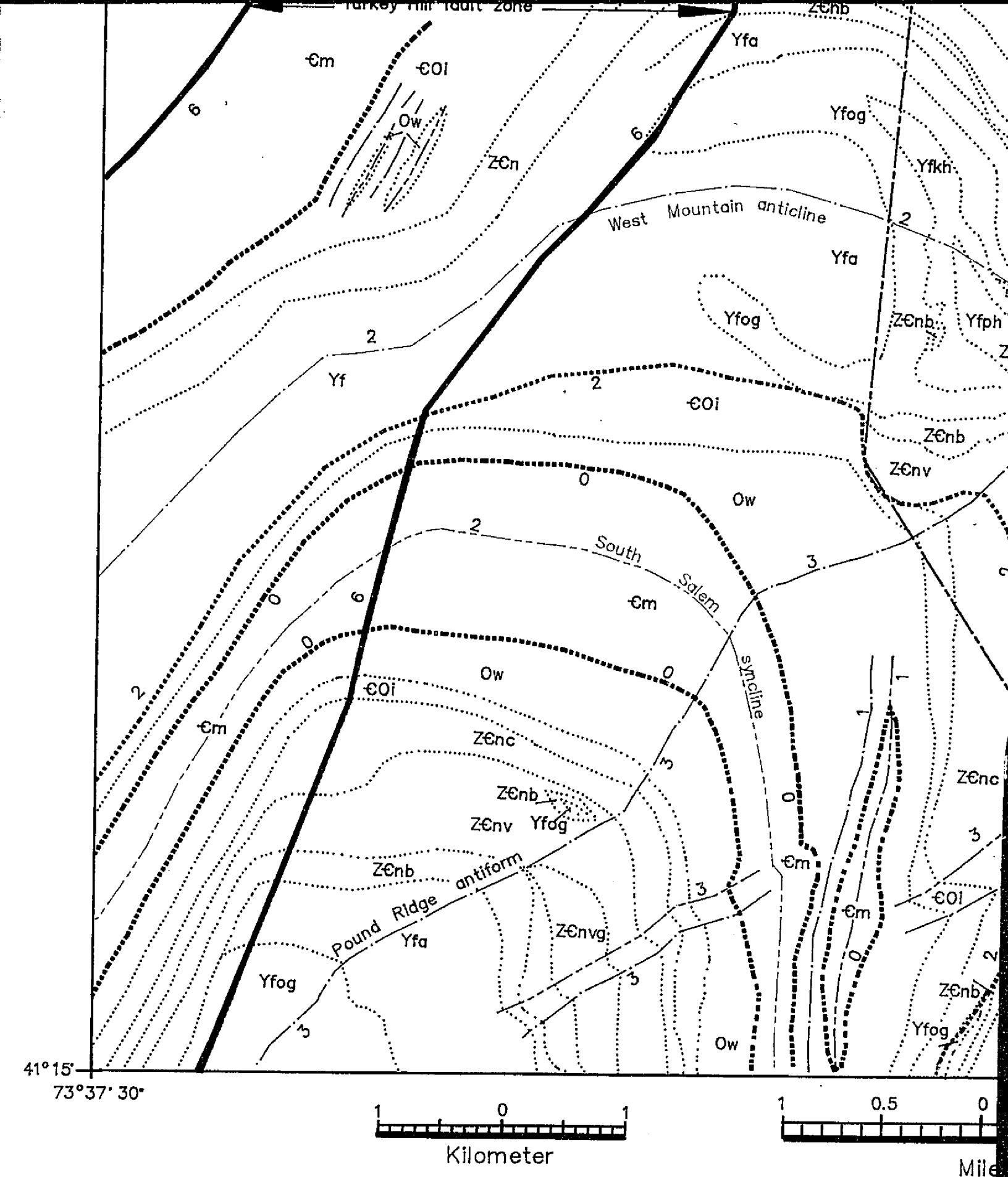
Turkey Hill fault zone
Z€nb
Yfa
€m
€Oi
Ow
Yfog
Z€n
Yfkh
West Mountain anticline
Yfa
Yfog
Z€nb
Yfph
Yf
€Oi
Z€nb
Z€nv
Ow
South Salem syncline
€m
Ow
€Oi
€m
Z€nc
Z€nb
Z€nv
Yfog
Z€nb
Pound Ridge antiform
Yfa
Z€nvg
Yfog
Ow
€m
€Oi
Z€nc
Z€nb
Yfog
41°15'
73°37'30"
1 0 1
Kilometer
1 0.5 0
Mile

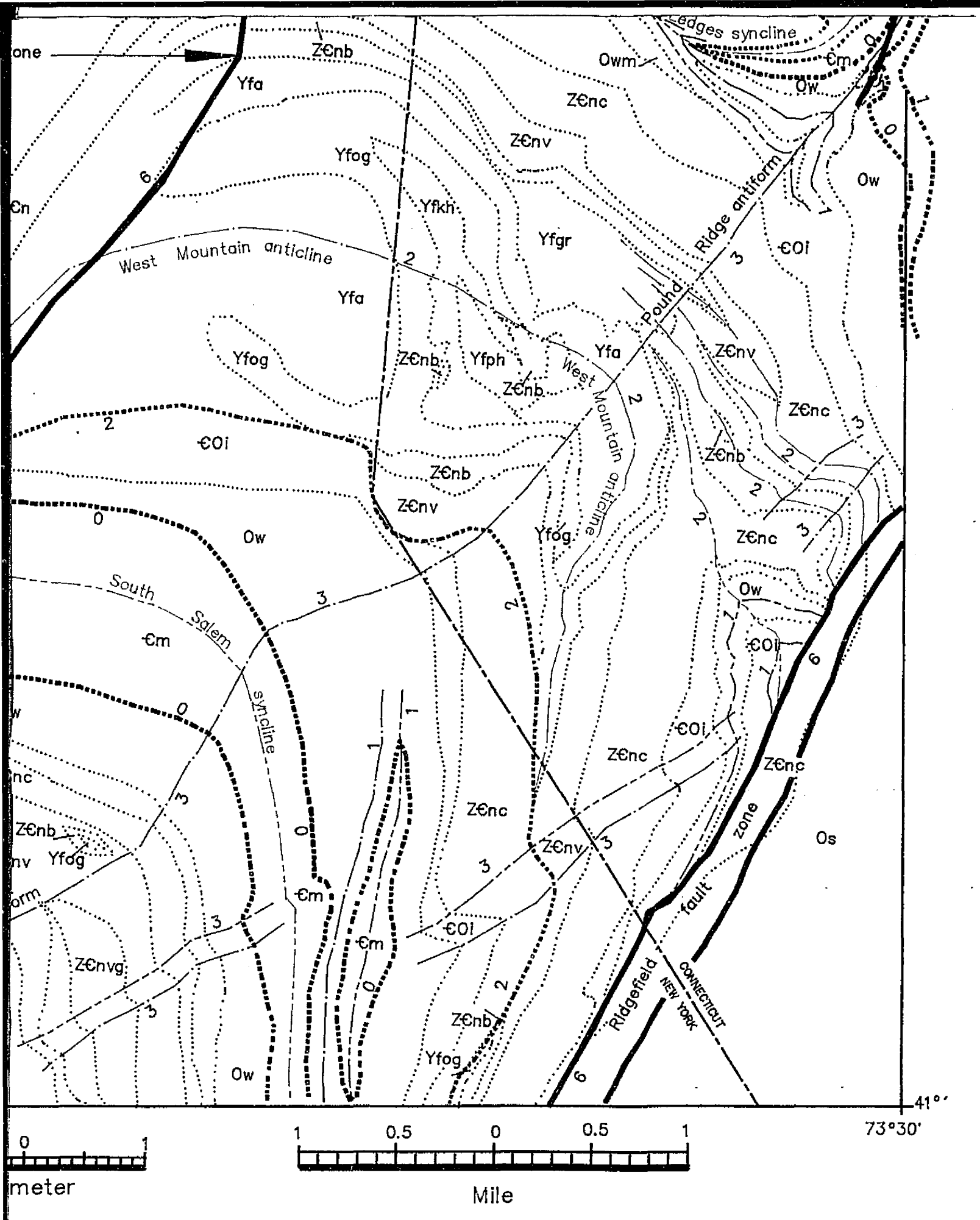
Edges syncline
Owm
Z€nb
Yfa
Z€nc
Z€nv
Yfog
Yfkh
Yfgr
Ridge antiform
Ow
€Oi
West Mountain anticline
Pound
Yfph
West Mountain anticline
€m
South Salem syncline
Z€nvg
fault zone
Ridgefield
CONNECTICUT
NEW YORK
Os
41°
73°30'
meter
Mile

PLEASE NOTE:

Oversize maps and charts are filmed in sections in the following manner:

LEFT TO RIGHT, TOP TO BOTTOM, WITH SMALL OVERLAPS

The following map or chart has been refilmed in its entirety at the end of this dissertation (not available on microfiche). A xerographic reproduction has been provided for paper copies and is inserted into the inside of the back cover.

Black and white photographic prints (17" x 23") are available for an additional charge.

University Microfilms International

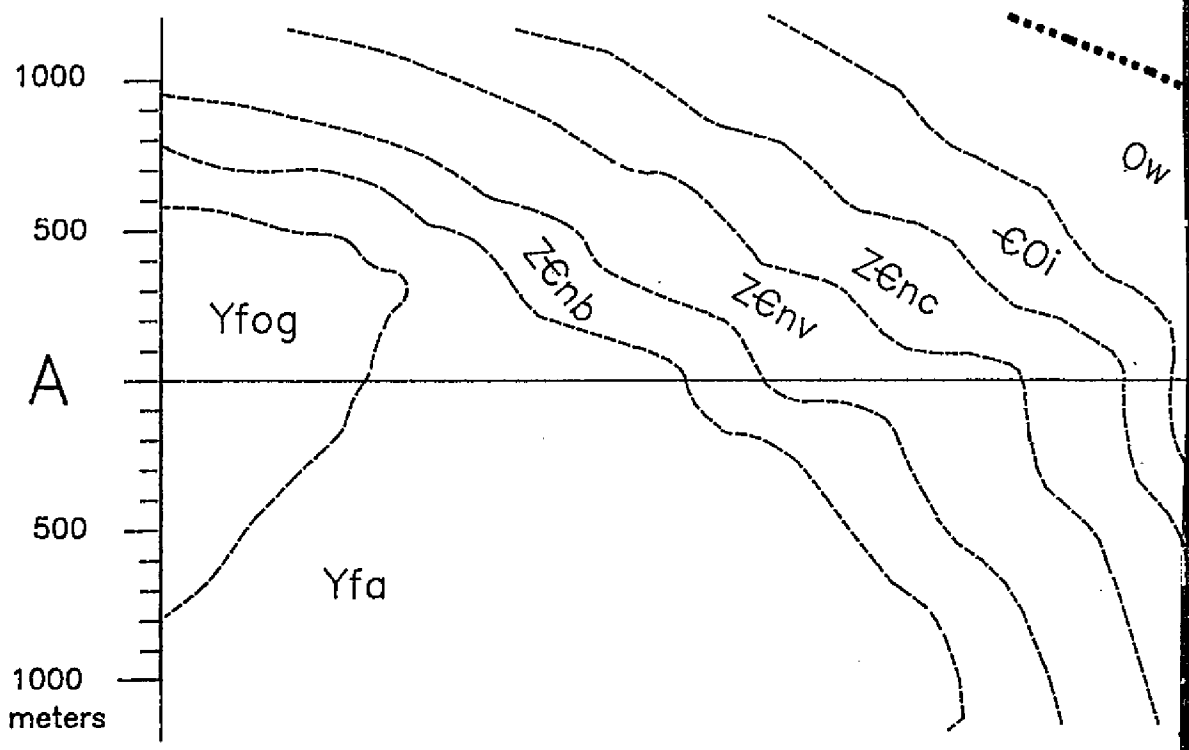

Pound Ridge Antiform

Intrusive Rocks

Os Siscowit Granite

Allochthonous Rocks

€Oh Hartland Formation

1

€m Manhattan Schist

0

Ow Walloomsac Schist

Owm Marble Member

PLATE V — G

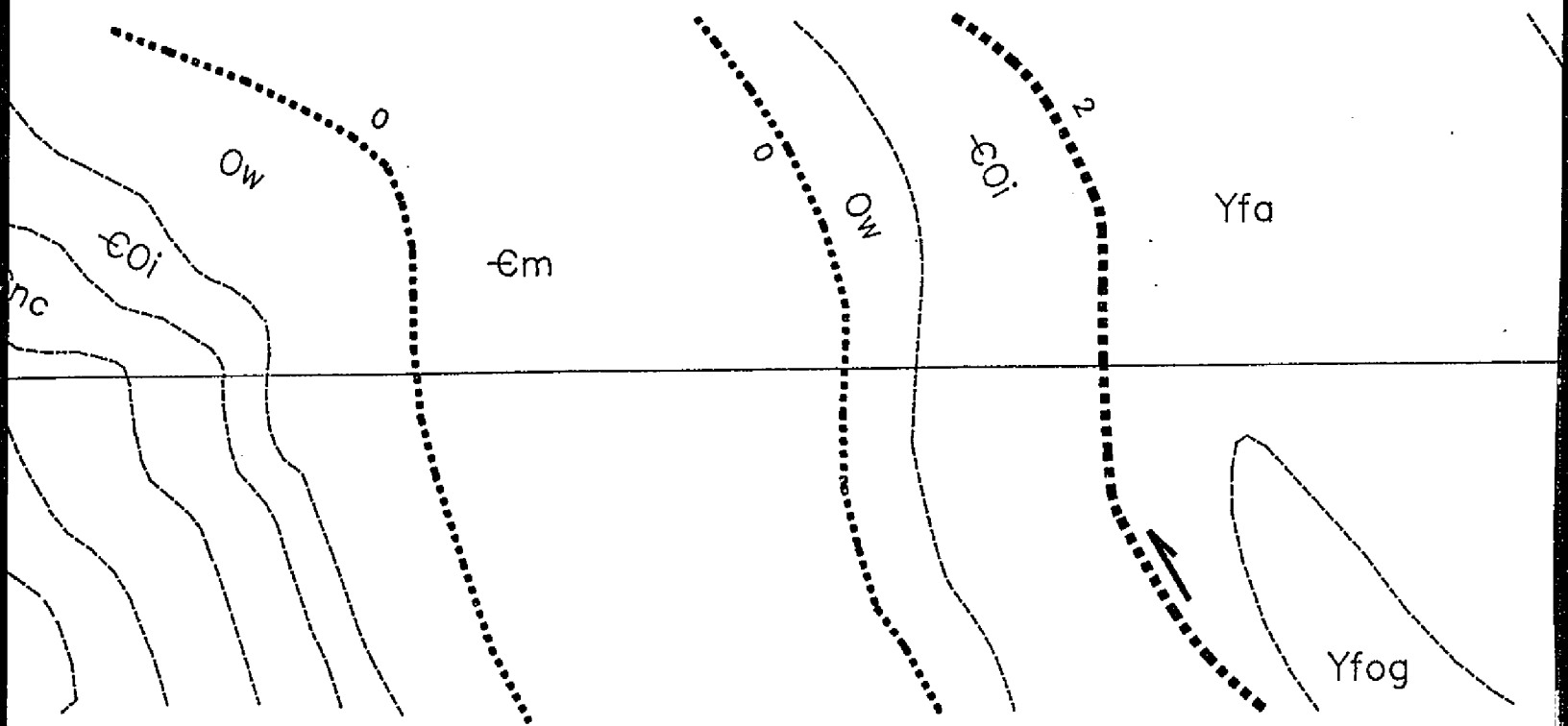

South Salem Syncline

We

V — GEOLOGIC CROSS SECTIONS

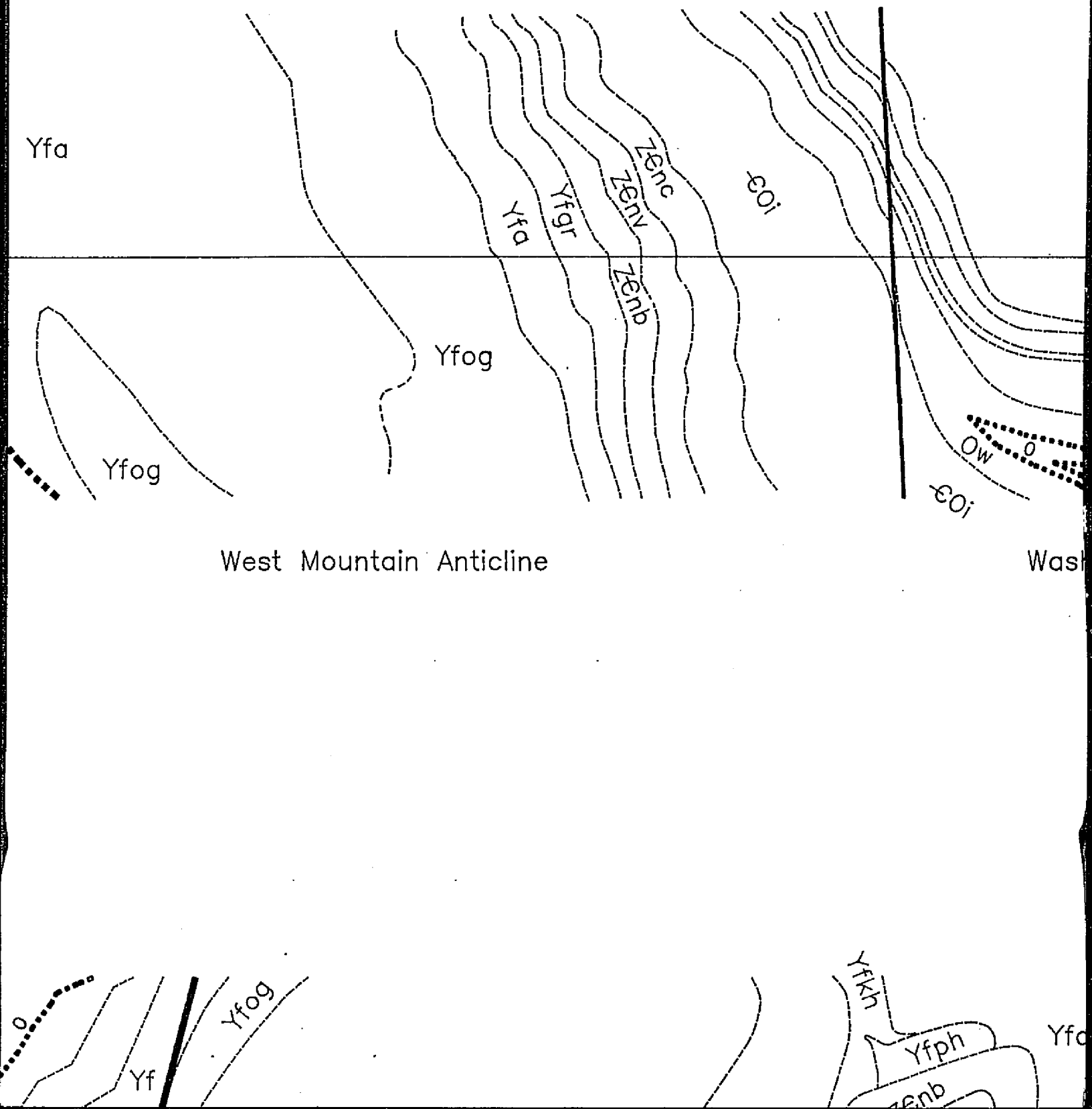

SECTIONS

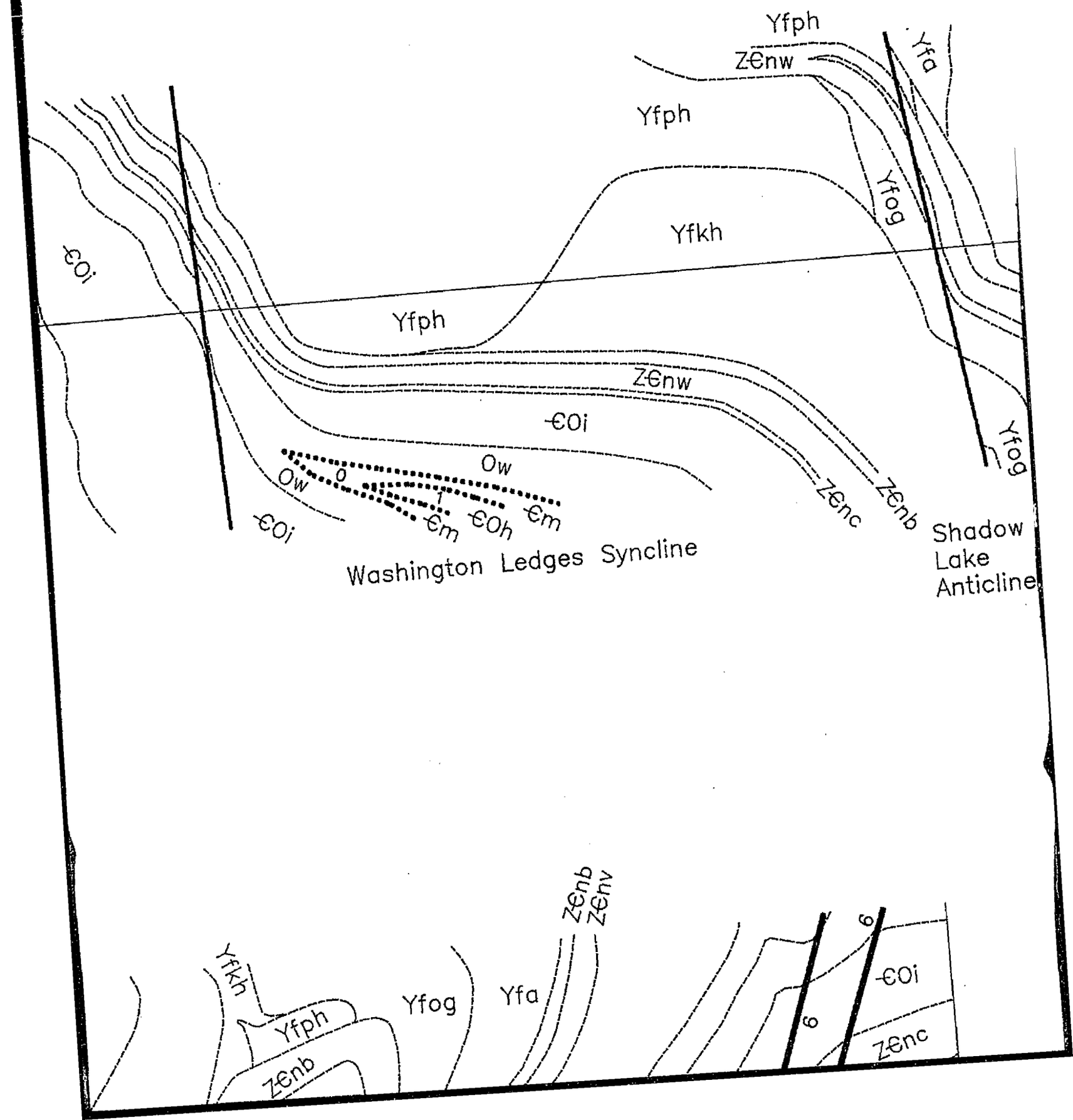
Yfph
Zϵnw
Yfa
Yfph
Yfog
Yfkh
ϵOi
Yfph
Zϵnw
ϵOi
Ow
Ow
0
1
ϵm
ϵOh
ϵm
Zϵnc
Zϵnb
Yfog
ϵOi
Washington Ledges Syncline
Shadow
Lake
Anticline
Yfkh
Yfph
Zϵnb
Yfog
Yfa
Zϵnb
Zϵnv
9
9
ϵOi
Zϵnc

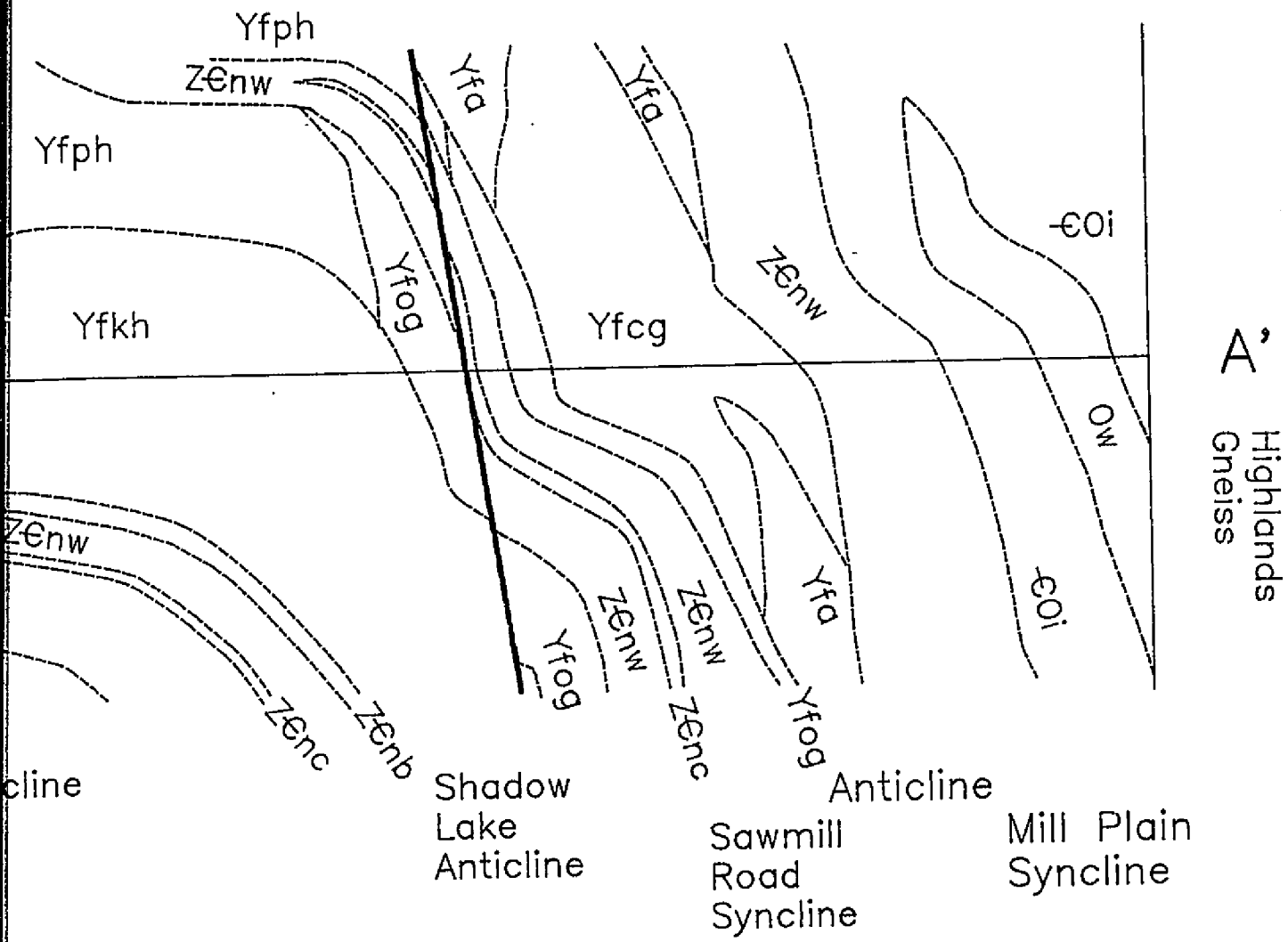
Yfph
Zenw
Yfph
Yfkh
Yfog
Yfa
Yfcg
Yfa
Zenw
-€Oi
Ow
A'
Highlands
Gneiss
Yfa
€Oi
Zenw
Zenw
Zenw
Yfog
Yfog
Zenc
Zenb
Zenc
cline
Shadow
Lake
Anticline
Anticline
Sawmill
Road
Syncline
Mill Plain
Syncline

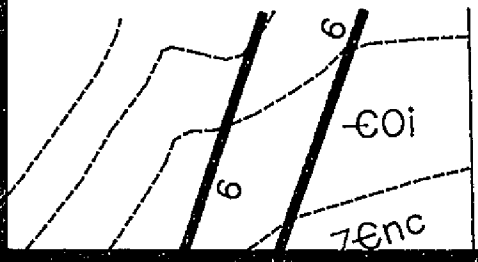
-€Oi
Zenc

meters

Pound Ridge Antiform

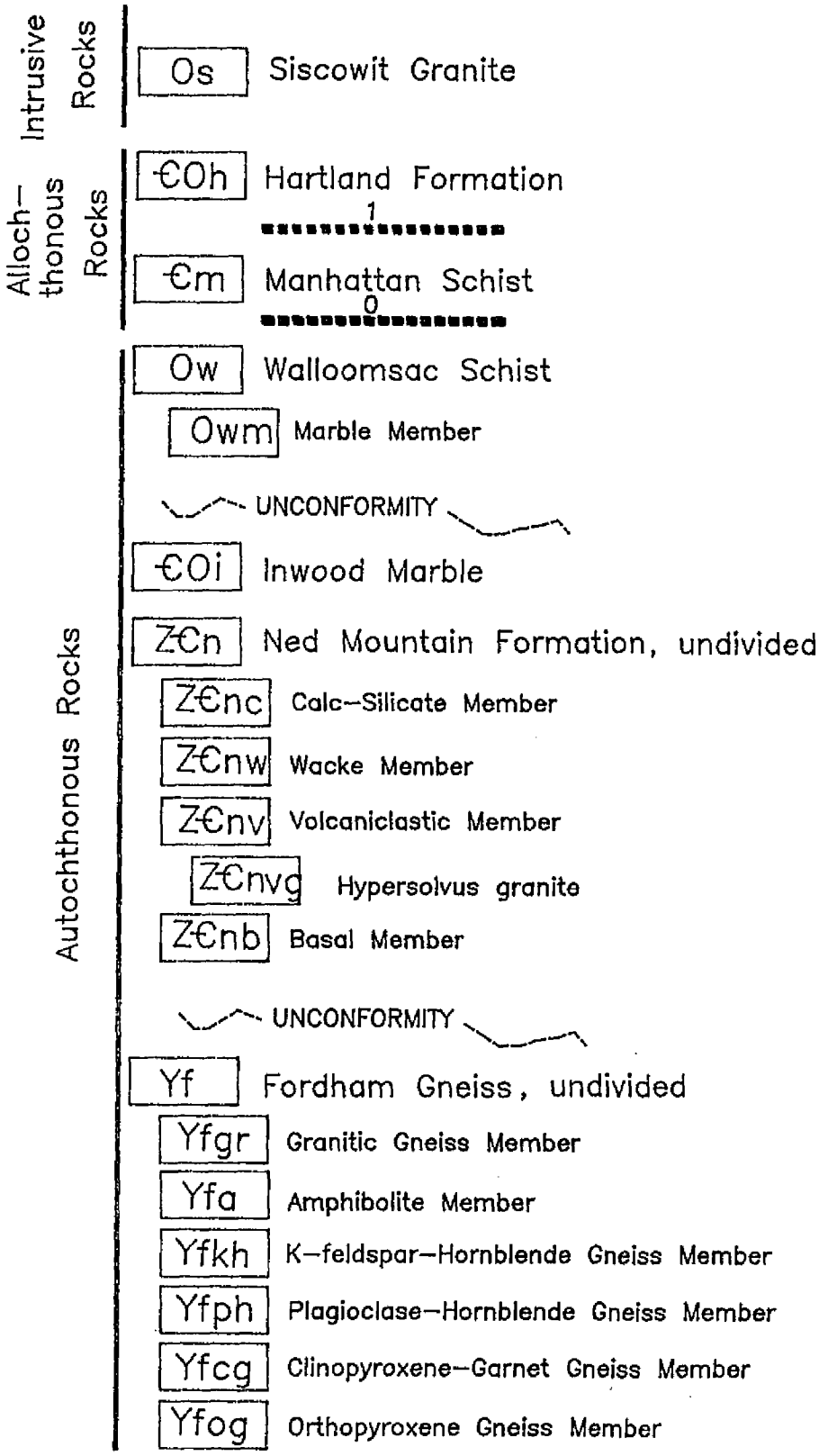

form

South Salem Syncline

te

ation

ist

chist

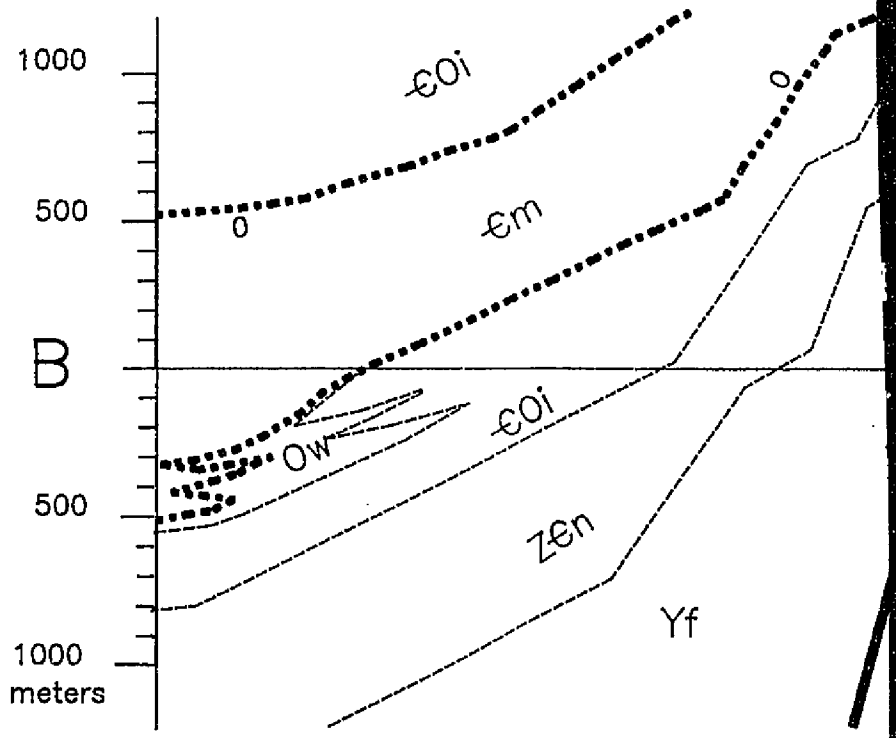

Turkey Hill Fault Zone

Formation, undivided

ember

ember

granite

s, undivided

Member

ber

blende Gneiss Member

blende Gneiss Member

arnet Gneiss Member

Gneiss Member

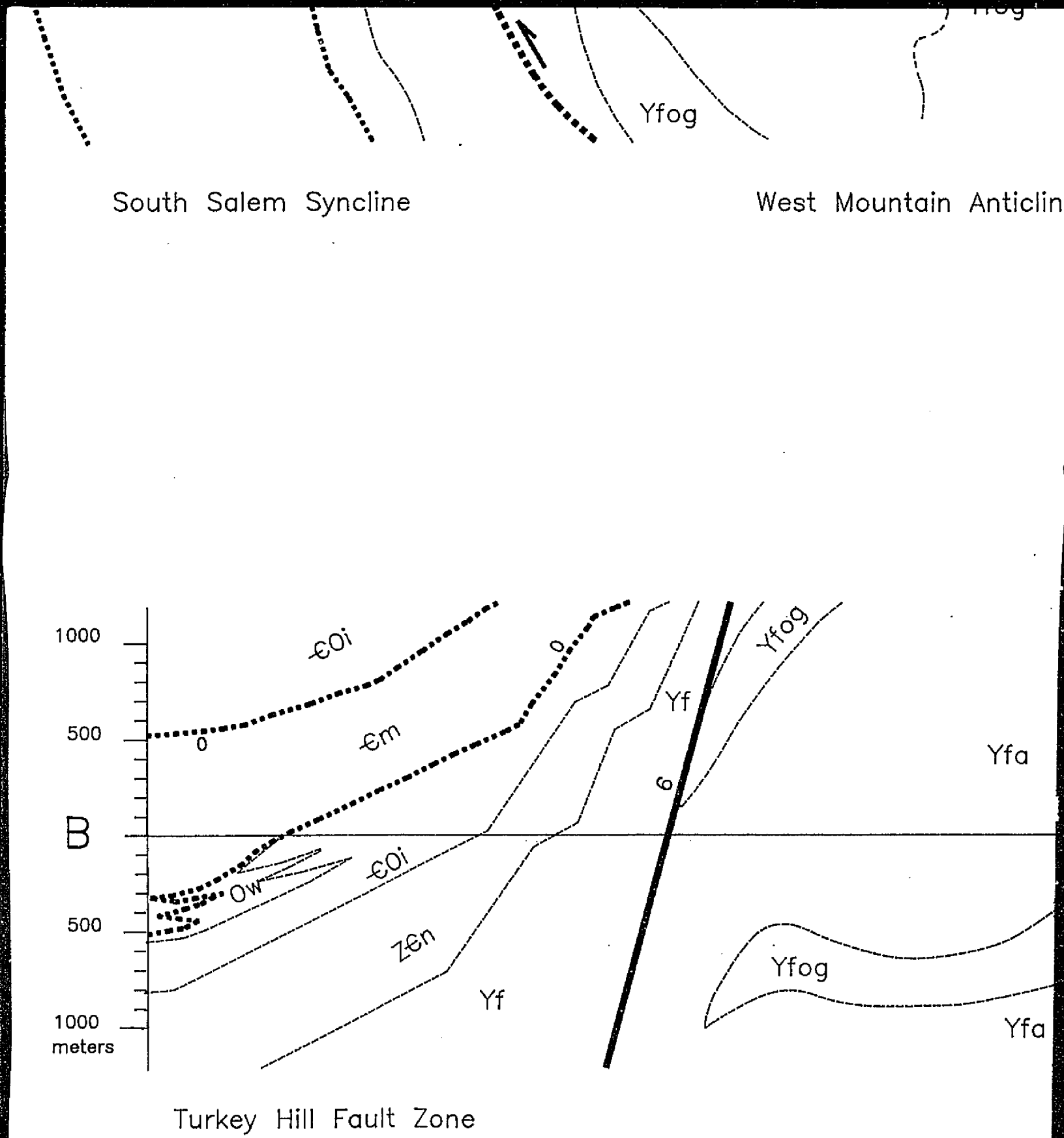

Turkey Hill Fault Zone

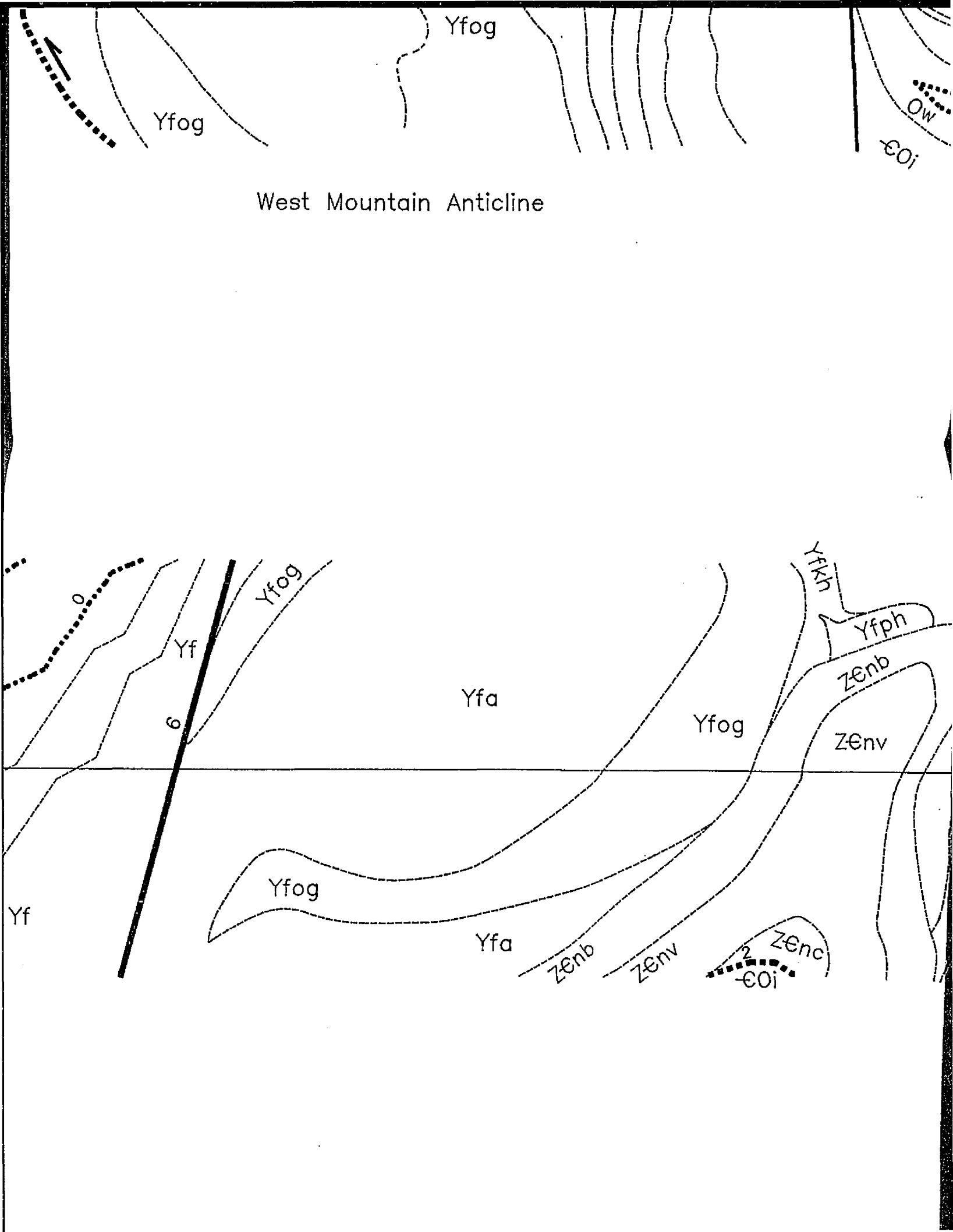
Yfog
Yfog
Ow
€Oi
West Mountain Anticline
O
Yf
Yfog
Yfkh
Yfph
Z€nb
Yfa
Yfog
Z€nv
Yf
Yfog
Yfa
Z€nb
Z€nv
Z€nc
2
€Oi

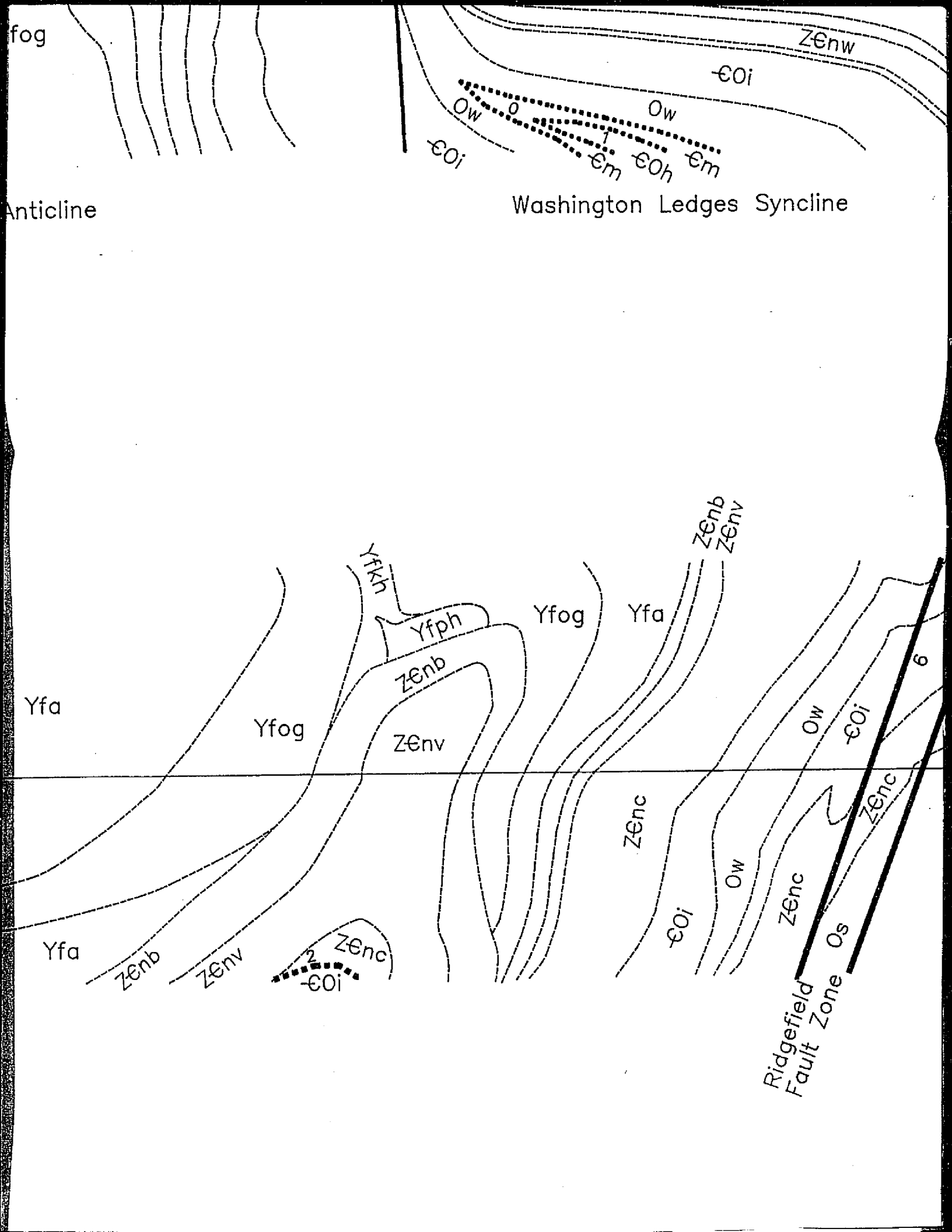
fog
Z€nw
€Oi
Ow
0
Ow
1
€Oi
€m
€Oh
€m
Anticline
Washington Ledges Syncline
Yfkh
Yfph
Yfog
Yfa
Z€nb
Z€nv
Yfa
Yfog
Z€nb
Z€nv
Z€nc
€Oi
Ow
6
Yfa
Z€nb
Z€nv
2
Z€nc
€Oi
Z€nc
€Oi
Ow
Z€nc
Os
Ridgefield
Fault Zone

Highlands
Gneiss

Zenw
Zenc
Zenb
Yfog
Zenw
Zenw
Zenc
Yfog
Yfa
€Oi
Ow

yncline

Shadow
Lake
Anticline

Anticline

Sawmill
Road
Syncline

Mill Plain
Syncline

B'

PLEASE NOTE:

Oversize maps and charts are filmed in sections in the following manner:

LEFT TO RIGHT, TOP TO BOTTOM, WITH SMALL OVERLAPS

The following map or chart has been refilmed in its entirety at the end of this dissertation (not available on microfiche). A xerographic reproduction has been provided for paper copies and is inserted into the inside of the back cover.

Black and white photographic prints (17" x 23") are available for an additional charge.

University Microfilms International

PLATE VI – MODEL FOR THE TACONIAN OROG
IN THE MANHATTAN PRONG

NORTHERN MANHATTAN PRONG

CENTRAL MANH

1. D_1 deformation (Early-M_1 metamorphism)

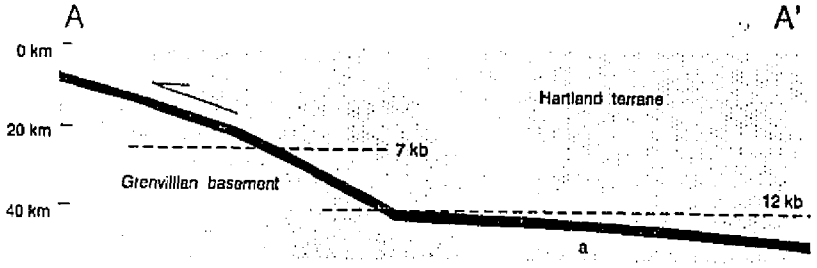

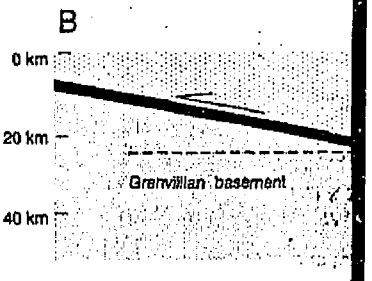

2. Post-D_1 intrusion of mafic complexes

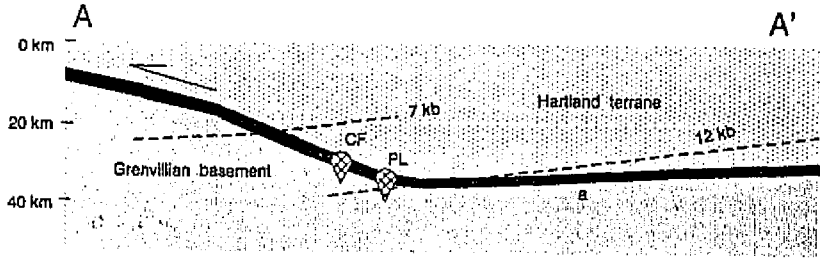

3. D_2 deformation

A. Cross Section A-A'

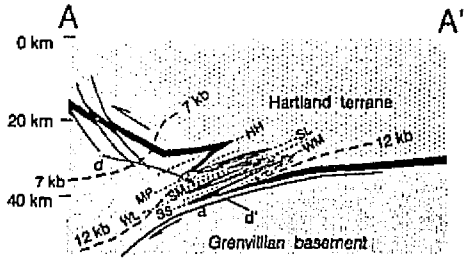

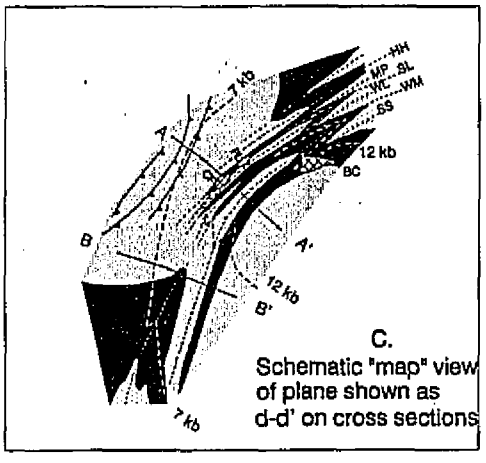

C. Schematic "map" view of plane shown as d-d' on cross sections

4. Post-D_2 warping--Intrusion of Cortlandt Comple

HH Hudson Highlands anticline

MP Mill Pond syncline

— MODEL FOR THE TACONIAN OROGENY IN THE MANHATTAN PRONG

ONG

CENTRAL MANHATTAN PRONG

D_1 deformation (Early-M_1 metamorphism)

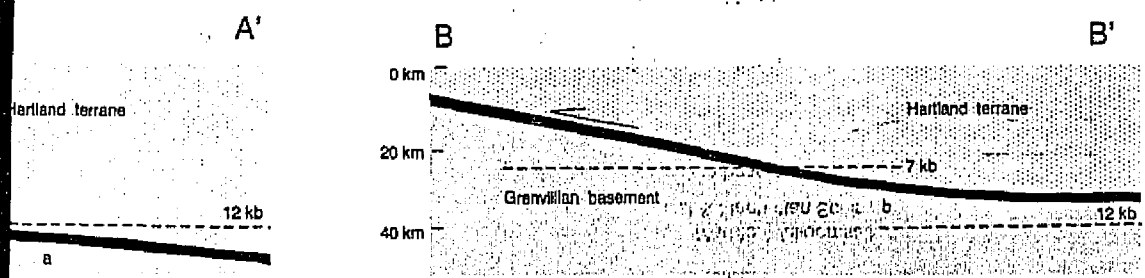

Post-D_1 intrusion of mafic complexes

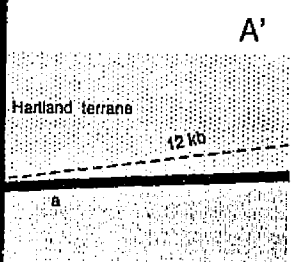

3. D_2 deformation

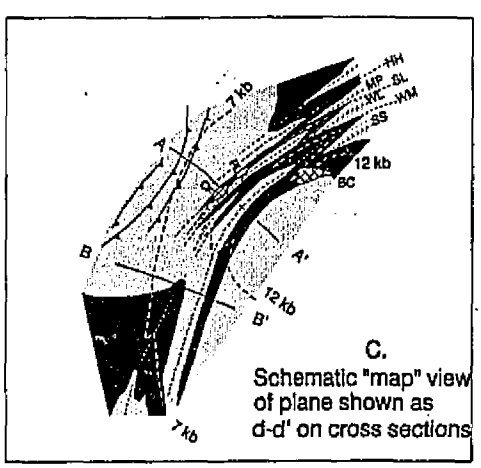

B. Cross Section B-B'

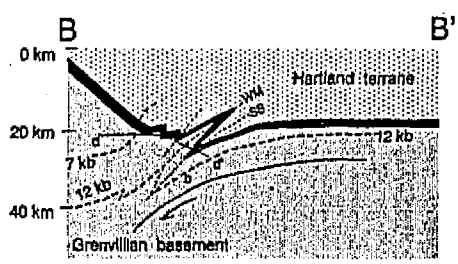

ost-D_2 warping--intrusion of Cortlandt Complex.

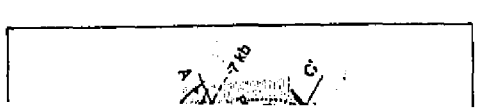

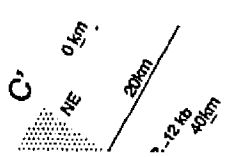

3. D_2 deformation

A. *Cross Section A-A'*

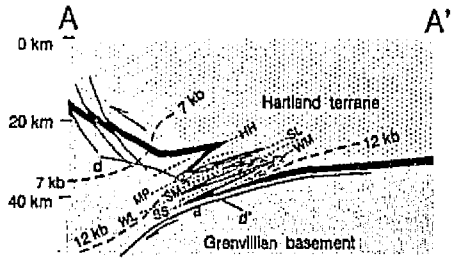

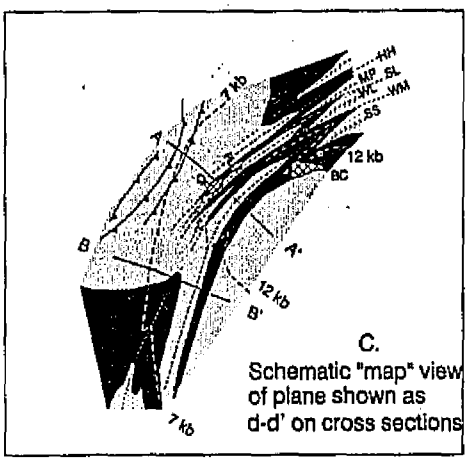

C. Schematic "map" view of plane shown as d-d' on cross sections

B. Cross Se

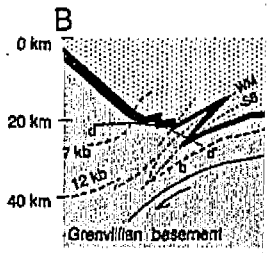

4. Post-D_2 warping -- Intrusion of Cortlandt Complex.

HH	Hudson Highlands anticline
MP	Mill Pond syncline
SM	Sawmill Road syncline
SL	*Shadow Lake anticline*
WL	Washington Ledges syncline
WM	West Mountain anticline
SS	South Salem syncline
CF	Croton Falls Complex
PL	Peach Lake Complex
BC	Bedford Complex
CC	Cortlandt Complex

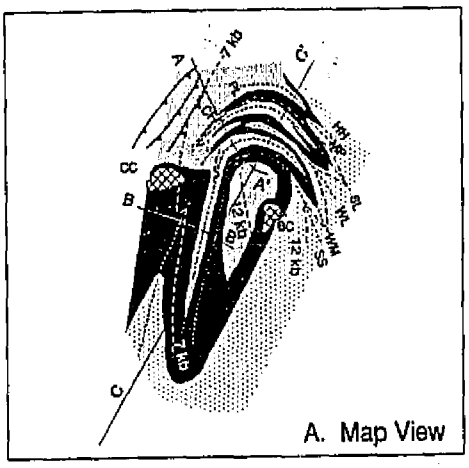

A. Map View

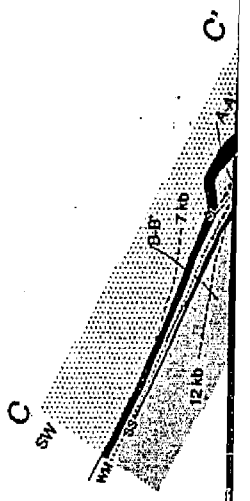

5. F_3 folding

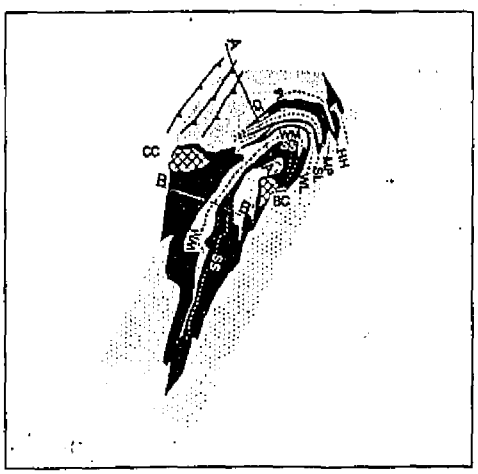

Mafic complexes

Hartland terrane

Inwood Marble, Walloomsac Schist & Manhattan Schist

Grenvillian basement

Thrust fault

F_2 hinge surfaces

Early-M_1 7 kb & 12 kb isobars

3. D_2 deformation

ction A-A'

A'

Hartland terrane

12 kb

an basement

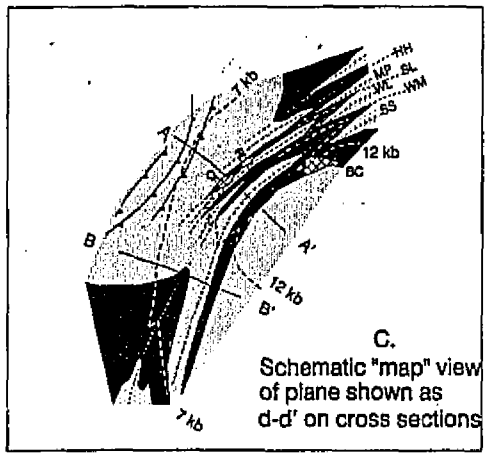

C. Schematic "map" view of plane shown as d-d' on cross sections

B. Cross Section B-B'

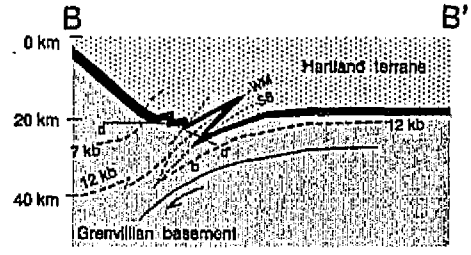

4. Post-D_2 warping--Intrusion of Cortlandt Complex.

anticline

ine

ine

syncline

cline

ce

ax

x

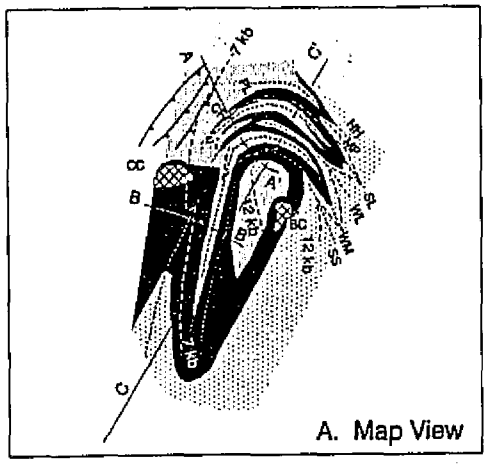

A. Map View

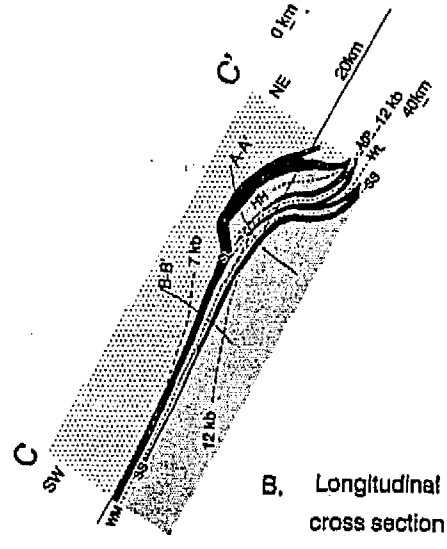

B. Longitudinal cross section C-C'

5. F_3 folding

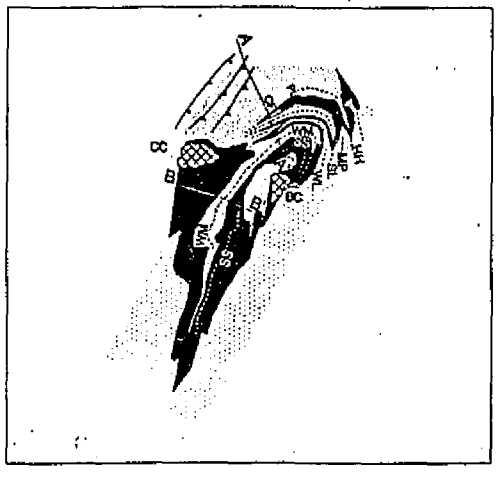

Mafic complexes

Hartland terrane

Inwood Marble, Walloomsac Schist & Manhattan Schist

Grenvillian basement

Thrust fault

F_2 hinge surfaces

Early-M_1 7 kb & 12 kb isobars

PART II-

ISOTOPICALLY-DEFINED BASEMENT BLOCKS OF THE NORTH-CENTRAL APPALACHIANS

ABSTRACT, Part II

Isotopic data (Sr, Pb, O, Nd) compiled from about 150 igneous bodies of Silurian to Carboniferous age underlying New England, New Brunswick, and eastern Quebec are used to distinguish five basement blocks. Isotopic compositions of igneous rocks from three of the blocks (Grenville, Central and Avalon) generally show wide variations, and include many distinctly continental values. Initial Sr ratios in each rise to at least .716. Pb initial ratios (from feldspars) often suggest "orogene" to "upper continental crust" magma sources. Negative ε Nd values are present. $\delta^{18}O$ values up to 12.6 (Avalon) and 13.3 (Central) indicate substantial inputs from sedimentary sources. Inheritance age data (such as xenocrystic zircon) suggest that the age of the Grenville basement is .9 to 1.4 Ga, the Central basement largely 1.4-1.8 Ga, and that the Avalon basement contains Middle Proterozoic and Archean components.

In contrast, plutons in two intervening regions (Boundary Mountains and Sebago) do not show the isotopic imprint of ancient continental crust. Zircon and Nd data are consistent with basements <750 Ma old. Sr initial ratios are <.706; Pb ratios lie between "mantle" and "orogene" values. $\delta^{18}O$ values rise only to 8.2 in the Boundary Mountains block and are mostly <10.0 in the Sebago block. In these two blocks, relatively low, restricted ranges of isotopic values occur in igneous rocks of varied bulk SiO_2 content. The Boundary Mountains and Sebago blocks are interpreted as arc terranes of Late Precambrian to Early Paleozoic age.

Crustal breaks inferred from seismic and gravity studies correspond well with the isotopically-defined basement boundaries. Thermochronological discontinuities coincide with several boundaries, suggesting that offsets occurred along them during Late Paleozoic to Mesozoic time. The existence and location of the five basement blocks offer important constraints for the tectonic history of the Appalachian orogen.

INTRODUCTION

Continents appear to have long histories of terrane accretion and growth. Discrimination of the discrete crustal fragments which comprise a continent is necessary for the complete and accurate reconstruction of its tectonic development. In this study, the isotopic compositions of igneous rocks are used to define the number and the nature of basement blocks in the north-central Appalachians. Data have been compiled on Sr initial ratios, Pb compositions, $\delta\ ^{18}O$ compositions, ε neodymium values and zircon inheritance ages from approximately 150 igneous bodies of Silurian to Carboniferous age. Isotopic data from these igneous bodies, whose geographical distribution is shown on Fig. 74, provide the basis for defining five zones (A, B, C, D, E).

Certain assumptions guided the way in which the isotopic zones were defined. First, it was assumed that melts derived from the mantle, and therefore potentially isotopically primitive, may intrude crustal blocks of any age. But reservoirs of isotopically distinct "crustal" character are expected only in ancient blocks, since these require lengthy separation from the mantle to evolve. Therefore, plutons intruding a block of ancient crust may display a broad range of isotopic characteristics, including distinct "crustal" values, while igneous rocks bodies within young crust should show a restricted range of comparatively mantle-like isotopic values.

When this logic is applied to a population of isotopic values, ancient material at depth ought to be detected, provided that this material has undergone partial melting and contributed to some magmas. When data from all the available isotopic systems (Sr, Pb, O, Nd) attest to a "crustal" character, confidence can be high that inputs from ancient crust are indeed present. If plutons of similar age and bulk chemical composition in adjoining regions have contrasting isotopic characteristics (one "crustal" and the other not), then juxtaposition of old and young crust can be inferred, so long as the regions have experienced comparable thermal histories. Misleading "crustal" values may occur as the result of shallow-level melting of ancient but allochthonous material in an orogenic belt, thus blurring some isotopic boundaries between old continental and

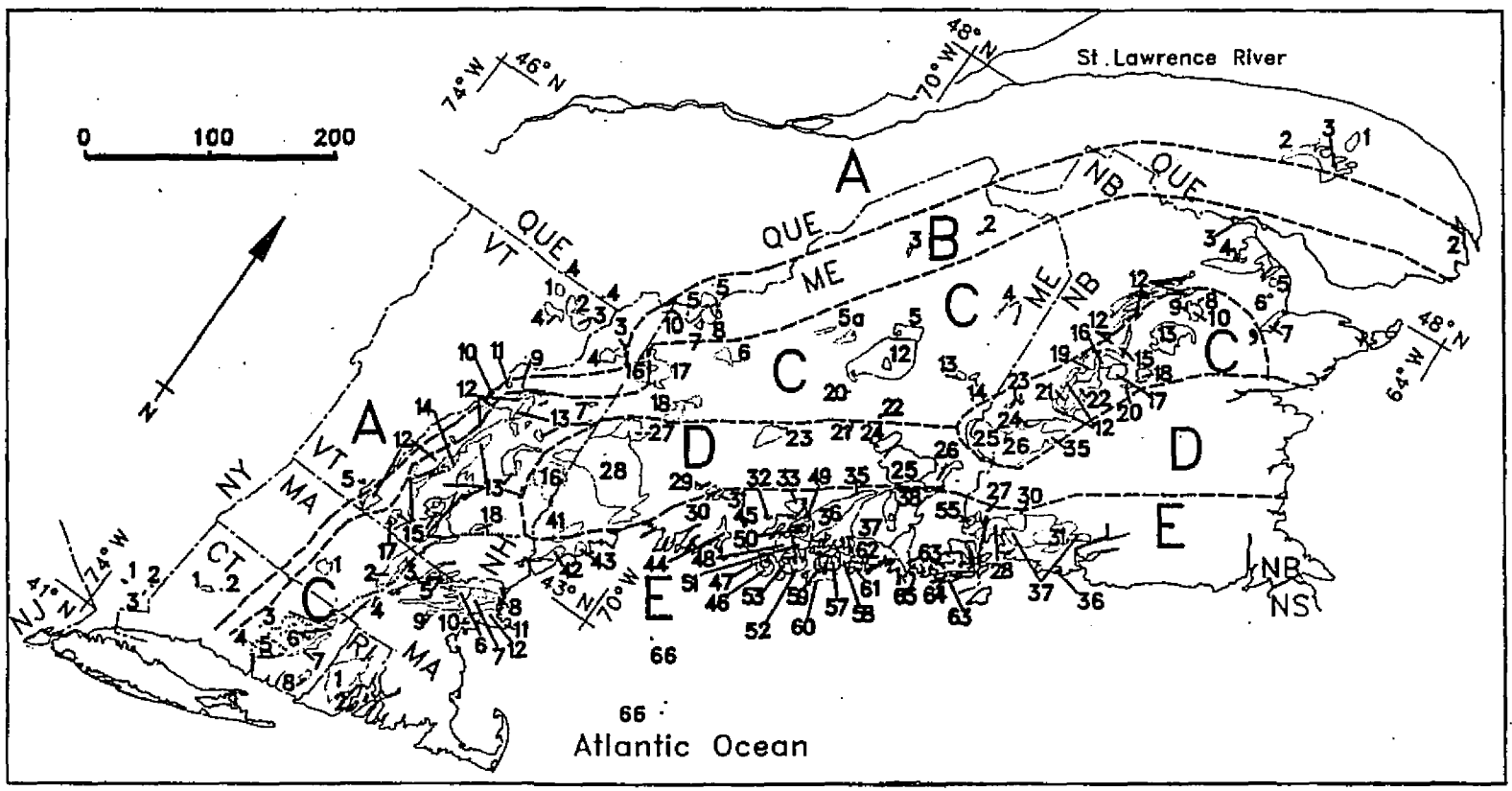

Fig. 74. Locations of the igneous bodies which provide isotopic data for this study. The igneous bodies are numbered separately in each state or province, and identified by name in Table 17. Isotopically-defined zones (A to E) are shown for reference, and their boundaries are indicated by dashed lines.

juvenile crustal blocks.

Previous work. Isotopic compositions of igneous rocks have provided evidence for the age and the nature of source materials in a variety of contexts. Within continents, isotopic compositions are often used to distinguish ancient crustal sources from younger mantle-derived ones. For instance, inputs from an older crust to arc magmas have been detected with Pb isotopes (Doe and Delevaux, 1973; Mukasa and Tilton, 1984; Barreiro, 1984; Housh, Bowring, and Villeneuve, 1989). The boundary between the ancient continental margin of the western United States and younger, arc-related terranes has been inferred from Sr initial ratios (Kistler and Peterman, 1973, 1978; Armstrong, Taubeneck, and Hales, 1977), ε Nd values (Farmer and DePaolo, 1983), and from Pb compositions (Zartman, 1974). A correspondence between plutonic Sr initial ratios of .706 and the stratigraphically defined continental edge has been recognized in Nevada (Elison, Speed, and Kistler, 1990). Juxtaposition of juvenile and continental terranes in South India (Krogstad and others, 1986) and in the Canadian Cordillera (Samson and others, 1989) has been demonstrated with Nd, Pb, and Sr isotopic data. In the southern Appalachians, O, Sr, and Pb isotopic compositions of Hercynian-aged granites in the Inner Piedmont reflect contributions from Grenville basement, whereas to the east, isotopic compositions from the Kings Mountain and Charlotte-Carolina Slate belts do not (Wenner, 1981; LeHuray, 1986).

Previous attempts to use isotopic compositions to define basements in the Northern Appalachians have focused on small areas and relied upon only one or two isotopic parameters. Andrew, Loiselle, and Wones (1983) studied O and Sr compositions in plutons of east-central Maine. Ayuso (1986) examined the Pb compositions of plutons of east-central and northern Maine, and Ayuso, Horan, and Criss (1988) investigated the O isotopic composition of plutons in northern Maine. Bevier (1987, 1988a) studied Pb compositions of plutons in New Brunswick. Wones and others (1981) considered Sr initial ratios as one of several criteria in their crustal subdivision of Maine. Aleinikoff and Moench (1987) analyzed the Pb compositions of plutons in

northern New Hampshire. Hayward has studied the Sr initial ratios, and O, Nd, and Pb isotopic compositions of several plutons in central New England (Hayward, 1983, 1989; Hayward, Gaudette, and Olszewski, 1988; Hayward, Olszewski, and Gaudette, 1990). Many others have performed Rb-Sr whole-rock age determinations, dated zircons using the U-Pb method, or investigated the O or Nd composition of individual igneous bodies. Table 17 summarizes the relevant data from most of the sources used in this paper.

TABLE 17

Isotopic Characteristics of Silurian to Carboniferous Igneous Rocks of the North-Central Appalachians

Zone	Map Number	Rock Unit	Radiometric Age	Method	Sr IR	Precamb. Inherit. Detected	Pb Ratios (/204Pb) 206Pb	207Pb	208Pb	$\delta^{18}O$	Reference
A	NY 1	Peekskill Granite	363±14	Rb-Sr	.7074						Mose & others, 1976
A	NY 2	Croton Falls granite	387±37	Rb-Sr	.7081						Brock & Mose, 1979
A	NY 3	Granite dikes, Manhattan Prong	343±9	Rb-Sr	.7091						Brock, Brueckner, & Brock, 1985 & unpub.data
A	NY 3	Granite dikes, Manhattan Prong	358±9	Rb-Sr	.7105						Brock, Brueckner, & Brock, 1985 & unpub.data
A	VT 1	Derby granodiorite	370±17	Rb-Sr	.7071	\					Arth & Ayuso, 1985; Ayuso & Arth, 1985
A	VT 1	Granite stock, Derby		Rb-Sr	.7125	\					Arth & Ayuso, 1985
A	VT 2	Echo Pond granodiorite		Rb-Sr	.707	\	18.13	15.53	37.98		Ibid.; Ayuso & Arth, 1985
A	VT 2	Echo Pond diorite		Rb-Sr	.704	/		to			Arth & Ayuso, 1985; Ayuso & Arth, 1985
A	VT 3	Nulhegan granodiorite	390±14	Rb-Sr	.7068	/	18.46	15.64	38.31		Arth & Ayuso, 1985; Ayuso & Arth, 1985
A	VT 4	Willoughby granite	376±9	Rb-Sr	.7068	/					Arth & Ayuso, 1985; Ayuso & Arth, 1985
A	VT 5	Black Mountain granite	326±17	Rb-Sr	.7118	Nd=>1.0 Ga	18.47	15.58	38.14*		Hayward, Gaudette, & Olszewski, 1988; Hayward, Olszewski, & Gaudette, 1990
A	VT 5	Black Mountain granite					18.60	15.67	38.54*		Hayward. Olszewski, & Gaudette, 1990
A	Que 1	McGerrigle plutonic complex	362±5	Rb-Sr	.71		18.02	15.52	37.80 - (range)		LaRocque, 1986; Whelan & Gariépy, 1986
A	Que 1	McGerrigle plutonic complex	382±8	Rb-Sr	.704		19.04	15.63	39.10 /		LaRocque, 1986; Whelan & Gariépy, 1986
A	Que 2	York River Fm. volcanics	380±3	Rb-Sr	.7041						LaRocque & Doig, 1984
A	Que 3	Lemieux Dome rhyolite	381±4	Rb-Sr	.7087						LaRocque & Doig, 1984 1984
A	Que 4	Stanhope dike swarm					18.20	15.56	38.00		Robert, Gariépy, & Whelan, 1988
A	Que 4	Stanhope dike swarm					18.40	15.64	38.30		Ibid.
B	Que 5	Spiders Lake granodiorite	368±1	Ar-Ar Hb			18.39	15.54	37.98	8.1	Heizler, Lux, & Decker, 1988; Ayuso, 1986; Ayuso, Horan, & Criss, 1988
B	Que 5	Spiders Lake granodiorite					18.03	15.54	37.94	8.1	Ayuso, 1986; Ayuso, Horan, & Criss, 1988
B	Que 5	Spiders Lake dike swarm					17.9	15.52	37.8		Robert, Gariépy, & Whelan, 1988
B	Que 5	Spiders Lake dike swarm					18.1	15.58	38.1		Ibid.
A	CT 1	Nonewaug Granite	383±5	Rb-Sr	.7165						Mose & Nagel, 1982
A	CT 2	Thomaston Granite	357±11	Rb-Sr	.706						Seidemann, 1980
C	CT 3	Granite dike, Glastonbury Gn.	354±10	Rb-Sr	.709						Brookins, 1980
C	CT 4	Folded pegmatite	348±15	Rb-Sr	.715						Ibid.
E	CT 5	Canterbury Gneiss	416±2	Rb-Sr	.7054						Pignolet, Grant, & Hickman, 1980
E	CT 5	Canterbury Gneiss	374±4	Rb-Sr	.7068						Ibid.
E	CT 6	Canterbury Gneiss	395±10	U-Pb Zir		No					Zartman & Naylor, 1984
E	CT 7	Canterbury Gneiss	392±9	Rb-Sr	.708						Ibid.
E	CT 8	Preston Gabbro	424±5	U-Pb Zir		No					Ibid.
C	MA 1	Belchertown Quartz Monzonite	380±5	U-Pb Zir		No					Ashwal & others, 1979
C	MA 2	Fitchburg Granite	402±11	Rb-Sr	.705						Zartman & Naylor, 1984
C	MA 3	Ayer Granite	433±5	U-Pb Zir		No					Ibid.
E	MA 4	Granite at Millstone Hill	372±7	Rb-Sr	.7060						Ibid.

TABLE 17, CONTINUED

Zone	Map Number	Rock Unit	Radiometric Age	Method	Sr IR	Precamb. Inherit.	Pb Ratios (/204Pb) 206Pb	207Pb	208Pb	$\delta^{18}O$	Reference
E	MA 5	Chelmsford Granite	399±6	Rb-Sr	.7102	Nd=625 Ma	18.34	15.49	38.02*	10.5-12.6	Hayward, 1989; Hayward, Gaudette, & Olszewski, 1988; Flagel & Hon, 1988; Hayward, Olszewski, & Gaudette, 1990
E	MA 5	Chelmsford Granite	389±5	U-Pb Zir		No	18.46	15.63	38.27*		Ibid; Zartman & Naylor, 1984
E	MA 6	Andover Granite (I)	455	Rb-Sr	.7043						Ibid.; Hill & others, 1984
E	MA 6	Andover Granite (II)	415	Rb-Sr	.7044						Zartman & Naylor, 1984; Hill & others, 1984
E	MA 7	Sharpners Pond Diorite	430±5	U-Pb Zir		No					Zartman & Naylor, 1984
E	MA 8	Newbury Volcanics	338±10	Rb-Sr	.7065						Fullagar & Bottino, 1968
E	MA 9	Indian Head Hill diorite	402±5	Rb-Sr	.7034						Hill & others, 1984
E	MA 10	Peabody Granite	359±24	Rb-Sr	.708						Zartman & Marvin, 1971
E	MA 10	Peabody Granite	380±15	U-Pb Zir		?					Zartman, 1977
E	MA 11	Cape Ann Granite (eastern)	450±20	U-Pb Zir		No					Ibid.; Zartman & Marvin, 1971
E	MA 11	Cape Ann Granite (eastern)	426±6	Rb-Sr	.703						Zartman & Marvin, 1971; Paige & Hon, 1988
E	MA 12	Cape Ann Granite (western)	375±15	U-Pb Zir		No					Zartman, 1977; Zartman & Marvin, 1971
E	RI 1	Scituate Granite	370±7	U-Pb Zir		No					Hermes & Zartman, 1985
E	RI 1	Scituate Granite	370	Rb-Sr	.705						Getty & Gromet, 1988
E	RI 2	East Greenwich intrusive suite	370±7	U-Pb Zir		No					Hermes & Zartman, 1985
A	NH 3	Volcanics at Clear Stream	434±8	U-Pb Zir		?1.5 Ga					Aleinikoff & Moench, 1985
A	NH 4	Long Mountain granite	350	U-Pb Zir#		to 1.8 Ga					Harrison, Aleinikoff, & Compston, 1987
A	NH 4	Long Mountain granite				D_MNd=1.5Ga					Ibid.
C	NH 7	Shelburne granite	406	Rb-Sr	.7058						Hayward, 1983
B-C	NH 9	Moody Ledge granite	422±4	U-Pb Zir		No	"mantle-like"				Aleinikoff & Moench, 1987
A	NH 10	Fairlee Quartz Monzonite	400	U-Pb Zir		Yes					Moench & Aleinikoff, 1987; Lyons, Aleinikoff, & Zartman, 1986
B	NH 11	French Pond granite	365±3	U-Pb Zir		No	"mantle-like"				Aleinikoff & Moench, 1987
C	NH 12	Bethlehem Gneiss	400±3	U-Pb Zir		Yes	"continental"				Ibid.
C	NH 12	Bethlehem Gneiss	396±78	Rb-Sr	.7065						Lyons & Livingston, 1977
C	NH 13	Kinsman Quartz Monzonite	402±19	Rb-Sr	.7107		"continental"				Ibid.; Aleinikoff & Moench, 1987
C	NH 13	Kinsman Quartz Monzonite	413±5	Sm-Nd		D_MNd=1.68Ga					Barreiro & Aleinikoff, 1985
C	NH 13	Kinsman Quartz Monzonite	400±6	U-Pb Zir		"preGrenville"					Harrison in Plank, 1987; Barreiro & Aleinikoff, 1985
C	NH 14	Sunapee granite	364±5	Rb-Sr	.7133						Hayward, 1989
C	NH 14	Sunapee granite	351±11	Rb-Sr	.7107						Lyons & Livingston, 1977
C	NH 14	Sunapee granite	354±5	U-Pb Zir#		1.0 Ga					Harrison, Aleinikoff, & Compston, 1987
C	NH 15	Spaulding Quartz Diorite	393±5	Rb-Sr	.7143						Lyons & Livingston, 1977
D	NH 16	Effingham granite	319±13	Rb-Sr	.7048						Hayward, 1989
C	NH 17	Fitzwilliam granite	383±6	Rb-Sr	.7090	D_MNd=.88Ga	18.34	15.49	38.02*	8.6-11.1	Hayward, 1989; Hayward, Gaudette, & Olszewski, 1988; Hayward, Olszewski, & Gaudette, 1990
							18.46	15.63	38.27*		
C	NH 18	Hooksett granite	400±7	Rb-Sr	.7066						Hayward, 1989

TABLE 17, CONTINUED

Zone	Map Number	Rock Unit	Radiometric Age	Method	Sr IR	Precamb. Inherit.	Pb Ratios (/204Pb) 206Pb	207Pb	208Pb	$\delta^{18}O$	Reference
B	ME 2	Deboullie granodiorite	(Devonian)				18.23	15.54	38.09		Ayuso, 1986; Ayuso, Horan, & Criss, 1988
B	ME 2	Deboullie granodiorite					18.22	15.54	38.07	7.4-7.7	Ibid.
B	ME 2	Deboullie granodiorite					18.17	15.55	38.04	7.4-7.7	Ibid.
B	ME 2	Deboullie syenite					18.41	15.53	38.37	7.5-7.9	Ibid.
B	ME 2	Deboullie syenite					18.25	15.54	38.08	7.5-7.9	Ibid.
B	ME 3	Priestley Lake granodiorite	(Devonian)				18.30	15.53	37.94	6.8-8.1	Ibid.
B	ME 3	Priestley Lake granodiorite					18.27	15.52	38.01	6.8-8.1	Ibid.
B	ME 3	Priestley Lake granodiorite					18.15	15.54	37.98	6.8-8.1	Ibid.
B	ME 3	Priestley Lake granodiorite					18.10	15.55	37.91	6.8-8.1	Ibid.
B	ME 3	Priestley Lake granodiorite					18.44	15.54	38.23	6.8-8.1	Ibid.
C	ME 4	Hedgehog volcanics	404±10	Rb-Sr	.706						Bottino & Fullagar, 1966; Sargent & Hon, 1981
C	ME 5	Traveler Rhyolite	349±10	Rb-Sr	.7100						Fullagar & Bottino, 1968; Rankin, 1968
C	ME 5a	Kineo rhyolite	406±24	Rb-Sr	.70919						Gaudette & others, 1990; Rankin, 1968
C	ME 6	Stratton granite	408±10	Rb-Sr	.70957						Ibid.
B	ME 7	Seven Ponds granodiorite	368±1	Ar-Ar			18.04	15.56	37.96	7.5-7.6	Heizler, Lux & Decker, 1988; Ayuso 1986;
							18.04	15.54	37.94	7.5-7.6	Ayuso, Horan, & Criss, 1988
B	ME 8	Chain of Ponds granodiorite	373±2	Ar-Ar			18.04	15.52	37.87	7.2-8.1	Heizler, Lux, & Decker, 1988; Ayuso, 1986; Ayuso, Horan, & Criss, 1988
B	ME 8	Chain of Ponds granodiorite					18.02	15.53	37.91	7.2-8.1	Ayuso 1986; Ayuso, Horan, & Criss, 1988
B	ME 8	Chain of Ponds granodiorite					17.96	15.56	37.93	7.2-8.1	Ibid.
B	ME 9	Hog Island granodiorite					18.09	15.51	37.96	7.8-8.2	Ibid.
B	ME 10	East Inlet quartz monzonite	430±4	U-Pb Zir		?					Eisenberg, 1981; Lyons, Aleinikoff, & Zartman, 1986
C	ME 12	Katahdin Granite	414±40	U-Pb Zir			18.35	15.59	38.13		Loiselle, Hon, & Naylor, 1983; Ayuso, 1986; Hon, 1980
C	ME 12	Katahdin Granite	388±5	Rb-Sr	.7083		18.38	15.59	38.15	7.2-12.4	Loiselle, Hon, & Naylor, 1983; Ayuso, 1986; Andrew, Loiselle, & Wones, 1983
C	ME 13	Pleasant Lake zoned pluton	402±6	Ar-Ar			19.13	15.58	38.20		Hubacher & Lux, 1987; Ayuso, 1986
C	ME 14	Hunt Ridge zoned pluton	402±6	Ar-Ar			18.27	15.59	38.14		Hubacher & Lux, 1987; Ayuso, 1986
B	ME 16	Umbagog quartz monzonite	384±6	U-Pb Zir		No	"mantle-like"				Aleinikoff & Moench, 1987
C	ME 17	Mooselookmeguntic Granite	371±6	Rb-Sr	.7065						Moench & Zartman, 1976
C	ME 18	Phillips granite	404±10	Rb-Sr	.71611						Gaudette & others, 1990
C	ME 20	Seboeis Complex	416±25	Rb-Sr	.7055						Loiselle & others, 1983
C	ME 20	Ebeemee granodiorite (Seboeis)	411±4	U-Pb Zir			18.40	15.59	38.18	11.2-12.6	Ibid.; Andrew, Loiselle, & Wones, 1983; Ayuso, 1986
D	ME 21	Norway Point gabbro (Seboeis)					18.34	15.58	38.06	7.4- 9.6	Ayuso, 1986; Andrew, Loiselle, & Wones, 1983
C	ME 22	Mattamiscontis granite "	410±4	U-Pb Zir	.7066		18.33	15.57	38.02	10.5-13.3	Ibid.; Loiselle & others, 1983; Ayuso, 1986
D	ME 23	Hartland granodiorite	360±8	Rb-Sr	.7056						Dallmeyer, van Breemen, & Whitney, 1982
D	ME 24	Center Pond diorite/granite	372±10	Rb-Sr	.7051						Loiselle & others, 1983; Scambos, Loiselle, & Wones, 1986

TABLE 17, CONTINUED

Zone	Map Number	Rock Unit	Radiometric Age	Method	Sr IR	Precamb. Inherit.	Pb Ratios (/204Pb) 206Pb	207Pb	208Pb	$\delta^{18}O$	Reference
D	ME 24	Center Pond diorite/granite					18.33	15.57	38.13		Ayuso, 1986
D	ME 24	Center Pond diorite/granite	380±5	U-Pb Zir			18.40	15.57	38.13	8.2- 9.4	Loiselle & others, 1983; Andrew, Loiselle, & Wones, 1983
D	ME 25	Passadumkeag River granite	381±4	Rb-Sr	.7041		18.26	15.57	38.09		Ayuso & others, 1984; Ayuso, 1986
										8.8- 9.2	Andrew, Loiselle, & Wones, 1983
D	ME 25	Passadumkeag River granite	388±6	U-Pb Zir		?	18.30	15.58	38.13		Ibid.; Ayuso & others, 1984; Ayuso, 1986
D	ME 26	Whitney Cove granite	379±5	Rb-Sr	.7055		18.25	15.56	38.29		Ayuso & others, 1984; Ayuso, 1986
D	ME 26	Whitney Cove granite	399±8	U-Pb Zir		?				9.0- 9.9	Ayuso & others, 1984; Andrew, Loiselle, & Wones, 1983
D	ME 27	Songo granodiorite-qtz.diorite	382±3	U-Pb Zir		No					Lux & Aleinikoff, 1985
D	ME 27	Songo granodiorite	382±34	Rb-Sr	.70528						Lux, Gibson, & Hamilton, 1989; Gibson & Lux, 1989
D	ME 28	Sebago granite	325±3	U-Pb Zir	.7031	No	18.47	15.58	38.14*		Aleinikoff, Moench, & Lyons, 1985; Hayward, Olszewski, & Gaudette, 1990
D	ME 28	Sebago granite	325±3	U-Pb Zir	.7053	No	18.60	15.67	38.54*		Aleinikoff, Moench, & Lyons, 1985; Hayward, Olszewski, & Gaudette, 1990
D	ME 28	Sebago granite	335±6	Rb-Sr	.7048	D_MNd=705Ma				7.5-11.1	Hayward, 1989; Hayward, Gaudette, & Olszewski, 1988
D	ME 29	Hallowell quartz monzonite	387±11	Rb-Sr	.705						Dallmeyer & van Breemen, 1981
D	ME 30	Togus quartz monzonite	394±8	Rb-Sr	.7049						Ibid.
D-E	ME 31	Threemile Pond granodiorite	393±15	Rb-Sr	.7058						Ibid.
D-E	ME 31	Threemile Pond granodiorite	381±14	Rb-Sr	.7065						Ibid.
E	ME 32	Northport granite					18.20	15.65			Eriksson, Hogan, & Williams, 1989
E	ME 32	Northport granite					18.72	15.69			Ibid.
E	ME 33	Mount Waldo granite	382±10	Rb-Sr	.705						Brookins in Wones, 1974; Brookins, 1976
E	ME 35	Parks Pond monzodiorite	384	Rb-Sr	.7099	Archean	18.28	15.66			Eriksson & Wones, 1983, 1985; Eriksson, Hogan, andWilliams, 1989; Williams, Eriksson, & Compston, 1986
E	ME 35	Parks Pond monzodiorite	387±8	U-Pb Zir		Archean	18.63	15.71			Ibid.; Eriksson, Hogan, & Williams, 1989
E	ME 36	Lucerne granite	371±21	Rb-Sr	.7077		18.38	15.62	38.18	5.8-11.3	Loiselle & others, 1983; Ayuso, 1986; Andrew, Loiselle, & Wones, 1983
E	ME 36	Lucerne granite	380±4	U-Pb Zir			18.89	15.67	38.58		Zartman & Gallego, 1979; Ayuso, 1986
E	ME 37	Cranberry Lake granite-Deblois	393±17	Rb-Sr	.7041		18.42	15.60	38.09	8.4-11.0	Loiselle & others, 1983; Ayuso, 1986; Andrew, Loiselle, & Wones, 1983
E	ME 37	Lead Mountain granite-Deblois	393±17	Rb-Sr	.7041		18.55	15.61	38.20	9.0-10.0	Ibid.; Loiselle & others, 1983; Ayuso, 1986
E	ME 37	Lead Mountain granite-Deblois					18.61	15.62	38.30		Ayuso, 1986
E	ME 38	Spruce Mountain granite								10.0	Andrew, Loiselle, & Wones, 1983
E	ME 40	Red Beach granite	385±6	Rb-Srmi	.7121						Spooner & Fairbairn, 1970
D	ME 41	Lyman granite	322±12	Rb-Sr	.7044	D_M=705Ma	18.49	15.63	38.39		Gaudette, Kovach, & Hussey, 1982; Hayward Gaudette, Olszewski, 1988; Michard-Vitrac, Albarede, & Allègre, 1981
E	ME 42	Webhannet granodiorite-granite	390±10	Rb-Sr	.7046						Gaudette, Kovach, & Hussey, 1982
E	ME 42	Webhannet granodiorite-granite	403±13	U-Pb Zir		No					Ibid.

TABLE 17, CONTINUED

Zone	Map Number	Rock Unit	Radiometric Age	Method	Sr IR	Precamb. Inherit.	Pb Ratios (/204Pb) 206Pb	207Pb	208Pb	$\delta^{18}O$	Reference
E	ME 43	Biddeford granite	341±12	Rb-Sr	.7067						Ibid.
E	ME 44	Waldoboro granite	367±4	Rb-Sr	.7123						Knight & Gaudette, 1987
E	ME 45	Union ultramafic complex	410±7	U-Pb Zir		No					Gaudette, 1981
E	ME 46	Vinalhaven granite	353±7	Rb-Sr	.705						Brookins, Berdan, & Stewart, 1973
E	ME 47	Vinalhaven Rhyolite	385±6	Rb-Sr	.7070						Ibid.
E	ME 48	Castine Volcanics	383±5	Rb-Sr	.7079						Ibid.
E	ME 49	Wallamatogus granite	363±15	Rb-Sr	.715		18.63	15.66	38.27		Brookins, 1976; Brookins in Wones, 1974; Ayuso, 1986
E	ME 50	South Penobscot diorite	394±15	Rb-Sr	.706						Brookins in Wones, 1974
E	ME 50	South Penobscot granite		Rb-Sr	.715		18.56	15.62	38.34		Brookins in Oliphant, 1969; Ayuso, 1986
E	ME 50	South Penobscot qtz. dior-gran	436±9	Rb-Sr	.70496						Stewart, Arth, & Flohr, 1988
E	ME 50	South Penobscot Suite	424±6	U-Pb Zir							Ibid.
E	ME 51	Sedgwick granite	387±15	Rb-Sr	.706						Brookins, 1976; Brookins in Wones, 1974;
E	ME 52	Oak Point granite (Deer Isle)	349±1	Rb-Sr	.7045		18.47	15.60	38.21		Brookins & Spooner, 1970; Ayuso, 1986
E	ME 53	Stonington granite (Deer Isle)	334±21	Rb-Sr	.7050						Brookins & Spooner, 1970; Hogan & Sinha, 89b
E	ME 54	Blue Hill granite	374±10	Rb-Sr	.707		19.21	15.66	38.51		Brookins, 1976; Brookins in Wones, 1974; Ayuso, 1986;
E	ME 55	Baring Granite	436	Rb-Sr	.705	D_MNd=1.1Ga					Jurinski & Sinha, 1989; Brueckner & Ludman, unpub. data
E	ME 57	Cadillac Mountain granite	361±35	Rb-Sr	.7039						Metzger & Bickford, 1972; Hogan & Sinha, 89b
E	ME 58	Bar Harbor Series volcanics	408±27	Rb-Sr	.7069						Metzger, Mose, & Nagel, 1982
E	ME 59	Southwest Harbor granite	373±12	Rb-Sr	.7056						Metzger, Mose & Nagel, 1982
E	ME 60	Cranberry Island volcanics	379±9	Rb-Sr	.7061						Brookins, Berdan, & Stewart, 1973
E	ME 61	Gouldsboro granite	377±19	Rb-Sr	.7077						Metzger, Mose, & Nagel, 1982
E	ME 62	Sullivan granite					18.47	15.61	38.09	8.7-10.7	Ayuso, 1986; Andrew, Loiselle, & Wones, 1983
E	ME 63	Quoddy Formation volcanics	411±15	Rb-Sr	.706						Fullagar & Bottino, 1968
E	ME 63	Dennys Formation volcanics	406±15	Rb-Sr	.705						Ibid.; Gates & Moench, 1981
E	ME 63	Pembroke Group volcanics	401±15	Rb-Sr	.704						Fullagar & Bottino, 1968; Gates & Moench, 1981
E	ME 64	Eastport Formation volcanics	403±5	Rb-Sr	.707						Bottino & Fullagar, 1966; Gates & Moench, 1981
E	ME 65	Flint Island volcanics	396±17	Rb-Sr	.7073						Metzger, Mose & Nagel, 1982
E	ME 66	Gulf of Maine granites	437±18	U-Pb Zir		No					Hermes, Ballard, & Banks, 1978
E	ME 67	Metaluminous granites (coastal)					18.00	15.52			Hogan, Jurinski, & Sinha, 1988
E	ME 67	Metaluminous granites (coastal)					19.20	15.61			Ibid.
E	ME 68	Peraluminous granites (coastal)				Model Pb	18.30	15.57			Ibid.
E	ME 68	Peraluminous granites (coastal)				~1.5 Ga	19.15	15.65			Ibid.
E	ME 69	Gabbros of coastal Maine					18.05	15.56			Ibid.
E	ME 69	Gabbros of coastal Maine					18.85	15.69			Ibid.
C	NB 3	Campbellton granite					18.29	15.59	38.01		Bevier, 1987
C	NB 4	Benjamin River pluton	370±30	Rb-Sr			18.41	15.58	38.07		Stewart, 1979; Bevier, 1987
C	NB 5	Antinouri Lake granite					18.21	15.59	38.08		Ibid.; Fyffe, Pajari, & Cherry, 1981
C	NB 6	Nicholas Denys granodiorite					18.24	15.59	38.04		Bevier, 1987; Fyffe, Pajari, & Cherry, 1981
C	NB 7	Pabineau Falls granite	373±5	U-Pb Zir#		to 1.8 Ga	18.28	15.61	38.09		Roddick & Bevier, 1988; Bevier 1987

TABLE 17, CONTINUED

Zone	Map Number	Rock Unit	Radiometric Age	Method	Sr IR	Precamb. Inherit.	Pb Ratios (/204Pb) 206Pb	207Pb	208Pb	$\delta^{18}O$	Reference
C	NB 7	Pabineau Falls granite	394±1	U-Pb Zir							Bevier, 1988a; Fyffe, Pajari, & Cherry, 1981
C	NB 8	Mount Elizabeth alkali granite	414$^{+11}_{-1}$	U-Pb Zir		Yes	18.57	15.70	38.42		Bevier & Whalen, 1990; Bevier, 1987; Fyffe, Pajari, & Cherry, 1981
C	NB 9	Mount Elizabeth syenite					18.47	15.67	38.31		Bevier, 1987
C	NB 10	Mount Elizabeth granite	417±2	U-Pb Mon			18.41	15.67	38.30		Bevier & Whalen, 1990; Bevier, 1987; Fyffe, Pajari, & Cherry, 1981
C	NB 12	Tobique Group volcanics	409±35	Rb-Sr	.7052						Fyffe & Cormier, 1979
C	NB 13	North Pole Stream Granite	378±7	Rb-Sr			18.54	15.67	38.25		Cormier in Fyffe, Pajari, & Cherry, 1981; Bevier, 1987
C	NB 13	North Pole Stream Granite	417±1	U-Pb Mon							Bevier & Whalen, 1990
C	NB 15	Redstone Mountain Granite	409±25	Rb-Sr	.7064		18.71	15.68	38.42		Fyffe & Cormier, 1979; Bevier, 1987
C	NB 16	Lost Lake Granite					18.34	15.66	38.26		Bevier, 1987
C	NB 17	Burnthill Granite	351±8	Rb-Sr			18.33	15.66	38.26		Crouse, 1981; Bevier, 1987; Fyffe, Pajari, & Cherry, 1981
C	NB 18	Dungarvon Granite					18.33	15.65	38.25		Bevier, 1987; Fyffe, Pajari, & Cherry, 1981
C	NB 19	Juniper Barrens Granite					18.35	15.67	38.25		Bevier, 1987
C	NB 20	Trout Brook Granite					18.36	15.69	38.38		Ibid.
C	NB 21	Becaguimec Lake Gabbro					18.35	15.70	38.36		Ibid.
C	NB 22	Nashwaak Granite					18.33	15.69	38.34		Ibid.; Fyffe, Pajari, & Cherry, 1981
C	NB 23	Gibson Granite					18.74	15.71	38.63		Bevier, 1987; Fyffe, Pajari, & Cherry, 1981
C	NB 24	Hartfield Tonalite	415±1	U-Pb Sph			18.35	15.66	38.22		Bevier & Whalen, 1990; Bevier, 1987; Fyffe, Pajari, & Cherry, 1981
C	NB 25	Skiff Lake Granite (Pokiok)	409±2	U-Pb Zir		?	18.33	15.67	38.30		Bevier & Whalen, 1990; Bevier, 1987; Fyffe, Pajari, & Cherry, 1981
C	NB 26	Hawkshaw Granite (Pokiok)	411±2	U-Pb Sph		?	18.33	15.66	38.23		Bevier & Whalen, 1990; Bevier, 1987; Fyffe, Pajari, & Cherry, 1981
E	NB 27	Tower Hill granite	415±15	Rb-Sr	.703						Butt & others, 1976; Fyffe, Pajari, & Cherry, 1981
E	NB 28	Bocabec Complex (St. George)	403±20	Rb-Sr	.7065						Cormier in Fyffe, Pajari, & Cherry, 1981
E	NB 30	Beech Hill granite	337±15	Rb-Sr	.719						Butt & others, 1976; Fyffe, Pajari,
E	NB 31	Mt. Douglas granite (St.George)	343±7	Rb-Sr	.7088						Cormier in Harding & others, 1988; Fyffe, Pajari, & Cherry, 1981
E	NB 35	Allandale Granite (Pokiok)	402±1	U-Pb Mon			18.37	15.67	38.27		Bevier & Whalen, 1990; Bevier, 1987
E	NB 36	Musquash Harbour Granite	392±55	Rb-Sr	.7187						Olszewski & Gaudette, 1982
E	NB 37	St. Croix-Mascarene granites					18.24	15.61	38.05		Bevier, 1988b
E	NB 37	St. Croix-Mascarene granites					18.67	15.65	38.35		Bevier, 1988b

Explanation of abbreviations
Hb = Hornblende; Mon = Monazite; Rb-Srmi = Rubidium-Strontium mineral isochron; Sph = Sphene; Zir = Zircon; Zir# = Zircon Ion Microprobe Analysis
Rb-Sr ages are whole-rock isochron ages unless otherwise specified.
* = the quoted range covers the combined values of two plutons.

Rb-Sr ages are calculated using Steiger & Jäger's (1977) recommended decay constants.

COMPILATION OF ISOTOPIC DATA

Sr, Pb, and O isotopic data were ranked from most "mantle-like" to most "crustal" and plotted on base maps (Figs. 75, 76, and 78). Pb data were also plotted on an evolution diagram (Fig. 77), and inheritance-age data were compiled on Fig. 80. The data sets are all mutually supporting and consistent with the basement zonation (A, B, C, D, E), although no single set of data is comprehensive enough to display the entire pattern.

Sr and Pb data. Strontium initial ratios (Sr IR) from whole-rock age determinations are the most abundant form of isotopic data in the Northern Appalachians. Sr IR of Silurian, Devonian, and some Carboniferous igneous bodies are listed in Table 17 and plotted on Fig. 75. These values are treated without distinction, since during the approximately 100 Ma span of time over which these igneous rocks sampled the basement, differences in Sr isotopic composition due to evolution were relatively small.

On Fig. 75, wide ranges of Sr IR values can be found in regions marked Zone A, C, and E. Each of these regions contains many igneous bodies having Sr IR greater than .706, and some over .710. These high initial ratios reflect long-standing enrichment in rubidium in the source region and are associated with a well-evolved upper continental crust. On the other hand, the region marked "D" contains a much more restricted range of compositions: plutons whose ages range from 381$\pm$4 Ma (Passadumkeag; Ayuso and others, 1984) to 322$\pm$12 Ma (Lyman; Gaudette, Kovach and Hussey, 1982) all have Sr IR under .706. This suggests the presence of a younger crust under Zone D.

There are no Sr IR yet available for Silurian to Carboniferous plutons in Zone B. However, data from Ordovician plutons in Oliverian domes of Zone B (Mascoma dome= .705 and Jefferson Dome= .70453; Naylor, 1969, and Foland and Loiselle, 1981) are consistent with a relatively young crust in this area, while gneisses in the Lebanon dome to the west (Zone A) may have

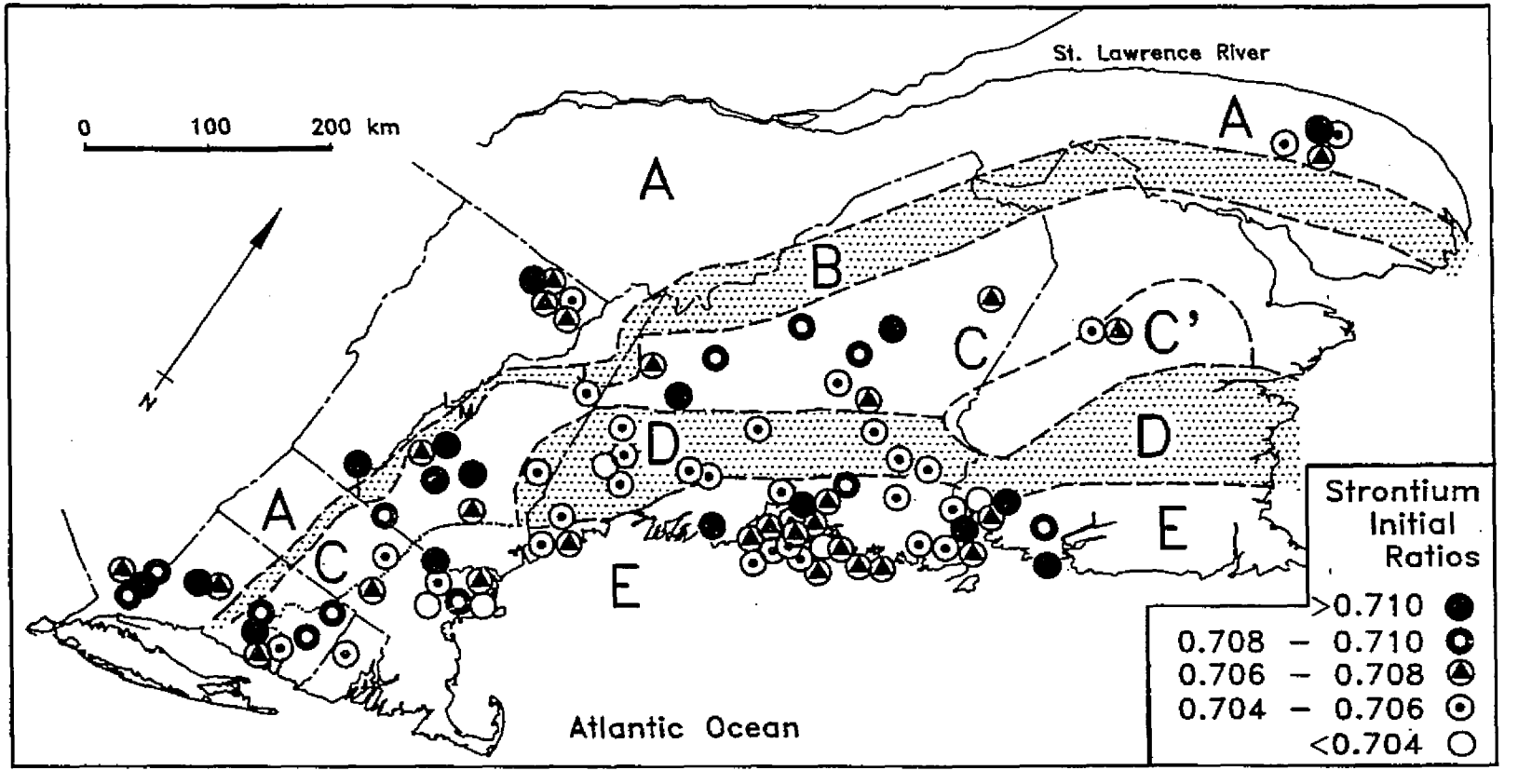

Fig. 75. Strontium initial ratios of Silurian to Carboniferous igneous rocks. Zones B and D are stippled. Letters represent Ordovician plutons in cores of certain Oliverian domes: "L"= Lebanon dome, "M"= Mascoma dome, "J"=Jefferson dome. Sources of data are listed on Table 17.

a higher Sr IR (.706±.002; Naylor, 1969).

Pb data from leached feldspars, which are listed on Table 17, are plotted in Figs. 76 and 77. Lead isotopic compositions of feldspars from igneous rocks approximate lead initial ratios (Pb IR) of the igneous bodies, on account of feldspar's low U/Pb ratio. Data shown on Figs. 76 and 77 are primarily restricted to plutons thought to be Devonian, although Silurian radiometric ages have been obtained on some (Table 17).

Pb evolution diagrams in Figs. 76 and 77 show $^{207}Pb/^{204}Pb$ and $^{206}Pb/^{204}Pb$ values predicted by Zartman and Doe (1981) for upper crust, orogene, and mantle settings. These figures show that Zones A, C, and E, which are characterized by a wide range of Sr IR, similarly show a great variety of lead compositions, including many distinctly crustal values. The central New Brunswick region is separated as subzone C' because its plutons show consistently high Pb isotopic ratios. Both Paleozoic and Precambrian plutons of Zone E in southeastern New Brunswick show highly radiogenic Pb compositions (Bevier, 1987). In contrast, Zone B is characterized by a restricted range of low values, suggesting a relatively young crust. This relatively young crust appears to continue from western Maine into northwestern New Hampshire along the Bronson Hill Anticlinorium, where Aleinikoff and Moench (1987) found "mantle-like" common leads in plutons, while continental Pb compositions are found both to the east and west (Fig. 76) (Aleinikoff and Moench, 1987; Arth and Ayuso, 1985).

Devonian plutons in the region marked Zone D likewise show a restricted range of Pb compositions (Figs. 76 and 77). In concordance with the restricted range of Zone D Sr IR, this points towards a young age for Zone D basement. The Carboniferous Lyman and Sebago granites appear to have significantly more radiogenic Pb compositions than those of the Devonian granites (Michard-Vitrac, Albarede, and Allègre, 1981; Hayward, Olszewski, and Gaudette, 1990). As will be discussed in a later section, inputs to the Carboniferous peraluminous granites from allochthonous, Pb-rich, supracrustal material derived from Zone C, as well as from Pb-poor, juvenile Zone D basement, appear to be responsible for the anomalous Pb compositions.

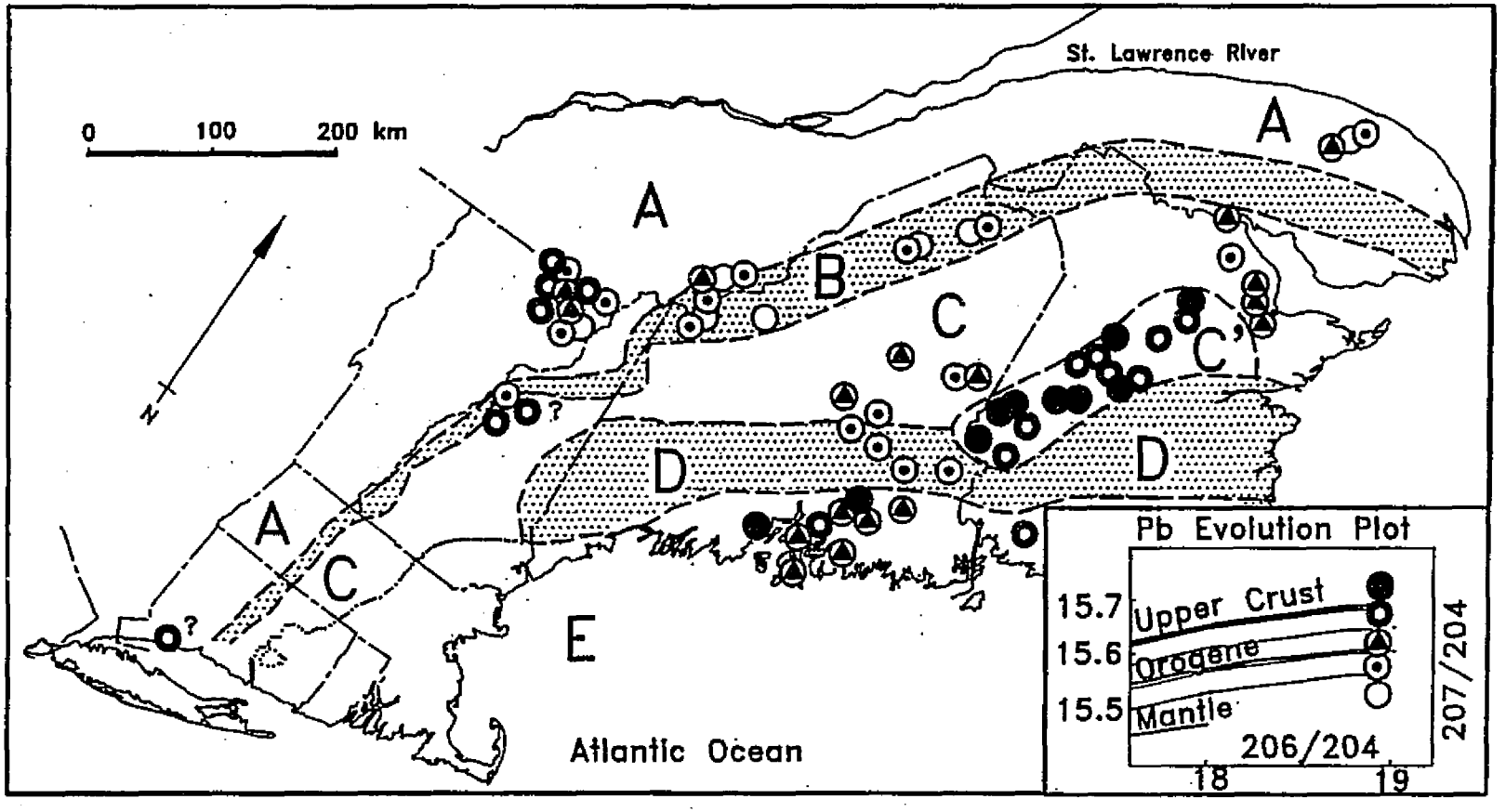

Fig. 76. Pb composition of feldspars from Devonian plutons. Pb evolution curves for upper crust, orogene, and mantle are from Zartman and Doe (1981). Data (listed on Table 17) are from Aleinikoff and Moench (1987); Arth and Ayuso (1985); Ayuso (1986); Ayuso and others (1988); Bevier (1987, 1988a); Eriksson, Hogan, and Williams (1989); Hogan, Jurinski, and Sinha (1988); Krogstad and others (1990); Robert, Gariépy, and Whalen (1988); and Whalen and Gariépy (1986). Symbols in New Hampshire represent the "continental" (but unspecified) values of the Kinsman Quartz Monzonite and Bethlehem Gneiss, and the "mantle" values of plutons from the northern Bronson Hill Anticlinorium (Aleinikoff and Moench, 1987). Where data density is high, some intermediate values are omitted.

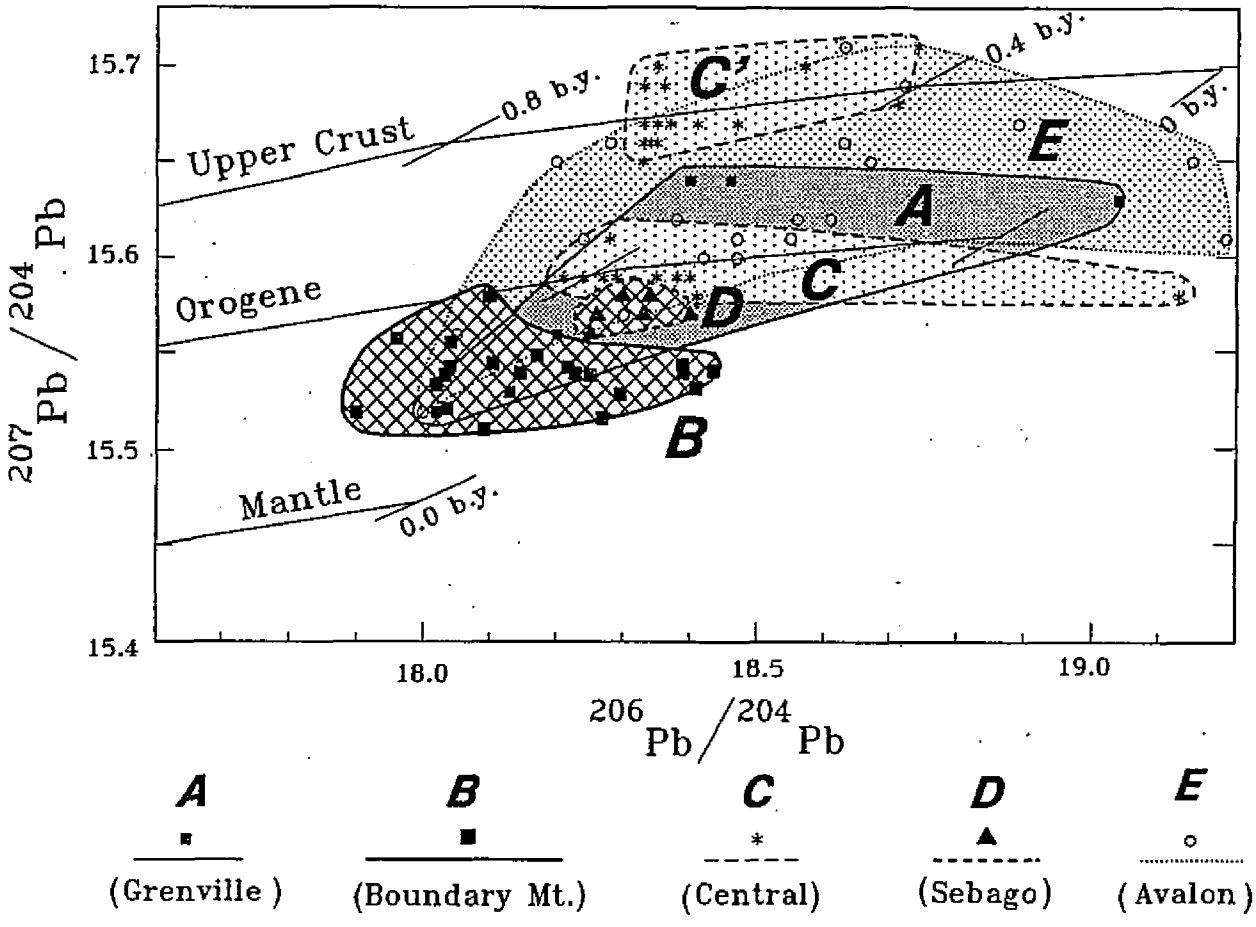

Fig. 77. Evolution plot of Pb compositions of feldspars from Devonian plutons. Sources for plotted data and evolution curves are listed in the caption for Fig. 76.

Oxygen data. Oxygen isotopic ratios of granitic rocks may reflect the relative contributions of sedimentary and mantle-derived source materials. $\delta\,^{18}O$ (‰) values over 10.0, particularly when combined with Sr IR>.706, are indicative of primarily sedimentary or continental crustal sources (e.g., James, 1981). Full ranges of reported values are given in Table 17; Fig. 78 shows the distribution of the maximum $\delta\,^{18}O$ values from whole-rock samples. The pattern seen for Sr and Pb is repeated here: in Zones C and E, maximum oxygen isotopic values are high and suggest substantial input of continental weathered material, while Zones B and D show lower and more mantle-like values. The relatively high maximum $\delta^{18}O$ value found for the Sebago two-mica granite (11.1; Hayward, 1989), along with its anomalously high Pb values, contrasts strikingly with its low SR IR and suggests contamination of melts derived from juvenile sources with crustal or sedimentary material. Zone B has the most mantle-like Pb and O compositions of any of the zones.

Neodymium data. ε neodymium values compare a sample's Nd composition with $^{143}Nd/^{144}Nd$ of chondritic meteorites, with 0 equivalent to a chondritic ratio. During partial melting, Nd is preferentially partitioned into liquid, and Sm into solid; as a result, over time, depleted mantle develops positive ε Nd values while negative ε Nd values evolve in continental crust.

ε neodymium data are presently available for only eight granitoids of Silurian to Carboniferous age in New England (Table 18). Whalen (1989) has analyzed Nd compositions of a number of unidentified granites in the Canadian Appalachians. The Nd data for Zones A, C, and E include several negative ε values (Table 18), and conform with the patterns inferred from Sr, Pb, and O isotopic compositions. An ancient crustal component dominates some plutons in each of these zones, although a variety of Nd values are present. No Nd data are available for Zone B. Nd compositions of two peraluminous plutons in Zone D have been studied: the Sebago and Lyman (Hayward, Gaudette, and Olszewski, 1988). Reported ε values for these two plutons show a wide

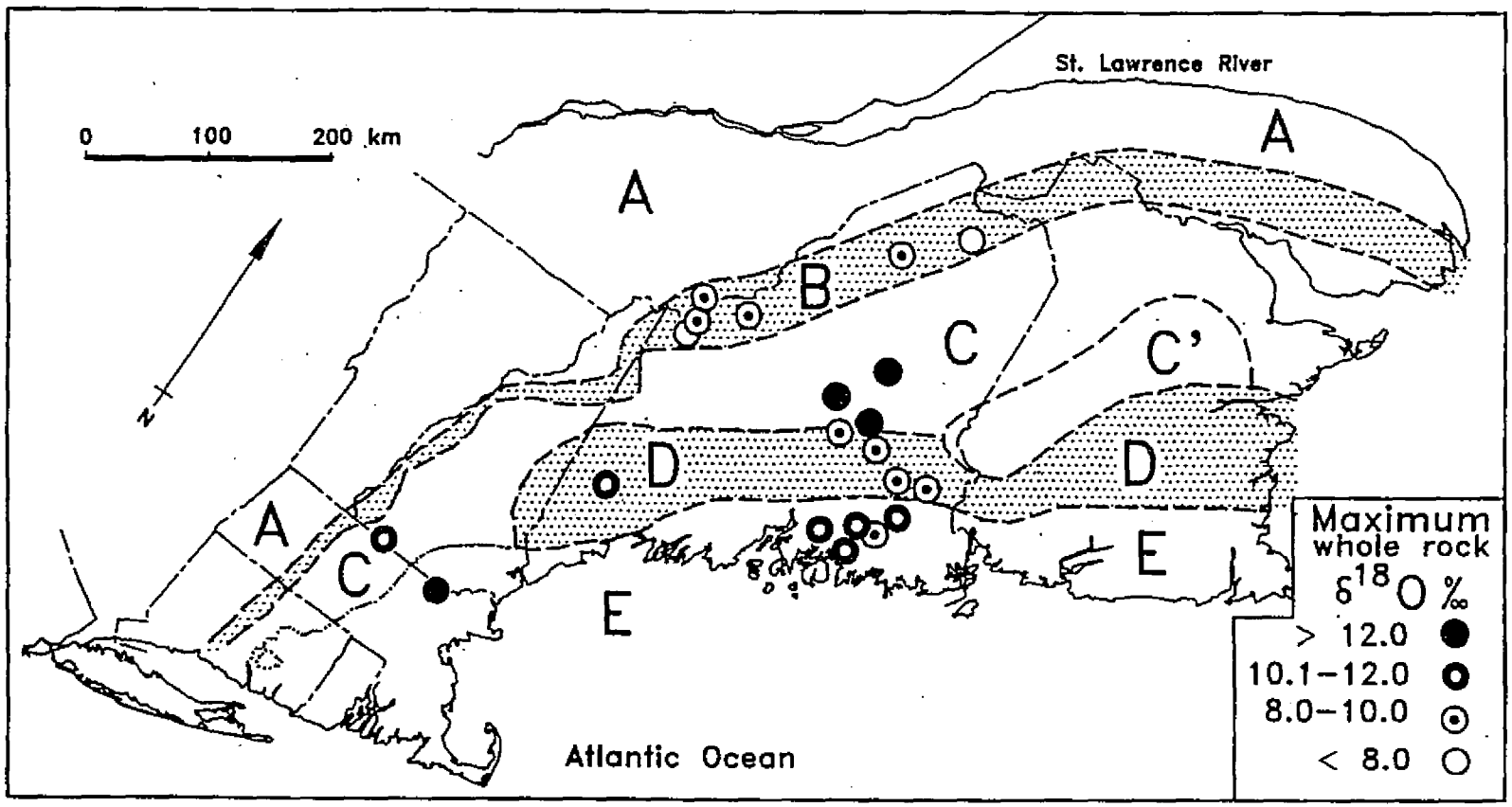

Fig. 78. Maximum whole-rock $\delta^{18}O$ compositions of Silurian to Carboniferous plutons. Data are from Andrew, Loiselle, and Wones (1983); Ayuso, Horan, and Criss (1988); and Hayward (1989).

TABLE 18

Isotopic Characteristics of North-Central Appalachian Igneous Rocks, Summarized by Basement Zone

	Zone A (Grenville)	Zone B (Boundary Mountains)	Zone C (Central)	Zone D (Sebago)	Zone E (Avalon)
$^{87}Sr/^{88}Sr$ Initial Ratios	0.704 - 0.7165	[Ordovician 0.7045 - 0.7051]	0.705 - 0.7161	0.7031 - 0.7056	0.703 - 0.719
$^{206}Pb/^{204}Pb$	18.02 - 19.04	17.96 - 18.44	18.21 - 19.13	18.25 - 18.44	18.00 - 19.21
$^{207}Pb/^{204}Pb$	15.52 - 15.64	15.51 - 15.58	15.57 - 15.71	15.56 - 15.58	15.52 - 15.69
$^{208}Pb/^{204}Pb$ (in feldspar; Devonian plutons)	37.80 - 39.10	37.80 - 38.37	38.01 - 38.63	38.06 - 38.29	38.05 - 38.58
Oxygen $\delta^{18}O$ (whole rock)		6.8-8.2	7.2 - 13.3	7.4 - 11.1	5.8 - 12.6
Neodymium ε	Vermont -8 to 0 (Black Mt.) -6 (Long Mt.) Quebec 0 to +8 (18 positive values)	No data available	New Hampshire -15 to +4(Fitzwilliam -4 (Kinsman) New Brunswick -4 to +5 (18 negative values & 5 positive values)	Maine -5 to +5 (Lyman) -10 to +10 (Sebago)	Maine -1 to +2.5 (Baring) New Brunswick -1 to +3 (5 negative values & 8 positive values

Isotopic values are for Silurian to Carboniferous igneous rocks unless otherwise specified.
Sources of Sr, Pb, and O data are given on Table 1; Nd data are from Barreiro and Aleinikoff (1985); Harrison, Aleinikoff, and Compston (1987); Hayward, Gaudette, and Olszewski (1988); Whalen (1989); and Brueckner and Ludman, pers. commun. (1990).
In Quebec and New Brunswick, the number of plutons giving negative and positive εNd values are noted.

spread (Sebago, +10 to -10; Lyman, +5 to -5) but appear to average zero. These ranges of isotopic values are difficult to interpret but may (like the Sr, Pb, and O compositions of these two-mica granites) be due to contributions from two very different sources, such as sediments derived from an ancient crust and a juvenile basement.

For some plutons, $^{143}Nd/^{144}Nd$ values alone are available. The Northeast Kingdom Batholith of Zone A shows continental values (.51187-.5120) (Arth and Ayuso, 1985). In Zone E, $^{143}Nd/^{144}Nd$ of the Sharpners Pond and Straw Hollow diorites suggest contamination of mantle melts with old crustal material (Hill and others, 1984).

COMPARISON OF ISOTOPIC AND SILICA COMPOSITIONS

Fig. 79 is a plot of bulk silica composition against Sr IR, initial $^{207}Pb/^{204}Pb$, and $\delta^{18}O$ values for the igneous rocks compiled here. The figure shows that the restricted ranges of Pb, Sr, and O isotopic compositions found in Zones B and D (heavy lines) occur in spite of a wide range of SiO_2 values, values generally comparable to those found in Zones A, C, and E. The restricted $^{87}Sr/^{86}Sr$ and $^{207}Pb/^{204}Pb$ values characteristic of Zone B and Zone D are independent of bulk silica composition, whereas there is a general correlation between increasing silica content and higher Sr IR for Zones A, C, and E. It appears that the crust underlying Zones B and D is isotopically more "primitive" and fundamentally distinct from the ancient continental crust under Zones A, C, and E.

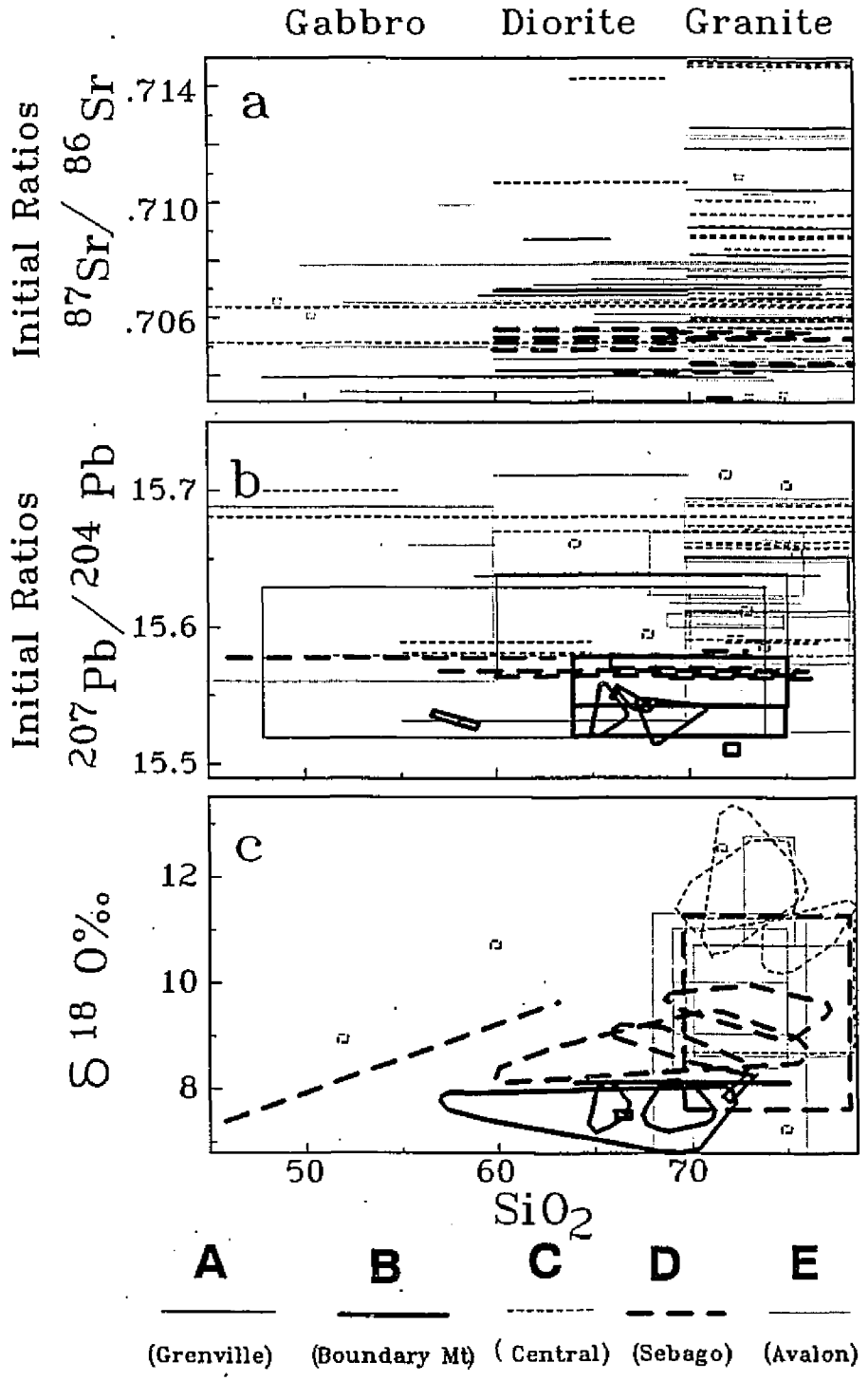

Fig. 79. Isotopic vs. bulk silica compositions of Silurian to Carboniferous igneous rocks, plotted by zone. a) whole-rock initial $^{87}Sr/^{86}Sr$ ratios vs. SiO_2; b) $^{207}Pb/^{204}Pb$ from feldspars vs. SiO_2 (Devonian plutons only); c) $\delta^{18}O$ compositions vs. SiO_2. Isotopic data and sources of compositional data are listed on Table 17. Igneous rock compositions are plotted by lithology where chemical analyses are not available.

INHERITANCE-AGE DATA

Xenocrystic zircons in plutons, detrital zircons, and Nd and Pb model ages provide indications of basement age for each of the crustal zones. Some populations of zircon show several age components; the oldest inheritance ages yet obtained from the Ordovician to Late Paleozoic igneous bodies are given in Fig. 80. Source-ages are subdivided into four groupings: 750 Ma or younger, .9 to 1.4 Ga, 1.4 to 1.8 Ga and greater than 1.8 Ga. Because the absence of an xenocrystic component provides useful negative evidence, zircons that have concordant Paleozoic ages (or with slight discordance apparently due to late Pb loss) are included with "750 Ma or younger" xenocrystic zircon. Outcrops of rock units with Middle Proterozoic radiometric ages are shown on Fig. 80 for comparison.

The distribution of these age indicators supports the interpretations that have made on isotopic grounds. In Zones B and D, where young crust had been inferred, no old (pre-750 Ma) xenocrystic zircon has been found. In Zone D, available data point towards relatively young basement: on the basis of Sr and Nd isotopic compositions, Hayward, Gaudette, and Olszewski (1988) propose that the sources of the (Carboniferous) Sebago and Lyman granites were derived from a depleted mantle-like source at 705 Ma.

Middle Proterozoic and Archean zircons do occur within diamictite of the Precambrian Chain Lakes Massif in Zone B and in correlative metagreywackes overlying Zone A in Quebec (Dunning and Cousineau, 1990; Olszweski, Gaudette, and Cheatham, 1990). However, general westward transport related to the Taconian orogeny has been inferred on both seismic (Unger, 1988; Spencer and others, 1989) and stratigraphic grounds (Boone and Boudette, 1989). The Chain Lakes Massif and related rocks, which are associated with Taconian-age mélanges (Boone and Boudette, 1989), are most readily interpreted as sialic material derived from ancient Zone C, and probably do not represent the basement of Zone B (in which they are located today).

In contrast, in Zones A, C, and E, where isotopic data are consistent with ancient crust,

Middle Proterozoic or older inheritance ages are common. Zone A is apparently the youngest of these continental fragments; inheritance ages there are generally between 0.9 and 1.4 Ga (Fig. 80). Older ages, locally present in eastern Zone A in New England (Fig. 80), are attributable to sediments derived from Zone C (see below). The 0.9 to 1.4 Ga range of ages seen in Zone A is also characteristic of the Grenvillian basement exposed in New York and New England. These ages are found in the Adirondack region (Chiarenzelli and McLelland, 1990; Daly and McLelland, 1991; Easton, 1986, and references therein); in the Green Mountains of Vermont (Aleinikoff and others, 1990); in the Hudson Highlands (Aleinikoff and Grauch, 1990; Helenek and Mose, 1984); in the Chester Dome (Karabinos and Aleinikoff, 1988) and in the Fordham Gneiss (Mose, 1982; Aleinikoff, 1985). Depleted-mantle Nd model ages on these rocks rarely exceed ~1.45 Ga (Daly and McLelland, 1991) and suggest that most of this portion of the Grenville province is juvenile. The only significantly older ages presently known are from detrital zircon found in the Hudson Highlands (Aleinikoff and others, 1982), in the northwestern Adirondacks (McLelland and others, 1988) and possibly in the Fordham Gneiss (Grauert and Hall, 1974). Looking to the northwest, the Grenvillian Central Granulite Terrane and Baie Comeau Segment of Quebec, west of the St. Lawrence River (Fig. 80), appear to be older than the Grenville of New England; Rb-Sr whole-rock studies give ages up to ~1.5 Ga (Frith and Doig, 1973; Barton and Doig, 1973, 1974), and depleted-mantle Nd model ages as old as 1.9 Ga are known (Hervet and others, 1990). However, the basement underlying the Paleozoic strata of Quebec southeast of the St. Lawrence River in Zone A may be similar in age to the Grenville of New York and western New England. Galenas hosted by Paleozoic sediments in this part of Quebec contain lead whose ultimate source was likely to have been Grenvillian feldspars (Schrijver and others, 1988). When the isotopic compositions of these leads are compared with Pb compositions of ~1.0 Ga feldspars of the Grenville province (Schrijver and others, 1988; Zartman and Wasserburg, 1969), they are most similar to leads from the Adirondacks, and they are distinctly more radiogenic than Pb from the Baie Comeau Segment. Either way, Zone A can be equated with Grenville basement.

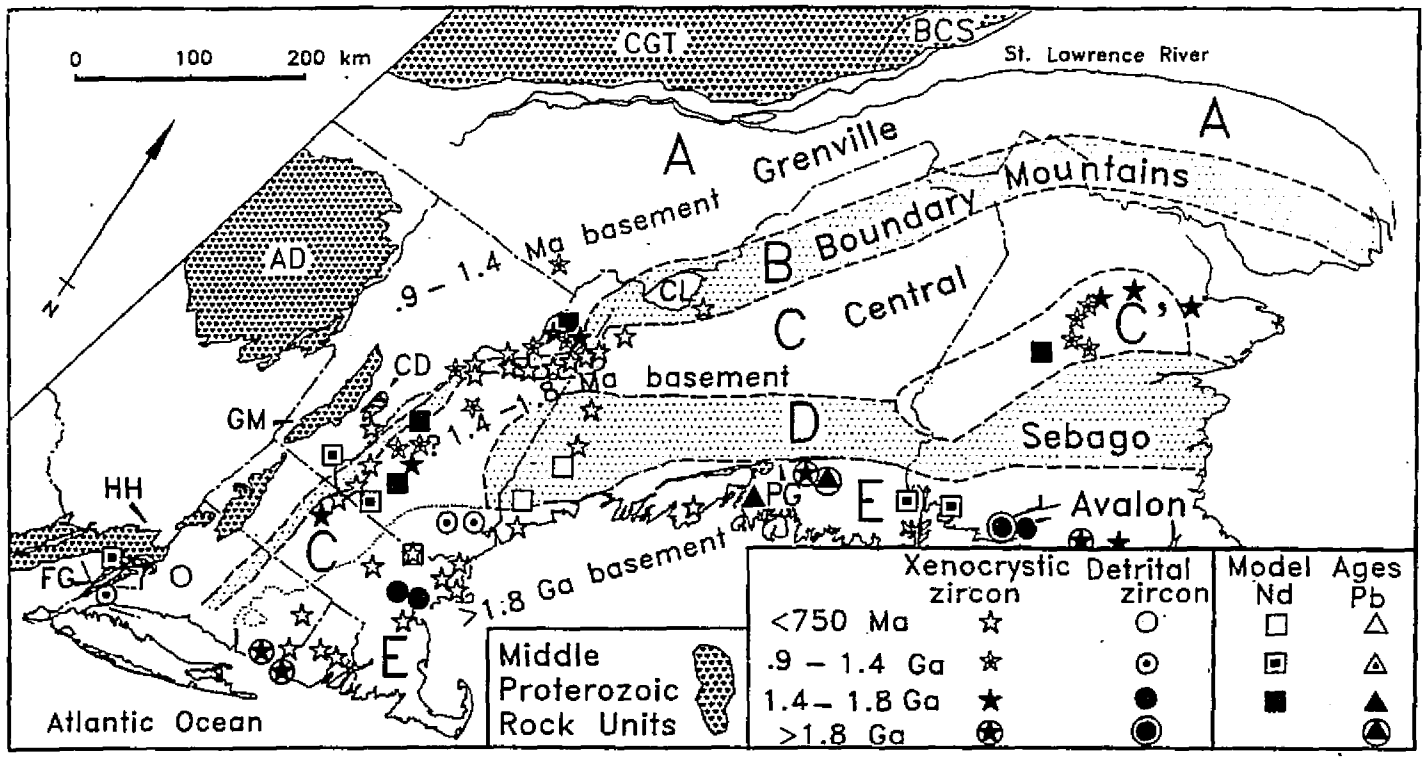

Fig. 80. Inheritance age data and Middle Proterozoic rock units of the Northern Appalachians. Precambrian massifs discussed in the text: AD= Adirondacks; BCS= Baie Comeau Segment; CD= Chester Dome; CGT= Central Granulite Terrane; CL = Chain Lakes; FG= Fordham Gneiss; GM= Green Mountains; HH= Hudson Highlands; PG= Passagassawakeag Gneiss. Paleozoic plutons whose zircon systematics show no Precambrian inheritance are included in the category "<750 Ma" zircon inheritance age. Nd ages shown are from depleted-mantle models, except for plutons in Vermont (Black Mountain) and Massachusetts (Chelmsford); all Nd data are from Paleozoic plutons. Nd symbols in New Brunswick represent populations of data (see Table 18). Data are from Table 17 plus Aleinikoff (1978); Bevier (1988a); Bevier and Barr (1990); Bevier, White, and Barr (1990); Dietsch and others (1989); Eriksson, Hogan, and Williams (1989); Fyffe, Barr, and Bevier (1988); Grauert and Hall (1974); Harrison, Aleinikoff, and Compston (1987); Hingston and Barreiro (1990); Hogan and Sinha (1989a); Hueber and others (1990); Lyons, Aleinikoff, and Zartman (1986); Olszewski (1980); Roddick and Bevier (1988); Shirey, Bender, and Horan (1988); Tucker and Robinson (1990); Whalen (1989); Zartman and Hermes, (1987); and Zartman and Leo (1985); Zeitler and others (1990). Unpublished zircon data of van Staal (Tetagouche volcanics; pers. commun., 1990) and Gariépy (Eastern Townships of Quebec; pers. commun., 1988) are also included. Data on some detrital zircon from allochthonous strata are omitted for clarity. Where multiple inheritance ages are reported, the oldest alone is shown.

Zone C contains older crust than does Zone A. Although no Middle Proterozoic basement is exposed in Zone C, 1.4 to 1.8 Ga zircon inheritance ages are reported in igneous rocks there (Fig. 80). Not only zircons, but the bulk of the crust may be of this age; the Kinsman Quartz Monzonite of New Hampshire, for example, has a 1.68 Ga depleted-mantle Nd model age (Barreiro and Aleinikoff, 1985). Input from Zone C basement to the Ordovician Ammonoosuc Volcanics of western New Hampshire (found on both Zone B and adjacent Zone C) is suggested by the Ammonoosuc's depleted-mantle Nd model ages of up to 1.7 Ga (Hingston and Barreiro, 1990). Metasediments of probable Zone C provenance (such as the Littleton Formation of New Hampshire) contain detrital zircon of 1.4-1.8 Ga ages (Harrison, Aleinikoff, and Compston, 1987). Because of westward transport during the Taconian and Acadian orogenies, some metasediments of Zone C origin have been emplaced onto Zones A and B. The Moretown Formation of Vermont, for instance, which contains zircons as old as 1.66 Ga (Karabinos, Kober, and Gromet, 1989) was thrust over Grenville basement during the Taconian orogeny (Stanley and Ratcliffe, 1985). Similarly, although the peraluminous Long Mountain granite of New Hampshire lies within Zone A (Fig. 74), it is probably the product of the anatexis of Zone C sediments (such as the Littleton Formation) and contains zircon with inherited component up to 1.8 Ga in age (Harrison, Aleinikoff, and Compston, 1987).

Inheritance ages from the Chain Lakes Massif and related rocks are consistent with an origin in Zone C. A number of zircon U-Pb ages there fall in the 1.4-1.8 Ga range (Naylor and others, 1973; Dunning and Cousineau, 1990; Olszewski, Gaudette, and Cheatham, 1990) as do both Sm-Nd and Rb-Sr model ages (Cheatham, Olszewski, and Gaudette, 1985). The recent detection of an Archean-aged zircon component in these same rocks (Olszewski, Gaudette, and Cheatham, 1990; Dunning and Cousineau, 1990) presents the possibility that further work will reveal Archean inheritance within Zone C.

A mosaic of different inheritance ages is present within Zone E (Fig. 80). Zircons show inheritance ranging in age from Late Proterozoic to Archean. Peraluminous granites from Maine

have Pb isotopic compositions that form a linear array and suggest ~1.5 Ga source materials (Hogan and Sinha, 1989a). A Late Archean inherited zircon component of about 2.7-2.8 Ga has been found in Permian granites in southern New England (Zartman and Hermes, 1987), in a Devonian granite in Maine (Williams, Eriksson, and Compston, 1986), and in igneous bodies of Late Precambrian age in New Brunswick (Bevier and Barr, 1990; Bevier, White, and Barr, 1990). Pb isotopic compositions from the 410 Ma Parks Pond pluton of Maine define a linear array suggestive of a 2.3 Ga source region (Eriksson, Hogan, and Williams, 1989). As in Zone C, there is no known outcrop of the source material of these ancient inheritance ages. The oldest rocks known in Zone E occur in Maine; there, Gaudette, Olszewski, and Cheatham (1983) obtained a 1360±68 Ma Rb-Sr whole-rock isochron for part of the Passagassawakeag Gneiss.

DISCUSSION OF ISOTOPIC AND INHERITANCE AGE CHARACTERISTICS

Three blocks of ancient continental crust (A, C, and E) and two younger terranes (B and D) have been defined. They are:

Zone A. Plutons in Zone A, the Grenville block, have a wide variety of Sr and Pb IR, including many continental values. Inheritance ages suggest a basement of .9 to 1.4 Ga age. Although the peak values of $^{207}Pb/^{204}Pb$ and $^{206}Pb/^{204}Pb$ are not as high as those found in the continental Zones C and E (Fig. 77), the greatest reported values of $^{208}Pb/^{204}Pb$ are found in Zone A (Table 18). Other leads of Grenville provenance such as the galenas of Gaspé (Schrijver and others, 1988), Appalachian Mississippi Valley-type deposits (Swinden, Lane, and Thorpe, 1988; Kesler and van der Pluijm, 1990) and feldspars of the Mount Rogers Formation of Virginia (LeHuray, 1984) show similar "excess" ^{208}Pb. Compared to Zones C and E, U was slightly depleted relative to ^{232}Th (parent of ^{208}Pb) in Zone A.

Zone B. Zone B plutons show the most mantle-like Pb and O isotopic values of any of the zones, despite fairly diverse bulk compositions. Ayuso (1986) and Ayuso, Horan, and Criss (1988) noted the distinctive character of Zone B plutons relative to the rest of Maine. $\delta\ ^{18}O$ values in Zone B plutons are all higher than those of the mantle (=6.0; Taylor, 1980) and reflect the contribution of a sedimentary (or crustal) component (Ayuso, Horan, and Criss, 1988). Pb compositions of Zone B Devonian plutons are similar to those of a 400 Ma "primitive orogene" (Zartman and Doe, 1981). No ancient xenocrystic zircons have been yet found in this zone. Zone B can, therefore, be interpreted as an arc terrane of Late Precambrian to Early Paleozoic age. Zone B is named the Boundary Mountains block after the Boundary Mountains Anticlinorium (Fig. 81). The Boundary Mountains block is defined primarily on the basis of data from Maine and northern New Hampshire, and is tentatively extrapolated northwards into Canada and southwards through

New England.

Zone C. Sr and Pb IR, $\delta\,^{18}O$ compositions, and ε Nd values here include many of distinctly crustal character. Inheritance age data indicate a basement at least partially 1.4 to 1.8 Ga old. Inheritance age, seismic, and geological evidence suggests that the Chain Lakes Massif of Maine was derived from Zone C. A Chain Lakes-like component did not, however, dominate the source of Zone C granites; the Pb compositions of Chain Lakes diamictite (Ayuso, Horan, and Criss, 1988) reflect severe depletion of U relative to Th and are not representative of Zone C, or of any other zone. Zone C, which occupies a middle position between continental Zones A and E, will be called the Central block.

Zone D. Zone D is named the Sebago block after its areally largest pluton. Although a variety of bulk compositions is represented here, including several peraluminous plutons, isotopic values (especially Sr IR) in Zone D tend to show a restricted range of relatively low values. According to Zartman and Doe's plumbotectonics model II, Pb compositions of Sebago block Devonian plutons approximate a 400 Ma orogene (Fig. 77). Available inheritance age data in the Sebago block are consistent with a basement younger than 750 Ma. The Bottle Lake and Center Pond plutons of Zone D contain sphene+magnetite assemblages, which suggests oxidized source materials; according to Andrew, Loiselle, and Wones (1983), a protolith of altered volcanic and volcaniclastic rocks would provide such a source and would explain the O and Sr compositions of the plutons. The Pb compositions of country rocks overlying the Sebago block are extremely radiogenic (Ayuso and others, 1982); they appear to have been derived from an ancient continental source, most likely the Central block (see discussion below). The Sebago block is isotopically well-defined in Maine and is inferred to continue eastwards through New Brunswick, although no igneous bodies are exposed. The distribution of the isotopic data suggest that the southwestern termination of the Sebago block lies within New Hampshire. Geological features of Siluro-

Devonian age appear to reflect the geometry of the Sebago block (see Part III). The Sebago block (like Zone B) probably originated as a Late Proterozoic to Early Paleozoic arc terrane.

Zone E. Zone E contains rocks commonly assigned to the Avalon tectono-stratigraphic zone, such as the Caledonia Highlands of New Brunswick and the Esmond-Dedham zone of southern New England (Fig. 81). These "Avalonian" regions cannot be distinguished from other portions of Zone E on the basis of existing isotopic data, so that all of Zone E is designated "Avalon" for the present purpose. (This usage is not intended to imply a uniform geologic history for all of "Avalon"; the Siluro-Devonian history of "Avalon" is discussed in Part III). A number of workers in eastern Maine have previously noted the major element and isotopic signature of well-evolved, ancient crust in Zone E (Avalon), and its geochemical contrast with the Sebago zone on the northwest side of the Norumbega fault (Wones and others, 1981; Loiselle and Ayuso, 1980; Andrew, Loiselle, and Wones, 1983; Ayuso, 1986). In Zone E, or Avalon, Sr and Pb IR and $\delta^{18}O$ compositions vary but all show many crustal values. Inheritance data point towards an ancient crust, which contains an Archean component.

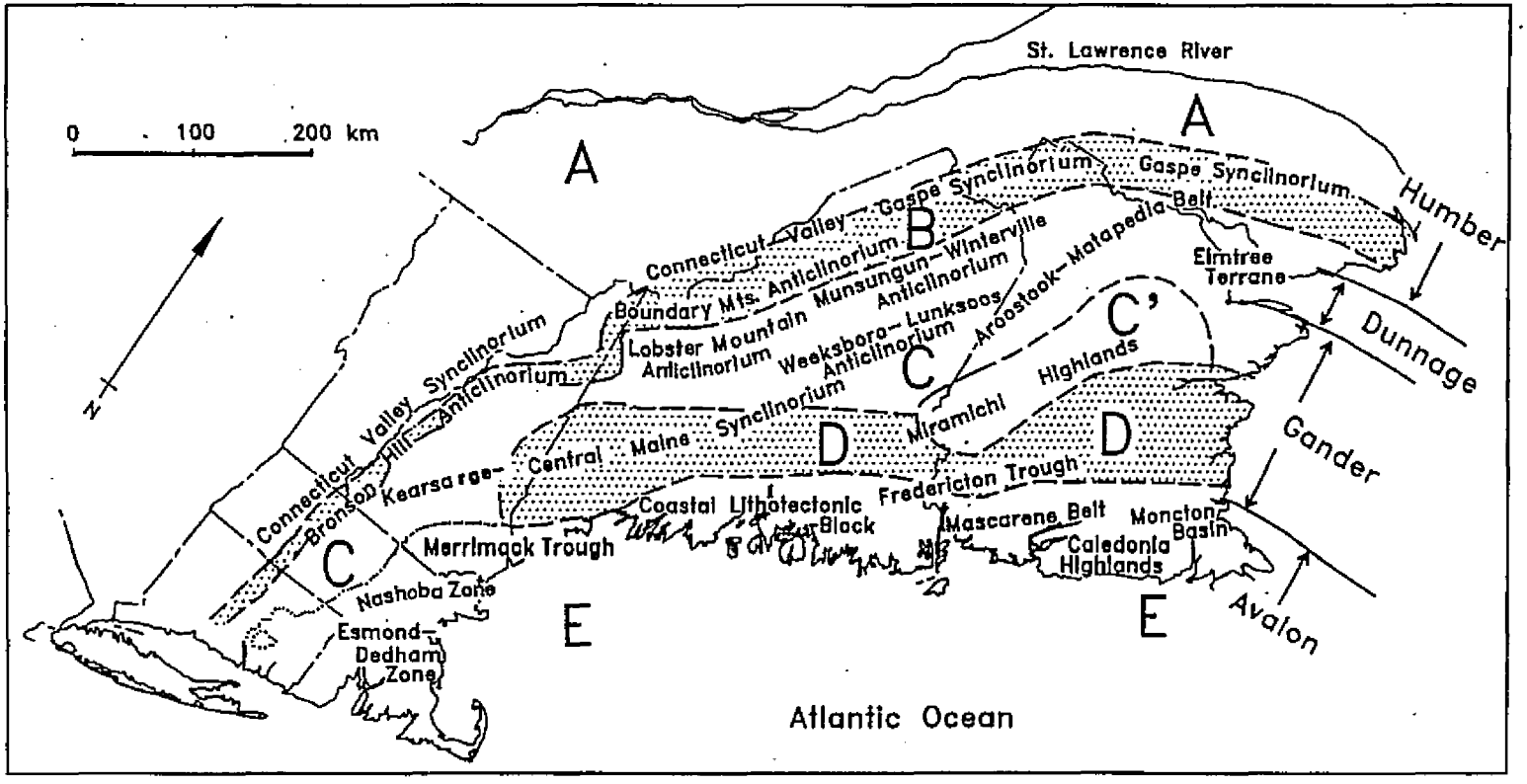

Fig. 81. Major stratigraphic subdivisions of the north-central Appalachians superimposed on the isotopically-defined basements. Williams' (1978) tectonostratigraphic zones are shown for comparison.

RELATIONSHIPS BETWEEN THE ISOTOPIC ZONES AND OTHER ASPECTS OF NORTHERN APPPALACHIAN GEOLOGY

COMPARISON OF ISOTOPIC AND TECTONOSTRATIGRAPHIC ZONES

Fig. 81 shows the relationship between the isotopically-defined blocks and supracrustal features, such as William's (1978) tectonostratigraphic zones and the major stratigraphic subdivisions of New England and New Brunswick. In general, only a limited correspondence exists between stratigraphic and isotopic terranes. The distribution of the rocks of the Kearsarge-Central Maine (KCM) Synclinorium can be used as an example. Early Silurian strata of the KCM Synclinorium appear to be distal correlatives of the shallow-water facies found in the Bronson Hill Anticlinorium (Zones B and C) (Moench and others, 1988; Hatch, Moench, and Lyons, 1983). The KCM Synclinorium, in addition to covering much of Zone C (Central), stretches over all of western Zone D (Sebago), so that Zone D has no obvious stratigraphic expression. Absence of correspondence between isotopic and stratigraphic terranes is also illustrated by the Miramichi Highlands, which overlie Central block (C) in New Brunswick, but are found inside Sebago (D) in Maine.

Allochthony of the supracrustal section may be responsible for the relationships seen in these examples. Mapping in Maine (Ludman, Hopeck, and Brock, in review; Ludman and Hopeck, 1988 and in review) indicates that several terranes, including the KCM Synclinorium and the Miramichi Highlands, have been tectonically transported eastwards. The presence of east-vergent thrusts in the shallow crust has been confirmed by seismic data (Ludman and others, 1990), so that the Miramichi Highlands in Maine appear to be allochthonous over Zone D. Similarly, structural east vergence reported in eastern New Hampshire (Eusden, Bothner, and Hussey, 1987; Eusden, 1989) suggests that the KCM Synclinorium is allochthonous over western Zone D. In some other

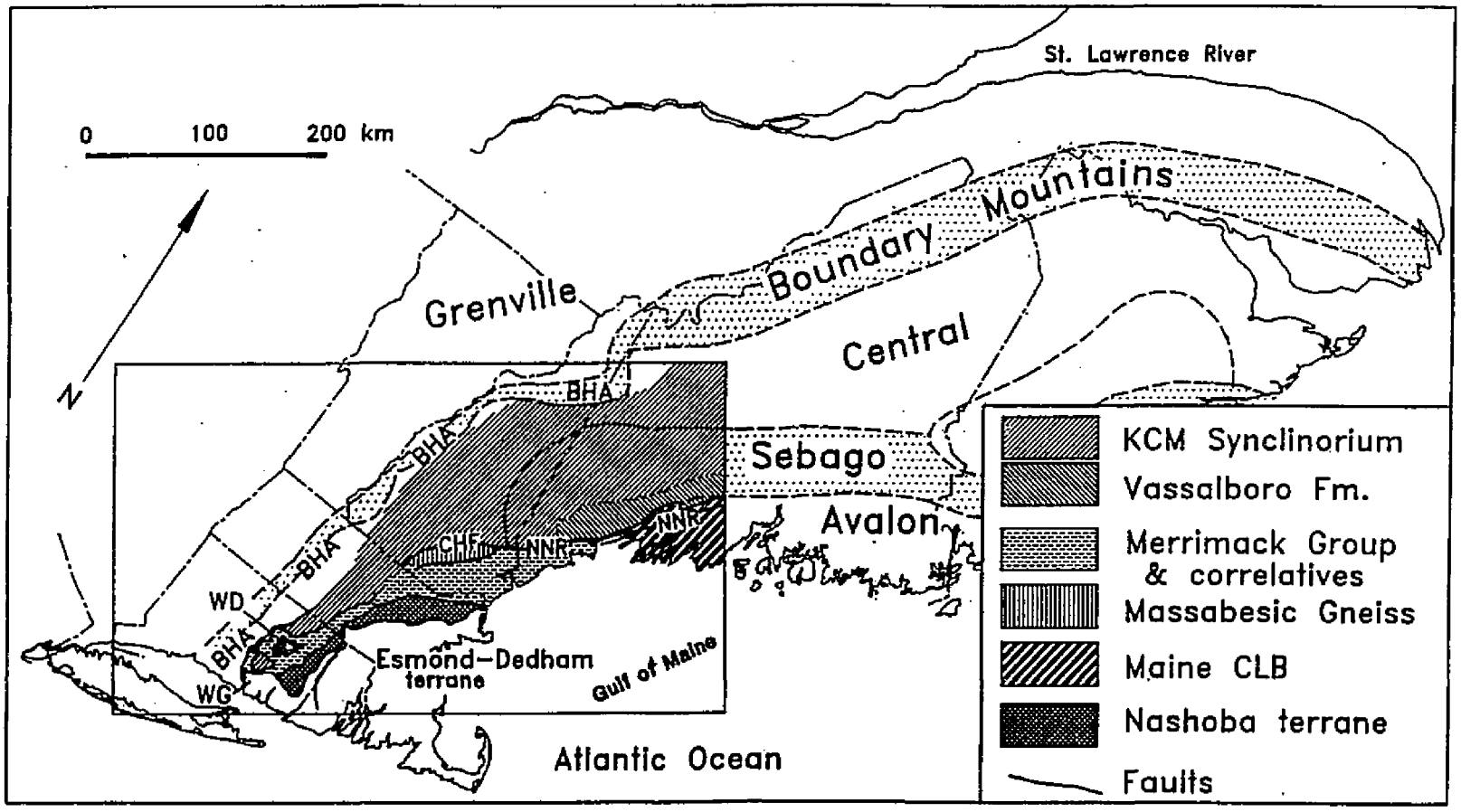

Fig. 82. Stratigraphic criteria used to determine the Central-Avalon (C-E) supracrustal block boundary. BHA= Bronson Hill Anticlinorium; CHF= Campbell Hill fault; CLB= Coastal Lithotectonic Block; KCM= Kearsage-Central Maine; NNF= Norumbega-Nonesuch River fault; WD= Willimantic dome; WG= Waterford Group. The KCM Synclinorium here includes the Brimfield Group of Connecticut. See text for discussion.

instances where stratigraphic and isotopic zones do not coincide, strata may have been deposited after accretion of underlying basements. This may be the case for the Connecticut Valley-Gaspé "Synclinorium", which received sediments in Silurian time (Hueber and others, 1990), and may have followed a zone of weakness along the Taconian Zone A (Grenville) - B (Boundary Mountains) suture (Fig. 84, Part III).

One isotopic boundary does closely correspond to an important stratigraphic break. Zone E, the Avalon block, contains the Coastal Lithotectonic Block (CLB) of Maine and the Merrimack Trough; whereas Zone D (Sebago) is overlain by the KCM Synclinorium (Figs. 81 and 82). The D-E isotopic boundary therefore separates strata that extend into or have correlatives as far west as Zones C (Central) and B (Boundary Mountains) from terranes whose correlatives are confined to easternmost North America.

Various linkages exist among the terranes of Zone E (Avalon). Some units of the Maine CLB may correlate with the Massabesic Gneiss of New Hampshire, or with the Nashoba Formation of the Nashoba terrane (Fig. 82) (Hussey, Bothner, and Thomson, 1986), and there are Silurian faunal links between coastal Massachusetts, New Brunswick, and Maine (Martinsson, 1970; Copeland and Berdan, 1977). Although the Merrimack Group was once equated with the Late Ordovician or Early Silurian Vassalboro Formation (Fig. 82), radiometric ages on post-tectonic plutons show that it is older (Zartman and Naylor, 1984; Gaudette and others, 1984; Hon and others, 1986). Links between the Merrimack Group and other terranes of Zone E (Avalon) include a possible gradational contact between the Merrimack Group (Berwick Formation) and the Massabesic Gneiss (Bothner and others, 1984) and the northwestern paleocurrent flow direction found in turbidites of the Merrimack Group's Kittery Formation (Rickerich, 1983; Hussey, Rickerich, and Bothner, 1984). Hutchinson and others (1988) inferred continuity of Avalonian terranes beneath the Gulf of Maine from magnetic and seismic reflection data.

To the south of the termination of the Sebago (D) block, the isotopically similar basements of the Central (C) and Avalon (E) blocks are in contact. These blocks are not readily dis-

tinguishable on isotopic grounds. However, the correspondence between the isotopic and stratigraphic boundaries of the Avalon block (E) in Maine discussed above provides a basis which can be used to extrapolate the western limit of the Avalon block southwards. Fig. 82 shows that on one side of this boundary are the KCM Synclinorium, its correlatives, and the Brimfield Group of Connecticut; on the other, the Massabesic Gneiss, the Merrimack Group, and its correlatives, such as the Paxton Group, Oakdale Formation, and Hebron Gneiss (Lyons, Boudette, and Aleinikoff, 1982; Zen and others, 1983; Hatch and others, 1984; Rodgers, 1985; Pease, 1989; Barosh and Moore, 1988). This Central (C)- Avalon (E) boundary, which is shown dotted on all the maps, must be a supracrustal boundary. It is unlikely to coincide with the Central-Avalon basement boundary for all or even most of its length. This supracrustal boundary is marked at the surface by recognized faults and ductile shear zones in New Hampshire (Campbell Hill Fault), Connecticut (Pease, 1989; London, 1988), and most of Massachusetts (Pease, 1989) as well as in Maine. In southern New England, gneisses to the east of this boundary (such as those of the Willimantic dome and the Waterford Group) have Avalonian affinities and ages and are distinct from gneisses of the nearby Bronson Hill Anticlinorium (Wintsch and Aleinikoff, 1987; Wintsch and Fout, 1982; Zartman, Hermes, and Pease, 1988).

SILURO-DEVONIAN THERMAL HISTORY AND THE ISOTOPIC ZONATION

The isotopic and petrologic characteristics of Silurian to Carboniferous igneous rocks in the continental Grenville (A), Central (C), and Avalon (E) blocks bear witness to diverse origins, and it can be safely assumed that a variety of source materials contributed to melts in each block. The question then arises: could the restricted isotopic compositions of the Boundary Mountains (B) and Sebago (D) blocks possibly be due to limitation of melting to discrete zones within these regions, and simply reflect lesser involvement of upper crustal materials?

To answer this question, we may consider whether the distribution of Acadian metamorphic grades is consistent with cooler crustal temperatures within the Boundary Mountains and Sebago zones than elsewhere. The Acadian orogeny dominated the Silurian to Carboniferous thermal history of the Northern Appalachians; the grade of Acadian regional metamorphism and amount of related crustal thickening should be good predictors of the extent of crustal melting. Yet, when the distribution of Acadian metamorphic grades (Part III, Fig. 94) and the isotopic zonation of the northern Appalachians are compared, no correspondence is evident. A thermal peak occurs in the Kearsarge-Central Maine Synclinorium, over both the Central (C) and Sebago (D) blocks, and metamorphic grade falls off to the northwest and southeast- into the Grenville (A) and the Avalon (E) blocks. Plutons of the Grenville block (A) display a "crustal" isotopic character in spite of this westward decrease in metamorphic grade. Clearly, the restricted isotopic ranges of plutons in the Sebago (D) and Boundary Mountains (B) blocks cannot be due to a cooler upper crust than that found in the neighboring Grenville (A) or Avalon (E) blocks.

Some correspondence does exist, however, between individual isotopic values and metamorphic grade within basement blocks. The most radiogenic Pb values in the Central block (C) are found in or near regions at amphibolite facies, in New Hampshire and in the western Miramichi Highland of New Brunswick (Zone C'). Pb compositions in the Sebago block show correspondence with metamorphic grade even more dramatically. As discussed earlier, the supracrustal section over the Sebago zone, composed largely of clastic sediments, is thought to have been allochthonously derived from the Central block (D). These cover rocks have very radiogenic Pb initial ratios (Ayuso and others, 1982). Clastic sediments are Pb-rich, while basalts and related arc rocks (which are inferred to exist in the buried Sebago basement) are Pb-poor; but a volcanic-arc basement would have the more abundant Sr. Therefore, where high temperatures led to partial melting of the allochthonous cover, resulting melts could add a radiogenic, Pb-rich component to a Sr-rich magma generated from juvenile Sebago crust at a deeper level. In Maine's Sebago zone, the two-mica granites (some of Carboniferous age) that occur at amphibolite-facies grade

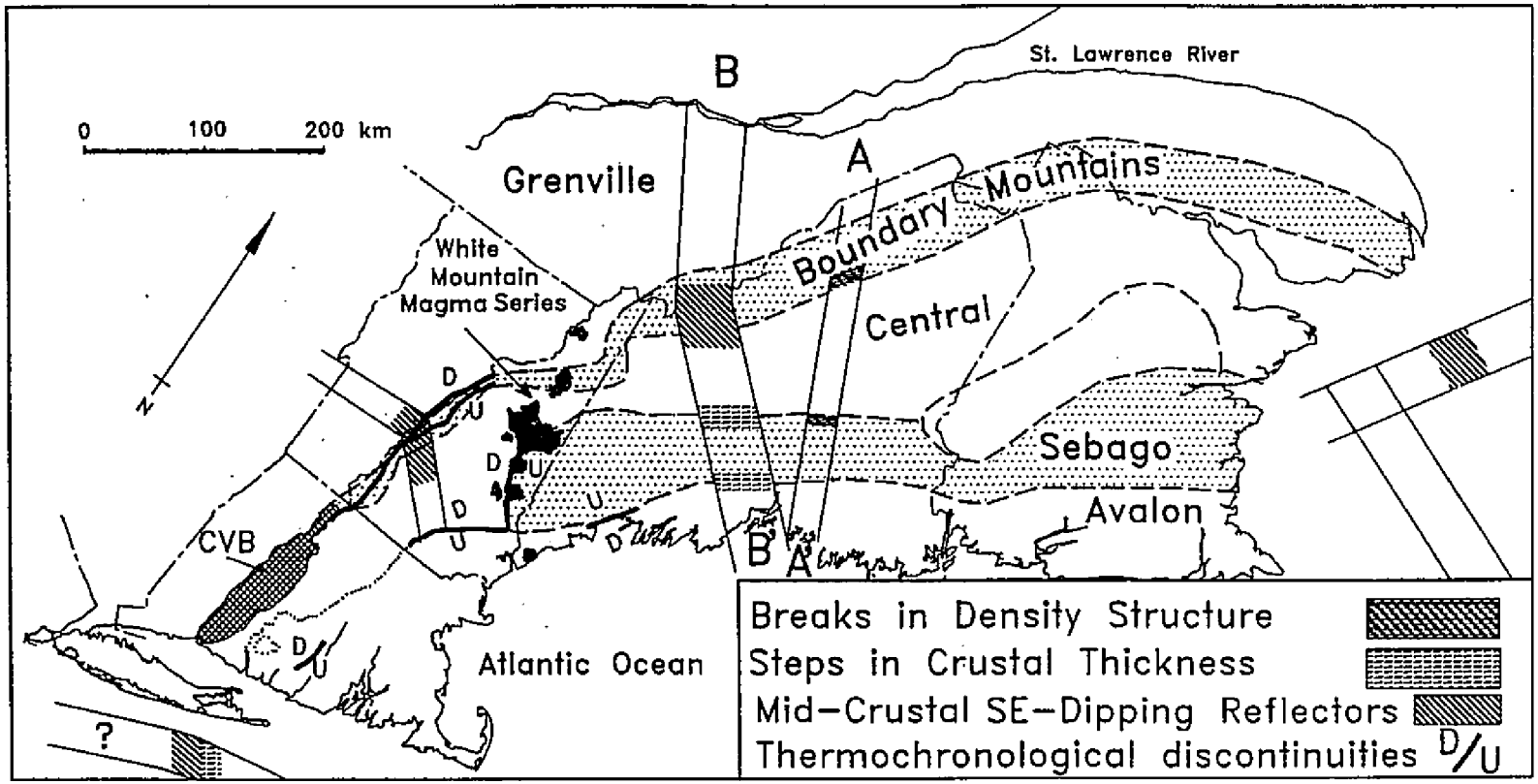

Fig. 83. Relationships between geophysical and thermochronological data and the isotopically-defined basement blocks. Density structure (along transect A-A') is from Hodge and others (1982). Seismic profiles are indicated by parallel lines, and locations of southeast-dipping reflectors at mid-crustal levels and steps in crustal thickness are shown in pattern. Seismic data are from Ando and others (1984); Marillier and others (1989); Phinney (1986); Spencer and others (1989); and Unger, Stewart, and Phillips (1987). Thermochronological discontinuites are from Eusden and Barreiro (1988); Harrison, Spear, and Heizler (1989); Lux and West (1989); Wintsch, Sutter, and Kunk (1989); and West and Lux (1989).

have more radiogenic leads (and higher $\delta^{18}O$ values) than the hornblende- and biotite-bearing granitoids found in greenschist-facies eastern Maine, but they share Sr IR $\leq$.7056.

GEOPHYSICAL AND PALEOGEOGRAPHICAL EVIDENCE FOR CRUSTAL BREAKS

Geophysical and paleogeographical evidence provide support for the existence of crustal breaks at the isotopic boundaries. For instance, Hodge and others (1982) studied the gravity field along the transect A-A' in Maine (Fig. 83); their analysis is consistent with juxtaposition of crustal fragments having contrasting density structures at two positions, on either side of the Central (C) block. The crust has been investigated by seismic reflection and/or refraction along several transects (Fig. 83); in every case, a region of southeast-dipping reflectors that cuts through the crust from shallow to deep levels has been identified. These reflectors are usually interpreted to represent the thinning margin of the Grenville block (Marillier and others, 1989; Spencer and others, 1989; Ando and others, 1984). On Fig. 83 the position of these reflectors is shown at midcrustal levels (4 to 8 seconds two-way relay time), or approximately 12 to 25 km depth. In three out of four cases, the east-dipping reflectors on these transects are found just southeast of the isotopic Grenville-Boundary Mountains boundary. On the southernmost transect, east-dipping reflectors appear to be some distance east of the Grenville boundary, but this reflector is associated with a Mesozoic rift basin (Hutchinson, Klitgord, and Detrick, 1985) and may be a relatively young feature. Seismic data also indicate two steps in crustal thickness along traverse B-B', Fig. 83 (Unger, Stewart, and Phillips, 1987). These steps are located on either side of the Sebago block (D).

The basement boundaries seem to have influenced the behavior of the crust during uplift and extension in Late Paleozoic to Mesozoic time. On Fig. 83, heavy lines denote thermochronological discontinuities; these discontinuites represent abrupt breaks in the isotopically-defined cooling history of the rocks. They are defined in most cases by contrasting $^{40}Ar/^{39}Ar$ mineral

ages (and patterns of ages) on either side of each line. One discontinuity (southeastern New Hampshire) is based on a ~100 Ma difference in monazite U-Pb ages (Eusden and Barreiro, 1988). A striking correspondence exists between the thermochronological discontinuites and isotopically-defined boundaries in central New England. At least some displacement on the boundaries seems to be Mesozoic; the position of the Connecticut Valley Basin relative to the boundaries (Fig. 83) suggests basement control. The trend of the Mesozoic White Mountain plutons, which is used to define one of the thermochronological discontinuites (Lux and West, 1989) itself apparently reflects control by the Sebago-Central basement boundary (Fig. 83). Structural control of the White Mountain magma trend was inferred previously by Foland and Faul (1977). Because the White Mountain magmas were intruded episodically over a ~130 Ma period, and show no geographic progression in ages, Foland and Faul (1977) proposed that a transform fault (possibly following an "ancient fracture") defined the White Mountain trend.

The metamorphic histories and the sequence of motions that gave rise to the thermochronological discontinuites may be complex, as they are, for example, along the New Hampshire-Vermont border (Spear and Harrison, 1990). In most cases, the precise origin of these discontinuites is not well understood. On Fig. 83, for illustrative purposes, the simplifying assumption is made that every discontinuity was the result of normal movement after a uniform metamorphic event, so that "D" represents the "down-dropped" side having the older cooling ages, and "U" represents the "uplifted" side having the younger ages.

The isotopically-defined blocks provide a new perspective from which to view the tectonic development of the north-central Appalachians. Paleontological and paleomagnetic studies provide evidence for separate existence of the Avalon block (E) and an North American block (A+B+C) during Late Ordovician to Early Devonian time. Acado-Baltic brachiopod and ostracode faunas of Silurian-Early Devonian age are known from the Avalon block (E) (Part III, Fig. 86) in New Brunswick, Maine, and northeastern Massachusetts (Boucot, Johnson, and Talent, 1967; Martinsson, 1970; Copeland and Berdan, 1977). During the same period, cosmopolitan or

Eastern Americas faunas lived on the Grenville (A), Boundary Mountains (B), and Central (C) blocks. Paleomagnetic studies confirm the separation of Avalon from North America during the pre-Acadian period (Van der Voo, 1988; Miller and Kent, 1988), and the proximity of the Central block (C) to North America (Wellensiek and others, 1988; Potts and others, 1990).

Igneous, structural, and metamorphic data from the north-central Appalachians of Siluro-Devonian age are compiled in Part III. The part played by each isotopically-defined basement block in the Early to Middle Paleozoic tectonic development of the region is examined there.

SUMMARY AND CONCLUSIONS, Part II

1. Five basement blocks can be distinguished in the Northern Appalachians on the basis of the isotopic compositions of Middle Paleozoic igneous rocks. The Sr, Pb, O and Nd compositions of the plutons and inheritance age indicators such as xenocrystic zircon yield internally consistent interpretations about the nature of each of the five basements.

2. Three of the blocks (Grenville (A), Central (C), and Avalon (E) are underlain by an ancient continental crust; plutons in these blocks show broad ranges of Sr, Pb, and O isotopic compositions and sometimes contain Middle Proterozoic or older zircons. The Central (C) and Avalon (E) blocks contain older material than does the Grenville basement (A) in this part of the Appalachians.

3. The two intervening zones, Boundary Mountains (B) and Sebago (D) do not have ancient continental crusts. Plutons in these zones show relatively narrow ranges of Sr, Pb, and O isotopic composition, even across a wide range of bulk chemical compositions. Inheritance of ancient (i.e., pre- 750 Ma) zircon is not known in these zones. Both of these blocks appear to be underlain by crust of arc origin, probably of Late Precambrian to Early Paleozoic age.

4. Tectonostratigraphic terranes are generally discordant with respect to the isotopically-defined blocks. The Avalon (E)- Sebago (D) boundary in Maine alone is approximately coincident with a stratigraphic break. The Central (C) and Avalon (E) blocks cannot be distinguished isotopically; a supercrustal boundary between them is defined instead.

5. The isotopically-defined boundaries coincide remarkably well with crustal breaks inferred from gravity and seismic reflection data. The presence of thermochronological discontinuities suggests that Late Paleozoic and Mesozoic displacements occurred preferentially along several of the boundaries.

6. The existence of the five distinct basements and their distribution in the subsurface has important implications for the Paleozoic tectonic development of the Northern Appalachians.

PART III-

EARLY TO MIDDLE PALEOZOIC ACCRETION HISTORY OF THE BASEMENT BLOCKS OF THE NORTH-CENTRAL APPALACHIANS

ABSTRACT, Part III

New England, New Brunswick, and eastern Quebec are underlain by five isotopically-defined basement blocks, consisting of two arc terranes (Boundary Mountains and Sebago blocks) and three continental terranes (Grenville, Central, and Avalon blocks) (Part II). Fundamental associations exist between most basement blocks and cover sequences; this permits paleomagnetic, paleobiological, stratigraphic, and igneous relationships to constrain the ages at which the basements were juxtaposed. Relationships between basement accretion and orogenic events are recognized: 1) accretion of the Boundary Mountains (BMB) and Central (CB) blocks occurred during the Late Cambrian to Early Ordovician Penobscottian orogeny; 2) the BMB-CB joined the Grenville block (GB) in the Late Ordovician Taconian orogeny; 3) Avalon remained separate from North America until the Acadian orogeny (Devonian time).

Belts of volcanic rocks of "indeterminate" or "arc" tectonic affinity existed along the (Siluro-Devonian) western margin of Avalon and the eastern margin of northern North America (GB-BMB-CB) before the Acadian orogeny, while igneous rocks with intraplate affinities were emplaced in the interiors of both plates. Strong geochemical similarities between the "indeterminate" rocks of the Appalachians and early Tertiary volcanics from the Patagonian Andes permit construction of a subduction model for the Siluro-Devonian Appalachians. Two subduction zones are inferred, one dipping west under northern North America and the other east under Avalon. These subduction zones indicate that ocean basins separated the Sebago block from both Avalon and North America in Silurian time: thus, two distinct plates were accreted to North America during the Acadian orogeny.

Features incorporated into the model for the Acadian orogeny proposed here include the ages of Acadian unconformities, timing of foreland-basin development, the distribution of tectonic vergence directions, and geographic distribution of metamorphic intensity. Three episodes of Acadian collision are inferred: 1) Sebago-Avalon, during earliest Devonian time, in eastern

Maine; 2) North America-Avalon, during late Early Devonian time, in southeastern New England; and 3) Sebago-North America, during Middle Devonian time, in central Maine. Southwest of the Sebago block in New England, this final episode of accretion was accompanied by the most severe shortening and highest grade of metamorphism of the Acadian orogeny.

INTRODUCTION

In Part II, five basement blocks underlying the north-central Appalachians were defined on the basis of isotopic and inheritance-age characteristics. Middle Paleozoic plutons in three of these blocks (Grenville, Central, and Avalon) show broad ranges of isotopic values, and often contain Middle Proterozoic or older xenocrystic zircons. These are inferred to be continental blocks, where a variety of isotopic reservoirs (including ancient continental crust) have contributed to magma generation. In contrast, plutons found in regions between the continental blocks (i.e., Boundary Mountains and Sebago blocks) lack signs of ancient inheritance and have characteristic, narrow ranges of isotopic values. The Boundary Mountains and Sebago blocks are inferred to be arc terranes of Late Precambrian to Early Paleozoic age. The purpose of this paper is to examine how the distribution of these basement blocks can constrain models of the Early to Middle Paleozoic tectonic development of the north-central Appalachians.

Three major Early to Middle Paleozoic orogenic events are recognized in the region: the Penobscottian orogeny (Late Cambrian-Early Ordovician), the Taconian orogeny (Late Ordovician), and the Acadian orogeny (Early to Middle Devonian). Of these events, probably the Acadian orogeny is the least understood. Tectonic models for the Acadian orogeny have postulated one subduction zone (Rodgers, 1981), two subduction zones (McKerrow and Ziegler, 1971; Bradley, 1983), or no subduction at all: for example, intra-plate convergence (Hall and Robinson, 1982), or accretion by means of longitudinal transport (Zen, 1983). Such diversity of opinion has stemmed in part from uncertainty over which (if any) terranes were accreted to North America in the course of the Acadian orogeny. The goals of this paper are 1) to determine the time at which each outboard basement block was accreted to Grenville (and thus which blocks participated in each major orogenic event) and 2) to re-examine the tectonics of the Acadian orogeny from the perspective of basement geometry. A tectonic model will be presented that uses the basement blocks identified in Part II and is consistent with the paleontologic, paleomagnetic, stratigraphic, structural, igne-

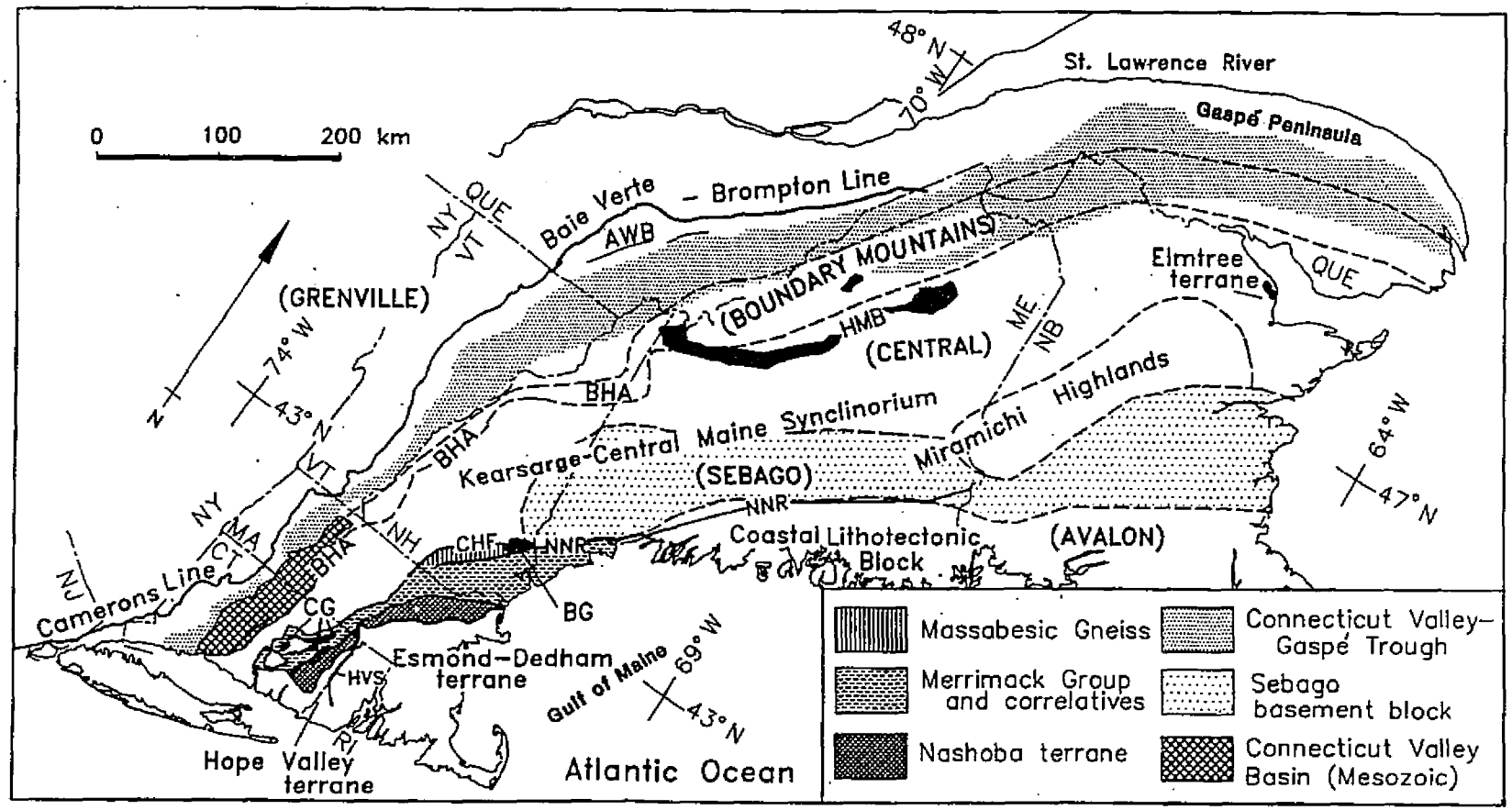

Fig. 84. Comparison of selected stratigraphic features with basement blocks of the Northern Appalachians. Boundaries of isotopically-defined basement blocks are dashed, and names of blocks are given in parentheses. Supracrustal features: AWB= Ascot-Weedon Belt; BG= Barrington granite; BHA= Bronson Hill Anticlinorium; CG= Canterbury Gneiss; CHF= Campbell Hill fault; CVB= (Mesozoic) Connecticut Valley Basin; HMB= Hurricane Mountain Belt; HVS= Hope Valley shear zone; NNR= Norumbega-Nonesuch River fault.

ous, and metamorphic records of the north-central Appalachians.

Basement-cover relationships. There is little correspondence between the boundaries of the isotopically-defined basement blocks and those of most tectonostratigraphic terranes in the Northern Appalachians (see Part II). Nevertheless, when the effects of shallow-level thrusting are taken in account, certain relationships between basement blocks and cover rocks can be inferred:

1) Cambro-Ordovician shelf- and slope-facies rocks of the North American (Laurentian) margin overlie much of the Grenville block (GB). Ophiolites of the Baie Verte-Brompton line (Fig. 84) are in tectonic contact with these Cambro-Ordovician cover rocks in Quebec: the Baie Verte-Brompton line defines the surface trace of the junction between North American and "oceanic" rocks (Williams and St-Julien, 1982). In central and southern New England, Cameron's Line and its extensions (Fig. 84) define the suture between the Cambro-Ordovician North American margin and exotic accretionary prism material (Hall and Robinson, 1982; Stanley and Ratcliffe, 1985). The Baie Verte-Brompton line and Cameron's Line are taken as boundaries that separate supracrustal rocks of Grenville- and Boundary Mountains- affinities.

2) The western boundary of Avalon-related terranes in Maine (Coastal Lithotectonic Block plus the Merrimack Trough) approximates the isotopic boundary of the Avalon block (Part II). This stratigraphic break, extended southwards, defines the supracrustal western limit of Avalon in New England (Fig. 84) (see Part II).

3) Strata that lie between the Baie Verte- Brompton line and the Avalon boundary are interpreted as cover related to either the Boundary Mountains or Central blocks. There is no known stratigraphic expression of the Sebago block; the supracrustal section presently above it appears to be allochthonous, derived from the Central block (Part II).

TIMING OF ACCRETION EVENTS

Penobscottian linkages. Geologic evidence indicates that the continental Central block (CB) and the Boundary Mountains block (BMB) were joined in Early Ordovician time. Boone and Boudette (1989) and Pollock (1989a) define a Boundary Mountains terrane which extends from the Baie Verte-Brompton line on the west (Fig. 84) to a mélange of Cambrian to Early Ordovician age on the east. This eastern mélange (Hurricane Mountain belt, Fig. 84) is thought to represent the suture between the Boundary Mountains terrane and the terrane ("Gander" or "Traveler") to which it was accreted during the Early Ordovician Penobscottian orogeny (Boone and Boudette, 1989; Pollock, 1989a). The Hurricane Mountain belt appears to be the supracrustal equivalent of the isotopically-defined boundary in Maine between the Boundary Mountains and Central basement blocks (Fig. 84).

A sliver of the BMB has been inferred to extend from northern New Hampshire and Maine southwards (see Part II) mostly along the Bronson Hill Anticlinorium (Fig. 84). Because the Hurricane Mountain mélange belt is essentially confined to Maine, the possibility arises that the BMB in Maine and its continuation in southern New England had separate origins. If so, the "juvenile" isotopic values of the BMB in southern New England might represent an Ordovician arc developed on the margin of the continental Central block, instead of defining an exotic, accreted terrane like the BMB of Maine. The Hurricane Mountain mélange is unconformably overlain by Middle Ordovician and older strata, indicating that the Central and Boundary Mountains isotopic blocks were joined before the Taconian orogeny (Boone and Boudette, 1989).

Extensive volcanism occurred over the CB of Maine during Middle to Late Ordovician time. Ordovician volcanics of the Tetagouche Group in the Miramichi Highlands (Fig. 84) have intraplate geochemical characteristics, and are interpreted as a back-arc equivalent of the Taconian arc (van Staal, 1987; Fyffe, Barr, and Bevier, 1988). In New Brunswick, ophiolitic rocks of the Elmtree terrane (Fig. 84) have been interpreted as fragments of an ensimatic back-arc basin (van

Staal, 1987), which was probably the product of local rifting of the CB.

Input from the ancient crust of the Central zone can explain the continental character of many Ordovician volcanic rocks. Inheritance ages and isotopic compositions of the Ammonoosuc Volcanics of New Hampshire (Hingston and Barreiro, 1990) and of the abundant Ordovician bentonites of the eastern half of the United States both show an ancient crustal component. Ordovician bentonites are known to contain xenocrysts of garnet and pyroxene, thought to be derived from a high-grade metamorphic basement during explosive eruptions (Samson and others, 1989; Delano and others, 1990). Xenocrystic zircon with a Middle Proterozoic (or older) inherited component have been found in bentonites (Samson and others, 1989). Apatite compositions suggest that the original ashes had $^{87}Sr/^{86}Sr$ of ~0.711 and probably negative ε Nd values (Samson and others, 1989). These age and isotopic characteristics are all compatible with a CB source.

Taconian linkages. There is general agreement that the Taconian orogeny took place when the Laurentian (Grenville) passive margin collided with an arc terrane along an east-dipping subduction zone (for example, Osberg, 1978; Hall and Robinson, 1982; Rowley and Kidd, 1981; Rodgers, 1981; Stanley and Ratcliffe, 1985). Paleomagnetic data from Maine suggest that this arc terrane, the composite Boundary Mountains-Central block (BMB-CB), was already proximal to North America in Middle Ordovician time (Wellensiek and others, 1988; Potts and others, 1990). Suturing of BMB-CB basement to Grenville seems to have taken place during Late Ordovician (Caradocian) time, along with Taconian deformation (Zen, 1967) and metamorphism (Hames, Sutter, and Ratcliffe, 1990). The Oliverian series plutons intruded along the Bronson Hill Anticlinorium during the Late Ordovician, while the Highlandcroft series plutons were emplaced in a belt to the west (Lyons, Aleinikoff, and Zartman, 1986; Zartman and Leo, 1985). The map distribution pattern of ancient xenocrystic zircon in these plutons appears to express the Grenville-Boundary Mountains basement boundary (Part II, Fig. 80).

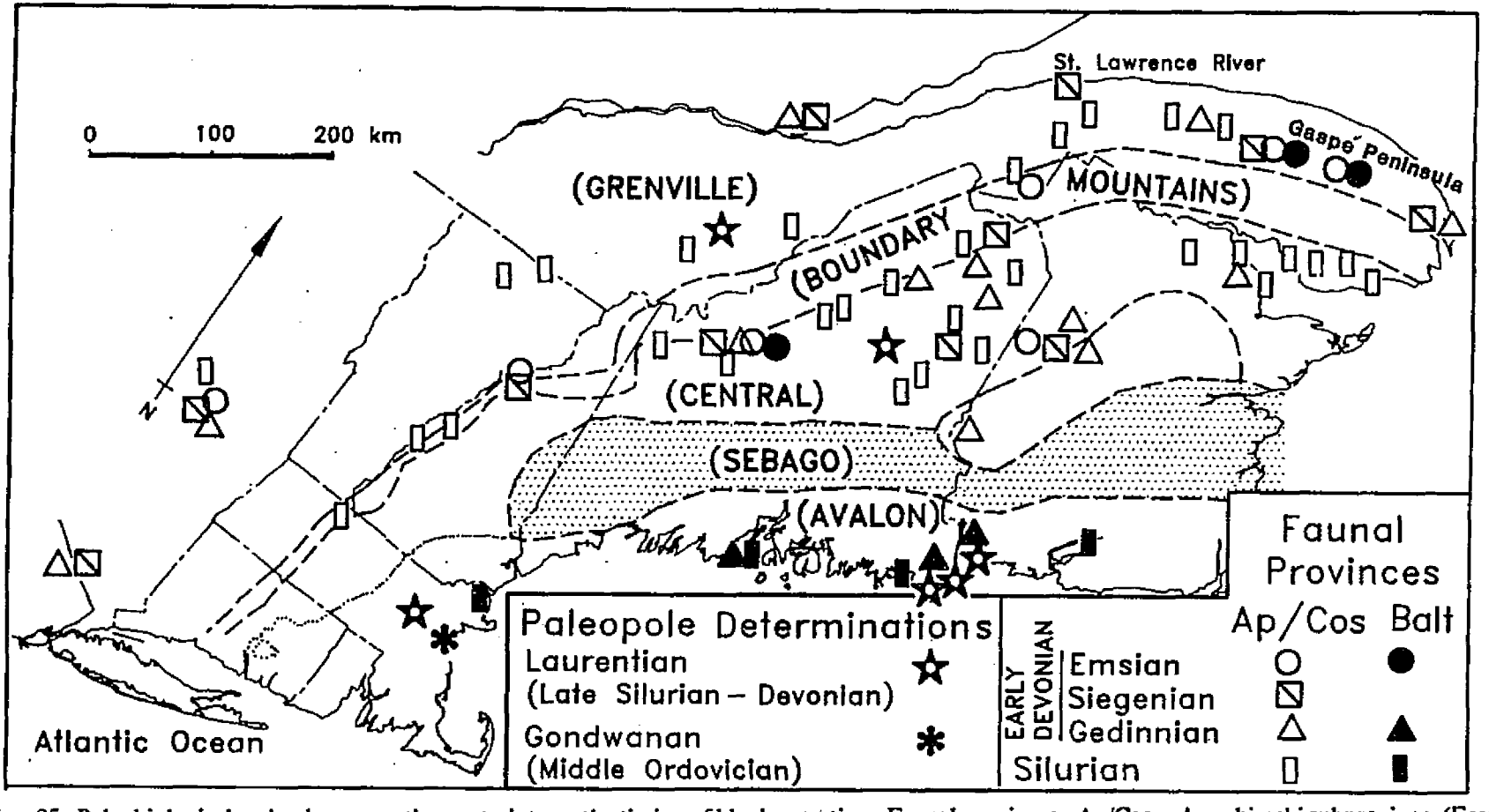

Fig. 85. Paleobiological and paleomagnetic constraints on the timing of block accretion. Faunal provinces: Ap/Cos= Appohimchi subprovince (Eastern Americas Realm), Siluro-Devonian ostracode and Early Devonian brachiopod faunas, plus cosmopolitan Silurian brachiopod faunas. Balt= Baltic (North European) Siluro-Devonian ostracode and brachiopod faunas. The Sebago basement block is stippled. Boundaries of basement blocks are dashed, and the supracrustal Avalon-Central boundary in southern New England is dotted. Faunal data are compiled from Berdan (1970, 1983); Boucot (1968); Boucot and Johnson (1967); Boucot, Johnson, and Talent (1967); Boucot and Rumble (1980); Boucot and Thompson (1963); Boucot and others (1958); Brookins, Berdan, and Stewart (1973); Copeland and Berdan (1977); Martinsson (1970); McGutcheon and Ruitenberg (1987); McKerrow and Ziegler (1971), and sources therein; Pickerill (1976); Shride (1976); St. Peter and Boucot (1981); Venugopal (1979); and Watkins and Boucot (1975). Paleomagnetic data are compiled from Kent and Opdyke (1980); Roy and Anderson (1981); Schutts and others (1976); Seguin, Rao, and Pineault (1982); Spariosu and Kent (1983); and Weisse, Haggerty, and Brown (1985).

Stratigraphic and faunal linkages among the Grenville, Boundary Mountains, and Central blocks confirm that these blocks had become joined during the Taconian orogeny. For example, a post-Taconian basin, the Connecticut Valley-Gaspé Trough, developed along the Grenville-Boundary Mountains (GB-BMB) basement boundary (Fig. 84), and was filled with Siluro-Devonian sediments (Hueber and others, 1990). The Silurian was a time of relatively cosmopolitan faunas, but an endemic North American beyrichiacean ostracode fauna appeared in Llandoverian (Early Silurian) time (Copeland and Berdan, 1977; Berdan, 1983). This fauna belongs to the Appohimchi subprovince (formerly the Appalachian Province) of the Eastern Americas Realm, and is found in northern New Brunswick, through western Maine, and south to Virginia. The Appohimchi brachiopod subprovince originated later, around the beginning of Ludlow (early Late Silurian) time (Johnson, 1979, p. 300; Boucot, 1975), and became increasingly distinct during the Early Devonian (Boucot, Johnson, and Talent, 1967). The Central, Boundary Mountain, and Grenville blocks shared these Appohimchi (and associated cosmopolitan) faunas (Fig. 85).

Closure of the Ordovician back-arc basin postulated in New Brunswick (van Staal, 1987) began by Late Ordovician time, with the onset of blueschist-facies metamorphism (van Staal and others, 1990). Closure was completed by Late Silurian time, when conglomerates were deposited over blueschist (Helmstaedt, 1971). The evidence suggests that the Grenville, Boundary Mountains, and Central blocks were welded into a single plate at some point between Late Ordovician and Late Silurian time, and formed a Silurian North America.

Post-Taconian paleogeography. The Avalon block (AB) apparently was not part of this Silurian North America. In eastern Maine, the Avalon region alone remained stratigraphically dissimilar to other lithotectonic belts after the Taconian orogeny (Ludman, Hopeck, and Brock, 1993). Siluro-Devonian ostracodes from the coastal region from New Brunswick to Massachusetts have Baltic (North European) provincial affinities (Martinsson, 1970; Copeland and Berdan, 1977), as do Early Devonian brachiopods (Boucot, Johnson, and Talent, 1967, p. 1240) (Fig. 85).

The distribution of animal communities and lithofacies in the north-central Appalachians demonstrates that two principal emergent or shallow-water areas were separated by deep water throughout the Silurian (McKerrow and Ziegler, 1971; Ziegler and Boucot in Berry and Boucot, 1970). This deep basin, known as the Fredericton Trough in New Brunswick and eastern Maine (McKerrow and Ziegler, 1971), separated the Eastern Americas and Baltic faunal realms. McKerrow and Cocks (1976) observed that the North American and North European faunal realms were convergent from Cambrian through Devonian time, and attributed this to gradually decreasing geographic separation. Migration between the faunal realms during late Early Devonian (Emsian) time is evinced by the earliest mixed (Appohimchi-Old World) brachiopod faunas, which occur on the Gaspé Peninsula of Quebec and in northwestern Maine (Fig. 85). Migration also occurred in the opposite direction: a beyrichiacean ostracode closely related to a North American form first appeared in Europe during the Siegenian (Early Devonian) (Berdan, 1983). Provinciality persisted in New England and adjacent Canada until the stratigraphic record was terminated by (Acadian-age) unconformities during Early to Middle Devonian time.

The paleomagnetic records are parallel to the faunal histories of the North American and Avalon blocks. The high Ordovician paleolatitudes of the Avalon terranes contrast with the equatorial position obtained from North America, and suggest a location somewhere on the margin of Gondwanaland (Van der Voo, 1988). The distance between the two plates diminished into Middle Paleozoic time, so that Late Silurian to Early Devonian paleopoles from North America and Avalon (including poles from localities shown on Fig. 85) do not seem to indicate significant latitudinal separation (Van der Voo, 1988; Miller and Kent, 1986). Paleopoles from Armorica and Baltica are also consistent with the assembly of an "Euramerica" plate with North America and Avalon by Early Devonian time (Van der Voo, 1982; Miller and Kent, 1988). Paleogeographic considerations point toward Devonian (and, therefore, Acadian) accretion of Avalon to North America.

Geologic evidence confirms the accretion of at least the western portion of the Avalon

block to North America during Early to Middle Devonian time. The western margin of the Avalon block (as it is defined in Part II), underwent Acadian deformation and metamorphism (Figs. 90 and 94). The Canterbury Gneiss, which consists of Early Devonian, sheet-like granitoids (Zartman and Naylor, 1984) was syntectonically intruded just east of the supracrustal Avalon-North America boundary in Connecticut (Fig. 84). The Norumbega-Nonesuch River-Campbell Hill fault zone, which closely follows the Avalon-North America block boundary (Part II), was "stitched" by the Barrington Granite (Fig. 84) at 364 Ma (Eusden and Barreiro, 1988). Acadian deformation in the Avalon block near the Maine-New Brunswick border is bracketed between deposition of the Early Devonian Eastport Formation and deposition of the unconformably overlying Late Devonian Perry Formation.

In contrast to terranes on the western margin of the Avalon Block, the more interior terranes of Avalon (Nashoba, Hope Valley, and Esmond-Dedham, Fig. 84) show little or no evidence of Acadian deformation or metamorphism. Acadian accretion does seem indicated for the Nashoba terrane, the westernmost of these terranes. It has possible stratigraphic links with southernmost coastal Maine (Hussey, Bothner, and Thomson, 1986) and Mississippian $^{40}Ar/^{39}Ar$ and mineral isochron ages (Hepburn, Hill, and Hon, 1987), suggesting Acadian metamorphism. Existing data also permit attachment of the Hope Valley terrane of southern New England to North America with the Acadian orogeny (O'Hara and Gromet, 1985). The Esmond-Dedham terrane of southeast New England, however, clearly has undergone post-Acadian displacement with respect to the remainder of the Avalon block (Skehan and Murray, 1980; Zartman and Naylor, 1984; O'Hara and Gromet, 1985). It seems likely that this Late Paleozoic displacement was not of enormous magnitude; there is no detectable latitudinal difference in the Late Devonian position of the Esmond-Dedham terrane, determined by Schutts and others (1976) and the Late Devonian positions of North America (Miller and Kent, 1986) or the Avalon plate (coastal Maine; Kent and Opdyke, 1980). Geophysical data suggest continuity of Avalonian crust between New Brunswick and Massachusetts under the Gulf of Maine (Hutchinson and others, 1988). It is probable that the

Esmond-Dedham terrane was somewhere in the proximity of North America by the end of the Acadian orogeny, though its final emplacement appears to be related to the Alleghenian tectonism (O'Hara and Gromet, 1985).

The one remaining isotopically-defined block, Sebago, is located between the Avalon and Central blocks. Accretion of the Sebago block to North America, therefore, could have taken place no earlier than the Late Ordovician (if it were synchronous with accretion of the Central block), and no later than the Middle Devonian (if accreted with Avalon). Because the Sebago block appears to be covered by allochthonous material derived from other blocks, no direct stratigraphic constraints are available on the age of its accretion. Structural, igneous, and metamorphic features related to the Acadian orogeny, which will be discussed in later sections, do provide a basis for inferring a Middle Devonian age for the accretion of the Sebago block to North America.

TECTONICS OF THE ACADIAN OROGENY

The basic tectonic elements of the Acadian orogeny consisted of 1) Silurian North America (GB-BMB-CB) 2) most (or all) of Avalon and 3) a possible Sebago plate. In order to reconstruct the framework in which these plates interacted, the post-Taconian, pre-Acadian igneous records of the Avalon and the North American plates are considered here.

PRE-ACADIAN (SILURO-DEVONIAN) IGNEOUS ROCKS

On Table 19, data on pre-Acadian igneous rocks of Silurian to Early Devonian age are compiled. Most of the igneous bodies accepted as pre-Acadian here are volcanic units, whose ages can be constrained stratigraphically. Silurian radiometric ages have recently been obtained on a number of plutons whose geologic relationships suggest younger emplacement ages. Such plutons have been excluded; those plutons listed on Table 19 have geologic relationships consistent with pre-Acadian emplacement. Silurian plutons of the Esmond-Dedham terrane are included, since the EDT is considered here as a fault-bounded fragment of the Avalon plate's interior.

Each of the igneous bodies listed on Table 19 has been assigned to the tectonic setting judged most consistent with the available (often limited) geochemical and petrographic data. Tectonic assignments were intentionally made in a conservative way, the choice of settings being 1) arc; 2) indeterminate; 3) transitional; and 4) intraplate. Rocks types judged to have "arc" affinities were restricted to (a) calc-alkaline, mafic to intermediate plutons with enriched LREE; (b) high-alumina basalt; and (c) largely calc-alkaline, unimodal, andesitic volcanic assemblages. Peralkaline, alkaline, and alkalic igneous bodies, along with (MORB-like) tholeiites having depleted LREE, were judged to have "intraplate" affinities. Volcanic assemblages which include mildly alkaline basalts were considered "transitional". Other rock types (including bimodal, calc-

TABLE 19.

Tectonic Affinities of Pre-Acadian Igneous Rocks, North-Central Appalachians

AVALON PLATE

Number	Class	Tectonic Setting	Rock Unit	AGE Stratigraphic	AGE Radiometric*		References
1	d	Indeterm.	Preston Gabbro		424±5	U-Pb Zir	Walker and Sclar, 1983; Zartman and Naylor, 1984
2	k	Indeterm.	Ayer Granite		433±5	U-Pb Zir	Zartman and Naylor, 1984
3	a	Arc	Indian Head Hill diorite		402±5	Rb-Sr	Hill and others, 1984
4	l	Indeterm.	Andover Granite		455	Rb-Sr	Hill and others, 1984; Zartman and Naylor, 1984;
					415	Rb-Sr	Collins and others, 1985
5	a	Arc	Sharpners Pond diorite		430±5	U-Pb Zir	Hill and others, 1984; Zartman and Naylor, 1984; Loftenius and Hon, 1987
6	b	Arc	Newbury Volcanics	Late Silurian	338±10	Rb-Sr	Shride, 1976; Hon and Thirlwall, 1985; Fullagar and Bottino, 1968
7	p	Intraplate	Cape Ann Granite		450±20	U-Pb Zir	Zartman, 1977; Zartman and Marvin, 1971
8	h	Indeterm.	Vinalhaven Rhyolite	Gedinnian	385± 6	Rb-Sr	Brookins, Berdan, and Stewart, 1973
9	h	Indeterm.	Thorofare Andesite	Late Silurian			Brookins, Berdan, and Stewart, 1973; Dow, 1965
10	f	Indeterm.	Castine Volcanics	Devonian	383±5	Rb-Sr	Pinette and Osberg, 1989; Brookins, Berdan, and Stewart, 1973
11	f,h	Indeterm.	Cranberry Island volcanics		379±9	Rb-Sr	Brookins, Berdan, and Stewart, 1973; Scherer, Pinet, and Seaman, 1990
12	h	Indeterm.	Bar Harbor Series volcanics		408±27	Rb-Sr	Metzger, Mose, and Nagle, 1982
13	h	Indeterm.	Flint Island volcanics	Silurian	396±17	Rb-Sr	Boucot in Metzger and Bickford, 1972; Metzger, Mose, and Nagle, 1982
14	e,i	Indeterm.	Pembroke Group volcanics	Silurian	401±15	Rb-Sr	Gates & Moench, 1981; Berry & Boucot, 1970; Fullagar & Bottino, 1968
15	e,i	Indeterm.	Dennys Formation volcan.	Silurian	406±15	Rb-Sr	Gates & Moench, 1981; Berry & Boucot, 1970; Fullagar & Bottino, 1968
16	f	Indeterm.	Quoddy Formation volcan.	Early Silurian	411±15	Rb-Sr	Gates & Moench, 1981; Berry & Boucot, 1970; Fullagar & Bottino, 1968
17	i	Indeterm.	Eastport Formation volcan.	Gedinnian	403±5	Rb-Sr	Gates & Moench, 1981; Berry & Boucot, 1970; Bottino & Fullagar, 1966
18	i	Indeterm.	Mascarene Group volcanics	Sil.-Gedinnian			Bailey and Matthew, 1876; Pickerill and Pajari, 1976 McCutcheon and Ruitenberg, 1987; Van Wagoner and Fay, 1988
19	p	Intraplate	Gulf of Maine granites		437±18	U-Pb Zir	Hermes, Ballard, and Banks, 1978

* Rb-Sr ages on this table have been calculated using Steiger and Jäger's (1977) recommended decay constants.

TABLE 19, CONTINUED

NORTH AMERICAN PLATE

Number	Class	Tectonic Setting	Rock Unit	AGE: Stratigraphic	AGE: Radiometric	References
20	r,q?	Intraplate	Standing Pond Volcanics	Siluro-Devon.	>423±4 U-Pb Zir	Hepburn, 1981, 1984; Hueber and others, 1990
21	j	Indeterm.	Shaw Mountain Fm. amphib.	Silurian		Carroll, Schneiderman, and Noblett, 1989; Boucot and Thompson, 1963
22	f	Indeterm.	Littleton Fm. volcanics (Tumble Dick Mountain)	Early Devonian	414±4 U-Pb Zir	Moench, 1989; Lyons and others, 1986 Moench and Aleinikoff, 1985; Aleinikoff and Moench, 1985
23	i	Indeterm.	Perry Mountain Fm. volcan.	Silurian	>412±2 U-Pb Zir	Moench, 1989; Moench and Aleinikoff, 1987; Hafner-Douglass 1987
24	f	Indeterm.	Rangeley Fm. volcanics	Early Silurian	434±8 U-Pb Zir	Moench and Aleinikoff, 1985; Aleinikoff and Moench, 1985
25	f	Indeterm.	Frontenac/Kidderville Fm.		>417 U-Pb Zir	Lyons and others, 1986; Green and Guidotti, 1968; Lyons, Zartman, and Aleinikoff, 1983
26	g	Indeterm.	Piscataquis Volcanic Belt	Early Devonian	406±24 Rb-Sr	Rankin, 1968, 1980; Neuman and Rankin, 1980; Gaudette and others, 1990
27	j	Indeterm.	Allagash Lake area volc.	Late Silurian		Pollock, 1989b
28	m?	Trans.?	Spider Lake Volcanics	Late Sil-E Dev.		Hall, 1970; Fitzgerald and Hon, 1989
29	m?	Trans.?	Ripohenous Dam area vol.	Late Sil-E Dev.		Fitzgerald and Hon, 1990
30	m	Trans.	Dockendorf Group volcan.	Gedinnian	404±10 Rb-Sr	Boucot and others, 1964; Sargent, Hon, and Roy, 1981; Bottino and Fullagar, 1966; Fitzgerald and Hon, 1989
31	n,o	Intraplate	Five-Mile Brook/Rocky Mt.	Late Silurian		Schwartz, Hon, and Roy, 1984
32	m	Trans.	Pointe aux Trembles/ Lac Raymond Fms.	Early Silurian		David and Gariépy, 1986
33	e	Indeterm.	Tobique Group (Millville)	Early Devonian		St. Peter, 1978; Dostal, Wilson, and Keppie, 1989
34	e	Indeterm.	(Wapske/New Denmark)	Early Devonian	409±35 Rb-Sr	St. Peter, 1978; Dostal, Wilson, and Keppie, 1989; Fyffe and Cormier, 1979
35	f	Indeterm.	Perham Group volcanics	Silurian		Boucot and others, 1964; Dostal, Wilson, and Keppie, 1989
36	m	Trans.	Chaleurs Group volcanics	Silurian		Greiner, 1970; Pajari, Rast, and Stringer, 1977; Dostal, Wilson, and Keppie, 1989; Skinner, 1974
37	m	Trans.	Dalhousie Group	Gedinnian		Howard, 1926; Pajari, Rast, and Stringer, 1977; Dostal, Wilson, and Keppie, 1989; Clarke, 1907
38	r	Intraplate	Pabos Suite	post Late Ord.		Bédard, 1986a
39	s	Intraplate	Ristigouche/Black Cape volcanics + dike suites	Late Silurian		Bédard, 1986a; Bourque and Lachambre, 1980; Laurent & Bélanger, 1984; Bélanger, 1982; Béland, 1958
40	s	Intraplate	McKay Lake-Mont Alexandre Raudin volc. + dike suites	Late Silurian		Bédard, 1986a; Bourque and Lachambre, 1980; Bélanger, 1980
41	q	Intraplate	York River Group volcan.	late Early Dev.	380±3 Rb-Sr	Bédard, 1986b; Boucot, Johnson, & Talent, 1967; LaRocque & Doig, 1984

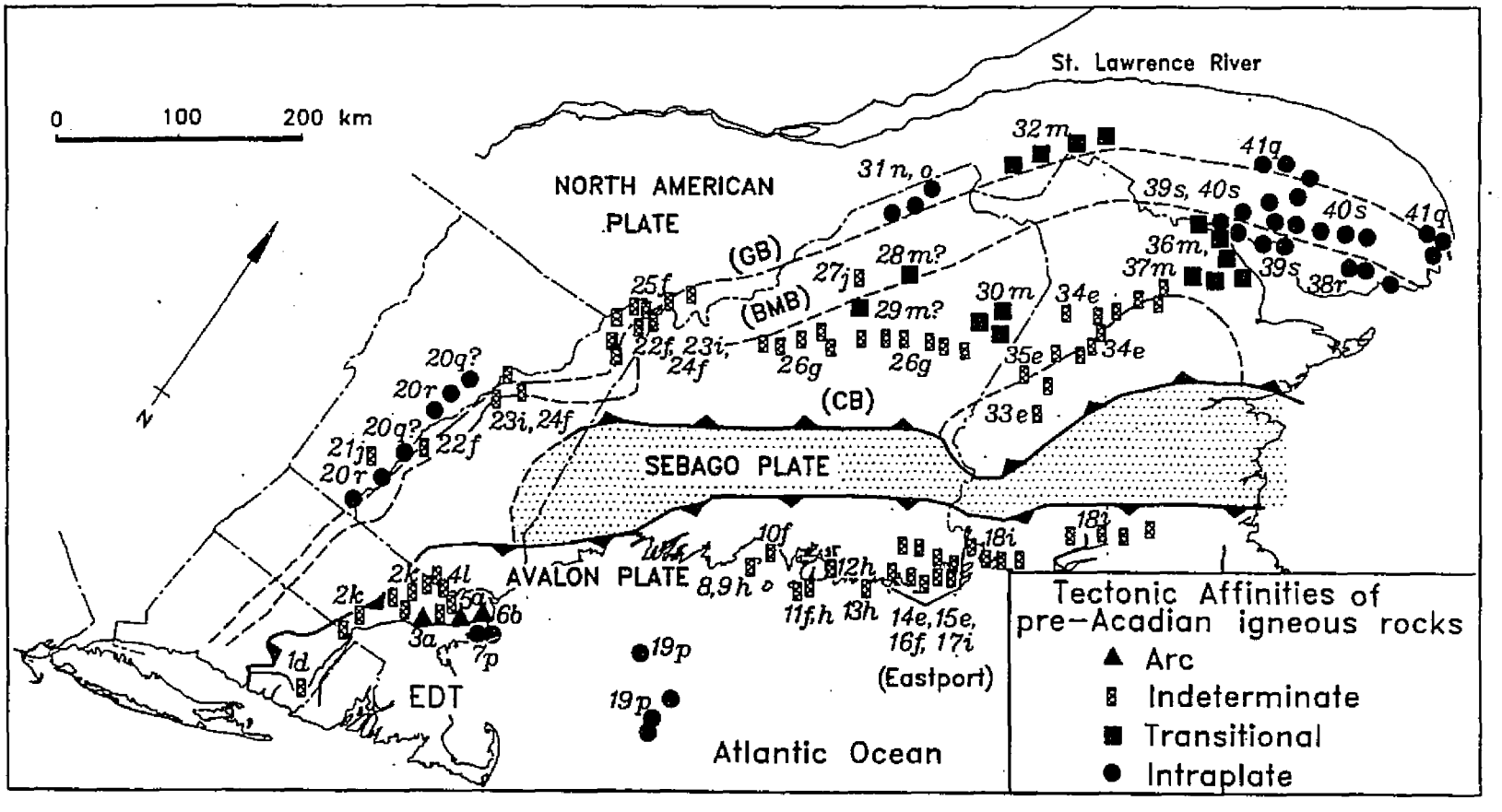

Fig. 86. Distribution and character of pre-Acadian igneous rocks. Names, ages, references for the igneous bodies are given in Table 19. Basement blocks: GB= Grenville; BMB= Boundary Mountain; CB= Central. Rock units: ARC AFFINITY: a- Calc-alkaline, mafic to intermediate plutons, with enriched LREE; b- High-alumina basalt; c- Unimodal volcanic suite, with calc-alkaline to tholeiitic andesite. INDETERMINATE AFFINITY: d- LREE enriched, mafic to intermediate plutons; e-Bimodal volcanics, calc-alkaline on AFM; f- Bimodal volcanics (no chemistry available); g- Metaluminous to peraluminous rhyolites; h- Felsic to intermediate volcanic suite (no chemistry available); i- Bimodal suite: tholeiitic basalt + felsic volcanics; j- Tholeiitic basalt to basaltic andesite; k- Quartz monzonite; l- Two-mica granite. TRANSITIONAL AFFINITY: m- Compositionally diverse volcanic suite, with basalts transitional to alkaline; n- Transitional to mildly alkaline basalt. INTRAPLATE AFFINITY: o- Peralkaline rhyolite; p- Alkalic granite; q-Alkali basalt; r- Tholeiite with depleted LREE; s- Hybrid alkali basalt, hawaiite, mugearite association.

alkaline volcanic suites, peraluminous rhyolites, and ordinary tholeiites) were assigned to the "indeterminate" category. These rock types are less strongly associated with a particular tectonic setting than are the rocks assigned to the "arc" and "intraplate" categories. Some rock units were assigned to the "indeterminate" category simply because few chemical data are available for them. All the rock types assigned to the "indeterminate" category here are listed in the caption of Fig. 86.

Fig. 86 shows the geographic distribution of the pre-Acadian igneous rocks along with their inferred tectonic settings. Pre-Acadian igneous activity evidently occurred within four belts, which are disposed about the Sebago block with mirror symmetry. Belts of igneous rocks having mostly "indeterminate" (and, in the Nashoba terrane, arc) affinity are present on the North American and Avalon blocks directly adjacent to the Sebago block. At a greater distance from the Sebago block, in interior regions of the plates, belts of "intraplate" igneous activity are found. A sharp break is present between the "indeterminate/arc" and "intraplate" belts on the Avalon block, a break which corresponds to the fault contact between the Esmond-Dedham terrane and the remainder of Avalon. On the North American plate, a region of "transitional", partially alkaline compositions occurs between the two. It appears that on both the North American and Avalon plates, contrasting tectonic settings existed in marginal and interior regions during the pre-Acadian period.

These parallel belts are most readily explained by a change from arc- to back-arc style igneous activity, and thus appear to be related to subduction. The paired igneous belts imply that one pre-Acadian subduction zone dipped eastwards under Avalon, and that the other dipped westwards under North America. On the North American block, the two distinct volcanic belts disappear and all Siluro-Devonian volcanic activity was minor to the south of the Sebago block. Subduction appears to have been limited to the northern portion of the North American plate. The distribution of the volcanic rocks suggests that a basin had existed between the North American plate and the Sebago block, and was closed by subduction during Siluro-Devonian time. "Indeterminate" and "arc" igneous activity seem to have been longer-lived on the Avalon plate;

Ordovician calc-alkaline igneous rocks of probable arc origin (Hon and others, 1986) are known, in addition to those of Silurian and Devonian age. A subduction setting has been inferred by earlier workers for several of the Siluro-Devonian "indeterminate", "arc", and "transitional" igneous suites (Rankin, 1968; Sargent, Hon, and Roy, 1981; Hill and others, 1984; Hon and Thirlwall, 1985; Hon and others, 1986; David and Gariépy, 1985; Fitzgerald and Hon, 1990), but intraplate origins have been suggested for other suites (Gates and Moench, 1981; Van Wagoner and Fay, 1988; Pinette and Osberg, 1989; Dostal, Wilson, and Keppie, 1989). Reluctance to infer a subduction setting for these rocks is due to the scarcity of unambiguous arc-related rock types and the absence of a clear "arc" signature on tectonic-discrimination diagrams. Discussion below suggests that arc settings are both permitted and probable.

The "intraplate" to "transitional" igneous belt transgresses the isotopic boundaries that defined the Grenville, Boundary Mountains, and Central blocks (Fig. 86). This supports the earlier conclusion that Grenville, Boundary Mountains, and (at least western) Central blocks acted as single plate during Silurian time. Some Early Silurian volcanic rocks of Quebec, particularly the "transitional" Pointe aux Trembles and Lac Raymond Formations (32m, Fig. 86) might conceivably be related to the subduction of the Ordovician back-arc basin of van Staal (1987). The Late Silurian and Early Devonian volcanic rocks of the North American plate most clearly define the two-belt pattern (Fig. 86 & Table 19). Closure of the inferred basin between the North American and Sebago plates may have taken place largely during this period.

AN ANDEAN ANALOG

Two contrasting belts of Mesozoic and younger igneous rocks crop out in South America (see Fig. 87). The compositionally diverse Cordillera, whose rocks are mostly of "arc" and "indeterminate" affinity in the sense used in this paper, occurs along the continental margin, while

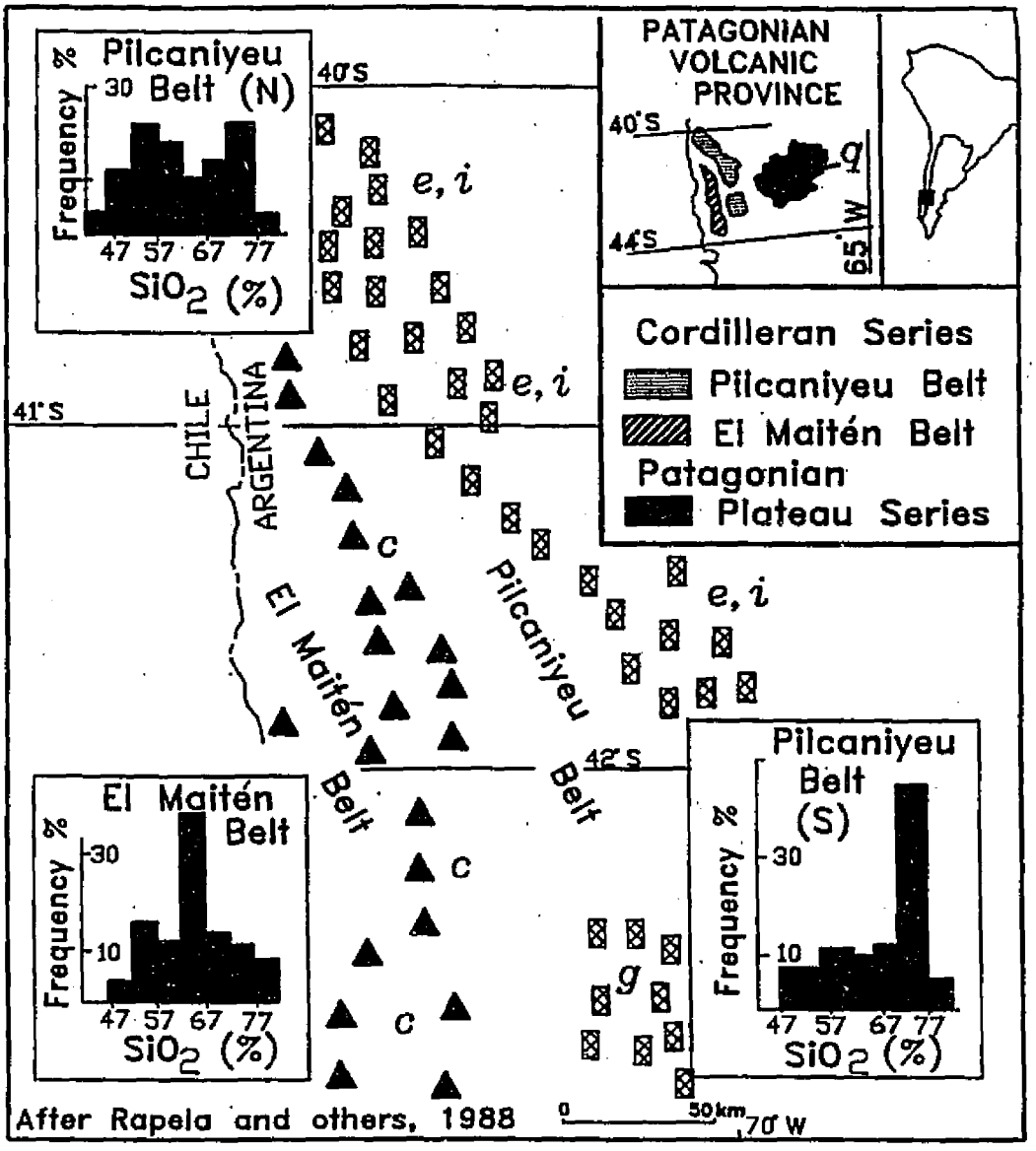

Fig. 87. Distribution and character of the Early Tertiary volcanic rocks of the Patagonian Volcanic Province. Rock categories (c, e, i, g, and q) are the same as on Fig. 3.

"intraplate" alkaline basalts are common in the region east of the Cordillera (Thorpe and others, 1982). Some parts of the Cordillera are dominated by "indeterminate" volcanics like those found in the Appalachian Siluro-Devonian section. Along the Mesozoic continental margin of Peru, for instance, tholeiitic to calc-alkaline mafic volcanism occurred in fault-bounded troughs (Atherton, Pitcher, and Warden, 1983; Pitcher, 1984) reminiscent of southern New Brunswick (Currie, 1988).

There are many parallels between the most common "indeterminate" rocks of the north-central Appalachians and those of the Early Tertiary volcanics of the Patagonian Cordillera between 40° and 42°30" S (Fig. 87). Two volcanic belts are present in the Patagonian Cordillera: the El Maitén Belt to the west, developed on relatively thin crust, and the Pilcaniyeu Belt, which overlies over thicker crust in the east (Rapela and others, 1988). The El Maitén Belt is largely composed of unimodal, andesitic volcanic rocks of "arc" affinity (Fig. 87), but the Pilcaniyeu Belt is dominated by "indeterminate" rocks. Rapela and others (1988) show that rhyolitic ignimbrites predominate in the southern Pilcaniyeu Belt (Fig. 87), as ignimbrites do in the Piscataquis belt of the North American plate (26g on Fig. 86). A bimodal suite of volcanic rocks characterizes the northern Pilcaniyeu Belt, similar to the bimodal suite which dominate large segments of the Siluro-Devonian Coastal Volcanic Belt of Maine (Avalon plate) and the Tobique Group of New Brunswick (North American plate, 33-34e). During Early Tertiary time, alkali basalts erupted in the back-arc region, the Patagonian plateau (Fig. 87) (Baker and others, 1981; Rapela and others, 1988), just as "intraplate" alkaline volcanism occurred during Early Devonian time in the interior of the North American plate.

Igneous rocks in many arc terranes, including the Patagonian Cordillera (Rapela and others, 1988), contain increasing amounts of K_2O (at constant SiO_2) with greater distance from the trench. This pattern is present among the Lower Devonian volcanic rocks of New Brunswick, where average K_2O increases with distance from the North American plate boundary (Fig. 88A). Average Rb and Rb/Sr of New Brunswick Siluro-Devonian volcanic rocks (Dostal, Wilson, and Keppie, 1989) also rise to the northwest, suggesting a deepening subduction zone.

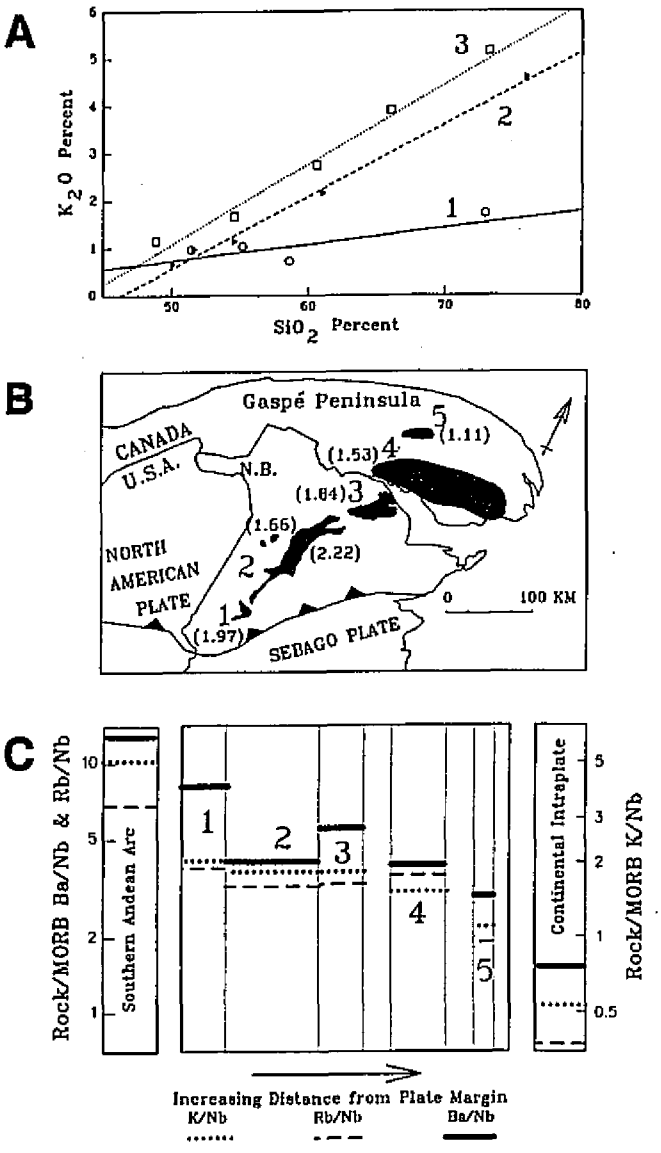

Fig. 88. Geochemical gradients found among North American volcanic rocks. A) K_2O vs. SiO_2 for Early Devonian "indeterminate" and "transitional" volcanic suites of New Brunswick (North American plate). K_2O increases with distance from Sebago plate. Locations are shown in Fig. 5B. Each data point is an average of several samples. Sources: Dostal, Wilson and Keppie (1989); Pajari, Rast, and Stringer (1977). B) Location map for data presented in Figs. 5A and 5C. 1= Tobique Group at Millville; 2= Tobique Group at Wapske/Odell and New Denmark; 3= Dalhousie Group; 4= Central and southern volcanic domains, Gaspé Peninsula (39-40 on Fig. 3); 5= York River Group. Average MORB-normalized K/Nb ratios of basalts are shown in parentheses. C) Average MORB-normalized K/Nb, Rb/Nb, and Ba/Nb ratios of "indeterminate" basalts (1, 2), "transitional" basalts (3), and ("uncontaminated") "intraplate" basalts (4, 5). Ratios from a Kenyan (Gregory Rift) alkali basalt (Baker and others, 1977) and a representative Andean calc-alkaline basalt (Hickey, Frey, and Gerlach, 1986) are given for comparison. Decreases observed in K/Nb, Rb/Nb, and Ba/Nb to the northwest parallel the shift towards "intraplate" rock types and contrasts with increases seen in K_2O and Rb in New Brunswick (Fig. 5A). Locations are shown in Fig. 5B. Data sources: 1-3, Dostal, Wilson, and Keppie (1989); 4-5, Bédard (1986 a & b).

Fig. 89 compares the "indeterminate" rocks of the Patagonian Andes (Pilcaniyeu Belt) and the Northern Appalachians. The most useful and comprehensive data presently available for the Avalon plate come from the Coastal Volcanic Belt at Eastport, Maine (Fig. 86) (Gates and Moench, 1981). The Castine Volcanics (10f on Fig. 86) have recently been studied by Pinette and Osberg (1989), but the data reveal significant alkali mobility and the original relationships between many elements have been obscured. For "indeterminate" rocks of the North American plate, Dostal, Wilson, and Keppie's (1989) study of the Tobique Group of New Brunswick currently provides the most complete data.

All three volcanic suites are subalkaline on a plot of $Na_2O + K_2O$ against SiO_2 (Fig. 89A). Although the suites are all largely calc-alkaline on an AFM plot (Fig. 89B), transitions to tholeiite are seen in the Coastal Volcanic Belt and the Pilcaniyeu Belt. Mg, Fe, Ti, and V trends found in basalts of the Tobique Group also reflect a tholeiitic character (Dostal, Wilson, and Keppie, 1989). When plotted on tectonic-discrimination diagrams, "indeterminate" rocks of the Pilcaniyeu Belt and the Northern Appalachians tend to occupy an ambiguous position (Fig. 89C). The Patagonian and the Appalachian volcanics may contain a greater "within-plate" lithospheric component than found in more typical continental-arc volcanic suites. On a MORB-normalized incompatible-element plot (Fig. 89D), basalts from the Pilcaniyeu and the El Maitén Belts of the Patagonian Andes contrast with basaltic andesite from the Central Volcanic Zone of the Andean Cordillera in failing to show depletion in P and Ti. "Indeterminate" Siluro-Devonian rocks from the Avalon plate (Coastal Volcanic Belt, Eastport area) and "transitional" volcanics from the North American plate (Chaleurs and Dalhousie Groups of New Brunswick) have P and Ti abundances similar to those of the Patagonian rocks (Fig. 89D).

In other respects, the MORB-normalized incompatible-element plots of "indeterminate" rocks from the Eastport area closely resemble those of the Andean Central Volcanic Zone. K, Rb, Ba and Th tend to be strongly enriched, and a sharply defined negative Ta-Nb anomaly is present (Fig. 89D). The Newbury Volcanics of Massachusetts (6b on Fig. 86), here assigned an "arc" affin-

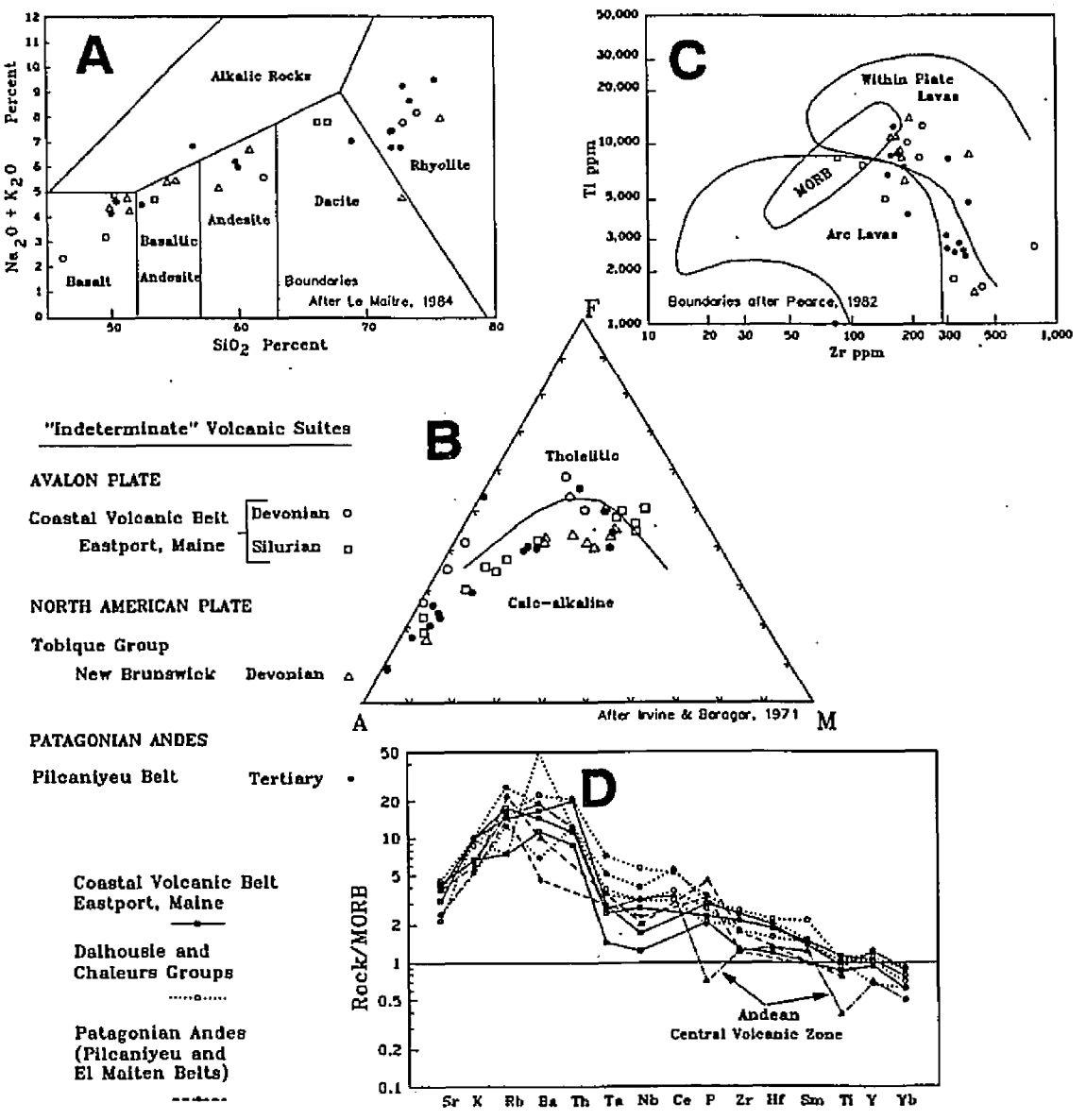

Fig. 89. Comparison of the "indeterminate" rocks of the Appalachians and the Patagonian Andes. A) Alkalies ($Na_2O + K_2O$) vs. SiO_2 for "indeterminate" volcanic suites of North American plate (Tobique Group), Avalon plate (Eastport area), and the Patagonian Andes (Pilcaniyeu Belt). Sources: Dostal, Wilson, and Keppie (1989); Gates and Moench (1981); Rapela and others (1988). B) AFM plot of the "indeterminate" volcanic suites. C) Ti vs. Zr plot of the "indeterminate" volcanic suites. D) MORB-normalized plot of incompatible elements for "indeterminate" (Coastal Volcanic Belt) and "transitional" (Dalhousie and Chaleurs Groups) suites of the Appalachians, compared with the "indeterminate" Patagonian Andes and "arc" rocks of the Andean Central Volcanic Zone. Diagram is after Pearce (1983). Data are from Gates and Moench (1981); Dostal, Wilson, and Keppie (1989); Rapela and others (1988); and Thorpe, Francis, and O'Callaghan (1984).

ity, are also reported to show a strong Ta-Nb anomaly (Hon and Thirlwall, 1985). Plots of the "transitional" Chaleurs and Dalhousie Group display a Ta-Nb anomaly as well, but it is less pronounced (Fig. 89D). In contrast, neither the alkaline nor the tholeiitic "intraplate" rocks of Gaspé conform to "arc" incompatible element abundance patterns (Bédard, 1986a). According to Gill (1981, p.138), a Ba/Ta ratio of >450 is the "single most diagnostic geochemical characteristic of arc magma"; reported values for "indeterminate" basalts of the Eastport area average 731, while "transitional" basalts of the Dalhousie and Chaleurs Groups average 460 and 514, and "intraplate" basalts of Gaspé average 265.

Incompatible-element abundances of North American Late Silurian-Early Devonian volcanic rocks appear to display the same subduction-related pattern seen in the overall rock distribution. The highest average MORB-normalized K/Nb, Rb/Nb, and Ba/Nb values are found closest to the plate margin and decrease towards the plate interior (Fig. 88B-C). Incompatible-element abundances of the York River Group in northern Gaspé (41q on Fig. 86) approach those of intraplate (continental) alkali basalts (Fig. 88B). Nakamura, Campbell, and Sun (1985) reported an analogous pattern west of the Japan Trench; normalized K/Ta+La values of both alkali and subalkaline basalts were found to decrease with distance from the plate margin. As Kuno (1966) observed that K_2O of Japanese volcanic suites increased with distance from the trench, clearly two distinct subduction-related mechanisms must be responsible. The decrease in K, Rb, and Ba enrichment (relative to Nb) of North American basalts likewise occurs in spite of the enrichment in K_2O and Rb with distance observed in the "indeterminate" and "transitional" rock suites (Fig. 88A). Zr/Nb ratios from Dostal, Wilson, and Keppie (1989) and Bédard (1986a, b) also suggest a subduction zone dipping under the North American plate. Zr/Nb of Lower Devonian volcanic rocks is highest in the Tobique Group ($Av._{basalts}$ ~ 17.4) (Fig. 88B), drops to ~ 12.4 in the Dalhousie Group, and is lowest (~ 11.4) on the Gaspé Peninsula. Late Silurian rocks in the region, such as the Perham Group (35f on Fig. 86), Chaleurs Group (36m) and volcanic rocks on the Gaspé Peninsula show the same geochemical trends as do the Early Devonian rocks.

Kay and Rapela (1987) related the temporal geochemical variations found among early Tertiary volcanic rocks of the Patagonian Andes to obliqueness of convergence. As the collision of Avalon with North America also appears to have been oblique on a regional scale (see discussion below), the Siluro-Devonian arcs of the north-central Appalachians were probably subjected to tension, which may account for their similar anomalous chemistry.

In addition to the arguments based on the chemistry and distribution of the igneous rocks, there is evidence from stratigraphy supporting the two-subduction zone model. The stratigraphic records of the "indeterminate" belts of both the Avalon and North American plates, like those of typical arc terranes, often display shoaling. On the Avalon plate, brachiopod communities display a general shallowing trend through Silurian time (Boucot and others, 1966; Watkins and Boucot, 1975) and a shift to subaerial Early Devonian deposition is locally recorded (Gates and Moench, 1981; Pickerill, Pajari, and Dickson, 1978). On the North American plate, uplift of parts of Maine, New Brunswick, and Quebec gave rise to the Salinic disconformity at approximately the Silurian-Devonian transition (Boucot, 1962; Boucot and others, 1964; Hall, 1970; Boone, 1970; Roy and Mencher, 1976; Roy, 1980; Bourque and others, 1988). This uplift may be related to either the onset of subduction or to an increase in subduction rate. Although clastic sediments blanketed much of the eastern North American plate during Early Devonian time, most eruptions of "indeterminate" volcanic rocks plate during Early Devonian time were subaerial (Rankin, 1968; St. Peter, 1982; L. R. Fyffe in Williams and others, 1985, p. 87).

In summary, the distribution of the pre-Acadian igneous rocks on the Avalon and northern North American plates into parallel "indeterminate" to "arc" and "transitional" to "intraplate" belts strongly suggests that subduction under both plates preceded the Acadian orogeny. K_2O versus SiO_2 and incompatible-element abundances of volcanic rocks (particularly from the North American plate) appear to reflect a similar shift in tectonic setting from plate margin to plate interior. The common "indeterminate" rock associations and their trace-element chemistry are within the range of compositions known from arc settings. An arc environment is also suggested

by the marked tendency towards uplift which preceded the Acadian orogeny in the "indeterminate" belts. Oblique subduction, under both plates, may best explain their pre-Acadian geologic records. According to this hypothesis, subduction would have 1) closed a basin between the North American and Sebago plates, and 2) resulted in accretion of Avalon to both the Sebago and North American plates. The distribution of igneous rocks inferred to be subduction-related suggests that the Sebago block acted independently of both the North American and Avalon plates during pre-Acadian time.

The distinctive, two-paired belts distribution of igneous rocks evident in the pre-Acadian period disappeared after the orogeny. Subsequent igneous activity did not conform to the pre-Acadian configuration, except for continuing peralkaline intrusion in the intraplate Esmond-Dedham terrane. Post-orogenic granitic plutons appeared in the "indeterminate" belts, in the North American "intraplate" region, and over the Sebago block alike. Clearly, the tectonic framework that had led up to the orogeny no longer was operative.

SEQUENCE AND TIMING OF ACADIAN ACCRETION EPISODES

Stratigraphic relationships constrain the sequence and timing of the accretion events which took place during the Acadian orogeny. Localized deformation and metamorphism most likely affected portions of the "arc" regions before the onset of Acadian accretion (e. g., the Nashoba terrane); thus, regionally developed unconformities, dated paleontologically, probably give the best indication of broad-scale deformation attributable to plate collision. West of the collisional zone, in the Appalachian Basin region of the North American interior, foreland basins shadowed the development of the Acadian orogenic belt. The locations of foreland basins regularly shifted southwestwards during Middle to Late Devonian time (Dennison, 1985; Ettensohn, 1985, 1987); oblique convergence with a dextral component between the North American and

Avalon plates has been inferred (Ettensohn, 1987). Ettensohn (1987) calculated that relative dextral plate movement averaged ~7 cm/year during Late Devonian time.

The earliest Acadian unconformities are found on the Avalon block in Maine and New Brunswick, where no fossils younger than earliest Devonian (Gedinnian) are known (Fig. 85). Deposition continued on the North American block into Siegenian, Emsian, or even (in the northwestern "intraplate" region) Middle Devonian time (Boucot, 1968; Poole and others, 1970; McGregor, 1973). The first Acadian collision is therefore likely to have involved the northern portion of the Avalon plate and the Sebago block (leaving the North American plate untouched) and probably took place in Maine during earliest Devonian (Gedinnian) time. A thickened, uplifted Sebago/Avalon plate would have lain proximally to North America from Gedinnian time onwards, and could have supplied the easterly-derived Early Devonian sediments (Moench and Pankiwskyj, 1987; Bradley and Hanson, 1989) of the Kearsarge-Central Maine Synclinorium's Madrid and Carrabassett Formations.

If relative dextral plate movement between Avalon and both North American and Sebago occurred at 7 cm/year, collision between Avalon and North America would have followed during late Early Devonian (Siegenian to Emsian) time. Stratigraphic constraints agree with this prediction, since Emsian fossils are found in the youngest pre-Acadian strata of central New England (Fig. 85). Radiometric ages confirm an Early Devonian age for initial Acadian deformation: early syntectonic igneous rocks of central New England give ~400 Ma Rb-Sr whole-rock ages (Lyons and Livingston, 1977). The oldest sediments of the Catskill Delta, the Esopus shale (Ettensohn, 1985), are also of Emsian age, suggesting that commencement of foreland-basin deposition in New York occurred in consequence of North America-Avalon collision.

A return to carbonate deposition in the Catskill region (Onondaga Limestone) during early Middle Devonian (Eifelian) time reflected relative quiet on the continental margin. The final episode of Acadian accretion, collision of the Sebago block with North America, is marked by the termination of pre-Acadian deposition in southeastern Quebec during Middle Devonian

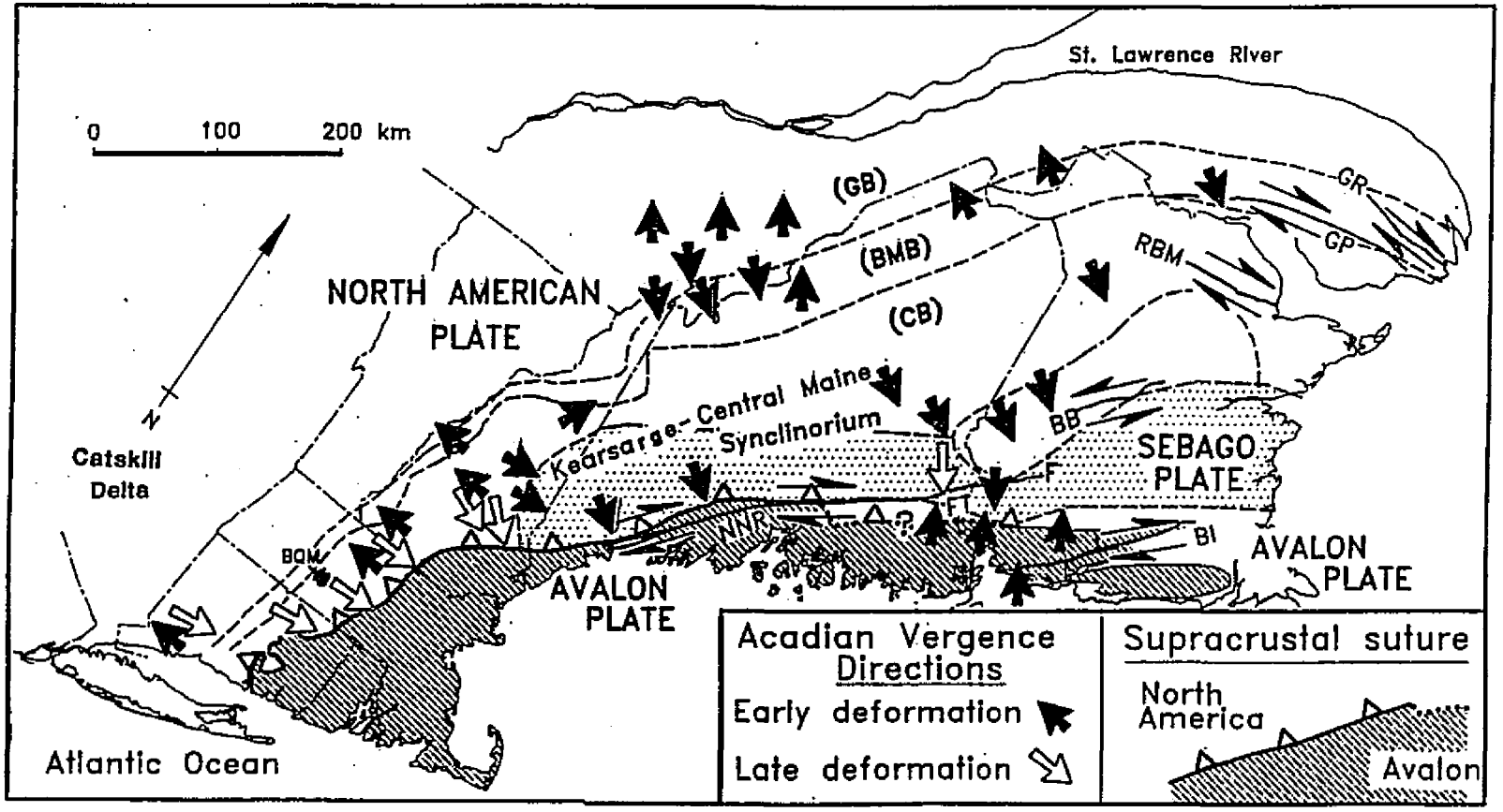

Fig. 90. Acadian structural features. Dominant Acadian vergence directions and selected strike-slip faults are shown. BB= Bamford Brook fault; BI= Belle Isle fault; BQM= Belchertown Quartz Monzonite; F= Fredericton fault; FT= Fredericton Trough; GP= Grand Pabos fault; GRF= Grande Rivière fault; NNR= Norumbega-Nonesuch River fault; RBM= Rocky Brook-Millstream fault. Basement blocks: GB= Grenville; BMB= Boundary Mountains; CB= Central. Structural data are compiled from: Bradley and Bradley (1988); Dieterich (1968); Eusden, Bothner, and Hussey (1987); Eusden (1989); Eusden (1990); Fyffe (1988); Fyffe and McLeod (1990); Hall and Robinson (1982); Hussey (1989); Keppie and others (1982); Ludman and Hopeck (1988); Ludman and Hopeck (in review); Ludman, Hopeck and Brock (in review); Marvinney (1989); McCutcheon (1981); Newberg (1986); Pease (1989); Robinson and others (1986); Rodgers (1981); Ruitenberg and McCutcheon (1987); Spencer and others (1989); Thompson and others (1968); Thompson (1985); Tremblay, St-Julien, and Labbé (1989); Trudel and Malo (1989).

(late Eifelian) time (Boucot, 1968). A post-Acadian molasse, the Mapleton Sandstone, was probably deposited slightly later (early Givetian, late Middle Devonian time) in northern Maine (Schopf in Boucot and others, 1964). The Sebago-North America collision coincided with the second (Hamilton) phase of the Catskill Delta and with the peak of clastic deposition in the New York region. Subsequently, the foreland basin migrated southwards (Ettensohn, 1985). The inferred sequence of accretion (and related depositional) events can be summarized this way: 1) Avalon-Sebago collision, during earliest Devonian (Gedinnian) time, in eastern Maine (provided source for Early Devonian sediments of central Maine); 2) Avalon-North American collision, during late Early Devonian (Emsian) time (first phase of Catskill deposition); 3) North America-Sebago collision, during Middle Devonian (late Eifelian) time (peak of deposition in the Catskill clastic wedge, New York region).

ACADIAN DEFORMATION

The two-subduction model forms a basis for predicting the principal tectonic vergence associated with each accretionary event during the Acadian orogeny. The Avalon-Sebago and Avalon-North America collisions should be primarily associated with west-vergent structures; the North America-Sebago collision with east-vergent structures. These predictions can be tested against the geologic record.

Fig. 90 shows Acadian-aged structural vergences compiled from the literature. The Avalon-North America supracrustal boundary in Maine and New Brunswick corresponds with a reversal of vergence direction. On the Avalon block, northwestern vergences predominate; on the North American side, southeastern vergences. These vergences accord with the presence of

oppositely-dipping subduction zones to the east and west of the Sebago block. Deeper into the North American plate (western Maine and Quebec), west vergences are common (Fig. 90). These areas contain older west-directed Taconian structures, many of which could have been reactivated during Acadian compression.

Tectonic stacking order can be used as an independent check on the sequence of plate accretions. Seismic data from the Sebago zone in eastern Maine suggest that shallow east-directed thrusts overlie buried west-vergent duplexes (Ludman and others, 1990). Late east-directed thrusting near the Sebago-Avalon boundary is suggested by the abundant west-dipping reflectors found there (Unger, Stewart, and Phillips, 1987). North American strata of the Kearsarge-Central Maine (KCM) Synclinorium, which overlie the Sebago block, were emplaced along southeast-directed thrusts (Ludman and Hopeck, 1988 and Ludman and Hopeck, in review). In eastern Maine near the Avalon-Sebago boundary, east-directed thrusts also emplaced strata of the Fredericton Trough (Fig. 90) on top of the Avalon block (St. Croix belt) (Ludman, Hopeck, and Brock, 1993). An Early Devonian Helderbergian brachiopod fauna has recently been recognized in slate of the Fredericton Trough in New Brunswick (A. J. Boucot, pers. commun., 1988), denoting a North American affinity for at least some Fredericton sediments. Thus, structural and seismic relationships seem to indicate that west-directed thrusting, presumably associated with the Avalon-Sebago collision, was followed by east-directed thrusts, along which North American strata were transported across the Sebago block and locally even onto the Avalon block. Emplacement of the North American strata over Sebago (shown schematically on Fig. 92) had been completed by 380-385 Ma (Middle Devonian), when they were intruded by a number of late syn-tectonic to post-tectonic plutons (Dallmeyer and van Breemen, 1981; Loiselle and others, 1983; Ayuso and others, 1984; Lux and Aleinikoff, 1985). Therefore, the sequence and timing of accretion events inferred from tectonic stacking order agrees with the stratigraphically-constrained sequence described earlier.

South of the Sebago block, the tectonic model predicts the earliest deformation to be west-

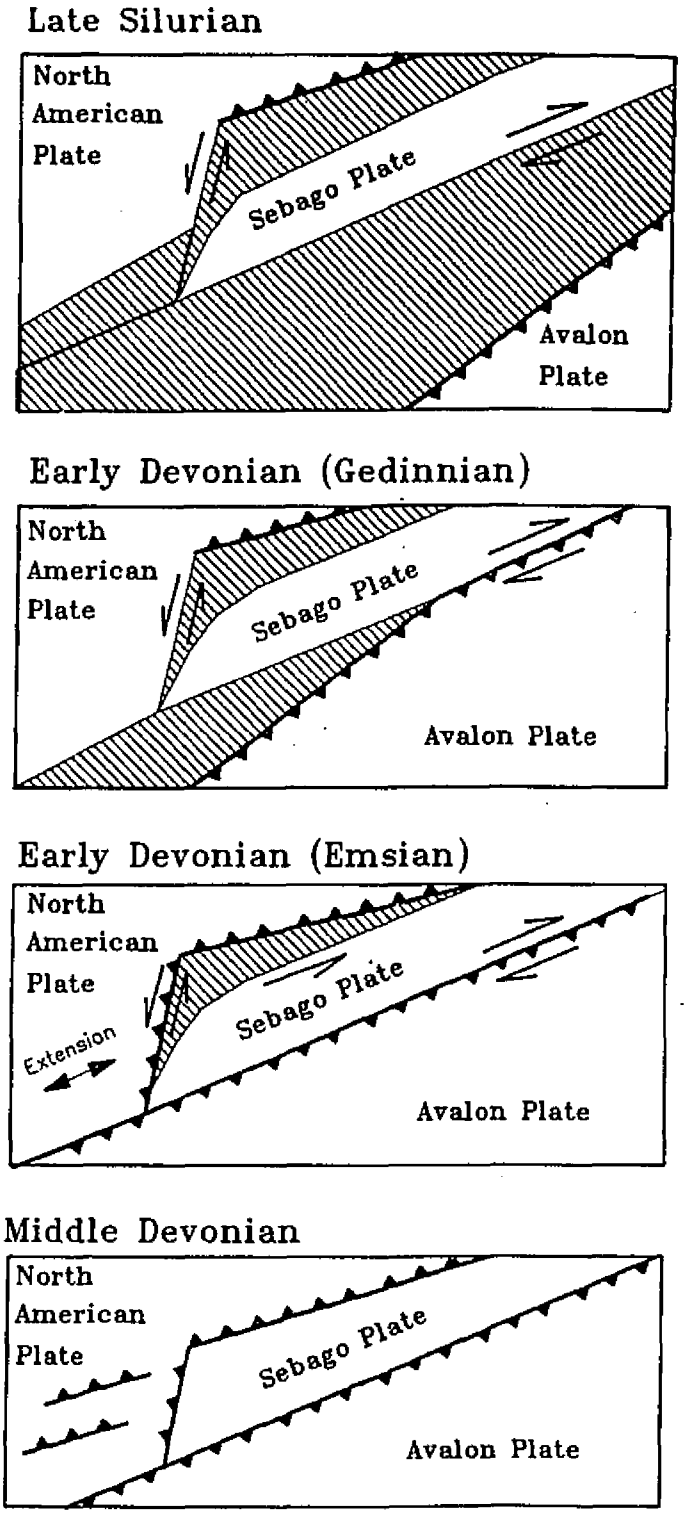

Fig. 91. Map-view schematic representation of the Acadian orogeny. Shading represents oceanic crust.

vergent structures associated with the Avalon-North America collision. Deformation of this kind has been recognized in central and southern New England (Fig. 90) (for example, Thompson and others, 1968; Hall and Robinson, 1982; Robinson and others, 1986). However, late Acadian structures of central Massachusetts and Connecticut verge to the east (Hall and Robinson, 1982; Rodgers, 1981). The location of these late east-vergent structures suggests that they are a continuation of structural trends further north related to the North America-Sebago collision (Fig. 90). This implies that closure of the basin that had separated the North American and Sebago plates resulted in substantial shortening of the North American plate to the southwest (Figs. 91 and 92).

Early west-vergent nappes of central New England were apparently emplaced in late Early Devonian time, during the Avalon-North America collision. East- vergent thrusting associated with the North America-Sebago collision probably followed during the early Middle Devonian (Eifelian). The intrusion of the Belchertown quartz monzodiorite (Fig. 90) at 380±5 Ma (U-Pb zircon) postdated early recumbent folding and preceded late (?) Acadian doming in central Massachusetts (Ashwal and others, 1979; Robinson and others, 1986). Its age is consistent with intrusion following North America-Sebago collision.

The data on vergence and stratigraphic constraints on ages of accretion lead to the following outline of events (Figs. 91 and 92):

1. Early Devonian (Gedinnian). Oblique collision between Sebago and Avalon begins in Maine, and is associated with west-vergent structures.

2. Late Early Devonian (Emsian). As collision progresses southwards, Avalon is accreted to North America along west-directed thrusts.

3. Middle Devonian. The basin between Sebago and North America is closed. North American strata are transported on east-directed thrusts. These thrusts propagate southwards and central and southern New England experiences severe shortening.

Not all Acadian-aged faults were thrusts. Strike-slip faults were an important component of Acadian deformation in some areas, particularly the Gaspé Peninsula (St. Julien, Malo, and

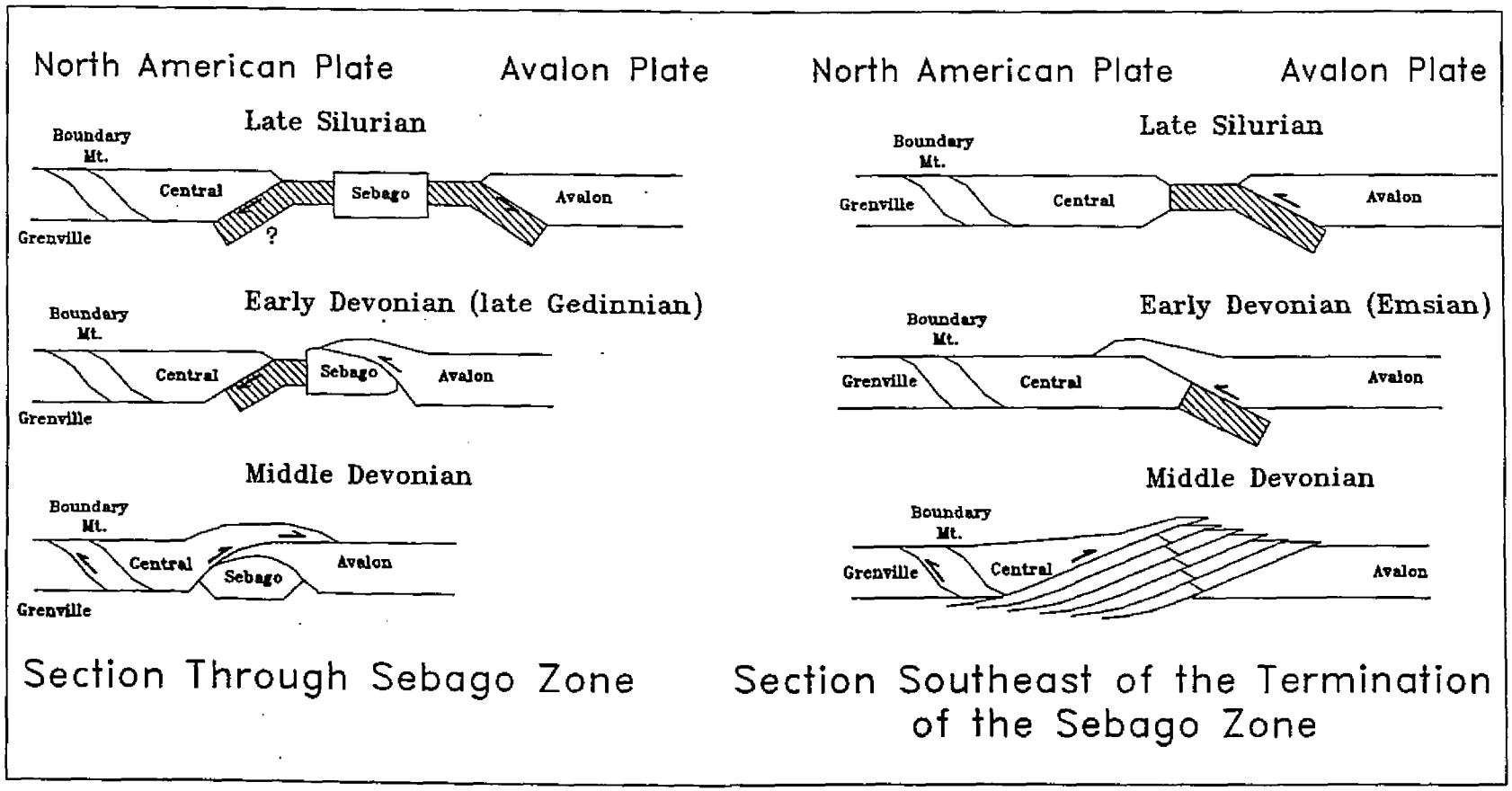

Fig. 92. Cross-sectional representation of the Acadian orogeny.

Kirkwood, 1988; Malo and Béland, 1989). Southeast-directed thrusting of Acadian age is also present in Gaspé. Both the thrusts and the dextral strike-slip faults are compatible with a north-west-southeast oriented maximum compressive stress (Trudel and Malo, 1989), and therefore can be attributed to the Sebago-North America collision.

A late Acadian strike-slip fault, the Norumbega-Nonesuch River fault, closely follows the southern Sebago block boundary in most of Maine (Fig. 90). Strike-slip faulting has also been recognized over the Sebago-Avalon boundary near the Maine-New Brunswick border, where the mapped Norumbega fault has swung northwards away from the block boundary (Ludman, pers. commun., 1991). Boundaries of the Sebago block are not well constrained in New Brunswick (see Part II), but a second strike-slip fault, Bamford Brook, follows the most northerly possible limit of the Sebago block there (Fig. 90). Interestingly, dextral motion is well documented on the Norumbega fault (Wones, 1978; Ludman, 1981; Johnson and Wones, 1984), while early Acadian sinistral motion occurred on the Bamford Brook fault (Fyffe, 1982). These fault motions raise the possibility that the Sebago block underwent northeastwards transport with respect to both the North American and Avalon plates during the Acadian orogeny. Cleavage orientations in strata overlying the Sebago block in New Brunswick support this proposition. Cleavage strikes ~030° over the northwestern part of the Sebago block, conforming to the inferred Sebago-North America boundary, but about 060° in the southern part, parallel to the Sebago-Avalon boundary. These orientations led Fyffe, Pajari, and Cherry (1981) to infer that the underlying crust had behaved as an independent block during the Acadian orogeny.

The geology of the Anatolian region in the eastern Mediterranean, related by Sengör and Yilmaz (1981), shares many of the elements that have been inferred here for Siluro-Devonian north-central Appalachians. The Anatolide/Tauride platform, a small plate like the Sebago block, was first accreted against a continental arc margin (analogous to the west boundary of Avalon) along the Pontide-Anatolide suture zone (Fig. 93). Later, this combined Eurasian plate collided with a second continent, the Arabian platform, along the Zagros-Bitlis suture zone (Fig. 93).

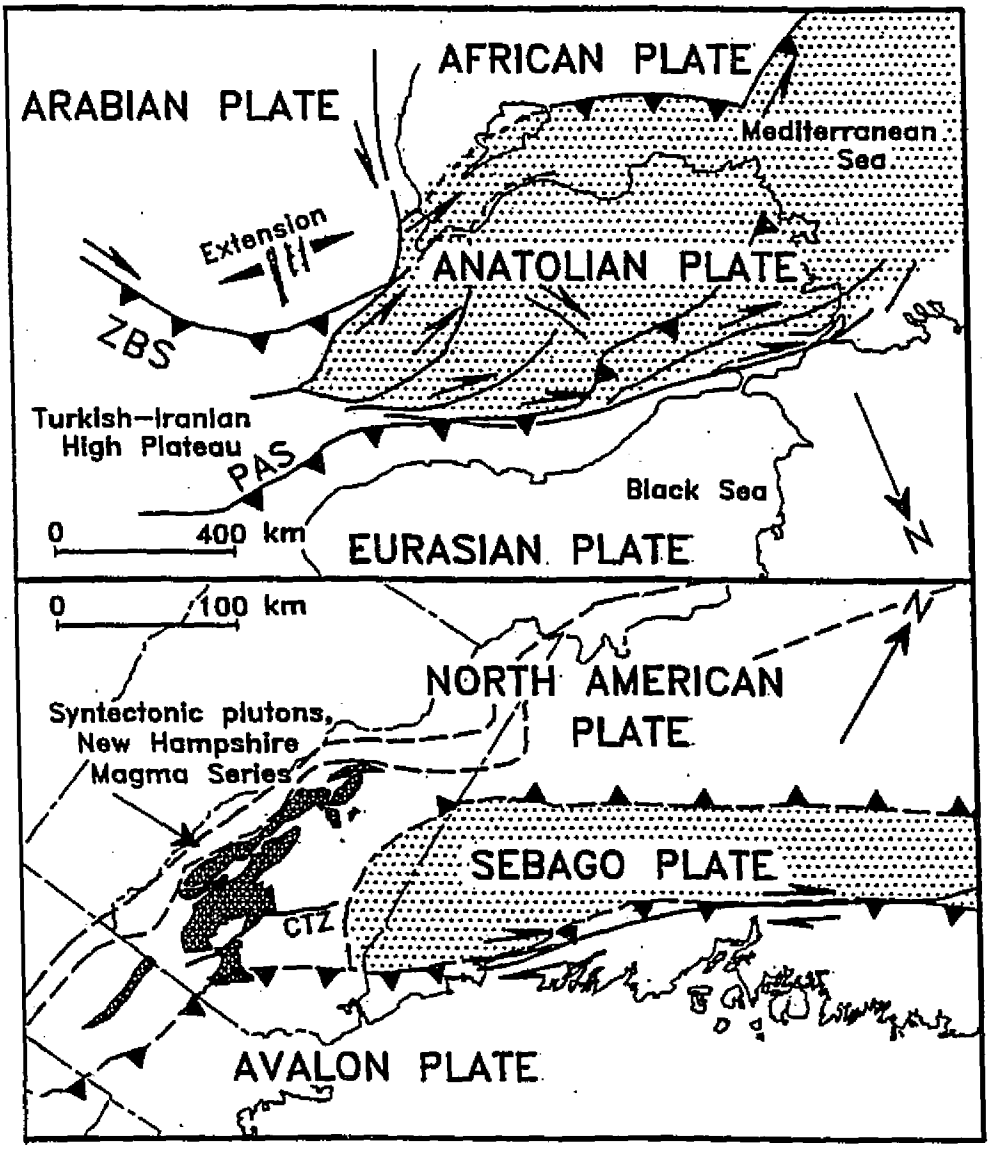

Fig. 93. Comparison of the present-day eastern Mediterranean with the proposed tectonic framework of the Acadian orogeny. Mediterranean geology based on Sengör and Yilmaz, 1981. ZBS= Zagros-Bitlis suture zone, PAS= Pontide-Anatolide suture zone. On North American plate, CTZ= Concord Tectonic Zone of Lyons, Boudette, and Aleinikoff (1982).

With continued convergence between the Arabian and Eurasian plates, the Anatolian plate (roughly coincident with the original Anatolide platform) became wedged out, and is still being extruded towards the west (Dewey and Sengör, 1979; Sengör and Yilmaz, 1981; Toksöz and others, 1989). These events seem to parallel the history of the north-central Appalachians, and suggest that the Anatolian region can serve as an analog for the Acadian orogeny.

Subsequent to the Eurasia-Arabia collision, and concurrent with extrusion of the Anatolian plate, extension occurred on the adjacent portion of the underthrust Arabian plate (Fig. 93). This extension resulted in alkaline volcanism (Sengör, Burke, and Dewey, 1978) and graben formation (Sengör and Yilmaz, 1981, quoting Sungurlu). Syn-Acadian intrusives of the New Hampshire Magma Series occur in the analogous region on the North American plate (Fig. 93). The chemistry of the Hardwick Tonalite, a member of the New Hampshire Magma Series, suggests that it was derived from an alkaline parent (Shearer and Robinson, 1988). Many plutons of the New Hampshire Magma Series were affected by the early west-vergent nappes and thrusts (Thompson and others, 1968; Nielson and others, 1976; Robinson and others, 1986), from which it appears that the peak of this magmatic event occurred early in the Acadian orogeny.

The Concord Tectonic Zone (Figs. 93 and 94) is a line marked by a series of possibly syn-Acadian mafic to ultramafic bodies (Lyons, Boudette, and Aleinikoff, 1982). The Concord Tectonic Zone projects southwest from the termination of the Sebago block, which suggests that these mafic/ultramafic plutons were intruded in an extensional environment related to the extrusion of the Sebago plate. The southeastern North American plate, adjacent to Sebago, seems to have been subjected to significant tension early in the Acadian orogeny (Fig. 91).

ACDADIAN METAMORPHISM

Metamorphism in orogenic belts can be related to tectonic thickening and to thermal perturbations. Relatively high metamorphic grades can be expected in areas of elevated heat flow and wherever tectonic thickening is greatest. Predictions about the distribution of Acadian metamorphic grades are inherent in the tectonic model outlined above and in Figs. 90 and 91. 1) According to the model, the Sebago block and the North American plate south of Sebago both underthrust continental arcs. These regions were at the core of the Acadian orogenic belt, and would have experienced the greatest degree of thickening. Due to the oblique nature of convergence, thickening related to collision with Avalon may have been relatively modest. 2) The arc regions of North America and Avalon would have undergone above average high heat flow and "Buchan" type metamorphism. 3) The North American plate south of the Sebago block experienced extension and associated high heat flow during Early Devonian time, along with west-verging deformation. In Middle Devonian time, additional shortening of this region was accompanied by east-vergent thrusting as Sebago was accreted to North America. (Figs. 91 and 92).

Fig. 94 shows the map distribution of Devonian metamorphic grades. In some areas, such as east of the Norumbega fault in southern Maine, uncertainty exists whether high-grade metamorphism is Acadian or whether it pertains to an older orogeny (Guidotti, 1989). Elsewhere, superimposed Late Paleozoic metamorphism or blanketing by younger sediments obscures the nature of Acadian metamorphism. Regions of "uncertain" grade are indicated on Fig. 94. In western New England, Acadian and Taconian metamorphic assemblages were distinguished by $^{40}Ar/^{39}Ar$ and K-Ar mineral ages (Clark and Kulp, 1968; Laird, Lanphere, and Albee, 1984; Sutter, Ratcliffe, and Mukasa, 1985; Dietsch and Sutter, 1987; Lanphere in Laird and Bothner, 1986; Burton, Kunk, and Ratcliffe, 1990; Hames, Sutter, and Ratcliffe, 1990).

The metamorphic record appears to conform well to the predictions based on the tectonic model:

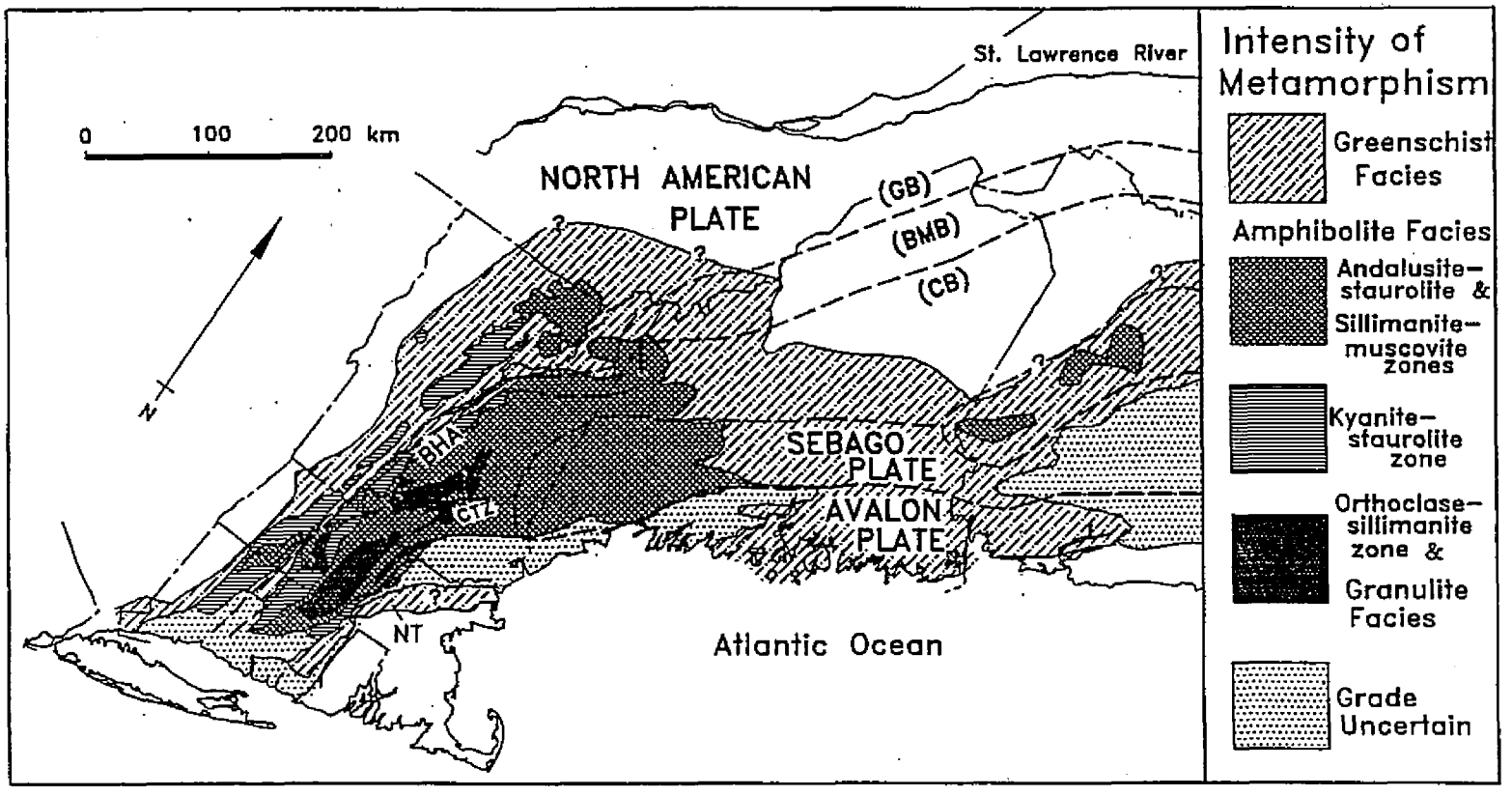

Fig. 94. Devonian metamorphism and thermal disturbance. Basement blocks: GM= Grenville; BMB= Boundary Mountains, CB= Central. NT= Nashoba terrane. CTZ= Concord Tectonic Zone of Lyons, Boudette, and Aleinikoff (1982). Metamorphic and thermal data are compiled principally from Fyffe (1982), Guidotti (in Osberg, Hussey, and Boone, 1985), Robinson (1986), and Williams and others (1972), with additional data from sources cited in the text, plus Currie (1988); Dietsch (1985); Eusden and Barreiro (1988); Fyffe, Barr, and Bevier (1988) (quoting Kalechitz, Lux, and Skinner); Hepburn, Olszewski, and Gaudette (1985); Nowlan, (1983); Rosenfeld and Eaton (1985); and Sutter and Ratcliffe, (1985).

1) In the modestly thickened northern portion of the region, peak metamorphic conditions tend to follow the buried Sebago block (Fig. 94). Acadian metamorphism dies out both to the east and west.

2) Low-pressure, greenschist to amphibolite facies metamorphism is found over most of the arc regions of North America and Avalon, though metamorphic grade falls off rapidly towards the interiors of the overriding plates (Fig. 94). The peak of metamorphism and related deformation appear to predate the Acadian orogeny in parts of the arc terranes (for instance, the Nashoba terrane; Zartman and Naylor, 1984). Nevertheless, lower-grade syn-Acadian metamorphism may also have occurred in these areas; for instance, the Carboniferous $^{40}Ar/^{39}Ar$ hornblende ages found in the Nashoba terrane (Hepburn, Lux, and Hill, 1987) suggest that metamorphic-range temperatures still existed there during the Acadian orogeny.

3) On the North American plate south of Sebago, metamorphic history strikingly corresponds with the model's predictions. Early metamorphism in the "extended" marginal region, associated with west-vergent deformation, was "Buchan" type and produced widespread andalusite (Robinson and others, 1986; Spear, 1986). Regions further west on the North American plate experienced a normal thermal gradient; Acadian metamorphism in western New England has been attributed to emplacement of hot thrust sheets from the east (Spear and Chamberlain, 1986; Spear, 1986; Chamberlain, 1986; Kohn and Spear, 1989). On the North American margin, early "Buchan" type metamorphism was followed by increased pressures ($\sim$6.3 kbar in central Massachusetts) and a lower thermal gradient (Tracy and Robinson, 1980; Robinson and others, 1982; Robinson and others, 1986). Peak metamorphic minerals in upper amphibolite and granulite grade rocks of central Massachusetts were overprinted by mylonitic fabrics that can be related to late east-vergent structures (Robinson and others, 1986).

The maximum amount of Acadian shortening took place within the North American block south of the Sebago zone. Kyanite-bearing metamorphic assemblages are essentially restricted to this region (Fig. 94). A welt of amphibolite-facies metamorphism continued to the northeast over

the Sebago block and adjoining regions (Fig. 94), but crustal thickening decreased dramatically north of Massachusetts (De Yoreo and others, 1989). Rocks presently exposed in central Massachusetts were buried at depths around 21 km (Robinson and others, 1986) while burial at around 10 km is indicated in western Maine (Holdaway, Dutrow, and Hinton, 1988).

Mélange, blueschist, and ophiolite, which have often led to recognition of subduction-related sutures, are largely absent from the Siluro-Devonian record of the north-central Appalachians. Devonian mélanges and olistostromes have been recognized in the Madrid and Carrabassett Formations of the Kearsarge-Central Maine Synclinorium and attributed to deposition in Acadian foredeep and accretionary prism settings (Hanson and Bradley, 1989; Bradley and Hanson, 1989). Blueschists are unknown. This is not surprising, since blueschist assemblages would be unlikely to survive metamorphic overprinting in the proposed two-subduction zone framework.

Recognition of ultramafic bodies along the postulated North America-Avalon suture would support the tectonic interpretation presented here, but such bodies might not be present. In the first place, ophiolite emplacement is an uncommon process and requires special conditions (for example, Edelman, 1988). Ophiolites do not seem to be created during continental collisions, but when found in continental sutures are relict from earlier events (Moores, 1982, p. 753). In addition, any ophiolite that had existed up to Early Devonian time may have been buried during the Acadian orogeny, as the Kearsarge-Central Maine Synclinorium was thrust over the Sebago block or as late east-directed thrusts emplaced North American strata over Avalon in central New England. Testing of the model proposed here will come with the continued mapping, geochemical investigation, paleomagnetic and paleontological study of the north-central Appalachians.

SUMMARY AND CONCLUSIONS, Part III

1. The major orogenic events of the north-central Appalachians (Penobscot, Taconic, and Acadian) can be understood as episodes in the accretion of the isotopically-defined basement blocks proposed in Part II.

2. The Central and most (or all ?) of the Boundary Mountains block were joined as the result of the late Cambrian-Early Ordovician Penobscottian orogeny of Maine. The composite Boundary Mountains-Central block, which experienced Middle to Late Ordovician arc and back-arc volcanic activity, was subsequently accreted to Grenville during the Taconian orogeny. Avalon remained paleomagnetically and faunally distinct from Silurian North America (Grenville-Boundary Mountains-Central plate) until Devonian time.

3. Igneous activity on the Avalon and the northern North American blocks occurred in two paired belts, which are disposed about the Sebago block with mirror symmetry. The inner belts consist of rocks with "indeterminate" to "arc" tectonic affinities; the outer belts, located in interior regions of the two plates, consist of "transitional" to "intraplate" igneous rocks. There are significant parallels in composition and in geologic setting between the "indeterminate" pre-Acadian igneous rocks and the early Tertiary volcanic rocks of the Patagonian Andes. Two pre-Acadian subduction zones can be inferred. One subduction zone dipped to the east under Avalon; the other, to the west under northern North America. K_2O, Rb, Rb/Sr, K/Nb, Rb/Nb, Ba/Nb and Zr/Nb of pre-Acadian volcanic rocks show gradients northwestwards from the North American plate boundary consistent with a deepening subduction zone. A basin separating North America and Sebago appears to have been closed by subduction under North America, implying separate existence of a Sebago plate before the Acadian orogeny. This Sebago block was later passively caught between the two colliding continental arcs.

4. The distribution of Acadian tectonic vergences and metamorphic grades, and the ages of Acadian clastic wedges and unconformities in Avalon and North America all appear to be consis-

tent with the following sequence of events (Figs. 90 and 91):

a. (Early Devonian- Gedinnian). Dextral-oblique collision between Avalon and Sebago in eastern Maine resulted in uplift and unconformity on the Avalon block. The thickened Sebago-Avalon block shed sediments westwards into the Kearsarge-Central Maine Synclinorium.

b. (late Early Devonian - Emsian). Collision progressed southwards until North America came in contact with Avalon. With continued convergence, most of the Sebago block was wedged out and transported northeastwards. The portion of North America southwest of Sebago experienced extension, intrusion, and high heat flow. West-directed thrusts brought these hot rocks deeper into North America. Earliest foreland basin deposition occurred in the Catskill Delta.

c. (Middle Devonian-late Eifelian). Sebago was accreted to North America. East-vergent structures associated with the North American subduction zone propagated southwards and helped accommodate continued shortening of the North American plate, as subduction of the basin separating Sebago and North America was completed. After a period of quiescence, Catskill Delta deposition in New York reached its peak, shadowing the growth of Acadian mountains.

The tectonic model for the Acadian orogeny presented here, founded upon isotopically-defined basement blocks, is consistent with a great number and variety of geological observations in the north-central Appalachians.

SUMMARY:

THE MANHATTAN PRONG IN CONTEXT OF APPALACHIAN OROGENIC HISTORY

The new findings in the Manhattan Prong presented in Part I can now be appraised from the standpoint of broad sweep of Northern Appalachian history, as presented in Parts II and III. In this summary, the Manhattan Prong is placed into regional perspective.

1. The Northern Appalachians are made up of five basement blocks. Three of these (Grenville, Central, and Avalon) are underlain by ancient continental material. Plutons in these blocks show broad ranges of isotopic characteristics, including many distinctly continental values. The intervening zones (Boundary Mountains and Sebago blocks) do not contain significant ancient crust. Plutons in these regions show a relatively narrow range of isotopic values. These two blocks are inferred to consist of Late Precambrian to Early Paleozoic arc terranes.

2. The Manhattan Prong lies on the Grenville block. The Fordham Gneiss represents the ancient continental basement, and partially retains billion-year-old textures and mineral assemblages.

3. The supercontinent containing North America (the Grenville block) underwent rifting during Late Precambrian to Early Cambrian time. The varied and complexly interfingered bimodal volcanic rocks, clastic sediments, and siliceous limestones of the Ned Mountain Formation were deposited during this interval.

4. A passive margin was established on eastern shore of North America during late Early Cambrian time. The dolomites of the Inwood Marble accumulated on the subsiding margin.

5. The Central and Boundary Mountains blocks were joined as the result of the late Cambrian to Early Ordovician Penobscottian orogeny of Maine. The combined Central-Boundary Mountains blocks developed a volcanic arc on its western margin.

6. North America (Grenville) began to collide with the Central-Boundary Mountains block around the beginning of Middle Ordovician time. Initial collision resulted in creation of a bulge in the North American margin. As the result of this bulge, an unconformity developed over the Inwood Marble.

7. Foundering of the margin followed uplift. The Walloomsac Schist was deposited in a euxinic, deepening basin. Metabasites in the Walloomsac Schist are probably mafic tuffs erupted from the approaching volcanic arc.

8. The northeastern Manhattan Prong was overthrust by the Central block (Hartland terrane) and buried to a depth of 40 kilometers or more early in the orogeny. High-pressure granulite assemblages developed, peaking with coexisting spinel + quartz + garnet + cordierite + rutile.

9. Moderate uplift followed the early high-grade metamorphism, and upper-amphibolite grade (M_2) metamorphism accompanied later phases of Taconian deformation. Early mineral assemblages were almost obliterated.

10. A volcanic arc was active on the western margin of the Avalon block during Silurian time. In Late Silurian to Early Devonian time, the Avalon block collided with the Sebago block. This was the first stage of accretion associated with the Acadian orogeny.

11. A second volcanic arc developed on the eastern margin of North America (Grenville-Boundary Mountains-Central block) during Late Silurian or Early Devonian time. This arc stood from New Hampshire through New Brunswick and faced the Sebago block.

12. During Early to Middle Devonian time, basins between North America and Avalon and between North America and Sebago were closed by subduction down the two trenches. Significant dextral transpression probably accompanied subduction. Collision led to intense metamorphism and deformation, especially in central and southern New England. The interiors of the two outlying plates (Grenville and Avalon) were relatively unaffected. To the west, the Manhattan Prong experienced little or no deformation.

13. As post-Acadian dextral motion between North America and Avalon continued into Mississippian time, the Manhattan Prong experienced extension. Water-rich magmas of the Carboniferous granite/pegmatite suite syntectonically infiltrated the Manhattan Prong, provoking extensive hydrothermally-driven greenschist- to middle-amphibolite facies M_3 retrogression.

14. The Alleghenian orogeny was the result of collision between North America and Africa during Carboniferous time. During the Pennsylvanian period, east-directed, low-angle thrusts developed under lower-greenschist facies conditions in the northern Manhattan Prong.

15. With the Alleghenian orogeny, the Wilson cycle which began with the deposition of the Ned Mountain Formation came to completion. During Mesozoic time, North America split off from a supercontinent yet again. The lamprophyre dike that intruded the Manhattan Prong at this stage marks the opening of a new Wilson cycle, and is analogous to the Eocambrian metabasite dikes that occur in the Fordham Gneiss.

REFERENCES CITED

Aaron, J. M., 1969, Petrology and origin of the Hardyston Quartzite (Lower Cambrian) in eastern Pennsylvania and western New Jersey: in Subitzky, S., ed., Geology of Selected Areas in New Jersey and Eastern Pennsylvania and Guidebook Excursions, Annual Meeting of the Geological Society of America, p. 21-34, Rutgers University Press, New Brunswick, New Jersey.

Agar, W. M., 1934, Granites and related intrusions of western Connecticut: American Journal of Science, v. 27, p. 354-373.

Alavi, M., 1975, Geology of the Bedford Complex and surrounding rocks, southeast New York: Contribution No. 24 (Ph. D. thesis), Department of Geology and Geography, University of Massachusetts, Amherst, Massachusetts, 117 p.

Aleinikoff, J. N., 1978, Structure, petrology, and U-Th-Pb geochronology in the Milford quadrangle, New Hampshire: Ph. D. thesis, Dartmouth College, 247 p.

Aleinikoff, J. N., 1985, Isotopic age and morphologic evidence for the age of the Fordham Gneiss: American Journal of Science, v. 285, p. 459-479.

Aleinikoff, J. N., and Grauch, R. I., 1990, U-Pb geochronologic constraints on the origin of a unique monazite-xenotime gneiss, Hudson Highlands, New York: American Journal of Science, v. 290, p. 522-546.

Aleinikoff, J. N., Grauch, R. I., Simmons, K. R., and Nutt, C. J., 1982, Chronology of metamorphic rocks associated with uranium occurrences, Hudson Highlands, New York-New Jersey, Geological Society of America Abstracts with Programs, v. 14, p. 1.

Aleinikoff, J. N., and Moench, R. H., 1985, Metavolcanic stratigraphy in northern New England--U-Pb zircon geochronology: Geological Society of America Abstracts with Programs, v. 17, p. 1.

Aleinikoff, J. N., and Moench, R. H., 1987, U-Pb geochronology and Pb isotopic systematics of plutonic rocks in northern New Hampshire: Ensimatic vs. ensialic sources: Geological Society of America Abstracts with Programs, v. 19, p. 1.

Aleinikoff, J. N., Moench, R. H., and Lyons, J. B., 1985, Carboniferous U-Pb age of the Sebago batholith, southwestern Maine: Geological Society of America Bulletin, v. 96, p. 990-996.

Aleinikoff, J. N., Ratcliffe, N. M., Burton, W. C., and Karabinos, P., 1990, U-Pb ages of Middle Proterozoic igneous and metamorphic events, Green Mountains, Vermont: Geological Society of America Abstracts with Programs, v. 22, p. 1.

Allison, I., and Ferguson, L. K., 1991, Agalmatolite: Indicator of Precambrian weathering?: Geological Association of Canada-Mineralogical Association of Canada-Society of Economic Geologists Program with Abstracts, v. 16, p. A2

Ando, C. J., Czuchra, B. L., Klemperer, S. L., Brown, L. D., Cheadle, M. J., Cook, F. A., Oliver, J. E., Kaufman, S., Walsh, T., Thompson, J. B, Jr., Lyons, J. B., and Rosenfeld, J. L., 1984, Crustal profile of mountain belt: COCORP deep seismic reflection profiling in New

England Appalachians and implications for architecture of convergent mountain chains: American Association of Petroleum Geologists Bulletin, v. 68, p. 819-837.

Andrew, A. S., Loiselle, M. C. and Wones, D. R., 1983, Granitic plutonism as an indicator of microplates in the Paleozoic of central and eastern Maine, Earth and Planetary Science Letters, v. 66, p. 151-165.

Armstrong, R. L., 1970, Geochronology of Tertiary igneous rocks, eastern Basin and Range Province, western Utah, eastern Nevada, and vicinity, U.S.A.: Geochimica et Cosmochimica Acta, v. 34, p. 203-232.

Armstrong, R. L., Taubeneck, W. H., and Hales, P. O., 1977, Rb-Sr and K-Ar geochronometry of Mesozoic granitic rocks and their Sr isotopic composition, Oregon, Washington, and Idaho: Geological Society of America Bulle tin, v. 88, p. 397-411.

Arth, J. G., and Ayuso, R.A., 1985, The Northeast Kingdom batholith, Vermont: Geochronology and isotopic composition of Sr, Nd, and Pb: Geological Society of America Abstracts with Programs, v. 17, p. 515.

Ashwal, L. D., Leo, G. W., Robinson, P., Zartman, R. E., and Hall, D. J., 1979, The Belchertown quartz monzodiorite pluton, west-central Massachusetts: a syntectonic Acadian intrusion: American Journal of Science, v. 279, p. 936-969.

Atherton, M. P., Pitcher, W. S., and Warden, V., 1983, The Mesozoic marginal basin of central Peru: Nature, v. 305, p. 303-306.

Ayuso, R. A., 1986, Lead-isotopic evidence for distinct sources of granite and for distinct basements in the northern Appalachians, Maine: Geology, v. 14, p. 322-325.

Ayuso, R. A. and Arth, J. G., 1985, Origin and evolution of calcalkaline plutons in the Northeast Kingdom batholith, Vermont: Geological Society of America Abstracts with Programs, v. 17, p. 516.

Ayuso, R. A., Arth, J. G., Sinha, A. K., Carlson, J., and Wones, D. R., 1984, Comparative geochronology in the reversely zoned plutons of the Bottle Lake Complex, Maine: U-Pb on zircons and Rb-Sr on whole rocks: Contributions to Mineralogy and Petrology, v. 88, p. 113-125.

Ayuso, R. A., Horan, M. F., and Criss, R. E., 1988, Pb and O isotopic geochemis try of granitic plutons in northern Maine: American Journal of Science, v. 288-A, p. 421-460.

Ayuso, R. A., Sinha, A. K., Arth, J. G., and Wones, D. R., 1982, Pb and Sr isotopic variation and constraints on granite sources in the Merrimack Synclinorium: Bottle Lake Complex, Maine: Geological Society of America Abstracts with Programs, v. 14, p. 436.

Badger, R. L., Sinha, A. K., and Gottfried, D., 1988, Failed and successful rifting in the Central Appalachians: nature of Late Precambrian magmatism: Geological Society of American Abstracts with Programs, v. 20, p. A124.

Bailey, L. W., and Matthew, G. R., 1876, Summary report of geological observations in New Brunswick: Geological Survey of Canada, Report of Progress for 1874-75, p. 84-89.

Baker, B. H., Goles, G. G., Leeman, W. P., and Lindstrom, M. M., 1977, Geochemistry and petrogenesis of a basalt-benmoreite-trachyte suite from the southern part of the Gregory Rift, Kenya: Contributions to Mineralogy and Petrology, v. 64, p. 303-332.

Baker, P. Rea, W., Skarmeta, J., Caminos, R., and Rex, D., 1981, Igneous history of the Andean Cordillera and Patagonian Plateau around latitude 46°S: Philosophical Transactions of the Royal Society, London, v. 303, p. 105-149.

Balk, R., 1936, Structural and petrologic studies in Dutchess County, New York: Structural and petrologic studies in Dutchess County, New York: Part I-Geologic structure of sedimentary rocks: Geological Society of America Bulletin, v. 47, p. 685-774.

Barosh, P. J., and Moore, G. E. Jr., 1988, The Paxton Group of southeastern New England: United States Geological Survey Bulletin 1814, 18 p.

Barreiro, B. and Aleinikoff, J. N., 1985, Sm-Nd and U-Pb isotopic relationships in the Kinsman Quartz Monzonite, New Hampshire: Geological Society of America Abstracts with Programs, v. 17, p. 3.

Barreiro, B. A., 1984, Lead isotopes and Andean magmagenesis: in Harmon, H. S. and Barreiro, B. A., eds., Andean Magmatism, Chemical and Isotopic Constraints: Shiva Publishing Limited, Cheshire, U. K., p. 21-30.

Barth, T. F. W., 1936, Structural and petrologic studies in Dutchess County, New York. Part II: Petrology and metamorphism of the Paleozoic rocks: Geologic Society of America Bulletin, v. 47, p. 775-850.

Barton, J. M. Jr., and Doig, R., 1973, Time-stratigraphic relationships east of the Morin anorthosite pluton, Quebec: American Journal of Science, v. 273, p. 376-384.

Barton, J. M. Jr., and Doig, R., 1974, Temporal relationships of rock units in the Shawinigan area, Grenville Province, Quebec: Canadian Journal of Earth Science, v. 11, p. 686-690.

Bell, G. K., 1936, Poundridge granite: Geological Society of America Proceedings (abstract), p. 65.

Belt, E. S., 1968, Post-Acadian rifts and related facies, eastern Canada, in Zen, E-an, White, W. S., Hadley, J. B. and Thompson, J. B. Jr., eds., Studies of Appalachian geology: Northern and maritime: New York, Interscience Publishers, p. 95-113.

Berdan, J. M., 1970, American ostracode zonation: in Berry, W. B. N., and Boucot, A. J., eds., Correlation of the North American Silurian Rocks: Geological Society of America Special Paper 102, p. 39-40.

Berdan, J. M., 1983, Biostratigraphy of Upper Silurian and Lower Devonian ostracodes in the United States: in Maddocks, R. F., ed., Applications of Ostracoda: Proceedings of the 8th International Symposium on Ostracoda, July 26-28, 1982, University of Houston, p. 313-337.

Berkey, C. P., 1907, Structural and stratigraphic features of the basal gneisses of the Highlands: New York State Museum Bulletin, v. 107, p. 361-378.

Berkey, C. P., 1911, Geology of the New York City (Catskill) Aquaduct: New York State Museum Bulletin, p. 146-283.

Berkey, C. P., and Rice, M., 1921, Geology of the West Point quadrangle, New York: New York State Museum Bulletins 225, 226, 152 p.

Berry, W. B. N. and Boucot, A. J., 1970, eds., Correlation of the North American Silurian rocks: Geological Society of America Special Paper 102, 289 p.

Bevier, M. L., 1987, Pb isotopic ratios of Paleozoic granitoids from the Miramichi terrane, New Brunswick, and implications for the nature and age of the basement rocks: in Radiogenic age and isotopic studies: Report 1: Geological Survey of Canada, Paper 87-2, p. 43-50.

Bevier, M. L., 1988a, U-Pb geochronologic studies of igneous rocks in New Brunswick, in Abbott, S. A., ed., Thirteenth annual review of activities: New Brunswick Department of Natural Resources and Energy, Minerals and Energy Division, Information Circular 88-2, p. 134-140.

Bevier, M. L., 1988b, Lead isotopic evidence for distinct sources of granite and for distinct basements in the northern Appalachians, New Brunswick: Geological Association of Canada Program with Abstracts, v. 13, p. A10

Bevier, M. L., and Barr, S. M., 1990, U-Pb age constraints on the stratigraphy and tectonic history of the Avalon terrane, New Brunswick, Canada: Journal of Geology, v. 98, p. 53-63.

Bevier, M. L., and Whalen, J. B., 1990, Tectonic significance of Silurian magmatism in Canadian Appalachians: Geology, v. 18, p. 411-414.

Bevier, M. L., White, C. E., and Barr, S. M., 1990, Late Precambrian U-Pb ages for the Brookville Gneiss, southern New Brunswick: Journal of Geology, v. 98, p. 955-965.

Bédard, J. H., 1986a, Pre-Acadian magmatic suites of the southeastern Gaspé Peninsula: Geological Society of America Bulletin, v. 97, p. 1177-1191.

Bédard, J. H., 1986b, Les suites magmatiques Paléozoïques de la Gaspésie: Ministère de l'Energie et des Ressources du Québec ET84-09, 111 p.

Béland, J., 1958, Région d'Oak Bay: Ministère des Mines du Québec RP-375, 12 p.

Bélanger, J., 1980, Les roches volcaniques du synclinal du Mont Alexandre: Ministère de l'Energie et des Ressources du Québec Rapport Préliminaire, 7 p.

Bélanger, J., 1982, Roches volcaniques Dévoniennes de la bande de Ristigouche: Ministère de l'Energie et des Ressources, Québec, Rapport Intérimaire DP-939, 13 p.

Billings, M. P., and Cleaves, A. B., 1934, Paleontology of the Littleton area, New Hampshire: American Journal of Science, 5th series, v. 28, p. 412-438.

Bird, J. M., and Dewey, J. F., 1970, Lithospheric plate-continental margin tectonics and the evolution of the Appalachian orogen: Geological Society of America Bulletin, v. 81, p. 1031-1060.

Bohlen, S. R., Dollase, W. A., and Wall, V. J., 1986, Calibration and applications of spinel equilibria in the system FeO-Al_2O_3-SiO_2: Journal of Petrology, v. 27, p. 1143-1156.

Bohlen, S. R., Wall, V. J., and Boettcher, A. L., 1983, Experimental investigations and geological applications of equilibria in the system FeO-TiO_2-Al_20_3-SiO_2-H_20: American Mineralogist, v. 68, p. 1049-58.

Boone, G. M., 1970, The Fish River Lake Formation and its environments of deposition; in Shorter contributions to Maine geology: Maine Geological Survey Bulletin, v. 23, p. 27-41.

Boone, G. M., and Boudette, E. L., 1989, Accretion of the Boundary Mountains terrane within the northern Appalachian orthotectonic zone: in Horton, J. W., Jr., and Rast, N., eds, Mélanges and Olistostromes of the U. S. Appalachians: Geological Society of America Special Paper 228, p. 17-42.

Bothner, W. A., Boudette, E. L., Fagan, T. J., Gaudette, H. E., Laird, J., and Olszewski, W. J., 1984, Geologic framework of the Massabesic Anticlinorium and the Merrimack Trough, southeastern New Hampshire: in Hanson, L. S., ed., Geology of the Coastal Lowlands, Boston, MA to Kennebunk, ME, New England Intercollegiate Geological Conference, Salem, Massachusetts, p. 186-206.

Bottino, M. L., and Fullagar, P. D., 1966, Whole-rock Rb-Sr age of the Silurian-Devonian boundary in northeastern North America: Geological Society of America Bulletin, v. 77, p. 1167-1175.

Bottino, M. L., and Fullagar, P. D., 1966, Whole-rock Rb-Sr age of the Silurian-Devonian boundary in northeastern North America: Geological Society of America Bulletin, v. 77, p. 1167-1175.

Boucot, A. J., 1962, Appalachian Siluro-Devonian: in Coe, K., ed., Some Aspects of the Variscan Fold Belt, 9th Inter-University Geological Congress, Manchester University Press, p. 155-163.

Boucot, A. J., 1968, Silurian and Devonian of the northern Appalachians: in Zen, E-An, White, W. S., Hadley, J. B., and Thompson, J. B. Jr., eds., Studies of Appalachian Geology: Northern and Maritime, Interscience Publishers, New York, p. 83-94.

Boucot, A. J., 1975, Evolution and extinction rate controls: Elsevier, Amsterdam, Oxford and New York, 427 p.

Boucot, A. J., and Johnson, J. G., 1967, Appalachian province Early Devonian palaeogeography and brachiopod zonation: in Oswald, D. H., ed., International Symposium on the Devonian System, v. II, Alberta Society of Petroleum Geologists, p. 1255-1267.

Boucot, A. J., and Rumble, D., III, 1980, Regionally metamorphosed (high sillimanite zone, granulite facies) Early Devonian brachiopods from the Littleton Formation of New Hampshire: Journal of Paleontology, v. 54, p. 188-195.

Boucot, A. J., and Thompson, J. B. Jr., 1963, Metamorphosed Silurian brachiopods from New Hampshire: Geological Society of America Bulletin, v. 74, p. 1313-1334.

Boucot, A. J., Field, M. T., Fletcher, R., Forbes, W. H., Naylor, R. S., and Pavlides, R., 1964,

Reconnaissance bedrock geology of the Presque Isle quadrangle, Maine: Maine Geological Survey, Quadrangle Mapping Series no. 2, 123 p.

Boucot, A. J., Johnson, J. G., and Talent, J. A., 1967, Lower and Middle Devonian faunal provinces based on brachiopoda: in Oswald, D. H., ed., International Symposium on the Devonian System, v. II, Alberta Society of Petroleum Geologists, p. 1239-1254.

Boucot, A. J., Johnson, J. G., Harper, C., and Walmsley, V. G., 1966, Silurian brachiopods and gastropods of southern New Brunswick: Geological Survey of Canada Bulletin 140, 45p.

Boucot, A. J., MacDonald, G. J. F., Milton, C., and Thompson, J. B. Jr., 1958, Metamorphosed Middle Paleozoic fossils from central Massachusetts, eastern Vermont, and western New Hampshire: Bulletin of the Geological Society of America, v. 69, p. 855-870.

Bourque, P.-A., and Lachambre, G., 1980, Stratigraphie du Silurien et du Dévonien basal du sud de la Gaspésie: Ministère de l'Energie et des Ressources du Québec Etude Spéciale ES-30, 123 p.

Bourque, P.-A., Gosselin, C., and Malo, M., 1988, Late Ordovician to Mid- Devonian paleogeography of the Gaspé-Témiscouata basin, Northern Appalachians: Geological Association of Canada Program with Abstracts, v. 13, p. A12-13.

Bowes, D., and Langer, A., 1969, Polyphase deformation in the schists of the Bronx, New York City: in Alexandrov, E., ed., Symposium on the New York City Group of Formations, 40th Annual Meeting of the New York State Geological Association, Queens College Press, Flushing, New York, p. 17-31.

Bradley, D., 1983, Tectonics of the Acadian orogeny in New England: Journal of Geology, v. 91, p. 381-400.

Bradley, D., and Bradley, L. M., 1988, Early Acadian W-directed thrusting in the Connecticut Valley-Gaspé Synclinorium, northern Maine, and its bearing on northern Appalachian plate kinematics: Geological Society of America Abstracts with Programs, v. 20, p. 9.

Bradley, D., and Hanson, L., 1989, Mélanges and turbidite facies of the Madrid Formation, Central Maine: in Berry, A. W. Jr., ed., Guidebook for Field Trips in Southern and West-Central Maine, New England Intercollegiate Geological Conference, Farmington, Maine, p. 183-199.

Bradley, D. C., 1982, Subsidence in late Paleozoic basins in the northern Appalachians: Tectonics, v. 1, p. 107-123.

Bradley, D. C., 1983, Tectonics of the Acadian orogeny in New England and adjacent Canada: American Journal of Science, v. 91, p. 381-400.

Brandon, J. P., 1981, Geology of the Ridgefield area, southwestern Connecticut and southeastern New York (M.S. thesis): Department of Geology and Geography, University of Massachusetts, 125 p.

Brock, P. C., 1989, Stratigraphy of the northeastern Manhattan Prong, Peach Lake quadrangle, New York - Connecticut: in Weiss, D., ed., Field Trip Guidebook, 61st Annual Meeting, New York State Geological Association, Middletown, New York, p. 1-27.

Brock, P. C., and Brock, P. W. G., 1981, Metamorphosed emery assemblages of the Croton Falls Mafic Complex, S. E. New York: Geological Society of America Abstracts with Programs, v. 13, p. 124.

Brock, P. C., and Brock, P. W. G., 1985b, Carboniferous (D_6) and Permian? (D_7) shear zones of the northern Manhattan Prong, S.E. N.Y.: Geological Society of America Abstracts with Programs, v. 17, p. 8.

Brock, P. C., Brueckner, H. K., and Brock, P. W. G., 1985, On the timing of orogenic events in the northern Manhattan Prong, S.E. N.Y.: Geological Society of America, Abstracts with Programs, v. 17, p. 7.

Brock, P. W. G., and Brock, P. C., 1983, The Fordham Gneiss of the northern part of the Manhattan Prong compared with the adjacent Highlands Gneiss, southeast N. Y.: Geological Society of America Abstracts with Programs, v. 15, p. 169.

Brock, P. W. G., and Brock, P. C., 1985a, The timing and nature of the Paleozoic deformation in the northern part of the Manhattan Prong, southeast New York: in Tracy, R.J., ed., Guidebook for fieldtrips in Connecticut and adjacent areas of New York and Rhode Island, 77th Annual Meeting, New England Intercollegiate Geological Conference, Yale University, New Haven, Connecticut, p. 241-275.

Brock, P. W. G., and Brueckner, H. K., 1978, Taconic, Acadian and younger deformation in the Croton Falls area, S.E. New York: Geological Society of America Abstracts with Programs, v. 10, p. 34.

Brock, P. W. G., and Mose, D. G., 1979, Taconic and younger deformation and metamorphism in the Croton Falls area, southeastern New York, Geological Society of America Bulletin, v. 90, Part I, p.705-707, and Part II, p. 1158-1195.

Brookins, D. G., 1976, Geochronologic contributions to stratigraphic interpretation and correlation in the Penobscot Bay area, eastern Maine: in Page, L. R., ed., Contributions to the Stratigraphy of New England, Geological Society of America Memoir 148, p. 129-145.

Brookins, D. G., 1980, Geochronologic investigations in central Connecticut: a reexamination of the pre-Triassic basement rocks: in Contributions to Geochronology in Connecticut II, State Geological and Natural History Survey of Connecticut, Report of Investigations No. 10, p. 21-35.

Brookins, D. G., and Spooner, C. M., 1970, The isotopic ages of the Oak Point and Stonington granites, eastern Penobscot Bay, Maine: Journal of Geology, v. 78, p. 570-576.

Brookins, D. G., Berdan, J. M. and Stewart, D. B., 1973, Isotopic and paleontologic evidence for correlating three volcanic sequences in the Maine Coastal Volcanic Belt, Geological Society of America Bulletin, v. 84, p. 1619-1628.

Burton, W. C., Kunk, M. J., and Ratcliffe, N. M., 1990, Muscovite and microcline $^{40}Ar/^{39}Ar$ ages from the Taconian- and Acadian- overprinted central Green Mountains, Vermont: Geological Society of America Abstracts with Programs, v. 22, p. 7.

Butt, K. A., Cherry, M. E., Cormier, R. F., and Fyffe, L. R., 1976, Igneous rocks of southwestern

New Brunswick: in Pajari, G. E., Jr., ed., Field Guide to the Geology and Plutonic Rocks of Southwestern New Brunswick and the Penobscot Bay Area of Maine, International Geological Correlation Program, v. 1, p. 1-38.

Button, A., 1979, Early Proterozoic weathering profile on the 2200 million year old Hekpoort Basalt, Pretoria Group, South Africa: preliminary results: University of Witwatersrand, Johannesburg, South Africa, Economic Geology Research Unit Information Circular #35, 38 p.

Button, A., and Tyler, N., 1981, The character and economic significance of Precambrian paleo-weathering and erosion surfaces in southern Africa: Economic Geology, v. 75, p. 686-709.

Carroll, W. E., Schneiderman, J. S., and Noblett, J. B., 1989, Petrology of the Ordovician (?) Barnard and Silurian Shaw Mountain amphibolites, Chester dome, Vermont: Geological Society of America Abstracts with Programs, v. 21, p. A285.

Cartwright, I., and Barnicoat, A. C., 1986, The generation of quartz-normative melts and corundum-bearing restites by crustal anatexis: petrogenetic modelling based on an example from the Lewisian of north-west Scotland: Journal of Metamorphic Geology, v. 4, p. 79-99.

Chamberlain, C. P., 1986, P-T paths in the root zone of the Fall Mountain nappe: constraints on the thermal budget of Acadian metamorphism: Geological Society of America Abstracts with Programs, v. 18, p. 8.

Chang, P. H., Ern, E. H. Jr., and Thompson, J. B. Jr., 1965, Bedrock geology of the Woodstock quadrangle, Vermont: Vermont Geological Survey Bulletin No. 29, 65 p.

Chase, P. J., and Brock, P. W. G., 1976, Sillimanite and sillimanite-orthoclase isograds in the Croton Falls quadrangle, southeast New York: Geologic Society of America Abstracts with Programs, v. 8, p. 149-150.

Chatterjee, N. D., and Froese, E., 1975, A thermodynamic study of the pseudobinary join muscovite-paragonite in the system $KAlSi_3O_8$-$NaAlSi_3O_8$- Al_2O_3-SiO_2-H_2O: American Mineralogist, v. 60, p. 985-993.

Cheatham, M. M., Olszewski, W. J., Jr., and Gaudette, H. E., 1985, The Chain Lakes Massif, west-central Maine; Northern Appalachian basement or suspect terrane?: Geological Society of America Abstracts with Programs, v. 17, p. 543.

Chiarenzelli, J. R., and McLelland, J. M., 1990, Age, subdivision, and origin of granitic rocks of the Adirondack Highlands, northern New York: Geological Society of America Abstracts with Programs, v. 22, p. 7.

Clark, G. S., and Kulp, J. L., 1968, Isotopic age study of metamorphism and intrusion in western Connecticut and southeastern New York: American Journal of Science, v. 266, p. 865-894.

Clark, G. S., and Kulp, J. L., 1968, Isotopic age study of metamorphism and intrusion in western Connecticut and southeastern New York: American Journal of Science, v. 266, p. 865-894.

Clarke, G. L., and Powell, R., 1991a, Proterozoic granulite facies metamorphism in the southeastern Reynolds Range, central Australia: geological context, P-T path and overprinting relationships: Journal of Metamorphic Geology, v. 9, p. 267-281.

Clarke, G. L., and Powell, R., 1991b, Decompressional coronas and symplectites in granulites of the Musgrave Complex, central Australia: Journal of Metamorphic Geology, v. 9, p. 441-450.

Clarke, G. L., Powell, R., and Guirand, 1989, Low-pressure granulite facies metapelitic assemblages and corona textures from MacRobertson Land, east Antarctica: the importance of Fe_2O_3 and TiO_2 in accounting for spinel-bearing assemblages: Journal of Metamorphic Geology, v. 7, p. 323-335.

Clarke, J. M., 1907, Some new Devonic fossils: New York State Museum Bulletin 107, p. 153-291.

Collins, R. D., Hill, M., Hon, R., and Hepburn, J. C., 1985, Petrographic and geochemical subdivisions of the Andover Granite, eastern Massachusetts: Geological Society of America Abstracts with Programs, v. 17, p. 12.

Copeland, M. J., and Berdan, J. M., 1977, Silurian and Early Devonian beyrichacean ostracode provincialism in northeastern North America: in Report of Activities, Part B; Geological Survey of Canada Paper 77-1B, p. 15-24.

Crouse, G. W., 1981, Geology of parts of the Burnthill, Clearwater and McKiel Brooks: New Brunswick Department of Natural Resources, Map Report 81-5, 46 p.

Currie, K. L., 1988, The western end of the Avalon Zone in southern New Brunswick: Maritime Sediments and Atlantic Geology, v. 24, p. 339-352.

Dadourian, P., 1979, Polyphase deformation and metamorphism in the northern part of the Manhattan Prong, Westchester and Putnam Counties, N. Y.: (M.A. thesis), Queens College, Flushing, N. Y., 108 p.

Dadourian, P., and Brock, P. W. G., 1979, Stratigraphic implications of differing metamorphic facies in the rocks of the Manhattan Prong in northern Westchester and southern Putnam Counties, N.Y.: Geological Society of America Abstracts with Programs, v. 11, p. 9.

Dallmeyer, R. D., 1975, $^{40}Ar/^{39}Ar$ release spectra of biotite and hornblende from the Cortlandt and Rosetown plutons, New York and their regional implications: Journal of Geology, v. 83, p. 629-643.

Dallmeyer, R. D., and Sutter, J. F., 1976, $^{40}Ar/^{39}Ar$ incremental-release ages of biotite and hornblende from variably retrograded basement gneisses of the northeastern-most Reading Prong, New York: their bearing on Early Paleozoic metamorphic history: American Journal of Science, v. 276, p. 731-747.

Dallmeyer, R. D., and van Breemen, O., 1981, Rb-Sr Whole-rock and $^{40}Ar/^{39}Ar$ mineral ages of the Togus and Hallowell quartz monzonite and Three Mile Pond granodiorite plutons, south-central Maine: their bearing on post- Acadian cooling history: Contributions to Mineralogy and Petrology, v. 78, p. 61-73.

Dallmeyer, R. D., Hermes, O. D., and Gil-Ibarguchi, J. I., 1990, $^{40}Ar/^{39}Ar$ mineral ages from the

Scituate Granite, Rhode Island: implications for Late Paleozoic tectonothermal activity in New England: Journal of Metamorphic Geology, v. 8, p. 145-157.

Dallmeyer, R. D., van Breemen, O., and Whitney, J.A., 1982, Rb-Sr whole-rock and $^{40}Ar/^{39}Ar$ mineral ages of the Hartland Stock, south-central Maine: A post-Acadian representative of the New Hampshire Plutonic Series: American Journal of Science, v. 282, p. 79-93.

Daly, J. S., and McLelland, J., 1991, Juvenile Middle Proterozoic crust in the Adirondack Highlands, Grenville province, northeastern North America: Geology, v. 19, p. 119-122.

Dana, J. D., 1873, On some results of the earth's contraction from cooling including a discussion of the origin of mountains and the nature of the earth's interior: American Journal of Science, v. 5, p. 423-443.

Dana, J. D., 1880, Limestone belts of Westchester County, New York: American Journal of Science, 3rd series, v. 20, p. 21-32, 194-220, 359-375, and 450-456.

Dana, J. D., 1881, Geological relations of the limestone belts of Westchester County, New York: American Journal of Science, v. 22, p. 103-119, 313-315, and 327-335.

David, J., and Gariépy, C., 1986, Geochemistry of the Lower Silurian Pointe aux Trembles and Lac Raymond formations, central Quebec Appalachians: a preliminary report: in Current Research, Part B, Geological Survey of Canada, Paper 86-1B, p. 131-140.

De Yoreo, J. J., Lux, D. R., Decker, E. R., and Osberg, P. H., 1989, The Acadian thermal history of western Maine: Journal of Metamorphic Geology, v. 7, p. 169-190.

Deer, W. A., Howie, R. A., and Zussman, J., 1992, An introduction to the rock-forming minerals (2nd edition): Longman Group Limited, Harlow, England, 696 p.

Delano, J. W., Shirnick, C., Bock, B, Kidd, W. S. F., Heizler, M. T., Putnam, G. W, Delong, S. E., and Ohr, M., 1990, Petrology and geochemistry of Ordovician K-bentonites in New York State: Constraints on the nature of a volcanic arc: Journal of Geology, v. 98, p. 157-170.

Dennison, J. M., 1985, Catskill delta shallow marine strata: in Woodrow, D. L., and Sevon, W. D., eds., The Catskill Delta: Geological Society of America Special Paper 201, p. 91-106.

Dewey, J. F., and Sengör, A. M. C., 1979, Aegean and surrounding regions: Complex multiplate and continuum tectonics in a convergent zone: Geological Society of America Bulletin, Part I, v. 90, p. 84-92.

Dieterich, J., 1968, Multiple folding in western Connecticut: A reinterpretation of structure in the Naugatuck-New Haven-Westport area: in Orville, P. M., Guidebook for Fieldtrips in Connecticut, New England Intercollegiate Geological Conference, New Haven, Connecticut, trip D-2, 13 p.

Dietsch, C. W., 1985, The geology of the Waterbury dome: in Tracy, R. J., ed., Guidebook for Fieldtrips in Connecticut and Adjacent Areas of New York and Rhode Island: New England Intercollegiate Geological Conference, New Haven, p. 1-23.

Dietsch, C., and Sutter, J., 1987, Tectonic and metamorphic evolution of western Connecticut as interpreted from $^{40}Ar/^{39}Ar$ data: Geological Society of America Abstracts with Pro-

grams, v. 19, p. 11.

Dietsch, C., Zartman, R. E., Kwak, L. M., and Aleinikoff, J. N., 1989, U-Pb zircon age constraints from deeply exposed polymetamorphic thrust sheets, southwestern New England Appalachians: Geological Society of America Abstracts with Programs, v. 21, p. A141.

Doe, B. R., and Delevaux, M. H., 1973, Variations in lead isotopic compositions in Mesozoic granitic rocks of California: A preliminary investigation: Geological Society of America Bulletin, v. 84, p. 3513-3526.

Dostal, J., Wilson, R. A., and Keppie, J. D., 1989, Geochemistry of Siluro-Devonian Tobique volcanic belt in northern and central New Brunswick (Canada): tectonic implications: Canadian Journal of Earth Science, v. 26, p. 1282-1296.

Dow, G. M., 1965, Petrology and structure of North Haven Island and vicinity, Maine: Ph.D. thesis, Urbana, University of Illinois, 146 p.

Drake, A. A., 1969, Precambrian and lower Paleozoic geology of the Delaware Valley, New Jersey-Pennsylvania: in Subitzky, S., ed., Geology of selected areas in New Jersey and Eastern Pennsylvania and guidebook of excursions, 1969 Annual Meeting of the Geological Society of America, Rutgers University Press, New Brunswick, New Jersey, p. 51-131.

Drake, A. A., 1984, The Reading Prong of New Jersey and eastern Pennsylvania: an appraisal of rock relations and chemistry of a major Proterozoic terrane in the Appalachians: in Bartholomew, M. J., ed., The Grenville event in the Appalachians and related topics, Geological Society of America Special Paper 194, p. 75-110.

Drake, A. A. Jr., Sinha, A. K., Laird, J. and Guy, R. E., 1989, The Taconic orogen: in Hatcher, R. D. Jr., Thomas, W. A., and Viele, G. W., eds., The Geology of North America, v. F-2, The Appalachian-Ouachita Orogen in the United States, Geological Society of America, Boulder, Colorado, p. 101-177.

Dunning, G. R., and Cousineau, P. A., 1990, U/Pb ages of single zircons from Chain Lakes Massif and a correlative unit in ophiolitic melange in Quebec: Geological Society of America Abstracts with Programs, v. 22, p. 13.

Easton, R. M., 1986, Geochronology of the Grenville Province; Part I: Compilation of data; Part II: Synthesis and interpretation: in Moore, J. M., Davidson, A., and Baer, A. J., eds., The Grenville Province, Geological Association of Canada Special Paper 31, p. 127-173.

Edelman, S. H., 1988, Ophiolite generation and emplacement by rapid subduction hinge retreat on a continent-bearing plate: Geology, v. 16, p. 311-313.

Eisenberg, R. A., 1981, Chronostratigraphy of metavolcanic and associated intrusive rocks of the Boundary Mountains Anticlinorium: Geological Society of America Abstracts with Programs, v. 13, p. 131.

Elison, M. W., Speed, R. C., and Kistler, R. W., 1990, Geologic and isotopic constraints on the crustal structure of the northern Great Basin: Geological Society of America Bulletin, v. 102, p. 1077-1092.

Eriksson, S. C., and Wones, D. R., 1983, The Parks Pond pluton, eastern Maine: Evidence for

cratonization or orogenic activity?: Geological Society of America Abstracts with Programs, v. 15, p. 118.

Eriksson, S. C., and Wones, D. R., 1985, The Parks Pond pluton: A mantle-derived mafic granite: Geological Association of Canada Program with Abstracts, v. 10, p. A17.

Eriksson, S. C., Hogan, J. P., and Williams, I. S., 1989, Ion microprobe resolu tion of age details in heterogeneous sources of plutonic rocks from a comagmatic province: Geological Society of America Abstracts with Pro grams, v. 21, p. A361.

Essene, E. J., 1983, Solid solutions and solvi among metamorphic carbonates with applications to geologic thermobarometry: in Reeder, R. J., ed., Carbonates: Mineralogy and chemistry, Reviews in Mineralogy v. 11, Mineralogical Society of America, Washington, D. C., p. 77-96.

Ettensohn, F. R., 1985, The Catskill delta complex and the Acadian orogeny: A model, in Woodrow, D. L., and Sevon, W. D., eds., The Catskill Delta: Geological Society of America Special Paper 201, p. 39-49.

Ettensohn, F. R., 1987, Rates of relative plate motion during the Acadian orogeny based on the spatial distribution of black shales: Journal of Geology, v. 95, p. 572-582.

Eusden, J. D., 1989, Stratigraphy, structure, and metamorphism across the "dorsal zone", central New Hampshire: in Bothner, W. A., ed., Guidebook for Field Trips in Southwestern New Hampshire, Southeastern Vermont, and North-Central Massachusetts, New England Intercollegiate Geological Conference, Keene, New Hampshire, p. 40-69.

Eusden, J. D., 1990, Sequence of deformation in the northern Presidential Range, New Hampshire: Geological Society of America Abstracts with Programs, v. 22, p. 14.

Eusden, J. D., and Barreiro, B., 1988, The timing of peak high-grade metamorphism in central-eastern New England: Maritime Sediments and Atlantic Geology, v. 24, p. 241-255.

Eusden, J. D., Bothner, W. A., and Hussey, A. M., Jr., 1987, The Kearsage-Central Maine Synclinorium of southeastern New Hampshire and southwestern Maine: Stratigraphic and structural relations of an inverted section: American Journal of Science, v. 287, p. 242-264.

Farmer, G. L., and DePaolo, D. J., 1983, Origin of Mesozoic and Tertiary granite in the western United States and implications for pre-Mesozoic crustal structure: 1. Nd and Sr isotopic studies in the geosyncline of the northern Great Basin: Journal of Geophysical Research, v. 88, p. 3379-3401.

Feakes, C. R., and Retallack, G. J., 1988, Recognition and chemical characterization of fossil soils developed on alluvium: a Late Ordovician example: in Reinhardt, J, and Siglio, W. R., eds., Paleosols and weathering through time: principles and applications: Geological Society of America Special Paper 216, p. 35-48.

Ferrill, B. A., and Thomas, W. A., 1988, Acadian dextral transpression and synorogenic sedimentary successions in the Appalachians: Geology, v. 16, p. 604-608.

Fettke, C. R., 1914, The Manhattan Schist of southeastern New York State and its associated

igneous rocks: New York Academy of Science Annals, v. 23, p. 193-260.

Fisher, D. W., 1977, Correlation of the Hadrynian, Cambrian and Ordovician rocks in New York State: New York State Museum Map and Chart Series Number 25, 75 p.

Fisher, D. W., Isachsen, Y. W., and Rickard, L. V., 1970, Geologic map of New York: State Museum and Science Service, Map and Chart Series, No. 15.

Fitzgerald, J. P., and Hon, R., 1989, Geology and geochemistry of the Spider Lake volcanic suite, north-central Maine: Geological Society of America Abstracts with Programs, v. 21, p. 14.

Fitzgerald, J. P., and Hon, R., 1990, Geochemistry of volcanic rocks from the Ripogenous Dam area, north central Maine: Geological Society of America Abstracts with Programs, v. 22, p. 15.

Flagel, S. F., and Hon, R., 1988, Petrogenesis of the peraluminous Chelmford Granite, Massachusetts: Geological Society of America Abstracts with Programs, v. 20, p. 18.

Fluhr, T. W., 1950, The Delaware aqueduct: some geological data: New York Academy of Sciences Transactions, v. 12, p. 182-186.

Fluhr, T. W., 1969, Recent engineering data on the New York City group of formations: in Alexandrov, E. A., ed., Symposium on the New York City Group of Formations, 40th Annual Meeting, New York State Geological Association, Queens College Press, Flushing, New York, p. 1-10.

Fluhr, T. W., and Bird, P. H., 1939, The problem of the quartzites: Delaware Water Supply News, v. 1, p. 67-68.

Foland, K. A., and Faul, H., 1977, Ages of the White Mountain intrusives- New Hampshire, Vermont, and Maine, USA: American Journal of Science, v. 277, p. 888-904.

Foland, K. A., and Loiselle, M. C., 1981, Oliverian syenites of the Pliny region, northern New Hampshire: Geological Society of America Bulletin, v. 92, Part I, p. 179-188.

Friedman, G. M., 1979, Sedimentary environments and their products: shelf, slope, and rise of proto-Atlantic (Iapetus) ocean, Cambrian and Ordovician periods, eastern New York State: in Friedman, G. M., ed., Guidebook, Joint Annual Meeting of New York State Geological Association (51st Annual Meeting) and New England Intercollegiate Geological Conference (71st Annual Meeting), Troy, New York, Rensselaer Polytechnic Institute, p. 47-86.

Frith, R. A., and Doig, R., 1973, Rb-Sr isotopic ages and petrologic studies of the rocks in the Lac St. Jean area, Quebec: Canadian Journal of Earth Sciences, v. 10, p. 881-899

Fullagar, P. D., and Bottino, M. L., 1968, Rb-Sr whole-rock ages of Silurian-Devonian volcanics from eastern Maine: EOS Transactions of the American Geophysical Union, v. 49, p. 346.

Fyffe, L., Barr, S. M., and Bevier, M. L., 1988, Origin and U-Pb geochronology of amphibolite-facies metamorphic rocks, Miramichi Highlands, New Brunswick: Canadian Journal of Earth Sciences, v. 25, p. 1674-1686.

Fyffe, L. R., 1982, Taconian and Acadian structural trends in central and northern New Brunswick: in St-Julien, P. and Béland, J., eds., Major Structural Zones and Faults of the Northern Appalachians, Geological Association of Canada Special Paper Number 24, p. 117-130.

Fyffe, L. R., 1988, Stratigraphic constraints on the timing of fault movements in New Brunswick: Maritime Sediments and Atlantic Geology, v. 24, p. 194-195.

Fyffe, L. R., and Cormier, R. F., 1979, The significance of radiometric ages from the Gulquac Lake area of New Brunswick: Canadian Journal of Earth Sciences, v. 16, p. 2046-2052.

Fyffe, L. R., and McLeod, M. J., 1990, Terrane boundaries in southwestern New Brunswick: Geological Society of America Abstracts with Programs, v. 22, p. 19.

Fyffe, L. R., Pajari, G. E., and Cormier, R.F., 1981, Rb-Sr geochronology of New Brunswick: Geological Society of America Abstracts with Programs, v. 13, p. 133.

Fyffe, L. R., Pajari, G. E., Jr., and Cherry, M. E., 1981, The Acadian plutonic rocks of New Brunswick: Maritime Sediments and Atlantic Geology, v. 17, p. 23-36.

Gale, L. D., 1839, Geological survey of the island of New York: Appendix C, Third Annual Report of the First Geological District of the State of New York, p. 177-199.

Ganguly, J., 1972, Staurolite stability and related parageneses: theory, experiments, and applications: Journal of Petrology, v. 13, p. 335-365.

Gapais, D., 1989, Shear structures within deformed granites: Mechanical and thermal indicators: Geology, v. 17, p. 1144-1147.

Gates, O., and Moench, R. H., 1981, Bimodal Silurian and Lower Devonian volcanic rock assemblages in the Machias-Eastport area, Maine: United States Geological Survey Professional Paper 1184, 32 p.

Gaudette, H. E., 1981, Zircon isotopic age from the Union ultramafic complex, Maine: Canadian Journal of Earth Sciences, v. 18, p. 405-409.

Gaudette, H. E., Bothner, W. A., Laird, J., Olszewski, W. J., and Cheatham, M. M., 1984, Late Precambrian/Early Paleozoic deformation and metamorphism in southeastern New Hampshire- Confirmation of an exotic terrane: Geological Society of America Abstracts with Programs, v. 16, p. 516.

Gaudette, H. E., Knight, D. R., Moura, C. A. V., and Olszewski, W. J., 1990, Evolution of the gabbro-granite belt, NW Maine. I: Timing of igneous activity: Geological Society of America Abstracts with Programs, v. 22, p. 20.

Gaudette, H. E., Kovack, A., and Hussey, A. M. II., 1982, Ages of some intrusive rocks of southwestern Maine, U.S.A.: Canadian Journal of Earth Sciences, v. 19, p. 1350-1357.

Gaudette, H. E., Olszewski, W. J., Jr., and Cheatham, M. M., 1983, Rb-Sr whole-rock ages of gneisses from the Liberty-Orrington anticline, Maine: The oldest (?) basement complex of the eastern margin, northern Appalachi ans: Geological Society of America Abstracts

with Programs, v. 15, p. 579.

Gay, A. L., and Grandstaff, D. E., 1980, Geochemistry and mineralogy of Precambrian paleosols at Elliot Lake, Ontario, Canada: Precambrian Research, v. 12, p. 349-373.

Geiser, P., and Engelder, T., 1983, The distribution of layer parallel shortening fabrics in the Appalachian foreland of New York and Pennsylvania: Evidence for two non-coaxial phases of the Alleghanian orogeny: in Hatcher, R. D. Jr., Williams, H., and Zietz, I., Contributions to tectonics and geophysics of mountain chains, Geological Society of America Memoir 158, p. 161-175.

Getty, S. R., and Gromet, L. P., 1988, Alleghanian polyphase deformation of the Hope Valley shear zone, southeastern New England: Tectonics, v. 7, p. 1325-1338.

G-Farrow, C. E., and Mossman, D. J., 1988, Geology of Precambrian paleosols at the base of the Huronian Supergroup, Elliot Lake, Ontario, Canada: Precambrian Research, v. 42, p. 107-139.

Gibson, D., and Lux, D. R., 1989, Petrographic and geochemical variations within the Songo pluton, western Maine: in Tucker, R. D., and Marvinney, R. G., eds., Studies in Maine Geology, V. 4: Igneous and Metamorphic Geology, Maine Geological Survey, p. 87-100.

Gill, J., 1981, Orogenic andesites and plate tectonics: Springer-Verlag, Berlin, 390 p.

Gold, D. P., 1967, Alkaline ultrabasic rocks in the Montreal area, Quebec: in Wyllie, P. J., ed., Ultramafic and related rocks: John Wiley & Sons, New York, p. 288-302.

Goldsmith, J. R., and Newton, R. C., 1969, P-T-X relations in the system $CaCO_3$-$MgCO_3$ at high temperatures and pressures: American Journal of Science, v. 267A, p. 160-190.

Goldsmith, J. R., and Newton, R. C., 1977, Scapolite-plagioclase stability relations at high pressure and temperatures in the system $NaAlSi_3O_8$-$CaAl_2Si_3O_8$-$CaCO_3$-$CaSO_4$: American Mineralogist, v. 62, p. 1063-81.

Gower, R. J. W., and Simpson, C., 1992, Phase boundary mobility in naturally deformed, high-grade quartzofeldspathic rocks: evidence for diffusional creep: Journal of Structural Geology, v. 14, p. 301-313.

Grandstaff, D. E., Edelman, M. J., Foster, R. W., Zbinden E., and Kimberley, M. M., 1986, Chemistry and mineralogy of Precambrian paleosols at the base of the Dominion and Pongola Groups (Transvaal, South Africa): Precambrian Research, v. 32, p. 97-131.

Grant, J. A., 1985, Phase equilibria in partial melting of pelitic rocks: in Ashworth, J. R., ed., Migmatites, Blackie & Son Limited, Glasgow, Scotland, p. 86-144.

Grauert, B., and Hall, L. M., 1973, Age and origin of zircons from metamorphic rocks in the Manhattan Prong, White Plains area, southeastern New York: Carnegie Institute Yearbook 72, p. 293-297.

Grauert, B., and Hall, L., 1974, Age and origin of zircons from metamorphic rocks in the Manhattan Prong, White Plains area, southeastern New York: Carnegie Institute Washington Year Book 72, p. 293-297.

Green, J. C., and Guidotti, C. V., 1968, The Boundary Mountains Anticlinorium in northern New Hampshire and northwestern Maine: in Zen, E-An, White, W. S., Hadley, J. B., and Thompson, J. B. Jr., eds., Studies of Appalachian Geology: Northern and Maritime, Interscience Publishers, New York, p. 255-266.

Greiner, H. R., 1970, Geology of the Charlo area, 21-0/16, Restigouche County, New Brunswick: New Brunswick Department of Natural Resources, Map Series 70-2, 18 p.

Gromet, L. P., 1989, Avalonian terranes and late Paleozoic tectonism in southeastern New England; Constraints and problems: in Dallmeyer, R. D., ed., Terranes in the Circum-Atlantic Paleozoic Orogens, Geological Society of America Special Paper 230, p. 193-211.

Gromet, L. P., and Robinson, P., 1990, Isotopic evidence for Late Paleozoic gneissic deformation and recrystallization in the core of the Pelham dome, Massachusetts: Geological Society of America Abstracts with Programs, v. 22, p. A368.

Guidotti, C. V., 1989, Metamorphism in Maine: an overview: in Tucker, R. D. and Marvinney, R. G., eds., Studies in Maine Geology, V. 3: Igneous and Metamorphic Geology, Maine Geological Survey, p. 1-17.

Hafner-Douglass, K., 1987, Metavolcanic rocks of the Piermont Allochthon and associated metadiabase dikes, Gardner Mountain area, northwestern New Hampshire: Geological Society of America Abstracts with Programs, v. 19, p. 16.

Hall, B. A., 1970, Stratigraphy at the southern end of the Munsungun anticlinorium, Maine: Maine Geological Survey Bulletin, v. 22, 63 p.

Hall, J., 1859, The natural history of New York, Part 6- Paleontology, J.3: Introduction, Van Benthuysen, Albany, N. Y., p. 1-85.

Hall, L. M., 1968a, Times of origin and deformation of bedrock in the Manhattan Prong: in Zen, E-an, White, W. S., Hadley, J. B., and Thompson, J. B., eds., Studies of Appalachian geology: Northern and maritime, Interscience Publishers, New York, p. 117-127.

Hall, L. M., 1968b, Bedrock geology in the vicinity of White Plains, New York: in Finks, R. M., ed., Guidebook to field excursions, 40th Annual Meeting, New York State Geological Association, Queens College, New York, p. 7-31.

Hall, Leo M., 1968c, Geology of the Glenville area, southwesternmost Connecticut and southeastern New York: in Orville, P.M., ed., Guidebook to fieldtrips in Connecticut, New England Intercollegiate Geological Conference, p. 1-12.

Hall, L. M., 1979, Basement-cover relations in western Connecticut and southeast New York: in Wones D. R., ed., The Caledonides in the U.S.A., International Geological Correlation Program Project 27, Virginia Polytechnic Institute and State University Memoir No. 2, Blacksburg, Virginia, p. 299-306.

Hall, L. M., and Robinson, P., 1982, Stratigraphic-tectonic subdivisions of southern New England: in St-Julien, P. and Béland, J., eds., Major Structural Zones and Faults of the Northern Appalachians, Geological Association of Canada Special Paper 24, p. 15-41.

Hames, W. E., Sutter, J. F., and Ratcliffe, N. M., 1990, Evidence for a 15 Ma duration of the Taconian collisional episode: Geological Society of America Abstracts with Programs, v. 22, p. 21.

Hansen, E., 1971, Strain facies: Springer-Verlag, New York, 207 p.

Hanson, L. S., and Bradley, D. C., 1989, Sedimentary facies and tectonic interpretation of the Lower Devonian Carrabassett Formation, north- central Maine: in Tucker, R. D., and Marvinney, R. G., eds., Studies in Maine Geology, V. 2: Structure and Stratigraphy, Maine Geological Survey, p. 101-125.

Harding, K. L., Morris, W. A., Balch, S. J., Lapointe, P. and Latham, A. G., 1988, A comparison of magnetic character and alteration in three granite drill cores from eastern Canada: Canadian Journal of Earth Sciences, v. 25, p. 1141-1150.

Harley, S. L., 1985, Paragenetic and mineral-chemical relationships in orthoamphibole-bearing gneisses from Enderby Land, east Antarctica: a record of Proterozoic uplift: Journal of Metamorphic Geology, v. 3, p. 179-200.

Harley, S. L., 1989, The origins of granulites: a metamorphic perspective: Geological Magazine, v. 126, p. 215-247.

Harrison, T. M., Aleinikoff, J. N., and Compston, W., 1987, Observations and controls on the occurrence of inherited zircon in Concord-type granitoids, New Hampshire: Geochimica et Cosmochimica Acta, v. 51, p. 2549-2558.

Harrison, T. M., and McDougall, I., 1980, Investigation of an intrusive contact, northwest Nelson, New Zealand- I, Thermal, chronological, and isotopic constraints: Geochimica et Cosmochimica Acta, v. 44, p. 1985-2003.

Harrison, T. M., Duncan, I. J., and McDougall, I., 1984, Diffusion of ^{40}Ar in biotite: temperature, pressure, and compositional effects: experimental results and geological implications: Geological Society of America Abstracts with Programs, v. 16, p. 531.

Harrison, T. M., Spear, F. S., and Heizler, M. T., 1989, Geochronologic studies in central New England II: Post-Acadian hinged and differential uplift: Geology, v. 17, p. 185-189.

Harwood, D. S., 1976, Clinopyroxene-plagioclase symplectite after omphacite and polymetamorphism of allochthonous rocks in northwestern Connecticut: Geological Society of America Abstracts with Programs, v. 8, p. 189.

Hatch, N. L., Jr., Moench, R. H., and Lyons, J. B., 1983, Silurian-Lower Devonian stratigraphy of eastern and south-central New Hampshire: Extensions from western Maine: American Journal of Science, v. 283, p. 739- 761.

Hatch, N. L., Jr., Zen, E-An, Goldsmith, R., Ratcliffe, N. M., Robinson, P., Stanley, R. S., and Wones, D. R., 1984, Lithotectonic assemblages as por trayed on the new bedrock geologic map of Massachusetts: American Journal of Science, v. 284, p. 1026-1034.

Hatcher, R. D., and Edelman, S. E., 1987. Macro-scale partitioning in the southern and central Appalachians: Thrusting and strike-slip as products of Alleghanian collision: Geological Society of America Abstracts with Programs, v. 19, p. 89.

Hatcher, R. D. Jr., 1987, Tectonics of the southern and central Appalachian internides: Annual Reviews of Earth and Planetary Sciences, v. 15, p. 337-362.

Hatcher, R. D. Jr., Thomas, W. A., Geiser, P. A., Snoke, W. A., Mosher, S., and Wiltschko, D. V., 1989, Alleghanian orogen, in Hatcher, R. D. Jr., Thomas, W. A., and Viele, G. W., eds., The Appalachian-Ouachita Orogen in the United States, The Geology of North America Volume F-2, Decade of North American Geology Project, Geological Society of America, p. 233-318.

Hayama, Y., 1959, Some considerations of the color of biotite and its relation to metamorphism: Journal of the Geological Society of Japan, v. 65, p. 21-30.

Hayward, J. A., 1983, Rb-Sr geochronology and the evolution of some peraluminous (two-mica) granites in New Hampshire: Geological Society of America Ab stracts with Programs, v. 15, p. 146.

Hayward, J. A., 1989, Implications of the Rb-Sr and O isotopic systematics and geochemistry of some two-mica granites in northern New England: in Tucker, R. D., and Marvinney, R. G., eds., Studies in Maine Geology, V. 3: Igneous and Metamorphic Geology, Maine Geological Survey, p. 53-66.

Hayward, J. A., Gaudette, H. E., and Olszewski, W. J., 1988, Isotopic characteristics of and constraints on parental sources of two-mica granites in northern New England: Geological Society of America Abstracts with Programs, v. 20, p. 26.

Hayward, J. A., Olszewski, W. J., and Gaudette, H. E., 1990, Pb isotopic geochemistry of two-mica granites in northern New England: Geological Society of America Abstracts with Programs, v. 22, p. 23.

Heizler, M. T., Lux, D. R., and Decker, E. R., 1988, The age and cooling history of the Chain of Ponds and Big Island Pond plutons and the Spider Lake granite, west-central Maine and Quebec: American Journal of Science, v. 288, p. 925-952.

Helenek, H. L., and Mose, D. G., 1984, Geology and geochronology of Canada Hill Granite and its bearing on the timing of Grenville events in the Hudson Highlands, New York: in Bartholomew, M. J., ed., The Grenville Event in the Appalachians and Related Topics: Geological Society of America Special Paper 194, p. 57-73.

Helmstaedt, H., 1971, Structural geology of Portage Lakes area, Bathurst-Newcastle district, New Brunswick: Geological Survey of Canada Paper 70-28, 42 p.

Hepburn, J. C., 1981, Rare earth element abundances in Siluro-Devonian metavolcanics, eastern Vermont and adjacent Massachusetts, Geological Society of America Abstracts with Programs, v. 13, p. 137.

Hepburn, J. C., 1984, Geochemical evidence for the origin of the Standing Pond Volcanics, eastern Vermont: Geological Society of America Abstracts with Programs, v. 16, p. 23.

Hepburn, J. C., Hill, M., and Hon, R., 1987, The Avalonian and Nashoba terranes, eastern Massachusetts, U.S.A.: an overview: Maritime Sediments and Atlantic Geology, v. 23, p. 1-12.

Hepburn, J. C., Lux, D. R., and Hill, M., 1987, $^{40}Ar/^{39}Ar$ Carboniferous cooling ages from the Nashoba terrane, eastern Massachusetts: Geological Society of America Abstracts with Programs, v. 19, p. 18.

Hepburn, J. C., Olszewski, W. J., and Guidotti, C. V., 1985, Metamorphism of tectonic terranes in the eastern marginal zone of the Appalachian orogen, New England: Geological Society of America Abstracts with Programs, v. 17, p. 608.

Hermes, O. D., and Zartman, R. E., 1985, Late Proterozoic and Devonian plutonic terrane within the Avalon zone of Rhode Island: Geological Society of America Bulletin, v. 96, p. 272-282.

Hermes, O. D., Ballard, R. D., and Banks, P. O., 1978, Upper Ordovician peralkalic granites from the Gulf of Maine: Geological Society of America Bulletin, v. 89, p. 1761-1774.

Hervet, M., Higgins, M. D., van Breemen, O., and Dickin, A., 1990, U-Pb age and Nd constraints on the Chicoutimi Gneissic Complex (CGC) at the southeast border of the Lac St. Jean Anorthosite Complex (LSJAC), Grenville Province, Quebec, Canada: EOS Transactions of the American Geophysical Union, v. 71, p. 661.

Hickey, R. L., Frey, F. A., and Gerlach, D. C., 1986, Multiple sources for basaltic arc rocks from the southern volcanic zone of the Andes (34-41^{o}S): trace element and isotopic evidence for contributions from subducted oceanic crust, mantle, and continental crust: Journal of Geophysical Research, v. 91, p. 5963-5983.

Hill, M. D., Hepburn, J. C., Collins, R. D., and Hon, R., 1984, Igneous rocks of the Nashoba block, eastern Massachusetts: in Hanson, L. S., ed., Geology of the Coastal Lowlands, Boston, MA to Kennebunk, ME, New England Intercollegiate Geologic Conference, p. 61-80.

Hingston, M., and Barreiro, B., 1990, A trace element and isotopic study of an Ordovician island arc in northern New England: Evidence for crustal in volvement: EOS Transactions of the American Geophysical Union, v. 71, p. 661.

Hodge, D. S., Abbey, D. A., Harbin, M. A., Patterson, J. L., Ring, M. J., and Sweeney, J. F., 1982, Gravity studies of subsurface mass distributions of granitic rocks in Maine and New Hampshire: American Journal of Science, v. 282, p. 1289-1324.

Hogan, J. P., and Sinha, A. K., 1989a, Isotopic characterization of peraluminous and metaluminous granitoid suites from the Coastal Maine Magmatic Province (CMMP): Implications for source region geometry and terrane accretion in eastern Maine: Geological Society of America Abstracts with Programs, v. 21, p. 23.

Hogan, J. P., and Sinha, A. K., 1989b, Compositional variation of plutonism in the Coastal Maine Magmatic Province: mode of origin and tectonic setting: in Tucker, R. D., and Marvinney, R. G. eds., Studies in Maine Geology, V. 4: Igneous and Metamorphic Geology, Maine Geological Survey, p. 1-33.

Hogan, J. P., Jurinski, J. B., and Sinha, A. K., 1988, Mineralogical, chemical and isotopic diversity in plutonic rock suites from the Coastal Maine Magmatic Province: Geological Society of America Abstracts with Programs, v. 20, p. A73.

Holdaway, M. J., and Lee, S. M., 1977, Fe-Mg cordierite stability in high-grade pelitic rocks based

on experimental, theoretical, and natural observations: Contributions to Mineralogy and Petrology, v. 63, p. 175-198.

Holdaway, M. J., Dutrow, B. L., and Hinton, R. W., 1988, Devonian and Carboniferous metamorphism in west-central Maine: The muscovite-almandine geobarometer and the staurolite problem revisited: American Mineralogist, v. 73, p. 20-47.

Holland, H. D., Feakes, C. R., and Zbinden, E. A., 1989, The Flin Flon paleosol composition of the atmosphere 1.8 BYBP: American Journal of Science, v. 289, p. 362-389.

Hon, R., 1980, Geology and petrology of igneous bodies within the Katahdin pluton: in Roy, D. C., and Naylor, R. S., eds., The Geology of Northeastern Maine and Neighboring New Brunswick, New England Intercollegiate Geological Conference, p. 65-79.

Hon, R., Bothner, W. A., Olszewski, W. J., Gaudette, H. E., Hepburn, J. C., Loftenius, C., and Dennen, W. H., 1986, Mid-Paleozoic calc-alkaline igneous rocks of the Nashoba block and Merrimack Trough: in Newberg, D. W., ed., Guidebook for Field Trips in Southwestern Maine, New England Intercollegiate Geologic Conference, Lewiston, Maine, p. 37-52.

Hon, R. and Roy, D. C., 1981, Magmatogenic and stratigraphic constraints on Acadian tectonism in Maine: Geological Society of America Abstracts with Programs, v. 13, p. 138.

Hon, R. and Thirlwall, M. F., 1985, Newbury volcanics- a Late Silurian island arc (?): Geological Society of America Abstracts with Programs, v. 17, p. 25.

Housh, T., Bowring, S. A., and Villeneuve, M., 1989, Lead isotopic study of Early Proterozoic Wopmay Orogen, NW Canada: Role of continental crust in arc magmatism: Journal of Geology, v. 97, p. 735-747.

Howard, W. V., 1926, Devonian volcanic rocks near Dalhousie, New Brunswick: Geological Society of America Bulletin, v. 37, p. 475-496.

Hubacher, F. A., and Lux, D. R., 1987, Timing of Acadian deformation in north eastern Maine: Geology, v. 15, p. 80-83.

Hueber, F. M., Bothner, W. A., Hatch, N. L., Jr., Finney, S. C., and Aleinikoff, J. N., 1990, Devonian plants from southern Quebec and northern New Hampshire and the age of the Connecticut Valley Trough: American Journal of Science, v. 290, p. 360-395.

Hussey, A. M. II, Bothner, W. A., and Thomson, J. A., 1986, Geological comparisons across the Norumbega Fault Zone, southwestern Maine: in Newberg, D. W., ed., Guidebook for Field Trips in Southwestern Maine, New England Intercollegiate Geological Conference, Lewiston, Maine, p. 53-78.

Hussey, A. M. II, Rickerich, S., and Bothner, W. A., 1984, Sedimentology and multiple deformation of the Kittery Formation in southwestern Maine and southeastern New Hampshire: in Hanson, L. S., ed., Geology of the Coastal Lowlands, Boston MA to Kennebunk, ME, New England Intercollegiate Geologic Conference, Salem, MA, p. 47-60.

Hussey, A. M. II, 1989, Lithotectonic stratigraphy, deformation, plutonism, and metamorphism, greater Casco Bay region, southwestern Maine: in Tucker, R. D., and Marvinney, R. G., eds., Studies in Maine Geology, V. 1: Structure and Stratigraphy, Maine Geological

Survey, p. 17-34.

Hutchinson, D. R., Klitgord, K. D., and Detrick, R. S., 1985, Block Island fault: A Paleozoic crustal boundary on the Long Island platform: Geology, v. 13, p. 875-879.

Hutchinson, D. R., Klitgord, K. D., Lee, M. W., and Trehu, A. M., 1988, U. S. Geological Survey deep seismic reflection profile across the Gulf of Maine: Geological Society of America Bulletin, v. 100, p. 172-184.

Irvine, T. N., and Baragar, W.R.A., 1971, A guide to chemical classification of the common volcanic rocks: Canadian Journal of Earth Sciences, v. 8, p. 523-548.

Jackson, R. A., and Hall, L. M., 1982, An investigation of the stratigraphy and tectonics of the Kent area, western Connecticut: in Joesten, R., and Quarrier, S. S., eds., Guidebook for fieldtrips in Connecticut and South Central Massachusetts, New England Intercollegiate Geological Conference, 74th Annual Meeting, University of Connecticut, Storrs, Connecticut, p. 213-246.

Jaffe, H. W., and Jaffe, E. B., 1989, Structure and petrology of the Precambrian allochthon, autochthon, and Paleozoic sediments of the Monroe area, New York: in Weiss, D., ed., Field Trip Guidebook, 61st Annual Meeting, New York State Geological Association, Middletown, New York, p. 29-49.

James, D. E., 1981, The combined use of oxygen and radiogenic isotopes as indications of crustal contamination: Annual Review of Earth and Planetary Science, v. 9, p. 311-344.

Johannes, W., 1968, Experimental investigation of the reaction forsterite + H_2O = serpentine + brucite: Contributions to Mineralogy and Petrology, v. 19, p. 309-315.

Johannes, W., 1985, The significance of experimental studies for the formation of migmatites: in Ashworth, J. R., ed., Migmatites, Blackie & Son Limited, Glasgow, Scotland, p. 36-85.

Johnson, J. G., 1979, Devonian brachiopod biostratigraphy: in House, M. R., Scrutton, C. T., and Bassett, M. G., eds., The Devonian World: Special Papers in Paleontology No. 23, p. 291-306.

Johnson, T. D., and Wones, D. R., 1984, Sense and mode of shearing along the Norumbega fault zone, eastern Maine: Geological Society of America Abstracts with Programs, v. 16, p. 27.

Jurinski, J. B., and Sinha, A. K., 1989, Igneous complexes within the Coastal Maine Magmatic Province: Evidence for a Silurian tensional environment: Geological Society of America Abstracts with Programs, v. 21, p. 25.

Karabinos, P., and Aleinikoff, J. N., 1988, U-Pb zircon ages of augen gneisses in the Green Mountain Massif and Chester Dome, Vermont: Geological Society of America Abstracts with Programs, v. 20, p. 29.

Karabinos, P., Kober, B., and Gromet, L. P., 1989, Applications of single- grain zircon evaporation analyses: Age discrimination in igneous suites and detrital grain studies: Geological Society of America Abstracts with Programs, v. 21, p. A268.

Kay, M., 1944, Geosynclines in continental development: Science, v. 99, p. 461-462.

Kay, M., 1947, Geosynclinal nomenclature and the craton: American Association of Petroleum Geologists Bulletin, v. 31, p. 1289-1291.

Kay, M., 1951, North American geosynclines: Geological Society of America Memoir 48, 143 p.

Kay, S. M., and Rapela, C. W., 1987, El volcanismo del Terciario inferior y medio en los Andes Norpatagónicos 40^{o}-42^{o}S: Fuente de origen de los magmas y su relación con variaciones in la oliciudad de la zona de subducción: in Coira, B., ed., International Symposium on Andean Volcanism, Actas, X Congreso Geológico Argentino, Tucuman.

Kent, D. V., and Opdyke, N. D., 1980, Paleomagnetism of Siluro-Devonian rocks from eastern Maine: Canadian Journal of Earth Sciences, v. 17, p. 1653-1665.

Keppie, J. D., Ruitenberg, A. A., Fyffe, L., McCutcheon, S., St-Julien, P. Skidmore, B., Béland, J., Hubert, C., Williams, H., and Bursnall, J., 1982, Structural map of the Appalachian Orogen in Canada: Memorial University of Newfoundland, Map No. 4, scale 1:200,000.

Kerrick, D. M., 1987, Fibrolite in contact aureoles of Donegal, Ireland: American Mineralogist, v. 72, p. 240-254.

Kerrick, D. M., 1990, The Al_2SiO_5 Polymorphs: Reviews in Mineralogy v. 22, Mineralogical Society of America, Washington, D. C., 406 p.

Kesler, S. E., and van der Pluijm, B. A., 1990, Timing of Mississippi Valley-type mineralization: Relation to Appalachian orogenic events: Geology, v. 18, p. 1115-1118.

King, P. B., 1959, The evolution of North America: Princeton University Press, Princeton, New Jersey, 189 p.

Kistler, R. W., and Peterman, Z. E., 1973, Variations in Sr, Rb, K, Na, and initial Sr^{87}/Sr^{86} in Mesozoic granitic rocks and intruded wallrocks in central California: Geological Society of America Bulletin, v. 84, p. 3489-3512.

Kistler, R. W., and Peterman, Z. E., 1978, Reconstruction of crustal blocks of California on the basis of initial strontium isotopic compositions of Mesozoic granitic rocks: United States Geological Survey Professional Paper 1071, 17 p.

Knight, D. R. and Gaudette, H. E., 1987, Rb-Sr age of the Waldoboro two mica granite, coastal Maine: Geological Society of America Abstracts with Programs, v. 19, p. 23.

Knopf, E. B., 1962, Stratigraphy and structure of the Stissing Mountain area, Dutchess County, New York: Stanford University Publications, Geological Sciences, v. 7, No. 1, 55 p.

Kohn, M. J., and Spear, F. S., 1989, Acadian pressure, temperature, and deformational history of west-central New Hampshire: hot thrusts over cold basement: Geological Society of America Abstracts with Programs, v. 21, p. 27.

Krogstad, E. J., Hanson, G. N., and Mezger, K., 1990, Possible Avalon Pb isotopic crustal signature in S. W. Connecticut: EOS Transactions of the American Geophysical Union, v. 71, p. 655.

Krogstad, E. J., Hanson, G. N., Rajamani, V, and Balakrishnan, S. 1986, Nd, Sr, and Pb isotopic evidence for separate, juxtaposed late Archean terranes, South India: EOS Transactions of the American Geophysical Union, v. 67, p. 1265.

Kumarapeli, P. S., Dunning, G. R., Pintson, H., and Shaver, J., 1989, Geochemistry and U-Pb zircon age of comenditic metafelsites of the Tibbit Hill Formation, Quebec Appalachians: Canadian Journal of Earth Science, v. 26, p. 1374-1383.

Kuno, H., 1966, Lateral variation of basalt magma type across continental margin and island arc: Bulletin of Volcanology, v. 29, p. 195-222.

Laird, J., and Bothner, W. A., 1986, Metamorphism in the northern Green Mountains of Vermont: in Robinson, P., and Elbert, D. C., eds., Field Trip Guidebook: Regional Metamorphism and Metamorphic Phase Relations in Northwestern and Central New England, Contribution No. 59, Department of Geology and Geography, University of Massachusetts, Amherst, Massachusetts, p. 11-36.

Laird, J., Lanphere, M. A., and Albee, A. L., 1984, Distribution of Ordovician and Devonian metamorphism in mafic and pelitic schists from northern Vermont: American Journal of Science, v. 284, p. 376-413.

LaRocque, C., 1986, Geochronology and petrology of north-central Gaspé igneous rocks, Quebec; unpublished M.Sc. thesis, McGill University.

LaRocque, C., and Doig, R., 1984, Geochemistry and geochronology of York River Formation volcanic rocks and associated intrusive of the Gaspé Peninsula, Quebec: Maritime Sediments and Atlantic Geology, v. 20, p. 114-115.

Laurent, R. and Bélanger, J., 1984, Geochemistry of Silurian-Devonian alkaline basalt suites from the Gaspé Peninsula, Quebec Appalachians: Maritime Sediments and Atlantic Geology, v. 20, p. 67-78.

Le Maitre, R. W., 1984, A proposal by the IUGS Subcommission on the Systematics of Igneous Rocks for a chemical classification of volcanic rocks based on the total alkali silica (TAS) diagram: Australian Journal of Earth Sciences, v. 31, p. 243-255.

Lefort, J.-P., 1984, Mise en evidence d'une virgation carbonifere induite par la dorsale Reguibat (Mauritanie) dans le Appalaches du Sud (U.S.A.). Arguments geophysiques: Bulletin Societe Geologique de France, v. 26, p. 1293-1303.

LeHuray, A. P., 1984, Lead and sulfur isotopes and a model for the origin of the Ducktown deposit, Tennessee: Economic Geology, v. 79, p. 1561-1573.

LeHuray, A. P., 1986, Isotopic evidence for a tectonic boundary between the Kings Mountain and Inner Piedmont belts, southern Appalachians: Geology, v. 14, p. 784-787.

Lessing, P., 1967, Petrology of the Poundridge leptite, Westchester County, New York: (Ph.D. thesis), Syracuse University, 69 p.

Lindsley, D. H., 1976, Experimental studies of oxide minerals: in Rumble, D. III, ed., Oxide Minerals, Reviews in Mineralogy Volume 3, Mineralogical Society of America, Washington, D. C., p. L61-L88.

Loftenius, C. J., and Hon, R., 1987, Petrology and geochemistry of the Sharpners Pond Quartz Diorite: Geological Society of America Abstracts with Programs, v. 19, p. 27.

Loiselle, M., Eriksson, S., Wones, D. R. and Sinha, A. K., 1983, Timing and emplacement of post-Acadian plutons in central and eastern Maine: Geological Society of America Abstracts with Programs, v. 15, p. 187.

Loiselle, M., Hon, R., and Naylor, R. S., 1983, Age of the Katahdin batholith, Maine: Geological Society of America Abstracts with Programs, v. 15, p. 146.

Loiselle, M. C., and Ayuso, R. A., 1980, Geochemical characteristics of granitoids across the Merrimack Synclinorium, eastern and central Maine: in Wones, D. R., ed., Proceedings, "the Caledonides in the USA", Blacksburg, Virginia, p. 117-121.

London, D., 1988, Characteristics and regional significance of the Cremation Hill ductile fault zone at the Bronson Hill-Merrimack boundary, south- central Connecticut: American Journal of Science, v. 288, p. 353-375.

Long, L. E., 1969, Whole-rock Rb-Sr age of the Yonkers gneiss, Manhattan Prong: Geological Society of America Bulletin, v. 80, p. 2087-2090.

Long, L. E., and Kulp, J. L., 1962, Isotopic age study of the metamorphic history of the Manhattan and Reading Prongs: Geological Society of America Bulletin, v. 73, p. 969-996.

Ludman, A., 1981, Significance of transcurrent faulting in eastern Maine and location of the suture between Avalon and North America: American Journal of Science, v. 281, p. 463-483.

Ludman, A., and Hopeck, J., 1988, Classification and significance of faults in eastern Maine; Field Trip Guide for the Summer Meeting of the Geological Society of Maine, 1988, p. 1-11.

Ludman, A., and Hopeck, J., in review, Classification and tectonic roles of faults in eastern Maine.

Ludman, A., Hopeck, J., and Brock, P. C., 1993 (in press), Nature of the Acadian orogeny in eastern Maine: in Roy, D. C., and Skeehan, J., eds., The Acadian Orogeny: Recent studies in New England, Maritime Canada, and the autochthonous foreland, Geological Society of America Special Paper 275.

Ludman, A., Hopeck, J., Domoracki, W. J., Coruh, C., and Doll, W. E., 1990, Seismic reflection evidence for the NW limit of Avalon in east-central Maine: Geological Society of America Abstracts with Programs, v. 22, p. 32.

Ludman, A., Hopeck, J. T., and Brock, P. C., in review, Nature of the Acadian orogeny in eastern Maine: in Roy, D. C., and Skeehan, J., eds., The Acadian Orogeny, Geological Society of America Special Paper

Luth, W. C., 1976, Granitic rocks: in Bailey, D. K., and Macdonald, R., eds., The evolution of the crystalline rocks, Academic Press, New York, p. 335-417.

Lux, D. R., and Aleinikoff, J. N., 1985, ^{40}Ar-^{39}Ar and U-Pb geochronology of the Songo pluton,

western Maine: Geological Society of America Abstracts with Programs, v. 17, p. 32.

Lux, D. R., and West, D. P., Jr., 1989, Late Paleozoic exhumation of northern New England: Implications from $^{40}Ar/^{39}Ar$ thermochronology: Geological Society of America Abstracts with Programs, v. 21, p. A141.

Lux, D. R., Gibson, D., and Hamilton, P. J., 1989, Geochronology of the Songo pluton, western Maine: in Tucker, R. D. and Marvinney, R. G., eds., Studies in Maine Geology, V. 4: Igneous and Metamorphic Geology, Maine Geological Survey, p. 101-114.

Lyons, J. B., Aleinikoff, J. N., and Zartman, R. E., 1986, Uranium-thorium-lead ages of the Highlandcroft Plutonic Suite, northern New England: American Journal of Science, v. 286, p. 489-509.

Lyons, J. B., and Livingston, D. E., 1977, Rb-Sr age of the New Hampshire Plutonic Series: Geological Society of America Bulletin, v. 88, p. 1808-1812.

Lyons, J. B., Bothner, W. A., Moench, R. H., and Thompson, J. B. Jr., eds., 1986, Interim Geologic Map of New Hampshire, scale 1:250,000.

Lyons, J. B., Boudette, E. L., and Aleinikoff, J. N., 1982, The Avalonian and Gander zones in central eastern New England: in St. Julien, P., and Béland, J., eds., Major Structural Zones and Faults of the Northern Appalachians, Geological Association of Canada Special Paper 24, p. 43-66.

Lyons, J. B., Zartman, R. E., and Aleinikoff, J. N., 1983, U-Pb ages of zircons from the Ordovician Highlandcroft Plutonic Suite and Silurian intrusives: Geological Society of America Abstracts with Programs, v. 15, p. 187.

Maggs, W. W., Cheney, J. T., and Spear, F. S., 1986, Probable retrograded eclogites in the Berkshire massif: Geological Society of America Abstracts with Programs, v. 18, p. 32.

Malo, M., and Béland, J., 1989, Acadian strike-slip tectonics in the Gaspé region, Quebec Appalachians: Canadian Journal of Earth Science, v. 26, p. 1764-1777.

Marillier, F., Keen, C. E., Stockmal, G. S., Quinlan, G., Williams, H., Colman-Sadd, S. P., and O'Brien, S. J., 1989, Crustal structure and surface zonation of the Canadian Appalachians: implications of deep seismic reflection data: Canadian Journal of Earth Sciences, v. 26, p. 305-321.

Marshak, S., and Tabor, J., 1989, Structure of the Kingston orocline in the Appalachian fold-thrust belt, New York: Geological Society of America Bulletin, v. 101, p. 683-701.

Martignole, J., and Sisi, J. C., 1981, Cordierite-garnet-H_2O equilibrium: A geological thermometer, barometer, and water fugacity indicator: Contributions to Mineralogy and Petrology, v. 77, p. 38-46.

Martinsson, A., 1970, Ostracodes- Correlation with Europe: in Berry, W. B. N., and Boucot, A. J., eds., Correlation of the North American Silurian Rocks, Geological Society of America Special Paper 102, p. 41-44.

Marvinney, R. G., 1989, Bedrock geology of the southeastern margin of the Connecticut Valley-

Gaspé Synclinorium in Somerset, County, Maine: in Berry, A. W. Jr., ed., Guidebook for Field Trips in Southern and West-Central Maine, New England Intercollegiate Geological Conference, Farmington, Maine, p. 212-237.

Mather, W. W., 1839, Third Annual Report on the Geology of the First Geological District of the State of New York: Albany, New York, p. 69-134.

Mather, W. W., 1843, Geology of New York, Part 1, Comprising the Geology of the First Geological District: Albany, New York, 653 p.

McCutcheon, S. R., 1981, Revised stratigraphy of the Long Reach area, southern New Brunswick: evidence for major, northwestward-directed Acadian thrusting: Canadian Journal of Earth Science, v. 18, p. 646-656.

McCutcheon, S. R., and Ruitenberg, A. A., 1987, Geology and mineral deposits, Annidale-Nerepis area, New Brunswick: New Brunswick Department of Natural Resources and Energy, Memoir 2, 5 plates, 141 p.

McGregor, D. C., 1973, Lower and Middle Devonian spores of eastern Gaspé, Canada: Palaeontographica, v. 142, p. 1-77.

McHone, J. G., 1978, Distribution, orientations, and ages of mafic dikes in central New England: Geological Society of America Bulletin, v. 89, p. 1645-1655.

McKerrow, W. S., and Cocks, L. R. M., 1976, Progressive faunal migration across the Iapetus Ocean: Nature, v. 263, p. 304-305.

McKerrow, W. S., and Ziegler, A. M., 1971, The Lower Silurian paleogeography of New Brunswick and adjacent areas: Journal of Geology, v. 79, p. 635-646.

McLelland, J., Chiarenzelli, J., Whitney, P., and Isachsen, Y., 1988, U-Pb zircon geochronology of the Adirondack Mountains and implications for their geologic evolution: Geology, v. 16, p. 920-924.

Mehnert, K. R., 1968, Migmatites and the origin of granitic rocks: Elsevier Publishing Company, New York, 393 p.

Merguerian, C., and Baskerville, C. A., 1987, Geology of Manhattan Island and the Bronx, New York City, New York: in Roy, D. C., ed., Northeastern Section of the Geological Society of America, Centennial Field Guide Volume 5, Decade of North American Geology Project, p. 137-140.

Merguerian, C., Mose, D., and Nagel, S., 1984, Late syn-orogenic Taconic plutonism along Cameron's Line, West Torrington, Connecticut: Geological Society of America Abstracts with Programs, v. 16, p. 50.

Merrill, F. J., 1890, On the metamorphic strata of southeastern New York: American Journal of Science, 3rd Series, v. 39, p. 383-392.

Merrill, F. J., 1896, The geology of the crystalline rocks of southeastern New York: New York State Museum Annual Report No. 50, Appendix A, p. 21-31.

Merrill, F. J., Darton, N. H., Hollick, A., Salisbury, R. D., Dodge, R. E., Willis, B., and Pressey, H. A., 1902, Description of the New York City District: U. S. Geological Survey, Atlas of the United States, New York City Folio, No. 83, 19 p.

Metzger, W. J., Mose, D. G., and Nagel, M. S., 1982, Rb-Sr whole-rock ages of igneous rocks in the vicinity of Mt. Desert Island, coastal Maine: Northeastern Geology, v. 4, p. 33-38.

Metzger, W. J. and Bickford, M. E., 1972, Rb-Sr chronology and stratigraphic relations of Silurian rocks, Mt. Desert Island, Maine: Geological Society of America Bulletin, v. 83, p. 497-504.

Michard-Vitrac, A., Albarede, F., and Allègre, C. J., 1981, Lead isotopic composition of Hercynian granitic K-feldspars constrains continental genesis: Nature, v. 291, p. 460-464.

Miller, J. D., and Kent, D. V., 1986, Synfolding and prefolding magnetizations in the Upper Devonian Catskill Formation of eastern Pennsylvania: Journal of Geophysical Research, v. 91, p. 12791-12803.

Miller, J. D., and Kent, D. V., 1988, Paleomagnetism of the Silurian-Devonian Andreas redbeds: Evidence for a Early Devonian supercontinent?: Geology, v. 16, p. 195-198.

Moench, R. H., 1989, Metamorphic stratigraphy and structure of the Connecticut Valley area, Littleton to Piermont, New Hampshire: in Lyons, J. B., Bothner, W. A., leaders, A Transect Through the New England Appalachians, International Geological Congress Field Trip Guidebook T162, p. 45-53.

Moench, R. H., and Aleinikoff, J. N., 1985, Metavolcanic stratigraphy in northern New England: Stratigraphic revisions: Geological Society of America Abstracts with Programs, v. 17, p. 54.

Moench, R. H., and Aleinikoff, J. N., 1987, The Piermont allochthon of northwestern New Hampshire: stratigraphic and isotopic evidence: Geological Society of America Abstracts with Programs, v. 19, p. 30.

Moench, R. H., and Zartman, R. E., 1976, Chronology and styles of multiple deformation, plutonism and polymetamorphism in the Merrimack Synclinorium of western Maine: in Lyons, P. C., and Brownlow, A. H., eds., Studies in New England Geology, Geological Society of America Memoir 146, p. 203-238.

Moench, R. H., Pankiwskyj, K. A., Boone, G. M., Boudette, E. L., Ludman, A., Newell, W. R., and Vehrs, T. I., 1988, Geologic map of western interior Maine: United States Geological Survey Miscellaneous Investigations Series, Map 1-1692, scale 1:250,000, 21 p.

Moores, E. M., 1982, Origin and emplacement of ophiolites: Reviews of Geophysics and Space Physics, v. 20, p. 735-760.

Morgan, G. B., and London, D., 1989, Experimental reactions of amphibolite with boron-bearing aqueous fluids at 200 MPa: implications for tourmaline stability and partial melting in mafic rocks: Contributions to Mineralogy and Petrology, v. 102, p. 281-297.

Mose, D. G., 1981, Avalonian igneous rocks with high initial $^{87}Sr/^{86}Sr$ ratios: Northeastern Geology, v. 3, No. 2, p. 129-133.

Mose, D. G., 1982, 1,300-million-year-old rocks in the Appalachians: Geological Society of America Bulletin, v. 93, p. 391-399.

Mose, D. G., and Hayes, J., 1975, Avalonian igneous activity in the Manhattan Prong, southeast New York: Geological Society of America Bulletin, v. 86, p. 929-932.

Mose, D. G., and Merguerian, C., 1985, Rb-Sr Whole rock age determination on parts of the Manhattan Schist and its bearing on allochthony in the Manhattan Prong, southeastern New York: Northeastern Geology, v. 7 No. 1, p. 20-27.

Mose, D. G., and Nagel, M. S., 1982, Chronology of metamorphism in western Connecticut: Rb-Sr ages: in Joesten, R., and Quarrier, S., eds., Guidebook for Fieldtrips in Connecticut and South-Central Massachusetts, Northeastern Intercollegiate Geologic Conference, Storrs, Connecticut, p. 247-262.

Mose, D. G., Ratcliffe, N. M., Odom, A. L. and Hayes, J., 1976, Rb-Sr geochronology and tectonic setting of the Peekskill pluton, southeastern New York: Geological Society of America Bulletin, v. 87, p. 361-365.

Mukasa, S. B., and Tilton, G. R., 1984, Lead isotope systematics in batholithic rocks of the Western and Coastal Cordilleras, Peru: in Harmon, R. S., and Barreiro, B. A., eds., Andean Magmatism, Chemical and Isotopic Constraints, Shiva Publishing Limited, Cheshire, U. K., p. 180-189.

Nakamura, E., Campbell, I. H., and Sun, S, 1985, The influence of subduction processes on the geochemistry of Japanese alkaline basalts: Nature, v. 316, p. 55-58.

Naylor, R. S., 1969, Age and origin of the Oliverian domes, central-western New Hampshire: Geological Society of America Bulletin, v. 80, p. 405-428.

Naylor, R. S., Boone, G. M., Boudette, E. L., Ashenden, D. D., and Robinson, P., 1973, Pre-Ordovician rocks in the Bronson Hill and Boundary Mountain Anticlinoria, New England, USA: EOS Transactions of the American Geophysical Union, v. 54, p. 495.

Nesbitt, H. W., and Young, G. M., 1989, Formation and diagenesis of weathering profiles: Journal of Geology, v. 97, p. 129-147.

Neuman, R. B., and Rankin, D. W., 1980, Bedrock geology of the Shin Pond-Traveler Mountain region: in Roy, D. C., and Naylor, R. S., eds., A Guidebook to the Geology of Northeastern Maine and Neighboring New Brunswick, New England Intercollegiate Geological Conference, Presque Isle, Maine, p. 86-97.

Newberg, D. W., 1986, The Norumbega Fault Zone between Bath and Freedom, Maine: in Newberg, D. W., ed., Guidebook for Field Trips in Southwestern Maine, New England Intercollegiate Geological Conference, Lewiston, Maine, p. 80-97.

Nielson, D. L., Clark, R. G., Lyons, J. B., Englund, E. J., and Borns, D. J.,1976, Gravity models and mode of emplacement of the New Hampshire Plutonic Series: in Lyons, P. C., and Brownlow, A. H., eds., Studies in New England Geology, Geological Society of America Memoir 146, p. 301-318.

Norton, M. F., 1959, Stratigraphic position of the Lowerre Quartzite: New York Academy of Science Annals, v. 80, p. 1148-1158.

Norton, M. F., and Giese, R. F. Jr., 1957, Lowerre quartzite problem: Geological Society of America Bulletin, v. 68, p. 1577-1580.

Nowlan, G. S., 1983, Biostratigraphic, paleogeographic, and tectonic implications of Late Ordovician conodonts from the Grog Brook Group, northwestern New Brunswick: Canadian Journal of Earth Science, v. 20, p. 651-671.

Oliphant, J. D., 1969, Geology of the igneous rocks in southeastern Penobscot township, Hancock County, Maine: M. S. thesis, University of Washington, 39 p.

Olszewski, W. J., Jr., 1980, The geochronology of some stratified metamorphic rocks in northeastern Massachusetts: Canadian Journal of Earth Sciences, v. 17, p. 1407-1416.

Olszewski, W. J., Jr., and Gaudette, H. E., 1982, Age of the Brookville Gneiss and associated rocks, southeastern New Brunswick: Canadian Journal of Earth Sciences, v. 19, p. 2158-2166.

Olszewski, W. J., Jr., Gaudette, H. E., and Cheatham, M. M., 1990, $^{207}Pb/^{206}Pb$ ages from the Chain Lakes Massif, N.W. Maine using single grain direct thermal ionization: Geological Society of America Abstracts with Programs, v. 22, p. 61.

Osberg, P. H., 1978, Synthesis of the geology of the northeastern Appalachians, U.S.A.: Geological Survey of Canada Paper 78-13, p. 137-146.

O'Hara, K., and Gromet, L. P., 1985, Two distinct Late Precambrian (Avalonian) terranes in southeastern New England and their Late Paleozoic juxtaposition: American Journal of Science, v. 285, p. 673-709.

Paige, M. L., and Hon, R., 1980, Geochemical study and tectonic setting of the Cape Ann Complex, northeast Massachusetts: Geological Society of America Abstracts with Programs, v. 20, p. 60.

Pajari, G. E. Jr., Rast, N., and Stringer, P., 1977, Paleozoic vulcanicity along the Bathurst-Dalhousie geotraverse, New Brunswick, and its relations to structure: in Barager, W. R. A., Coleman, L. C., and Hall, J. M., eds., Volcanic Regimes in Canada, Geological Association of Canada Special Paper 16, p. 111-124.

Paterson, S. R., Vernon, R. H., and Tobisch, O. T., 1989, A review of criteria for identification of magmatic and tectonic foliations in granitoids: Journal of Structural Geology, v. 11, p. 349-363.

Pearce, J. A., 1982, Trace element characteristics of lavas from destructive plate boundaries: in Thorpe, R. S., ed., Andesites: Orogenic Andesites and Related Rocks, J. Wiley and Sons, Inc., Chichester, United Kingdom, p. 525-548.

Pearce, J. A., 1983, Role of the sub-continental lithosphere in magma genesis at active continental margins: in Hawkesworth, C. J., and Norry, M. J., eds., Continental Basalts and Mantle Xenoliths, Shiva Press, Nantwich, United Kingdom, p. 230-249.

Pease, M. H., Jr., 1989, Correlation of the Oakdale Formation and Paxton Group of central Massachusetts with strata in northeastern Connecticut: United States Geological Survey Bulletin 1796, 20 p., 1 plate.

Perchuk, L. L., and Lavrent'eva, I. V., 1983, Experimental investigation of exchange equilibria in the system cordierite-garnet-biotite: in Saxena, S. K., ed., Kinetics and equilibria in mineral reactions, Springer-Verlag, New York, p. 199-239.

Pettijohn, F. J., Potter, P. E., and Siever, R., 1973, Sand and sandstone: Springer-Verlag, New York, 618 p.

Philpotts, A. R., 1970, Mechanism of emplacement of Monteregian intrusions: Canadian Mineralogist, v. 10, p. 395-410.

Phinney, R. A., 1986, A seismic cross section of the New England Appalachians: the orogen exposed: in Barazanyi, M., and Brown, L., eds., Reflection seismology; the continental crust: American Geophysical Union Geodynamic Series 14, p. 157-172.

Pickerill, R. K., 1976, Significance of a new fossil locality containing a Salopina community in the Waweig Formation (Silurian - uppermost Ludlow/ Pridoli) of southwest New Brunswick: Canadian Journal of Earth Sciences, v. 13, p. 1328-1331.

Pickerill, R. K., and Pajari, G. E., Jr., 1976, The Eastport formation (Lower Devonian) in the northern Passamaquoddy Bay area, southwest New Brunswick: Canadian Journal of Earth Sciences, v. 13, p. 266-270.

Pickerill, R. K., Pajari, G. E., Jr., and Dickson, W. L., 1978, Geology of the Lower Devonian rocks of Passamaquoddy Bay, southwest New Brunswick: in Ludman, A., ed., Guidebook for Field Trips in Southeastern Maine and Southwestern New Brunswick, New England Intercollegiate Geological Conference, Queens College Press, New York, p. 38-56.

Pignolet, S., Grant, N. K., and Hickman, M. H., 1980, Rb-Sr geochronology of the Honey Hill fault area, eastern Connecticut: Geological Society of America Abstracts with Programs, v. 12, p. 77.

Pindell, J., and Dewey, J. F., 1982, Permo-Triassic reconstruction of western Pangaea and the evolution of the Gulf of Mexico-Caribbean region: Tectonics, v. 1, p. 179-211.

Pinette, S. R., and Osberg, P. H., 1989, Geochemical aspects of volcanic rocks on islands in east Penobscot Bay: in Tucker, R. D., and Marvinney, R. G., eds., Studies in Maine Geology, V. 3: Igneous and Metamorphic Geology, Maine Geological Survey, p. 91-110.

Pitcher, W. S., and Read, H. H., 1963, Contact metamorphism in relation to manner of emplacement of the granites of Donegal, Ireland: Journal of Geology, v. 71, p. 261-296.

Pitcher, W.S., 1984, Phanerozoic plutonism in the Peruvian Andes: in Harmon, R. S., and Barreiro, B. A., eds., Andean Magmatism: Chemical and Isotopic Constraints, Shiva Publishing Limited, Cheshire, United Kingdom, p. 152-167.

Pollock, S. G., 1989a, Mélanges and olistostromes associated with ophiolitic metabasalts and their significance in Cambro-Ordovician forearc accretion in the northern Appalachians: in Horton, J. W., Jr., and Rast, N., eds., Mélanges and Olistostromes of the U. S. Appala-

chians, Geological Society of America Special Paper 228, p. 43-64.

Pollock, S. G., 1989b, Late Silurian basaltic volcanism and associated shallow water sedimentation, northern Maine: Geological Society of America Abstracts with Programs, v. 21, p. 59.

Poole, W. H., Sanford, B. V., Williams, H. and Kelley, D. G., 1970, Geology of southeastern Canada: in Douglas, R. J. W., ed., Geology and Economic Minerals of Canada, Geological Survey of Canada Economic Geology Report no. 1, p. 227-304.

Potts, S., Van der Voo, R., Van der Pluijm, B., and Johnson, R., 1990, Paleomagnetism of the Bluffer Pond Formation in the Munsungun-Winterville Anticlinorium of northern Maine: EOS Transactions of the American Geophysical Union, v. 71, p. 491.

Prasad, N., and Roscoe, S. M., 1991, Geochemical and mineralogical features of sub-Huronian paleosols, their formation and significance to atmospheric evolution during the Huronian period: Geological Association of Canada- Mineralogical Association of Canada-Society of Economic Geologists Program with Abstracts, v. 16., p. A101.

Prucha, J. J., 1956, Geology of the Brewster magnetite district of southeastern New York: New York State Museum and Science Service, Geological Survey Circular 43, 48 p.

Prucha, J. J., 1959, Field relationships bearing on the age of the New York City Group of the Manhattan Prong: New York Academy of Science Annals, v. 80, p. 1159-1169.

Prucha, J. J., Scotford, D. M., and Sneider, R. M., 1968, Bedrock geology of parts of Putnam and Westchester Counties, New York and Fairfield County, Connecticut: New York State Museum and Science Service, Map and Chart Series No. 11, 26 p.

Purdy, J. W., and Jager, E., 1976, K-Ar ages on rock forming minerals from the central Alps: University of Padua Memoir, v. 30, p. 1-31.

Rainbird, R. H., Nesbitt, H. W., and Donaldson, J. A., 1990, Formation and diagenesis of a sub-Huronian saprolith: comparison with a modern weathering profile: Journal of Geology, v. 98, p. 801-822.

Rankin, D. W., 1968, Volcanism related to tectonism in the Piscataquis volcanic belt, an island arc of Early Devonian age in north-central Maine: in Zen, E-An, White, W. S., Hadley, J. B., and Thompson, J. B., Jr., eds., Studies of Appalachian Geology: Northern and Maritime, Interscience Publishers, New York, p. 355-369.

Rankin, D. W., 1968, Volcanism related to tectonism in the Piscataquis Volcanic Belt, an island arc of early Devonian age in north-central Maine: in Zen, E-An, White, W., S., Hadley, J. B., and Thompson, J. B., Jr., eds., Studies in Appalachian Geology, Northern and Maritime: Wiley Interscience, New York, p. 355-369.

Rankin, D. W., 1976, Appalachian salients and recesses: Late Proterozoic continental breakup and opening of the Iapetus Ocean: Journal of Geophysical Research, v. 81, p. 5605-5619.

Rankin, D. W., 1980, The Traveler Rhyolite and its Devonian setting, Traveler Mountain area, Maine: in Roy, D. C., and Naylor, R. S., eds., A Guidebook to the Geology of Northeastern Maine and Neighboring New Brunswick, New England Intercollegiate Geological

Conference, Presque Isle, Maine, p. 98-113.

Rankin, D. W., Drake, A. A. Jr., Glover, L. III, Goldsmith, R., Hall, L. M., Murray, D. P., Ratcliffe, N. M., Read, J. F., Secor, D. T. Jr., and Stanley, R. S., 1989, Pre-orogenic terranes, in Hatcher, R. D., Thomas, W. A., and Viele, G. W., eds., The Appalachian-Ouachita orogen in the United States, The Geology of North America Volume F-2, Decade of North American Geology Project, Geological Society of America, p. 7-100.

Rapela, C. W., Spalletti, L. A., Merodio, J. C., and Aragón,E., 1988, Temporal evolution and spatial variation of early Tertiary volcanism in the Patagonian Andes (40^{o}-$42^{o}30'$S): Journal of South American Earth Sciences, v. 1, p. 75-88.

Ratcliffe, N. M., 1968, Stratigraphic and structural relations along the western border of the Cortlandt intrusives: in Finks, R. M., ed., Guidebook to field excursions, 40th Annual Meeting, New York State Geological Association, Queens College, New York, p. 197-220.

Ratcliffe, N. M., 1979, Adaption and redefinition of the Sherman Marble and regional correlations of Plymouth and Sherman-type marbles in Vermont and Massachusetts, in Changes in stratigraphic nomenclature by the U. S. Geological Survey: U. S. Geological Survey Bulletin 1482A, p. A79-A84.

Ratcliffe, N. M., 1987, High TiO_2 metadiabase dikes of the Hudson Highlands, New York and New Jersey: Possible Late Proterozoic rift rocks in the New York Recess: American Journal of Science, v. 287, p. 817-850.

Ratcliffe, N. M., and Knowles, R. K., 1969, Stratigraphic relations along the western edge of the Cortlandt intrusives and their bearing on the Inwood-Manhattan problem: in Alexandrov, E., ed., Symposium on the New York City Group of Formations, 40th Annual Meeting of the New York State Geological Association, Queens College Press, Flushing, New York, p. 49-53.

Ratcliffe, N. M., Bender, J. F., and Tracy, R. J., 1983, Tectonic setting, chemical petrology and petrogenesis of the Cortlandt Complex and related igneous rocks of southeastern New York State: Guidebook Field Trip 1, Geological Society of America, 101 p.

Ratcliffe, N. M., Buden, R. V., and Burton, W., 1985, Ordovician ductile deformation zones in the Hudson Highlands and their relationship to metamorphic zonation in the cover rocks of Dutchess County: in Tracy, R.J., ed., Guidebook for fieldtrips in Connecticut and adjacent areas of New York and Rhode Island, 77th Annual Meeting, New England Intercollegiate Geological Conference, New Haven, Connecticut, p. 25-60.

Reed, J. C. Jr., 1955, Catoctin Formation near Luray, Virginia: Geological Society of America Bulletin, v. 66, p. 871-896.

Retallack, G., 1986, Reappraisal of a 2200 Ma-old paleosol near Waterval Onder, South Africa: Precambrian Research, v. 32, p. 195-232.

Rickerich, S. F., 1983, Sedimentology, stratigraphy, and structure of the Kittery Formation in the Portsmouth, N. H., area: Master's thesis, University of New Hampshire, 115 p.

Robert, F., Gariépy, C., and Whalen, J. B., 1988, Pb-isotope geochemistry of the Topsails, Mt.

McGerrigle and East Townships granitoid intrusives: Geological Association of Canada Program with Abstracts, v. 13, p. A104.

Robinson, P., 1986, Introduction (to guidebook), in Robinson, P. and Elbert, D. C., eds., Field Trip Guidebook: Regional Metamorphism and Metamorphic Phase Relations in Northwestern and Central New England, Contribution No. 59, Department of Geology and Geography, University of Massachusetts, Amherst, Massachusetts, p. 1-10.

Robinson, P., and Tucker, R. D., 1991, Implications of new U-Pb zircon and monazite ages in the Bronson Hill anticlinorium,Massachusetts: Proterozoic source regions, a major overthrust, and Acadian versus Carboniferous metamorphism:Geological Society of America Abstracts with Programs, v. 23, p. A310.

Robinson, P., Tracy, R. J., Hollocher, K. T., and Dietsch, C. W., 1982, High grade Acadian metamorphism in south-central Massachusetts: in Joesten, R., and Quarrier, S. S., eds., Guidebook for Fieldtrips in Connecticut and South Central Massachusetts, New England Intercollegiate Geologic Conference, Storrs, Connecticut, p. 289-340.

Robinson, P., Tracy, R. J., Hollocher, K. T., Schumacher, J. C., and Berry, H. N. IV, 1986, The central Massachusetts metamorphic high, in Robinson, P., and Elbert, D. C., eds., Field Trip Guidebook: Regional Metamorphism and Metamorphic Phase Relations in Northwestern and Central New England, Contribution No. 59, Department of Geology and Geography, University of Massachusetts, Amherst, Massachusetts, p. 195-266.

Roddick, J. C., and Bevier, M. L., 1988, Conventional and ion microprobe U-Pb ages of two Paleozoic granites, Miramichi terrane: Geological Association of Canada Program with Abstracts, v. 13, p. A105.

Rodgers, J., 1968, The eastern edge of the North American continent during the Cambrian and Early Ordovician, in Zen, E-an, White, W. S., Hadley, J. B., and Thompson, J. B. Jr., eds., Studies of Appalachian geology: Northern and maritime: Interscience Publishers, New York, p. 141-149.

Rodgers, J., 1970, The tectonics of the Appalachians: Interscience Publishers, New York, 271 p.

Rodgers, J., 1981, The Merrimack synclinorium in northeastern Connecticut: American Journal of Science, v. 281, p. 176-186.

Rodgers, J., 1985, Bedrock geological map of Connecticut: Connecticut Geological and Natural History Survey, scale 1:125,000.

Rodgers, J., Gates, R. M., and Rosenfeld, J. L., 1959, Explanatory text for preliminary geologic map of Connecticut, 1956: Connecticut State Geological and Natural History Survey Bulletin 84, 64 p.

Rosenfeld, J. L., and Eaton, G. P., 1985, The Middle Haddam area, Connecticut, revisited: in Tracy, R. J., ed., A Guidebook for Field Trips in Connecticut and Adjacent Areas of New York and Rhode Island, New England Intercollegiate Geologic Conference, New Haven, Connecticut, p. 277-295.

Rowley, D. B., and Kidd, W. S. F., 1981, Stratigraphic relationships and detrital compositions of the medial Ordovician flysch of western New England: Implications for the tectonic

evolution of the Taconic Orogeny: Journal of Geology, v. 89, p. 199-218.

Roy, D. C., 1980, Tectonics and sedimentation in northeastern Maine and adjacent New Brunswick: in Roy, D. C., and Naylor, R. S., eds., A Guidebook to the Geology of Northeastern Maine and Neighboring New Brunswick, New England Intercollegiate Geological Conference, Presque Isle, Maine, p. 1-21.

Roy, D. C., and Mencher, E., 1976, Ordovician and Silurian stratigraphy of northeastern Aroostook County, Maine: in Page, L. R., ed., Contributions to the Stratigraphy of New England, Geological Society of America Memoir 148, p. 25-52.

Roy, J. L., and Anderson, P., 1981, An investigation of the remanence characteristics of three sedimentary units of the Silurian Mascarene Group of New Brunswick, Canada: Journal of Geophysical Research, v. 86, no. B7, p. 6351-6368.

Rutherford, M. J., 1969, An experimental determination of iron biotite-alkali feldspar equilibria: Journal of Petrology, v. 10, p. 381-408.

Sacks, P. E., and Secor, D. T. Jr., 1990, Kinematics of Late Paleozoic continental collision between Laurentia and Gondwana: Science, v. 250, p. 1702-1705.

Samson, S. D., McClelland, W. C., Patchett, P. J., and Gehrels, G. E., 1989, Nd isotopic evidence for ancient continental material between juvenile terranes of the Canadian Cordillera: EOS Transactions of the American Geophysical Union, v. 70, p. 485.

Samson, S. D., Patchett, P. J., Roddick, J. C., and Parrish, R. R., 1989, Origin and tectonic setting of Ordovician bentonites in North America: Isotopic and age constraints: Geological Society of America Bulletin, v. 101, p. 1175-1181.

Sargent, S. L., Hon, R., and Roy, D. R., 1981, Dockendorf Group-Early Devonian calc-alkaline volcanism of "Andean type" in northeastern Maine: Geological Society of America Abstracts with Programs, v. 13, p. 174.

Sargent, S. L. and Hon, R., 1981, Dockendorf Group-Early Devonian Calc- Alkaline volcanism of "Andean type" in northeastern Maine: Geological Society of America Abstracts with Programs, v. 13, p. 174.

Scambos, T. A., Loiselle, M. C., and Wones, D. R., 1986, The Center Pond pluton: the restite of the story (phase separation and melt evolution in granitoid genesis): American Journal of Science, v. 286, p. 241-280.

Scherer, E, Pinet, P., and Seaman, S., 1990, Bimodal compositional clustering of tephra and flows in the Cranberry Island Series of coastal Maine: Geological Society of America Abstracts with Programs, v. 22, p. 67.

Schrijver, K., Marcoux, E., Beaudoin, G., and Calvez, J. Y, 1988, Pb-Zn occurrences and their Pb-isotopic signatures bearing on metallogeny and mineral exploration-Paleozoic sedimentary rocks, northern Appalachians, Quebec: Canadian Journal of Earth Sciences, v. 25, p. 1777-1790.

Schuchert, C., 1925, Significance of Taconic orogeny: Geological Society of America Bulletin, v. 36, p. 343-350.

Schuchert, C., 1930, Orogenic times of the northern Appalachians: Geological Society of America Bulletin, v. 41, p. 701-724.

Schutts, L. D., Brecher, A. Hurley, P. M., Montgomery, C. W., and Krueger, H.W., 1976, A case study of the time and nature of paleomagnetic resetting in a mafic complex in New England: Canadian Journal of Earth Sciences, v. 13, p. 898-907.

Schwartz, W. D., Hon, R., and Roy, D. R., 1984, Trace element geochemistry of Silurian bimodal magmatism in northern Maine: Geological Society of America Abstracts with Programs, v. 16, p. 62.

Scotford, D. M., 1956, Metamorphism and axial plane folding in the Pound Ridge area, New York: Geological Society of America Bulletin, v. 67, p. 1155-1198.

Seguin, M. K., Rao, K. V., and Pineault, R., 1982, Paleomagnetic study of Devonian rocks from Ste. Cecile-St. Sébastien region, Quebec Appalachians: Journal of Geophysical Research, v. 87, p. 7853-7864.

Seidemann, D. E., 1980, K-Ar and Rb-Sr dates for the Reynolds Bridge Gneiss and a post-metamorphic Thomaston granite dike at Reynolds Bridge, Connecticut: Contributions to Geochronology in Connecticut, II, State Geological and Natural History Survey, Report of Investigations No. 10, p. 13-19.

Selverstone, J., and Chamberlain, C. P., 1990, Apparent isobaric cooling paths from granulites: Two counter examples from British Columbia and New Hampshire: Geology, v. 18, p. 307-310.

Sengör, A. M. C., and Yilmaz, Y., 1981, Tethyan evolution of Turkey: A plate tectonic approach: Tectonophysics, v. 75, p. 181-241.

Sengör, A. M. C., Burke, K., and Dewey, J. F., 1978, Rifts at high angles to orogenic belts: Tests for their origin and the upper Rhine Graben as an example: American Journal of Science, v. 278, p. 24-40.

Shanmugam, G., and Lash, G. G., 1982, Analogous tectonic evolution of the Ordovician foredeeps, southern and central Appalachians: Geology, v. 10, p. 562-566.

Shearer, C. K., and Robinson, P., 1988, Petrogenesis of metaluminous and peraluminous tonalites within the Merrimack Synclinorium: Hardwick Tonalite, central Massachusetts: American Journal of Science, v. 288-A , p. 148-195.

Shirey, S. B., Bender, J. F., and Horan, M. F., 1988, Sr, Nd, Pb, and O isotopes and trace elements in 440 Ma mafic alkaline complexes: Evidence for a Proterozoic subcontinental mantle beneath eastern North America: EOS Transactions of the American Geophysical Union, v. 69, p. 524.

Shride, A. F., 1976, Stratigraphy and correlation of the Newbury Volcanic Complex, northeastern Massachusetts: in Page, L. R., ed., Contributions to the Stratigraphy of New England, Geological Society of America Memoir 148, p. 147-177.

Sinha, A. K., and Zietz, I., 1982, Geophysical and geochemical evidence for a Hercynian magmatic

arc, Maryland to Georgia: Geology, v. 10, p. 593-596.

Skehan, J. W., and Murray, D. P., 1980, Geologic profile across southeastern New England: Tectonophysics, v. 69, p. 285-319.

Skinner, R., 1974, Geology of Tetagouche Lakes, Bathurst and Nepisiguit Falls map-areas, New Brunswick, with emphasis on the Tetagouche Group: Geological Survey of Canada Memoir 371, 133 p.

Spariosu, D. J., and Kent, D. V., 1983, Paleomagnetism of the Lower Devonian Traveler Felsite and the Acadian orogeny in the New England Appalachians: Geological Society of American Bulletin, v. 94, p. 1319-1328.

Spear, F. S., 1986, P-T paths in central New England: The evolution of a paired metamorphic belt: Geological Society of America Abstracts with Programs, v. 18, p. 68.

Spear, F. S., and Chamberlain, C. P., 1986, Metamorphism and tectonic evolution of the Fall Mountain nappe complex and adjacent Merrimack Synclinorium, in Robinson, P. and Elbert, D. C., eds., Field Trip Guidebook: Regional Metamorphism and Metamorphic Phase Relations in Northwestern and Central New England, Contribution No. 59, Department of Geology and Geography, University of Massachusetts, Amherst, Massachusetts, p. 121-143.

Spear, F. S., and Cheney, J. T., 1989, A petrogenetic grid for pelitic schists in the system SiO_2-Al_2O_3-FeO-MgO-K_2O-H_2O: Contributions to Mineralogy and Petrology, v. 101, p. 149-164.

Spear, F. S., and Harrison, T. M., 1990, Post Acadian uplift history of central New England from detailed petrologic and $^{40}Ar/^{39}Ar$ studies: Geological Society of America Abstracts with Programs, v. 22, p. 71-72.

Spencer, C., Green, A., Morel-a-l'Huissier, P., Milkereit, B., Luetgert, J., Stewart, D., Unger, J., and Phillips, J., 1989, The extension of Grenville basement beneath the northern Appalachians: results from the Quebec-Maine seismic reflection and refraction surveys: Tectonics, v. 8, p. 677-696.

Spooner, C. M., and Fairbairn, H. W., 1970, Relation of radiometric age of granitic rocks near Calais, Maine, to the time of Acadian Orogeny: Geological Society of America Bulletin, v. 81, p. 3663-3670.

Stanley, R. S., and Ratcliffe, N. M., 1985, Tectonic synthesis of the Taconian orogeny in western New England: Geological Society of America Bulletin, v. 96, p. 1227-1250.

Steiger, R. H., and Jäger, 1977, Subcommission on geochronology: convention on the use of decay constants in geo- and cosmochronology: Earth and Planetary Science Letters, v. 36, p. 359-362.

Stewart, D. B, Arth, J. G., and Flohr, M. J. K., 1988, Petrogenesis of the South Penobscot Intrusive Suite, Maine: American Journal of Science, v. 288-A, p. 75-114.

Stewart, R. D., 1979, The geology of the Benjamin River Intrusive Complex: M.Sc. thesis, Carleton University, Ottawa, Ontario, 126 p.

Stormer, J. C., 1975, A practical two feldspar thermometer: American Mineralogist, v. 60, p. 667-674.

Storre, B., 1970, Stabilitatsbedingungen Grossular-furender Paragenesen im System CaO-Al_2O_3-SiO_2-CO_2-H_2O: Contributions to Mineralogy and Petrology, v. 29, p. 149-162.

St-Julien, P., Malo, M., and Kirkwood, D., 1988, Acadian wrench fault tectonics in the Gaspé Peninsula: Geological Society of America Abstracts with Programs, v. 20, p. 73.

St. Peter, C., 1978, Geology of head of Wapske River, map-area J/13: New Brunswick Department of Natural Resources, Mineral Resources Branch, Map Report 78-1, 24 p.

St. Peter, C., 1982, Geology of Juniper-Knowlesville-Carlisle area, New Brunswick map-areas I-16, I-17, I-18: New Brunswick Department of Natural Resources, Mineral Resources Branch, Map Report 82-1, 82 p.

St. Peter, C., and Boucot, A. J., 1981, Age and regional significance of brachiopods from the Temiscouata Formation of Madawaska County, New Brunswick: Maritime Sediments and Atlantic Geology, v. 17, p. 88-95.

Sutter, J. F., Ratcliffe, N. M., and Mukasa, S. B., 1985, $^{40}Ar/^{39}Ar$ and K-Ar data bearing on the metamorphic and tectonic history of western New England: Geological Society of America Bulletin, v. 96, p. 123-136.

Swinden, H. S., Lane, T. E., and Thorpe, R. I., 1988, Lead-isotope compositions of galena in carbonate-hosted deposits of western Newfoundland: evidence for diverse lead sources: Canadian Journal of Earth Sciences, v. 25, p. 593-602.

Taterka, B.D., 1987, Bedrock Geology of Central Park, New York City: Contribution 61, (M.S. thesis), Department of Geology and Geography, University of Massachusetts, Amherst, Massachusetts, 84 p.

Tauvers, P. R., 1982, Basement-cover relations in the Lincoln area, Vermont: (M. S. thesis), University of Vermont, Burlington, Vermont, 177 p.

Taylor, H. P., Jr., 1980, The effects of assimilation of country rocks by magmas on $^{18}O/^{16}O$ and $^{87}Sr/^{86}Sr$ systematics in igneous rocks: Earth and Planetary Science Letters, v. 47, p. 243-254.

Thomas, W. A., 1977, Evolution of Appalachian salients and recesses from reentrants and promontories in the continental margin: American Journal of Science, v. 277, p. 1233-1278.

Thomas, W. A., 1991, The Appalachian-Ouachita rifted margin of southeastern North America: Geological Society of America Bulletin, v. 103, p. 415-431.

Thompson, A. B., 1976, Mineral reactions in pelitic rocks: II. Calculation of some P-T-X (Fe-Mg) phase relations: American Journal of Science, v. 276, p. 425-454.

Thompson, J. B., Jr., Robinson, P., Clifford, T. N., and Trask, N. J., Jr., 1968, Nappes and gneiss domes in west-central New England: in Zen, E-An, White, W. S., Hadley, J. B., and Thompson,J.B. Jr., eds., Studies of Appalachian Geology: Northern and Maritime, p.

203-218, Interscience Publishers, New York.

Thompson, J. B. Jr., 1957, The graphical analysis of mineral assemblages in pelitic schists: American Mineralogist, v. 42, p. 842-858.

Thompson, J. B. Jr., 1972, Lower Paleozoic rocks flanking the Green Mountain anticlinorium: in Doolan, B. L., and Stanley, R. S., eds., Guidebook to field trips in Vermont, 64th Annual Meeting New England Intercollegiate Geological Field Conference, Burlington, Vermont, University of Vermont, p. 215-229.

Thompson, P. J., 1985, Stratigraphy, structure, and metamorphism in the Monadnock quadrangle, New Hampshire: Contribution No. 58, (Ph.D. thesis), Department of Geology and Geography, University of Massachusetts, Amherst, 191 p., 8 plates.

Thorpe, R. S., Francis, P. W., and O'Callaghan, L., 1984, Relative roles of source composition, fractional crystallisation and crustal contamination in the petrogenesis of Andean volcanic rocks: Philosophical Transactions of the Royal Society of London, v. A310, p. 675-692.

Thorpe, R. S., Francis, P. W., Hammill, M., and Baker, M. C. W., 1982, The Andes: in Thorpe, R. S., ed., Andesites: Orogenic Andesites and Related Rocks, p. 187-205, John Wiley & Sons, New York.

Tillman, J. E., 1981, Fault zones and seismicity in western Connecticut and southeastern New York: John Hopkins University, Applied Physics Laboratory, 57 p.

Toksöz, M. N., Oral, M. B., and Barka, A., 1989, Tectonic deformation in the eastern Mediterranean and Caucasia due to collision of the Arabian and Eurasian plates: EOS Transactions of the American Geophysical Union, v. 70, p. 1372.

Tracy, R. J., and Robinson, P., 1980, Evolution of metamorphic belts: information from detailed petrologic studies: in Wones, D. J., ed., The Caledonides in the U.S.A., I.G.C.P. project 27, p. 189-195, Virginia Polytechnic Institute and State University, Blacksburg, Virginia.

Tremblay, A., St-Julien, P., and Labbé, J.-Y., 1989, Mise à l'evidence et cinématique de la faille de La Guadeloupe, Appalaches du sud du Québec: Canadian Journal of Earth Sciences, v. 26, p. 1932-1943.

Trudel, C., and Malo, M., 1989, Analyse structurale des failles acadiennes de la région de Matapedia (Gaspésie), Appalaches du Québec: Geological Association of Canada Program with Abstracts, v. 14, p. A40.

Tucker, R. D., and Robinson, P., 1990, Age and setting of the Bronson Hill magmatic arc: A reevaluation based on U-Pb zircon ages in southern New England: Geological Society of America Bulletin, v. 102, p. 1404-1419.

Tullis, J., and Yund, R. A., 1985, Dynamic recrystallization of feldspar: a mechanism of ductile shear zone formation: Geology, v. 13, p. 238-241.

Tullis, J., and Yund, R. A., 1991, Diffusion creep in feldspar aggregates: experimental evidence: Journal of Structural Geology, v. 13, p. 987-1000.

Tyler, N., 1979, Correlation, stratigraphic relations, and geochemistry of the Ventersdrop Supergroup in the Derdepoort area, west-central Transvaal: University of the Witwatersrand, Johannesburg, South Africa, Economic Geology Research Unit Information Circular #131, 25 p.

Unger, J. D., 1988, Orientation of the decollement surface beneath the Chain Lakes Massif: results of a 3-D seismic reflection study: Geological Society of America Abstracts with Programs, v. 20, p. 77.

Unger, J. D., Stewart, D. B., and Phillips, J. D., 1987, Interpretation of migrated seismic reflection profiles across the northern Appalachians in Maine: Geophysical Journal of the Royal Astronomical Society, v. 89, p. 171-176.

Van der Voo, R., 1982, Pre-Mesozoic paleomagnetism and plate tectonics: Annual Reviews of Earth and Planetary Science, v. 10, p. 191-220.

Van der Voo, R., 1988, Paleozoic paleogeography of North America, Gondwana, and intervening displaced terranes: Comparisons of paleomagnetism with paleoclimatology and biogeographical patterns: Geological Society of America Bulletin, v. 100, p. 311-324.

van Staal, C. R., 1987, Tectonic setting of the Tetagouche Group in northern New Brunswick: implications for plate tectonic models of the northern Appalachians: Canadian Journal of Earth Sciences, v. 24, p. 1329-51.

van Staal, C. R., Ravenhurst, C. E., Winchester, J. A., Roddick, J. C., and Langton, J. P., 1990, Post-Taconic blueschist suture in the northern Appalachians of northern New Brunswick, Canada: Geology, v. 11, p. 1073-1077.

Van Wagoner, N. A., and Fay, V. K., 1988, Stratigraphy and volcanology of a portion of the Lower Devonian volcanic rocks of southwestern New Brunswick: in Current Research, Part B, Geological Survey of Canada, Paper 88-1B, p. 69-78.

Venugopal, D. V., 1979, Geology of Debec Junction-Gibson Millstream-Temperance Vale-Meductic Region, map-areas G-21, H-21, I-21, and H-22: New Brunswick Department of Natural Resources, Mineral Resources Branch, Map Report 79-5, 36 p.

Waldron, K. A., and Tracy, R. J., 1986, P-T relationships in Taconian regional metamorphism and post-orogenic contact metamorphism, northern Manhattan Prong, New York: Geological Society of America Abstracts with Programs, v. 18, p. 74.

Walker, A. T., and Sclar, C. B., 1983, Petrochemistry of the Preston Gabbro of southeastern Connecticut: tectonic implications: Geological Society of America Abstracts with Programs, v. 15, p. 118.

Watkins, R. and Boucot, A. J., 1975, Evolution of Silurian brachiopod communities along the southeastern coast of Acadia: Geological Society of America Bulletin, v. 86, p. 243-254.

Webb, G. W., 1969, Paleozoic wrench faults in Canadian Appalachians: American Association of Petroleum Geologists Memoir 12, p. 754-786.

Weisse, P. A., Haggerty, S. E., and Brown, L. L., 1985, Paleomagnetism and magnetic mineralogy of the Nahant Gabbro and Tonalite, eastern Massachusetts: Canadian Journal of Earth

Sciences, v. 22, p. 1425-1435.

Wellensiek, M. R., Van der Voo, R., van der Pluijm, B. A., and Johnson, R., 1988, Paleomagnetism of Middle Ordovician volcanics in the Weeksboro-Lunksoos Lake Anticlinorium, north-central Maine: EOS Transactions of the American Geophysical Union, v. 69, p. 337.

Wenner, D. B., 1981, Oxygen isotopic compositions of the late orogenic granites in the southern Piedmont of the Appalachian Mountains, U.S.A., and their relationship to subcrustal structures and lithologies: Earth and Planetary Science Letters, v. 54, p. 186-199.

West, D. P., Jr., and Lux, D. R., 1989, Evidence for Late Paleozoic-Early Mesozoic extensional tectonism along the Norumbega fault zone, southwestern Maine: Geological Society of America Abstracts with Programs, v. 21, p. A141.

Whalen, J. P., 1989, Nature of Canadian basement terranes as inferred from a Nd isotopic transect: Geological Society of America Abstracts with Programs, v. 21, p. A201.

Whalen, J. P., and Gariépy, C., 1986, Petrogenesis of the McGerrigle plutonic complex, Gaspé, Quebec: a preliminary report: in Current Research, Part A, Geological Survey of Canada, Paper 86-1A, p. 265-274.

Whiting-Goldberg, M. A., 1977, Geology of the northern half of the Mount Vernon quadrangle, southeastern New York: (M. A. thesis), Queens College, Flushing, New York, 98 p.

Williams, G. L., Fyffe, L. R., Wardle, R. J., Colman-Sadd, S. P., and Boehner, R. C., 1985, eds., Lexicon of Canadian Stratigraphy, Volume VI- Atlantic Region: Canadian Society of Petroleum Geologists, Calgary, Canada, 572 p.

Williams, H., 1978, Tectonic lithofacies map of the Appalachian orogen: Memorial University of Newfoundland Map No. 1a, scale 1:2,000,000.

Williams, H., and St-Julien, P., 1982, The Baie Verte-Brompton Line: Early Paleozoic continent ocean interface in the Canadian Appalachians: in St-Julien, P., and Béland, J., eds., Major Structural Zones and Faults of the Northern Appalachians, Geological Association of Canada Special Paper 24, p. 177-207.

Williams, H., Gillespie, R. T., and Van Breemen, O., 1985, A late Precambrian rift-related igneous suite in western Newfoundland: Canadian Journal of Earth Science, v. 22, p. 1727-1735.

Williams, H., Kennedy, M. J., and Neale, E. R. W., 1972, The Appalachian structural province: in Price, R. A., and Douglas, R. J. W., eds., Variations in Tectonic Styles in Canada, Geological Association of Canada Special Paper 11, p. 181-261.

Williams, H., Turner, F. J., and Gilbert, C. M., 1982, Petrography- An introduction to the study of rocks in thin section (2nd. ed.): W. H. Freeman and Company, New York, 626 p.

Williams, I. S., Eriksson, S. C., and Compston, W., 1986, Application of inherited zircons to terrane accretion: an example of Archean zircons from the Coastal Belt of Maine: Geological Society of America Abstracts with Programs, v. 18, p. 790.

Wilson, J. T., 1966, Did the Atlantic close and then re-open?: Nature, v. 211, p. 676-681.

Winkler, H. G. F., 1974, Petrogenesis of metamorphic rocks (3rd. ed.): Springer-Verlag, New York, 320 p.

Wintsch, R. P., and Aleinikoff, J. N., 1987, U-Pb isotopic and geologic evidence for Late Paleozoic anatexis, deformation, and accretion of the Late Proterozoic Avalon terrane, south-central Connecticut: American Journal of Science, v. 287, p. 107-126.

Wintsch, R. P., and Fout, J. S., 1982, Structure and petrology of the Willimantic dome and the Willimantic fault, eastern Connecticut: in Joesten, R., and Quarrier, S. S., eds., Guidebook for fieldtrips in Connecticut and South Central Massachusetts, Northeastern Intercollegiate Geological Conference, Storrs, Connecticut, p. 465-482.

Wintsch, R. P., and Sutter, J. F., 1986, A tectonic model for the Late Paleozoic of southeastern New England: Journal of Geology, v. 94, p. 459-472.

Wintsch, R. P., Sutter, J. F., and Kunk, M. J., 1989, $^{40}Ar/^{39}Ar$ thermochronology applied to terrane accretion in southeastern New England: Geological Society of America Abstracts with Programs, v. 21, p. A141.

Wissig, G. C. Jr., 1970, Bedrock geology of the Ossining Quadrangle, New York: (Ph.D. thesis), Syracuse University, 186 p.

Wones, D. R., 1974, Igneous petrology of some plutons in the northern part of the Penobscot Bay area: in Osberg, P. H., ed., Northeastern Intercollegiate Geological Conference Guidebook for Fieldtrips in East-central and North-central Maine, p. 99-125.

Wones, D. R., 1978, Norumbega fault zone, Maine: United States Geological Survey Summary of Technical Reports VIII, National Earthquake Hazards Reduction Program, p. 108-111.

Wones, D. R., Loiselle, M., Ayuso, R. A., Sinha, A. K., Scambos, T. A., and Andrew, A., 1981, Source models for Caledonian plutons, eastern and central Maine: Geological Society of America Abstracts with Programs, v. 13, p. 184.

Zartman, R. E., 1974, Lead isotopic provinces in the Cordillera of the western United States and their geologic significance: Economic Geology, v. 69, p. 792-805.

Zartman, R. E., 1977, Geochronology of some alkaline rock provinces in eastern and central United States: Annual Review of Earth and Planetary Sciences, v. 5, p. 257-286.

Zartman, R. E., and Doe, B. R., 1981, Plumbotectonics- The model: Tectonophysics, v. 75, p. 135-162.

Zartman, R. E., and Gallego, M. D., 1979, Radiometric ages: Compilation B, United States Geological Survey: in Marvin, R. F., and Dobson, S. W., eds., Isochron West, The Bulletin of Isotopic Geochronology, no. 26, p. 18-19.

Zartman, R. E., and Hermes, O. D., 1987, Archean inheritance in zircon from late Paleozoic granites from the Avalon zone of southeastern New England: an African connection: Earth and Planetary Science Letters, v. 82, p. 305-315.

Zartman, R. E., and Leo, G. W., 1985, New radiometric ages on gneisses of the Oliverian domes in

New Hampshire and Massachusetts: American Journal of Science, v. 285, p. 267-280.

Zartman, R. E., and Marvin, R. F., 1971, Radiometric age (Late Ordovician) of the Quincy, Cape Ann, and Peabody Granites from eastern Massachusetts: Geological Society of America Bulletin, v. 82, p. 937-958.

Zartman, R. E., and Naylor, R. S., 1984, Structural implications of some radiometric ages of igneous rocks in southeastern New England: Geological Society of America Bulletin, v. 95, p. 522-539.

Zartman, R. E., and Wasserburg, G. J., 1969, The isotopic composition of lead in potassium feldspars from some 1.0-b.y. old North American igneous rocks: Geochimica et Cosmochimica Acta, v. 33, p. 901-942.

Zartman, R. E., Hermes, O. D., and Pease, M. H., Jr., 1988, Zircon crystalliza tion ages, and subsequent isotopic disturbance events, in gneissic rocks of eastern Connecticut and western Rhode Island: American Journal of Science, v. 288, p. 376-402.

Zartman, R. E., Hurley, P. M., Krueger, H. W., and Giletti, B. J., 1970, A Permian disturbance of K-Ar radiometric ages in New England: Geological Society of America Bulletin, v. 81, p. 3359-3374.

Zbinben, E. A., Holland, H. D., Feakes, C. R., and Dobos, S. K., 1988, The Sturgeon Falls paleosol and the composition of the atmosphere 1.1 GaBP: Precambrian Research, v. 42, p. 141-163.

Zeitler, P. K., Barreiro, B., Chamberlain, C. P., and Rumble, D. III, 1990, Ion-microprobe dating of zircon from quartz-graphite veins at the Bristol, New Hampshire, metamorphic hot spot: Geology, v. 7, p. 626-629.

Zen, E-an, 1967, Time and space relationships of the Taconic allochthon and autochthon: Geological Society of America Special Paper 97, 107 p.

Zen, E-an, 1983, Exotic terranes in the New England Appalachians-limits,candidates, and ages: A speculative essay: in Hatcher, R. D., Jr., Williams, H., and Zietz, I., Contributions to the Tectonics and Geophysics of Mountain Chains, Geological Society of America Memoir 158, p. 55-81.

Zen, E-an, Goldsmith, R., Ratcliffe, N. L., Robinson, P. and Stanley, R. S., 1983, Bedrock geologic map of Massachusetts: United States Geological Survey, Washington, D. C., scale 1:250,000.

PLATE I—

GEOLOGICAL MAP OF PARTS OF THE PEACH LAKE AND BREWSTER QUADRANGLES, NEW YORK AND CONNECTICUT

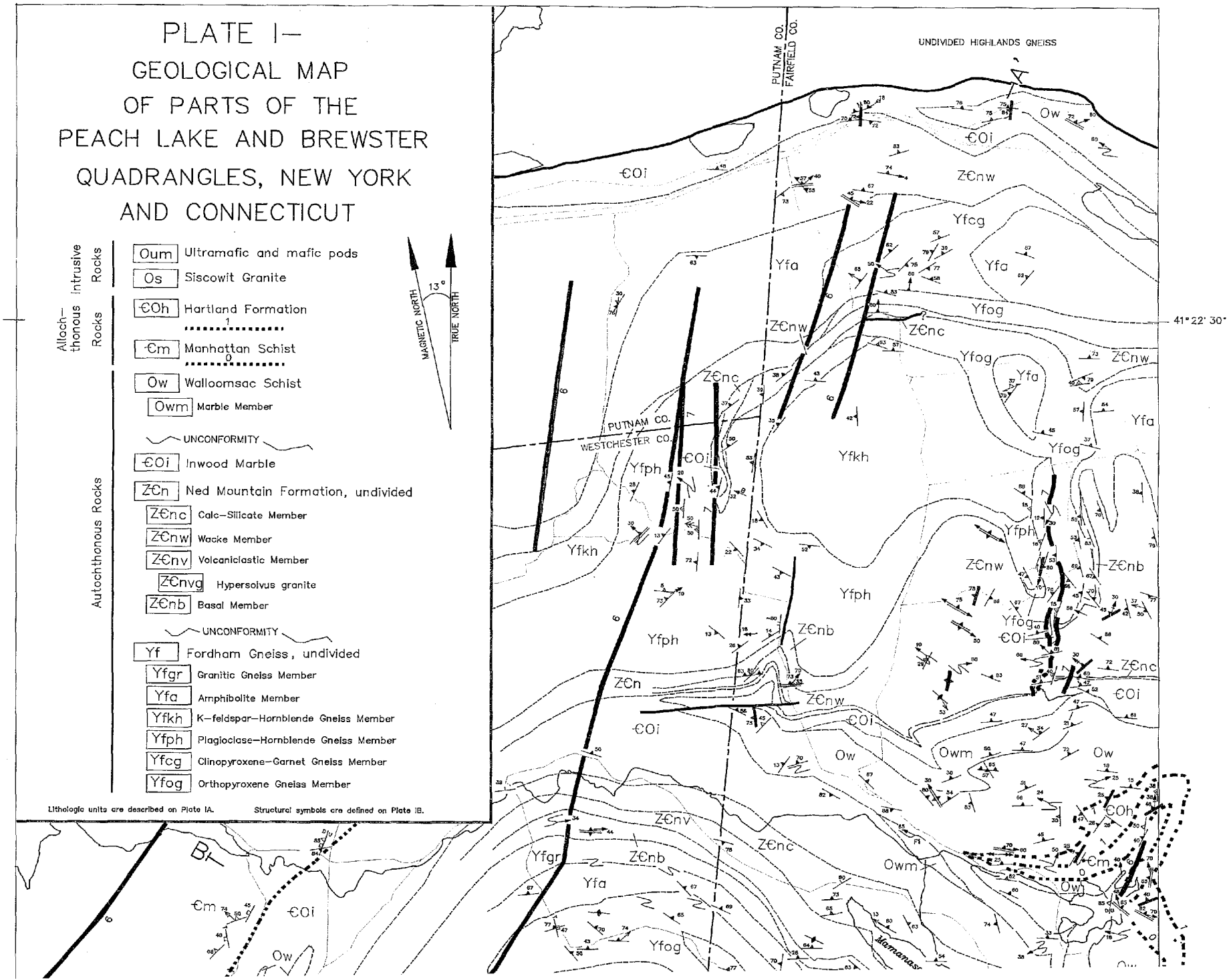

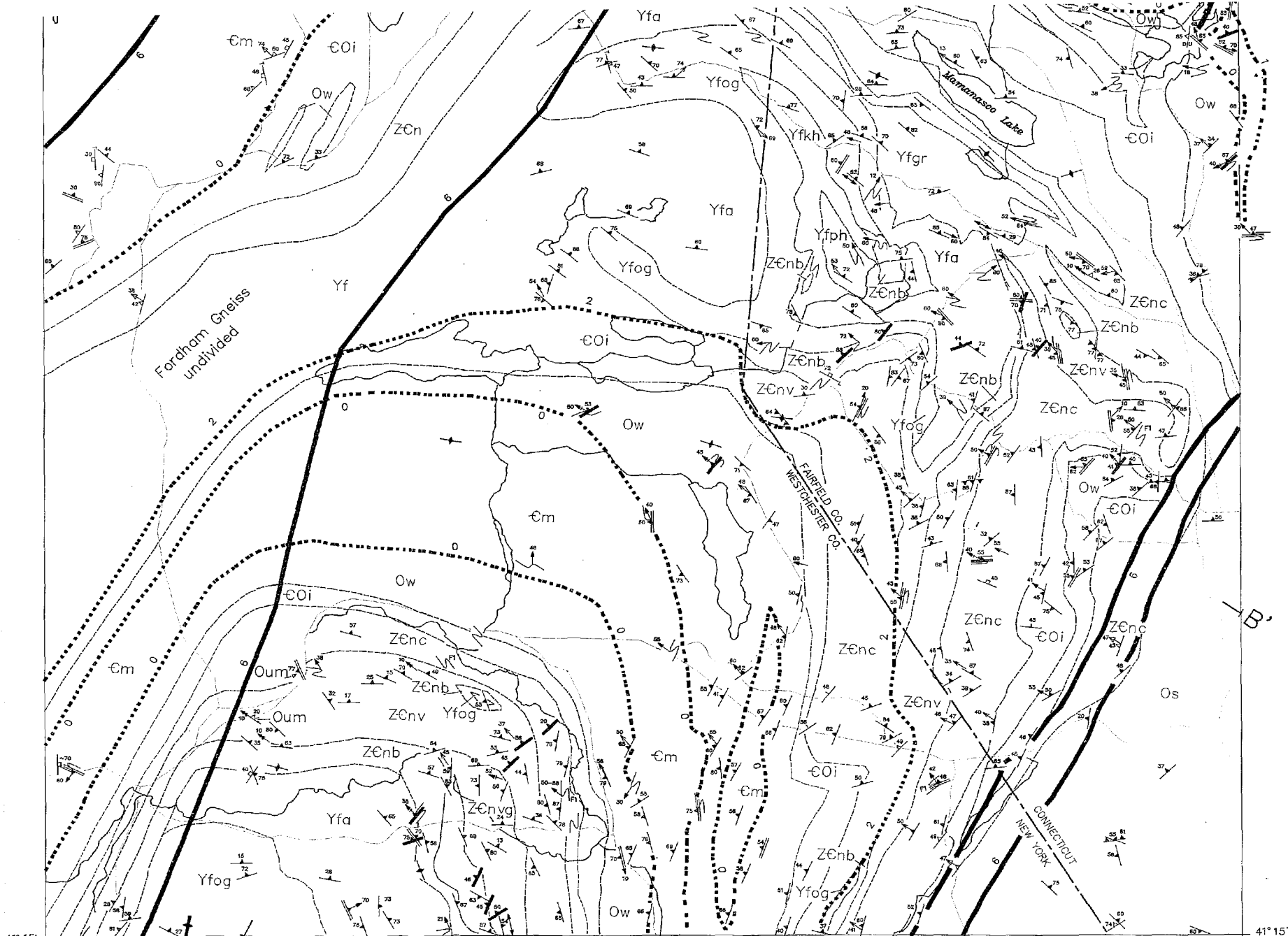

SCALE 1:24000

Selected roads

For identification of roads and landmarks, see Plate III.

1 0.5 0 0.5 1 MILE

1 0.5 0 0.5 1 KILOMETER

Geology by Pamela Chase Brock, 1992.

BROCK, PAMELA J.
9325069 © 1993

PLATE IA– EXPLANATION OF LITHOLOGIC UNITS

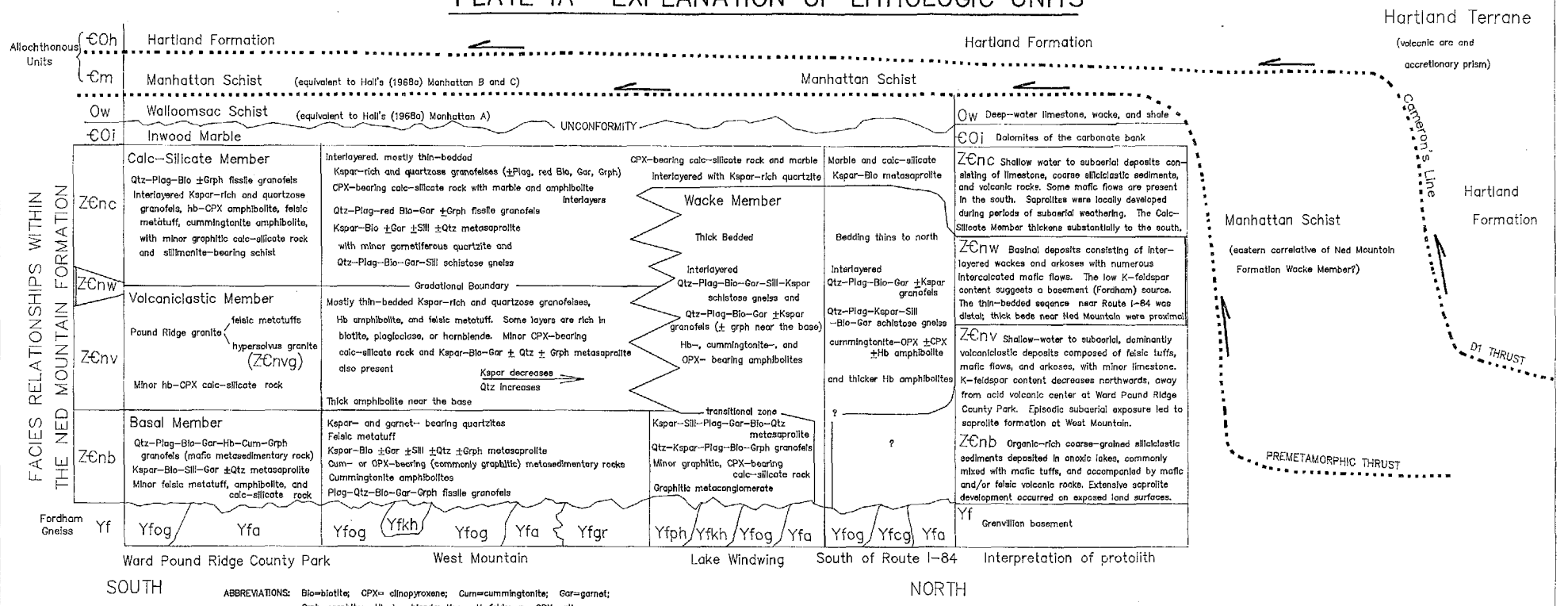

ABBREVIATIONS: Bio=biotite; CPX= clinopyroxene; Cum=cummingtonite; Gar=garnet; Grph=graphite; Hb=hornblende; Kspar=K–feldspar; OPX=orthopyroxene; Qtz=quartz; Sill=sillimanite.

INTRUSIVE ROCKS

MESOZOIC

Lamprophyre

Dark green, fine–grained, porphyritic lamprophyre dike less than 0.5 meter in thickness. Biotite phenocrysts are abundant and display a flow foliation parallel to dike contacts.

MISSISSIPPIAN

Mississippian Granite Suite

Very small bodies of tourmaline–bearing, two–mica white granite, pink microcline–rich pegmatite, and white albitic pegmatite. Cleavages defined by muscovite +/– biotite are commonly present. Aluminous host rocks are typically retrograded to muscovite–rich schists.

Os Siscowit Granite

Medium to coarse–grained, pinkish–weathering, pale beige granite and granitic gneiss. Foliation is variably developed;

AUTOCHTHONOUS UNITS

CAMBRO–ORDOVICIAN

Ow Wallloomsac Schist

Rusty–weathering, poorly bedded, migmatitic quartz–plagioclase K–feldspar–biotite garnet–sillimanite schistose gneiss and biotite–garnet–sillimanite–quartz–feldspar schist. Well–bedded, graphitic, quartz–plagioclase–biotite granofels, calcareous marble, and calc–silicate rock are present near the base. The typical reddish biotite gives many rocks a distinctive red cast. Bedding varies from several centimeters to greater than one meter in thickness. The Walloomsac Schist contains minor hornblende (+/–) clinopyroxene amphibolite and a few very thin beds of cummingtonite amphibolite.

Owm Marble Member

The marbles and calc–silicates of the Walloomsac Schist are distinguished as the Marble Member where their thickness in outcrop permits.

€Oi Inwood Marble

Well–bedded white, tan, and greenish magnesian marble with calcareous interlayers. Silica–poor magnesian beds consist of dolomite, +/– phlogopite, calcite, olivine, and spinel. The more siliceous of the magnesian beds contain calcite–olivine–diopside–phlogopite. Scattered interbeds of brown phlogopite–calcite schist, white quartzite, and dark diopside–rich amphibolite are locally present.

PROTEROZOIC Y

Yf Fordham Gneiss

Yfgr Granitic Gneiss Member

Coarse–grained, poorly layered, light grey, hornblende–bearing granitic gneiss with abundant clots of magnetite, one– to three–millimeters in diameter. Amphibolitic interlayers are also present.

Yfa Amphibolite Member

Massive hornblende–rich amphibolite with minor leucocratic quartz–feldspar–biotite +/– hornblende gneiss. Small amounts of pyroxene are commonly present in both the mafic and leucocratic layers. Contacts with with Yfog, Yfcg, and Yfph are gradational.

Yfkh K–feldspar–Hornblende Gneiss Member

Leuco– to mesocratic, coarse–grained, well–layered, K–feldspar–plagioclase–quartz–hornblende +/– clinopyroxene gneiss with amphibolitic interlayers.

Yfph Plagioclase–Hornblende Gneiss Member

ALLOCHTHONOUS UNITS

CAMBRO–ORDOVICIAN

€Oh Hartland Formation

Well–bedded sequence of thick, dark grey to black, hornblende–, cummingtonite–, or orthopyroxene–bearing amphibolites, thick white quartz–plagioclase–biotite–garnet granofelses, and thin (~10 centimeter) layers of white granofels rhythmically interbedded with grey quartz–feldspar–biotite–garnet–sillimanite schistose gneiss.

€m Manhattan Schist

Poorly bedded, migmatized, dark grey quartz–plagioclase–K–feldspar–biotite–garnet–sillimanite schistose gneiss and white quartz–plagioclase–biotite–garnet granofels, with interlayers of hornblende amphibolite.

ORDOVICIAN

Os Siscowit Granite

Medium to coarse–grained, pinkish–weathering, pale beige granite and granitic gneiss. Foliation is variably developed; micas are generally aligned, and quartz ribbons locally prominent. Biotite is ubiquitous, and secondary muscovite is generally present. Contains metasedimentary xenoliths and garnet–biotite schlieren.

Oum Ultramafic and mafic pods

Isolated pods of grey to black mafic and ultramafic rock, each less than two meters in diameter. Pods consist of olivine–phlogopite hornblendite (partially converted to unfoliated amphibolite) or garnet–hornblende amphibolite.

PROTEROZOIC Z– CAMBRIAN

Silica–poor magnesian beds consist of dolomite, +/– phlogopite, calcite, olivine, and spinel. The more siliceous of the magnesian beds contain calcite–olivine–diopside–phlogopite. Scattered interbeds of brown phlogopite–calcite schist, white quartzite, and dark diopside–rich amphibolite are locally present.

Z€n Ned Mountain Formation

See diagram above for description of geographical and facies–related variations

Z€nc Calc–Silicate Member

Z€nw Wacke Member

Z€nv Volcaniclastic Member

Z€nb Basal Member

PROTEROZOIC Y

Yfkh K–feldspar–Hornblende Gneiss Member

Leuco– to mesocratic, coarse–grained, well–layered, K–feldspar–plagioclase–quartz–hornblende +/– clinopyroxene gneiss with amphibolitic interlayers.

Yfph Plagioclase–Hornblende Gneiss Member

Coarse–grained, well–layered, leuco– to mesocratic plagioclase–quartz–hornblende +/– clinopyroxene gneisses with amphibolitic interlayers.

Yfcg Clinopyroxene–Garnet Gneiss Member

Massive, poorly layered, generally melanocratic, green– or red–and–green clinopyroxene–garnet–plagioclase–quartz gneiss. Irregular black patches occur where hornblende has replaced clinopyroxene and garnet.

Yfog Orthopyroxene Gneiss Member

Coarse–grained, well–layered, leuco–to mesocratic orthopyroxene–bearing gneisses with dark hornblende–rich interlayers, cross–cut in places by orthopyroxene–bearing granite. Dark grey or greenish when fresh; beige or pinkish when weathered.

C

Poorly bedded, migmatized, dark grey quartz–plagioclase–K–feldspar–biotite–garnet–sillimanite schistose gneiss and white quartz–plagioclase–biotite–garnet granofels, with interlayers of hornblende amphibolite.

PLATE IB– EXPLANATION OF STRUCTURAL SYMBOLS

PLANAR FEATURES

Strike and dip

	Vertical	Inclined
Bedding		35
Foliation		46
Cross–cutting foliation		55

Hinge surfaces and refoliation zones

F1		47 F1
F2 and unspecified age		63
F3		37
F4		12

Fabrics in late faults and shear zones

- S6 cleavage and sense of displacement, where available. 65 D U
- Cleavage in D7 shear zone 25
- Late (post–F3) mylonite zone (exact age uncertain) M 81
- Brittle fault cleavage 87
- Tourmalinized fractures 42 T

LINEAR FEATURES

Trend and plunge

	Horizontal	Inclined
Quartz rod (age unspecified)		44
Boudin line		51

Hinge lines

F1		F1 54
F2 and unspecified age		43
F3		42
F4		11

- Intersection of D6 with older foliation 33
- L7 mullion and quartz rods 36
- Slickensides 7

FOLD STYLE AND CROSS–CUTTING RELATIONSHIPS

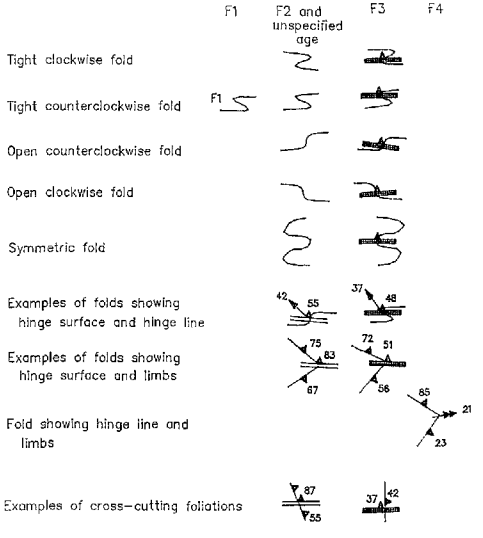

(Intersections of structural symbols are plotted at the outcrop location. The centers of fold symbols are plotted at the outcrop location.)

CONTACTS AND FAULTS

- Tightly constrained contacts
- interpolated contacts
- 0 Premetamorphic thrust
- 1 Cameron's Line (D1 thrust)
- 2 D2 thrust
- 6 D6 fault zone
- 7 D7 thrust
- Brittle fault

BROCK, PAMELA J.
9325069 © 1993

Plate II—A. Map showing truncation of Fordham Gneiss lithologies beneath the Ned Mountain Formation.

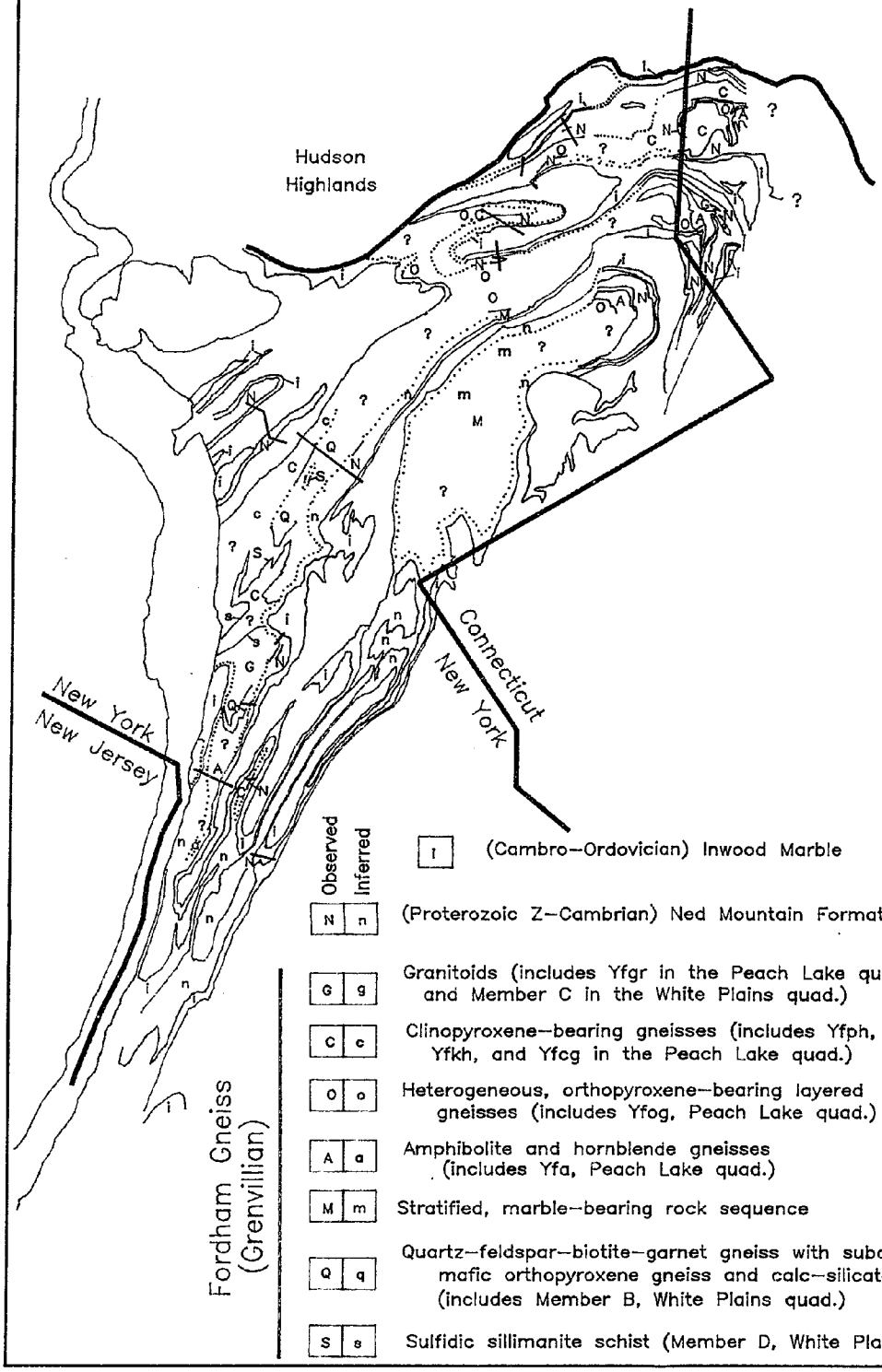

Plate II—B. Location map for trans
outside of the study

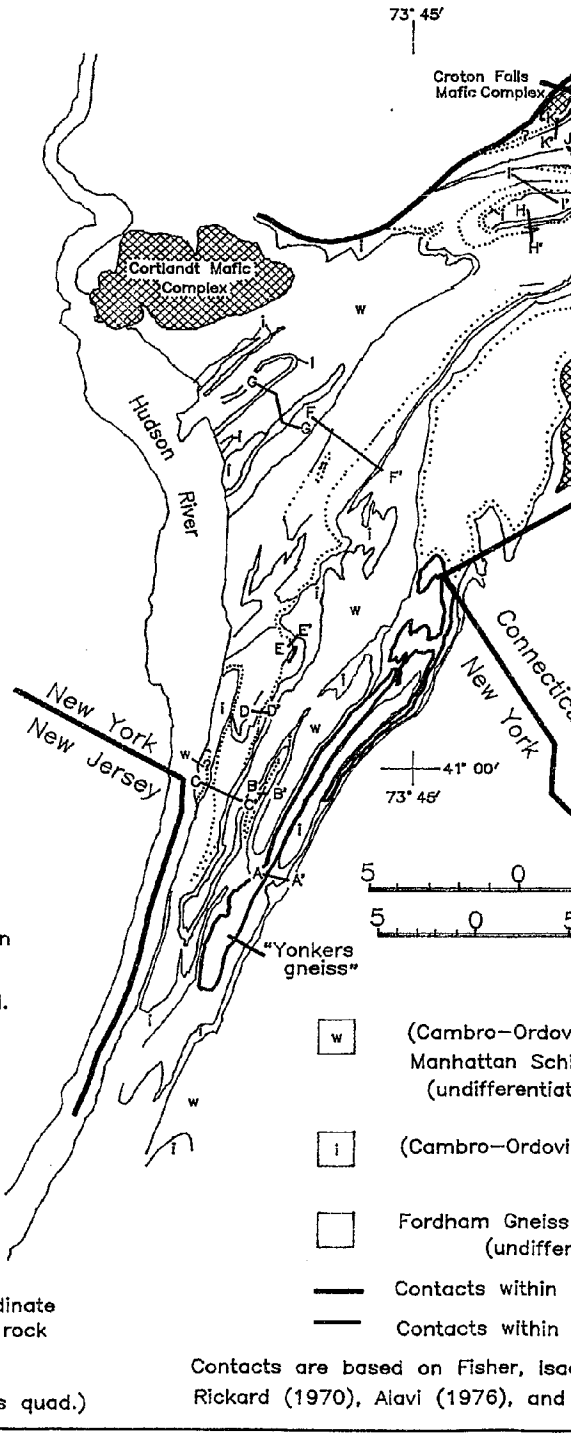

BROCK, PAM
9325069 ©

ap for transects examined
the study area.

Plate II–C. Map showing subdivisions of the Ned Mountain Formation.

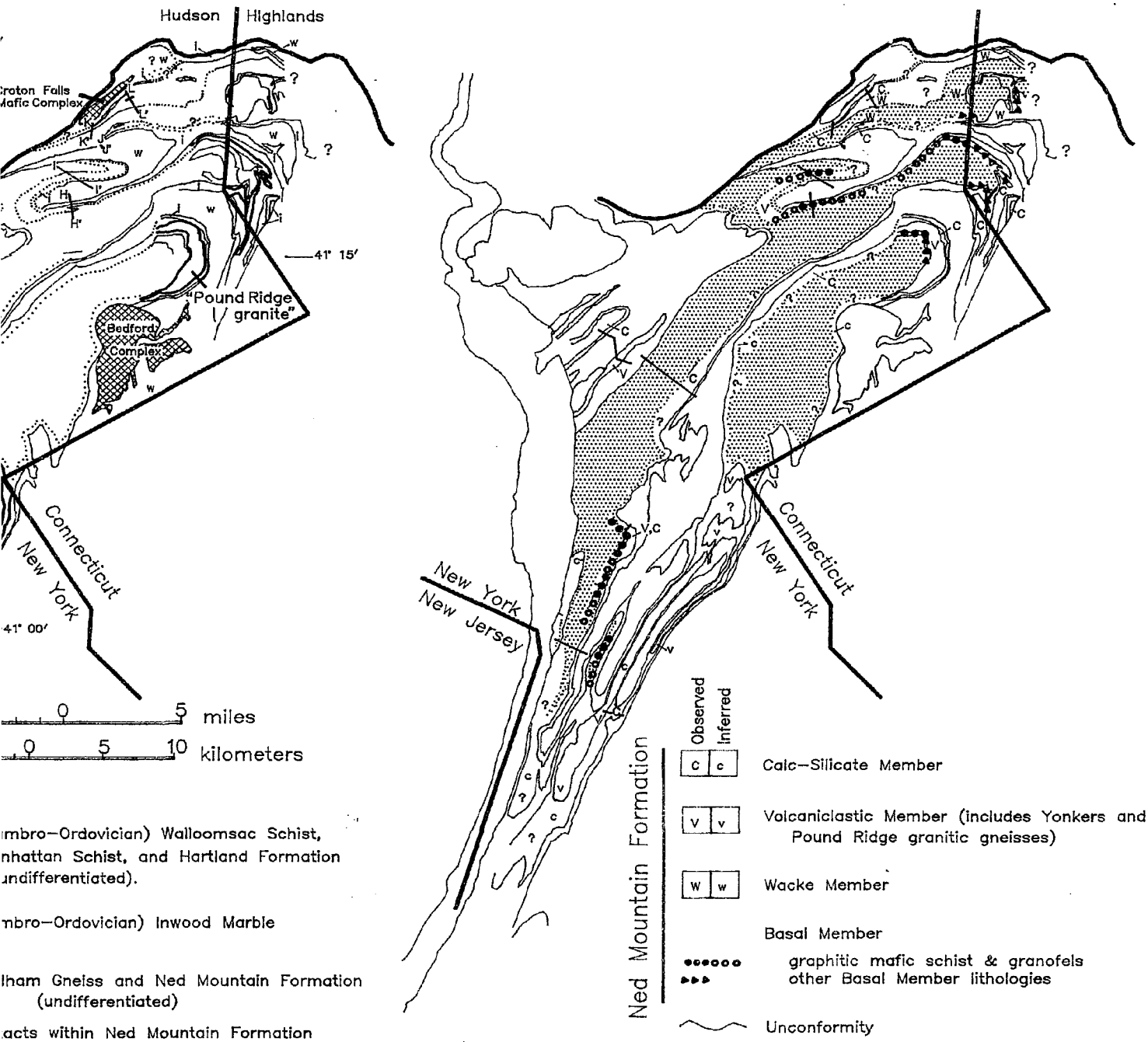

mbro–Ordovician) Walloomsac Schist,
nhattan Schist, and Hartland Formation
undifferentiated).

mbro–Ordovician) Inwood Marble

lham Gneiss and Ned Mountain Formation
(undifferentiated)

acts within Ned Mountain Formation

acts within Fordham Gneiss

Fisher, Isachsen and
(1976), and new mapping.

NOTE: See Plate I for more detail on lithologic subdivisions in the study area.

, PAMELA J.
69 © 1993

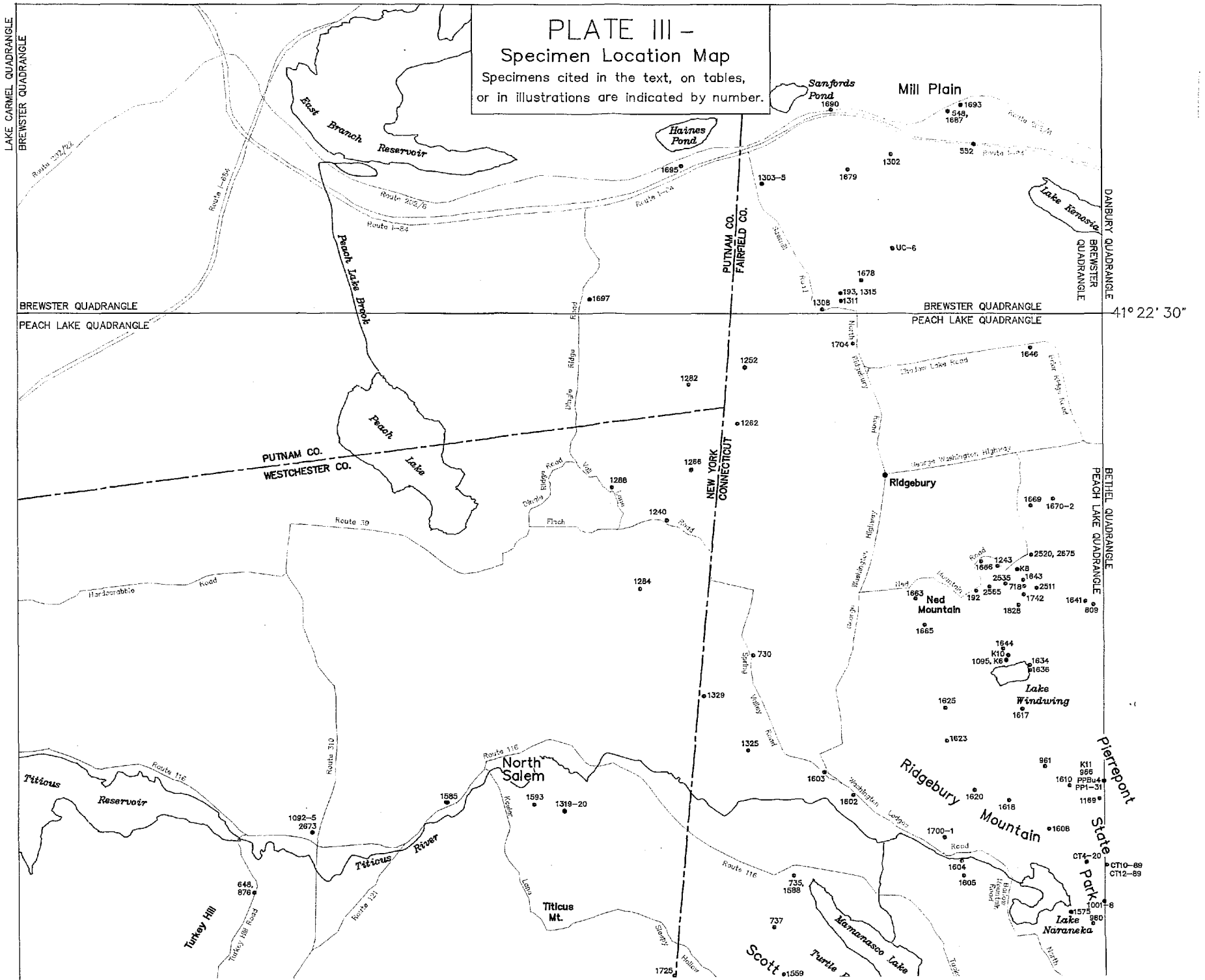
PLATE III –
Specimen Location Map
Specimens cited in the text, on tables, or in illustrations are indicated by number.
LAKE CARMEL QUADRANGLE
BREWSTER QUADRANGLE
DANBURY QUADRANGLE
BETHEL QUADRANGLE
PEACH LAKE QUADRANGLE
41° 22' 30"
PUTNAM CO.
WESTCHESTER CO.
PUTNAM CO.
FAIRFIELD CO.
NEW YORK
CONNECTICUT
Sanfords Pond
Haines Pond
East Branch Reservoir
Peach Lake Brook
Peach Lake
Lake Kenosia
Mill Plain
Ridgebury
Ned Mountain
Ridgebury Mountain
Lake Windwing
Lake Naraneka
Pierrepont State Park
North Salem
Titicus Reservoir
Titicus River
Titicus Mt.
Turkey Hill
Scott
Mamanasco Lake
Route 116
Route 35
Route 121
Route 310
Route 1-84
Route 202/6
Route 202/35
Dingle Ridge Road
Flint Road
Hardscrabble Road
Sperry Valley Road
Washington Ledges Road
Turkey Hill Road
Lonn Road
Stanley Hollow Road
Ridgebury Road
Shadow Lake Road
Briar Ridge Road
George Washington Highway
Ned Mountain Road
Ridgebury Mountain Road
1092–5
2673
1319–20
1585
1593
1303–5
1679
1695
1697
1678
1193, 1315
1311
1308
1704
1252
1282
1262
1286
1240
1284
1329
1325
730
1603
1602
1620
1618
1608
1700–1
1604
1605
735,
1588
737
1725
1559
1575
980
1001–8
CT4–20
CT10–89
CT12–89
1646
1669
1670–2
2520, 2675
1666
1243
K8
2535
1643
718
2511
1663
192
2565
1742
1641
809
1828
1685
1644
K10
1095, K6
1634
1636
1625
1617
1623
961
K11
966
1610
PPBu4
PP1–31
1169
648,
876
1302
552
1693
549,
1687
1690
UC–6

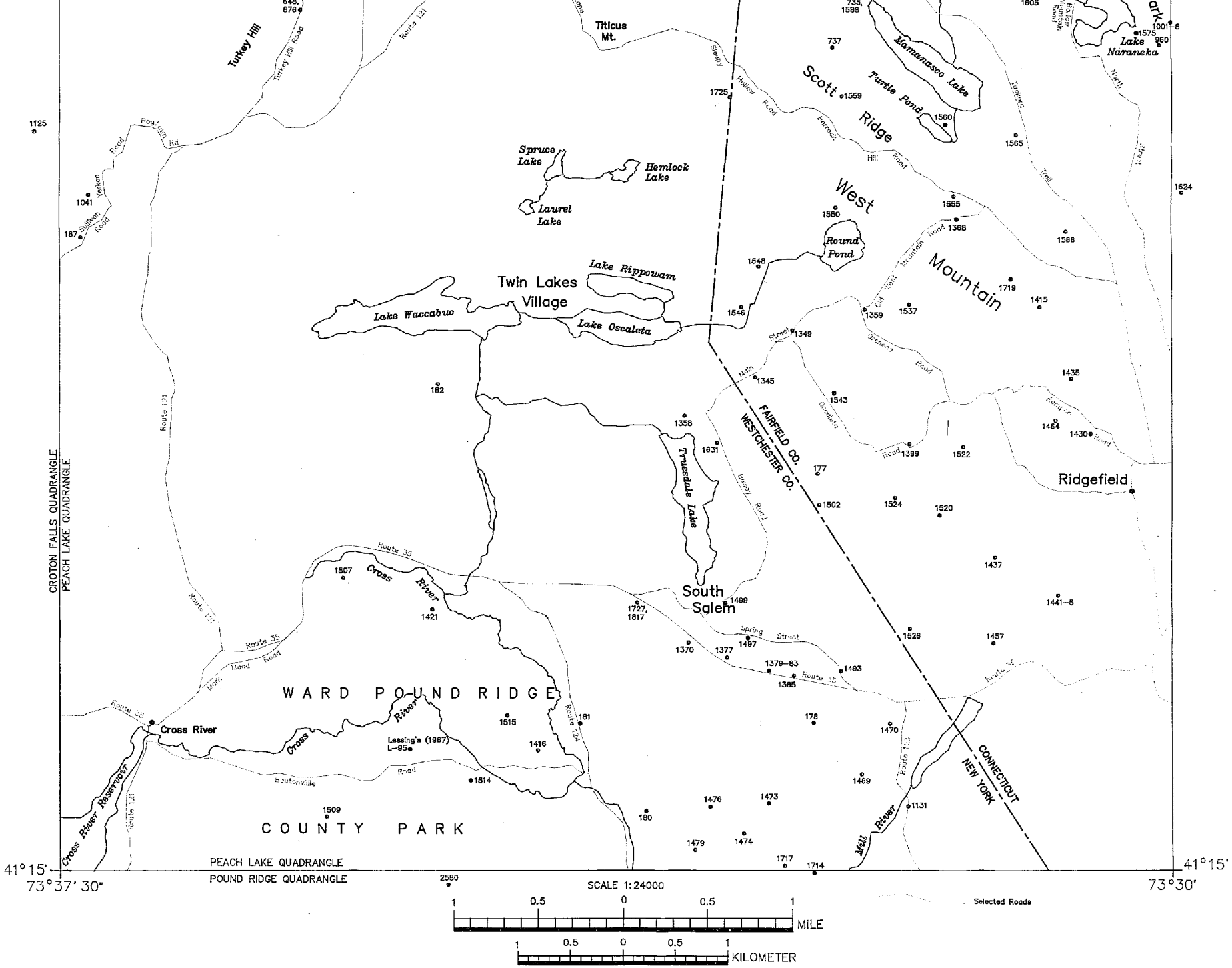

BROCK, PAMELA J.
9325069 © 1993

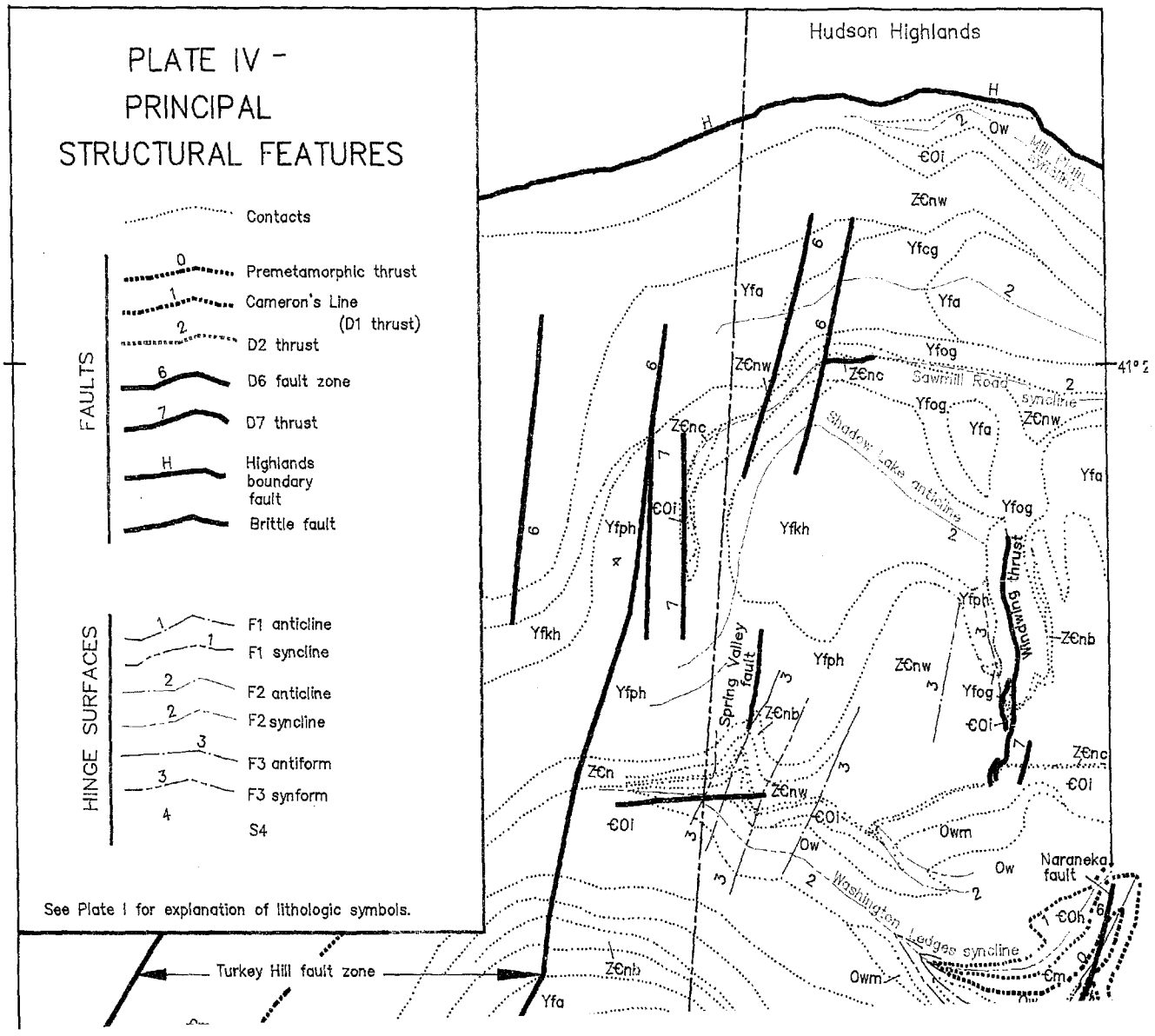
PLATE IV -
PRINCIPAL
STRUCTURAL FEATURES
Contacts
FAULTS
0 Premetamorphic thrust
1 Cameron's Line (D1 thrust)
2 D2 thrust
6 D6 fault zone
7 D7 thrust
H Highlands boundary fault
Brittle fault
HINGE SURFACES
1 F1 anticline
1 F1 syncline
2 F2 anticline
2 F2 syncline
3 F3 antiform
3 F3 synform
4 S4
See Plate I for explanation of lithologic symbols.
Hudson Highlands
Turkey Hill fault zone
Spring Valley fault
Mahopac thrust
Shadow Lake anticline
Sawmill Road syncline
Washington Ledges syncline
Naraneka fault
41° 2
Yfa
Yfkh
Yfph
Yfcg
Yfog
Z€nw
Z€nc
Z€nb
Z€n
€Oi
€Oh
€m
Owm
Ow

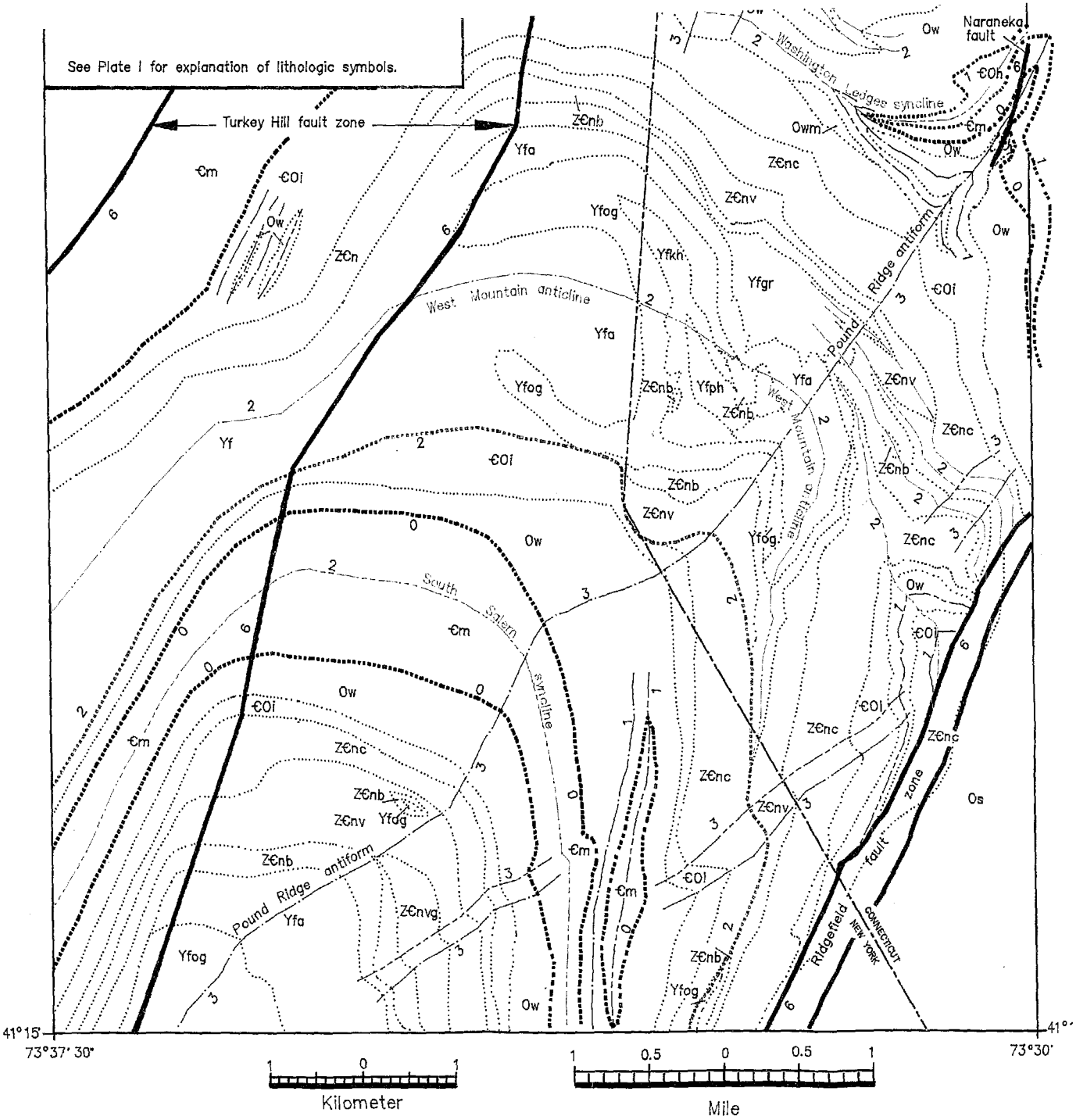

BROCK, PAMELA J.
9325069 © 1993

PLATE V — GEOLOGIC

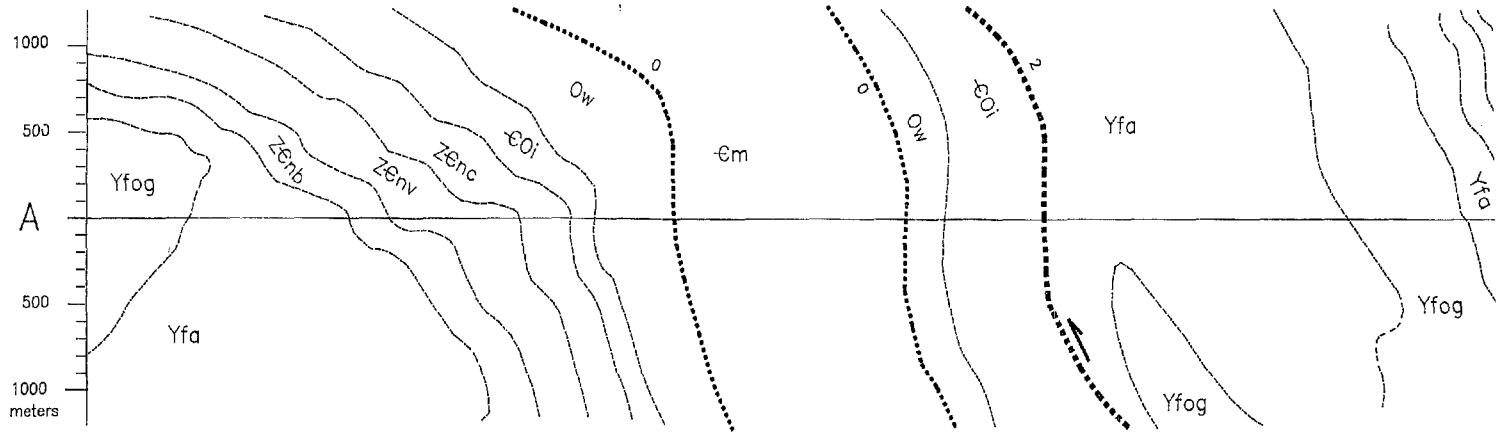

Pound Ridge Antiform

South Salem Syncline

West Mountain Anticline

Intrusive Rocks
- Os — Siscowit Granite

Allochthonous Rocks
- €Oh — Hartland Formation
- 1
- €m — Manhattan Schist
- 0

Autochthonous Rocks
- Ow — Wallomsac Schist
  - Owm — Marble Member
- UNCONFORMITY
- €Oi — Inwood Marble
- Z€n — Ned Mountain Formation, undivided
  - Z€nc — Calc-Silicate Member
  - Z€nw — Wacke Member
  - Z€nv — Volcaniclastic Member
    - Z€nvg — Hypersolvus granite
  - Z€nb — Basal Member
- UNCONFORMITY
- Yf — Fordham Gneiss, undivided
  - Yfgr — Granitic Gneiss Member
  - Yfa — Amphibolite Member
  - Yfkh — K-feldspar-Hornblende Gneiss Member
  - Yfph — Plagioclase-Hornblende Gneiss Member
  - Yfcg — Clinopyroxene-Garnet Gneiss Member
  - Yfog — Orthopyroxene Gneiss Member

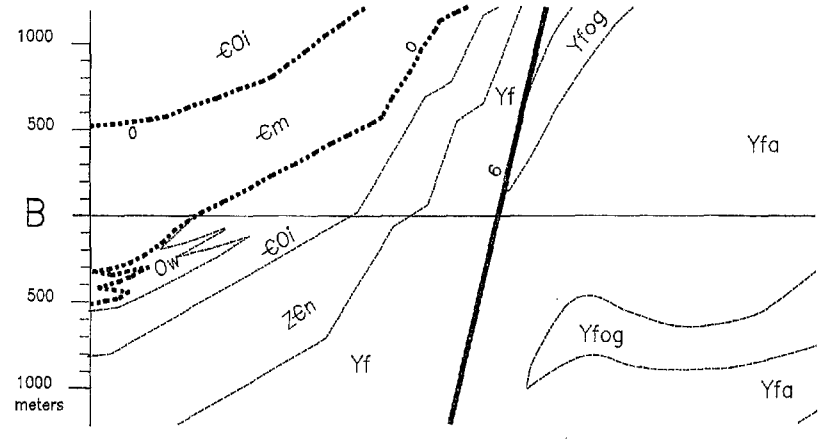

Turkey Hill Fault Zone

BROCK, PAMELA J.
9325069 © 1993

LOGIC CROSS SECTIONS

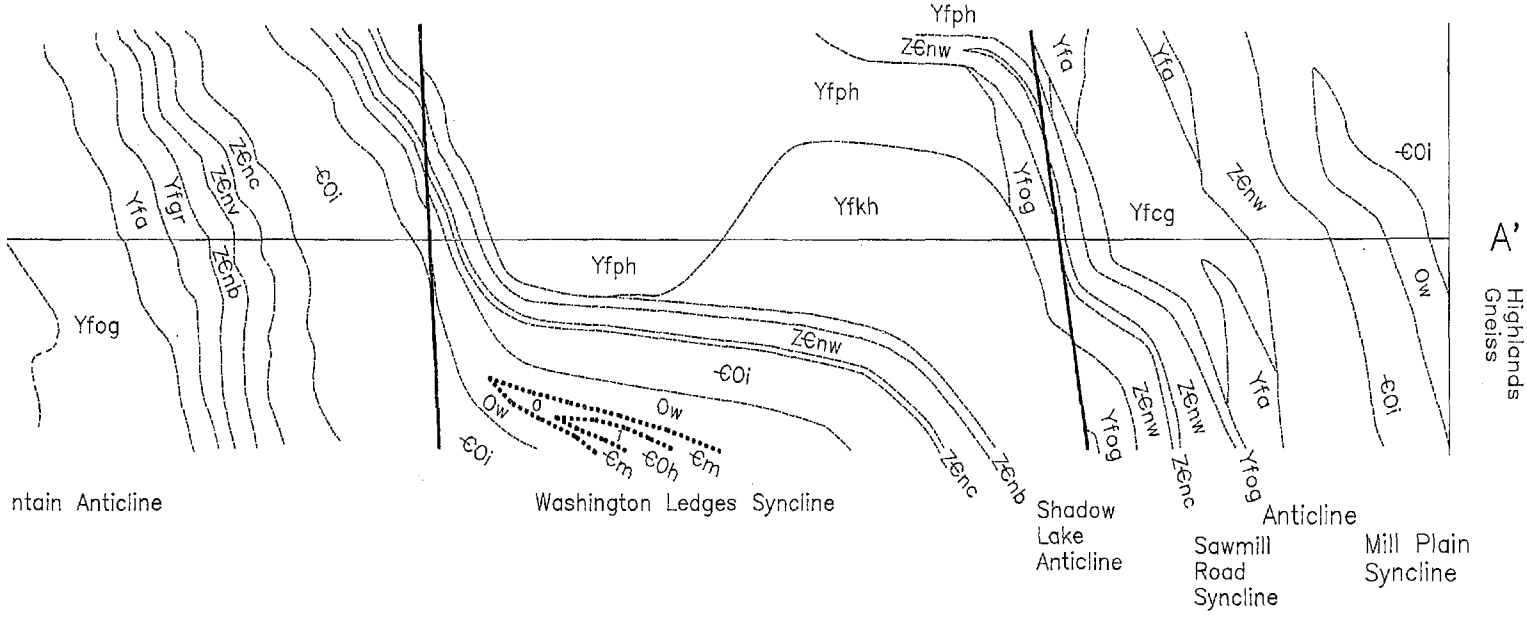

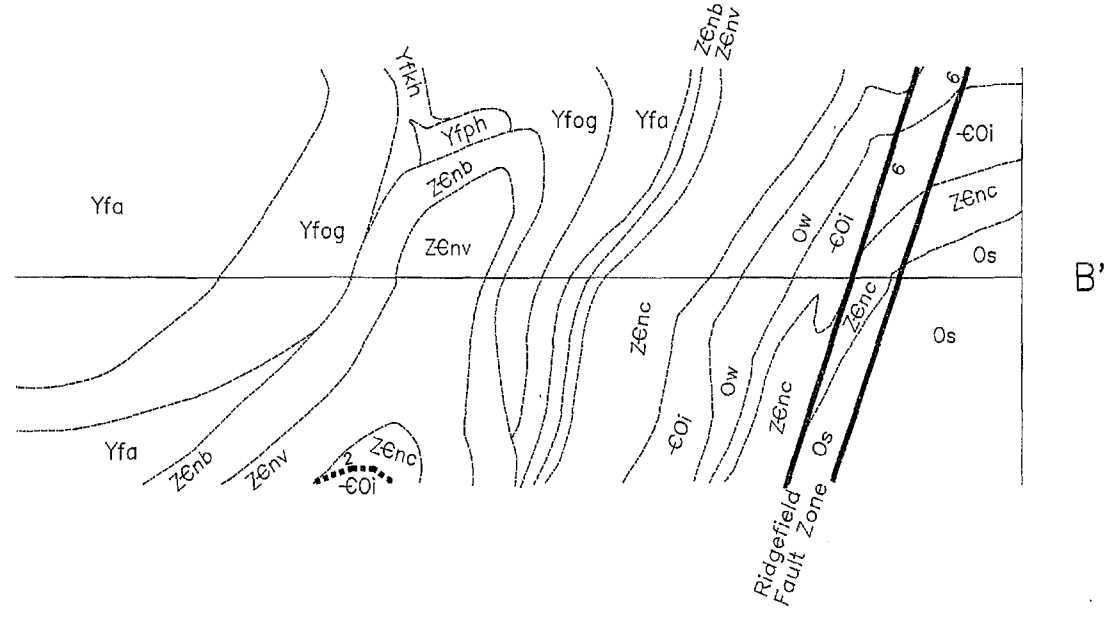

A J.
03

PLATE VI — MODEL FOR THE TACONIAN OROGENY IN THE MANHATTAN PRONG

NORTHERN MANHATTAN PRONG

CENTRAL MANHATTAN PRONG

1. D_1 deformation (Early-M_1 metamorphism)

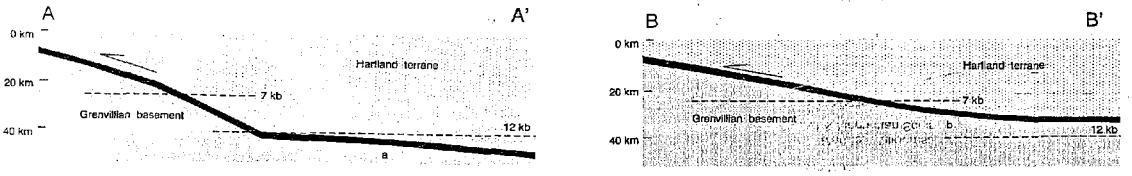

2. Post-D_1 intrusion of mafic complexes

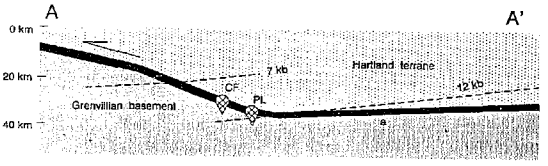

3. D_2 deformation

A. Cross Section A-A'

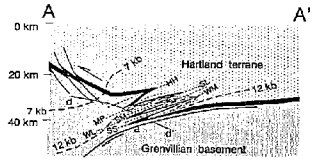

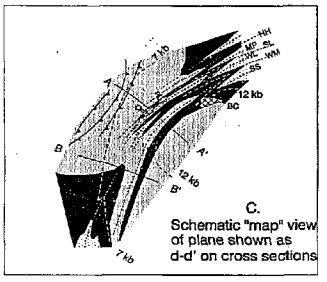

C. Schematic "map" view of plane shown as d-d' on cross sections

B. Cross Section B-B'

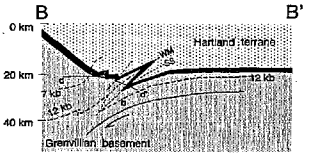

4. Post-D_2 warping -- Intrusion of Cortlandt Complex.

HH	Hudson Highlands anticline
MP	Mill Pond syncline
SM	Sawmill Road syncline
SL	Shadow Lake anticline
WL	Washington Ledges syncline
WM	West Mountain anticline
SS	South Salem syncline
CF	Croton Falls Complex
PL	Peach Lake Complex
BC	Bedford Complex
CC	Cortlandt Complex

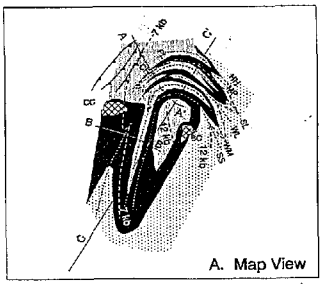

A. Map View

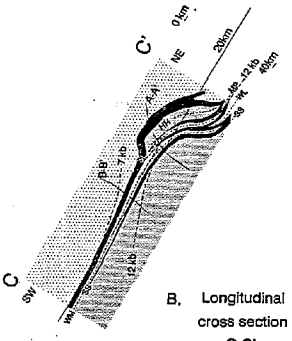

B. Longitudinal cross section C-C'

5. F_3 folding

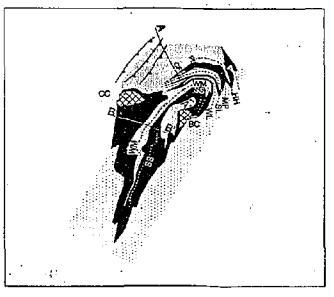

Mafic complexes

Hartland terrane

Inwood Marble, Walloomsac Schist & Manhattan Schist

Grenvillian basement

Thrust fault

F_2 hinge surfaces

Early-M_1 7 kb & 12 kb isobars

BROCK, PAMELA J.
9325069 © 1993